International **Rotating** **Equipment** Conference

8th EFRC Conference

Pump Users
International Forum 2012

Compressor Users
International Forum 2012

EFRC
EUROPEAN FORUM
for RECIPROCATING
COMPRESSORS

EFRC Conference 2012

Düsseldorf, 27th–28th September 2012

PROCEEDINGS

Sponsored by

Contents

EFRC

EUROPEAN FORUM
for RECIPROCATING
COMPRESSORS

CONVENE WHERE EUROPEAN HISTORY WAS WRITTEN

In the past the Hofburg was a stage for world political and cultural history. Maria Theresia, Joseph II and Metternich lived and worked at the Hofburg, while Mozart, Beethoven, Liszt and Strauss made music here. Emperor Franz Joseph I gave the Hofburg its present day appearance.

Today the Hofburg is one of the world's best-loved conference centers and You will have the chance to convene here with the leading minds of the reciprocating compressor industry and to determine the future of your compressors. Here where European history has been determined.

EUROPEAN FORUM for RECIPROCATING COMPRESSORS

Save the date:
9th EFRC Conference
September 17th - 19th, 2014
Vienna

FITTING PERFECTLY

FOR YOUR NEEDS OF FLOW CONTROL.

NEA
BLUEPOCKET

NEA
BLUEPOCKET
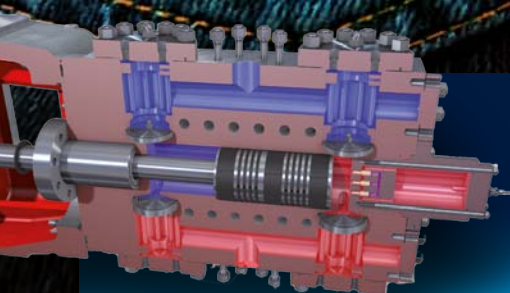
Innovation of a new generation of dynamic clearance pocket for all types of NEA reciprocating compressors. Retrofitable.
Energy management at prime settings.

Learn more at Booth A10

NEUMAN & ESSER GROUP

8th Conference of the EFRC
September 27th / 28th, 2012, Düsseldorf

EFRC

EUROPEAN FORUM for RECIPROCATING COMPRESSORS

Nonlinear multi-axial fatigue analysis of a threaded crosshead to piston rod connection of a reciprocating compressor using the Brown-Miller algorithm

by:

Riccardo Traversari	**Alessandro Rossi**	**Marco Faretra,**
Rotating Machinery Design Manager	**Rotating Machinery Design Engineer**	**Mechanical Engineering Consultant**
Compression Service Technology	**Compression Service Technology**	**Hypertecs s.r.l.**
Florence	**Florence**	**Casalecchio di Reno (Bo)**
Italy	**Italy**	**Italy**
riccardo.traversari@cstfirenze.com	alessandro.rossi@cstfirenze.com	marco.faretra@hypertecs.it

8th Conference of the EFRC
September 27th / 28th, 2012, Düsseldorf

Abstract:

The crosshead to piston rod threaded connection is one of the most critical parts of the whole reciprocating compressor. Traditionally, this critical connection is dimensioned by the classic method of the "Load/Deformation diagram" or "triangle of the elasticity's" to evaluate mean and fluctuating stresses on the thread and then the relevant safety factor with the specific Smith fatigue diagram.

A better approach is to make a Finite Element Analysis, which can be performed simulating the threaded connection as a cylindrical surface, neglecting the real thread geometry or, even better, simulating the real thread geometry. But, even the more refined elastic FEM fatigue analysis, with Von Mises monoaxial equivalent stress, typically estimates stresses that often exceed the material yield strength in the thread root radius, thus resulting in unrealistically poor safety factors even in the subsequent fatigue analysis. Also a biaxial fatigue analysis for infinite life in the linear range shows the same problem even for well proven applications.

This paper, after a review of the aforementioned methods, describes a new advanced approach to the design of the threaded connection of the crosshead to piston rod based on an elastic-plastic, multi-axial nonlinear, non proportional FEA, using the Brown-Miller algorithm with the Morrow correction of the mean stress. This new calculation method allows taking in the correct consideration also the possible local plastic deformations, evaluating their real effect on the thread strength.

Nonlinear multi-axial fatigue analysis of a threaded crosshead to piston rod connection of a reciprocating compressor using the Brown-Miller algorithm, *Riccardo Traversari, Alessandro Rossi, Marco Faretra;* COMPRESSION SERVICE TECHNOLOGY, HYPERTECS S.R.L.

1   Introduction

The connection between the piston rod and the crosshead is one of the critical points in a reciprocating compressor. In fact many failures at this point are reported in the literature[1] and it has been always a matter of great attention by the design engineers of these machines. The main reason for this criticality is that this connection implies some areas of stress concentration, metallic contacts and movement.

Recently, in order to monitor this area of the compressor, specific diagnostic systems have been developed to detect as soon as possible conditions of potential damage.

2   Various types of piston rod to crosshead connection

The various manufacturers have utilized various solutions for this connection and some of them have utilized different solutions for the various size of machine and in different times. Also the API Standard 618[2] take into consideration this connection and give some directives for the design.

A quick and schematic summary of the most popular solutions is reported in Figure 1.
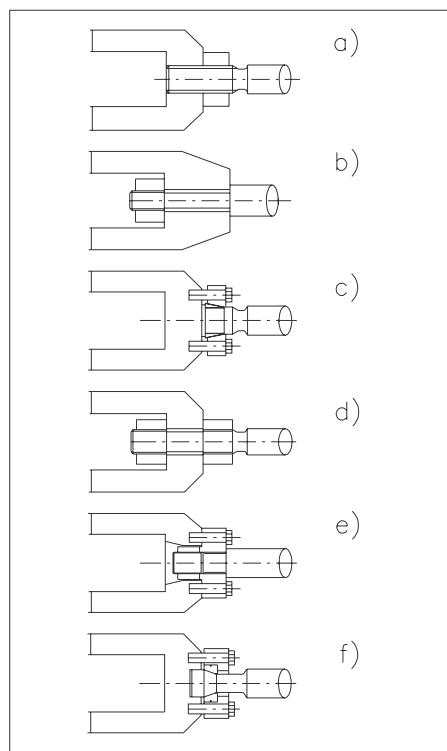
Figure 1: Various type of piston rod to crosshead connection

Solutions a), b) and c) are the typical designs reported also by the API Standard. Solution a) provides for a long thread on the extremity of the piston rod which is screwed into the crosshead body by rotating the piston and is preloaded by tightening an external nut. This solution was widely utilized in the past but as it is rather difficult, particularly with large rods, to tighten the external nut, the preload achieved was often insufficient and that caused loosening of the connection with consequent fatigue failure. This solution has nowadays more limited application to the rather small piston rod sizes.

Solution b) is an improvement as it positions the threaded portion of the piston rod in a more protected location where, due to the much more elastic preloaded shank, it is subject to much lower stress fluctuation. This solution is conceptually good and has, in addition, a smaller nut to be tightened, but the internal position of the nut requires to find a way to tighten it properly.

Solution c) has still a thread in the non protected area but it reduces the tightening risk as it delegates the connection to the crosshead body to a series of multiple smaller bolts, normally four or six, which are easier to be tightened by torque wrench to achieve the proper preload.

Solution d) is also an improvement of solution a) as it increases somewhat the elasticity of the preloaded portion of the rod but it still keep the risk of insufficient tightening, especially for large sizes.

Solution e) is similar to solution b) where the problem to tighten the nut is solved by introducing a flange, to which the shank is tightened externally and connecting the flange, as in solution c), to the crosshead body with bolts of smaller size.

Solution f) has eliminated the thread which is substituted by a conical clamping. The piston rod is fastened to the crosshead body through a multibolt flange as in solutions c) and e). This solution has the advantage to eliminate the thread but the disadvantage to introduce the mating of two conical surfaces which is not easy to be obtained.

Many other similar solutions or combination of the above described ones have been adopted by the various manufacturers. As a general comment one can say that it has been clearly understood that, whatever solution is utilized, the main protection against fatigue failures is a correct tightening of the connection. It is for this reason that API in their 618 Standard have specified that "the tightening procedure shall assure a minimum preload in the connection equal to 1.5 times the maximum allowable continuous rod loading".

Nonlinear multi-axial fatigue analysis of a threaded crosshead to piston rod connection of a reciprocating compressor using the Brown-Miller algorithm, *Riccardo Traversari, Alessandro Rossi, Marco Faretra;* COMPRESSION SERVICE TECHNOLOGY, HYPERTECS S.R.L.

3 Traditional calculation approach

The traditional approach to the calculation of the connection between threaded piston rod to the crosshead is based on the classic "Load/Deformation diagram" or "Triangle of Elasticity's" of bolted joints reported by most of the books of Machine Design, for instance the Mascinen Elemente of G. Niemann & others[3]. A typical example of this diagram is shown in Figure 2, where:

α= Stiffness of the parts subject to tension
β= Stiffness of the compressed parts
P= Preload
F_T= External operating force (Tension)
F_C=External operating force (Compr.)
ΔF= Total amplitude of the fluctuating force on the parts subject to tension
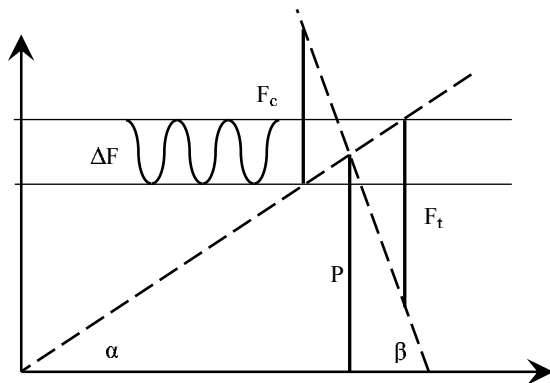
Figure 2: Load/deformation diagram

The Load/Deformation diagram is very useful to determine the total amplitude of the fluctuating force ΔF on the threaded area as, dividing this by the screw root area, one obtains the fluctuating stress on the thread that is then compared with the allowable fatigue limit of the threads of the specific material and production technology (simply cut, ground, rolled, etc).

A problem of this type of approach is that, due to the squat dimensions of the components of the connection crosshead to piston rod, it is rather difficult to determine the values of α and β. Figure 3 shows a typical piston rod to crosshead connection where the areas of influence of the tightening force is shown. The shaded area is deriving by the assumption that the preload propagates from the area of application of the force toward the contact zone in conformity to the Roetscher cone of influence of 30°. Consequently the stiffness of the compressed parts must be calculated as that of an average cylinder represented in Figure 3 with a dotted line.
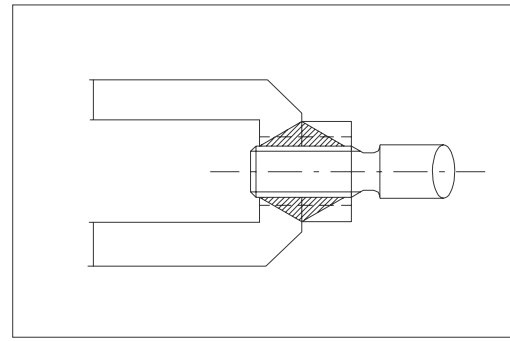
Figure 3: Cone of influence representation

Another uncertainty comes from the determination of the area where the external force is applied as the relevant point of application determines a modification of the Load/Deformation diagram[3] and then the value of the fluctuating force on the thread.

Although this method has allowed for several decades to design reasonably good connections and it is still good for the preliminary sizing of this important area of the reciprocating compressors, a better approach is necessary for a more precise stress analysis.

4 A better approach: Finite Element Analysis (FEA)

Nowadays a more advanced approach can be used in simulating the crosshead to piston rod connection. In fact in paragraph 3 it has been shown that it is not always simple to state a reliable model based on the "De Saint Venant" theory due to the fact that the components are often squat. For example, in this particular study (see Figure 4) the rod region between the flange (that is bolted to the crosshead body) and the nut can be hardly evaluated as a slim beam subject to tension, while the other pulled parts, other than the compressed ones, to be considered in the Load/Deformation diagram, are hard to be determined in a reliable way.

All these limits can be overcome by means of the FEA, but also this method has his own problems and has to be used, in the crosshead simulation, with great care and doing the due considerations, as it will be shown in the following.

The very first approach in simulating the crosshead to piston rod connection (but it is a very general consideration to do, dealing with FEA) is to represent the geometry of the actual parts to be studied. Usually who performs the FEA study has to choose the "depth of detail" to be used in the model. Not every detail of the real part can be represented in the 3D model, and, less evident but

Nonlinear multi-axial fatigue analysis of a threaded crosshead to piston rod connection of a reciprocating compressor using the Brown-Miller algorithm, *Riccardo Traversari, Alessandro Rossi, Marco Faretra;* COMPRESSION SERVICE TECHNOLOGY, HYPERTECS S.R.L.

not less important, not every detail is useful to be represented. In our case, the main aspect is the threaded connection between the rod and the flange. The approach can be double: modelling the real thread geometry or neglecting it.

4.1 Connection simulation neglecting the real thread profile
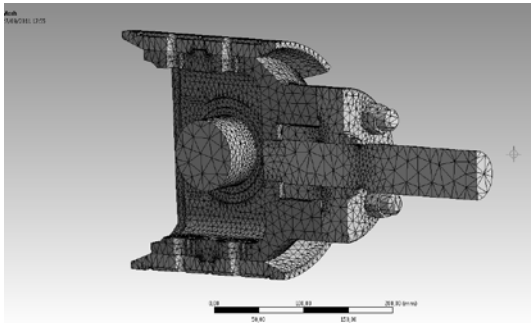
Figure 4: 3D model neglecting thread geometry of the rod

The easier approach is, for sure, simplifying the threaded connection by neglecting the real thread geometry and considering the threaded part of the rod as a cylinder with a diameter equal to the thread root area (see Figure 4). One way to calculate the fatigue safety coefficient of the thread from the stress distribution obtained by the FEA (see Figure 5), run with the above simplification, is to do it manually by computing the average stress across the virtual cylinder section and entering its mean value and fluctuation during the compression cycle, into the Smith diagram relevant to the specific material and thread manufacture technology.
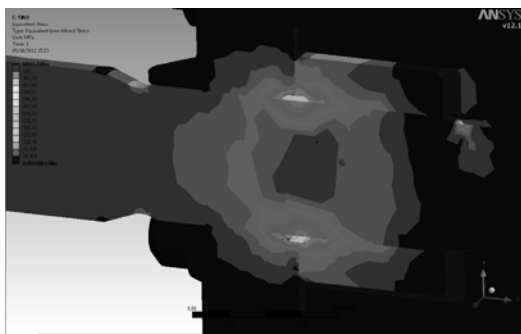
Figure 5: Stress distribution neglecting threads

This approach, although introducing an important approximation, has the advantage of evaluating quite well the stiffness of the various parts of the connection and is "something in the middle" between the traditional manual approach and the fully computational one. As it will be seen in the following, this method allows to avoid some problems that arise with the fully computational way.

4.2 Connection simulation with the real thread profile
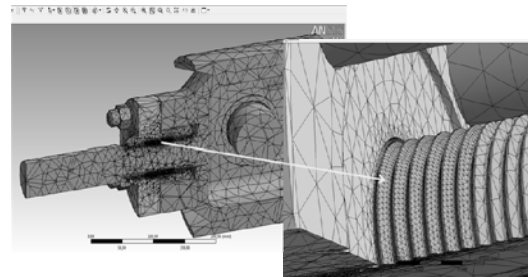
Figure 6: 3D model representing the real thread geometry

This approach considers the real shape of the thread in the 3D model to be analyzed (see Figure 6). It seems this to be the most complete and accurate approach, but an important aspect is related to the particular shape of the thread. As a matter of fact, although one generally speak of a thread to be tightened at an average nominal stress related to the thread root area, the FEA static analysis done with an elastic model of the materials shows that at the thread root, even if in a very superficial surface, the stress is much higher than the average nominal and may be close to the yield point of the material, or exceed it. For instance, in the case under examination, the stress at the root resulted 950 N/mm^2 while the yield stress of the material was 600 N/mm^2 (see Figure 7).
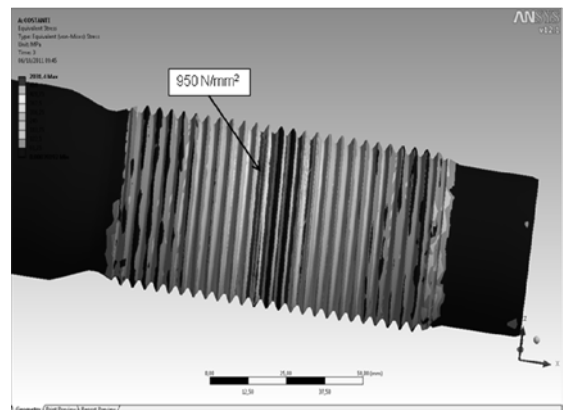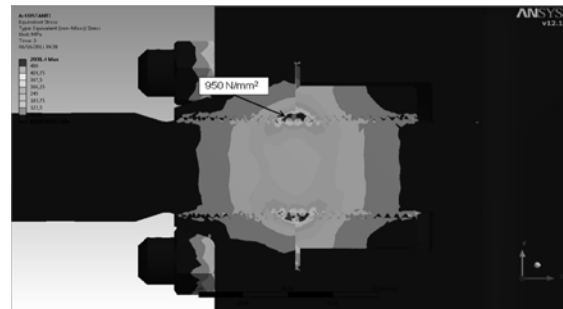
Figure 7: Elastic FEA shows 950 N/mm^2 at root

In the real situation this is all but a problem. In fact the surface material that yields causes a local redistribution of the stress that has just the effect to transfer the load to the area surrounding the one plastically deformed. But the problem is that, in such a situation, it is not possible to perform a conventional FEA fatigue analysis because it would give misleading and pessimistic results. In fact, see Figure 8, the fatigue analysis performed with the Dang Van method[4], shows that, in the preloaded part of the piston rod, in spite of an average nominal stress on the thread root area of 250 N/mm^2 and a stress fluctuation of 10 N/mm^2 the thread results to have a fatigue safety coefficient less than 1 and close to 0.5 for infinite life, which is not realistic.
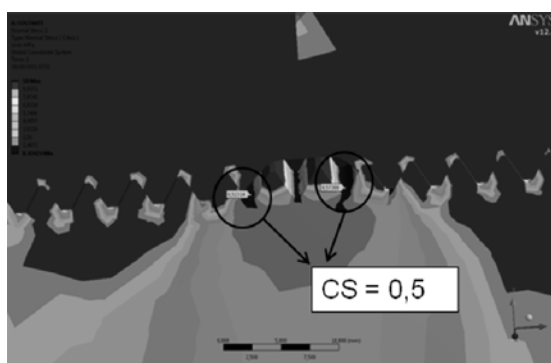
Figure 8: Dang Van safety coefficient of the preloaded part of the piston rod

On the contrary, for the really problematic region, that is the first thread close to the flange on the piston side, the same method gives a much higher fatigue safety coefficient of 1.55.
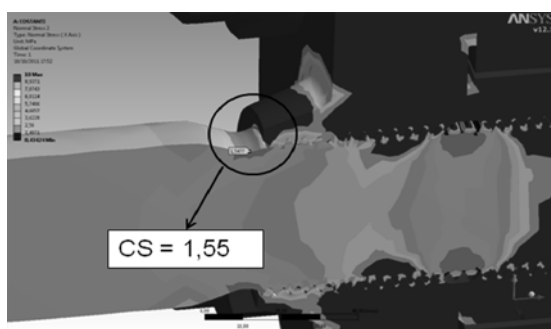
Figure 9: Dang Van coefficient of the first thread

This result is clearly unrealistic. This is the main reason why usually it is preferred to neglect the real thread geometry and make this calculation according to the system described in para 4.1.To achieve a better understanding of the stress distribution on this type of connection and at the same time a more realistic fatigue safety coefficient it is necessary to move to a more advanced method that is described in the following.

5 Fatigue coefficient determination

5.1 Various methods for fatigue resistance evaluation

The fatigue analysis is fundamental in the design process of mechanical components since fatigue failure is the principal cause of damage of mechanical structures subject to time-varying loads.

Considering the implications that the fatigue resistance of components has in regard to the economic success of a product and safety issues, many researchers, starting with Wöhler (1860), have dedicated much efforts to the implementation of criteria that predict the behaviour of components subject to mechanical loads varying in time. The criteria for fatigue analysis were mainly developed considering a uniaxial state of stress and were mostly based on curves of resistance stress - number of cycles.

In the following one presents three of the most known criteria that have been proposed to assess the fatigue strength in the case of multiaxial stress states that occur in the machinery components.

5.2 Monoaxial approach with equivalent stress according to Von Mises

Numerous investigators have attempted to correlate multiaxial fatigue test data using parameters originally developed for static yield under complex stress states. The benefit of such an approach is that simple uniaxial tests would be sufficient to completely describe fatigue behaviour under any combination of complex loading.

Although many yield criteria have been suggested, the most popular theory is the octahedral shear stress theory, normally called von Mises theory, which can be computed as:

$$\Delta\sigma_{eq} = \frac{1}{\sqrt{2}}\left[(\Delta\sigma_1 - \Delta\sigma_2)^2 + (\Delta\sigma_2 - \Delta\sigma_3)^2 + (\Delta\sigma_3 - \Delta\sigma_1)^2\right]^{\frac{1}{2}}$$

This equation is valid only for proportional or in-phase loading as in case of non proportional or out-of-phase loading (i.e. that implies the variation of the direction of principal stresses during the load cycle) it happens that:

$$\Delta\sigma_1 - \Delta\sigma_3 \neq \Delta(\sigma_1 - \sigma_3)$$

so that no unique definition of the shear stress exists.

5.3 Multiaxial linear approach according to Dang Van

The development of computational techniques based on finite elements and the need to have multiaxial, non proportional fatigue analysis criteria, has stimulated research and nowadays several studies are now available in this regard[5][6][7][8]. Dang Van[9] proposed a model that considers that the nucleation of a crack happens at the microscopic grain dimension scale.

His method deals with a two size scale:

- A macroscopic scale, that is related with the elementary volume surrounding a point where the fatigue analysis is to be performed. This size scale is of the order of dimension of a strain gage or a FEM element, i.e. of a few millimeters. This is the scale that can be investigated with the traditional techniques.
- A microscopic grain dimension (much smaller of a FEM element, of the order of 10^{-4} mm).

The values of stresses and strains of macroscopic and microscopic areas are different from each other, but the Dang Van[10] method states a relationship among them, so that by means of a tool such as FEA, that investigates the macroscopic ones, also the microscopic can be evaluated, and the fatigue safety coefficient calculated.

The assumption at the base of the criterion is that no fatigue failure occurs if the component is stabilized in a state of elastic shakedown, which entails the fact that residual stresses must be constant in time and the stress must remain in the elastic range.

Practically the criterion prescribes to compare the fatigue limit of the material $\tau(t) + a\,\sigma_h(t) = b$, where a and b are experimental coefficients related to the material, with the loading pattern of the microscopic stress. As one can see from Figure 10 there is no fatigue failure when the loading path is kept within the area defined by the two lines of the fatigue limit.

5.4 Multiaxial nonlinear approach using the Brown-Miller algorithm with the Morrow correction of the mean stress

The Brown-Miller method[11] of fatigue evaluation is a multiaxial non proportional method that evaluates the "life" of a part calculating the number of cycle within which that part does not fail. The Brown-Miller algorithm proposes that the maximum fatigue damage occurs on the plane which experiences the maximum shear strain amplitude, and that the damage is a function of both these shear strain and the strain normal to this plane (see Figure 11).
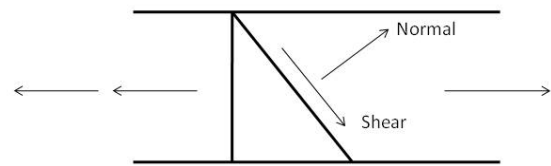
Figure 11: The Brown-Miller method

The Fe-safe[12] software, that was utilized by the authors for the case study reported in para. 6 offers, among other fatigue evaluation criteria, a method based on the Brown-Miller algorithm[13] modified by Morrow to take into account the mean stress. This method allows to take into account also the following parameters[14]:

- the strain hardening coefficient K'
- the strain hardening exponent N'
- the fatigue strength exponent (Basquin's exponent) b
- the fatigue strength coefficient σ_f'
- the fatigue ductility exponent (Coffin-Mason exponent) c
- the fatigue ductility coefficient ε_f'
- the surface finish
- the machining type (grounding, rolling, etc.)

Figure 10: The Dang Van method

Nonlinear multi-axial fatigue analysis of a threaded crosshead to piston rod connection of a reciprocating compressor using the Brown-Miller algorithm, *Riccardo Traversari, Alessandro Rossi, Marco Faretra;* COMPRESSION SERVICE TECHNOLOGY, HYPERTECS S.R.L.

6 Final elastic-plastic FEA and Brown-Miller fatigue analysis of the crosshead to piston rod connection

As it has been seen in the previous paragraphs, the correct way to manage a complex situation, such the case of a threaded crosshead to piston rod connection, involves several aspects to be taken into account, such as:

- geometry (detailed or simplified)
- model of internal stress distribution and their variation during the load cycle application to be considered in the FEA study (equivalent monoaxial or multiaxial)
- simulation of the real behaviour of the material including its plastic phase: σ/ε curve of the material (real yielding curve or simply elastic)
- fatigue evaluation method to be considered (i.e. proportional or non proportional)

To take into account, for a robust engineering design, of all above features for our case study, the FEA was repeated utilizing advanced software capable of evaluating also the plasticity situations. The elastic-plastic behaviour of the material was considered as bilinear isotropic hardening as shown in Figure 12.
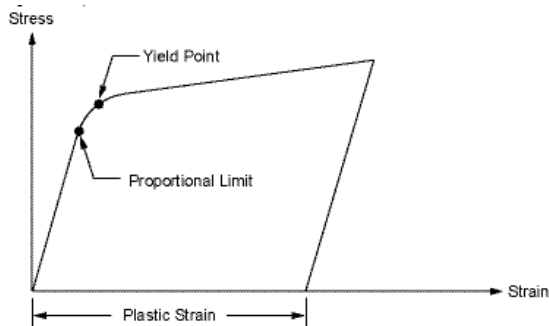
Figure 12: σ/ε curve of bi-linear isotropic materials

The results of the new FEA on the 3D model simulating the real thread profile and considering an elastic-plastic behaviour of the material show that the stress level in the root radius is, roughly half of the one calculated considering a pure elastic behaviour of the material: the maximum value is 480 N/mm^2 against 950 N/mm^2 (see Figure 13).
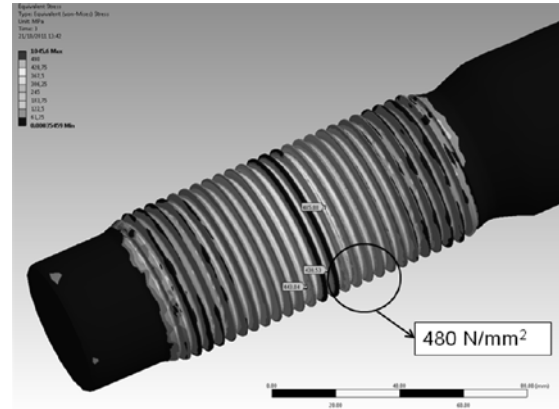
Figure 13: Elastic-plastic FEA shows 480 N/mm^2 at root radius

In fact the better FEA model shows that there is a redistribution of the stress in the layers underneath the surface of the thread (see Figure 14).
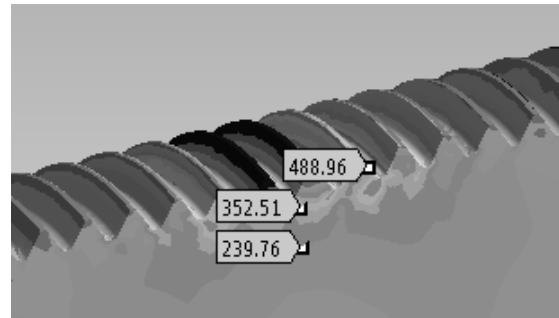
Figure 14: Stress yielding redistribution due to surface material

The fatigue analysis was performed using the Brown-Miller algorithm described in para. 5.4. The results of this fatigue analysis, performed considering the same load conditions of the previous ones, shows a more consistent situation as shown in Figure 15.
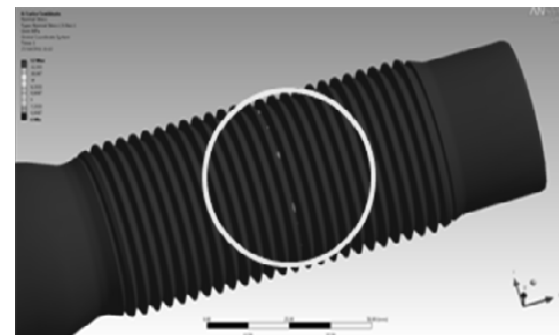
Figure 15: Points with 10^{10} cycle life

23

Nonlinear multi-axial fatigue analysis of a threaded crosshead to piston rod connection of a reciprocating compressor using the Brown-Miller algorithm, *Riccardo Traversari, Alessandro Rossi, Marco Faretra;*
COMPRESSION SERVICE TECHNOLOGY, HYPERTECS S.R.L.

The few points in the root radius highlighted in the picture show a life of 10^{10} cycles. In fact the method calculates a life duration and does not state, as f.i. Dang Van method, the "infinite life" condition. However, that duration can be considered as "infinite life" for the practical application: a typical rotation speed for such machine is 600 rpm, that are 315360 cycles/year, therefore 10^{10} cycles are 31.7 years of continuous service, while the life of the whole machine is something like 20 to 30 years.

7   Conclusion

When one utilize simple tools as the "Load/Deformation diagram" and Von Mises criterion one has to make guesses about the geometry of the components, work on macro means of stresses but with the advantage of having solid reference points given by the fatigue tests on the threads made by many researchers.

Going deeper into the micro stress analysis, f.i. with the FEA, allows to have a better knowledge of how the material is loaded but one must avoid to "believe" the results in a fideistic way and, on the contrary, have awareness of the limits of the tools that are being utilized. The state of stress that comes out of the calculation must be interpreted by the operator and compared with his experience and possibly with other similar methods. Also the evaluation of the potential damage that a certain state of stress can cause shall be deeply considered and the most appropriate fatigue evaluation method selected for the specific application.

For the case study the methods that have shown to be more consistent were the elastic-plastic FEA and the Brown-Miller/Morrow based fatigue evaluation criterion.

References

[1] Detection of concealed damages in early stages on reciprocating machinery, Eike Drewes, Prognost System GmbH, Rheine, Germany, 4th Conference of the EFRC June 9th/ 10th, 2005

[2] API 618, Reciprocating Compressors for Petroleum, Chemical, and Gas Industry Services, Edition: 5th

[3] Maschinen-Elemente Band 1: Konstruction und Berechnung von Verbindungen, Lagern, Wellen, G. Niemann, Est Springer, 1983

[4] Criterion for high cycle fatigue failure under multiaxial loading, in biaxial and multiaxial fatigue, Dang Van, K., et al., Mechanical Engineering Publication, London, pp.459-478, 2003

[5] Multiaxial Fatigue of an Induction Hardened Shaft. Cordes, T., Lease, K. s.l., SAE International, 1999

[6] Modern Metal Fatigue Analysis. Draper, J. s.l. EMAS Publications, 2008

[7] Locati, L. La fatica dei materiali metallici. Milano Ulrico Hoepli, 1950

[8] Socie, D.F., Marquis, G.B. Multiaxial Fatigue. s.l. SAE International, 1999

[9] High cycle fatigue and a finite element analisys Dang Van, B., Papadopoulos, D. 3, pp.397-411, s.l. Fatigue Fract. Eng. Mater. Struct., 1995, Vol. 18

[10] Dang Van, K., Paradopoulos, I.V. High-cycle Metal Fatigue: From Theory to Applications (CISM International Centre for Mechanical Sciences). s.l. Springer Verlag GmbH, 1999

[11] A theory for fatigue failure under multiaxial stress-strain conditions, Brown, M.W., and Miller, K.J, Proceedings of the Institute of Mechanical Engineers, Vol. 187, 1973, 745-756

[12] Fe-safe user guide – Safe technology - http://www.safetechnology.com

[13] Developing a durability by design process, John Draper, ASME Advances in Modeling, Analysis, and Simulation of Manufacturing Processes, October 4-7, 2009, Purdue University, West Lafayette

[14] A critical plane approach to multiaxial fatigue damage including out-of-phase loading, Ali Fatemi, Darrel F. Socie, Fatigue & Fracture of Engineering Materials & Structures Volume 11, Issue 3, pages 149–165, March 1988

Advanced multilevel solution of journal paths in reciprocating compressors including bearing deformation

by:

P.N. Duineveld, B. Brogle

Technology Department

Howden Thomassen Compressors BV

Rheden, The Netherlands

pd@thomassen.com

C.H. Venner, S. van Loo

Department of Mechanical Engineering

Faculty of Engineering Fluid Dynamics

University of Twente

Enschede, The Netherlands

8th Conference of the EFRC
September 27th / 28th, 2012, Düsseldorf

Abstract:

In compressor bearing analysis and design to determine the journal paths and film thicknesses traditionally the Mobility method is used. This method is computationally very cheap and well suited for practical engineering as it uses predetermined expressions relating the bearing force to the eccentricity and loading conditions. However, these expressions are restricted to a particular bearing type and effects which may be crucial under extreme loads such as bearing deformation cannot be taken into account. For this purpose an alternative approach is presented in this paper. A numerical solution approach has been developed solving the full two dimensional Reynolds equation for the pressure at every moment in time during loading cycle and the journal paths. The approach allows taking into account arbitrary bearing shapes deformations, constant, as well as varying in time. To allow use in a practical design environment optimally efficient Multigrid techniques are used for the numerical solution of the equations such that realistic cases can be considered on small scale computers which are commonly available. In this paper the method is explained, validated, and some first results are presented illustrating the effect of bearing deformation on the journal path.

Advanced multilevel solution of journal paths in reciprocating compressors including bearing deformation,
P.N. Duineveld, B. Brogle, C.H. Venner, S. van Loo; HOWDEN THOMASSEN COMPRESSORS BV,
UNIVERSITY OF TWENTE

1 Introduction

In bearing analysis for compressor design traditionally the Mobility Method (Booker, 1971, Moes 2000) is used to predict the bearing pressure field in the journal path computation. This is a very reliable and easy to use, computationally cheap method which is still widely applied nowadays, see e.g. (Moes, 2000) for an application to reciprocating machinery. Current trends in design are towards more extreme loading conditions (higher forces/ratings) which will increase to a level where the effect of bearing deformation induced by forces may have a significant effect on the film thickness in the bearings and on the journal paths. As a result of these forces the bearings will elongate in the direction of the force, i.e. the bearing shapes will tend to be elliptic with the major axis of the ellipse directed along the load. This effect may be detrimental or beneficial to the minimum film thickness along the journal path. A disadvantage of the mobility method is its inflexibility to take into account variations in bearing shape. In that case new mobility functions have to be "developed" e.g. from numerically pre-computed solutions of the Reynolds equation for the given bearing shape and for the many possible values of eccentricity and speed.

In order to gain more insight into the effects of bearing deformation on journal path and film thickness in reciprocating compressors a full numerical solution approach has been developed. This has become feasible since computer power has increased tremendously and nowadays advanced numerical solution algorithms allow very quick numerical solution of the Reynolds equation. The full numerical solver has full flexibility regarding the bearing shape, ranging from pre-chosen shapes such as circular or elliptic to full dynamic shape changes along the journal path. An additional advantage is the possibility to incorporate effects of groove patterns in the bearing.

In this paper the novel approach is described. Next, for some characteristic cases the results are compared with results presented in the literature and results obtained using the Mobility Method. Finally the results of bearing deformation on the journal path and minimum film thickness are shown for an example reciprocating compressor application.
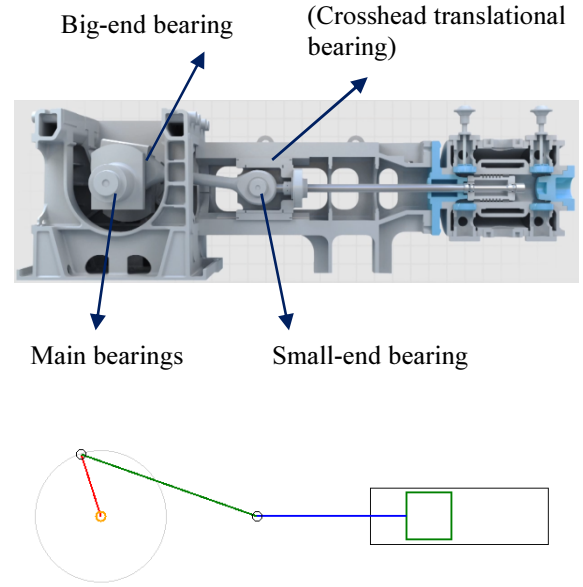
Figure 1: Model and schematic of crank mechanism reciprocating compressor including main bearings, big- and small-end connecting rod bearings and crosshead translational bearings

2 Theoretical Model

The theoretical model consists of two equations. First the Reynolds equation relating pressure to film thickness (gap shape) and its time derivative. Secondly, an equation of motion for the journal center. When inertia effects are neglected, this is simply a force balance equation which equates the momentary external load to the integral over the generated pressure field. This equation determines the momentary value of the eccentricity.

Let x be the circumferential direction and y the direction along the journal surface in the lubricant film, h the gap height or film thickness, U the entrainment velocity, and η the dynamic viscosity of the lubricant, the Reynolds equation is given by:

$$\frac{\partial}{\partial x}\left(h^3 \frac{\partial p}{\partial x}\right) + \frac{\partial}{\partial y}\left(h^3 \frac{\partial p}{\partial y}\right) = 6\eta \frac{\partial}{\partial x}(h\overline{U}) + 12\eta \frac{\partial h}{\partial t}$$

Where h is derived from the eccentricity ε :

$$h(x,t_0) = c\{1 + \varepsilon \ \cos(x/R)\}$$

Using: $\quad H = \frac{h}{c}, \quad P = \frac{pc^2}{12\eta\overline{U}R}, \quad \theta = \frac{x}{R}, \quad Y = \frac{y}{B}$

The Reynolds equation is written dimensionless:

$$\frac{\partial}{\partial \theta}\left(H^3 \frac{\partial P}{\partial \theta}\right) + \frac{R^2}{B^2}\frac{\partial}{\partial Y}\left(H^3 \frac{\partial P}{\partial Y}\right) = \frac{1}{2}\frac{\partial H}{\partial \theta} + \frac{\partial H}{\partial T}$$

Advanced multilevel solution of journal paths in reciprocating compressors including bearing deformation,
P.N. Duineveld, B. Brogle, C.H. Venner, S. van Loo; HOWDEN THOMASSEN COMPRESSORS BV,
UNIVERSITY OF TWENTE

The equation relating motion of the three bearings one encounters in reciprocating machinery (see Figure 1) is given by:

$$\overline{U} = \frac{\omega_c R}{2}\left[H - Z\frac{\cos\phi_c}{\sqrt{\frac{l^2}{r^2} - \sin^2\phi_c}}\right]$$

A cavitation condition is introduced by assuming p=0 in cavitated regions. This is justified since the vapor pressure is small compared to pressure of the liquid. Refer to Figure 2.

The force balance equation which determines the eccentricity is written as:

$$F_\theta = f_\theta\frac{c^2}{12\eta BU_a R^2} = \int_0^{2\pi}\int_0^B P(\theta,Y)\cos\theta\,dYd\theta$$

$$F_Y = f_Y\frac{c^2}{12\eta BU_a R^2} = \int_0^{2\pi}\int_0^B P(\theta,Y)\sin\theta\,dYd\theta$$

In this equation f_θ and f_Y are the dimensional applied loads and $P(\theta,Y)$ is the pressure of the bearing liquid. Note that the bearing eccentricity does not explicitly appear in the force balance equation.

The following boundary conditions apply:
- P(Y=0) = P(Y=width)=0
- P(Q=0) = P(Q =2π)
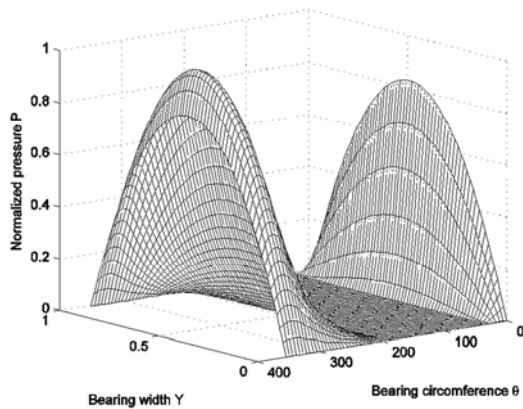
Figure 2: Characteristic pressure profile in the lubricant film in a bearing as a function of the angular and width coordinates. Note that the solution is periodic in the angular coordinate. The zero pressure region is the "cavitated" region

3 Numerical solution

The first step for numerical solution is to discretize the continuous equations, i.e. at each point of a computational grid covering the domain the continuous equation is approximated by an algebraic equation relating the values of the unknowns in neighboring points of the grid. For simplicity in the present study a finite difference method has been used with a second order central differencing of the pressure flow terms (Venner & Lubrecht, 2000) and a first order discretization of the wedge and squeeze term. The result is an implicit algebraic system of equations for the unknowns to be solved for the pressure and the eccentricity at each instant in time. The advantage of the implicit scheme is its stability. The first order discretization provides sufficient accuracy. However, it can quite easily be replaced by a higher order discretization.

Starting with an initial position the pressure field is solved. Subsequently a timestepping procedure is used. At each timestep the pressure field and the eccentricity are solved iteratively. For this purpose a Gauss-Seidel line relaxation method is used for the pressure, alternated with modification of the eccentricity using the residual of the force balance condition. Multigrid techniques, see (Venner & Lubrecht, 2000), are used to accelerate convergence of the iterative process.

The principle of Multigrid methods is to optimally exploit the convergence behavior of an iterative scheme to obtain a fast solution algorithm. Most iterative solution algorithms are slow to converge, in particularly when the mesh size of the grid is small, whereas mostly dense grids are required for an acceptable accuracy. The error reduction per iteration is generally $1-O(h^2)$ when h is the mesh size of the grid. The reason for this slow convergence is the very poor reduction given to error components that slowly vary over the grid (smooth components). To the contrary, high frequency components are very efficiently reduced. As a result already after a few iterations the remaining error is smooth. Multigrid techniques exploit this characteristic behavior of the iterative process by, rather than continuing on the same grid, resort to solving an approximation to the smooth remaining error on a coarser grid, i.e. typically with a mesh size twice larger. As the number of points on this grid is smaller and the convergence speed higher this can be done computationally more efficient. Besides, the equation from which the error must be solved is the same and the same iterative procedure can be used.

Advanced multilevel solution of journal paths in reciprocating compressors including bearing deformation,
P.N. Duineveld, B. Brogle, C.H. Venner, S. van Loo; HOWDEN THOMASSEN COMPRESSORS BV,
UNIVERSITY OF TWENTE

When an approximation to the error has been obtained on the coarse grid it is used to correct the solution on the fine grid, and some additional iterations are performed to remove remaining high frequency error components. This process is referred to as a "coarse grid correction cycle".

When the coarser grid is still too fine to quickly solve the problem one can introduce even coarser grids. The result is a recursive procedure in which, to solve the equations on a target grid, a series of coarser grids is used to accelerate convergence. The resulting "coarse grid correction cycle" can easily be designed such that an error reduction of an order of magnitude per cycle is obtained independent of the number of nodes on the target grid. The total work involved in the cycle is only a little more than the actual few iterations carried. Hence, problems with dense grids can be solved very efficiently on smalls scale computers. Figure 6 gives a schematic of a coarse grid correction cycle.
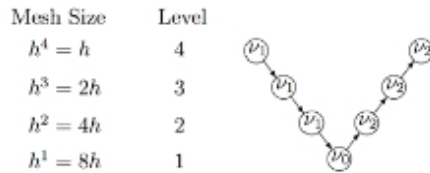
Figure 3: Schematic representation of a multigrid coarse grid correction cycle for the case of 4 grids (levels)

In the developed solver a number of these coarse grid correction cycles are used per time step to solve the system of discretized equations to a prescribed accuracy.

4 Validation

To verify the correctness of the results and the developed method two steps have been taken. The first is to investigate convergence of the solution of the discrete equation to a limit with decreasing mesh size and timestep in a manner consistent with the order of discretization. As an example in the figures 4 and 5 the x-eccentricity as a function of time is shown for the main bearing of a typical compressor obtained using different mesh sizes and timesteps in the calculations. It should be noted that in this case x refers to the (x,y) Cartesian coordinate system in which the center of the journal moves, rather than the coordinate system in the lubricant film used in the Reynolds equation. The solutions shown in the figures were obtained using a mesh size in both directions and a timestep that is each time refined by a factor two. Figure 4 shows the result of an entire load cycle. Figure 5 shows an enlargement.
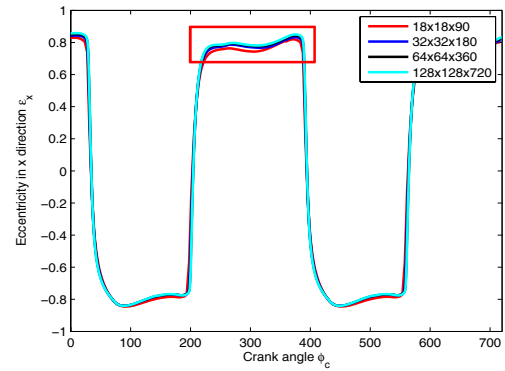
Figure 4: Eccentricity in x-direction for four different grid/time settings
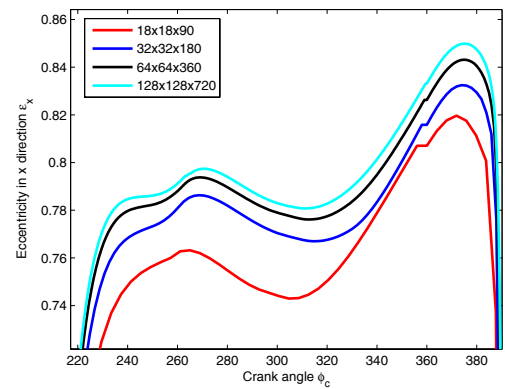
Figure 5: Zoomed part of x-eccentricity

From these figures it can clearly be seen that the solution converges. At each moment in time the difference between the results obtained using increasingly finer meshes and smaller timesteps decreases by a factor two with each refinement. With this it is shown that first order convergence is indeed the case. This is in accordance with the first order discrization in time. The observed behavior is also used to obtain an error/accuracy estimate.

Next, for a representative case taken from the literature the results are compared with results obtained using the mobility method. This is in fact an error indicator for the mobility method as solving the full system of equations for the specific bearing by definition is more accurate. The case chosen is often referred to in the scientific literature: The journal orbit of a connecting rod bearing of a four stroke Ruston and Hornsby 6 VEB-X Mk III (Campbell, 1967) diesel engine. This case was taken for comparison and the journal path is given in the figure below.

Advanced multilevel solution of journal paths in reciprocating compressors including bearing deformation,
P.N. Duineveld, B. Brogle, C.H. Venner, S. van Loo; HOWDEN THOMASSEN COMPRESSORS BV,
UNIVERSITY OF TWENTE
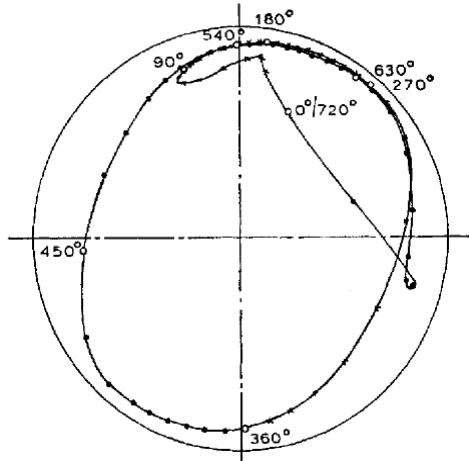
Figure 6: Journal path for a given load case from measurements (Campbell, 1967)

Using the same load shape the orbit was computed with the mobility method, yielding the results presented in Figure 7. The solution obtained using the full numerical solution algorithm is presented in Figure 8. In the computation the bearing is assumed to be rigid.

From this comparison it can be seen that the journal path obtained with the mobility method agrees well with the full numerical results, and also with results shown in the literature. which in fact is a demonstration of the remarkable accuracy of the mobility method. The computed values of the minimum film thickness for the different methods also agreed quite well with the measurements.
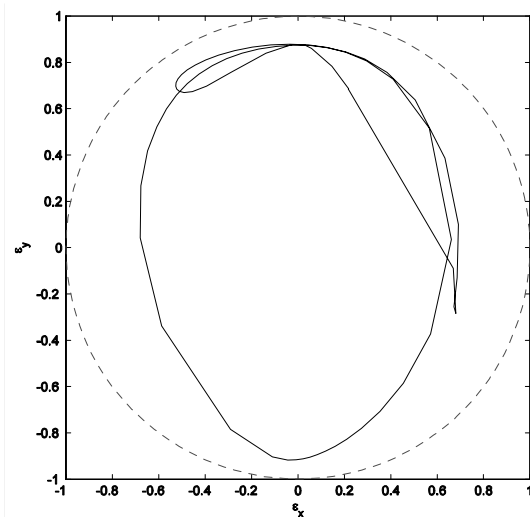
Figure 7: Journal path for a Ruston and Hornsby diesel engine computed with a mobility method
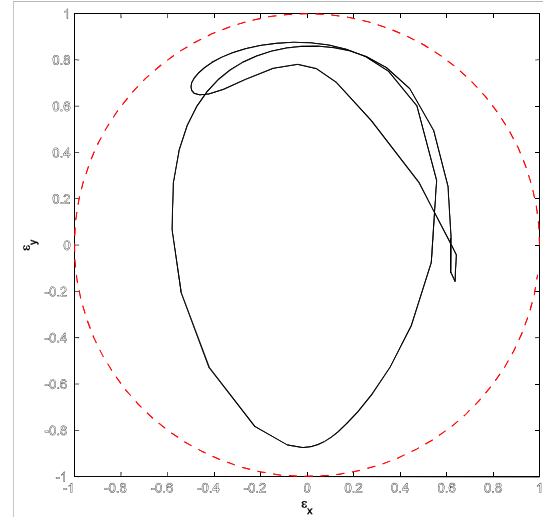
Figure 8: Journal path for a Ruston and Hornsby diesel engine computed using the full Reynolds solver

5   Bearing Deformation

So far the bearing shell was considered to be perfectly circular. In practice however, a bearing subjected to a dynamic loading cycle will not remain circular but undergo elastic deformations. In fact, a perfectly circular bearing will not be encountered at all in practice. When the loads are not too large the effects of elastic deformation on the journal path will not be large. However, when the loads increase, shape changes of the bearing shell may no longer be negligible. Hence, when designing for more extreme conditions bearing deformation may either augment or diminish lubrication conditions.

In reciprocating compressors bearing deformation is governed by external loads and not by the pressures in the film like in elastohydrodynamic lubrication (ball bearings). This allows for a significant simplification, eliminating additional iterative loops.

The developed computational methodology allows straightforward incorporation of arbitrary bearing shell shapes. In theory deformations of bearings can take all kinds of shapes. As an example case the deformation of a connecting rod is calculated using FEM, refer to Figure 9, and the bearing shell shape function derived from this is given in Figure 10.

Advanced multilevel solution of journal paths in reciprocating compressors including bearing deformation,
P.N. Duineveld, B. Brogle, C.H. Venner, S. van Loo; HOWDEN THOMASSEN COMPRESSORS BV,
UNIVERSITY OF TWENTE
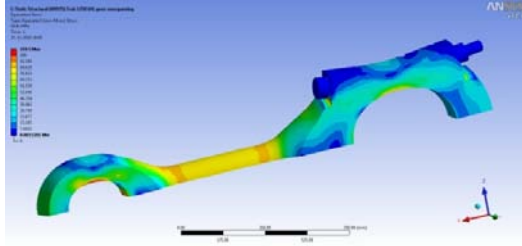
Figure 9: Stresses and displacements in a connecting rod
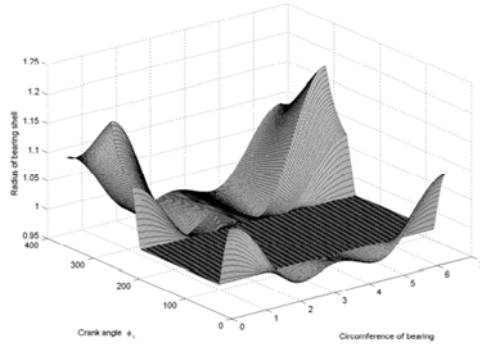
Figure 10: Surface graph of amplitude of an elliptically deforming bearing as a function of crank angle (time)

The flat part of the shape function represents compression of the shaft, where no bore elongation is imposed due to the force acting directly on the stiff part of the bore directly pushing onto the shaft.

The stiffness is such that for initial calculations it is legitimate to approximate the deformation as pure elliptical, such that a gap function can be generated without the application of for example FEM for obtaining the exact gap shape.

To mimic the shape of a connecting rod bore, an elliptic geometry function was derived, which deforms with the load function. In Figure 11 the unit clearance circle and its one-sided clearance is represented.
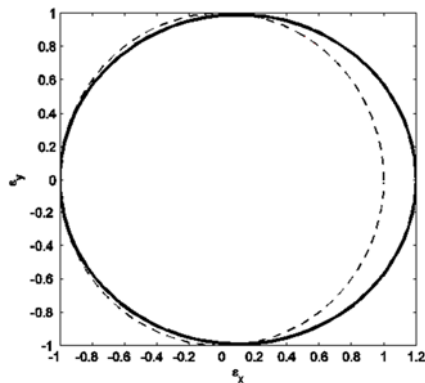
Figure 11: Comparison of the clearance circle of a circular bearing and of an elliptically deformed bearing

The developed Full Numerical Reynolds Solver (FNRS) solver can incorporate any bearing shell deformation. A data file with deformed shape data from FEM analysis can be used as input or use can be made of the elliptical approximation of the deformation allowing very quick calculations without having to make a full FEM analysis for each case.

6 Results

For a characteristic highly loaded example load case, refer to Figure 12, the journal path for the small-end bearing is calculated making use of the FNRS in combination with the in time flexible pre-defined geometry. Results of this calculation are given in Figure 13 and Figure 14 (center in clearance circle).
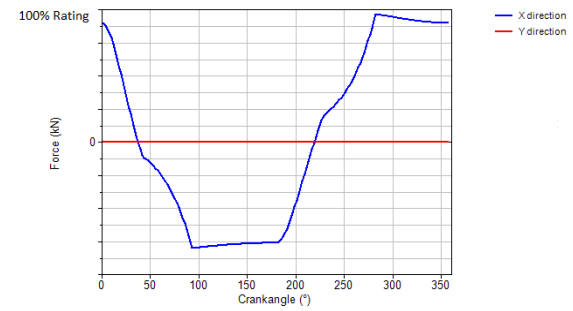
Figure 12: Pinload (small-end) diagram for example load case
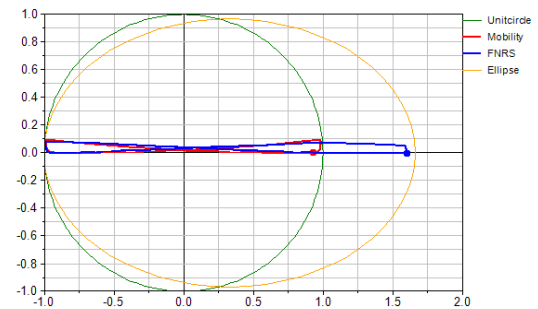
Figure 13: Small-end orbit, comparison of results obtained for the example machine assuming an undeformed and deformed bearing respectively
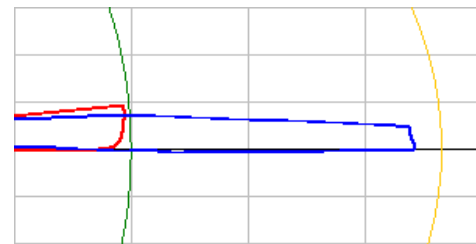
Figure 14: Zoomed in orbits of Figure 13, restricted by inner (undeformed) and outer limits of clearance circle

The maximum elastic elongation was 33% of the clearance and the side contraction 3.3%, yielding the following numerical values for the elongated side:

	Rigid mobility	Rigid FNRS	Elastic FNRS
Minimum film thickness	1.79 μm	1.67 μm	1.98 μm
Difference	+7.2%	(=100%)	+18.6%

7 Discussion

The increase in film thickness effect is easily understood: for obvious reasons the necessary clearance initiates a difference in radius under fully rigid conditions when flexibility is added, at least locally the radii of journal and bearing are a better match, distributing the load over a larger area (lower hydrodynamic pressure, and thicker film). Likewise results were also reported by (Attia Hili, et al, 2010).

It was discovered that for typical compression cycles minimum film thickness calculated approximately 5% less when using the rigid FNRS, since this is viewed as the more reliable method it is concluded that the previously used mobility method typically overestimated the minimal film thickness for rigid geometries especially in small-end bearings, this may be related to a high squeeze-film component.

However, when deformation is taken into account film thickness improves significantly, for typical cases somewhere from 10% - 20% limited by the needed strength and thus limited flexibility of the connecting rod. The elastic effect is most effective if the deformation approaches the radial clearance. Unfortunately this is just a one-sided effect as one bore side is stiff, and thus the minimal film thickness remains with this side, pre-assuming a symmetrical loading. One can however take advantage of the increased film thickness at the flexible side by tailoring the compressor duties accordingly. However too much, and specifically unnatural deformation does ultimately collapse film thickness.

8 Conclusion

Design optimization and analysis of reciprocating compressor bearings is no longer limited by the limitations of the traditionally used (rigid) Mobility Method. A novel approach has been developed based on full numerical simulations of the pressure field from the Reynolds equation incorporating a complete description of the bearing shape. This Full Numerical Reynolds Solver (FNRS) allows very detailed simulations with short calculation times.

The bearing deformation in response to the loading can be incorporated in the form of estimated pre-computed elliptic shapes or taken from detailed FEM analysis. The efficiency of the approach even allows taking into account the effects of groove patterns on the journal path and the analysis of the effects of surface defects or fabrication errors.

The method is very flexible which also allows the calculation of translational slider bearings (crosshead) and 3D asymmetric bearing shapes.

During the design or assessment of bearings deformations can now be taken into account. It could be shown that bearing flexibility can be advantages, and flexibility may be taken into consideration and/or tailored when bearings or compressor duties are designed.

The newly developed advanced method is included in Thomassen proprietary software which allows for more accurate calculations of bearings including deformation of the bearing shell. In the end this will lead to more efficient and reliable designs of bearings and compressors.

Advanced multilevel solution of journal paths in reciprocating compressors including bearing deformation, *P.N. Duineveld, B. Brogle, C.H. Venner, S. van Loo;* HOWDEN THOMASSEN COMPRESSORS BV, UNIVERSITY OF TWENTE

9 Bibliography

Attia Hili, M., Bouaziz, M., Maatar, T., Fakhfakh, M., & Haddar, M. (2010). *Hydrodynamic and Elastohydrodynamic studies of cylindrical journal bearing.* Tunisia: Mechanical Modelling and Production Research Institute (U2MP), National School of Engineers of Sfax (ENIS).

Booker, J. (jan. 1971). Dynamically loaded Journal Bearings: Numerical application of the mobility method. *Trans. ASME*, S. p168-176.

Campbell, J. e. (1967). *Bearings for Reciprocating Machinery: a Review of the Present State of Theoretical, Experimental and Service Knowledge.* Proc. Instn Mech Engrs 182(3A): p. 23.

Ciuff, R., Fusi, A., & Rossi, A. (Oct. 2011). A practical mathematical model for reciprocating compressor plain bearing design. *Compressor tech II*, S. 94.

DuBois, G., & Ocvirk, F. (1954). The Short Bearing Approximation for Plain Journal Bearings. *ASME Paper 54*, Lub-5.

Moes, H. (2000). *Lubrication and Beyond.* Enschede: University of Twente.

Ocvirk, F. (1952). *Short Bearing Approximation for Full Journal Bearings.* Washington D.C.: Technical note 2808, Nat. Adv. Comm. for Aeronautics.

Sommerfeld, A. (1904). Zur Hydrodynamischen Theorie der Schmiermittelreibung. *Zeitschrift fuer Mathematic und Physik 50*, 97-155.

Venner, C., & Lubrecht, A. (2000). Multilevel Methods in Lubrication. In D. Dowson. Elsevier.

CFD Evaluation of Pressure Losses on Reciprocating Compressor Components

by:

Guido Pratelli
Lead Engineer / Technologist
GE Oil & Gas – Nuovo Pignone
Via F. Matteucci 2, 50127, Florence, Italy
T: +39 055 458 9667
F: +39 055 423 2800
E. guido.pratelli@ge.com

Alberto Babbini
Lead Engineer / Technologist
GE Oil & Gas – Nuovo Pignone
Via F. Matteucci 2, 50127, Florence, Italy
T: +39 055 423 2587
F: +39 055 423 2800
E: alberto.babbini@ge.com

Francesco Balduzzi
Ph.D. Student - University of Florence
Via S. Marta 3, 50139, Florence, Italy
T: +39 055 4796 402
F: +39 055 4796 342
E: balduzzi@vega.de.unifi.it

Giovanni Ferrara
Assistant Professor - University of Florence
Via S. Marta 3, 50139, Florence, Italy
T: +39 055 4796 402
F: +39 055 4796 342
E: ferrara@vega.de.unifi.it

Riccardo Maleci
Contract Researcher - University of Florence
Via S. Marta 3, 50139, Florence, Italy
T: +39 055 4796 402
F: +39 055 4796 342
E: maleci@vega.de.unifi.it

Luca Romani
Ph.D. Student - University of Florence
Via S. Marta 3, 50139, Florence, Italy
T: +39 055 4796 402
F: +39 055 4796 342
E: romani@vega.de.unifi.it

8th Conference of the EFRC
September 27th / 28th, 2012, Düsseldorf

Abstract:

Reciprocating compressor efficiency is driven by the pressure losses generated at suction and discharge. While the valves are the major contributors to these losses, a key role is played by other components along the cylinder suction and discharge paths.

CFD simulations of complete systems are a viable solution for prediction of total pressure losses. On the other hand, these simulations require noticeable man work for set-up; moreover, the results are dependent on the specific geometric and fluid-dynamic parameters chosen for the calculation.

Recent studies have suggested that an approach based on superposition of effects is suitable for the prediction of pressure losses caused by the different components. Valve geometries are replaced by equivalent porous regions, thus providing a great simplification of the model and enhancing productivity due to the possibility of evaluating different configurations without having to re-construct and re-mesh the geometries.

In this paper, the same approach is presented and applied to one specific, real-world case. Total pressure losses are computed by a steady-state CFD simulation of a complete configuration of cylinder equipped with 16 valves and other components (cylinder head, liner, valve unloaders, cages etc.), at suction and discharge condition.

Calculation of the P-V cycle inside the cylinder is performed taking into account the loss coefficients obtained at previous step. Comparison with measured data is provided in order to support the validity of this approach.

CFD Evaluation of Pressure Losses on Reciprocating Compressor Components, *Guido Pratelli, Alberto Babbini, Francesco Balduzzi, Giovanni Ferarra, Riccardo Maleci, Luca Romani;* GE OIL & GAS

1 Introduction

The quantification of pressure losses generated at suction and discharge phases is essential to predict the compressor working cycle. There is a legacy of decades of studies on performance of compressor valves, regarded as the main source of pressure losses, with databases available to OEMs and valve manufacturers.

It is also well-known that the components present on suction and discharge flow paths (cylinder liner, cylinder head, valve cage, valve unloaders etc.) as well as the cylinder geometry itself, play a substantial role in interfering with the fluid-dynamics of valve and thus increasing the pressure losses generated by the valve. This is especially true for those designs where the clearance volume has been minimized in order to increase volumetric efficiency; in these cases the narrow gas passages between the cylinder chamber and the valve (here and below denominated "valve pocket") determine a noticeable restriction to the gas flow path. Also, depending on cylinder construction technique (i.e., cast iron/steel vs. forged) and peculiar design, the geometry of the gas ducts from the valve to the cylinder flanges (here and below denominated "suction/discharge ducts") can be fairly complex, thus contributing significantly to the overall losses.

The availability of an accurate and flexible tool to predict overall pressure losses is a key factor to increase the design robustness of compressors, guaranteeing to the Customer the maximum affordability of operational data, and is also a fundamental driver for the development of new products with always increasing focus on energy efficiency.

In this paper, an original simulation approach developed jointly by GE Oil & Gas and University of Florence is described and applied to a particular application. The case analysed is the first stage of a four-stages unit, which compresses pure carbon dioxide from atmospheric pressure up to 150 bar. The unit has four cylinders, one for each stage. First stage cylinder is an iron casting, having one of the largest diameters among all Nuovo Pignone RCs, equipped with four suction and four discharge valves for each end.

The choice of a CO_2 service as a test case, is due to the molecular weight of the process gas, one of the highest among the usual services; for this reason, a remarkable contribution to the total absorbed power of the fluid-dynamic losses is expected. The accurate prediction of pressure losses in this peculiar case was therefore considered technically challenging for the application of the proposed method.

2 Nomenclature

A_v	Valve's geometric flow area
BC	Boundary condition
BDP	Bottom dead position
CE	Crank end of the cylinder
D_v	Valve fit diameter
EFA	Valve's effective flow area
F	Resistance loss coefficient
HE	Head end of the cylinder
k	Turbulent kinetic energy
K_s	Valve flow coefficient, defined as EFA / A_v. In this paper is also recalled as "global K_s", in this case it is meant the K_s of a theoretical valve which concentrates the overall losses of valve and cylinder components.
L_v	Valve length (excl. unloader)
m′	Mass flow rate
P	Instantaneous mean pressure inside cylinder
P_{01}	Total pressure upstream of the valve
P_2	Static pressure downstream of the valve
P_s	Suction pressure at cylinder flange
P_d	Discharge pressure at cylinder flange
TDP	Top dead position
U_x	Axial flow velocity through porous region
V	Instantaneous volume inside cylinder
y^+	Dimensionless wall distance
γ	Ratio of heat capacities
Δp_x	Pressure difference across porous region, in axial direction
ρ	Density
ρ_1	Density upstream of the valve
ω	Specific dissipation rate

3 Background

In this section a brief introduction to the available tools and methods is presented, without the ambition to provide a comprehensive state-of-the-art of current technology.

A traditional approach to the aforementioned problem is to make use of semi-empirical parametric correlations, based on experimental studies, for determining pressure losses due to the valve pocket, based on few geometrical parameters; an example is provided in the referenced paper[1].

CFD Evaluation of Pressure Losses on Reciprocating Compressor Components, *Guido Pratelli,*
Alberto Babbini, Francesco Balduzzi, Giovanni Ferarra, Riccardo Maleci, Luca Romani; GE OIL & GAS

This approach has the advantage of being very easy to adopt, while its limitation lies mainly in the generality of the method, which has proven to be hardly applicable to some specific, real-world cases. Conversely, the necessity of reducing technical risk has sometimes led to adoption of conservative designs.More recently, studies based on advanced CFD techniques have shown the possibility of performing simulations of unsteady flow through the complete configuration of valves and cylinder components[2]. This approach has certainly the advantage of providing detailed information of the fluid dynamics over the computed domain; however, its downsides are the remarkable amount of man-work and computational resources needed for setting-up and running the calculation, as well as the limited applicability of the results to the specific simulated case.

More in general, the CFD simulation of the complete configuration of cylinder components and valves presents a series of practical and technical challenges, some of which are here below listed.

- The computational domain shall include the geometry of all components along the gas flow path. Sometimes these geometries are simply not available, e.g. when the OEM is not the owner of the valve design, but makes use of a third-party product.

- The difference in typical dimensions between the valve channels and the cylinder geometry can be very high. This complicates the mesh, due to the need of accounting for different length scales, and generally leads to increase in number of elements.

- The valve geometrical features (e.g. valve lift) are typically "free" design parameters subject to tailoring and fine-tuning depending on the specific application. The necessity to iterate the whole process of geometry creation and meshing, each time one of the valve parameters is changed, makes optimization a very costly task.

- Benchmark with experimental data is crucial in order to tune the numerous set-up parameters of a CFD calculation. Direct comparison of the simulation results is not possible, unless detailed experimental data coming from appropriate test-bench campaigns is available. Comparison of the globally averaged flow properties with the much more accessible P-V cycle data is an indirect validation and therefore, in the authors' opinion, not sufficient by itself for a robust assessment.

- Since the flow inside the cylinder is inherently unsteady, the most straightforward computational approach should be an unsteady simulation. Use of moving or dynamic meshes is needed to account for piston movement. These techniques require a remarkable computational cost, which makes them practically unaffordable for industrial use, and relegates them to demonstrative cases. Use of steady-state simulations would be a viable alternative, but the discrepancy between steadiness of the calculation and unsteadiness of the problem shall be overcome by specific considerations.

Having considered the above mentioned limitations, GE Oil & Gas together with the University of Florence have developed an original approach to predict the losses generated by cylinder components independently from the evaluation of the flow field within the valve. This method, based on the assumption of mutual independence between the distinct sources of losses (so-called superposition of effects principle), consists of substituting the valve with an equivalent porous region that generates a localized pressure drop together with a straightening of the flow.

The authors have thoroughly described this approach in another paper[3]. Briefly, the validation of the method is based on multiple levels; the first one is the benchmark between the CFD simulation of the valve and the bench test data of the same valve, which drives the selection of the numerous computational parameters of the simulation (mesh sizes, turbulence model, etc.).

The second level is the "virtual" validation of the valve simplified model (porous region) vs. the complete model of the same valve, aforementioned. The simulation of the cylinder components follows the same approach chosen for the valve model, thus providing an "indirect" validation of the simulation against the experimental data. In other words, the same CFD method used for the valve, validated by comparison with experiments, is reasonably assumed to be suitable for simulation of the flow inside cylinder, as well.

The third level is the validation of the superposition of effects hypothesis; this has been performed by means of sensitivity studies, which have demonstrated the effective independency of the losses generated by the various sources, upstream and downstream the valve.

The fourth level, which is an original contribution yet not reported in the previous paper, is the validation of the overall pressure losses (steady-state) against the P-V cycle data (unsteady) available from field measurements, by means of the simplified dynamic model described in chapter 5.

In Figure 1 a schematic representation of the overall conceptual scheme is depicted.
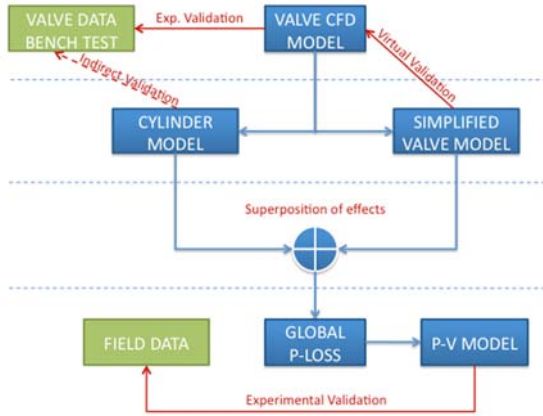
Figure 1: Model Conceptual Scheme

4 CFD Evaluation of Pressure Losses

A CFD simulation of the case described in Chapter 1 has been performed in order to evaluate the overall pressure losses at different conditions, comparing the various sources generated by the cylinder components upstream and downstream the valves.

The fluid domain of the cylinder is symmetrical, divided into different zones (head end, crank end, suction and discharge ducts, porous regions); the split parts are depicted in Figure 2. Valves are located at both cylinder effects, four (2 suction + 2 discharge) for each effect in the split domain. All the cylinder components in contact with the gas are represented. The piston is located in an intermediate position, where it does not mask the valve pocket.
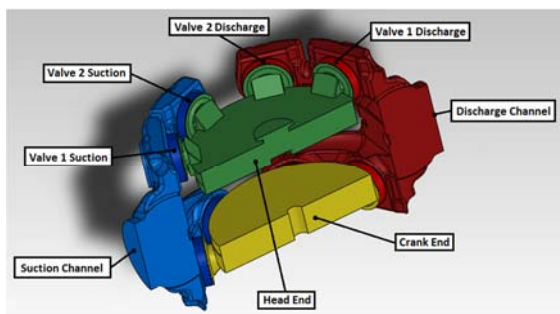
Figure 2: Computational domain

4.1 Modelling of porous regions

Porous regions are zones of the fluid domain for which, in the CFD solver, a sink term is added to the standard Reynolds-Averaged Navier-Stokes equation, according to the Darcy-Forchheimer equation[4]. In the model here described, porous regions have the same overall dimensions (diameter D_v and length L_v) than the valves installed in the reference application.

In this approach, the porous region characteristics are resumed in a single parameter F, called the resistance loss coefficient; this parameter is defined as the loss coefficient per unit length along the flow direction, according to the following equation:

$$\Delta p_x = (\frac{1}{2}\rho F U_x^2) L_v$$

In other words, the parameter F is defined so as to generate in the porous region the same pressure losses than the valve which it shall represent. This coefficient can be calculated simply from the valve design data (D_v, L_v and EFA), which are always available to the compressor manufacturer.

4.2 Simulation settings

An unstructured tetrahedral mesh of the split domain has been adopted, with prismatic layers on the solid walls; y^+ of the cell adjacent to wall has been chosen consistently with the wall function requirements; direct solution of the BL viscous sublayer has proven not necessary.

Global and local mesh parameters have been set up by means of a "goal driven" sensitivity analysis, in order to choose the optimal element size according to the expected flow path and the need to minimize the computing time. The total number of elements is approximately 15 million (depending on the specific case), with nearly 1:1 ratio between number of tetrahedral and prismatic elements. A cylindrical domain has been added to the discharge duct outlet (visible in Figure 6), in order to avoid reversed flows at the BC and accelerate convergence.

Four distinct cases have been run to simulate all the compressor effects, i.e. the suction and the discharge phases of both HE and CE. Domain zones are activated or deactivated according to each case. The BCs have been set so as to simulate the flow at the mean piston velocity, consistently with the mass flow actually seen by the valve during the most significant part of its opening time.

CFD Evaluation of Pressure Losses on Reciprocating Compressor Components, *Guido Pratelli,*
Alberto Babbini, Francesco Balduzzi, Giovanni Ferarra, Riccardo Maleci, Luca Romani; GE OIL & GAS

The simulation is a steady RANS with k-ω turbulence model, according to the modelling best practices already tuned on valve model. The simulated fluid is ideal CO (perfect gas).The computational cost required to perform the simulations on a desktop workstation, in terms of total CPU time, is reported in Figure 3. The time needed for actually running the simulations (few hours per run) demonstrates the remarkable cost-efficiency of the proposed method.

Calculation Times [CPU sec]		
	Suction	Discharge
Head End	1.20E+06	1.10E+06
Crank End	1.91E+06	1.37E+06
System description		
CPU	2 X INTEL Xeon (6-core) E5645 @ 2.40 GHz with 48 GB RAM	
OS	SUSE LINUX 2.6.34.10-06-desktop	

Figure 3: CPU times and system description

4.3 Results

In the following Figures (from 4 to 11) the calculated streamlines for the various simulations are presented, aiming to provide a visual understanding of the gas flow paths. Streamlines are coloured as a function of velocity magnitude; colour scale is not provided.
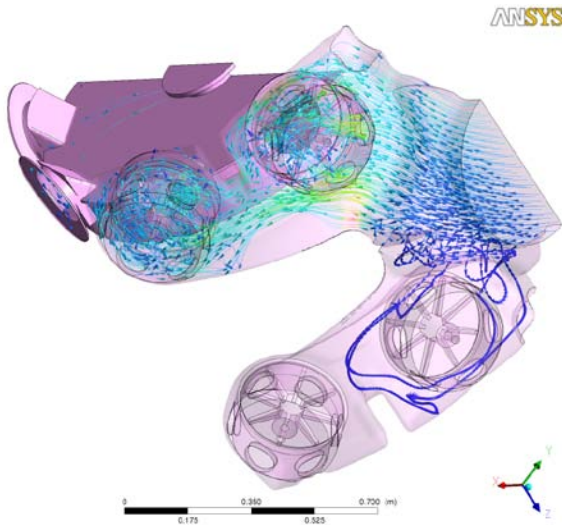
Figure 4: Streamlines of suction phase, HE
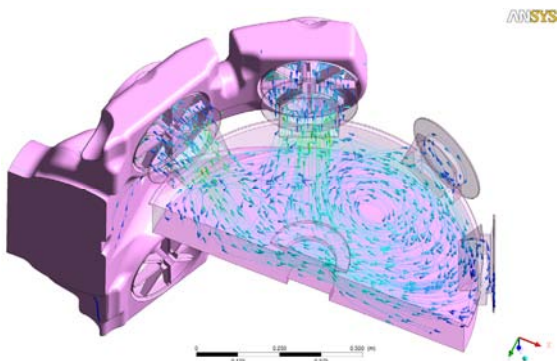
Figure 5: Streamlines of suction phase, HE
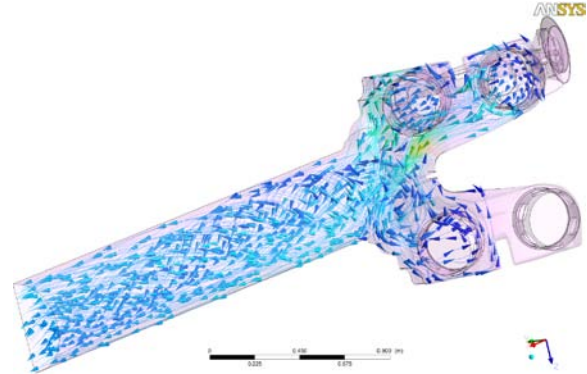
Figure 6: Streamlines of discharge phase, HE
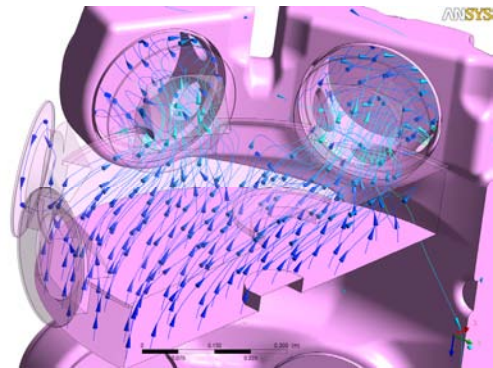
Figure 7: Streamlines of discharge phase, HE
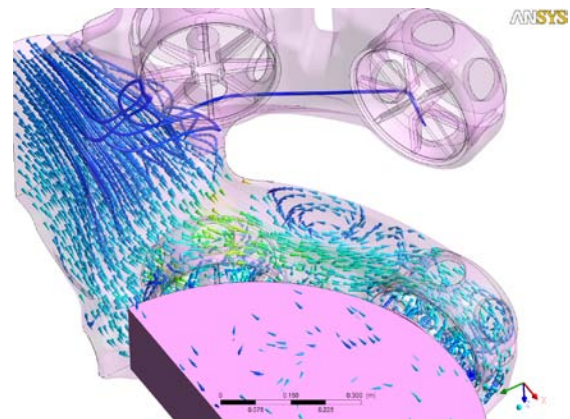
Figure 8: Streamlines of suction phase, CE
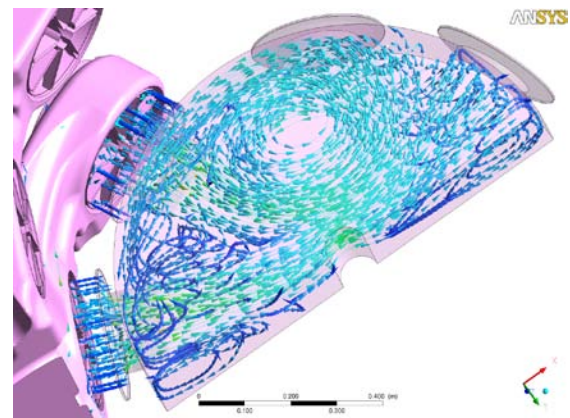
Figure 9: Streamlines of suction phase, CE

CFD Evaluation of Pressure Losses on Reciprocating Compressor Components, *Guido Pratelli, Alberto Babbini, Francesco Balduzzi, Giovanni Ferarra, Riccardo Maleci, Luca Romani;* GE OIL & GAS
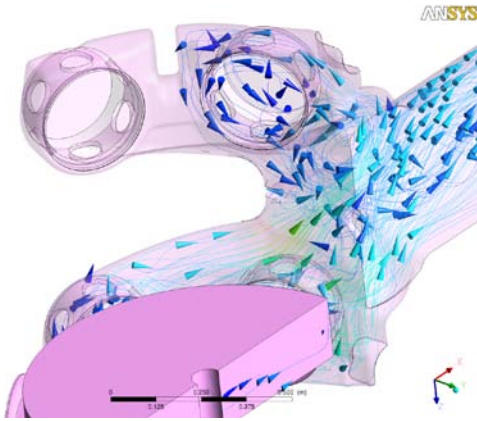
Figure 10: Streamlines of discharge phase, CE
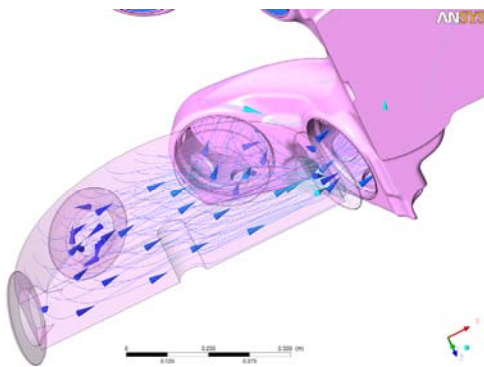
Figure 11: Streamlines of discharge phase, CE

By calculating the mass flow averaged pressure drops upstream, across and downstream the valves, a clear understanding of the contribution of the single components to the overall losses can be achieved. The distribution of relative pressure losses (defined as the ratio between local and total pressure drops, in percentage) for the various cases is presented in plots from Figure 12 to Figure 15.
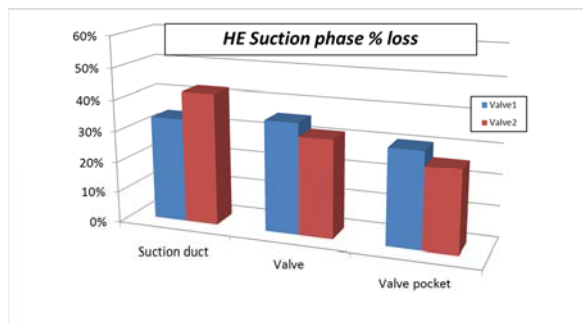
Figure 12: Relative pressure losses, suction, HE
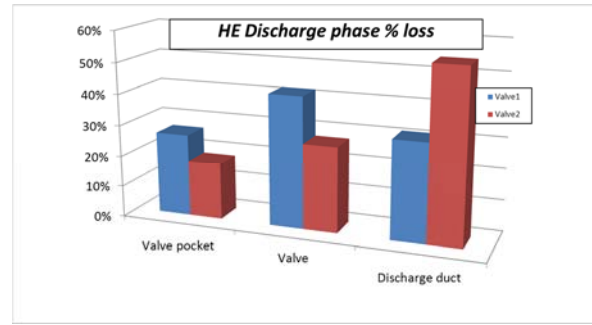
Figure 13: Relative pressure losses, discharge, HE
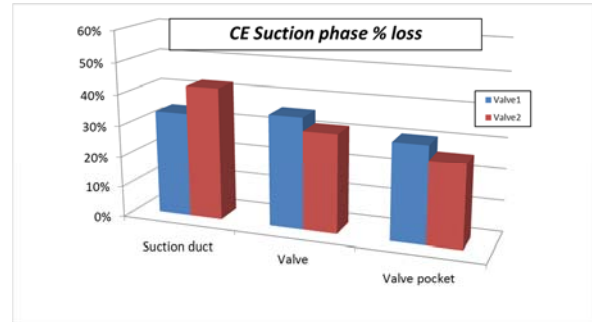
Figure 14: Relative pressure losses, suction, CE
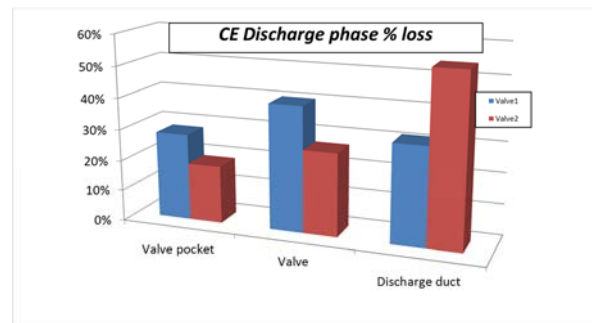
Figure 15: Relative pressure losses, discharge, HE

By analysing these results, it appears clear that, though the valves play a key role in determining the overall losses, a major contribution is due to the other cylinder components. In particular, the suction and discharge ducts have a noticeable influence, especially at discharge phase and for the outboard valves, due to the longer and more complex flow path from the valve to the cylinder flange.

The valve pocket losses appear to be significant, and generally higher at suction than at discharge; this is regarded as due to the "funnel-shaped" geometry of the valve pocket, that generates higher losses at suction (divergent channel) than at discharge (convergent channel).

However, the computation of relative pressure losses somewhat hides the real contribution of the valve pocket, inasmuch as the main effect of the valve pocket is to restrict the flow field across the valve, concentrating it near to the valve centre and

38

CFD Evaluation of Pressure Losses on Reciprocating Compressor Components, *Guido Pratelli,*
Alberto Babbini, Francesco Balduzzi, Giovanni Ferarra, Riccardo Maleci, Luca Romani; GE OIL & GAS

"masking" the outer circle; this appears evident in Figure 16 and Figure 17. Since the pressure losses are roughly proportional to the square of velocity, the reduction in passage area, accelerating the flow, leads to a significant increase of pressure loss across the valve. This behaviour is supposed to well reproduce the real fluid-dynamic interaction between the valve and the valve pocket.
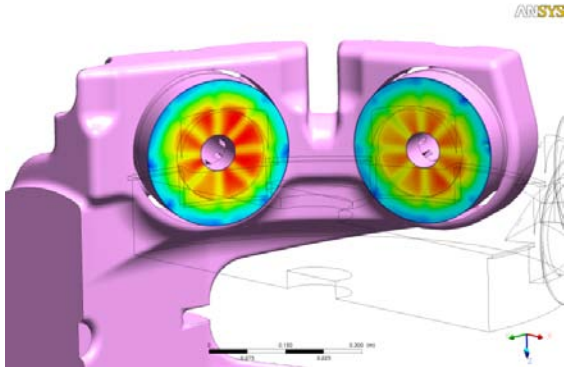
Figure 16: Velocity magnitude distribution at valve inlet, suction, HE
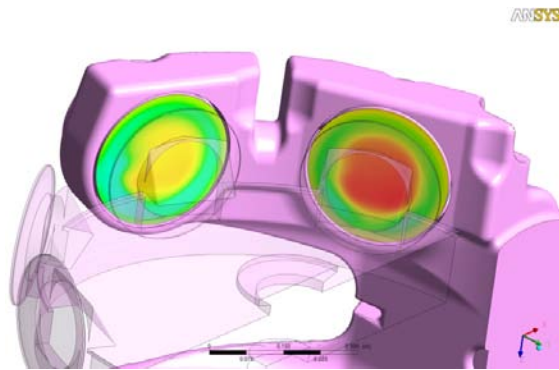
Figure 17: Velocity magnitude distribution at valve outlet, discharge, HE

It is worth noticing the significant differences in pressure losses between inboard and outboard valves, evident in all cases but especially at discharge conditions (see Figure 13 and Figure 15). As already mentioned, the gas flow path through the cylinder ducts is longer for the outboard valves, leading to higher pressure losses. Conversely, there is a reduction in mass flow through those valves, being the total pressure difference from cylinder chamber to flange, constant for all valves. A plot of mass flow through each valve is provided in Figure 18, while the table at Figure 19 provides a comparison between the relative reduction of mass flow and pressure losses.
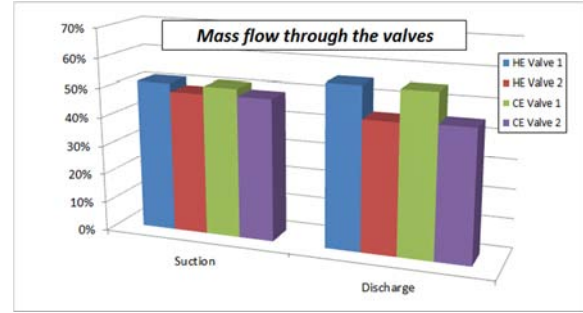
Figure 18: Mass flow through each valve as a percentage of the total mass flow

Valve2 vs Valve1		Mass Flow	Pressure Loss
Suction	HE	-5.46%	-11.83%
	CE	-4.81%	-10.34%
Discharge	HE	-19.66%	-37.96%
	CE	-18.51%	-33.47%

Figure 19: Comparison of relative reduction of mass flow and pressure losses between the valves

The relative reduction of the flow coefficient K_s (defined as the ratio between effective flow area and geometric flow area of the valve) due to the effect of cylinder components, respect to the value for the stand-alone valve, is provided in Figure 20. The global K_s parameter is crucial to determine the P-V cycle of the compressor stage (see Chapter 5); it is worth noting that, being K_s roughly proportional to inverse square of the pressure losses, the order of magnitude of its relative changes may appear underestimated.

Ks change		Suction	Discharge
HE	Valve1	-27.16%	-11.24%
	Valve2	-26.54%	-10.18%
CE	Valve1	-27.41%	-8.61%
	Valve2	-26.89%	-9.34%

Figure 20: Global K_s change as a percentage, relative to the value of stand-alone valve.

5   Comparison with experimental data

As previously recalled, the simulated cases represent a real application of a CO_2 compressor. In order to validate the approach at a global level, it has been developed a simple numerical model able to simulate the compressor stage P-V cycle; this model has been implemented in Matlab environment.

CFD Evaluation of Pressure Losses on Reciprocating Compressor Components, *Guido Pratelli,*
Alberto Babbini, Francesco Balduzzi, Giovanni Ferarra, Riccardo Maleci, Luca Romani; GE OIL & GAS

The P-V cycle is divided in 4 distinct phases: suction, compression, discharge and re-expansion; each phase is modelled as a consecution of stationary states. The simulation starts at 0° crank angle (TDP), and evolves progressively up to 360°; at each time step the program makes a comparison between the pressure inside the cylinder (P) and the pressures defined at the suction flange (P_s) and at the discharge flange (P) in order to judge which is the correct phase according to following rules:

- If $P < P_s$, the suction valves open and the gas enters inside the cylinder;

- If $P > P$, the discharge valves open and the gas exits the cylinder;

- If $P_s < P < P$, all valves are closed and the gas that is inside the cylinder is compressed or expanded depending on the piston movement direction.

Spring constant of valves are accounted for in order to accurately predict the opening angle, however the valve dynamics is not modelled ("ideal valve").

During the suction and discharge phases the program calculates the mass flow through the valves, as a function of the instantaneous pressure inside the cylinder, according to the following formula based on adiabatic, isentropic, compressible gas flow in a convergent nozzle:

$$\dot{m} = K_s \cdot A_v \cdot \sqrt{\left[\frac{2\gamma}{\gamma-1}\right]\left\{\rho_1 \cdot P_{01} \cdot \left[\left(\frac{P_2}{P_{01}}\right)^{\frac{2}{\gamma}} - \left(\frac{P_2}{P_{01}}\right)^{1+\frac{1}{\gamma}}\right]\right\}}$$

The calculated data of pressure over time is plotted in Figure 21 against P-V charts collected on field by means of pressure transducers installed directly on the machine at both cylinder ends. Being not possible to install PT directly inside the cylinder bore, they were connected to the bore through apposite ducts accessible from outside. These ducts generate pressure pulsations, which have been eliminated in post-processing phase using a low-pass filter, in order to eliminate the high frequency oscillations with negligible influence on the measured cycle.

The numerical model is calibrated by imposing P_s and P as equal to the instantaneous values of pressure measured inside the cylinder at TDP and BDP (assuming zero flow, thus pressures equalisation).
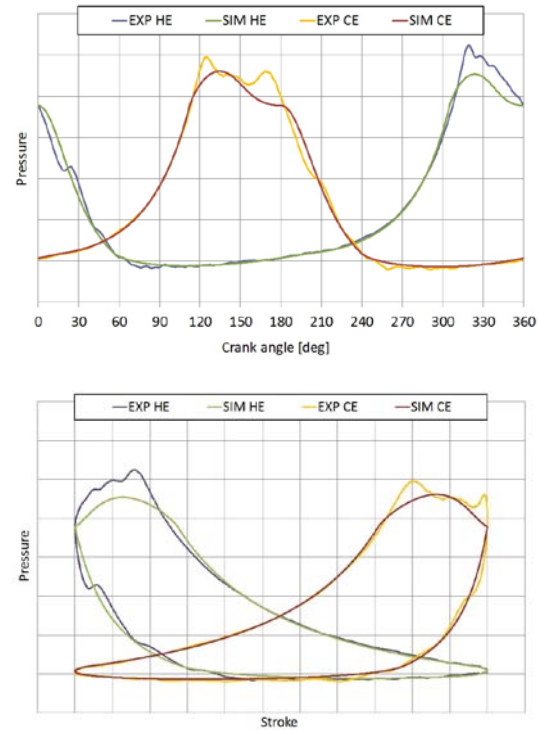
Figure 21: Comparison between experimental data and simulation results.

By analysing the P-V plots, it is evident the close agreement between the two data sets; this allows to consider the validation of the model as fully satisfactory. The only detectable differences between the model and the experiments lies in a limited underestimation of pressure during the discharge phase, while during the suction phase the two data sets are almost indistinguishable. This discrepancy could be explained by the valve dynamics effect, which are not considered in this simplified model. Anyway, since the dynamic phenomena are limited to a small portion of the cycle period (part of the valves' opening period), its effects are considered negligible.

As a quantitative evaluation of the agreement between experiment and simulation, the relative difference between the adsorbed energies has been calculated for both HE and CE, resulting respectively about 5% and 3.8%. The estimated discharge temperature is about 3.6°C higher than the one obtained from field data; it shall be pointed out that heat exchange with environment and tempered water is not accounted for.

6   Conclusion

In this paper, an original approach, aimed to predict the overall pressure losses generated during the operation of a reciprocating compressor by means of the replacement of the valves by an equivalent porous region, has been presented.

This method has been applied to the simulation of a real-world application (first stage of a large CO_2 compressor) in order to test its functionality; comparison of the results against field data for the same application is provided in order to validate the method itself.

However, it is pointed out that this simplified approach is not just a technical demonstrator, but – due to the noticeable cost-efficiency of the process, compared to the complete unsteady CFD simulation of the compressor cycle – it turns out to be an accurate yet practical tool to predict compressor performances, that can be used during all phases of the product development.

Moreover, the basic conceptual foundation behind it – the possibility to separately evaluate the contribution of the various cylinder components to the overall losses – is of much value to the industry, because it provides a key to predict the performances of a particular cylinder configuration at early design stage, independently from the valves that will be installed in the specific applications.

References

Bauer F., *Valve losses in Reciprocating Compressors.* International Compressor Engineering Conference at Purdue University, Indiana, USA, 1988.

[2] Traversari R., Rossi A., Faretra M., *Thermo-fluid-dynamic design of Reciprocating Compressor Cylinders by Fluid Structure Interaction (FSI).* Proc. of the ASME PVP Conference, Baltimore, Maryland, United States, 2011.

Balduzzi F., Ferrara G., Babbini A., Pratelli G., *CFD evaluation of the pressure losses in a reciprocating compressor: a flexible approach.* Proc. of the ASME 11th ESDA Conference, Nantes, France, 2012, in press.

[4] Versteeg H. K., Malalasekera W., *An introduction to computational fluid dynamics.* The finite volume method. Longman, England, 1995.

8th Conference of the EFRC
September 27th / 28th, 2012, Düsseldorf

SESSION 32: OPERATION & MAINTENANCE

EFRC

EUROPEAN FORUM
for RECIPROCATING
COMPRESSORS

Steel Casting Defects – An Issue for both, Compressor Users and Manufacturers

By

Gerard Zima
Group Refining Maintenance Advisor

SLOVNAFT, a.s.
Bratislava, Slovakia

Gerard.Zima@SLOVNAFT.sk

and

Ilya Asser
Sales Engineer

NEAC Compressor Service GmbH & Co. KG
Uebach-Palenberg, Germany

Ilya.Asser@NEAC.de

8th Conference of the EFRC
September 27th / 28th, 2012, Dusseldorf

Abstract:

The paper touches a difficult issue of steel casting quality. A particular user experience with casting defects of pressure containing machinery parts from refinery praxis is outlined. The difficulties from such defects arising for the user are demonstrated as well as its repair procedure in such cases. It shows also the problem from the compressor manufacturer's point of view and how to deal with casting defects. For the particular case the paper shows the technical process of repairing the leaking compressor cylinder and technical solutions to prevent recurrence of errors in the new cast cylinder quality. A typical example is presented which also highlights the need for close and good user and manufacturer cooperation.

OPERATION & MAINTENANCE

Steel Casting Defects – An issue for both, Compressor Users and Manufacturers, *Gerard Zima, Ilya Asser, SLOVNAFT, NEAC COMPRESSOR SERVICE*

1   Introduction

Reciprocating compressors are playing a key role in refinery processing technologies. They are principally used in two applications: mostly as make-up compressors and sometimes also as recycle compressors. The task of the make-up compressor is supplying compressed gas in the required quantity and pressure to any kind of process or in order to maintain some level of circuit pressure. The role of the recycling compressor is to circulate gas in the reaction circuit e.g. in a refining technology. It is obvious that compressors in refining technology processes are as important as the heart in a human body. In case of a compressor stop the process cannot continue "to stay alive" comparable to the human body in case of heart stoppage. The uninterrupted continuous compressor operation is a crucial factor of reliable operation in most refining technologies.

A compressor is a relatively complex mechanism. It contains a number of moving parts which are subject to natural "wear and tear", and these are the main cause for necessary maintenance performance. The replacements of valves, piston and guide rings as well as seals are typical examples of such maintenance activities. Significantly less frequently but more severe cases are the failures of static parts of the compressor. Particularly serious are the disorders that cause loss of tightness and integrity of the pressure containing parts such as compressor cylinders. Such disorders not only cause long-term compressor outages and expensive repairs, but may also result in significant threat to the safety of people and devices in the vicinity of the equipment.

2   Cylinder casting defects and leaks - compressor user view

Below several cases of dangerous casting defects and leaks are described which really caused user problems and losses. The sharing of these experiences can be useful and supporting for other users and manufacturers to avoid similar issues which are every time unpleasant for all parties being involved.

2.1   SLOVNAFT's first experiences with insufficient quality of cast cylinders (1997)

Slovnaft did not face leakage problems at compressor cylinders until the construction of new production units started at the end of the nineties. In previous decades there were two or three disorders caused by wrong operation (frozen cooling water), but not by insufficient quality or design. Cylinders were considered absolutely trouble-free compressor parts, which were not kept as spares. The problems started only since the production and delivery of large reciprocating compressors – all hydrogen - for various new production units

2.2   Reformer unit compressors

The first major incident was encountered in the workshop test of a reciprocating make-up compressor for the reformer production unit.

After the usual and successful four hour test run a visual inspection of a randomly selected cylinder, which was also part of the agreed testing and acceptance, was performed.

It was a real shock, literally, when a cavity as big as a child's fist, appeared in the rear cylinder head – see Figure 2.2.1.

Figure 2.2.1: Reformer compr. cylinder porosity

Of course, after this finding, Slovnaft requested to open all cylinders. The findings confirmed the presence of numerous surface pores and fault indications also on other parts, particularly at cylinder heads.

Steel Casting Defects – An issue for both, Compressor Users and Manufacturers, *Gerard Zima, Ilya Asser, SLOVNAFT, NEAC COMPRESSOR SERVICE*

Basic parameters of compressors are shown in Table 2.2.2.

Type	Horizontal, 4 cranks, 2 stages, double acting	
Function	1°Make-up	2°Make-up
Medium	94%H2+HC	94%H2+HC
Flow	66400 M3/H	65800 M3/H
Pressures	0.57/1.54 MPa	1.44/3.6 MPa
Temperatures	40/120°C	40/120°C
Power	5.5 MW	

Table 2.2.2: Reformer compressor parameters

The manufacturer stated that he is aware of shortcomings, but according to his experience it does not affect the performance of the compressor. Of course, the cylinders successfully had met the pressure test and helium leakages test as well. Slovnaft had, however, objections because not only compressor efficiency is the issue, but also safety, long-term reliability and lifetime. From the outside visible porosity Slovnaft had doubts about the internal material quality. Therefore a new cylinder was manufactured and delivered by the manufacturer as spare. Due to the long delivery time the compressor was started with the porous cylinder. After one year of operation the leakage occurred in the area of lubrication hole. After retightening of the lube tube connection inside of cylinder material, the cylinder was tight.

2.3 Further experiences

Further incidents with cylinder casting quality occurred in line with the construction of two additional new production units. In both cases manufacturers had faced problems with the delivery of high quality castings from foundries. Cylinders did not meet test requirements due to presence of porosities and cracks which led to not successful hydro tests. Several cylinders were therefore scrapped already during the compressors production phase by the producers themselves.

2.4 Last experiences with failures during operation

2.4.1 LC Finer hydrogen compressors

Three large hydrogen reciprocating compressors are operated in the LC finer unit. These machines have combined functions: The first stage serves as the make-up and three additional as the recycle compressor. The basic parameters are shown in Table 2.4.1.1.

Type	Horizontal, 4 cranks, 4 stages, double acting			
Function	1°Make-up	2°- 4° Recycle		
Medium	97 % H2 + HC	92% H2 + HC		
Flow	2740 kg/h	9230 kg/h		
Pressures	1.6/2.4 MPa	5.2 MPa	11,1 MPa	20,1 MPa
Temperatures	30/55°C	35/110°C	25/110°C	25/100°C
Power	5.2 MW			

Table 2.4.1.1: LC finer compressor parameters

A very difficult situation emerged when cracks in the areas of valve seats were discovered during planned maintenance - see Figures 2.4.1.1 and 2.4.1.2.
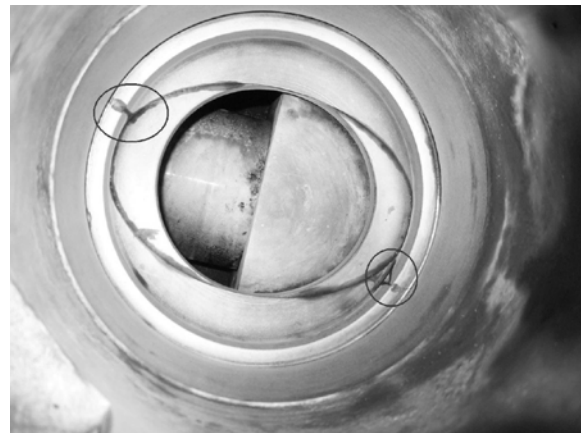
Figure 2.4.1.1: Transverse valve seat cracks

Figure 2.4.1.2: Circumferential valve seat crack

More detail examination revealed that cracks had propagated in to the inner cylinder bore below the liners – see Figure 2.4.1.3.

One of the liners was also cracked. Cracks appeared on the third and fourth stages of all three compressors.

OPERATION & MAINTENANCE

Steel Casting Defects – An issue for both, Compressor Users and Manufacturers, *Gerard Zima, Ilya Asser,*
SLOVNAFT, NEAC COMPRESSOR SERVICE

Figure 2.4.1.3: Crack propagated into cyl. bore

Since delivery time of new cylinders was very long and the production unit - being one of the critical refinery units - could not be shut down for such a long time Slovnaft had to perform a repair of the cylinder - even with the risk being related to such a repair.

Finally the unique repair by welding was realized, which allowed the repair of one compressor within three months after finding a failure and to shorten risky operation until the delivery of the new spare cylinders for two more compressors.

The scope of repair is visible in Figures 2.4.1.4 and 2.4.1.5, where the scope of grinded defected material is shown.

Figure 2.4.1.4: Scope of removed material – St. 3

This case was not primarily a cylinder material quality issue; the root cause was related to the insufficient seats thicknesses and excessive torque.
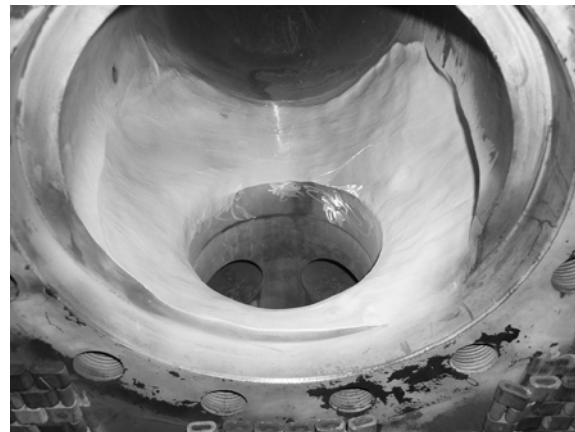
Figure 2.4.1.5: Scope of removed material – St. 4

However during the repair of the third stage cylinder, which is made of cast steel, again a significant material porosity was discovered which was causing leaks during the pressure test - again at the location of lube tubes passing inside the cylinder – Figure 2.4.1.6.

Figure 2.4.1.6: Porous area - cast cylinder - St. 3

This porosity also appeared on the new spare cylinders, where after half a year of operation were leaks of hydrogen into cooling water passage. Finally it was repaired by application of sealed tube – see Figure 2.4.1.7.

Steel Casting Defects – An issue for both, Compressor Users and Manufacturers, *Gerard Zima, Ilya Asser, SLOVNAFT, NEAC COMPRESSOR SERVICE*
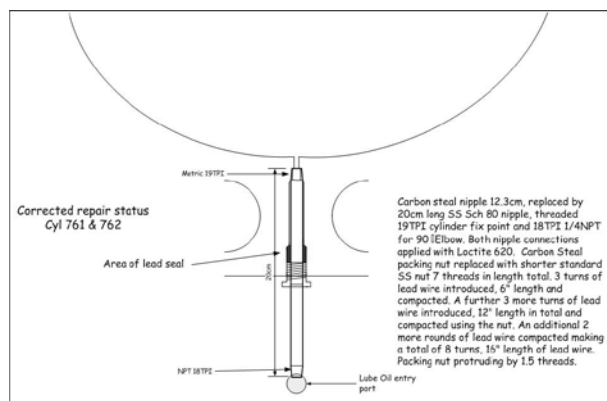
Figure 2.4.1.7: Leak area repair by sealed tube

2.4.2   HDS7 hydrogen compressors

The HDS7 is the next of critical refinery unit because it is producing diesel being one of the most important refinery products. There are two Make-up reciprocating compressors operated. Basic parameters are shown in Table 2.4.2.

Type	Horizontal, 2 cranks, 2 stages, double acting	
Function	1°Make-up – PSA inlet	2° Make-up – two gas inlets (1°+ CCR5)
Medium	99.9% H_2	94% H_2 + HC
Flow	504 kg/h	3252 kg/h
Pressures	1.5/3.2 MPa	2.8/6.92 MPa
Power	982 kW	

Table 2.4.2.: HDS7 Compressor parameters

It is one of the above mentioned cases where the compressor manufacturer faced repeatable problems with low quality of cast cylinders delivered by the foundry.

Consequently it complicated also compressors putting into the operation in refinery due to time delay and leakages on site. The problem became critical again in late 2010, when an additional leak of the second stage cylinder and later of the spare cylinder too was identified. This caused a long-term operation of the unit without the stand-by compressor, which meant a reduced reliability and availability of the unit. Because again, like the LC Finer, it was not possible to shut down the unit and delivery time of the new cylinder was long, the emergency repair needed to be done. Additionally Slovnaft discussed design and technological changes of the new cylinder with the compressor manufacturer since an expensive purchase of the original unreliable cylinder design and manufacturing was not acceptable.

Slovnaft noted with appreciation the willingness of the manufacturer to seek the necessary adjustments and ensure their implementation. This user-manufacturer collaboration gave rise to a new cylinder, in which Slovnaft expects a much higher reliability and lifetime than before. Testing and implementation of the new cylinder into operation in May 2012 was successful. Detailed description of the old cylinder repair and modifications for a new cylinder is explained in the chapter 3.

2.5   Summary of user problems associated with poor quality of cast cylinders

Low-quality cast steel cylinders and the resulting compressor malfunctions are causing for user really serious difficulties.

- Significantly reduced operational safety

It is easily understandable that the escape of flammable, explosive and toxic gas outside of cylinders space is a huge risk to the environment. Refinery hydrogen gas is composed mostly of hydrogen, which is highly explosive, of hydrocarbons, which are flammable and hydrogen sulphide which is toxic. Their escape is a high risk.

- Significantly reduced reliability and availability of equipment

Each failure requires repair and thus the equipment disabling from the operation.

- Significant loss of production

As leaking compressors cannot be in a long and safe operation, it indicates the need to reduce operational performance or complete unit shutdown. Such losses are high. For example, the daily loss of the LC Finer unit shutdown is about several hundred thousand Euros. Losses of HDS7 are similar.

- Significant increase in maintenance costs

It is due to the cost of emergency cylinder repairs, the costs of forced buying new cylinders as well as the expenses for disassembly and assembly of the compressor.

- Loss of confidence

Problems of this type, especially when repeated, cause users doubts to the quality of the compressor as a whole. On the one hand, it is the natural reaction of people; on the other hand, this is a

OPERATION & MAINTENANCE

Steel Casting Defects – An issue for both, Compressor Users and Manufacturers, *Gerard Zima, Ilya Asser,*
SLOVNAFT, NEAC COMPRESSOR SERVICE

negative fact. Confidence to the equipment and its manufacturer is an important element of the successful operation, maintenance, and mutual cooperation

3   Cylinder casting defects and leaks – compressor manufacturer view

Casting technology – as typically applied for the production of cylinders for reciprocating compressors – ever since and still today incorporates the risk of casting defects. As much as possible the raw cast cylinder bodies are checked for such defects but it cannot be ruled out that "soft" casting sections become obvious only in the run of machining, during the pressure test or even after some time when the cylinder has done a number of hours in true operation.

The application of sound casting technology including professional casting simulation techniques can minimize or even completely avoid such defects.

3.1   NEA/NEAC's experiences with poor quality of cast cylinders

If a casting defect emerges during the last round of machining or even later, when the pressure and leak testing is performed, a lot of time and money is already spent - and lost. The supplier of the cast raw cylinder will provide for a new piece but not for the extra machining and testing – and not for the potential significant delay in delivery time for the complete machine which may result in tremendous contractual commercial penalties.

Since process gas compressors cylinders are usually made as per specific requirements – typically the diameter, stroke, number of valves and pressure rating – it had been common in the past to utilize an existing cylinder casting pattern and modify such to fit for the new task.

In the past little attention was paid to check if the modified pattern was suitable for casting. The responsibility was with the casting company anyway; because "they know how to do it". That procedure has proven not to be beneficial with regard to potential casting defects.

Casting defects had never been a regular occurrence but even if happening occasionally the extra effort to correct the same had always been unpleasant as outlined above.

NEUMAN & ESSER (NEA) therefore decided:

- To utilize only reliable and proven cylinder series which are, once defined, not altered.

- To apply casting simulation techniques to optimize the pattern and riser system prior to the actual casting

- To involve only few knowledgeable casting companies

- To switch to cylinder blocks from forged and cast material with consequentially extended machining effort even for applications where a simple grey cast iron would do; just to avoid the permanent risk of casting defects due to the complex cylinder geometry with its various cooling water compartments and gas passages.

3.2   Performed repair

For the particular case demonstrated here Figure 3.2.1 depicts the cylinder which had the porous sections and where leaks were encountered.

Figure 3.2.1: Cylinder from GS-C 25

Steel Casting Defects – An issue for both, Compressor Users and Manufacturers, *Gerard Zima, Ilya Asser, SLOVNAFT, NEAC COMPRESSOR SERVICE*

Figure 3.2.2: Porous section

Figure 3.2.2 shows the cylinder with the identified and marked porous spots at the bottom of the cylinder. In the run of the helium pressure test numerous bubbles emerged from the casting surface (Figure 3.2.3)

Figure 3.2.3: Helium bubbles from cylinder

The sectional drawing in Figure 3.2.4 identifies the exact position where the bubbles had been detected and where the repair needed to be done.
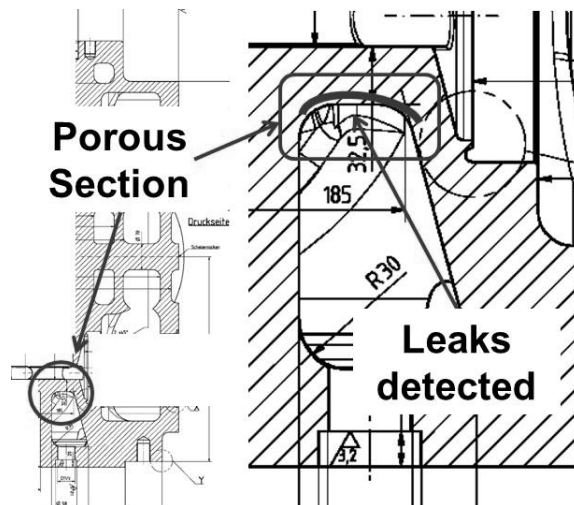
Since cylinder material is GS-C25 welding of the cast iron was possible.

Figure 3.2.5 is the view inside the cylinder towards the area with the defects after a section of the cylinder bottom part had been cut off.
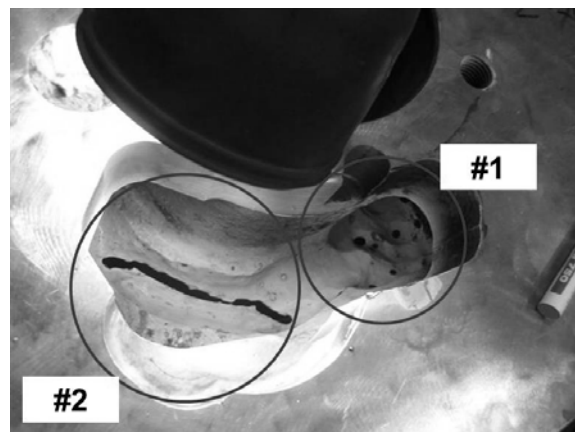
Figure 3.2.5: Cut off cylinder bottom section

Figure 3.2.6 and Figure 3.2.7 are zoom details from Figure 3.2.5 with a clear view inside the casting structure and its porous area.

Steel Casting Defects – An issue for both, Compressor Users and Manufacturers, *Gerard Zima, Ilya Asser, SLOVNAFT, NEAC COMPRESSOR SERVICE*

Figure 3.2.6: Detail #1 of Figure 3.2.5

Figure 3.2.7: Detail #2 of Figure 3.2.5

Figure 3.2.8 shows the cylinder bottom view after the repair procedure and dimension check had been finalized; and the cylinder was then prepared for the next pressure and leak test.

Figure 3.2.8: Repaired cylinder

In the end the full mechanical capabilities had been regained and the cylinder was fit for purpose again.

3.3 Root cause analysis

Starting from the original geometry (Figure 3.3.1) a casting technology analysis was conducted to find potential reasons for the cylinder leaks.
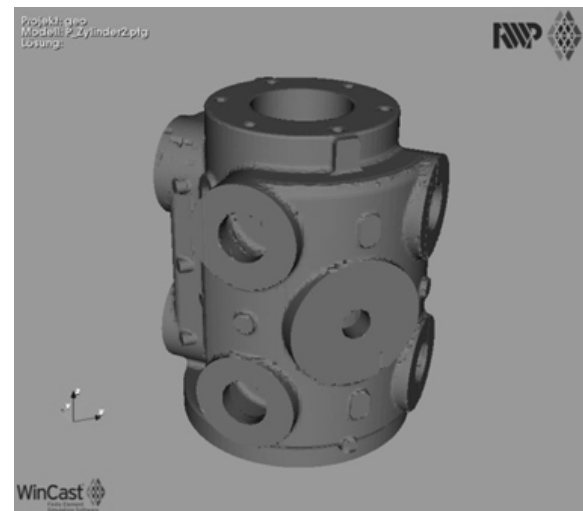
Figure 3.3.1: Original geometry

For the as-built casting system a solidification simulation was performed. It can be noted that the principle solidification runs in direction of the riser

The temperature pattern (Figure 3.2.2) shows the elevated temperature of the riser.
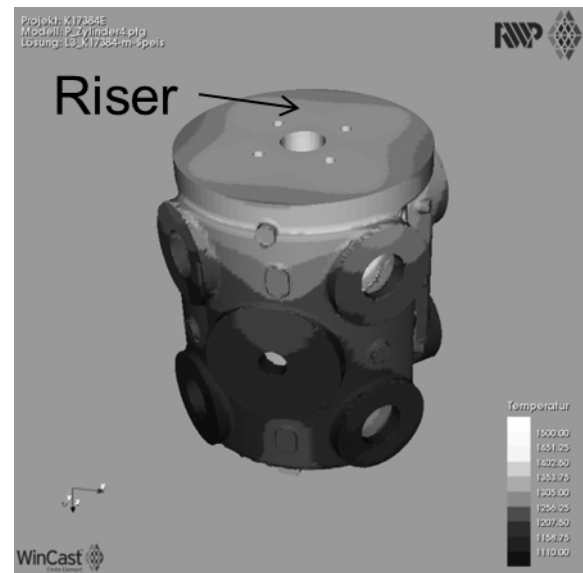
Figure 3.3.2: Temperature pattern

Despite the solidification being directed towards the riser some feeding defects are occurring in the red marked sections (Figure 3.2.3). These can result in a less dense casting matrix.

Steel Casting Defects – An issue for both, Compressor Users and Manufacturers, *Gerard Zima, Ilya Asser, SLOVNAFT, NEAC COMPRESSOR SERVICE*
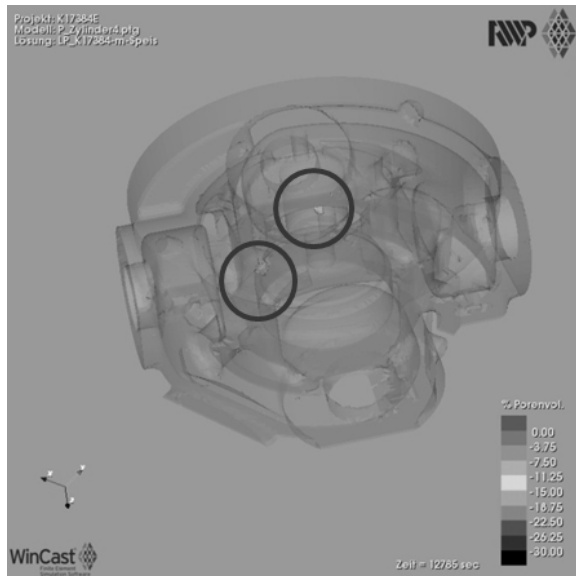
Figure 3.3.3: Highlighted defects

For clarification purposes a sectional drawing of the cylinder is added (Figure 3.3.4) with different colours assigned to the various casting cores.
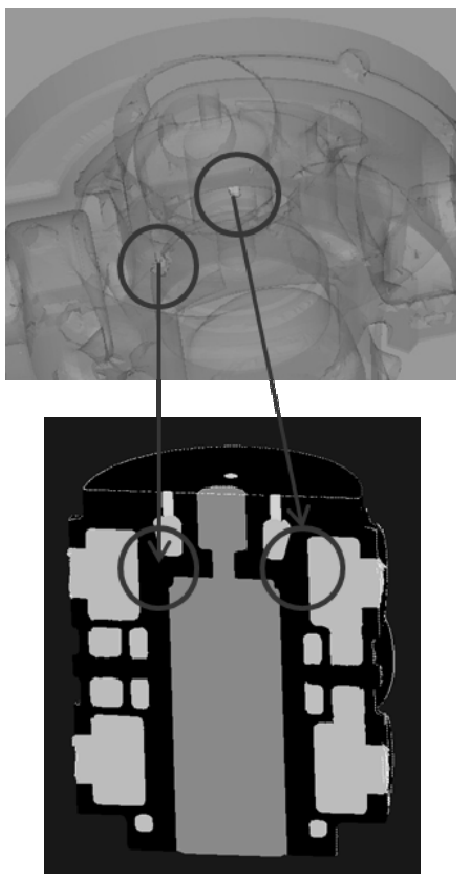
Figure 3.3.4: Cylinder sectional drawing

The potential defects are highlighted again.

3.4   Modifications to avoid the defects

To make the geometry a little more appropriate to the casting procedure some geometrical dimensions had been adjusted (Figure 3.4.1 and 3.4.2)
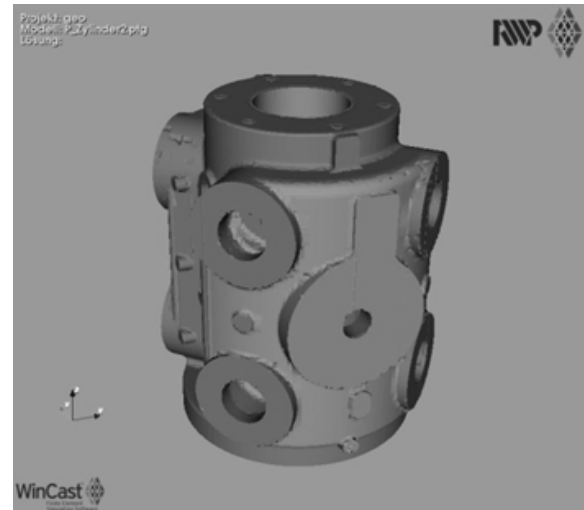
Figure 3.4.1: Optimized geometry (1)
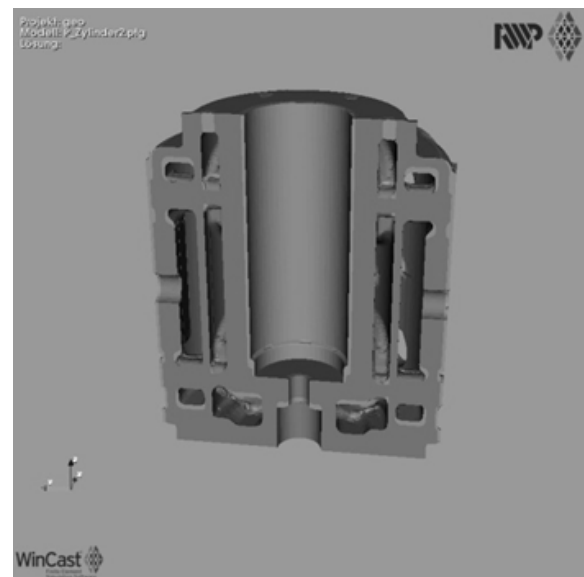
Figure 3.4.2: Optimized geometry (2)

Sections of optimized geometry are highlighted in light brown (beige).

Through the optimized geometry and a modified casting technology the hot spots were moved into the riser (Figure 3.4.3).

51
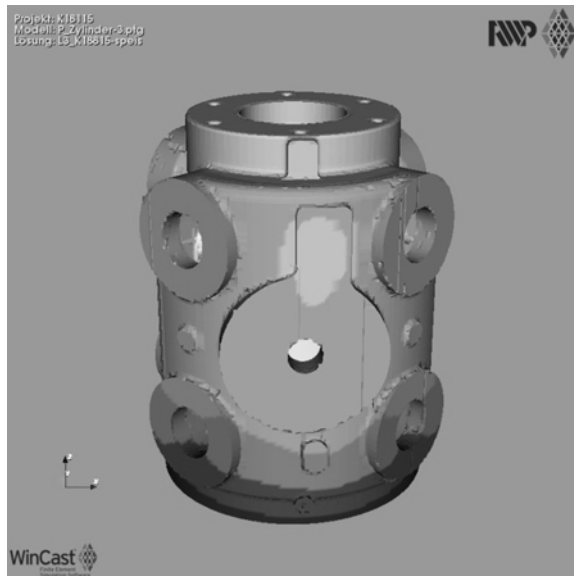
Figure 3.4.3: Optimized temperature pattern

The temperature pattern of the optimized design depicts the difference versus the initial pattern (Figure 3.2.2).
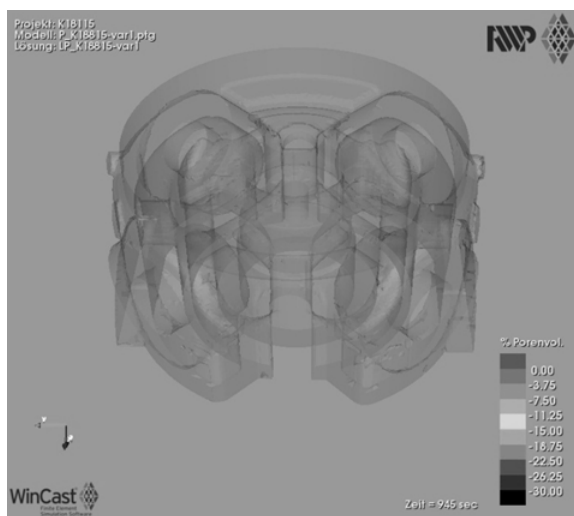
Figure 3.4.4: Casting without defects

The above described alterations have the effect that the initially critical sections are now free from any defect (Figure 3.4.4). Leaks have no longer to b anticipated.

3.5 Solution applied for the new SLOVNAFT cylinder

Main improvements applied for the new cylinder for Slovnaft:

1. Optimized cylinder geometry based on simulation and expert analysis

2. Improved technological risers design for correct solidification in the area of final cylinder.

3. Selection of different foundry with more reliable quality

4. Application of more careful inspection of manufactured quality

4 Lessons learned

Cylinder design and casting procedure to render cast pieces without defects is based on the following:

1. Cylinder pattern series are utilized which have proven to render reliable castings.

   Continued and repeated casting pattern alterations are the death for the casting quality. Once the pattern is set it shall not be modified – or it must be treated like a new development with a consequential check procedure as outlined below.

2. Prior to the actual cylinder casting the casting technology and the riser systems are optimized together with the casting company; and with an external casting expert if the casting company does not have the simulation know-how.

3. Casting simulations are performed to define an optimized and proper casting procedure.

4. Patterns for grey cast iron and nodular iron must not be utilized for cast steel – and vice versa – since their casting systems differ from each other. No switching between both without adjustment and sound check of the casting pattern.

5. Only few and knowledgeable casting companies shall be involved who know the pattern series and its characteristics. With those partners the experience is shared.

OPERATION & MAINTENANCE

Steel Casting Defects – An issue for both, Compressor Users and Manufacturers, *Gerard Zima, Ilya Asser, SLOVNAFT, NEAC COMPRESSOR SERVICE*

All new NEUMAN & ESSER cylinders which had been developed and cast as per the latest design and sizing procedure have been free from defects, because the series had been optimized together with casting experts through accompanied simulation techniques.

From user point of view:

1. The reliable material quality of all pressure containing parts is crucial.

2. The open, effective and active approach and technical support and cooperation given by compressor manufacturer is expected and required in case of occurred problems.

3. The only easy original copied manufacturing and delivery of spare cylinders and cylinder heads without removal of repeated problems reasons is not acceptable.

4. Discussion and subsequent selection of most reliable cylinder design and material sub-vendor in phase of new compressor delivery is suitable.

5. The efficient quality plan for cylinder manufacturing looking also the material inside quality is necessary.

SLOVNAFT considers safe, reliable and cost effective equipment operation as one of crucial business target. The above described experiences are understood as strong learning which will apply for future activities.

5   Conclusion

Through casting technology simulations - which are state of the art these days and regularly applied – it is not only possible but has been achieved to create cylinder casting geometries (even with complex configuration) and casting procedures in a way that defects can reliably be avoided.

If the number of casting patterns in the cylinder series is reduced to a minimum, the shape of the raw cylinder is kept as simple as possible and available tools are utilized, uneven cooling of the cast piece as well as unfavourable temperature patterns – which are leading to soft and porous casting sections – are prevented and casting defects are occurrences of the past.

In spite of all above effort and in line with the experience the using of nodular cast iron for low pressure application and fabricated/machined cylinders for medium and high pressure application instead of problematic cast steel application looks as meaningful decision for compressor end users – especially for larger compressor sizes.

3D-Laser Form and Position Verification before and after Repair of complex Compressor Parts

Markus Weber
Senior Engineer Compressors - Rotating Equipment

BASF SE, GTF/TE - U427
Ludwigshafen, Germany

Markus.A.Weber@BASF.com

and

Stefan Damberg
Project Engineer

NEAC Compressor Service GmbH & Co. KG
Uebach-Palenberg, Germany

Stefan.Damberg@NEAC.de

8th Conference of the EFRC
September 27th / 28th, 2012, Dusseldorf

Abstract:

This paper focuses on 3D-laser form and position verification before and after repair of complicated compressor parts with considerable heat intrusion. The subject discussed here is a cylinder for a reciprocating compressor which had to be cut and welded to eliminate a section with too small wall thickness. In order to confirm the reproducibility of the welding, prior to the actual repair the procedure was tested utilizing 3D-laser equipment for the dimension check before and after the procedure. The result will show significant deformation of the cylinder mating surface towards the frame which could easily be made visible only from the laser model. Based on the true 3D cylinder shape, obtained from the laser scanning, decisions can be made concerning final machining to bring the cylinder back to its proper form.

3D-Laser Form and Position Verification before and after Repair of complex Compressor Parts, *Markus Weber, Stefan Damberg, BASF, NEAC COMPRESSOR SERVICE*

1   Introduction

BASF SE is the world-wide largest chemical company with it's headquarters in Ludwigshafen at the Rhine. The BASF SE headquarter (Figure 1.1) in Ludwigshafen consists of over 2.000 buildings and spreads out over 10 km², being the largest inter-dependent chemistry area of the world belonging to a single company. A wide pipeline network enables efficient supply of the plants with raw materials and energy. In the production group intermediate materials for the followers are produced just in time.

Figure 1.1: BASF SE Plant in Ludwigshafen

BASF SE in Ludwigshafen is operating various reciprocating compressors of different ages. There are compressors running recently being built in 2011 just as recips manufactured in the late 30s of last century. Due to good maintenance and broad detail knowledge how to operate these machines also the "grandpas" do a very reliable and efficient job within BASF SE.

Sometimes, however, issues are occasionally encountered which are initially puzzling; particularly when machines, which have been running trouble-free for decades, are suddenly showing never before experienced damage.

Such as the incident with a two stage ethylene compressor manufactured by Borsig; located in the production plant at BASF SE site in Ludwigshafen.

2   The Compressor

In that production plant four identical compressors are operated. The machines are of two stage design and they compress ethylene from 1 bar(abs) up to 21 bar(abs). First commissioning took place in 1938. Since then the compressors are running quite reliably. Figure 2.1 gives an impression of the compressor hall where the machines are located.
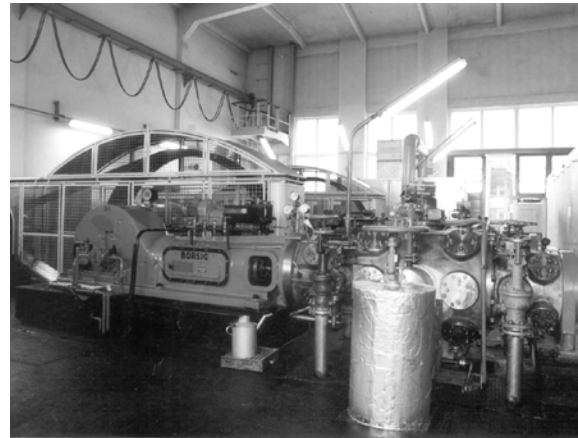
Figure 2.1: Compressor Shop

Figure 2.2 shows the specification of the reciprocating compressor.

- **Reciprocating Compressor**
  Manufacturer Borsig, Type DVA 1340
  Since 1938 in C_2H_4 (Ethylen) Service

  - 2 Stages, horizontal, double acting
  - Capacity   1,30 to/h
  - Suction pressure   0,9 bar a
  - Discharge pressure   21,0 bar a
  - Speed   165 rpm
  - Material grade   stainless steel (1.4581)
                        ni-resist 3 (EN JL 3011)

Figure 2.2: Compressor Specification

The picture below (Figure 2.3) allows a closer view towards the compressor unit.
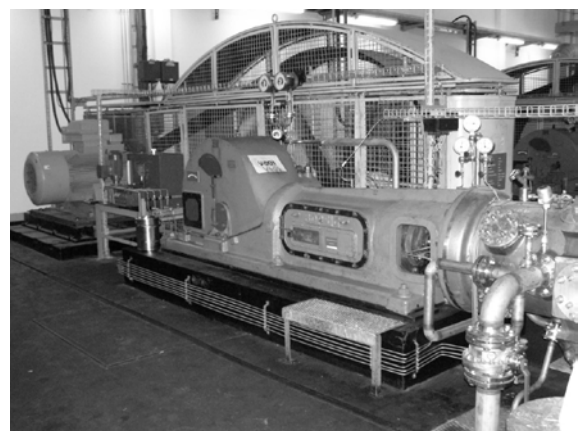
Figure 2.3: View towards the Frame

In the early 90s process parameters altered slightly.

OPERATION & MAINTENANCE

3D-Laser Form and Position Verification before and after Repair of complex Compressor Parts, *Markus Weber, Stefan Damberg, BASF, NEAC COMPRESSOR SERVICE*

As a consequence traces of hydrofluoric acid were detected in the condensate which partially caused massive corrosive attack in the suction side of the 1st and 2nd stage cylinders (refer to Figure 2.4).
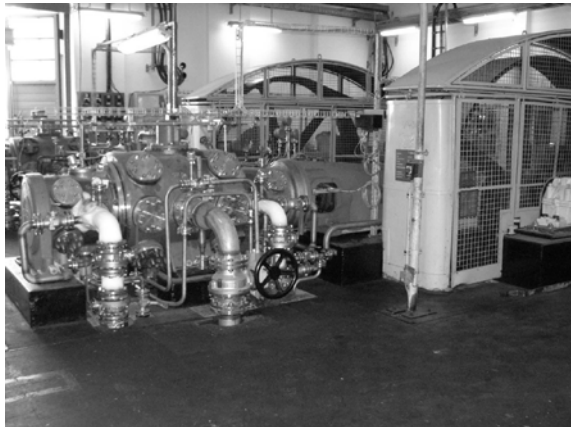
Figure 2.4: View at Suction Side, 2nd stage

Due to local undercut of the thickness of pressurized cylinder walls the original grey cast iron cylinders had to be replaced. To achieve a better corrosion resistance the new cylinders were manufactured from stainless steel casting (material no. 1.4581).

3 Design Considerations linked to long-term Operation Experience

Some details of the original cylinder had needed modification. In order to be able to conduct the necessary material testing after the casting and due to different casting requirements the cylinder walls had to be designed as a welded construction.

Figure 3.1 shows one of the cylinder fabrication drawings with the welding locations (red lines) to fit the parts together.
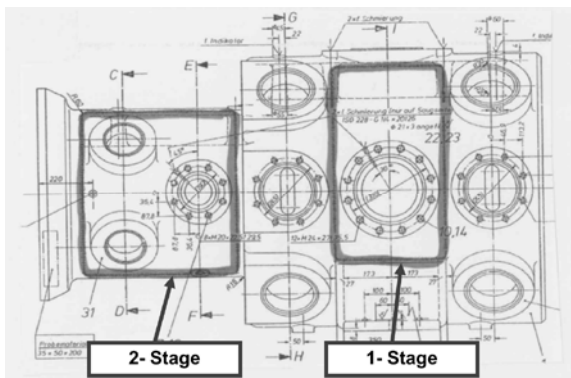
Figure 3.1: Drawing with welding Locations

On the left two pictures of the quartet in Figure 3.2 the main cylinder body can be seen. On the right two pictures the second part was put on the main body with welds already being prepared.

Figure 3.2: New Cylinder - Preparation of Welds

After several years of operation of these stainless steel cylinders, despite their increased resistance to corrosion, some corrosive attack was detected at critical locations of the cylinders; such as gaps, seams and cavities.

With continuous operation it also became evident that heat affected zones from repair or manufacturing welding showed a reduced corrosion resistance. In the heat affected areas selective attack occurs at crystal boundaries of the material matrix which leads to macroscopic-granular removal of material and, thus, creates a rough and porous structure which may no longer be gas tight.

Based on the described findings over some three years two cylinders needed replacement again. Resulting from these operation experience design modification were developed to avoid areas of endangered corrosive attack. The specification said that the cylinder shall be free from gaps, such as threads, and cavities.

Additionally it was agreed with the manufacturer to perform solution annealing, after all welding work had ended, according to specific time and temperature parameters to prevent micro structural changes in the heat affected zones and, hence, to maintain the corrosive resistance for the complete piece.

4 The Case – Cylinder 2nd Stage

In the run of a revision at one of the cylinders being built as per "old" design, which had been in operation for some 5 years, the traditionally screwed-in condensate drain should for above described reasons be replaced by a welded nozzle

OPERATION & MAINTENANCE

3D-Laser Form and Position Verification before and after Repair of complex Compressor Parts, *Markus Weber,*
Stefan Damberg, BASF, NEAC COMPRESSOR SERVICE

connection. Therefore the cylinder was dis-assembled and thoroughly cleaned from product sticking to the walls.

During the inspection a line-shape groove was found at the suction side of the crank end 2nd stage cylinder near the heat affected zone where part of the cylinder wall had been welded to the main cylinder body.

The defect is visible between the 06:00 o´clock (Figure 4.1) and the 12:00 o'clock position (Figure 4.2).

Figure 4.1: Suc. Chamber, 2-stage; 6:00 o'clock
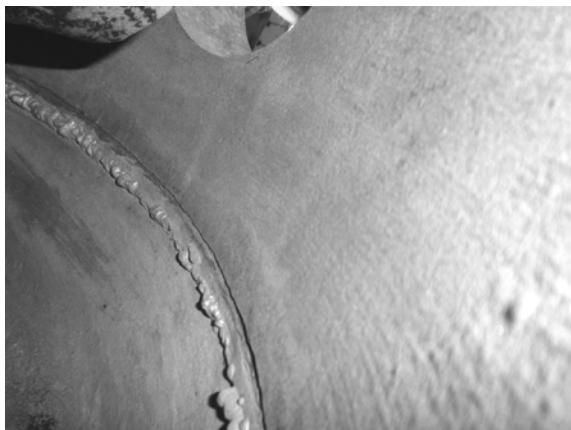
Figure 4.2: Suc. Chamber, 2-stage; 12:00 o´clock

In Figure 4.3 the location of the defect is indicated from the outside of the cylinder body.

Figure 4.3: Position of the Defect

Over a length of some 500 mm the wall thickness was reduced from 30 mm to 11 mm. The calculation, taking the notch related stress concentration into consideration, revealed that the minimum wall thickness had nearly been reached.

The root cause is presumably corrosion in conjunction with an initial small seam left over from the manufacturing process.

With the definition of time frames for checking the groove depth the cylinder was released for further operation.

5   Remedy Options

Disregarding the actual expenses for the remedy it is more the loss of production that counts when options are evaluated.

5.1   New Cylinder

The procurement lead time for a new cylinder is typically in the range of 6 to 12 months.

No matter if a new cylinder shall be purchased or not it became immediately clear that any kind of repair option had to be assessed with regard to the

OPERATION & MAINTENANCE

3D-Laser Form and Position Verification before and after Repair of complex Compressor Parts, *Markus Weber, Stefan Damberg, BASF, NEAC COMPRESSOR SERVICE*

above time frame and expenses in comparison with the expected loss of production.

To bridge the delivery time a repair concept for the flawed cylinder was to be defined.

5.2   Cylinder Repair

The time range for the repair was estimated to be some 3 to 4 weeks. In comparison with the above 6 to 12 months for the new cylinder that immediately superseded any thought about the additional repair expenses versus the production losses.

The focus was put on following alternative procedures:

1.   Welding from the inside.

2.   Cutting out of the particular wall piece; casting of a new wall section and welding to the main body (comparable to the manufacturing process of a new cylinder).

3.   Cutting a groove from the outside, prepare a welding V-gap and fill-up with welding material.

Option A was rejected since access to the relevant area is limited and optimal welding preparation therefore hardly possible.

Option B and C were kept in the focus.

For each of the potential repair procedures heat related deformation in conjunction with internal material stress through the heat intrusion had to be considered.

Since welding is part of the manufacturing process from design perspective the deformation was taken into consideration through material allowances. The cylinder with the defect, however, had already been machined to final dimensions. Therefore the material allowances are no longer available.

Stress relief heat treatment must be regarded with serious doubt because functional dimensions of the cylinder would most likely get out of tolerable range; the cylinder would presumably become useless.

Therefore the amount of deformation - from the extensive welding being necessary - was of the essence to evaluate the amount of machining after the welding and if it was at all possible to regain the required shape of the cylinder without cutting off too much at location where machining option were

limited; e. g. without taking the risk to reduce wall thicknesses too much elsewhere just because the original surface quality needed to be reached again.

From thoughts above finally option C was favoured.

For demonstration purposes before scrapping operations had stored an old cylinder which had earlier been sorted out because of severe corrosion (Figure 5.2.1).
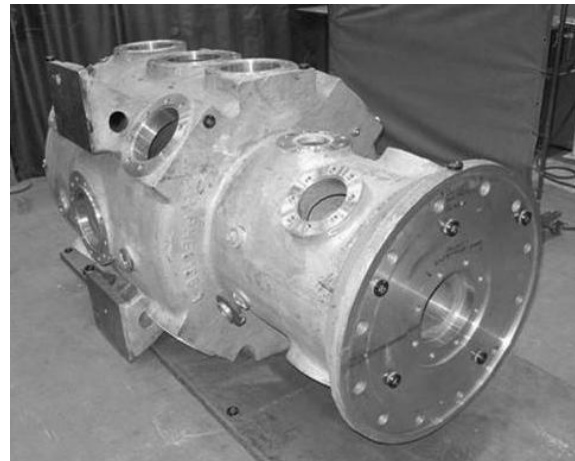
Figure 5.2.1: Old Cylinder 2nd Stage

That opened the possibility to test the selected repair procedure at this old cylinder prior to the "hot" execution.

Through the "test repair" including exact measurement of the functional dimensions it became possible to predict the deformation and quantify the expected dimension off-set as well as the internal material stress. Furthermore welding parameters for the later execution can be optimized from these findings.

When selecting an adequate measurement technique the on-site laser scanning was preferred versus traditional measuring tools.

Reasons for the decision:

▪   Omission of transportation between welding location and machining tools.

▪   Prevention of alignment and adjustment errors.

▪   Accuracy of the 3D-laser equipment.

To avoid that operation of the compressor turns into a "blind flight" the temporary repair has to be performed according to the latest "state of the art" through companies who know how to do it; accompanied with documentation that is "court-proof".

OPERATION & MAINTENANCE

3D-Laser Form and Position Verification before and after Repair of complex Compressor Parts, *Markus Weber, Stefan Damberg, BASF, NEAC COMPRESSOR SERVICE*

6   Deformation Check Procedure with 3D-Laser Application

BASF SE and NEAC some years ago (see EFRC 2003 presentation "An old product still fresh") started collaborating with the use of laser measurement equipment for better and faster definition of geometrical and trigonometrical issues of reciprocating compressors.

Since NEAC Compressor Service now owns and operates the 3D-laser equipment and has the experience to conduct laser dimension, form and position measurements of reciprocating compressor parts BASF SE decided to partner again with NEAC for the described investigation.

Regarding Borsig compressors built up to 1995 by Borsig Berlin, NEAC Compressor Service since 2003 is OEM providing technical support for repairs and spare parts.

6.1   Cylinder Welding and Laser Equipment

Figure 6.1.1 shows the unusable scrap-cylinder being utilized for the "test repair" and following deformation check.
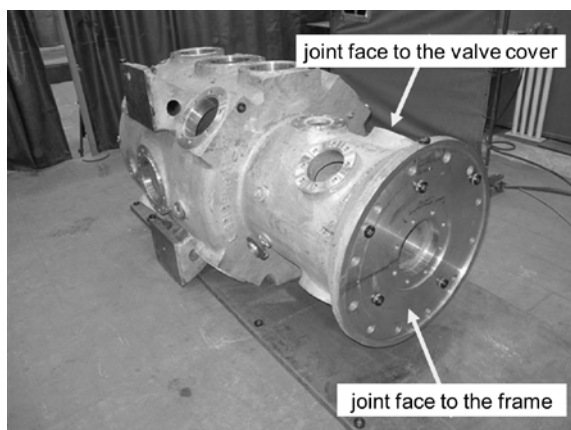
Figure 6.1.1: Unusable Cyl. for the "Test Repair"

The machined faces with the true form and position as required for installation were the reference points and faces before and after the welding

Figure 6.1.2 shows the 3D-laser equipment utilized by NEAC in front of the relevant cylinder.

Figure 6.1.2: 3D-Laser Equipment

The 3D-laser source which launches the laser beam towards the body identifies each measuring location through reflection of the beam back to the transmitter. The length (distance) between each scanning point as well as its angle is recorded. Through multiple point by point scanning of the body surface a full size scanning model is created through application of complex software which collects and evaluates the laser measurement data.

Since laser measurement requires "eye-contact" between the laser source and the scanning point the laser equipment has to be moved to various positions. Figure 6.1.3 shows the 2nd position at the other side of the cylinder to continue the scanning.

OPERATION & MAINTENANCE

3D-Laser Form and Position Verification before and after Repair of complex Compressor Parts, *Markus Weber, Stefan Damberg, BASF, NEAC COMPRESSOR SERVICE*

Figure 6.1.3: 3D-Laser Check – Cyl. Flange

After the scanning of the original shape had been finalized and the scanning model was created the cylinder was cut at the point where the later to be repaired cylinder has the defect (Figure 6.1.4) and the weld was prepared for repair- exactly as it shall later be done at the other cylinder.

Figure 6.1.4: Weld Preparation

Afterwards the repair welding was performed (Figure 6.1.5) with result shown in Figure 6.1.6.

Figure 6.1.5: Welding in Progress

Figure 6.1.6: Welded Joint

The repaired cylinder was then scanned with the 3D-laser again to verify in which way and how much the various faces were deformed.

6.2   Test Results

Through the 3D-laser measurement a scanning model of the relevant important machined faces was created. Figure 6.2.1 shows the condition of the original cylinder prior to any repair activity. This was the basis for further evaluation with the same results after the repair welding.
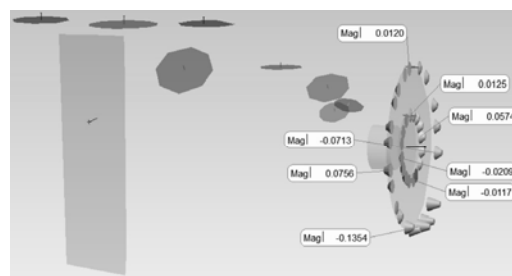
Figure 6.2.1: Reference Measurement

OPERATION & MAINTENANCE

3D-Laser Form and Position Verification before and after Repair of complex Compressor Parts, *Markus Weber, Stefan Damberg, BASF, NEAC COMPRESSOR SERVICE*

When the "test repair" had been conducted as outlined in the previous chapter the 3D-laser scanning was repeated. The results of the 2nd scan is shown in Figure 6.2.2 where – in comparison with Figure 6.2.1 – it is immediately obvious what happened to the cylinder flange face.
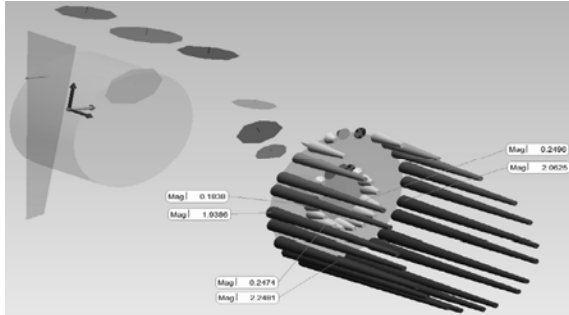
Figure 6.2.2: Deformation after Welding Process

The same investigation was done to all other faces which are of importance for the proper shape and integrity of the cylinder body.

With the 3D-laser equipment it is possible to immediately verify form and position when the relevant piece is still mounted in the machining tool.

Summary from the 3D-Laser measurement after the welding performance:

- Deformation of joint face to the valve cover: max. 0.3 mm.

- Out-of-roundness internal bore for the stuffing box: 0.9 mm.

- Deformation of joint face to the frame: max. 2.3 mm.

- Angular misalignment of the joint face to the frame: max. 0.8°.

Results:

- Deviations are well known after the laser measurement.

- Internal stress in the cylinder material.

- Necessity of additional work on functional surfaces.

- Improvement if equalization of the deformations is possible, without minimizing the strength properties of the components.

- Check if stress-relief heat treatment is possible.

Based on above results the impact of the necessary repair welding and consequential machining can now exactly be assessed and planned.

7 Lessons learned

To provide for all the above it is essential to involve the OEM for the following:

1. Material specialists are necessary for the damage and repair option assessment which then needs to be introduced into the current component configuration with evaluation through the OEM.

2. Form and position verification through laser measurement is necessary and accurate results can be provided in shortest time. Their check versus the dimensions as per design drawings can only be done by the OEM being in possession of the relevant documents.

3. If the repair assessment as well as the form and position verification results in the proposal to conduct a design change or optimization this can best be performed with or by the OEM.

8 Conclusion

Through the application of 3D-Laser technology it is possible and comparably easy:

- To detect deformation of parts and pieces due to welding.

- To assess the amount of internal stress as a result from heat intrusion.

- To determine the amount of additional machining work after welding.

- To check if stress-relief heat treatment is possible.

The impact of the necessary repair welding and consequential machining can exactly be planned to minimized down time of the machine and keep production losses on a low level.

Field Assessment of Overall RMS Vibration Guidelines for Reciprocating Compressors

by:

Howes, Brian
Chief Engineer, Beta Machinery Analysis
Calgary, Canada
bhowes@betamachinery.com
and
Tom Stephens
Senior Equipment Specialist, Ariel Corporation
Mt. Vernon, USA
tstephens@arielcorp.com

8th Conference of the EFRC
September 27th / 28th, 2012, Düsseldorf

Abstract:

The EFRC has prepared an overall RMS vibration guideline for reciprocating compressors. The intent is to have this guideline approved as an ISO standard. To assess the accuracy and robustness of this guideline, the authors have completed field studies on a range of compressor installations. These field tests compare the proposed guideline to other vibration parameters and measurement approaches. This paper will present the findings from these field assessments and conclusions regarding the proposed standard.

Field Assessment of Overall RMS Vibration Guidelines for Reciprocating Compressors, *Brian Howes, Tom Stephens;* BETA MACHINERY ANALYSIS, ARIEL CORPORATION

1   Introduction

A new vibration guideline has been proposed for the monitoring of reciprocating compressors, and associated piping. It was first published in 2008 at the 6th EFRC Conference in Dusseldorf. Efforts are currently ongoing to incorporate the EFRC limit into ISO standard 10816-8.

The EFRC Guideline makes use of root mean square overall (RMS OA) vibration measurements in terms of acceleration, velocity and displacement. Zones of vibration are defined in terms of subjective ratings of the integrity of parts of the compressor.

The user of a vibration guideline is likely to be attracted to a method that is easy to use and interpret. The proposed RMS Guideline meets this need because simple handheld instruments can be used to collect the data.

One paper has been published since the introduction of the new guideline at the 7th EFRC Conference. The conclusion of the paper was that most measured vibrations were in acceptable zones. This result was consistent with the long-term satisfactory operation of the machines measured. The purpose of this paper is to evaluate the guideline with more field data, including compressors with problem vibrations. Comparisons of RMS measurements to spectral measurements will be shown.

Author Howes has used a guideline based on individual frequency components – a spectral guideline that has been used globally for the past 40 years by compressor manufacturers and compressor users. Assessments of integrity of the new RMS OA Guideline and the older Spectral Guideline will be compared.

In most cases the two approaches provide similar results and this tends to validate the usefulness of the EFRC Guideline.

Data from five different compressors are included in the analysis. Refer to Table 1 below for a brief description of the units. Also, comments based on decades of experience analyzing reciprocating compressors by the authors will be provided.

The evaluation highlighted the challenges in applying RMS data. This paper illustrates how different vibration instrumentation can result in significantly different RMS Overall data. Accounting for these differences is very important when investigating vibration problems.

Example Number	Model	Speed (rpm)	Driver	Maximum Frequency (Hz)
1	JGA4	1200	Engine	250
2	JGK2	1000 - 600	Electric	500
3	JGC6	1000 - 800	Engine	200
4	JGU6	745	Electric	1000
5	JGD4	1000 - 600	Electric	1000

Table 1: Compressors from Field

Another important topic addressed in the paper is Crest Factor (CF). This parameter is useful to supplement the RMS result in order to identify problems, especially when the EFRC screening guideline produces marginal or high vibrations. Field data is used to illustrate how CF will vary for the same RMS value.

Certain areas important to all reciprocating compressor systems, such as, pressure relief valves and small bore connections, are not included in the guideline.

The EFRC Guideline requires that spectral data be used for further analysis in the event that vibrations exceed the RMS Guideline. Recommendations are provided for spectral analysis since no details are provided in the guideline.

2   Definition of Vibration Measurement Terms

In this paper, the following types of vibration measurement will be discussed:
- **RMS Overall** can be obtained from two sources and the results will be different:
  - i.   Time waveforms, or from simple handheld data collectors.
  - ii. Spectral data (frequency based results) obtained from more complex spectrum analyzers
- **Amplitudes of individual frequencies**. These data are obtained from spectral analysis, which is the required approach when analyzing vibration data for troubleshooting, or when vibration exceeds the EFRC Guideline.
- **Crest Factor (CF)** (Peak Overall divided by RMS). This parameter characterizes the vibration waveform. For the same RMS, a large CF is an indication that the likelihood of fatigue failures will be higher than if the CF is low.
- **Peak Overall**. This measure of the highest vibration is related to fatigue failure. Peak data is obtained from time waveforms, using two methods – ISO and non-ISO.

OPERATION & MAINTENANCE

Field Assessment of Overall RMS Vibration Guidelines for Reciprocating Compressors, Brian Howes,
Tom Stephens; BETA MACHINERY ANALYSIS, ARIEL CORPORATION

In theory, the time and spectral methods of calculating RMS OA should give the same result. An example from the data where this is not true is discussed.

3 RMS Data Analysis – Reconciling Two Methods

At the beginning of the analysis of the data, it was assumed that the process would be simple. In fact, pitfalls were discovered.

A spectrum analyzer was used to collect the vibration data. Various maximum frequencies were used. In all cases, the minimum analyzer frequency was zero, rather than the 2 Hz specified in the EFRC Guideline – a limitation of the analyzer.

During the evaluation, it was determined that RMS OA value from a time waveform or a spectrum was not always the same. See Figure 1 below for data from four selected test points. The blue line compares the ratio of the two approaches (RMS T/RMS F):

- RMS T = RMS calculated from time waveform data.
- RMS F = RMS based on spectra (frequency) data (spectra)
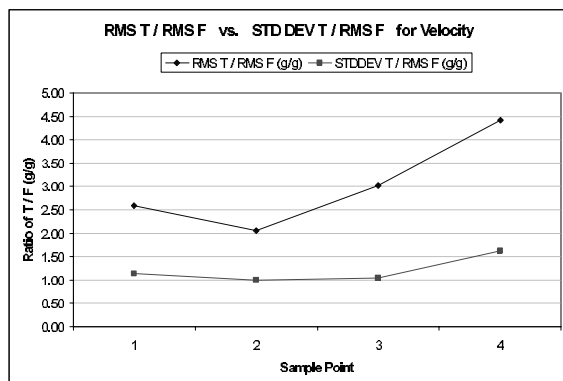
Figure 1: Ratios of Time vs. Frequency Domain RMS Calculations.

The difference varies between 200% and 400%. Different analyzer measuring devices account for the differences, due to these reasons:

- Velometers vs. accelerometers can produce differences: Accelerometers required digital time domain integration to create vibration results compared to velometers.
- Filtering low frequency data (or not) will produce large differences. Some hardware does not filter low frequencies (below 2 Hz).

This illustrates that methods and test equipment can produce large differences.

Correcting RMS Data

If a different method is used compared to the ERFC defined procedure, then the data will likely need to be corrected.

Correction of this problem was achieved by using the standard deviation of the time waveform instead of the RMS, based on the definition below:

$$RMS^2 = mean^2 + standard\ deviation^2$$

The RMS OA mentioned in the EFRC Guideline document is expected to have a mean value of the time waveform approaching zero. Usually, high pass filtering the data above 2 Hz will achieve that goal (which is captured in the frequency range of 2-1000 Hz in the proposed standard).

If data are not filtered then using the standard deviation will correct the problem (see red line in Figure 1).

4 Spectral Vibration Guideline Used to Compare with EFRC RMS Guideline

The purpose of a vibration guideline is to provide a screening tool for identifying "areas of concern". Generally, these guidelines are derived empirically, although vibration guidelines can also be derived from finite element models of specific geometries. A vibration guideline should always be slightly conservative.

Spectral guidelines are available and in common use for reciprocating compressors. One such guideline has been used by author Howes' company for about 45 years (covering all parts covered by the EFRC Guideline). Over the years, it has been adopted by compressor manufacturers and compressor users around the world.

This Spectral Guideline can be summarized for piping and dampers as the lesser of 10 mils pp (.09 mm RMS) or 1 ips peak (18 mm/sec RMS) at any frequency up to 500 Hz. The limits are multiplied by constants for different parts of the compressor: 0.7 for cylinders and 0.5 for frames. Foundations, considered a special case, are assessed based on limits of 0.05 ips peak (.9 mm/s RMS) for vertical and 0.1 (1.8) for horizontal plane vibrations[1] A special case of the Spectral Guideline is for frequencies above 125 Hz on relief valves (and other parts that are sensitive to internal fretting or vibratory loosening, such as gate valves). An acceleration limit is defined as 2 g peak (14 ms^{-2} RMS). Allowing increased severity over 2 g peak is not recommended.

Field Assessment of Overall RMS Vibration Guidelines for Reciprocating Compressors, Brian Howes,
Tom Stephens; BETA MACHINERY ANALYSIS, ARIEL CORPORATION

For the subjective analysis of vibration severity used in this paper, we have added zones to permit comparison with the RMS OA Guideline, as shown in Table 2. No distinction is made between cylinder directions. Foundation zone boundaries are 50%, 100% and 150% of the limits mentioned above.

Note that the frequency below which displacement becomes the defining measurement is 100/PI Hz (about 31 Hz, compared to 10 Hz for the RMS).

Zone Boundary	Frame	Cylinder	Damper or Pipe
	Velocity from 31 to 500 Hz in/sec peak (mm/s RMS)		
A/B	.25 (4.5)	.35 (6)	.5 (9)
B/C	.5 (9)	.7 (13)	1 (18)
C/D	.75 (14)	1.05 (19)	1.5 (27)
	Displacement below 31 Hz Mils pp (mm RMS)		
A/B	2.5 (.02)	.35 (.03)	5 (.045)
B/C	5 (.045)	7 (.06)	10 (.9)
C/D	7.5 (.07)	11 (.1)	15 (.14)

Table 2: Spectral Guideline Zone Boundaries

5   Field Data Compared to both EFRC and Spectral Guidelines

Using the comparison boundary zones defined in Table 2, a limit comparison study has been completed. Figures 2 to 5 compare the two methods for many data points collected from the compressor examples. The data is velocity readings (inches per second, IPS).

The shaded boxes represent data points that show similar results between the two guidelines. Data outside these shaded boxes represent areas where the guidelines produce different recommendations.

In most cases, the two methods produce similar results and confirm that the EFRC Guideline is effective in screening for condition.

There are relatively small differences between the methods, as highlighted by the black circles. In all cases the EFRC Guideline results in a slightly more conservative assessment than the Spectral Guideline – a good result.
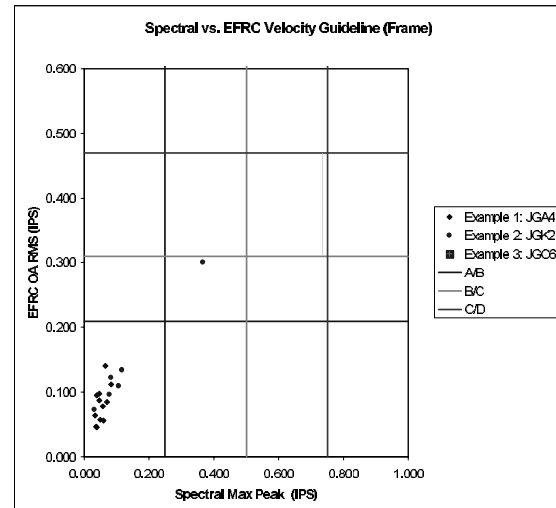
Figure 2: Compressor Frame
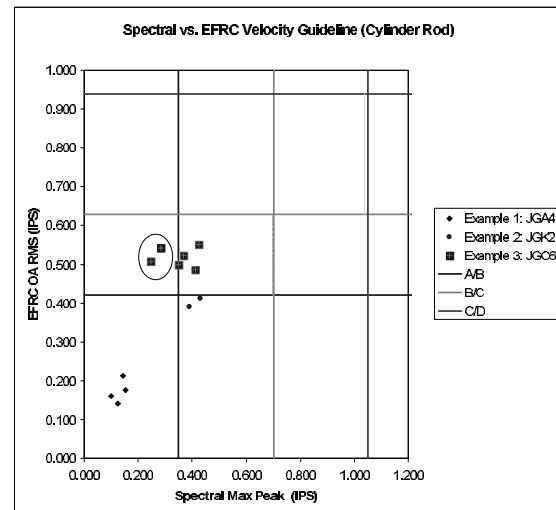
Figure 3: Cylinder Rod
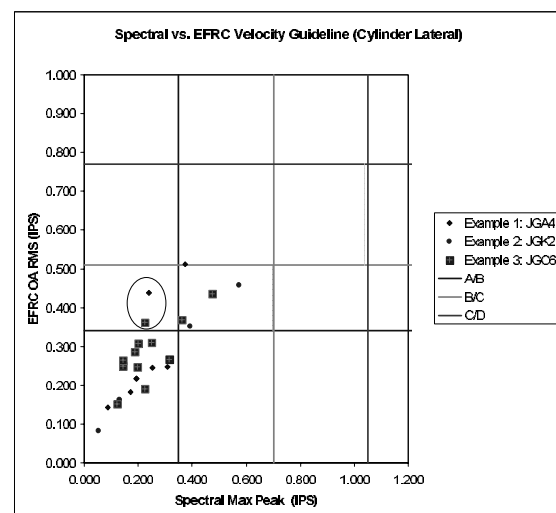
Figure 4: Cylinder Lateral

OPERATION & MAINTENANCE

Field Assessment of Overall RMS Vibration Guidelines for Reciprocating Compressors, Brian Howes,
Tom Stephens; BETA MACHINERY ANALYSIS, ARIEL CORPORATION
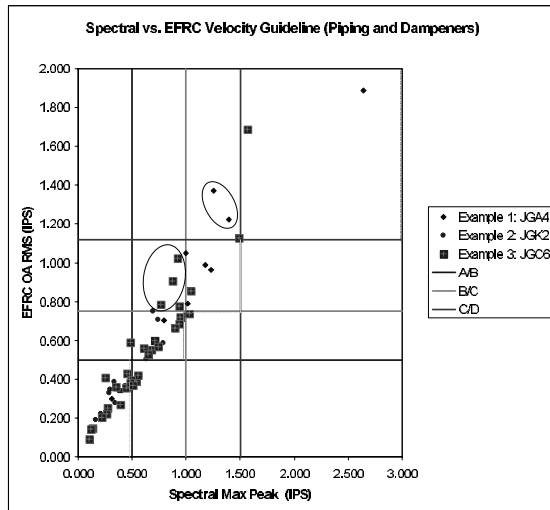
Figure 5: Piping and Dampers (Pulsation Bottles)

6   Comments on Velocity, Acceleration, Displacement

The evaluation in this paper presents velocity data which is the most common approach for reciprocating compressors.

Displacement data is used for low frequency measurements (below 30 Hz). This would apply to pipe & pulsation vessels (dampers) on slow speed compressors. This paper did not compare the two guidelines in this region. Table 3 shows a comparison of displacement guideline boundaries. Our experience shows that the EFRC displacement limits could result in unacceptably high stresses in damper to cylinder nozzles. More information must be reviewed to confirm this concern.

Location	Description	Units	Horizontal compressors		
			A/B	B/C	C/D
Foundation	EFRC	mm RMS	0.032	0.048	0.072
	EFRC (Converted)	mil p(P-P)	3.56	5.35	8.02
Frame (top)	EFRC	mm/s RMS	0.084	0.127	0.191
	EFRC (Converted)	in/s pPk	9.35	14.14	21.27
	Spectral Guideline	in/s Pk		5	
Cylinder	EFRC (Lateral)	mm/s RMS	0.139	0.207	0.31
	EFRC (Rod)	mm/s RMS	0.17	0.255	0.382
	EFRC (Lateral - Converted)	in/s pPk	15.48	23.05	34.52
	EFRC (Rod - Converted)	in/s pPk	18.93	28.40	42.54
	Spectral Guideline	in/s Pk		7	
Dampers/Piping	EFRC	mm/s RMS	0.202	0.302	0.454
	EFRC (Converted)	in/s pPk	22.49	33.63	50.56
	Spectral Guideline	in/s Pk		10	
EFRC Guidelines are for Overall RMS values from 2-1000 Hz					
EFRC (Converted) values are mils P-P from pseudo-peak (RMS * sqrt(2))					
Spectral Guidelines are for any discrete frequency <31 Hz					

Table 3: Comparison of Displacement Levels

Acceleration data is applicable for higher frequency applications such as relief valves (above 125 Hz). In this region, the EFRC Guideline could be overly conservative for other parts of the compressor system.

Based of 10 years of field analysis, Author Howes evaluated acceleration spectral guidelines. The guideline was 2 g peak acceleration for all parts of the compressor and piping. Howes discovered that too many problem areas were erroneously flagged by this guideline.   The conclusion was that for reciprocating compressors, velocities below 1 ips peak above 125 Hz are not a problem, and acceleration should only be used when evaluating relief valves and other components that are sensitive to fretting damage.

7   OEM vs. EFRC Guidelines

In practice, the user should also follow guidelines provided by compressor manufacturers.

Author Stephens represents a major OEM who currently employs a frequency bandwidth limited (10-250 Hz) overall peak limit covering the foundation, frame and cylinders. Different levels are provided for frames of varying load capacity. The EFRC Guidelines are less conservative for the smaller frames, and slightly more conservative for the larger frames. In general, the velocity guideline levels are comparable to the EFRC Guidelines. See Table 4 for details.   Given that these particular compressors typically operate above 10 Hz, the displacement measure is not employed (nor recommended). Acceleration measures are also not used nor recommended.

Location	Description	Units	Horizontal compressors		
			A/B	B/C	C/D
Foundation	EFRC	mm/s RMS	2	3	4.5
	EFRC (Converted)	in/s pPk	0.11	0.17	0.25
	Spectral Guideline	in/s Pk		0.1	
	OEM Guideline (Medium)	in/s Pk		0.15	
	OEM Guideline (Large)	in/s Pk		0.2	
Frame (top)	EFRC	mm/s RMS	5.3	8	12
	EFRC (Converted)	in/s pPk	0.3	0.45	0.67
	Spectral Guideline	in/s Pk		0.5	
	OEM Guideline (Medium)	in/s Pk		0.4	
	OEM Guideline (Large)	in/s Pk		0.5	
Cylinder	EFRC (Lateral)	mm/s RMS	8.7	13	19.5
	EFRC (Rod)	mm/s RMS	10.7	16	24
	EFRC (Lateral - Converted)	in/s pPk	0.48	0.72	1.09
	EFRC (Rod - Converted)	in/s pPk	0.6	0.89	1.34
	Spectral Guideline	in/s Pk		0.7	
	OEM Guideline (Medium)	in/s Pk		0.8	
	OEM Guideline (Large)	in/s Pk		1	
Dampers/Piping	EFRC	mm/s RMS	12.7	19	28.5
	EFRC (Converted)	in/s pPk	0.71	1.06	1.59
	Spectral Guideline	in/s Pk		1	
EFRC Guidelines are for Overall RMS values from 2-1000 Hz					
EFRC (Converted) values are in/s pseudo-peak (RMS * sqrt(2))					
Spectral Guidelines are for any discrete frequency from 31-500 Hz					
OEM Guidelines are for Overall Peak values from 10-250 Hz					

Table 4: Comparison of Velocity Guidelines

As earlier discussed, problems due to high vibration are usually a result of motions in the 10-250 Hz frequency range. Higher frequencies are usually a result of impacting and can result in very high true peak measurements, so the band limiting was employed to focus on the frequencies of interest and make the response information less sensitive to impulsive responses. Often, this provides similar effects as an RMS measure, and it is common for people to employ these OEM limits with pseudo-peak measurements or devices.

OPERATION & MAINTENANCE

Field Assessment of Overall RMS Vibration Guidelines for Reciprocating Compressors, Brian Howes, Tom Stephens; BETA MACHINERY ANALYSIS, ARIEL CORPORATION

8 Crest Factor (CF) as a Tool to Assist Vibration Analysis

One challenge with using RMS measurements is that RMS value does not indicate the vibration profile. The vibration profile can be important in analyzing reciprocating compressor issues.

Here are two examples which could have the **same RMS** value:

i. A vibration signature containing many harmonics, all having low amplitudes. For a reciprocating compressor this may not represent a risk of fatigue failure. This example would have a low CF.

ii. A vibration signature containing impulsive responses or two or more large amplitude peaks. Due to the process of averaging the entire spectrum, the resulting RMS value would be the same as (i). This signature, however, could pose a much higher risk of fatigue failure. This situation would have a higher CF.

While the EFRC will provide an effective screening tool, it could be enhanced by using CF data – especially if the screening results are in the marginal or high zones.

CF is the ratio of Peak Overall to RMS. CF for a sinusoid is always 1.414. CF is 1.0 for a square wave.

Figure 6 illustrates how CF can vary while RMS OA remains constant. The chart plots increasing numbers of frequency components (peak single frequencies). If the peak amplitude of the individual spectral components are added arithmetically as peak values, then a worst case Peak OA curve results.

The CF starts out at 1.414 for a single frequency peak and climbs to over 4 with 9 peaks combined. In reality, it is unlikely that this worst case situation will occur.
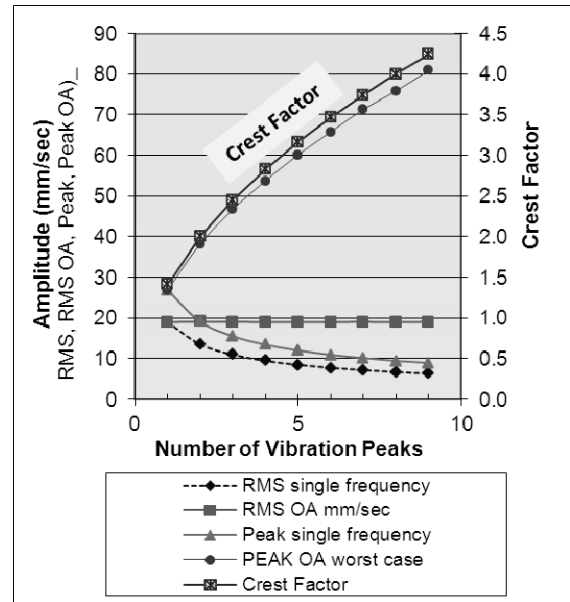
Figure 6: Crest Factor vs. RMS OA for Complex Spectra

Our observations of the variability of CFs from measurements of vibrations (see Figure 7) are that typical CFs are in the order of 2 to 3.5 (occasionally, as high as 4 have been seen). This maximum CF of 3.5 from the test data seems to be consistent with the "worst case" calculations above.
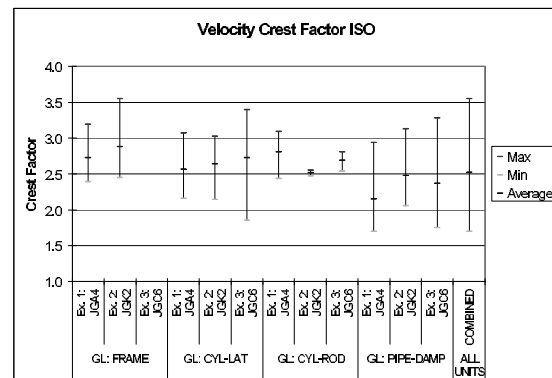
Figure 7: Crest Factors from Measured Data

The two methods of calculating peak amplitude of a complex time waveform are:

- Absolute value of the mean to maximum or minimum (ISO definition), or
- Peak to peak divided by 2. This is a commonly provided measurement by spectrum analyzers.

Figure 8 compares the two methods. A ratio of 1.0 would mean the methods were the same. Ratios as high as 1.3 can be seen in the figure.

Field Assessment of Overall RMS Vibration Guidelines for Reciprocating Compressors, Brian Howes, Tom Stephens; BETA MACHINERY ANALYSIS, ARIEL CORPORATION
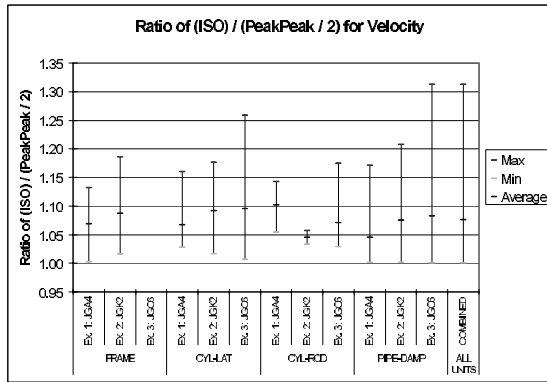
Figure 8: Comparison of Peak Measurements by Calculation Method

This observation caused us to calculate all CFs using the ISO definition of peak for this paper. It should be noted that this method will be conservative compared to a PP/2, especially if it is used to calculate a P-P value for fatigue analysis.

9   Justification for Crest Factor

Fatigue failures can occur on machinery and piping components. Peak stress is used to predict fatigue-inducing stresses. As a result of this relationship between peak stress and fatigue, peak vibrations (and CF) are valuable for evaluating vibration.

In a previous published paper[2] by Howes, a piping failure associated with a plunger pump is described in which the overall peak amplitude was very high, while the peaks at orders of pump speed in the spectrum of the vibrations (and by extension the RMS OA amplitude) were low. In other words, the CF was high. The Spectral Guideline used by Howes' company failed to detect this problem. An RMS OA guideline, we assert, would also have failed to predict a problem in this case.

Based on this example, it would seem prudent to consider peak amplitudes as well as either RMS or Spectral measurements when the guideline assessment is at a point in the Marginal Zone. CF is a convenient way to do this if normal ranges of CF for reciprocating compressor vibrations are known.

10   Caution: Pseudo-Peak is a Confusing Term

Over 50 years ago, a major manufacturer of vibration instrumentation created confusion by calculating pseudo-peak overall measurements (RMS OA times the square root of 2) rather than "true" Peak Overall. Instrumentation is available for purchase today that perpetuates this confusion.

Pseudo-peak overall measurements provide no additional information compared to RMS measurements. Caution is urged, therefore, when using guidelines based on peak readings. Vibration analysts are recommended to check their instrumentation to determine if peak or pseudo-peak data is provided.

11   Collecting RMS and Spectral Data

For the purpose of measuring overall vibration data on a reciprocating compressor and its associated piping to conform to the EFRC Guideline, the following settings are suggested on a spectrum analyzer:

- Maximum frequency: 1000 Hz (to conform to EFRC Guideline)
- Minimum frequency: 2 Hz (or, if 0, use Standard Deviation instead of RMS OA when using time waveforms to determine RMS OA)
- Flat-top Window (for amplitude accuracy)
- Bins between orders of run speed: at least 6 (to prevent leakage between orders during Spectral RMS calculations)

In our experience, vibration data of interest on reciprocating compressors is usually limited to a maximum frequency of between 200 and 500 Hz. An advantage of using 1000 Hz as a maximum frequency is that the sample period is lower, allowing for faster updates of measurements as compressor speed is varied.

The time period of the sample, based on the recommended settings above, will be significantly greater than one revolution of a reciprocating compressor crankshaft.

Averaging could be used to eliminate some of the low frequency and random components that can be present in real data.

12   Conclusion

- The analysis of field data confirms that the EFRC Guidelines based on RMS OA compares favorably to Spectral Guidelines in the velocity region. Either guideline could be used as a screening tool.

- The EFRC Guideline does not currently address small bore piping. A new guideline for small bore piping should be added to the standard. The current pipe guideline should be used for small bore attachments until a formal level is defined. Small bore attachments have the greatest propensity to fail due to fatigue. Typically, these components tend to have CFs

OPERATION & MAINTENANCE

Field Assessment of Overall RMS Vibration Guidelines for Reciprocating Compressors, Brian Howes,
Tom Stephens; BETA MACHINERY ANALYSIS, ARIEL CORPORATION

at the lower end of the range mentioned above. This makes the use of RMS OA for small bore piping assessment attractive (simple and reasonably conservative).

- Use of the EFRC displacement limits on dampers (also referred to as bottles) for low speed (below 600 rpm) compressors should be checked against guidelines derived from stress estimates to avoid damper-to-cylinder nozzle failures. Our experience suggests the RMS displacement limits for this special case are too high. More field data analysis is required.

- Use of the EFRC acceleration limits may result in overly conservative assessments of compressor parts.

- The EFRC Guideline currently does not apply to relief valves and other components sensitive to acceleration. In our opinion, another "part" guideline is required, since relief valves are an integral part of all reciprocating compressor installations. We recommend an acceleration guideline for relief valves, etc. as shown in Table 5 below. The velocity guideline should be the same as for piping.

Horizontal compressors m/s^2			Vertical compressors m/s^2		
Key zones			Key zones		
A/B	B/C	C/D	A/B	B/C	C/D
8	12	18	8	12	18
1.15 g pk	1.73 g pk	2.6 g pk	1.15 g pk	1.73 g pk	2.6 g pk

Table 5: Suggested Relief Valve Guideline

- CFs for reciprocating compressors and the attached piping tend to be in the range of 2 to 3.5, with an average less than 2.5, typically. RMS OA values near zone boundaries can be assessed further by examining the corresponding CF.

- Limiting overall vibration readings to a frequency band tends to lower the measured CFs.

- Spectral RMS OA values from spectrum analyzers are more accurate (consistent) than time waveform RMS OA values (without filtering or DC removal). RMS data that has not been filtered (below 2 Hz), will likely have mean values in the time waveform that are not zero. Thus, the data should be corrected by using Standard Deviation instead of RMS OA.

- Peak measurements using the ISO and the peak-to-peak/2 methods can give significantly different results. The ISO method will always give higher peak values.

- Instrumentation users should be careful to understand how RMS and peak measurements are calculated. Caution should be exercised when using pseudo-peak overall data (RMS times 1.414).

- Users of spectrum analyzers should test how their instruments calculate RMS OA and peak values against the methods defined in the EFRC Guideline.

13   Acknowledgements

References

[1] Irish, K & Walker, W. P. (1969). Foundations for Reciprocating Machines. London: Butler and Tanner Ltd.

[2] Howes, Brian C, Berg, Lyle, & Zacharias, Valerie. Incorrect Valve Selection on Plunger Pumps Results in Undetected High Frequency Vibration and Costly Failures, A Case Study. Proceedings from Canadian Machinery Vibration Association Proceedings, 1996

8th Conference of the EFRC
September 27th / 28th, 2012, Düsseldorf

EFRC

EUROPEAN FORUM
for RECIPROCATING
COMPRESSORS

Tasnee Petrochemical Complex

EFFICIENT MAINTENANCE OF THE WORLD'S LARGEST LDPE COMPRESSOR TRAIN

by:

Yousef Al-Shammari

Reliability & Integrity Department

Jubail Industrial City

Kingdom of Saudi Arabia

Email: y.alshammari@tasnee.com

8th Conference of the EFRC
September 27th / 28th, 2012, Düsseldorf

Abstract:

Tasnee operates the world's largest single frame reciprocating compressor in LDPE service. The LDPE production line consists of a 6-throw 7 MW Booster Primary and a 12-cylinder 27,5 MW Secondary Hyper. The two case studies describe how monitoring information supports essential maintenance decisions: when to safely shut down the compressors, where to open the machines and what measures are to be taken to allow a re-start of operation in the shortest possible time. These experience reports provide an in-depth look in the daily routine of state-of-the-art compressor operation with a special focus on maintenance efficiency.

Efficient Maintenance Of The World's Largest LDPE Compressor Train, *Yousef Al-Shammari;*
TASNEE PETROCHEMICAL COMPLEX

Introduction

The Tasnee facility has 5 different plants. Next to the PDH (Propane Dehydrogenation), EC (Ethylene Cracker), PP (Polypropylene) and HDPE (High Density Polyethylene), the Low Density Polyethylene (LDPE) plant is in operation since 2009. The Tasnee LDPE process is designed for 400 KTA.
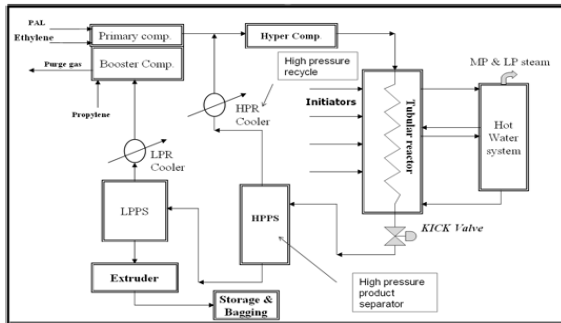
The LDPE production line consists of a 6-throw 7 MW Booster Primary and a 12-cylinder 27,5 MW Secondary Hyper.

1 Case 1 Insufficient Pressure on 2nd stage on hyper compressor during start-up phase

The first case is based on the Hyper machine (Secondary Compressor), where in October 2011, during a start-up phase, the pressure on the 2nd stage was insufficient and the compressor was not able to deliver the pressure to the Tubular Reactor. The 1st stage produced the maximum pressure but the 2nd stage failed to produce the required plant pressure. As a consequence, the production process had been stopped.

The Secondary Compressor is a Traverse Hyper with a design mass flow of 160 000 kg/h and volume of 126.860 Nm³/hour by an process suction pressure of 276 bar(a) and a discharge pressure of 2651 bar(a).
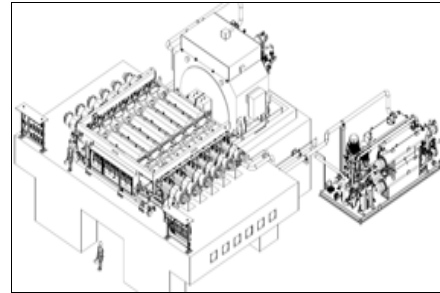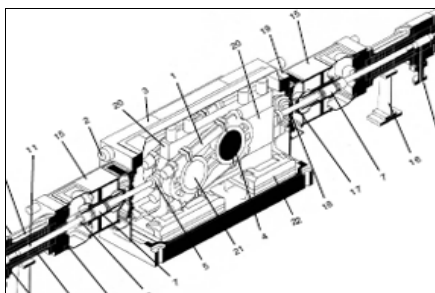
The machine has on each stage 6 single acting cylinders, so that this 2-stage Hyper has 12 compression chambers.
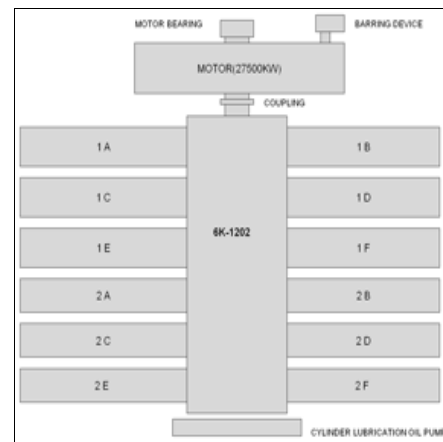
The machine at site:
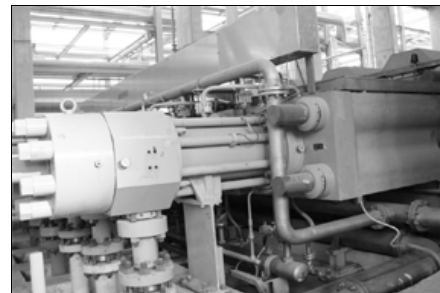
Tasnee uses PROGNOST®-NT for condition monitoring and safety protection. With the system it is possible to continuously analyse the condition of the machine. The compressor is equipped with, besides frame vibration velocity sensors, acceleration sensors at the cylinder head and at the intermediate crosshead slide on each cylinder. The plunger displacement in x/y direction is visible as well as an orbit data set. Both are automatically analysed.
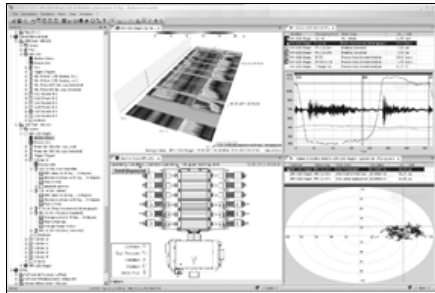
Nevertheless, the dynamic pressure inside the compression chamber can be shown by an indirect measurement (strain gauge rings).

PV diagrams of TASNEE
Hyper compressor measured
by strain gauge rings
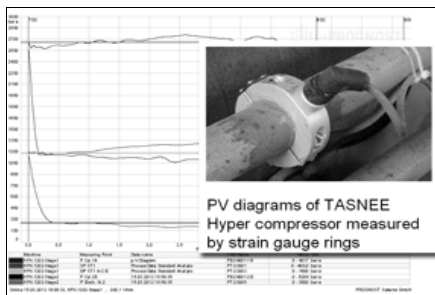
But what was happened Oct 16, 2011?

After a standard plant shut down for maintenance actions, the 1st stage had it's maximum discharge pressure, but the 2nd stage was not able to build up the pressure. The plant had a safe shut down to open the 2nd stage cylinder 2E for confirmation of a central valve failure. The maintenance team at site decided this after the final evaluation of the pV-diagram analysis. The following picture shows the failure mode.
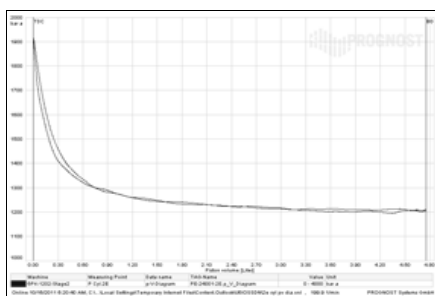
The next screenshot shows, at the same time, the pressure signal over volume of another cylinder 2F.
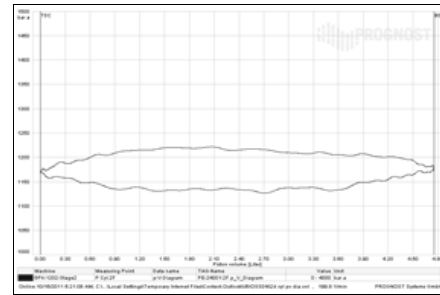
The findings after opening cylinder 2E

The suction valve pin was found damaged and it moved from its actual position. Imprints of the pin were visible on the suction valve seat. This movement and the gap created between the suction valve seat has caused the gas to short circuit back to the suction side and restricted the pressure to increase.
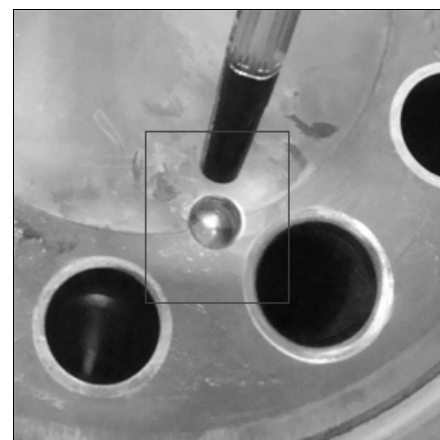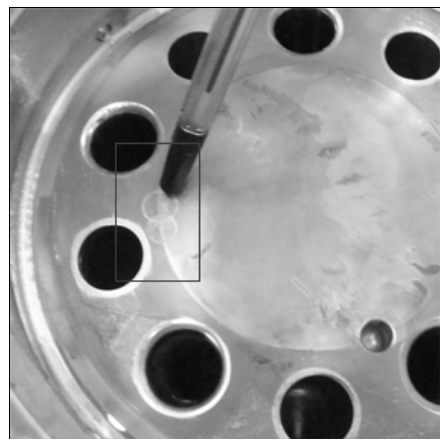
Conclusion

The final conclusion was, that the team at site made the right decision to stop the machine shortly to re-open only the cylinder 2E. This was committed by the diagnostic work and a previously maintenance work, where this central valve was replaced as well. The pV-diagram analysis was the key for this decision.

2   Case 2 High Crosshead vibration on booster compressor

A 2nd case should be highlighted in addition. This time a problem was identified at the Booster Primary compressor. The next picture gives the general arrangement:
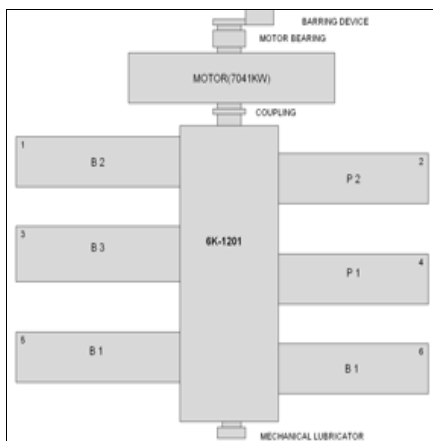
This machine is a 5-stage 6-cylinder double acting piston compressor with 7 MW. The following picture is showing the side view of the compressor with the 1st stage booster cylinder and the two primary stages.

In this case the problem occurred inside one compression chamber of the 1st stage cylinders. The operators were alarmed by the PROGNOST®-NT monitoring system after a machine start-up, where

the compressor was not in maintenance. A lot of Safety Alerts, caused by the CHS vibration, came in. The following picture shows the log book of the PROGNOST®-NT system.

From the protection module of the system, only pre-alarms were generated, so the machine was not shut down automatically. After analysing the data during this start up- period, the Condition Monitoring group of Tasnee recommended to stop the process and open the cylinder for inspection, because the vibration amplitude increased dramatically.
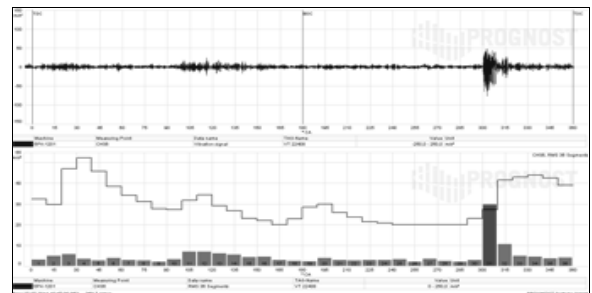
On July 26, the machine was stopped and the crosshead clearance checked and found normal. During this check, the compression chambers were not opened and inspected. After re-start of the compressor, the vibration was still on the same amplitude and again only pre-alarms were issued by the system.

The monitoring system did not send alarms any more and the operators decided to run the machine but monitor the situation very carefully. The following trend picture is showing that the vibration amplitude stabilized over time.

Efficient Maintenance Of The World's Largest LDPE Compressor Train, *Yousef Al-Shammari;*
TASNEE PETROCHEMICAL COMPLEX
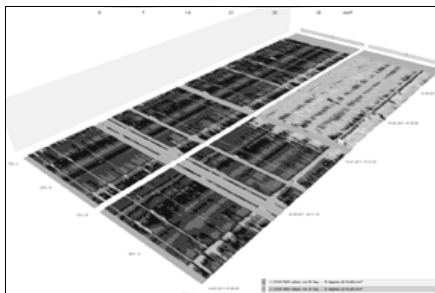
The final learning for Tasnee was, that with he help from the PROGNOST®-NT monitoring system and their detailed information, it was possible to run the Booster compressor safely until the planned shutdown.

In this condition it was able to run the machine until the next planned shutdown in October. During this scheduled stop, the machine was checked in detail and a lot of polymer coating on valves and cylinder spacer were found.
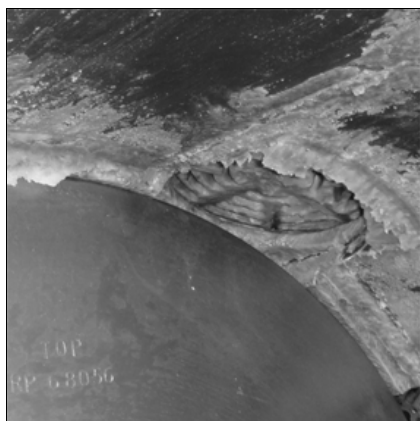
Maintenance practices and experienced failure modes in Air Liquide plants – Protection and monitoring systems

by:

Bertheloot Luc & Grillhofer Wolfgang
Rotating Machinery Expert Group
Air Liquide

luc.bertheloot@airliquide.com; wolfgang.grillhofer@airliquide.com

8th Conference of the EFRC
September 27th / 28th, 2012, Düsseldorf

Abstract:

Air Liquide is operating about 250 reciprocating piston compressors of several OEMs and different types and age with shaft power between 10kW and 4100kW in different plants in Europe. More than 40 compressors require a shaft power of more than 1000kW. The gases which are compressed are so called air gases as oxygen, nitrogen and the inert gases, carbon monoxide and dioxide, syngas, hydrogen and mixtures of mentioned gases. Air Liquide has developed standard maintenance strategies based on the type of gases and machine criticality. This paper and presentation shall give an overview on the maintenance philosophy of the different kind of compressors running with different type of gases as also the maintenance applied on the auxiliary equipment as the stepless volume flow control systems, etc. Based on our gathered experience we want to give an overview on failure analysis results, on compressor type and/or production specific failures and on lessons learned. Furthermore the value of protection and monitoring systems shall be discussed, especially which failures can be detected and avoided with state of the art protection systems and where are the limits from Air Liquide experience point of view.

CONDITION MONITORING

Maintenance practices and experienced failure modes in Air Liquide plants – Protection and monitoring systems, *Luc Bertheloot, Wolfgang Grillhofer;* AIR LIQUIDE

1   Introduction

For the hydrogen and air gas production Air Liquide has a large number of different reciprocating piston compressors in operation. Especially where high discharge pressures are needed or mentioned gases must be provided with low volume flow or light gases as hydrogen are compressed still the reciprocating type is used.

Furthermore there are still older plants in operation which are using reciprocating piston compressors instead of possible other types.

From maintenance point of view experience has shown that one important parameter is the type of sealing the piston to the cylinder. While especially for the light hydrogen gas compressors with piston rings are used, a lot of compressors with labyrinth pistons are installed for providing the air gases. Figure 1 below gives an overview on the population of the compressors for the mentioned gases classified in groups with and without piston rings. 41% of the installed compressors of mentioned gases are piston ring free machines, also known as laby compressors. The hydrogen compressors do have piston rings and represent 59% of the whole population taking into account nitrogen, oxygen, nitrogen / oxygen mixtures and hydrogen.
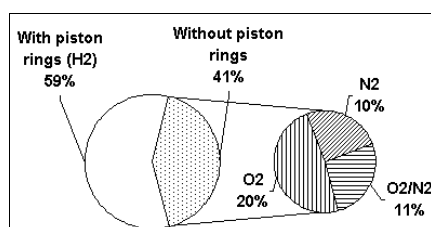
Figure 1: Reciprocating piston compressor population, types with piston rings and without piston rings

The groups mentioned above do comprise all the compressors from 14kW to 4100kW which is currently the most powerful installation for a hydrogen reciprocating piston compressor in an European Air Liquide plant.

In order to give an idea about the distribution from power point of view the compressors were also classified in groups >=100kW & <500kW, >=500kW & <1000kW and >=1000kW, please refer to the figure 2.
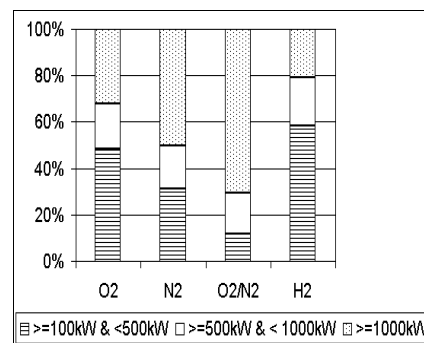
Figure 2: Reciprocating piston compressor power and gas classification

The goal of Air Liquide in the past was to work out and to agree on general maintenance procedures to ensure highest possible reliability and availability for the machines.

By setting up such general rules based on the operation experience Air Liquide has now the tool to reach and to keep the reliability and availability targets.

In the following section 2 an overview on the agreed maintenance strategy is given. In section 3 the experiences with monitoring and protection systems are described. Section 4 summarizes four cases of typical failure modes and their possible root causes as well as the conclusions for Air Liquide.

2   Air Liquide maintenance strategy

When taking into account the whole machinery population, i.e. including also the turbo- and cryogenic machines, Air Liquide has implemented a combination of time based and condition based maintenance based on the target getting best machine reliability and highest availability values.

Due to the long experience of operating different reciprocating piston compressor types of different OEMs in different conditions it was possible to optimise the general OEM maintenance plans.

Furthermore the development of new parts and new materials made it possible to adapt the original strategy.

2.1   Maintenance interval and activities

2.1.1   Guideline

As the production processes ask for compressing different gases as air, hydrogen, nitrogen, oxygen, syngas and carbon monoxide at different operating

CONDITION MONITORING

Maintenance practices and experienced failure modes in Air Liquide plants – Protection and monitoring systems,
Luc Bertheloot, Wolfgang Grillhofer; AIR LIQUIDE

parameters it is obvious that different maintenance intervals must be applied.

Other criterions are if the cylinder is lubricated or dry and if the compressor is equipped with piston rings or not.

As seen in the past the cylinder wear parts, i.e. piston rings, rider rings, valves and the piston rod packings have still a shorter lifetime due to wear than the driving or gear parts as the crosshead, connecting rod bearings and crankshaft bearings. This fact results in two different maintenance packages. The first is the minor maintenance comprising the cylinder wear parts and the second is the major maintenance also taking into account the driving or gear parts.

The maintenance guideline gives a limit for the MTBM for both maintenance packages. Experience has shown that the MTBM for the major maintenance is within a bandwidth of two to six times the MTBM for minor maintenance. Influencing factors for this bandwidth are different gases, design with or without piston rings and experienced problems.

The decision when to schedule respective maintenance within the bandwidth mentioned above is done after an assessment of the machine condition.

The input for this assessment is / are

- the general machine behaviour experienced by operating people,

- the machine history,

- the trends of operating parameters,

- the oil analysis results,

- the vibration analysis results and

- the performance measurements.

2.1.2   Machine behaviour and history

Based on the gathered information from the operating people together with the documented machine history it can be decided if it is a critical machine or not. So detected weaknesses will call for more stringent maintenance intervals thus resulting in intervals closer to the lower limit.

2.1.3   Operating parameter trends

Non critical compressors are equipped with the standard instrumentation allowing trending the stage suction and discharge temperatures and pressures. However, it is the intention to equip the critical and big compressors as used for hydrogen compression also with sensors measuring the valve temperatures.

2.1.4   Oil analysis

Air Liquide has developed and implemented a strong oil analysis program. The standard is to analyse the oil twice a year and to trend the changes of the analysis results. The figure below presents the oil analysis tests as standardised for the reciprocating piston compressors installed in European plants.

Description	Method		Unit
	1st choice	Alternative	
Kinematic viscosity @ 40 °C	ASTM D 445	DIN 51550	mm²/s
Color	ASTM D 1500	ISO 2049	ASTM Colour
TAN (Total acid number, potentiometric titration)	ASTM D 664	DIN 51558	mgKOH/g
Multi-elements analysis by Inductively Coupled Plasma (ICP)	ASTM D 5185		mg/kg
Appearance	Visual		C/Clear
			B/Bright
			L/Limpide
			D/Dark
			+
			P/Particles
Water Content (Carl Fisher)	ASTM 6304C	ISO 3733	mg/kg

*Figure 3: Air Liquide oil analysis standard tests
         for reciprocating piston compressors*

For each parameter limits were identified which are based on the experience and the oil supplier information. It is important to point out here that in a first step the parameter changes within a defined time period must be checked. Of course the absolute values must be also within a defined limit.

A continuously review process has for example resulted in the question if the standard analysis can reliably detect bearing failures. We had already cases in the past where we have found white metal particles in the lower part of the crankcase although the oil analysis indicated a good compressor condition.

To plan the duration of the stop correctly and also to make a correct budget it is important to be able to predict the overhaul type a number of months before the overhaul, i.e. following major or minor maintenance. It was and will be necessary to adapt our predictive maintenance plan for the piston compressors to achieve this. Apparently the oil analysis was not the good indicator for this bearing problem what was surprising to our opinion.

For the future we are planning short stops a number of months before the overhaul and to open the crankcase for a visual inspection of the condition of the oil (traces of white metal, water in the oil, etc.).

2.1.5   Vibration monitoring

A parameter which can give additional information about the machine behaviour is vibration. It is the nature of reciprocating machines that the vibration behaviour is different compared to turbo compressors.

However, it is also a parameter which should not be neglected when doing the machine assessment for defining the next maintenance activities.

Here we can talk about three levels of vibration protection/monitoring used in Air Liquide plants in the past.

As a basic level can be seen those compressors where a vibraswitch is installed. Of course with such a device it is not possible to monitor the vibration.

A second level of vibration protection/monitoring is realized by permanently installed velocity transducers and / or accelerometers at defined positions, e.g. at the crosshead, at the cylinder head or at the crankcase. These systems which are storing the history information can be used for trending and analysis.

It can be possible that significant defects will not be detected if the transducer is not directly located on the critical spot. In section 4 one case is described where we have exactly seen this behaviour. Several transducers at different positions are necessary to perform a correct surveillance.

State of the art online monitoring and protection systems do represent the third and last level. As the systems used by Air Liquide are monitoring the vibration levels depending on the crankshaft angle it is possible to detect parts condition changes. Additionally these systems are equipped with rod drop sensors for the big and critical horizontal hydrogen compressors. Rod drop measurements and accelerometers installed at each crosshead do complete the online monitoring. A screenshot of the DCS screen of one of our biggest hydrogen compressors with two stages and six cylinders is shown with these above mentioned mechanical parameters in figure 6.

 In paragraph 3 an overview is given showing when and which vibration protection and monitoring systems were installed on which reciprocating piston compressor types in Air Liquide plants.

2.1.6   Performance measurement

As wear on cylinder parts and piston rod packings do influence the performance and flow, a performance check can give first information about possible problems with those parts.

A general practical approach to check the performance is to monitor the kWh/Nm³ ratio of the compressor. Especially on machines not equipped with permanent monitoring systems this approach is applied. Alternatively also the motor current trend in combination with the discharge pressure and discharge temperature trends can be observed.

Compressors with an electric motor power above 1MW can be assessed by using the online trending feature of a web based SCADA system, refer also to figure 4. This diagram shows the motor current, the discharge pressure und the discharge temperature trends of a two stage hydrogen compressor with six cylinders covering an operation period in 2011.
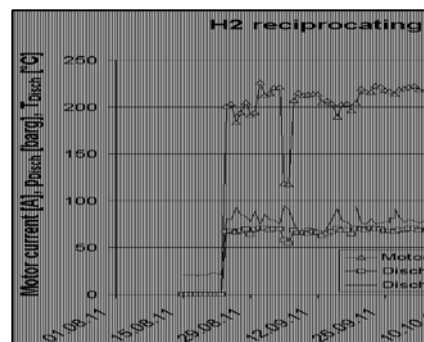
Figure 4: Performance trending with SCADA

As an alternative when the compressor is equipped with suitable equipment, p/V diagrams will be gathered and the development over time will be checked, refer also to the next picture figure 5. As usual with this method a comparison with the theoretical p/V diagrams was done.
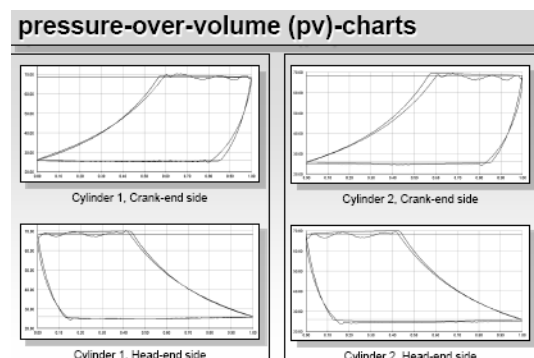
Figure 5: Performance trending using p/V charts

CONDITION MONITORING

Maintenance practices and experienced failure modes in Air Liquide plants – Protection and monitoring systems, *Luc Bertheloot, Wolfgang Grillhofer;* AIR LIQUIDE

On the hydrogen compressor with two stages and six cylinders we have installed a state of the art monitoring system, refer also to figure 6. The valve temperatures are included in the trending which is absolutely necessary for a reciprocating piston compressor with such a number of suction and discharge valves from our point of view. Also the leakage measurements are continuously recorded.
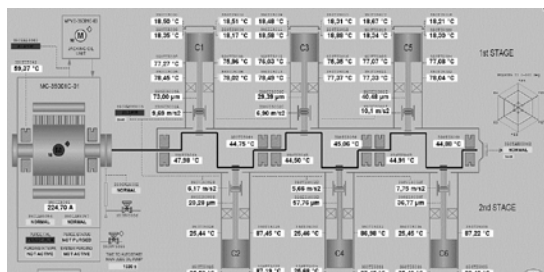
Figure 6: State of the art online monitoring system

In any case it must be sure that the period of performance evaluation is representative, i.e. no start up, no operation on by-pass, etc. and that the delivery pressure is experienced as normal.

2.2 Maintenance interval influencing parameters

Although Air Liquide has now the knowledge about optimised maintenance intervals and actions due to the focus on reliability and availability, these intervals are also influenced by other factors.

The main factors are

- production requirements,

- different lifetime of different wear parts and

- additionally installed regulation systems.

2.2.1 Production requirements

A main point in praxis is the possibility of stopping a compressor from production point of view. For plants where the gas production unit is directly connected to the customer, it is necessary to coordinate stops of production influencing machines with customer maintenance actions, e.g. shut downs.

Some Air Liquide plants are part of a pipeline network. Then it is possible to coordinate respective gas production of the other plants in order to compensate the outage of the plant with the maintenance. Influencing facts are also if stand by machines are available, if the gas production plant is connected to a pipeline network or if back up systems of the produced gases are available.

2.2.2 Different wear parts lifetime

Experiences do confirm that compressor valves, piston rings and packings lifetime are dictating the applied minor maintenance interval. From users point of view an extended lifetime of one part of this group due to latest development is nice to know, but does not help too much as the compressor must be shut down because of shorter lifetime of the other components. At this point Air Liquide wants to point out that parts and compressors for respective gases and conditions should always be developed also under the focus of optimized compressor maintenance intervals.

For sure the minimum lifetime of cylinder wear parts and packings expected by Air Liquide for non lubricated compressors, dry hydrogen, carbon monoxide and wet gases is 8000hrs.

For other gases and conditions 12000 to 24000hrs or more should be reached for the cylinder wear parts and packings.

2.2.3 Additionally installed regulation systems

Especially the larger hydrogen compressors in the HYCO plants must fulfil the demand of flexibility from volume flow point of view. In order to avoid additionally energy losses and restrictions in reachable operating points due to bypass operating conditions or stepwise flow control, these Air Liquide compressors are mainly equipped with stepless, electro-hydraulically actuated control systems.

Such advantages from operating point of view must be compared to the challenges from maintenance point of view as this system is technically more complicate compared with simpler bypass or variable clearance pocket control systems.

Based on the experience from the operation of such control systems a combination of predictive inspections and time based maintenance actions was developed.

A weekly visual inspection of the actuators and the additional equipments gives first hints of possibly developing failures. When it was agreed to perform minor or major compressor maintenance the control system condition will be evaluated a defined time before the compressor maintenance.

3 History and overview on monitoring and protection systems in Air Liquide plants

The vibration monitoring and surveillance has shown an important evolution in the last 40 years. In the beginning of the years 1970 the reciprocating compressors were only equipped with vibraswitches. These compressors were mainly vertical laby compressors compressing air gases. These compressors had also a limited capacity. Only a few of these mainly critical piston compressors were equipped with vibration transducers to realize a better compressor protection. The main vibration related maintenance activities on these compressors were detailed vibration/pulsation analysis to solve rupture problems of piping, supports and coolers due to the lack of adequate pulsation dampeners.

Only the last 10 years also with the introduction of the automatic data acquisition in the plants, more sophisticated protection and monitoring systems have been introduced.

Nowadays for a new compressor we select from the systems as described in the following.

Vibration protection and/or monitoring for reciprocating piston compressors consist of different levels:

- Vibraswitch system

The vibraswitch trips the compressor if the vibration behavior exceeds a predetermined level. This indicator is mainly sensible for shocks and is not a precise vibration detector. It is also not free from errors and wrong calibration. To avoid unnecessary trips on a critical piston compressor it is perhaps necessary to install a second one or a third one to come to a voting system 2oo2 or even 2oo3.

This vibraswitch is installed on 95% of Air Liquide reciprocating piston compressors. These compressors have a limited capacity. The minimum requirement is that the system is regularly (frequency: during each minor overhaul) checked and calibrated so that a serious deterioration can be detected.

- Vibration behavior followed up by velocity transducer or accelerometer

The measurement is more precise, alarm and trip levels can be determined with more precision. These levels can be defined on a m/s2 or g scale or on a mm/s RMS basis and trending is possible in the DCS. The measured vibration levels are strongly depending on the place where the accelerometer is installed. It could be possible that significant defects will not be detected if the transducer is not directly located on the critical spot. Several transducers are necessary to perform a correct surveillance.

- Vibration follow up by a monitoring-/protection system designed for reciprocating compressors

The highest level is a system based on velocity transducer, accelerometer and keyphasor measurements. The measured level is compared with a reference curve and these levels are also depending on the crank angle. The basic challenge on piston compressors is that the vibration levels are strongly varying dependent on the moment of the measurement (valve opening and closing, changing direction of movement of the piston, etc…)

These systems can also be equipped with rod drop measurements for horizontal piston compressors in addition to the accelerometers installed on the crosshead or /and on the cylinder covers or the velocity transducer installed on the crankcase. Cylinder pressure measurements together with the keyphasor signal will allow for pV trending.

- Vibration follow up by periodic measurements

To our opinion it has not much sense to do periodic vibration measurement on a piston compressor as it is done on a turbo compressor.

It is difficult to make a correct evaluation of the lifetime of the wear parts, i.e. piston rings, packings, etc. by this method. These parts must still be replaced on a periodic basis. Only condition based maintenance on piston compressors is not possible.

There is a very important portion of the vibrations caused by gas pulsations. The vibration levels cannot be correlated directly with a mechanical behavior.

It can however be of some interest to measure periodically the motor, coupling and mechanical oil pump, i.e. the real rotating parts of the piston compressor.

Trouble shooting can still be necessary in case of problematic running of some compressors. In this case vibration and pulsation measurements are necessary. Many of these old compressors are

Maintenance practices and experienced failure modes in Air Liquide plants – Protection and monitoring systems,
Luc Bertheloot, Wolfgang Grillhofer; AIR LIQUIDE

installed with only pulsation dampeners at the inlet of the compressor or sometimes also at the third stage outlet. Installing interstage pulsation dampeners afterwards causes a very high cost and is sometimes difficult to do. The problems influence highly the reliability of the coolers (bundles, tube failures, etc.). This situation has to be evaluated case by case and naturally oxygen compressors have some priority. Solutions which are not studied in detail with the support of objective measurement should be avoided.

4 Discussion of failure modes experienced by Air Liquide

4.1 Case 1: Broken big end bearing bolt

A first example of a failure mode on a hydrogen piston compressor with a power of 3MW and two stages installed in an unmanned plant (during the nights and the weekends) is shown hereafter.

On this compressor a state of the art monitoring system has been installed (a vibraswitch and rod drop measurement system were already installed before).

In figure 7 stored data from the compressor is shown. At 07:06 a.m. the compressor runs under good conditions. The vibrations at crosshead stage 1 have a maximum of approximately 30 m/s2. The peaks displayed with the light graph are taken at the cylinder head and have much higher amplitudes.
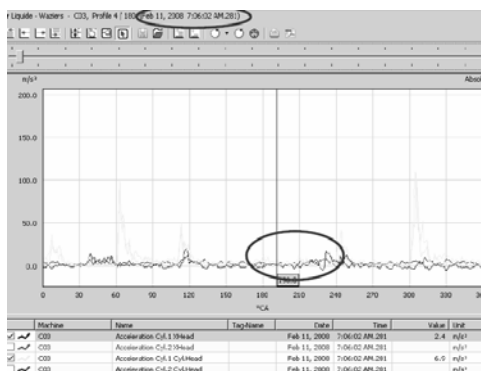
Figure 7: Acceleration signals of stage 1/crosshead (dark) and cylinder head (light)/07:06am

At 07:08am the damage at the big end bearing bolt occurs. High vibrations are recorded especially at the crosshead sensor stage 1, which is the sensor closest to the defect bearing (5,5 times magnified vibrations=167.8 m/s2), for the trends refer also to figure 8 below.
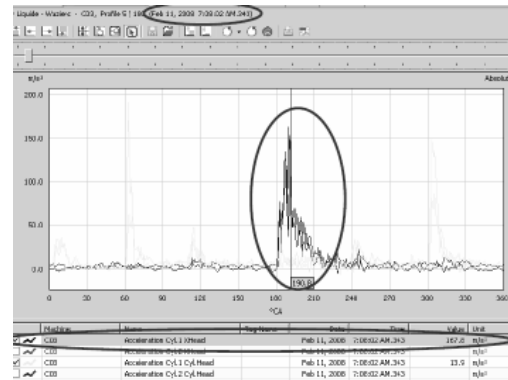
Figure 8: Acceleration signals of stage 1/crosshead (dark) and cylinder head (light)/07:08am

At 07:10am the significant vibrations are reduced (see figure 9)
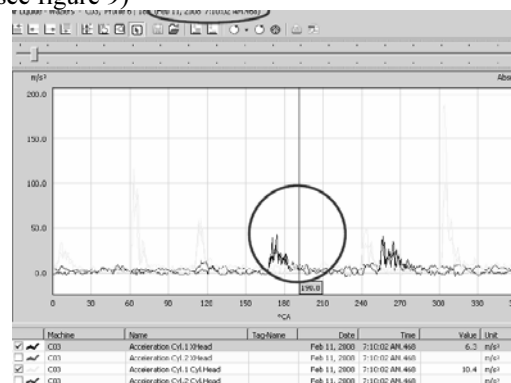
Figure 9: Acceleration signals of stage 1/crosshead (dark) and cylinder head (light)/07:10am

The failure of the big end bearing bolt of the first stage connecting rod which is shown in figure 10 was correctly detected by the accelerometer installed at the crosshead of the first stage.

It was evidently a high shock with important amplitude which damaged also the cover of the crankcase. It can be noted that this defect was not detected by the vibraswitch as this was installed on the crankcase but at an important distance away of the spot where the damage occurred.
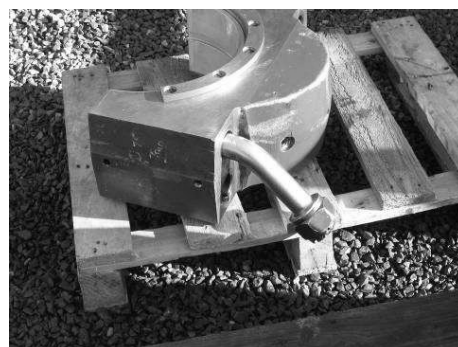
Figure 10: Broken big end bearing bolt

Maintenance practices and experienced failure modes in Air Liquide plants – Protection and monitoring systems,
Luc Bertheloot, Wolfgang Grillhofer; AIR LIQUIDE

4.2 Case 2: Broken piston rod

A second damage on the same compressor was experienced a number of years later.

The first signal was at the 5th of July on 12:12:58 h with a complete normal behavior of the vibration levels on the crosshead of the first stage; refer to the first screenshot of figure 11.
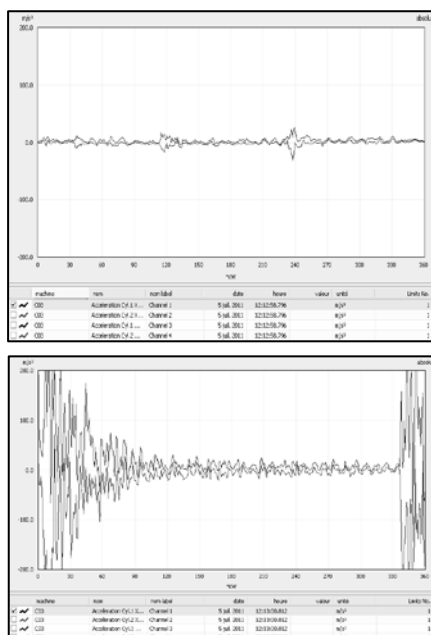
*Figure 11: Acceleration signal at the crosshead at
12:12:58h and at 12:13:00h (trip)*

The second print shown above is taken at 12:13:00h with the trip of the compressor due to a high level detected with the vibraswitch. The piston rod was broken at the crosshead connection which is shown in figures 12 and 13. No indication was found on the vibration picture of the accelerometer on the crosshead before the trip of the compressor by the vibraswitch. The same conclusion could be made for the accelerometer on the cylinder head of the first stage.
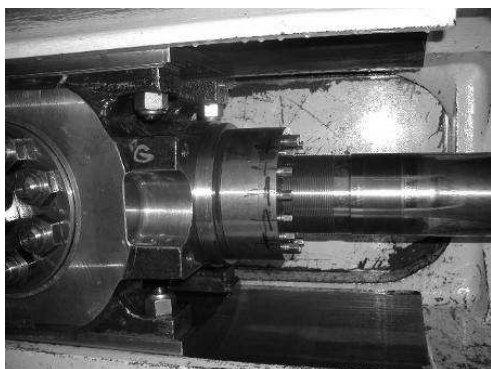
*Figure 12: Multi bolt tensioned piston rod to
crosshead connection*

Figure 13: Broken piston rod

In contradiction with the first incident, the monitoring system has not given any early warning of the problem and apparently the system is insensitive to detect this type of important problem.

It could be observed by the rod drop measurements that this type of defects can be detected earlier (10 minutes before the breakdown) by the rod drop system as shown in the following diagram in figure 14. The top black line represents the measured rod drop signal. A couple of minutes before the breakdown a significant increase can be recognized, refer to the position marked by the black arrow.
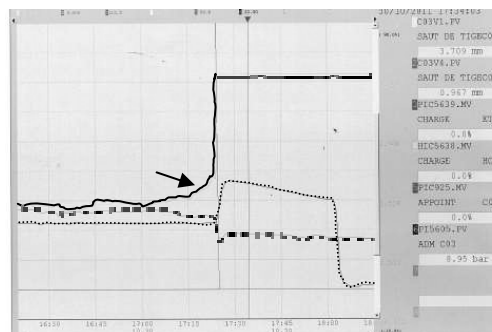
Figure 14: Rod drop measurements

After discussion with the OEM, the following statement was given: "This applies to users of compressors and integral engine-compressors that have a conventional piston rod to crosshead attachment whereby the piston rod screws into the crosshead and where the piston rod is over 3.5 inches utilizing a Multi Bolt Tensioner. This warning is also intended to warn and advise compressor users that they may experience fatigue cracking of the piston rod when it is not properly installed and/or maintained.

Regarding the supernut, it is now known that at maximum rod load conditions a higher percentage of the crosshead load is carried through the threads rather than the face of the crosshead compared with a conventional jamnut. There have been some isolated instances where piston rod threads have been found to be cracked. Usually one or two three threads close to the end of the crosshead face.

83

CONDITION MONITORING

Maintenance practices and experienced failure modes in Air Liquide plants – Protection and monitoring systems,
Luc Bertheloot, Wolfgang Grillhofer; AIR LIQUIDE

This can occur on rare occasions when the multi-bolt tensioner is not installed or maintained in line with the procedure. Failure to strictly comply with the procedure may prevent the multi-bolt from performing resulting in potential damage to piston rod thread. It is even more important on highly loaded units, or units prone to process upset, which could result in an overload of the compressor ratings. The multi-bolt tensioner is more sensitive to this type of upset."

The OEM has advised to install a hydraulic nut instead of multi bolt tensioner but also with a lower preload. This gives a greater safety margin against the material limits as clearly shown in the Goodman diagram in figure 15. The prestress on the rod is reduced from 2.5 times the maximum continuous rod load (MACRL) to 1.75 MACRL.
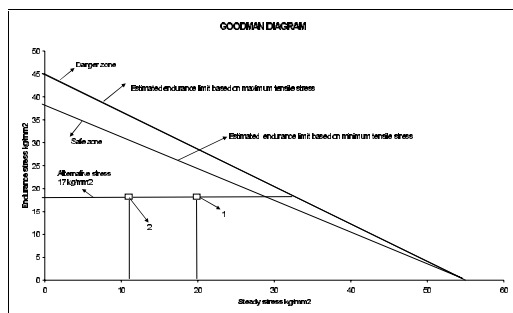
Figure 15: Goodman diagram: Position 1 is the stress situation with the multi bolt tensioner connection; Position 2 is the stress situation with the hydraulic nut.

4.3 Vibration-pulsation problem cases

Other cases more frequently encountered are vibration and pulsation problems on existing piston compressors. The main consequences of such problems are not located on the compressor parts itself but rather on the auxiliary equipment as coolers and piping. A first example is a big one stage booster compressor with 4 cylinders. The discharge pulsation dampeners were positioned horizontally in line with the discharge piping. The nominal discharge pressure is 64 bar but it was impossible to run at this condition. Already at an outlet pressure of 50 bar (inlet 25 bar) the cylinders were vibrating heavily and the compressor was making a lot of noise. This compressor was in operation for a long time in this reduced condition until final solution has been brought to this. The vibration behavior was followed by permanently installed accelerometers.

As shown in figure 16 a much bigger suction dampener has been installed to reduce the vibration at the suction piping and a flexible piping system was mounted between the cylinders and the dampener. It has to be noted that the original

suction dampener had a volume of 380 liters and was replaced by a volume of 1000 liters!

Figure 16: A suction dampener with increased volume was installed with flexible steel piping

Important elements were also the discharge pulsation dampeners shown in figure 17. A study performed by the OEM has shown that dynamic forces with a high frequency of 10 times the running speed were caused by these discharge pulsation dampeners.

Figure 17: Discharge pulsation dampener in original horizontal position

The solution proposed by the OEM was finally to use the same pulsation dampeners but to position these bottles in a vertical way. All these important modifications have finally solved the vibration problems on this compressor.

Another similar problem was on a network laby compressor N2/O2 40 bar, 3 stages. High vibration levels (more than 100 mm/s RMS) were measured on the discharge bottle of the third stage. Air Liquide accepts for good condition a maximum of 20 mm/s RMS. Frequency measurements show a dominant frequency at 56.5 Hz. Pulsation measurements have also indicated the same frequency with an amplitude of 0.72 bar peak-to-peak. The end user has tried to reinforce the structure but finally a new pulsation dampener with a bigger volume and other dimensions was chosen. In oxygen applications we always avoid the use of baffle plates inside this dampener.

Maintenance practices and experienced failure modes in Air Liquide plants – Protection and monitoring systems,
Luc Bertheloot, Wolfgang Grillhofer; AIR LIQUIDE

As already stated before simple and even so called "miraculous" solutions as shown in the figure 18 should be avoided. The installation of such a dilatation joint doesn't stop the transfer of the vibrations in the piping due to the fact that this equipment doesn't present any damping of the vibrations and that vibrations are also transferred by the pulsations. This type of solutions can only cause further catastrophic failures.

Figure 18: Bad solution for avoiding transfer of vibrations

4.4 Case 4: Packing ring seal failure

A complete different failure was noted in cases where the wear parts failed before the expected lifetime. In the Air Liquide applications for hydrogen at high pressures in non-lube, the sealing elements are the most critical parts. In the particular case mentioned here below, the sealing elements in the pressure packing were subject to a premature failure, refer also to figure 19.

The main reasons for the premature failure were the choice of the coating on the piston rods and type of roughness applied on this coating in contact with the sealing elements. Apparently the material 86%WC, 10%Co and 4%Cr is too brittle and the formation of the PTFE film is too rapidly and limits the heat transfer to the piston rod. Another material 87%WC and 13%Co and another roughness profile should avoid the premature wear. Further investigation on this subject is to our opinion still necessary and need confirmation. The basic is to have a lifetime of minimum 8000 continuous running hours and hopefully with the necessary improvement a final running lifetime of these wear elements can be obtained of 12000 to 14000 running hours.

Figure 19: Failure of the sealing elements in the pressure packing

5 Conclusions

It is worthwhile to mention that the maintenance intervals on dry running reciprocating piston compressors are still far away from the three years uninterrupted running as it was mentioned a number of years ago by respective OEMs and suppliers. The important maintenance work and high cost of this maintenance is certainly one of the major drawbacks to use this type of compressors. In spite of the development of very sophisticated synthetic materials the progress in the lifetime for dry running compressors is limited. Sure it is depending on a number of process parameters, for example the discharge pressure, the discharge temperature, etc., on the nature of the gas as e.g. dry bone gas or wet gas and the design parameters as the piston speed and used materials.

We tried to point out that from our operating experience point of view the selection process for wear parts and materials seems still not to be a straight forward process. Especially when it depends on the counterparts designs and materials.

One big advantage of the developments in the last years was certainly the high flexibility (important turndown) with the installation of the stepless volume flow control systems. This performance in terms of regulating the volume flow cannot be obtained for the turbo compressors.

Concerning the compressor online monitoring and protection systems which were developed the last years, it is also the opinion of the authors that there is still a lot of work to be done to obtain a good reliability and to provide systems which are able to detect the whole range of defects. It is our experience that accelerometer based systems are not always the most reliable ones.

In this document we have tried to explain that some important defects were not visible with the used online monitoring system.

On older reciprocating compressors a trouble shooting complete vibration and pulsation analysis can bring a significant improvement with a limited number of modifications but it cannot be generalized in all cases.

As the main target for these machine types is to get best reliability and highest availability also under the aspect to minimize the maintenance costs, the maintenance strategy was optimized taking into account all the aspects as pointed out in this paper.

Automatic shutdown caused by dynamic piston-rod position analysis saved compressor

by:

Uwe Ladwig
Plant Maintenance Department
YARA Brunsbüttel GmbH
Brunsbüttel
Germany
Uwe.Ladwig@Yara-com

8th Conference of the EFRC
September 27th / 28th, 2012, Düsseldorf

Abstract:

YARA operates a horizontal process gas compressor in CO_2 service, feeding an urea plant. This compressor is equipped with a piston rod position sensor - taken as a shutdown parameter. This case study describes how the monitoring system detected a loosened cylinder/housing connection. Only the piston rod position sensor initiated a safety shutdown, the more common crosshead vibration shutdown was not involved in the case, and would not have avoided damages.

1   Introduction

YARA Brunsbüttel GmbH is a production site of YARA International, located in the north of Germany, in the area of the Kiel Canal and the river Elbe.

The plant consists of two production lines:

- Ammonia: 2200 metric tons per day

- Urea: 2000 metric tons per day

YARA Brunsbüttel has operated two identical 4-throw reciprocating compressors in carbon dioxide service since 1978. The compressor, involved in this case study, was installed in 2008 for capacity extension of the urea plant. For full load of the urea plant all of them have to run.

Since 2001, when an on-line condition monitoring system was installed on both "1978" compressors, numerous component failures have been detected by the system including: rider band wear, valve problems and loose components (valve cages, etc.)

In 2002 the automatic machinery protection function of the system limited additional consequential damages caused by a piston rod failure, utilizing crosshead acceleration as the only shut down parameter. A complete loss of the machine was avoided, but there were still heavy damages (for instance a cracked mainframe) during the stopping sequence.

In 2006 piston rod position signals from the existing rod drop probes were added to the machinery protection function, initiated by YARA from the experience of 2002, that piston rod movement increased in rapidly short time prior complete failure.

In 2007 we had a successful automatic shutdown in the moment, when the piston rod was partial fractured, before complete breakage. No secondary damage occurred.

This case was presented at the EFRC conference 2008.

In Jan. 2012 the monitoring system avoided successfully potential major cost-intensive damages to the additional "2008" compressor by detecting the cracking of cylinder connection bolts 1st. stage and the out of position movement of the cylinder. The machine was automatically tripped prior to complete failure, using peak-to-peak rod run out analyses.

2   Monitoring system equipment

The 3 compressors are equipped with a "Prognost" monitoring system.

The system has 5 sensors at each stage/crank:

1. Acceleration crosshead (shut down)
2. Piston rod position (shut down)
3. Acceleration cylinder
4. Dynamic cylinder pressure head end
5. Dynamic cylinder pressure crank end
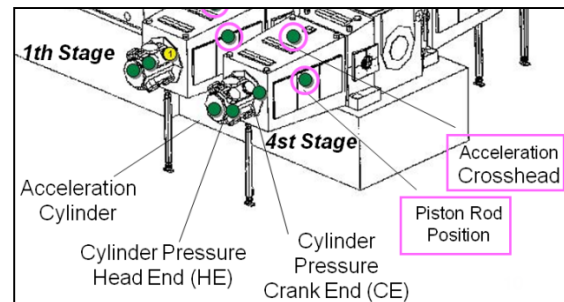
Figure 1: Sensor positions

The system was installed in 2001. The automatic shutdown at the crosshead casing was installed from the beginning. The second shut down criteria, piston rod position, was set in operation 2006.

3   Machine and process data

The described machine has the following technical and process data:

Machine type:	4-throw, horizontal, double-acting, 4-stage
Stroke:	250 mm (9,8 in.)
Piston diameter:	1000, 520, 270, 135 mm (39, 20, 11, 5 in.)
Speed:	425 RPM
Power:	1,162 KW (1,558 HP)
Year of manufacture:	2008
Medium:	CO_2 (~98.8%)
Suction pressure:	1.0 bar (15 psig)
Discharge pressure:	170 bar (2,466 psig)
Flow rate:	5,000 Nm3/h
Capacity control:	by HydroCom (Hörbiger)

Automatic shutdown caused by dynamic piston-rod position analysis saved compressor, *Uwe Ladwig;* YARA BRUNSBÜTTEL GMBH

Figure 2: CO_2 Compressor

4 Automatic trip of compressor

On January, 3rd 2012, at 2:46:46 pm, the compressor tripped automatically due to high piston rod run out at cylinder 1st stage.

4.1 Findings at compressor

All connecting bolts between crank-side cylinder cover and cylinder were broken. The cylinder moved out of position.
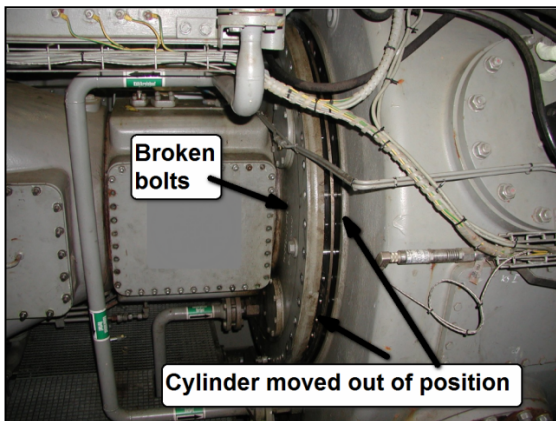
Figure 3: Cylinder 1st stage after shut down
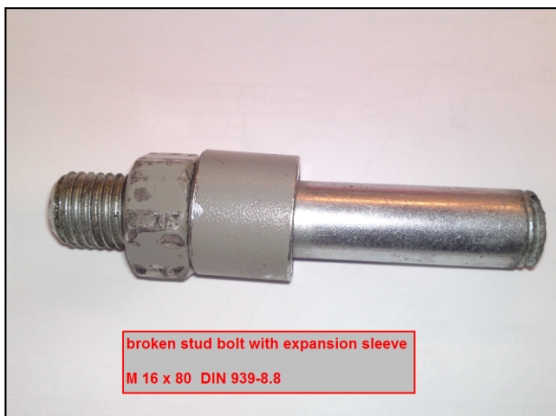
Figure 4: broken stud bolt

Figure 5: broken stud bolt fracture surface
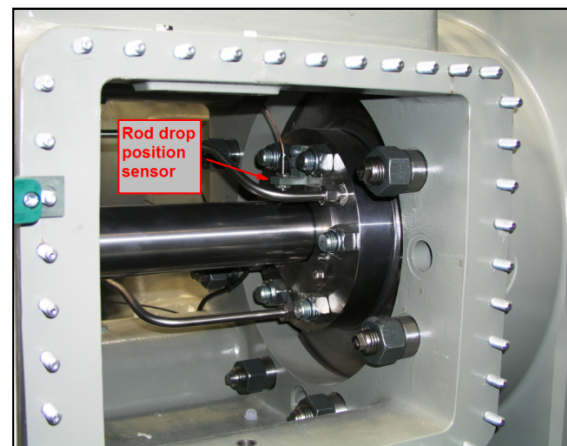
Figure 6: involved rod drop sensor

Automatic shutdown caused by dynamic piston-rod position analysis saved compressor, *Uwe Ladwig;*
YARA BRUNSBÜTTEL GMBH

4.2   Shutdown sequence in the monitoring system

The first alert of high piston rod movement occurred

3rd January 2012
- 14:46:42 first pre-alert
- 14:46:44 second pre-alert
- 14:46:45 third pre-alert
- **14:46:46 shut down signal**
- 14:46:51 machine stood still

4.3   Data analyse of shutdown

The Prognost screenshot shows the normal behaviour of the piston rod and crosshead vibrations 2:46 hours before the incident.
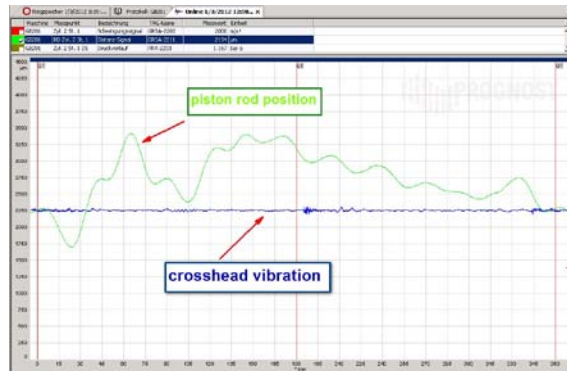
Figure 7: piston rod movement and crosshead vibration 2hours 46 min before incident (1 revolution, 360°crank angel)

The next figure (8) shows the shutdown (safety) limits, generated from the peek to peek value of 8 45° segments of piston rod position. Operation behavior is still "normal"
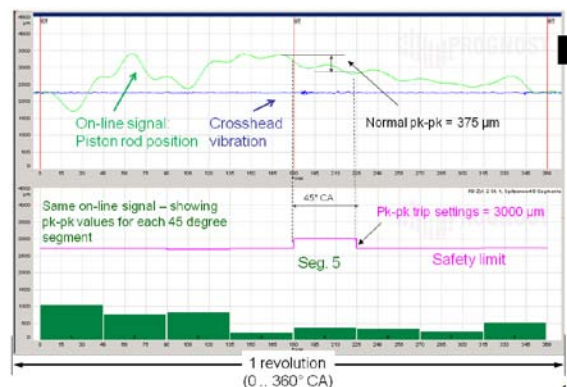
Figure 8: Definition of piston rod position analysis, peak-to-peak, 8 segments, normal operation

Please note:

The crosshead vibration is still unchanged, while the piston rod movement is partly out of the measuring range!
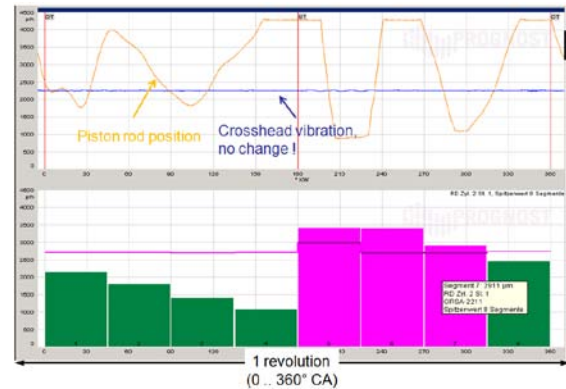
Figure 9: Definition of piston rod position analysis, peak-to-peak, 8 segments, TRIP

Figure 10 shows the development of the rod-drop movement exemplarily for segment 7.
There was a small increase of the rod-drop movement 10 minutes before the incident, but far below the safety limits.
Only 4 seconds before the shutdown the rod-drop movement increased heavily.
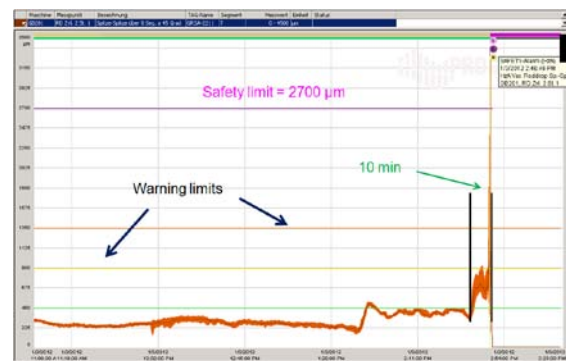
Figure 10: Data Analysis - 4 hr Trend Rod Position - Segment 7 (270-315 deg CA)

5   Conclusion

Due to the shutdown in the right moment no further damages at the compressor occurred.

After 24 hours of repair (replacing the bolts) the compressor was back in operation.

Using crosshead vibration as a shutdown parameter, modern reciprocating machinery protection systems can limit consequential damages, but damages are not completely avoidable.

Automatic shutdown caused by dynamic piston-rod position analysis saved compressor, *Uwe Ladwig;* YARA BRUNSBÜTTEL GMBH

By using rod position as a shutdown parameter, it is possible to detect the development of a slightly out of position moved cylinder (due to broken stud bolts, which was not detectable by vibration) and a successfully trip before it fails completely.

Automated machine monitoring systems with rod position shut down functions lead to lower cost of production and maintenance and higher plant efficiency.

Assumed, the cylinder would have been heavily damaged in this case (without rod-drop shut down) and had been replaced, we would have had at least 3 months of production loss, which means in this case: 18,600 tons of urea. The price of urea is volatile, end of March 2012 it was around 400 US$ per metric ton.

8th Conference of the EFRC
September 27th / 28th, 2012, Düsseldorf

EFRC

EUROPEAN FORUM
for RECIPROCATING
COMPRESSORS

VO**RWE**G GEHEN

Biogas injection into transport grids – a new interesting field for compressor manufacturers

by:

Dirk Sattur

and Thomas Oelkrug

Department Assetservice Gas

RWE Deutschland AG

Dortmund

Germany

dirk.sattur@rwe.com

8th Conference of the EFRC
September 27th / 28th, 2012, Düsseldorf

Abstract:

Since April 2008 the German grid regulator published several changes in the gas grid access ordinance for connecting biogas upgrading plants to the public transport grid. By separating carbon dioxide and hydrosulfide from biogas that is produced in larger biogas plants, the efficiency and the heat to power coefficient is enhanced. After the upgrading phase biogas is equal in gas quality to conventional natural gas with the exception of the right calorific value in the corresponding transport grid. For this reason the next step is the conditioning of the biogas with ambient air and liquefied petroleum gas. Of course the most important point is the compression to operating pipe pressure. Nearly eighty injection plants are operating in Germany at the end of 2011 and forecasts are perspecting a fast growing field of business. Finally the government is aiming for a total substitution of 6 % of whole natural gas consumption in Germany in the year 2020 by biogas, that is equivalent to 750 injection plants operating in the field. Therefore a flexible reciprocating compressor that operates with special attributes concerning the requirements of biogas applications is the heart of an upgrading and injection plant. The connection of an experienced industry with a sector of green energy is a future business for compressor makers. The paper deals with the perspectives of biogas in detail, selection criteria for reciprocating compressors and a side view in an existing projected and already built facility. Let´s go green in compressor business will play a future role in the R&D –activities of reciprocating compressor makers.

Biogas injection into transport grids – a new interesting field for compressor manufacturers, *Dirk Sattur, Thomas Oelkrug;* RWE DEUTSCHLAND AG

1   Introduction

RWE Deutschland is part of the RWE Group, a leading European supplier of gas, electricity and water which also has upstream gas interests. The entire RWE Group generated €53 billion in revenue in 2011, producing 3 bcm of gas and supplying eight million gas customers.

RWE Deutschland is an operating parent company which oversees six regional energy companies as well as distribution grids, grid servicing, gas storage and metering in Germany. It employs more than 21,000 people and 2010 sales revenue was €18.5 billion. The company also forms partnerships with German municipalities – it has eight majority participations in municipal utilities and more than 70 minority participations. Business and residential customers are supplied with gas, electricity, water and services as well as energy efficiency consultancy and development schemes. It has gas storage capacity of 1.5 bcm, which is equivalent to the annual consumption of 600,000 households.

RWE Deutschland's operating principles are based on providing a secure, reliable energy supply day and night and ensuring security complies with international standards. The company is steadily investing in the expansion and maintenance of gas, electricity and water grids and has been driving the development of new technologies, in particular environmentally friendly electricity storage solutions and of course all kinds of biogas applications concerning the gas grid. In 2007 RWE Deutschland was confronted with the first demand for biogas injection in gas grid of the company´s subsidiary by a local supplier that also operates several biogas plants. Since 2007 the political environment, especially for renewable energy had changed very quickly.

2   Political environment for biogas

2.1   New Gas Network Access Ordinance

The parameters for the injection of biogas in Germany will be defined as a result of the implementation of the government's integrated energy and climate program, whereby the target is to exploit a potential of 6 per cent (60 bn kWh) of today's natural gas consumption in Germany by the year 2020 and 10 per cent (100 bn kWh) by 2030. This objective is defined in an amendment to the Gas Grid Access Ordinance, which came into full effect on September 3rd, 2010, and regulates the grid access for both suppliers and grid operators concerning biogas applications around the gas grid.

The target had first been defined in 2008. A new part 11a "separate treatments for biogas according the injection into gas grids" was added. Biomethane can be used not only for standard heating applications, but also for cogeneration, where the resulting energy is subsequently fed into the grid to profit from the feed-in tariffs under the Renewable Energy Sources Act (EEG), and in natural gas powered vehicles. A number of interesting business models can be developed to exploit the wide-ranging possibilities for its use. The market players involved have recognized this trend and are positioning themselves strategically in this new business field. The goal of 6 billion cubic meters of biogas by 2020 requires the construction of roughly 1,000 medium-sized (700 cm/h) or 2,000 smaller (350 cm/h) biomethane plants, equaling about 100-200 plants per year.

2.2   Actual situation given by the regulator in Germany

By the end of 2011, about 80 plants are feeding into the German gas grids with a total hourly feed-in capacity of 64,000 cubic meters of biomethane. A clear growth trend can be recognized. Related to that, conservative estimates call for an investment of 10 –12 € billion in plant technology till 2030. Roughly around 7 per cent of whole investments are directly connected to compressor technologies. main steps is shown.
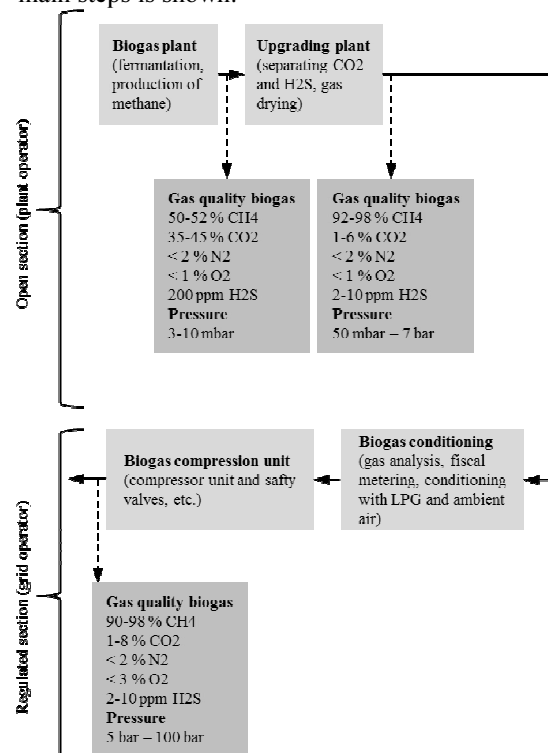
Figure 1: overview of upgrading and injection process with cut surface between biogas plant and grid operator

Biogas injection into transport grids – a new interesting field for compressor manufacturers, *Dirk Sattur, Thomas Oelkrug;* RWE DEUTSCHLAND AG

Changes in the Gas Grid Access Ordinance brought a clear cut surface between the gas grid operator and the biogas plant operator concerning operating costs, investments and in addition a uniform technical concept for the engineering of biogas injection plants. In figure 1, a chart of the biogas upgrading process is shown.

3 Technical process from production to injection

3.1 Upgrading process

Up to 2006 raw biogas was only co-generated to produce heat and electricity. To further enhance the usage of the produced heat the upgrading and injection of biogas into gas grids was developed.

Before the raw biogas can be fed into the gas grids it has to be upgraded from raw biogas to biomethane. The so called biogas upgrading plants (BGU) separates water, carbon dioxide and hydrogen sulphide from the biogas. A standard configuration for raw biogas quality that is directly produced in the fermenter contains 50 to 55 per cent methane, 1 to 2 per cent of oxygen, traces of nitrogen and up to 45 per cent of carbon dioxide. Probably the hardest problem to handle is the high amount of hydrogen sulphide, it can raise up to 400 ppm which depends on substrate used for gas production in the fermenter. Several physical and chemical processes can be used for the separation of the carbon dioxide. The pressure swing adsorption and the water scrubbing is the most common technology for biogas upgrading. Essential to these upgrading technologies is the compression of biogas up to 10 bar_g for the separation of the unwished associated gases. Due to the fact that the grid operator uses a reciprocating compressor in his injection facility there are several other smaller compressor working in the whole plant. After the upgrading process the former raw biogas changes its gas configuration extensively.

The share of methane raises to 92 to 99 per cent and only a maximum of 1 per cent oxygen is part of the now called biomethane. With an additional sulphur removal scrubber in the upgrading plant shares of hydrogen sulphide are down by 5 ppm. Because of that injection plants can be built in carbon steel and don't need the usage of stainless steel in comparison to the biogas plant. The produced biomethane is, as we mentioned, a nearly purified and non-smelling natural gas whose calorific value can be compared to high caloric natural gas. The upgraded biomethane then is adjusted according to the calorific value, wobbe index and pressure of the injection grid. These facilities are called biogas conditioning and injection plants (BGI).

In 2006 the first plants to upgrade and feed in biomethane into the grid were put into operation. In April 2008 the technical directive VP 265-1 of the German Technical and Scientific Association for Gas and Water (DVGW) for the upgrading and injection of biogas was enacted and therefore harmonizing the technical standards and requirements for biogas upgrading and injection.

3.2 Conditioning process

The function of the biogas conditioning and injection plant is the fiscal metering (flow, energy) of the upgraded biogas, the adjustment of the calorific value and the Wobbe-Index (conditioning) by adding ambient air and/or liquid petroleum gas (LPG) and the compression of the biomethane according to the grid pressure by a reciprocating compressor and the injection into the gas grid.
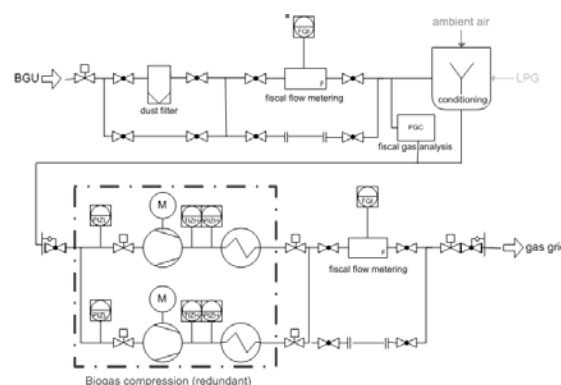
Figure 2: flow sheet biogas conditioning and injection plant (BGI)

As you can see in figure 2, the biomethane is transported to the safety valve at the entrance of the plant. First it is flowing through a filter to separate dust particles. In the second step the gas flow is metered.

3.1 Fiscal metering and conditioning

For the trading of the upgraded and/or injected biomethane on the gas market according to its energy content the fiscal metering of the biomethane before and after the conditioning is essential. The injected biomethane can be virtually discharged at any point of the German gas grid and therefore traded diversified in an own accounting grid. The biomethane flow is usually measured with rotary pistons flow meters, that are insusceptible to gas pulsation caused by reciprocating compressors. If the flow increases to a certain amount, turbine or ultrasonic flow meters must be used. A process gas chromatograph (PGC) analyses the composition of the biomethane before compression to calculate the right amount of additional ambient air and/or

DESIGN & ENGINEERING

Biogas injection into transport grids – a new interesting field for compressor manufacturers, *Dirk Sattur, Thomas Oelkrug;* RWE DEUTSCHLAND AG

liquefied petroleum gas to create the relevant calorific value and Wobbe-Index of the gas grid. Which more or less depends on low or high caloric natural gas in the grid. The amount of ambient air and/or liquefied petroleum gas depends more or less on the low calorific value of the natural gas in the grid.

3.3 Biomethane compression and injection

The German Gas Grid Access Ordinance requires an availability of the BGI plant of 96 per cent per anno. This requirement is usually met with the erection of a 100 % redundancy concerning compressor and compressor range. The biogas compressor is therefore the essential part of the BGI plant.

The compressor is usually integrated into the BGI process after the fiscal metering and after the conditioning of the biomethane as you can see in figure 2. This specific tie point prevents high pressure samples enter the gas analysis (PGC). It also simplifies the conditioning with air and/or LPG, because you can use simple air screw or reciprocating compressors up to 10 bar$_g$ for the injection of the needed ambient air through the gas agitator. The air has to be dried and filtered before entering the conditioning process. LPG can then be added either due to ambient evaporation or can be pumped and afterward electrically evaporated as needed during the conditioning process.

Usually the compressors are integrated into the BGI process as a pre-packaged unit (plug and play) from the respective manufacturers. Inlet and outlet flanges are screwed to the respective BGI plant pipes. The manufacturers electrical wiring, instrumentation and control system of the compressors is implemented into the overall wiring and control system of the BGI plant, normally by a profi-bus system.

4 Requirements for biogas compressors

4.1 Flow control

The requirements on biogas compressors are versatile.

The biogas flow from the BGU plant can vary significantly from 20 – 100 %. This requires a bypass and a frequency control system of the compressor alongside with the option of suction valve lifting. As a general rule the flow is automatically controlled by the suction pressure. If

the biogas flow from the BGU trough the BGI decreases, the suction pressure will drop and the electric engine will be throttled by the frequency control system. As already mentioned above, below 50 per cent of maximum flow other technical options have to be used to prevent the deactivation of the BGI. Due to the fact that you cannot stop the fermentation process a deactivation of the BGI will mean to burn the biomethane to an excess gas burner.

To guarantee the 96 per cent availability, that is postulated by the regulator and to secure controllability you can choose a redundancy concept of 2 x 100 per cent or 3 x 50 per cent. If you choose a concept with 3 x 50 per cent you emphasize more the principal of controllability, if you choose 2 x 100 per cent you emphasize more the principal of availability with less investment and maintenance costs. To furthermore secure the availability of 96 per cent minimal maintenance intervals should not go below 8.000 hours of operation a year for each compressor.

The pressure ratio from the BGU plant to the gas grid can vary from approximately 1 to 70. The suction pressure range spreads from 1 to 10 bar$_g$ and on the other hand the discharge pressure ranges from 16 to 84,5 bar$_g$, which normally describes the pipe pressure at the gas grid . Therefore single or multiple stage reciprocating compressors are needed corresponding with the upgrading process and the grid pressure. In figure 3 an exemplary calculation of operating conditions for a v-type reciprocating biogas compressor are shown. Especially the maximum temperature at inlet and the pressure at suction side are in focus.

OPERATING CONDITIONS (EACH MACHINE)			
● SERVICE OR ITEM NO.	Design 11-49	Design 13-49	Design 15-49
● STAGE	1	1	1
○ NORM. OR ALT. CONDITIONS			
○ CERTIFIED PT. ( ) MARK ONE			
● MOLECULAR WEIGHT	16.88	16.88	16.88
● Cp/Cv (K) @ 65°C OR __0__°C	1.30	1.30	1.30
○ INLET CONDITIONS: AT INLET TO: ○ PULSE DEVICES ○ COMPRESSOR CYLIND			
NOTE: ○ SIDE STREAM TO ____ STAGE(S), THESE IN			
● PRESSURE bar g @ PULL. SUPP INLT	11.00	13.00	15.00
■ PRESSURE bar g @CYL FLANGE	10.91	12.90	14.88
● TEMPERATURE (°C)	35.00	35.00	35.00
● REF. SIDE STREAM TEMPS (°C)			
■ COMPRESSIBILITY (Zs)	0.986	0.983	0.980
INTERSTAGE: INTERSTAGE Δ P INCL. ○ PULSE DEVICES ○ PIPING ○ COOLERS ○ SE			
◉ Δ P BETWEEN STAGES, %/(bar)	/	/	/
DISCHARGE CONDITIONS: AT OUTLET FROM ○ PULSE DEVICE ○ COMP. CYL. FLANC			
■ PRESS bar g @ CYL. FLANGE	49.57	49.57	49.57
● PRESS bar g @ PUL. SUPP. OUTLET	49.00	49.00	49.00
■ TEMP., ADIABATIC, °C	174.85	156.88	141.24
■ TEMP., PREDICTED, °C	163.65	148.18	134.85
■ COMPRESSIBILITY (Z2) OR (Zavg)	0.992	0.988	0.984
*REQUIRED CAPACITY, RATED FOR PROCESS, AT INLET TO COMPRESSOR, NO NEGATIVE TOL			
○ kg/h CAPACITY SPECIFIED	1059.41	1361.90	1674.18
IS ● WET ○ DRY			
○ m³/h (1013mbar & 0°C) 3)	1406.55	1808.16	2222.76
*MFGR.'S RATED CAPACITY (AT INLET TO COMPRESSOR) & kW @ CERTIFIED TOLERANCE OF ± 3			
◉ kg/h CAPACITY SPECIFIED	1092.17	1404.02	1725.96
IS ● WET ○ DRY			
◉ INLET m³/h	150.13	162.59	172.54
◉ m³/h (1013 mbar & 0°C)	1450.05	1864.08	2291.51
◉ kW / Stage (Indicated)	95	105	114
☐ TOTAL kW @ COMPRESSOR SHAFT	107	118	128

Figure 3: operating conditions for biogas plant Dorsten (Source: NEUMAN & ESSER Group, 2011)

DESIGN & ENGINEERING

Biogas injection into transport grids – a new interesting field for compressor manufacturers, *Dirk Sattur, Thomas Oelkrug;* RWE DEUTSCHLAND AG

Biogas upgrading plants (BGU's) can also work close to atmospheric pressure (e.g. amine scrubbers). It can therefore be feasible to implement an initial air blower before the main compression inside the BGI plants to prevent the forming of negative pressure, leading to a low suction pressure shut-down of the compressor unit. BGU plants with scrubber technology (amine or water scrubber) produce a biomethane saturated with water.

4.2   Gas drying and cooling system

Usually the gas grid operator will dry the biomethane before entering the compressor unit. Otherwise the forming of a high amount of condenser water inside the cylinder is possible. The combination of high temperatures, condenser water or gas hydrates from higher hydrocarbons (e.g. wrong LPG combination) and a chemical reaction with the biomethane can speed up corrosion and erosion inside the compressor. If there isn´t a gas drying system before the compressor, every single stage of the compressor needs a demister unit. To secure a safe operation it can also be implemented in the cooling unit.

To prevent oil from entering the gas grid the transport system operator prefers non lubricated reciprocating compressors. Otherwise oil filters and oil absorbers have to be integrated into the BGI plants securing a maximum oil ratio of 0,1 mg per cm biogas.

Beside the drying, cooling of the compressed biomethane is also very important. Outlet temperatures of approximately 150 °C have to be cooled down to max. 45 °C at the entrance to the pipe system because otherwise the polyethylene pipe coating will be damaged. With the preset temperature of around 30 to 40 °C of biomethane at the inlet of the compressor in some cases an additional water chiller has to be installed to handle the small ΔT. Especially in the summer when the temperature raise to 30 °C or more outside.

4.3   Pulsations and vibrations

Because of the fiscal metering, gas grid operators try to limit gas pulsations, especially to turbine flow meters to 1 % peak-to-peak to guarantee the accuracy. Otherwise the pulsation might be the reason for an additional acceleration of the turbine flow meter. Pulsation sources interact with pipe system and travel up and downstream of the plant. The pulsation source can be characterised by amplitude and frequency. To avoid pulsation waves the pipe system has to be designed with a large volume. In addition a static damping study can help to design pulsation dampers correctly. Normally it

is much too expensive to do dynamic approach 2 studies including the pipe system compared with the investment of small scaled compressors.

Even more important than to avoid pulsation is to prevent vibrations travel from the compressor skid to the whole pipe system. After frequencies that cause vibrations are identified often they can be faded out. Due to the fact that in projection phase the natural resonance of the compressor is identified you can optimize your system by using the frequency converter. The control unit is programmed to cut through this special frequencies. In biogas plants you can find several solutions to solve problems caused by vibrations. The less expensive one is probably to uncouple the compressor from the stiff piping system of the plant with flexible steel tubes. The more effective one is to have a separated baseplate for the compressor, so that the compressor can deduce unbalanced moments into the base plate. The second one of cause do not work in containers, where the force of gravity is deduced into the container framework.

BGI plants are usually installed into containers or smaller ready-mix concrete buildings. To prevent any vibrations accessing the container or building, as already mentioned, it is necessary to prevent the forming of vertical forces originating from the compressors that effect the container framework.

Smaller boxer-type   compressors with their horizontal forces can be viewed as "mass free" and can be implemented into the BGI process with less investment in reducing vibration and pulsation.

4.3   Gas leakage

The Renewable Energy Sources Act (EEG) prohibits methane losses during the upgrading and injection process greater than 0,5 % of the flow. The compressor units therefore have to be equipped with leakage free crankcase cover gaskets. If this is not possible a leakage collector and compressor has to be implemented into the process. Usually it is not feasible to re-inject the leakage gas in a low pressure and already LPG conditioned biogas section of the BGI plant. In some cases leakage gas can be used in heating systems to support the fermentation process in the biogas plant. Another possibility is to inject smaller amounts of leakage gas directly in a low pressure distribution grid that is near the plant (e.g. under 200 mbar).

Biogas injection into transport grids – a new interesting field for compressor manufacturers, *Dirk Sattur, Thomas Oelkrug;* RWE DEUTSCHLAND AG

5   Conclusion

The paper tries to describe the technical process from the raw biogas production through the upgrading and conditioning of the biomethane. It summarizes the requirements given by the operator for a feasible biogas compressor which are:

- Wide range of flow

- Intelligent cooling and drying system

- Preferred a non-lubricated compressor

- Maximum pulsation peak-to-peak 1 %

- Prevent unbalanced moments on container framework

- Smart gas leakage system or compression proof chassis to suction pressure

- Minimum availability of 96 per cent of operations hours

- A 24/7 running compressor with minimum maintenance intervals of 8000 hours

After Germany started the injection of biomethane into gas grids, other European countries are already on their way to receive similar legislations given by the government. Especially France, the Netherlands and Great Britain but also Poland and the Czech Republic are confronted with larger biogas projects. The experience made in German projects can directly be implemented in other projects in Europe and help to prevent mistakes in projection. For reciprocating compressor manufacturers it is an interesting market working together with the production of sustainable and renewable energy and it is growing every day. There is no other compressor design that can keep up with the strong and flexible attributes of smaller reciprocating compressors. Let us do a step in a green future for compressor manufacturers.

6   Annex

In the Annex a list of existing plants with initial start of operation and flow capacity is shown.

City	Status	Initial start of operation	Flow capacity [cm³/h]
Aicha (Osterhofen)	under construction	2012	750
Aiterhofen	in operation	2009	1,000
Altena/Bahrdorf	in operation	2011	380
Alteno	under projection	2012	350
Altenstadt/Hessen	in operation	2012	600
Altenstadt/Schongau	in operation	2009	690
Angermünde	in operation	2010	650
Anklam	under construction	2012	1.500
Apensen	under construction	2012	350
Arneburg	under construction	2012	700
Arnschwang	in operation	2010	690
Barleben	under construction	2012	350
Barsikow	in operation	2011	350
Bergheim/Paffendorf	under projection	2012	600
Bergheim/Steinheim	under projection	2013	300
Berlin-Ruhleben	under construction	2012	490
Blankenhain	in operation	2011	650
Blaufelden	in operation	2010	210
Borken / Münsterland	under projection	2013	750
Brandis	under projection	2013	700
Bruchhausen-Vilsen	in operation	2011	370
Brumby	under construction	2012	700
Brunne	in operation	2011	300
Burgrieden	in operation	2008	300
Dannenberg	in operation	2010	200
Dargun	in operation	2011	1.140
Darmstadt	in operation	2008	150
Darmstadt 2nd stage	under construction	2012	700
Dorsten	under construction	2012	1.300
Drögennindorf	under construction	2011	250
Ebsdorfergrund	under construction	2012	500
Eggertshofen/Freising	in operation	2010	220
Eggolsheim	under construction	2012	400
Eich in Kallmünz	in operation	2011	600
Eimbeckhausen	under construction	2012	350
Einbeck	in operation	2009	500
Erdeborn	under projection	2013	350
Ettlingen	in operation	2008	330
Feldberg	under projection	2012	350
Forchheim im Breisgau	in operation	2010	530
Forst (Lausitz)	under projection	2012	1.350
Fürth/Seckendorf	in operation	2011	800
Gangkofen	under projection	2013	350
Gardelegen	under projection	2012	350
Godenstedt	in operation	2009	300
Gollhofen-Ippesheim	under construction	2012	620
Graben/Lechfeld	in operation	2008	500
Grabsleben	in operation	2010	350
Gröden	under construction	2012	400
Groß Kelle	in operation	2011	250
Guben	under projection	2012	750
Güstrow	in operation	2009	5.000
Güterglück	in operation	2009	650
Hage	under construction	2012	350
Hahnennest	in operation	2012	350
Haldensleben	under projection	2013	700
Hamburg	in operation	2011	300
Hankensbüttel	in operation	2011	350
Hardegsen	in operation	2009	500
Heidenau	under projection	2012	380
Heitersheim/Breisgau	under projection	2012	500
Hellerwald/Boppard	under construction	2012	680
Hohenhameln Mehrum	under construction	2012	750
Holleben II	in operation	2011	700
Homberg/Efze	in operation	2010	350
Horn - Bad Meinberg	in operation	2009	1,000

Biogas injection into transport grids – a new interesting field for compressor manufacturers, *Dirk Sattur, Thomas Oelkrug;* RWE DEUTSCHLAND AG

Industriepark Höchst	in operation	2011	1,000
Jürgenshagen	under construction	2011	380
Kannawurf	under construction	2013	700
Karben	under construction	2012	350
Karft	in operation	2011	550
Kerpen	in operation	2009	550
Ketzin	in operation	2008	200
Kißlegg-Rahmhaus	in operation	2010	300
Fulda	under construction	2012	280
Fulda 2nd stage	under construction	2013	310
Klein Schulzendorf	under construction	2012	350
Klein Wanzleben	under construction	2012	700
Könnern 1	in operation	2007	650
Könnern 2	in operation	2009	1.500
Lanken/Wotersen	in operation	2009	410
Lehma	in operation	2012	600
Leizen	under construction	2012	380
Lenzen	under projection	2012	600
Lichtensee	under construction	2012	700
Loop	under projection	2013	550
Lüchow	in operation	2009	650
Maihingen	in operation	2008	560
Malstedt	in operation	2011	370
Mammendorf	under construction	2012	380
Marienthal	under projection	2012	380
Marktoffingen	under construction	2012	350
Merzig	in operation	2011	550
Müden (Aller)	under construction	2012	350
Mühlacker	in operation	2007	500
Neukammer 2	in operation	2010	1,050
Neuss am Niederrhein	in operation	2010	165
Niederndodeleben	in operation	2009	650
Oberriexingen	under construction	2011	380
Oschatz	under construction	2012	700
Osterby	in operation	2012	350
Ottersberg	under projection	2012	650
Palmersheim	in operation	2011	350
Pliening	in operation	2006	485
Pohlsche Heide	in operation	2010	350
Pritzwalk-Neudorf	under construction	2012	700
Ramstein	in operation	2011	350
Rathenow	in operation	2009	520
Rätzlingen	under projection	2012	380
Reimlingen	under projection	2013	700
Rhede	in operation	2010	500
Röblingen am See	under construction	2012	650
Ronnenberg	in operation	2008	300
Rosche	under projection	2012	380
Roßwein/Haßlau	in operation	2011	700
Sachsendorf	in operation	2011	350
Sargard (Rügen)	under construction	2012	660
Schöllnitz	under construction	2012	700
Schöpstal	in operation	2011	700
Schuby	in operation	2011	1,000
Schwandorf 2	in operation	2008	1,000
Schwarme	under projection	2012	350
Schwedt	in operation	2010	3,500
Schwedt 2nd stage	under construction	2012	3,500
Seehausen	under projection	2013	700
Semd (Groß-Umstadt)	in operation	2010	210
Senftenberg	under projection	2012	1,000
Staßfurt	under projection	2013	350
Straelen	in operation	2006	550
Stresow	in operation	2011	650
Stülpe	under projection	2013	750
Tangstedt/Bützberg	in operation	2011	350
Tuningen	in operation	2009	250
Unsleben	in operation	2010	350
Vettweiß	under construction	2012	550
Werlte	in operation	2007	340

Wetschen	in operation	2010	700
Willingshausen	in operation	2010	350
Wittenburg	under projection	2011	350
Wölfersheim	under construction	2012	750
Wohnzach (Hallertau)	under construction	2012	1.000
Wriezen	in operation	2011	650
Wunstorf	under projection	2013	350
Wüsting	in operation	2009	700
Zeven	in operation	2009	125
Zittau	under construction	2012	550
Zörbig	in operation	2010	2,500
Zörbig 2nd stage	in operation	2012	2,500
Zschornewitz	under projection	2012	700
Zülpich	under projection	2012	400

Figure 4: overview biogas upgrading and injection plants in Germany end of 2011 by location, status and capacity flow rate[1]

References

[1]Deutsche Energie-Agentur GmbH (dena); Date: 8/2011; Biogas Partner – a joint initiative

[2]European Commission; Energy Efficiency: Attainability of Climate Goals; www.europa.eu, KOM/2008/0772, Information of the European Commission, 13. November 2008, Decision of the EU-Parliament, 17. December 2008

[3]Kolbenmaschinen – Kolbenpumpen, Kolbenverdichter, Brennkraftmaschinen; Küttner, Eifler, Schlücker, Spicher, Will; 7th edition, vieweg+taubner, 2009

Efficient Compressor Drives for the Smart Power Grid

by:

Siggberg Anders

Pumping & Compression, Power Plants

Wärtsilä Finland Oy

Vaasa

Finland

anders.siggberg@wartsila.com

8th Conference of the EFRC
September 27th / 28th, 2012, Düsseldorf

Abstract:

For many years electric motors have traditionally been considered an industry standard for driving compressors in more developed countries with heavier infrastructures. These regions are accessing increasing renewable power such as wind and solar, and in many situations the primary electric utility grids become unstable for starting up big electrically driven machines, such as compressors in for example underground gas storage projects. This is augmented on a country specific basis; with decisions for phasing out nuclear power plants in Germany will even increase the problem. Modern gas or dual fuel diesel combustion engines offers a credible and proven solution for the dilemma. With fast start-up times, high reliability and low emissions, gas engines can be the optimal solution for the future power grid of Europe. In fact, even the toughest emission limits can be met with state-of-the-art control systems and modern exhaust gas after treatment. Gas engines offers the highest efficiency on the market today, even when the power grids suffers from black outs.

A feasibility study of a dual drive in a smart power grid will also be presented.

1 Introduction

The fairly stable electricity market until the unbundling and privatization starting in the 1990's will continue to undergo drastic changes during the years ahead. With the increasing public concern for the climate change, renewable power generation is seen as one of the most significant measures to decrease emissions. There are a number of different future power generation scenarios available by various organisations, however in this paper the most viable scenario is not the key item. The significant item is that the variable renewable power generation will increase substantially, and probably even higher than the expectations. Thus the figures to highlight the future renewable power generation share is limited to a few, focusing on the European installed power generation mix 2008 and the scenario 2030 (Figure 1).
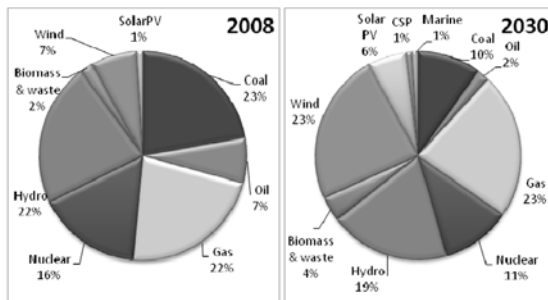
Figure 1: European installed Power Generation capacity mix 2008 and scenario 2030 [1]

In Europe, with clear political support from the European Council, the prospected increase in variable renewable power generation is dramatic with almost 340 GW or 30 % (wind 23% and solar PV 6%) of the generation mix in 2030 (1200 GW).

From the important low emission aspect, renewable power generation from wind and solar is an important player. However, from a production and demand balance perspective there are some challenges:

• Variability - Wind and solar have a natural volatility

• Predictability - Wind forecasting can be made, but typical errors are 5-25%

• Dispatch ability - With some restrictions for wind and solar

Considering these challenges and the high electricity supply availability taken for granted, traditional power generation need to adapt and increase flexibility, new generation technologies must be analysed and alternative methods and (ancillary) markets introduced. Markets where not only energy produced is remunerated, but also regulation capability, speed of response and capacity reserve payments are essential ingredients.

2 Challenges in the smart grid

The basic idea with smart power grids is that a consumer gets informed when there is excess power in the grid. Excess power is usually cheaper than the normal tariffs. If a consumer wants to start up big electric motors he might not get the permissions unless there is excess power, for example during a windy day.

Big consumers with flexibility are also needed to stabilize the grid. Gas compression applications might not be the most suitable consumer for stabilizing the electric grid. In Europe, seasonal underground gas storages fill the caverns during summer time when the gas is cheap, not only when the wind is blowing but also during days without wind. During winter time when there is a big need of power and heat the storages are withdrawn, even during days with wind.

The reason for the needed balancing power in a grid can easily be understood when looking at the output power that wind turbines generate at different wind speed, figure 2. Below wind speeds of 10 m/s the turbine is only producing half of its rated power, and at wind speeds greater than 25 m/s the wind turbine is automatically shut-down in order to protect itself.
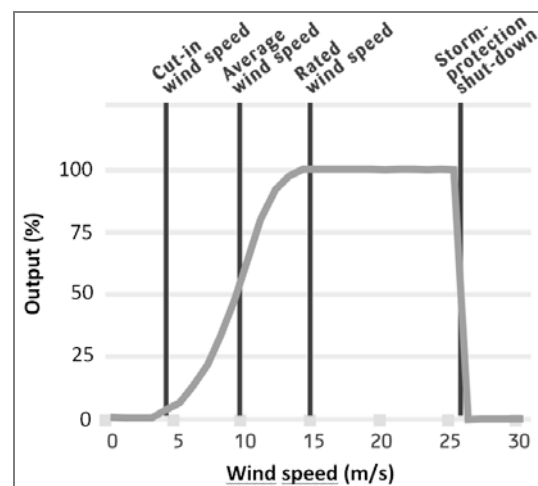
Figure 2: Output power from a wind turbine as a function of wind speed [2]

In countries with a high degree of electricity generated from wind power, the demand of power is not met with the electricity generated from wind power. This can be illustrated with an example from Denmark, the country with the largest relative amount of wind power in the world (Figure 3).
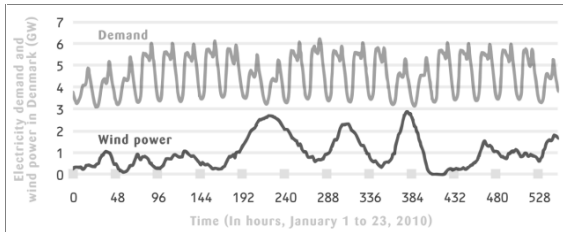
Figure 3: Electricity demand and wind power in Denmark, January 2010 [3]

Some suggested solutions for balancing a power grid are:

1   Regulation by conventional generation

2   Buffering (energy storage)

3   Demand control

4   Removing big consumers

A well designed compressor station can balance the grid by using previously mentioned solutions 1, 3 and 4. Furthermore, if the compressor station is at a natural gas storage facility, it can also act as a balancing plant. Electricity is not stored in a gas storage, but if the compressor drives are electrical the station will have a similar balancing effect on the grid as electricity storage. This is of course applicable only if the gas price is reasonable low at the same time as the electricity. Figure 4 shows that there is no clear correlation between the electricity and gas price, the gas price is much more stable than the electricity price, even though there is no global natural gas market as such. For this reason gas storages with electric drives cannot balance the grid as such as there is no need for compression at the same time as there is surplus electricity.
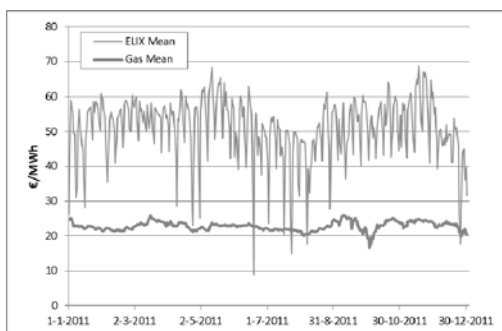
Figure 4: 2011 daily average electricity price (ELIX) and an average daily gas price (average of NCG, Gaspool, TTF and Zeebrügge [4]

3   Modern gas engines as compressor drives

In 1992, Wärtsilä started the development of lean-burn, spark-ignited Otto cycle gas engines. The first 34SG gas engines were released in 1995 and today the latest generation takes the power of the W34SG series up to 10 MW. In compressor applications the engine operates with variable speed between 525-750 rpm. The efficiency of the W34SG is the highest of any spark-ignited gas engines today. The natural gas fuelled, lean-burn, medium-speed engine combines high efficiency with low emissions. This is achieved applying state-of-the-art technology with features including:

- use of a lean gas mixture for clean combustion

- individual cylinder combustion control and monitoring, providing even load on all cylinders

- stable combustion, ensured by a high-energy ignition system and pre-combustion chamber

- self-learning and self-adjustable functions in the control system.

The W34SG is a well proven technology with more than 620 units running worldwide in on-shore applications and a total accumulated installed power of 5300 MW.
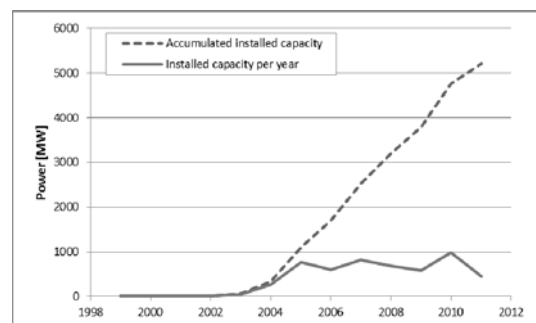
Figure 5: Installed on-shore W34SG gas engines

3.1   Flexibility

Modern reciprocating engines have embedded intelligent control systems that ensure fast reactions to change. Typical start-up time from stand still to synchronisation is within one minute and the time needed to reach 100% output is only 5 minutes, meaning that the loading takes place at a 25% / minute rate (Figure 6). In continuous operation, sudden power system frequency drops can be conquered by even faster reactions to change and

rapid loading, ensuring excellent support for Primary and Secondary Frequency Support as outlined by many Transmission System Operators (TSOs). In a variable environment, fast unloading is also a desired factor and unloading in only one minute allows for rapid balancing of surplus power from renewable energy sources. With a less predictable environment, multiple start and stops, cyclic loading and unloading and generating set reactions in seconds, not minutes or hours, will be a daily routine. Such new operational patterns should be possible while maintaining high efficiency and low maintenance impact. Reciprocating engines are agile and support these desired features.
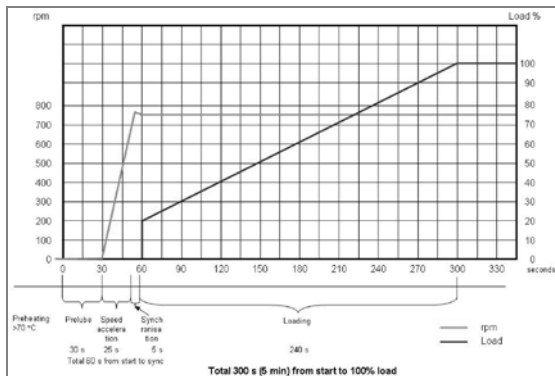
Figure 6: Start-up and loading time of the W34SG gas engine

3.2 Efficiency

Since the economic crash of 2008 and the following worldwide depression/recession, all stakeholders have to be more aware of project economics and the significant impact that can be realised with more whole life efficient products and services of compressor drives. Figure 7 shows the guaranteed operating field of the W34SG compressor drive, including the efficiency in the limiting points. The engine reaches its maximum efficiency at the lowest allowed speed (525 rpm) and full load. The lowest efficiency point can be found at the maximum speed (750 rpm) and minimum load (30 %). The figure shows that by using variable speed flow control one can improve the overall efficiency even from the rated point.
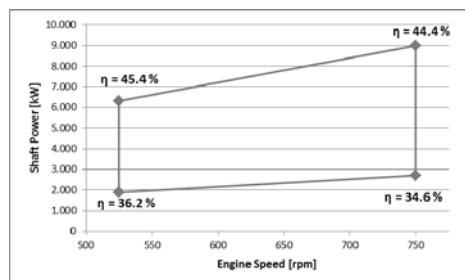
Figure 7: W20V34SG compressor drive gas engine operating envelope

3.3 Emissions

The main parameters governing the rate of NO_X formation in internal combustion engines are peak temperature and residence time. The temperature is reduced by the combustion chamber air-fuel ratios: the higher the air-fuel ratio the lower the temperature and consequently the lower the NO_X emissions.

In the W34SG engine, the air-fuel ratio is high and uniform throughout the cylinder, due to premixing of the fuel and air before introduction into the cylinders. Maximum temperatures and subsequent NO_X formation are therefore low, since the same specific heat quantity released by combustion is used to heat up a larger mass of air. Benefiting from this unique feature of the lean-burn principle, the NO_X emissions from the W34SG are extremely low, and comply with the most stringent existing NO_X legislation.

4 Dual drives

To fully utilize the potential and benefits of both electric drives and gas engines one should consider dual drives where both a compressor and a generator are connected to a gas engine at the same time. This setup is illustrated in Figure 8 where the gas engine is to the left, connected with a clutch to the generator in the middle, which again, is connected via another clutch to the compressor to the right in the figure. The generator shaft goes through the generator and is sized to take the full load and torque of the compressor. The dual drive setup gives the altruistic possibility to generate electric power simultaneously to compression, or act as a normal power plant during seasonality when there is no project phase or economic benefit for compression.
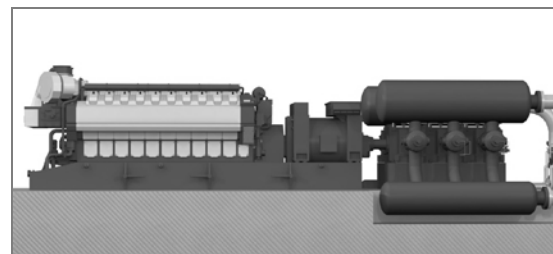
Figure 8: A dual drive setup with a gas engine driving both a compressor and a generator

The dual drive system has the following five discrete running modes:

1. **Mechanical compression**. Generator spinning unloaded. Variable speed.

2. **Electrical compression**. Engine de-clutched. Fixed speed.

3. **Compression and power generation** simultaneously. Compressor and generator are sharing the power from the gas engine. Applicable running mode for a gas storage during part flow or when the compressor for some reason does not load the engine to 100 %. Fixed speed.

4. **Compression with fuel sharing**. Gas engine and electric motor are sharing the load from the compressor. Fixed speed. Might be an applicable running mode if the TSO want to dump a certain power but not as much as the compressor needs, the gas engine is used for delivering the rest of the needed shaft power.

5. **Power generation**. Compressor de-clutched. Fixed speed.

An additional benefit is that a soft starter is not needed for the electric drive, as the compressor can be started with the gas engine and switched to electric drive at full speed.

During critical project/programme management periods when compression is of most importance, i.e. cavern filling periods, the operator can switch to gas mode and run the compressors in island mode independent from the electrical HV/MV grid.

The dual drive gives flexibility to the smart power grid. During periods with no compression work, the plant can act as peaking power plant with start up times far faster than combined cycle gas turbines. The owner can get extra income by selling the capacity reserve, even though it would not be used.

During periods of excess power in the grid, the station can utilize the generator as a motor and stabilize the grid by doing electrical compression work.

A minor drawback with this type of dual drive basis of design is perhaps the higher investment costs compared to a normal compressor station. On the other hand, the dual drive is not only a compression station but also a power plant, a fact that turns the total investment costs to the advantage of the dual drive.

With increasing energy prices it gets even more important than before to operate on the cheapest available fuel and to have the possibility to constantly optimize and change the fuel strategy as the market price changes, in all short, mid and long term project life cycles. Another key factor is to maximize the utilization of the investments and obtain a better return of capital employed (ROCE). Equating this, simply in a gas storage it means to be able to do something useful with the installed rotating equipment capacity also during periods when no compression work takes place.
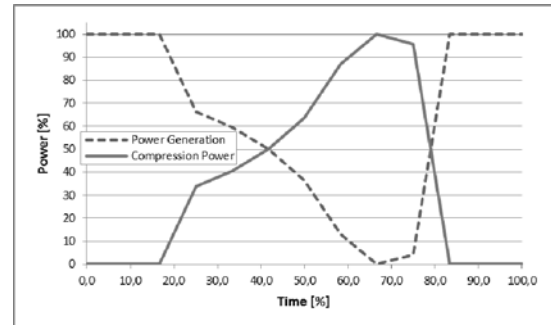
Figure 9: Compression power and power generation example running profile of a dual drive in a seasonal gas storage

5   Dual drive feasibility

In order to quantify the possibilities a dual drive setup gives, the fuel cost for each running mode throughout a year was calculated. For this white paper the year 2011 was selected as reference. The electricity price was taken from ELIX on an hourly basis and daily average prices were calculated. Gas prices for NCG, Gaspool, TTF and Zeebrügge was taken on a daily basis from NCG. [5] A daily average gas price was calculated based on all four gas markets and the calculated value was used throughout the study to represent a universal gas price.
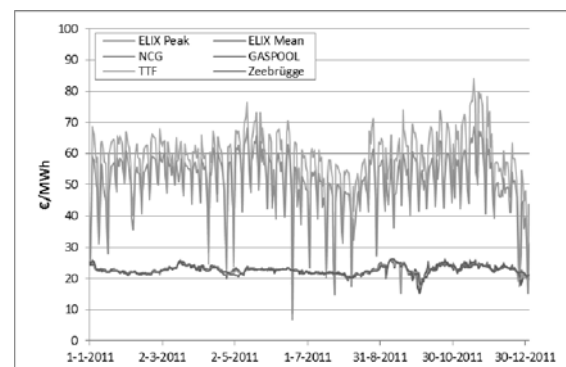
Figure 10: Electricity and gas prices during 2011

For each day the maximum fuel consumption was calculated for the mechanical drive gas engine and the electric motor, assuming a 10 MW compressor, 100 % load and a 24 h/day running profile. For the gas engine a shaft efficiency of 44.4 % was used and for the electric motor 96 %. In order to make the results more readable, the trend was sorted with respect to the electricity price, making it a duration curve. The final result is shown in Figure 11. The total fuel cost for the year was calculated to 4,48 M€ for the gas engine and 4,63 M€ for the electric motor. With a dual drive one could always choose the cheaper drive, decreasing the total cost to 4,24 M€. A yearly saving of 240 000 € compared to a pure gas engine and 390 000 € compared to a pure electric motor.

The price for own electricity generation was calculated for each day and compared to the market spot price. For the generator the same efficiency was used as for the electric motor.
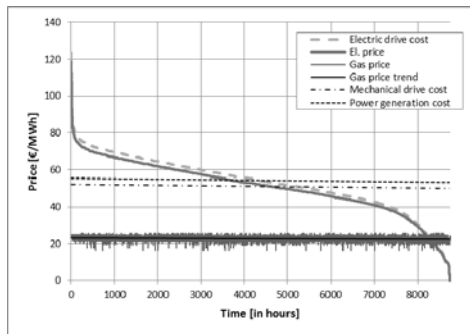
Figure 11: Electricity price duration curve for 2011 with corresponding gas price. Fuel cost curves for electric drive, gas engine drive and power generating set added

As Figure 11 shows, the mechanical drive fuel costs are lower than the electric drive 59 % of the year, and own power could be generated to a lower price than the market during 44 % of the year.

As these calculations show the theoretical maximum fuel costs, we also wanted to look more in detail if the dual drive is used purely for peaking. The peaking potential can be illustrated with the average daily price trend, Figure 12.
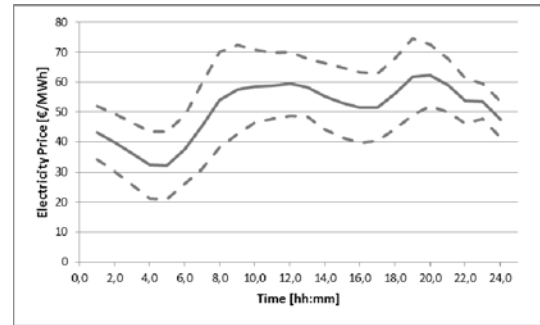
Figure 12: Daily electricity price trend, average for 2011 including standard deviation

During winter the morning and afternoon peaks grows, which of course gives an indication of the potential income electricity generation could offer. Figure 13 is an example of the record high day of 2012.
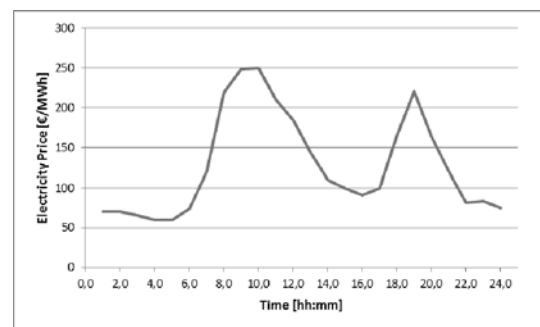
Figure 13: Hourly electricity price, 10.2.2012

In this study, factors like running profiles of the compressor station was not taken into account as these depend on the type of installation, among other factors. Transmission costs of both electricity and gas were also left outside the scope of the study. Only the possibilities of dual drives have been presented and it is left to each and every compressor owner to decide how the concept is applicable on their installations.

6   Conclusion

For big seasonal storages gas engines are superior when comparing efficiency and flexibility, features that are crucial for consumers in the smart power grid. By installing gas engines as compressor drives instead of electric motors, the smart power grid will be more stabilized as there will be less and smaller peak consumers. By using the gas from the pipeline as fuel, the stations will be independent from the fluctuations in the more unstable primary HV power grids.

The big advantages of balancing the power grid and optimizing fuel costs of a compressor station comes when installing both a gas engine and an electric generator to drive the same compressor. This setup

gives the possibilities to act as a high profit peaking power plant during seasons when no compression work is taking place.

For smaller day-to-day storages electric motors might be as suitable as gas engines because of the ability to absorb excess power from the grid and thereby stabilize the grid. This feature is, however, only of advantage if the gas spot price is low at the same time as there is excess power available.

As the smart power grids gets implemented in Europe and the share of renewable power generation grows, the potential revenues of utilizing compressor stations for other work than pure compression will grow. The higher the interaction of the compressor station with the grid is, the bigger are the potential savings.

7   Acknowledgements

It is not possible to completely cover such a broad topic in a paper of this type. For those who are interested in smart power grids and power generation the freely available hardback book electronic copy of "Smart Power Generation" [6] is strongly recommended.

In this paper we have limited the basis of design to underground gas storages as examples for the implementation of gas engines to the smart power grid, but other compression applications could be considered as well.

References

[1] World Energy Outlook 2010 IEA, www.iea.org

[2] Klimstra, Jacob and Markus Hotakainen, ´**Smart Power Generation**´, Avain, Helsinki, 2011, ISBN 978 951 692 846 6, www.smartpowergeneration.com

[3] Klimstra, Jacob and Markus Hotakainen, ´**Smart Power Generation**´, Avain, Helsinki, 2011, ISBN 978 951 692 846 6, www.smartpowergeneration.com

[4] European Power Exchange, www.epexspot.com

[5] NetConnect Germany, www.net-connect- germany.de

[6] Klimstra, Jacob and Markus Hotakainen, ´**Smart Power Generation**´, Avain, Helsinki, 2011, ISBN 978 951 692 846 6, www.smartpowergeneration.com

Non-lubricated Moderate Speed Reciprocating Compressors in a Hydrogen Plant

by:

Benjamin F. Williams
Process Application and Account Manager
Ariel Corporation
Mount Vernon, Ohio
USA
bwilliams@arielcorp.com

Laurent Richaume
Rotating Equipment Team Manager
Air Liquide Engineering & Construction
Champigny-Sur-Marne Cedex
France
Laurent.RICHAUME@airliquide.com

8th Conference of the EFRC
September 27th / 28th, 2012, Düsseldorf

Abstract:

In 2007 Air Liquide made the decision to purchase and install packaged, non-lubricated, moderate speed compressors for the hydrogen and natural gas feed services in a hydrogen plant supplying a refinery in South America. The compressors have been operating successfully for over two years. This case study will include a description of the compressor selections and details on the operational history.

Non-lubricated Moderate Speed Reciprocating Compressors in a Hydrogen Plant, *Benjamin F. Williams, Laurent Richaume;* ARIEL CORPORATION, AIR LIQUIDE ENGINEERING & CONSTRUCTION

1   Introduction

Since the early 1990's; emission regulations throughout the world have led to increased demand for hydrogen. That is because hydrogen is required for many desulphurization processes. Industrial gas companies have constructed a number of Hydrogen plants throughout the world to meet the demands of the refining and petrochemical industries.

The majority of reciprocating compressors used in these hydrogen plants have been lubricated, long stroke, slow speed types. This is due to historical preference and the perception that these are the most reliable compressors available. It should be noted that other types of reciprocating compressors have also been used successfully in these facilities. These include vertical compressors and horizontal, short stroke, moderate speed types.

Although lubricated compressors are the most common type used in these facilities; there are times that the design of the hydrogen plant or its components cannot tolerate oil carryover in the gas stream. In those cases; the decision must be made whether to use a lubricated compressor with a downstream coalescing (oil removal) system or a non-lubricated (dry piston) compressor.

When determining lubricated vs. non-lubricated compressors; among the items that need to be considered are the impact of oil downstream of the compressor, initial and life cycle cost and frequency of required maintenance. Typically non-lubricated compressors will have a higher initial capital cost due to the higher cost of wear part materials. Non-lubricated compressors typically require more frequent maintenance than a lubricated compressor.

In 2007, Air Liquide made the decision to purchase packaged, non-lubricated, horizontal, balanced opposed, short stroke, moderate speed reciprocating compressors for the natural gas feed and hydrogen product services at a new hydrogen plant they were constructing in Campana, Argentina.

The hydrogen plant went on-line in November 2009. This paper describes the compressor selections, provides a brief overview of their design characteristics and summarizes their operational history.

2   Air Liquide Campana

2.1   Hydrogen Production Unit

Air Liquide built a new hydrogen unit (steam methane reformer technology) in Campana, Buenos Aires, Argentina. The unit supplies hydrogen and steam to the Esso Petrolera Argentina refinery for use in the production of gasoline.

Prior to this project; Air Liquide would typically purchase vertical, slow speed compressors for this type of facility. The decision to purchase moderate speed, short stroke compressors for the Campana project was based on delivery, compact packaging and capital cost. Spare parts availability and references for similar applications also contributed to the decision to purchase moderate speed reciprocating compressors.

The decision to use non-lubricated compressors for both the natural gas feed and hydrogen product services was based on differing requirements. Primarily; the natural gas feed service required non-lubricated compressors to prevent oil contamination of the Air Liquide process and process equipment. The hydrogen compressors needed to be non-lubricated due to Air Liquide customer requirements.

Figure 1: Campana, Buenos Aires, Argentina[1]

2.2   Compressor Requirements

2.2.1   Natural Gas Feed

P suction (BarA)	11
P discharge (BarA)	41
Gas specific gravity	0.5727
Capacity required (Nm3/hr.)	6800

Figure 2: Feed gas compression requirements

2.2.2   Hydrogen Product

P suction (BarA)	28
P discharge (BarA)	54
Gas specific gravity	0.0741
Capacity required (Nm3/hr.)	15400

Figure 3: Hydrogen compression requirements

DESIGN & ENGINEERING

Non-lubricated Moderate Speed Reciprocating Compressors in a Hydrogen Plant, *Benjamin F. Williams, Laurent Richaume;* ARIEL CORPORATION, AIR LIQUIDE ENGINEERING & CONSTRUCTION

3   Compressor Selections

Air Liquide purchased two 100% capacity, non-lubricated, non-cooled, short stroke, moderate speed, electric motor driven reciprocating compressors for each service. (Typically, Air Liquide will purchase either two 100% or three 50% units for their hydrogen plants.)

Following are a brief description of the compressor selections and details on the calculated performance of each.

3.1   Natural Gas Feed

Non-lubricated, short stroke, moderate speed, two stage, two throw compressor driven by a 500 kW, 750 RPM squirrel cage induction motor.

Cylinder Data:	Stage 1	Stage 2
Cylinder bore dia., mm	358.78	244.48
Cylinder MAWP, BarG	56.2	87.6

Compressor Performance Calculations

Stage	1	2
Calculated flow Nm3/hr.	6876	6860
Gas specific gravity (S.G.)	0.5727	0.5726
Ratio of Specific Heat "N"	1.2864	1.2938
Suction pressure (BarA)	11	21.72
Suction temperature (C)	37.1	40
Discharge pressure (BarA)	22.15	41
Discharge temperature (C)	96	96

3.2   Hydrogen Product

Non-lubricated, short stroke, moderate speed, two stage, two throw compressor driven by a 500 kW, 750 RPM squirrel cage induction motor.

Cylinder Data:	Throw 1	Throw 2
Cylinder bore dia., mm	244.48	244.48
Cylinder MAWP, BarG	87.6	87.6

Stage	1
Calculated flow Nm3/hr.	15503
Gas specific gravity (S.G.)	0.0741
Ratio of Specific Heat "N"	1.4047
Suction pressure (BarA)	28
Suction temperature (C)	45
Discharge pressure (BarA)	54
Discharge temperature (C)	119

4   Compressor Design Characteristics

As noted previously, the compressor frame models are the same for both services. The following overview applies to both the natural gas feed and hydrogen product compressors; unless otherwise noted.

4.1   Compressor Frames

Model – JGT/2
Compressor stroke (mm) – 114.3
Piston rod diameter (mm) – 50.8
Rated speed (RPM) - 1500
Operating speed (RPM) – 744
Average piston speed (mps) – 2.8
Rated tension rod load (kN) – 165
(Average calculated tension rod loads were 119 kN and 103 kN, respectively)
API-618 Type "C" distance pieces
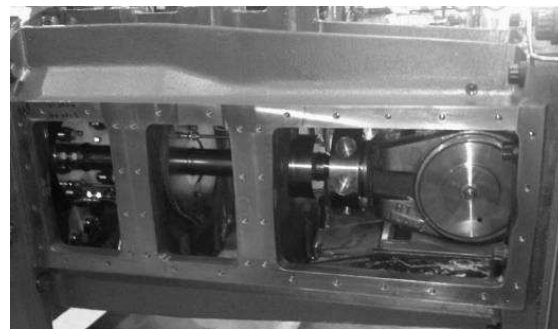
Figure 4: API-618 type "C" distance piece

4.2   Cylinder Bodies

Material - ASTM A395 ductile iron
Non-cooled
Unlined - ion-nitride hardened to approximately 57 Rc.
Surface finish – 0.15 micro-meters

*- meters per second

DESIGN & ENGINEERING

Non-lubricated Moderate Speed Reciprocating Compressors in a Hydrogen Plant, *Benjamin F. Williams, Laurent Richaume;* ARIEL CORPORATION, AIR LIQUIDE ENGINEERING & CONSTRUCTION

4.3   Piston and Rod Assemblies

Piston material - ASTM A48 Class 30 gray iron
                (2 piece)
Piston rod material - Low alloy carbon steel with
                tungsten carbide coating.
Surface finish – 0.2 micro-meters

Piston wear bands
        1 piece, angle cut
        Pressure balanced
        0.035 N/mm2 wear band loading
        Special polymer alloy for oil free service.

Piston rings
        1 piece angle cut
        Special polymer alloy for oil free service.

Figure 5: NL piston assembly

4.4   Packing

Water cooled packing case- carbon steel
Packing purged with nitrogen
Combination of cut and uncut packing ring sets
Special polymer alloy for oil free service
Intermediate and wiper packing sets include buffered packing rings.
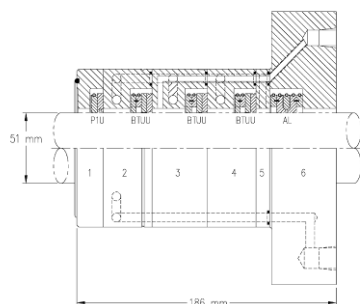
Figure 6: Pressure packing case

4.5   Valves

Natural gas feed compressor
        Non-metallic plate valve
        2.59 mm lift

Hydrogen compressor
        Non-metallic concentric ring valve
        0.99 mm lift

Designed for non-lubricated service
Head end valve depressor type suction valve unloaders.
Thermocouples for monitoring discharge valve temperatures.

5   Operating History

The compressors are operating on a rotational basis; generally the units are switched every six months. The natural gas compressors are run at 100% capacity; the hydrogen compressors operate at 50% load.

As of March 2012 – The plant had been in operation for approximately 18,000 hours total. The individual compressor operating hours were as follows:

Natural gas feed
        Unit 1 – 12086 hours
        Unit 2 – 6726 hours
Hydrogen
        Unit 1 – 9202 hours
        Unit 2 – 9334 hours

5.1   Inspection Results

Inspections have been performed on two of the compressors; one hydrogen and one natural gas feed. Each had approximately 9,300 hours run-time at the time of the inspections.

5.1.1   Running Gear

The running gear for both compressors was inspected and all clearances were within specified tolerances.

5.1.2   Cylinder Inspection Results

Visual and dimensional inspections were performed on each cylinder. A brief summary of these inspections follows:

DESIGN & ENGINEERING

Non-lubricated Moderate Speed Reciprocating Compressors in a Hydrogen Plant, *Benjamin F. Williams, Laurent Richaume;* ARIEL CORPORATION, AIR LIQUIDE ENGINEERING & CONSTRUCTION

Piston and Piston Rod Assemblies

Figure 7: Campana hydrogen compressor piston after 9300 hours of operation

Piston Rods (Nominal Dimension – 50.8 mm)

Piston rods were inspected for damage and wear. Rod diameters (as measured in Figure 8) all were acceptable; 50.76 to 50.78 mm. All piston rods were cleaned and reinstalled, with no repairs needed.
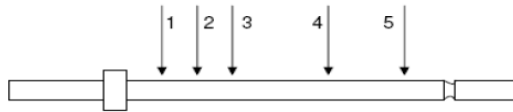
Figure 8: Piston rod inspection points

Pistons

Piston ring grooves and wear band grooves were inspected. All groove widths and depths were within new tolerance.

Piston Rings and Wear Bands

Piston ring and wear band radial thickness, side clearance and end gaps were measured. All showed normal wear. The hydrogen compressor piston rings (PR) and wear band (WB) measurements are shown in Figure 9, along with the same measurements for the new replacement rings and wear bands.

Dimension (mm)	Cylinder 1	Cylinder 2	New
WB Radial Thickness	8.8-9.2	8.8-9.2	9.6
WB Width	40.8	40.8	40.8
WB End Gap	10.5	10.5	7.0
PR Radial Thickness	9.3	9.3	9.3
PR Width	11.5-11.9	11.5-11.9	12.9
PR End Gap	8.0	8.0	8.0

Figure 9: Piston ring and wear band measurements

It is a common perception that cooled cylinders are needed for critical service machines; particularly non-lubricated types. As noted previously; the cylinders on these moderate speed compressors are non-cooled. The worn piston ring and wear band dimensions shown in Figure 9 are within the manufacturer's acceptable range. These rings and wear bands could have been re-installed. However, as spare piston rings and wear bands were available, the decision was made to replace them.

Cylinder Bore Dimensions
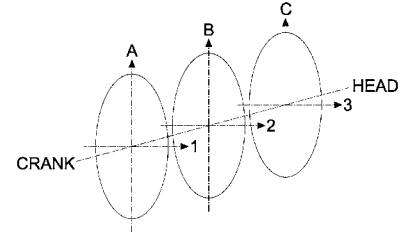
Figure 10: Cylinder bore measuring points

Dimension (mm)	NG Feed Stage 1	NG Feed Stage 2	Hydrogen Cylinder 1	Hydrogen Cylinder 2
A	358.80	244.52	244.05	244.05
1	358.78	244.50	244.00	244.02
B	358.90	244.89	244.09	244.10
2	358.84	244.97	244.05	244.11
C	358.78	244.51	244.11	244.11
3	358.78	244.52	244.05	244.11

Figure 11: Cylinder bore diameters recorded during inspections

Packing Rings

The packing rings showed normal wear. However, there were some broken springs and packing rings in one of the hydrogen compressor packing cases (See Figure 12). All packing cases were cleaned up and packing rings were replaced with rings of the same material.

Figure 12: Packing ring set – shows broken spring and packing rings

DESIGN & ENGINEERING

Non-lubricated Moderate Speed Reciprocating Compressors in a Hydrogen Plant, *Benjamin F. Williams, Laurent Richaume;* ARIEL CORPORATION, AIR LIQUIDE ENGINEERING & CONSTRUCTION

Valves

Due to the rotating speeds of moderate speed reciprocating compressors; a common industry concern is the number of times the compressor valves open and close; as compared to those of a longer stroke, slow speed compressor. In this case; the compressor valves are cycling at 744 times per minute. The valves for both units were inspected and all valves looked good. The valves were re-installed in both compressors. Air Liquide plans to replace the valves at the 16,000 hour inspection.

6   Conclusion

Moderate speed compressors have performed well in hydrogen and natural gas feed services at an Air Liquide hydrogen plant in Argentina. After 9300 hours of operation, two of the four compressors were inspected and the cylinder wear parts (piston trim, packing and non-metallic valve components) showed little or no wear. This can be attributed to a number of things, including clean, dry gas at the compressor suction, wear part material selection, conservative design and application, as well as reduced piston speeds.

In simple terms; piston speed affects the "rubbing parts". Although the rotating speed is higher than "normal" for these types of applications; the short stroke, moderate speed compressors installed at Campana have very conservative piston speeds. The low piston speeds have a very positive effect on the life of the wear parts.

Although the valves in these cylinders cycle more often than what would be considered "typical" for the industry; these valves were found to be in very good condition and were reinstalled for continued use.

It is important to note that the moderate speed compressors detailed herein use non-cooled, unlined cylinders. The commonly held industry viewpoint is that cylinder cooling and liners are necessary for successful operation; especially in those applications requiring non-lubricated compressors. However, as the inspection results described in this article show; there is an alternative design suitable for these applications.

With a conservative design and application; along with proper material selection and package design; moderate speed reciprocating compressors are very well suited for use in critical services, such as hydrogen plants.

7   References

[1] Google Maps – Map of Campana, Argentina

- Dimensional data included herein was taken from Air Liquide inspection / maintenance reports dated 22 June 2011 and 27 December 2011.

Acknowledgements

8th Conference of the EFRC
September 27th / 28th, 2012, Düsseldorf

PROGNOST Systems GmbH

Bridging the gap between safety protection and condition monitoring

by:

Eike Drewes

PROGNOST Systems GmbH

Rheine, Germany

Email : eike.drewes@prognost.com

8th Conference of the EFRC
September 27th / 28th, 2012, Düsseldorf

Abstract:

In the reciprocating machinery industry it is still common that users safety protection equipment and condition monitoring is strictly separated. Machine operators frequently face a time consuming troubleshooting with minimum diagnostic data e.g. from the DCS system. Since many years flight data recorders are a common standard in the aviation industry to perform post-incident analyses of aircraft accidents. Such data recorders are also available for protection systems now and could be used to upgrade the diagnostic information.

The paper describes how transient data recorders built into a protection system can not only support the post-incident failure analysis, but even more can be used to provide on-demand information of the compressor condition. They can be used to improve the traditional snapshot monitoring program that is still widely in place on reciprocating machines and deliver information whenever it is required without waiting time for an analyst to come and take the measurement. Whenever they are closely integrated to the protection system, they are much more cost efficient than full equipped condition monitoring systems and close the gap between equipment protection and online condition monitoring.

1 Maintenance strategies and condition monitoring of machines

When operating rotating machinery different maintenance strategies are applied. The simplest method is to run a machine until it stops due to a failure. This method, known as run-to-failure method, is still widely applied, but bears the risk that a comparably small damage can cause rather large consequential damages. Whether this method is acceptable depends on the criticality of the machine and on the availability of spared machine capacity.

When certain wear processes in the machine are well understood and the timely progress of wear is known, those parts should be replaced shortly before their lifetime is reached to maximise use of the wear potential and prevent component failures (Preventive Maintenance).

However, the lifetime of many components of reciprocating compressors such as valves and bearings is not subject to linear wear making it difficult to decide on the best time to replace a component mainly on completed operating hours. Maintenance decisions on components that are experiencing non-linear wear are challenging and can not be made time based. It requires monitoring of certain parameters that allow judgement on the component's condition and an estimation of the best time to replacement. This is called Predictive Maintenance.
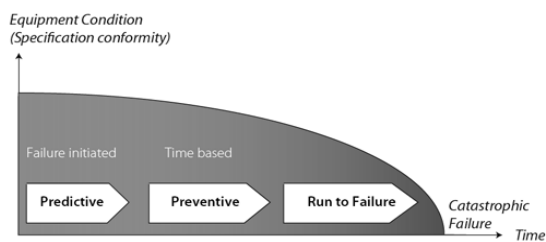
Fig. 1: Basic maintenance strategies

Which maintenance strategy is applied depends mainly on two parameters:
    a)   the criticality of the machine
    b)   the availability of a spare compressor

The total population of machines can be grouped in three main categories.
    Category I   Critical, unspared
    Category II   Critical, spared
    Category III   Uncritical, spared
    Category IV   Uncritical, unspared
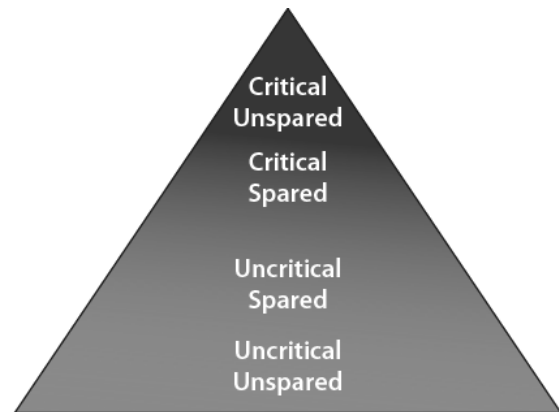
Fig. 2: Proportion of machinery in the four categories of criticality

Generally the more critical a machine the less acceptable it is to run it to failure or to rely on preventive maintenance, because an unexpected failure with a machine shutdown has a negative effect on the production or safety. The availability of a stand-by compressor will reduce the requirement for predictive maintenance, but has no effect on the level of safety that is required i.e. it may be acceptable to pay for a costly repair that is a rare event, but a gas leak with an explosion and fatality can not be accepted.

2 The gap between protection and condition monitoring

Especially uncritical and spared reciprocating compressors are still operated without or with a minimum of protection. Regardless of the maintenance strategy most of the critical reciprocating compressors are equipped with at least basic protection typically using frame vibration, low lube oil pressure and discharge gas temperature. The number of primary damages is large, so that a complete coverage of all imaginable primary damages would require an almost indefinite amount of monitoring parameters. Therefore a compromise between limitation of consequential damage and amount of protection parameters is widely practiced. Depending on the degree of the acceptable damage the protection parameters are determined.

An overall guideline on the on the essential protection parameters e.g. can be obtained from the API618. However, this should be considered as the bare minimum and does not reflect all recent experiences of the industry.

Bridging the gap between safety protection and condition monitoring, *Eike Drewes;* PROGNOST SYSTEMS GMBH

Condition	Alarm	Shutdown
High gas discharge temp for each cylinder	X	X
Low frame lube-oil pressure	X	X
Low frame lube-oil level	X	--
Cylinder lubricator system failure	X	--
High oil-filter differential pressure	X	--
High frame vibration	--	X
High level in separator	X	X
Jacket water system failure	X	--

Tab. 1: API 618 4th edition: Minimum Alarm and Shutdown Requirements for Reciprocating Compressors

Frame vibration is typically considered a parameter that provides basic information on the mechanical condition of the compressor. However, in the past years it has been widely accepted that frame vibration is not sufficient for mechanical safety protection. Monitoring vibration impacts on the crosshead slide has been recognized as a better method detecting all major mechanical problems of the motion work. Recent experience has also shown that piston rod failures can only be prevented by monitoring dynamic piston rod position (piston rod run out). Only if a piston rod failure is considered an acceptable damage crosshead slide vibration is sufficient for mechanical protection.
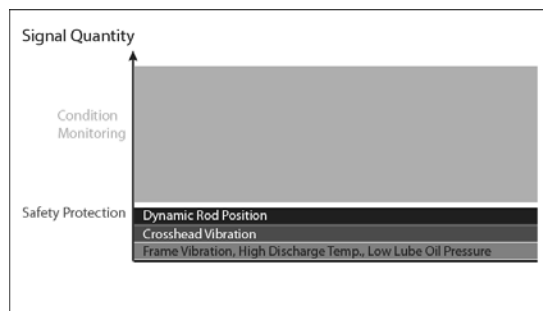
Fig. 3: Typical methods of safety protection for recip compressors

Protection systems are typically designed to work based on simple but reliable RMS parameters e.g. RMS vibration. Some of the values are transferred to DCS systems, but most protection parameters such as low frame lube pressure or low suction pressure are not useful to provide diagnostic information for preventive or predictive maintenance.

Piston rod position is a parameter that is directly "located" at the gap between protection and condition monitoring. The two different parameters, vertical piston rod position to indicate rider ring wear piston rod run out indicating the mechanical health of the piston rod and its connections are coming from the same sensor and signal. It is economical to use both parameter, one for protection and one for condition monitoring. However, in most applications only one parameter is used, either for protection or for condition monitoring.

3 How can the gap between protection and condition monitoring be bridged?

Bridging the gap between condition monitoring and protection systems means using monitoring sensors for both purposes. This is more economic and increases the quality of both protection and condition monitoring. One way to bridge the gap is to save high frequency signal data for detailed analysis in a memory attached to the protection system. The aviation industry has introduced flight data recorders since decades, however, it is only used in post mortem analysis. But why should recorded data only be used when a damage has occurred?

Using the protection sensors for condition monitoring purposes is one option, another option is increasing the frequency and signal quantity of monitoring sensors and continuously recording the data for on demand diagnostic purposes.
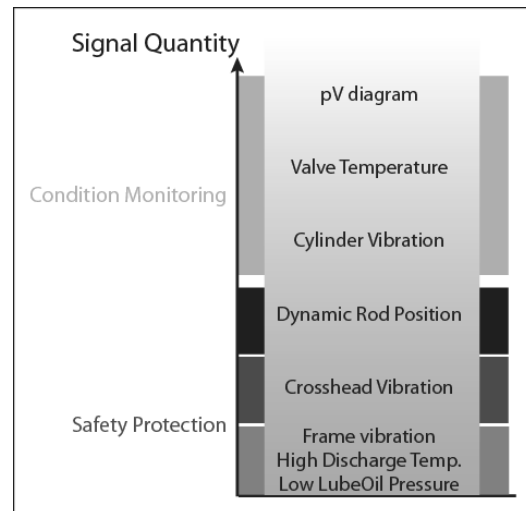
Fig. 4: Typical levels of safety protection and condition monitoring for recip compressors

Reciprocating compressor diagnostic condition monitoring is typically based e.g. on p-V diagram analysis and cylinder vibration or vibration monitoring of crankshaft bearings. Primarily information on the condition of components such as

suction/discharge valves with comparably high failure rates is collected. This is often done with periodic snapshot monitoring in order to save investment cost for sensors, cables and diagnostic systems. However, trended data is providing continuous information with a much higher diagnostic quality as compared to a periodical snapshot data collection (Offline Monitoring).

The diagnostic quality of condition monitoring data is defined by two variables: quantity of signals/sensors time the signal is available /frequency of the recordings.

The diagnostic quality of offline monitoring can not be improved by increasing the number of monitored sensors indefinitely. Adding some of the offline sensor positions to a permanent data recorder will add diagnostic quality, because it allows on demand access to online data and gapless trended data. The information always results from the same sensors and can be obtained without a risky activity of personnel in the field operating a portable data collector. This is a particular advantage offshore, where the deployment of people is always a matter of logistics.
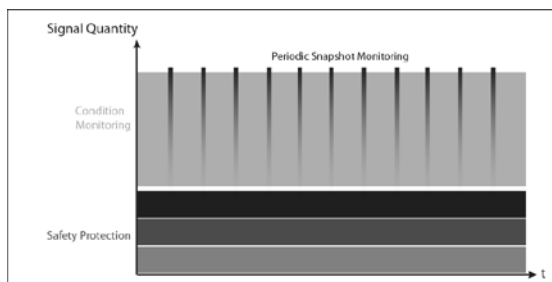
Fig. 5: Stretching diagnostic quality

4   What is the cost benefit compared to condition monitoring systems?

Online monitoring is often considered too costly for uncritical and spared machines. Investment cost are coming from six areas:
a) sensors
b) field wiring
c) data acquisition systems
d) computerised server and monitoring systems
e) monitoring and diagnostic software
f) analyst know how

Online data recorders have a competitive price advantage in three out of six points:
b) Field wiring
d) computerised server and monitoring systems
e) monitoring and diagnostic software

These three areas typically cause more than 60% the total investment. This underlines that permanent data recorders may provide a significant upgrade in diagnostic quality at an economic scale.

Today modern protection systems offer the opportunity to be expanded by high frequency data recorders. The data acquisition platform is common, but the data recording does not interfere with the protection function. In case of a machine shutdown all important instrumentation is available for on demand analysis. While portable offline data collection often comes too late such data is recorded gapless and therefore always is available for the critical moment in time. This way answers on what has caused the shutdown can be obtained immediately and the gap between condition monitoring and protection can be overcome.

5   Summary

Today still a large portion of the population of reciprocating compressors is operated without condition monitoring and even protection systems. Depending on the maintenance strategy and the criticality of the machine both technologies are used. There is currently a gap between protection and condition monitoring resulting from the installed monitoring sensors either used for protection or condition monitoring purposes. Additionally large amount of diagnostic information is collected with portable data collectors. The quality of the condition monitoring and diagnostics can be improved by using online data recorders with the modern protection systems that offer the possibility of detailed root cause analysis in case of shutdown alarms or on demand data analysis at any time when required for diagnostic purposes. This is provides a significant increase in the diagnostic quality at a competitive price compared to offline monitoring with portable analysers. This option should be considered whenever installing new equipment or existing monitoring and protection hardware is upgraded.

Digital communication technologies have arrived at condition monitoring systems for reciprocating compressors

by:

Stachel Klaus
Product Management
klaus.stachel@hoerbiger.com

Locken Tomas
Research & Development
tomas.locken@hoerbiger.com

HOERBIGER Compression Technology
TechGate Tower 15th floor
Donau-City Strasse 1
1220 Vienna, Austria

8th Conference of the EFRC
September 27th / 28th, 2012, Düsseldorf

Abstract:

Traditional condition monitoring systems comprise of sensors that are installed at the compressor and electronic processing units that are mounted in the cabinet room. The analog high frequency output signal of vibration, indicator pressure and rod-position sensors are each wired by instrumentation cables to the processing units. This is in contrast to other applications in process industry where digital communications like remote I/Os and field bus have been used for data transfer and safety systems for many years. Compared to analog signal transmission the digital data transfer based on remote I/Os reduces costs, has less limits regarding installation, is more robust against interferences and allows for the implementation of self-monitoring technologies to ensure data integrity. Up to now remote I/Os have been available only for relatively slow signals and therefore not suitable for real-time compressor condition monitoring systems. This paper presents the new technology for the digital transfer of high frequency signals and compares both technologies – analog and digital – based on a user perspective.

Digital communication technologies have arrived at condition monitoring systems for reciprocating compressors,
Klaus Stachel, Tomas Locken; HOERBIGER COMPRESSION TECHNOLOGY

1   Introduction

Digital communication technologies like Profibus, Foundation fieldbus and Modbus have become very common for process control and data exchange. This is because many transmitters or other devices share the same set of cables rather than requiring a dedicated set of cables per device as in the case of parallel signal transmission. Moreover, several parameters can be communicated per device in a fieldbus network whereas only one parameter can be transmitted on an analog connection.

In the past, safety automation had to be "hard-wired" and based on "relay" technology due to existing international standards. This changed with the advent of a new standard – IEC 61508 – specifying how microcontrollers and software have to be designed for use in safety applications. This triggered the development for example of PROFIsafe, which was to integrate safety into the existing standard fieldbus technologies. Today, fieldbus technologies are used for applications which must meet safety-relevant standards like IEC 61508.

However, all industrial fieldbus systems have been designed for process control and have data transmission rates that are relatively low; for example Profibus PA offers a rate of maximum 31.25 kBit/s. Hence, existing field bus systems are not suitable for compressor condition monitoring systems with remote analysis of high dynamic data like vibration in time-wave form, indicator pressure and piston rod displacement. So in the past condition monitoring systems have used analog signal transmission from the sensor via the barriers to the monitoring rack in the safe zone.

2   Layout of traditional systems

With traditional condition monitoring systems several and different type of sensors are installed at the compressor and are wired individually to the barriers and signal conditioners in a cabinet. These interfaces are further linked to the monitoring electronic processing units.
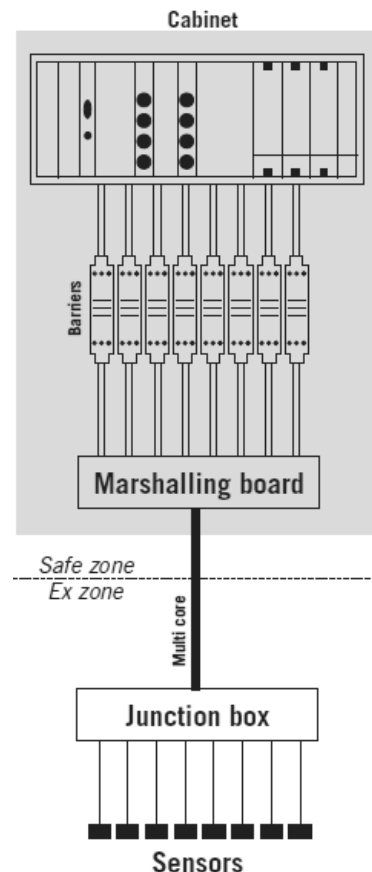
Figure 1: Traditional system layout

The field instruments typically installed on reciprocating compressors for condition monitoring are accelerometers and velocitymeters for vibration monitoring, indicator pressure transmitters for performance and rod-load monitoring and rod-drop transmitters for rider ring wear and piston-rod run-out monitoring.

All these types of transmitters are intrinsically safe, since the compressors are mostly installed in the hazardous area. A device termed intrinsically safe is designed to not contain any components that produce sparks or which can hold enough energy to produce a spark of sufficient energy to cause an ignition. This is achieved by ensuring that only low voltages and currents enter the hazardous area, and that all signal wires are protected by safety barriers.

Accelerometer and rod-drop transmitters have voltage as electrical output, whereas velocitymeters and indicator pressure transmitters provide typically a current signal.

Operation of accelerometers over long cables affects frequency response and introduces noise and distortion when an insufficient current is available to drive cable capacitance. The maximum frequency that can be transmitted over a given cable length is a function of the cable impedance and the ratio of

CONDITION MONITORING

Digital communication technologies have arrived at condition monitoring systems for reciprocating compressors,
Klaus Stachel, Tomas Locken; HOERBIGER COMPRESSION TECHNOLOGY

the peak signal voltage to the current available from the signal conditioner

Although Integrated Circuit Piezoelectric (ICP) type accelerometers provide a high voltage, low impedance output well-suited for driving long cables through harsh environments the maximum cable length is limited to around 300meters.

The following chapters present an electronic development that allows users of condition monitoring systems to benefit from state-of-the-art communication technologies and to push the limit of maximum cable length further to support modern process plant layouts.

3 Digital communication

Digital communication is today a proven technology and has been used in many application areas for a long time. The area perhaps most known is the telecom industry where digital communication has been the standard for products over the last 40 years.

In the automotive industry the CAN-bus has been the standard bus for transferring information between different parts of the vehicle. In recent years also optical buses have been introduced when the amount of data transferred and speed requirements has increased.

Within the industrial applications bus types like CAN and RS-485, Modbus or Profibus protocols are used traditionally. More recently also Ethernet has made its way into these applications.

When it comes to safety aspects the fly-by-wire technology used within the aircraft industry has proven that even for highly safety critical applications digital communication is the preferred option to use.

3.1 System Overview CIU²- FTIM²

Before describing the features in more detail, the system layout enabling digital high-speed communication between transmitter and electric processing unit is introduced.

Figure 2 shows the system overview including the base unit CIU² (Central Interface Unit) and the transmitter interface module FTIM² (Fast Transmitter Interface Module). In total the base unit can handle up to six transmitter interface modules at the same time. As shown by the figure this is a distributed system where the parts sometimes are located with a long distance from each other. The CIU² and FTIM² are physically connected together

by an industrial Ethernet CAT (category) 7 or higher cable to ensure best possible transfer of signals.
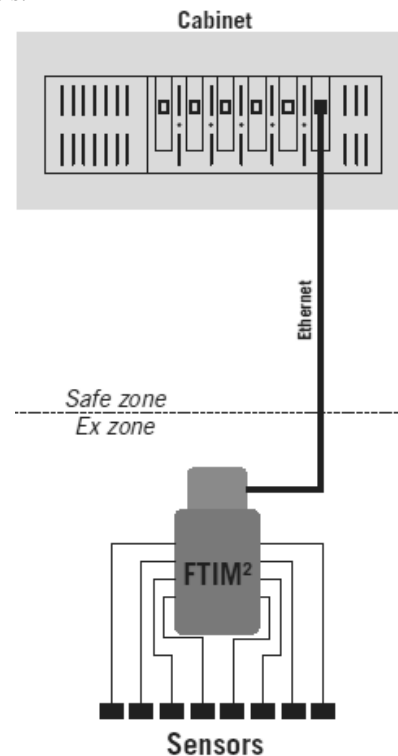
Figure 2: System layout with digital communication between field devices and cabinet

3.2 Power over Ethernet

For distributed systems the power supply needs to be solved in an economic, reliable and safe way. At compressor plants where it is preferred not to have individual power sources located close to the distributed units, the best option is to supply power from the base unit through the same cables that is used for data communication. This technology called Power over Ethernet (PoE) is today common and well proven for various applications like remote cameras, Ethernet phones and other network accessories. A big advantage is that the equipment can be installed where it is most suitable for operation without consideration of available power supply or even the need pulling additional power cables.

PoE is defined and specified through the standard IEEE 802.3af. It is a robust and safe way to connect remote end devices and have data exchange and power at the same time through the same cable. It is an attractive choice when the power consumption is modest and the application requires long cable runs. The standard also sets specific requirements for the cable used to ensure correct functionality and low level of disturbances.

CONDITION MONITORING

Digital communication technologies have arrived at condition monitoring systems for reciprocating compressors,
Klaus Stachel, Tomas Locken; HOERBIGER COMPRESSION TECHNOLOGY

In the HOERBIGER compressor monitoring system PoE is implemented in full compliance with the standard IEEE 802.3af for the power supply of the distributed FTIM² located close to the compressor. The base unit CIU² is the power distributer and supplies each FTIM² with power individually through an industrial Ethernet cable. This enables the CIU² to have full individual control of the power supplied and also to diagnose and act on errors such as short cut, over- and under voltage to ensure safety and reliability. When an error has been detected the power is turned of immediately and is not turned on again until demanded.

3.3 Data transmission and control

For any digital data transmission to take place there needs to exist an electrical interface to transfer the data and a protocol that defines the structure of the information sent and received.

For the data transmission between FTIM², placed remotely at the compressor, and CIU² an extended version of the electrical interface RS485 is implemented and used.

Figure 3: FTIM² certified by ATEX, FM, CSA

Extended RS485 means that a special hardware component is used to handle the long distances required for the data transmission. This component also offers high ESD protection and failsafe operation. Since distances of up to five hundred meters are required for the data transmission this would not be possible without the advanced hardware component without the use of repeaters.

The protocol for the data transmission is based on S/PDIF according to the standard IEC 60958. This protocol supports Bi-phase marked code which means that data and clock information are combined and leads to a self synchronized data stream. This is essential for the synchronisation of the data traffic flowing between the CIU² and the FTIM².

The digital communication channel between the two units is capable of handling speeds up to 4 Mbit/s. This high capability is needed in order to transfer

the large amount of data that are measured by the FTIM² during one revolution. The sampled data is pre-processed by the FTIM² and then packaged and sent in frames to the CIU².

Figure 4: Base unit CIU² / 335 x 260 x 100mm

The transmission path is implemented as a point-to-point connection. To achieve high safety and availability of the data transferred, two separate transmission channels are used. The main channel is used to send and receive data between the units under normal condition. The second channel is used as a retransmission channel for fault handling to avoid loss of data or congestion on the main channel.

The data flow consists of two main parts – Firstly a request message from the CIU² containing timing information and a request for the sampled sensor data. Secondly the corresponding response message from the FTIM².

In figure 5 it can be seen how the data sampled from sensors are divided into data packages. The packages are called segments. Each compressor revolution of sampled sensor data consists of several segments.

The data sent/received is carried within a frame to achieve highest possible safety in terms of not loosing any data and to detect if data has been corrupted during the transfer. Each segment of sampled data is divided into four of these frames to further increase the integrity of the sent segment (package). How the data from one segment is divided can be seen in figure 6.
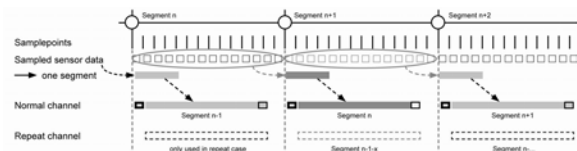
Figure 5: Data sampled into segments and repeat channel.

CONDITION MONITORING

Digital communication technologies have arrived at condition monitoring systems for reciprocating compressors,
Klaus Stachel, Tomas Locken; HOERBIGER COMPRESSION TECHNOLOGY
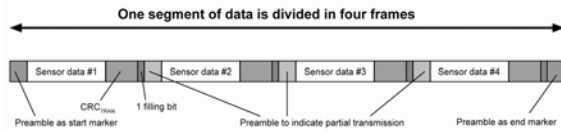
Figure 6: One segment of data divided in frames.

Each frame consists of a preamble describing the type of message, the sampled sensor data followed by a checksum calculation (CRC$_{TRAN}$) securing the data integrity. At the end a preamble is added to the last frame to indicate the segment end.

The CRC detects if the data sent has been corrupted in anyway during the transfer. The way to do this is to calculate a unique number out of the data you are about to send. First this is done by the transmitting unit (FTIM²), and this calculated number (CRC$_{TRAN}$) is included in the frame. When the frame is received the same calculation is done by the receiving unit (CIU²) on the data package. The two CRC values are then compared and if not identical the data is corrupted and the transmission has failed. When a transmission failure is detected the second channel is activated and a retransmission of the faulty segment is initiated.

The initiation of retransmission is done immediately and the lost segment is sent in parallel on the spare channel during the following normal transmission of data.

3.4 Fault detection and monitoring

As already mentioned previously the power lines are monitored individually and as soon as failures are detected actions are taken to secure safe and reliable operation. The data transferred over the same cable is protected by the CRC calculation to detect any corrupted parts of the transmission.

In addition to these fault detection strategies for the data and power the HOERBIGER monitoring system has other self monitoring functionalities of its components. All sensors are continuously monitored for several error conditions. These are errors like the sensor being unreachable or operated outside the measurement range, if the sensor gets stuck in any position or if voltage and current levels are outside the defined limits. The FTIM² evaluates the sensor performance and sends the status information together with the measured sensor data on the digital communication lines back to the CIU².

All key hardware components like FPGA and CPU in the FTIM² and the CIU² are all monitored to detect any malfunction that can limit the performance of the system.

The CIU² evaluates continuously the status information and updates the system TRUST signal indicating if the system can be trusted or not. As soon as any safety related failures are detected the TRUST signal is removed and indicated to the user.

The system fulfils the requirements of IEC 61508 / 61511 (SIL) for machinery protection and is certified by TÜV Rheinland, Germany.

3.5 Processing and storage of digital information

To have the data in digital format gives a wide range of possibilities for processing and storage. All digital sensor data received by the CIU² is stored for further processing on the CIU² itself. The sensor data received consist of two main parts - status information (already described in 3.4) and the actual reading from the sensor.

The sensor data is stored in a buffer designed to hold a minimum of five hundred revolutions of data for each sensor. The size of the buffer is predefined why the exact number of revolutions stored depends on the number of input channels (sensors) configured. When the buffer is full the oldest information is removed according to FIFO (First In First Out) in order for new data to fit into the buffer. After the initial control to ensure that the data received is complete and without errors the data processing starts with the Event Manager. Here the sensor data are checked against the two types of limit levels (alarm and safety alarm). These are limit sets configured by the user to monitor and protect the compressor. For each sensor a total of sixteen limit sets can be configured. Every limit set for dynamic signals can have up to 360 individual limit values over one revolution – a feature designed to monitor vibrations in the most effective and reliable way.
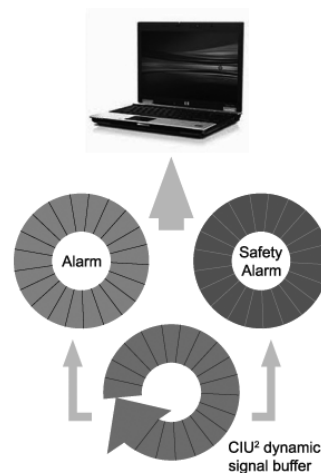
Figure 7: Dynamic signal buffer on CIU².

CONDITION MONITORING

Digital communication technologies have arrived at condition monitoring systems for reciprocating compressors,
Klaus Stachel, Tomas Locken; HOERBIGER COMPRESSION TECHNOLOGY

In the event of a limit violation resulting in an alarm or safety alarm the latest 500 revolutions of the compressor crankshaft of sensor data surrounding the event will be stored and saved in a separate event buffer on the CIU². This functionality of storing important digital data gives numerous possibilities for processing of the information in later stage. The complete content of the event buffer can be downloaded into a PC application by the maintenance supervisor or reliability engineer for evaluations and analysis.

4   Comparison of both technologies

In general, when data is transmitted a certain amount of noise may enter into the signal. Noise can be natural or manmade for instance lightning, cell phones, starting of large electric consumers or operation of frequency converters. Electrical interference may result into incorrect compressor performance assessment or at the worst into nuisance alarms and compressor trips. Although noise and interference cannot be completely removed in the transmission of an analog signal, with good engineering and proper installation, many of the effects of noise and interference can be reduced (shielding cables, twisted pairs). But analog transmission especially of voltage signals always bears some risk of signal interference.

Voltage signals are filtered by the impedance of the wire. While digital transmissions are also degraded, slight variations do not matter since they are ignored as long as they are within the tolerance for binary zero and one when the signal is received. With an analog signal, variances cannot be distinguished from the signal and so provide a kind of distortion. In a digital signal, similar variances will not matter, as any signal close enough to a particular value will be interpreted as that value. Techniques such as check sum calculations are used to detect errors and guarantee error-free communication through redundancy or retransmission.

Beside higher accuracy and robustness against interferences digital communication of dynamic signals offers following advantages through all stages of a project:

Installation and commissioning phase

- Reduced wiring, and therefore, easier project engineering, fewer engineering hours and less documentation.

- Adding further signals at later stage does not require extension of central infrastructure like cabinets.

- Less number of cables, cable routes, terminal blocks and marshalling boards.

- Less barriers in the cabinet, since barriers are incorporated in the FTIM.

- Faster implementation and commissioning.

- Lower costs for installation of cables, cable connection, and checking.

- Reduced faults in implementation.

- Less space required .

- Allows for increased cable length compared to analog techniques - thus supporting modern plant design concepts.

Operation phase

- Higher transmission reliability due to redundant channels.

- Digital communication is more sustainable to noise.

- Plausibility checks can be done to confirm the data transmission integrity.

- Communication of processed measurement value and sensor status from field to monitoring system.

Maintenance phase

- Less training required, since less complex system layout and fewer parts is included in the system.

- Quicker identification of problems.

5   Conclusion

Performance monitoring and adequate machinery protection systems allow for assessing the condition of the compressor while it runs, support maintenance decisions and protect valuable assets. Repair work can be planned in better way and spare parts can be organized in time. Most important: downtime can be reduced which results in increased production.

It is expected that the utilisation of digital communication technologies will be the future path for premium condition monitoring and protection systems for reciprocating compressors.

Localization of reciprocating compressor components faults using on-line dynamic correlation of impulsive vibration signatures with calculated forces and displacements at individual running gear components

by:

Rossi Gaia
Application Engineer
GE Measurement & Control
Italy
gaia.rossi@ge.com

8th Conference of the EFRC
September 27th / 28th, 2012, Düsseldorf

Abstract:

Vibration monitoring is essential for detection of failures at running gear components (connecting rod, crosshead, piston rod and piston) of critical reciprocating compressors in the petroleum, chemical and gas industry service; however, the complex vibration signature resulting from the characteristic impact events at the running gear presents some unique interpretation challenges for early failure identification. As components failure modes differ significantly from case to case, different approaches have been considered by specialists, ranging from empirical to first principles based methods, to associate a vibration pattern with a failure mode. Advances in diagnostic and signal processing technologies provide powerful real-time analytics for identification of mechanical malfunctions. Developments in data analysis demonstrate the value of correlating events in vibration signal with parameters derived from on-line cylinder pressure measurement and kinematic analysis of rod loads and vertical force at crosshead to localize the source of the failure independently of load conditions at early stages, avoiding escalation into secondary damage and reducing cost of repair and of extended unplanned downtime.

Localization of reciprocating compressor components faults using on-line dynamic correlation of impulsive vibration signatures with calculated forces and displacements at individual running gear components,
Gaia Rossi; GE MEASUREMENT & CONTROL

1   Introduction

In the recent years, an increasing number of users decided to adopt a health management program for critical reciprocating compressors, where a crucial role is played by an on-line monitoring system consisting of transducers, monitoring hardware and diagnostic software to analyze compressor parameters, to provide essential information for machine management and support an effective Condition Based Maintenance program

This trend responds to the need of implementing a predictive maintenance approach to reduce maintenance costs and improve safety availability, cost and regulatory compliance. Trending and alarming on casing vibration only is not adequate for such approach, therefore technology focus is on advanced analysis tools for early malfunction identification though dynamic behavior analysis and move away from just trend monitoring for safety shutdown and move up to predictive analytics.

In particular for reciprocating compressors in oil and gas services, asset criticality determines the monitoring strategy. The methodologies for machine protection and for machine condition assessment are different. For example, while casing vibration transducers connected to control system will provide a trip in emergency, they do nothing towards providing information for evaluating machine health and malfunction type and managing below the trip level. Condition Based Maintenance programs employ condition monitoring systems with the aim of scheduling "informed" maintenance when it is most cost-effective and precedes functional failure.

However, when it comes to monitoring and protection requirements for reciprocating compressors in process plants, standards are not very comprehensive nor do they all agree.

Over the last years, the majority of equipment manufacturers, users, and experts have been increasingly in agreement about considering crosshead vibration an essential parameter for monitoring and protection, to complement the traditional frame vibration monitoring as specified in API 618 standard current release. Nevertheless, at this time the relevant international standards provide very limited insight on this subject. This article aims to provide clarification on some basic concepts.

2   Vibration analysis on reciprocating compressors

Years of field experience have demonstrated that techniques which may be well understood for analyzing rotating machinery vibration produce confusing results when applied to reciprocating machinery.

The reason is the different source of these vibrations and how the system responds. Vibration associated with rotational speed is the dominant motion on industrial rotating machines and this synchronous behavior allowed the direct application of these concepts towards addressing common machinery malfunctions, as rotor unbalance. The typical vibration frequencies observed with those common malfunctions generally occur between a quarter of running speed and twice running speed and correlate excellently with machine mechanical conditions. Consequently, principles and diagnostic methodologies are broadly accepted and harmonized among the machinery diagnostic collectivity.

This is not quite true for reciprocating compressors. Vibration analysis of these machines creates some unique challenges, because many forcing functions produce a complex signature in the vibration measurement that makes any attempt of using standard analysis techniques used for rotating equipment ineffective.

2.1   Compressor Frame Vibration

Vibration measured on reciprocating compressor frame results essentially from the response of the mechanical system to the main forces and moments that are occurring in the machine at running conditions, as:

- Gas load forces, acting on the piston and stationary components at 1x and at whole multiples of running speed, generally significant up to 10x, in the alternating direction of the piston rod travel. For large process compressors, those are typically the largest contributor to piston rod and compressor frame load.
- Reciprocating and rotating masses unbalance. These are predominant at 1x and 2x compressor speed.
- Gas unbalance forces in the pulsation bottles, pulsation at the cylinder nozzle area and on piping.

As a consequence, the extent of vibration is inherent with the reciprocating compressor design and its response to all the applied forces and moments. This causes these machines to generally vibrate more than a comparable rotating machine in normal conditions.

Figure 1 shows that many harmonics are produced by the complex shape a of frame vibration (velocity) waveform.

Localization of reciprocating compressor components faults using on-line dynamic correlation of impulsive vibration signatures with calculated forces and displacements at individual running gear components,
Gaia Rossi; GE MEASUREMENT & CONTROL
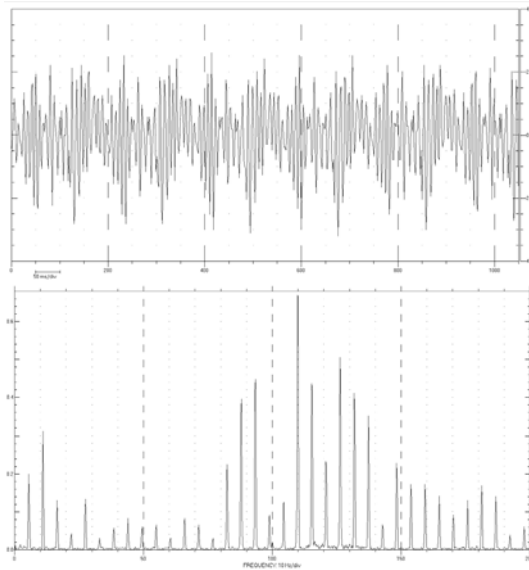
Figure 1: Frame velocity timebase waveform and related spectrum, full load conditions

Monitoring frame vibration with a velocity transducer is appropriate to detect an increase of these rotation-related forces (due to gas load or inertial imbalance, foundation looseness, excessive rod load). The preferred transducer location is on the side of the frame in the direction of piston rod travel, on the centerline of the crankshaft main bearings where dynamic load is transmitted. The magnitude for a filtered frame velocity signal is usually low (less than 7 mm/s RMS); however, at low frequencies, even small amplitudes of measured velocity may correspond to large amounts of displacement.

On the other hand, measuring only frame vibration can be insufficient, as the increase in frame velocity from incipient failures developing at the running gear or cylinder assembly will be small and typically covered by the larger vibration contribution due to machine movement. By the time the malfunction has been detected by the frame velocity transducer and the compressor shut down, major secondary damage may have already occurred. Malfunctions as liquid or debris carryover, loose piston or piston nut, loose crosshead nut, loose liner, typically manifest themselves with impacts transmitted at the crosshead.

Frame and crosshead vibration measurements are different in principle and related benefits as will be discussed.

2.2 Vibration monitoring and Impact Monitoring

Analysis of reciprocating compressor vibration is complex due to the nature of the generated signals

and conventional analysis of broad band time based waveforms and spectra are of limited value. Vibration transducers monitoring rotating machinery generate stationary signals; this means they have constant frequency content over the revolution as Figure 2 shows.
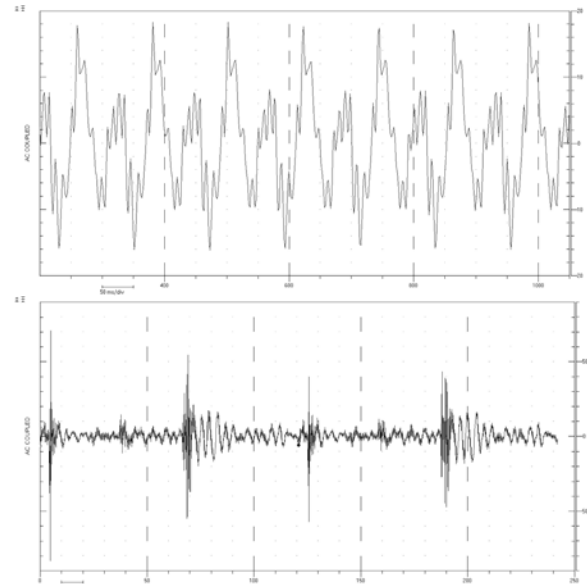
Figure 2: Example of stationary and non-stationary signal (waveform of motor bearing vibration and compressor crosshead vibration)

In contrast, seismic transducers on reciprocating compressors generate both stationary and non-stationary content. In particular, the signal generated by an accelerometer placed vertically on a crosshead guide is characterized by different frequencies with different amplitudes at different points in the revolution. The right end plot in Figure 2 shows a typical crosshead vibration waveform. The signal shows high amplitude, short duration "peaks" followed by a "ring down" that occur irregularly during a revolution. This signal is not filtered so the transducer is picking up the widest range of frequencies (Typically from 10Hz to 30 kHz).

These acceleration peaks can be referred to as response to impulse events occurring during compressor normal operation (valve opening and closing, gas flow noise, crosshead pin impacts at rod load reversal). Impulses due to mechanical knocks excite the structural resonances of the machine components that result in high frequency, free vibration and the characteristic impact/ring-down profile.

As said, the main purpose of vibration readings on the compressor frame is to detect vibration related to periodic forces. Whilst the overall frame

vibration increase is certainly a concern, the primary interest of crosshead acceleration monitoring is detecting vibration peaks associated with structure response to impulsive events. Conditions that increase the excitation of such resonances are generated by the developing faults as fractured or loose components or excess clearances. Loose rod nuts, loose bolts, excessive slipper clearance, worn pins as well as liquid in the process can be detected at early stages of development using crosshead impact monitoring, thus allowing appropriate countermeasures and avoiding potential catastrophic consequences.

Considering the occurrence rate and consequences of such type of failures, of all vibration measurements that can be applied on such compressors, crosshead vibration is probably the most effective protection measurement available, if correctly employed.

While crosshead acceleration has proven itself to be a sound measurement for detecting mechanical malfunctions, industry has little experience in applying and analyzing it, resulting in increased risks of false or missed alarms, and poor diagnostic value from diagnostic systems. Reference 1[1] presents some guidelines on proper transducer installation, settings, filter and signal processing.

2.3   Crosshead vibration analysis

So, how to determine the nature and severity of an impulse/impact event from a crosshead acceleration signal waveform?

When viewed in the time domain, the non-stationary crosshead vibration signal looks like multiple disconnected events; therefore diagnostic methodologies as spectral analysis provide little value due to the discontinuous frequencies.

The most appropriate analytic methodology is based on signal timing. An online condition monitoring system will synchronize the vibration signal with crankshaft rotation to associate vibration peaks to the piston position along the stroke. Individual monitoring and alarming of crank angle "bands" will allow association of peaks to the problem area.

For example, a crosshead vibration peak occurring when piston is travelling towards close to the top dead center can be related to liquid or debris ingression in the chamber. When piston moves towards its top dead center, the impact with the non-compressible material will generate an impulse event. The monitoring system will then raise an alarm at the corresponding monitored band (for

example, starting 10 crank angle degrees before top dead center and ending 10 degrees after). Figure 3 shows a liquid ingestion event as detected by crosshead accelerometer and relative graphic representation of piston position.
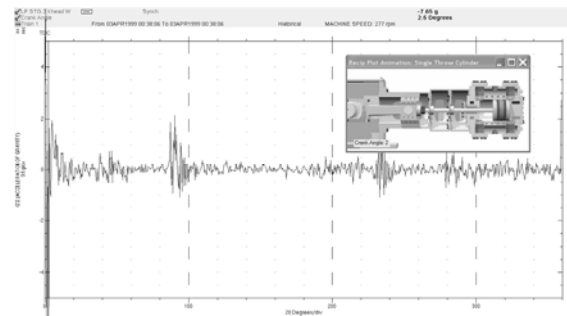
Figure 3:   Crosshead acceleration vs. crank angle, showing high peak at top dead center. The horizontal axis represents crankshaft degrees of revolution where 0° indicates top dead center

3   Diagnostic methodology

Even when peaks' position in crank angle domain is tracked, the large number of mechanical events occurring in a reciprocating compressor cylinder and running gear components present a real challenge for those attempting to determine the source of a knock. An additional challenge is represented by the variable operating conditions as operating pressures or compressor capacity regulation that frequently occur in these applications and generate different vibration patterns that need to be appropriately identified to avoid wrong diagnoses and missing an early failure detection.

Historical data based pattern recognition using segmented vibration data results in an unwieldy set of data given by the combination of the number of stages, load conditions, and failure patterns leading by several hundreds of patterns for a single machine, without considering the issues as concurrent malfunction events and stepless unloader operation.

To overcome these limitations, dynamic cylinder pressure measurement is key to provide real time load-tracking data analysis and positive identification of mechanical problems. This methodology relies on accurate online synchronization of vibration and pressure data with crank position reference.

Cylinder pressure measurement has long been recognized as an essential tool for cylinder performance and valve malfunctions analysis (for

Localization of reciprocating compressor components faults using on-line dynamic correlation of impulsive vibration signatures with calculated forces and displacements at individual running gear components, *Gaia Rossi;* GE MEASUREMENT & CONTROL

example through Pressure vs. Volume diagram analysis), however the ability to correlate events in the crosshead acceleration waveform with events in the pressure and rod load curves has great value in simplifying the diagnosis of mechanical failures as well.

From cylinder pressure, the monitoring system provides online calculation of piston rod loads, adding very valuable information on both machine potentially harmful operating conditions and on identification failures at running gear components as well, as will be described further.

Firstly let us clarify on the main forces derived from cylinder pressure measurement available in the online monitoring system.

3.1 Rod load

Forces due to the acceleration of the reciprocating masses (piston and rod assembly, crosshead assembly including pin) and the gas pressures in the cylinder place the piston rod under alternating tensile and compressive forces.

The combination of the gas loads and inertia loads evaluated at the crosshead pin in the direction of piston motion is the "combined rod load" as defined in API-618 5th edition[2] and it varies continuously throughout the revolution from minimum to maximum values.

The gas rod load for an operating cylinder on a typical process compressor with double-acting cylinders can be calculated by the monitoring system in real time, by multiplying the cylinder pressure measured at each degree of revolution by the active area of each piston face (blue line in Figure 4). The red line in Figure 4 shows the inertia force contribution as calculated from the reciprocating masses (piston assembly, rod and crosshead assembly) and speed. The resultant curve as algebraic sum of the gas and inertia forces is the green line in Figure 4 representing the combined rod load at crosshead pin.
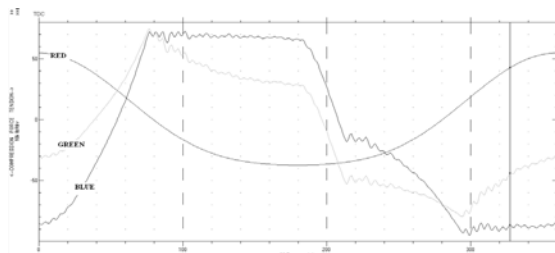
Figure 4: Gas force (blue line), inertia force (red) and combined force (green) vs. crank angle

Online rod load monitoring has great value in assessing machine stress by continuous calculation of maximum rod load as well as rod load reversal values for each degree of revolution.

A robust and reliable monitoring system must be capable of online combined rod load calculation, monitoring the peak rod forces (compression and tension) for each cycle in addition of other important parameters as in Table 1.

Monitoring System Outputs from Dynamic Cylinder Pressure Channel (for each crankshaft revolution)
Suction pressure
Discharge pressure
Maximum Pressure
Minimum Pressure
Compression Ratio
Peak Rod Load – Tension
Peak Rod Load – Compression
Degrees of Rod Load Reversal

Table 1: Outputs from online monitoring system

Fast developing catastrophic damage to crosshead pin and small end bearing can occur when rod load reversal is absent or heavily reduced, so rod load reversal must also be calculated and monitored directly by the protection system to allow reliable and prompt alarming. Several factors affect the actual rod load, including decreasing line pressures, process changes, improper operation of unloaders, valve failures, ring failure, process upsets, and machinery modifications.

At the same time, rod load curves are a key element for diagnostics, enabling association of knocks and impacts in vibration signal to a specific component malfunction.

3.2 Tracking load reversal points to detect mechanical malfunctions

The concept behind the diagnostic methodology is that impacts captured by a crosshead vibration transducer originate in the component that experiences a change in direction of force. If an impulse event can be correlated with a force change on a particular component, then the fault lies with that component.

In Figure 5, the combined rod load forces at the crosshead pin transition from compression to tension, and vice-versa twice during revolution (as shown by the green dots). This is when the crosshead pin moves from one side of the bushing to the other. When excessive clearance develops between the crosshead pin and bushing, a rapid build-up of velocity must be absorbed by the

CONDITION MONITORING

Localization of reciprocating compressor components faults using on-line dynamic correlation of impulsive vibration signatures with calculated forces and displacements at individual running gear components, *Gaia Rossi;* GE MEASUREMENT & CONTROL

bushing, resulting in a knock at the point where the combined rod load crosses the neutral axis. Therefore, knocks that occur near the point of combined rod load reversal typically indicate looseness or problems within the crosshead assembly.
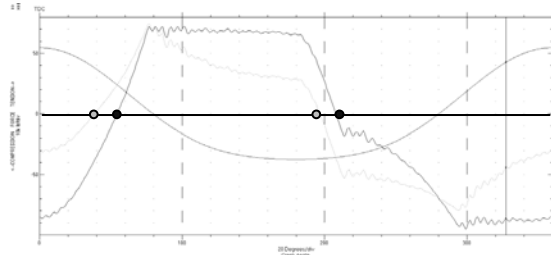
Figure 5: Gas force (dark dot) and combined force (clear dot) reversal points

The same would not happen in the case of a loose piston to rod connection, or a piston ring slap. Knocks caused by these malfunctions are not influenced by the reciprocating mass force so the knock will occur at gas load reversal points (shown by the blue dots on Figure 5).

Diagnostic tools automate this analytic principle to provide real-time identification of such malfunctions.

The online condition monitoring system processes pressure and force waveforms, then determines the location of each potential impact event and stores the corresponding crank angle. This algorithm accounts for compressor load changes (for example by means of clearance pocket unloaders). The degrees of crank angle at which the zero-force crossings occur are dynamically tracked and stored and a band in the associated crosshead acceleration waveforms is established. As these bands follow, or track, the condition of the cylinder they may be referred to as "tracking bands." The evaluation algorithm then establishes alarm levels within each associated vibration waveform band based on the impact event location.

For example, Figure 6 shows green, yellow, and red threshold band alarms for acceleration at the gas reversal points. If the impulse event amplitudes in all bands move into the yellow region, the system generates a piston-looseness "Alert" alarm. If all impulse event amplitudes move into the red region, the system generates a piston-looseness "Danger" alarm as in Figure 7 case.
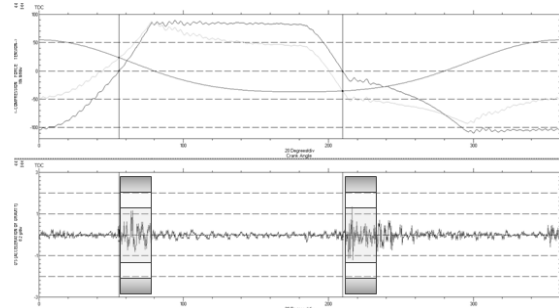
Figure 6: Rod Load Forces, crosshead acceleration and tracking bands

The algorithm processes in the same way also piston rod vibration measurement, as supporting evidence for the detection of a loose piston assembly.
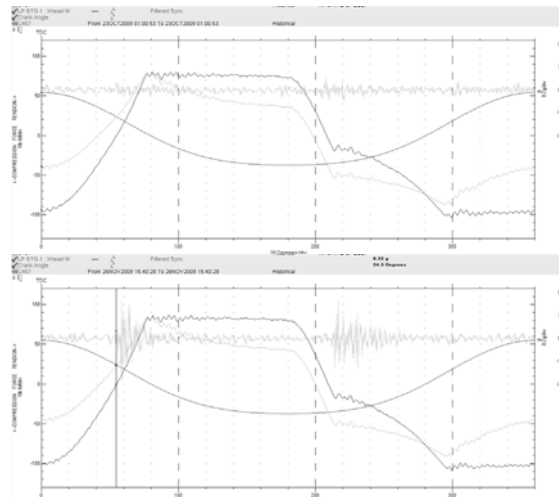
Figure 7: Crosshead vibration impacts at gas load reversal before and during a Piston Looseness event identified for an API 618 type compressor in make-up hydrogen service[3]

As a large amount of data is available to the user to review, automated diagnosis proves of great value in quick and accurate failures identification and since correlation is based on online load values, it is not dependent on process conditions as load and reversal points are continuously calculated and tracked.

4   Secondary forces at the crosshead

From the combined rod load calculated by the monitoring system, another interesting parameter can be obtained and used for further vibration characterization that is secondary force at the crosshead.

CONDITION MONITORING

Localization of reciprocating compressor components faults using on-line dynamic correlation of impulsive vibration signatures with calculated forces and displacements at individual running gear components,
Gaia Rossi; GE MEASUREMENT & CONTROL
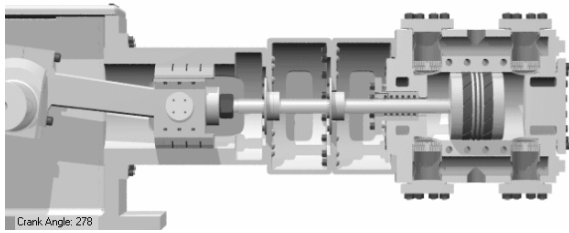
Figure 8: connecting rod, crosshead, piston and rod assembly

The crosshead (see schematic in Figure 8) transmits axial load to the piston through the piston rod and absorbs the dynamic forces produced in a direction perpendicular to the horizontal axis of the motion. Crosshead secondary motion takes place across the clearance between crosshead and crosshead guide and it is caused by the thrust force induced by the connecting rod that changes its direction depending on its position, so that the crosshead moves towards and impacts against the inner surface of the crosshead lower and upper guide periodically. The clearance between crosshead and crosshead guide is very small, but large enough to periodically induce the crosshead's secondary motion and consequent impact-induced vibration. Figure 9 shows the balance of forces acting at the crosshead.

The force acting at the crosshead can be estimated directly from cylinder pressure and running gear mass. Hydrodynamic forces from oil film interaction are typically calculated at design and study stage with high level of complexity and for evaluation of this practical approach have not been considered.

At each position in the stroke, the horizontal force in the connecting rod balances out the force generated at the piston rod. As the crankshaft turns both the connecting rod angle and the combined inertial and gas loads vary. In addition, the location of the crosshead with respect to crankshaft rotation also affects the vertical force acting on the crosshead.
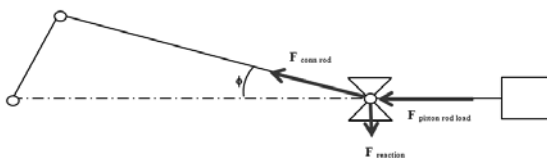
Figure 9: Balance of forces at the crosshead

As the connecting rod does not lie in the horizontal position, the force exerted by the connecting rod produces both horizontal (to counter the gas and inertia forces acting on the wrist pin) and a vertical force. The vertical force lies in the negative (downward) or positive (upward) direction. If the

vertical positive force exceeds the weight of the crosshead and piston rod, the crosshead will move upward vertically against the upper guide. Therefore, considering the combined forces, when the connecting rod is not in the horizontal position, there are cases when eventually the crosshead will impact either on upper or lower guide based on the direction of the resulting force. Such impact is one of the sources of vibration in reciprocating compressors.
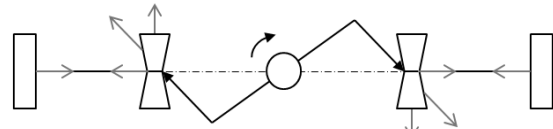
Figure 10: Up- and down- running crossheads

For a double-acting cylinder on a horizontal reciprocating compressor as represented in Figure 10, on the right throw the vertical force will most often act downward during the stroke. Similarly, the opposed crosshead on the left side will most often act against the upper guide rail. For both cases, the vertical force at the crosshead acts in expected direction respectively upwards and downward for most of the stroke. However, for a small time period in either case, the force does act opposite of the expected direction.

4.1 Examples for different compressor loads

Figure 11 shows data for an API 618 type compressor opposite throws at full load, (respectively first and second stage of fuel gas compression service) as seen on the diagnostic software. Vertical force at crosshead is showing matching patterns yet in opposite direction for down-running and up-running crossheads.
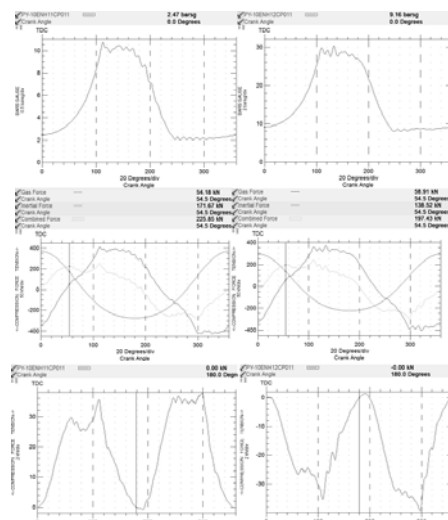
Figure 11: Cylinder pressure, rod load and vertical force at full load at opposing throws

CONDITION MONITORING

Localization of reciprocating compressor components faults using on-line dynamic correlation of impulsive vibration signatures with calculated forces and displacements at individual running gear components, *Gaia Rossi;* GE MEASUREMENT & CONTROL
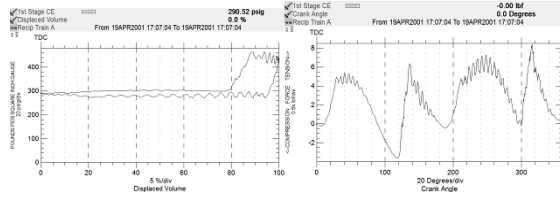
Figure 12: Cylinder pressure and vertical force at part load with suction valve stepless unloader
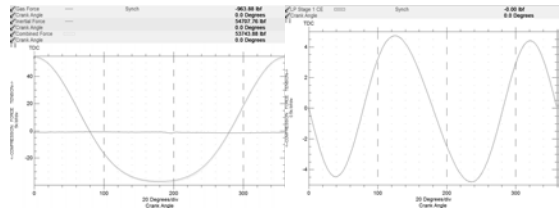
Figure 13: Rod load and vertical force at no load

When stepless unloader devices operate, the patterns may vary considerably. An up-running crosshead, as a consequence of its weight, may be subject to detach from the sliding surface close to the dead centers and at different locations during the stroke. Figure 12 shows cylinder pressure and crosshead vertical force during suction valve stepless unloader action. The pattern for vertical force is quite dissimilar from the one at full capacity and crosshead may actually transition from the opposite rails more times.

Figure 13 shows vertical force on a down-running crosshead during no load test run. Here only inertial force gives contribution to the combined load plot. Again, "down-running" classification no longer describes the behavior of crosshead.

However, vertical force plots are not sufficient to give an indication of the actual crosshead position; motion needs to be estimated from vertical force from kinematic analysis. Interaction with oil film has been neglected in this practical approach.

Based on Figure 9 representation of a crank slider mechanism, as gas pressure builds on the piston and the crank slider moves, the crosshead pin reacts to the forces. The piston rod assembly in the picture exerts a force on the crosshead pin pulling it toward the crankshaft. The horizontal reaction component or connecting rod force will be $-F_{\text{piston rod load}}$ and the vertical component will be $-F_{\text{piston rod load}} \tan\Phi$

With the online force and mass of the crosshead, piston rod and connecting rod, the instantaneous crosshead vertical acceleration at each coordinate can be calculated. Knowing the time interval separating the ordinates, the crosshead vertical velocity and displacement can be calculated as

integrated values with constraints given by the crosshead guides clearances.

Calculated Vertical Position plots in Figures 14, 15 and 16 represent an approximation of crosshead position (upper or lower rail) and the transition from one rail to the other. If an impact event can be correlated to these points, the root cause of failure can be related to crosshead slap problem by impacts due to increased clearances and wear.

Figures 14 to 16 show the resulting plots for the same compressor cases described in Figures 11 to 13. The Impulse Impact plot represents the estimated impact location.

Motion can be estimated for different load conditions and correlation between the estimated crosshead motion and the impact events at the crosshead during crosshead slap malfunctions can be analyzed.
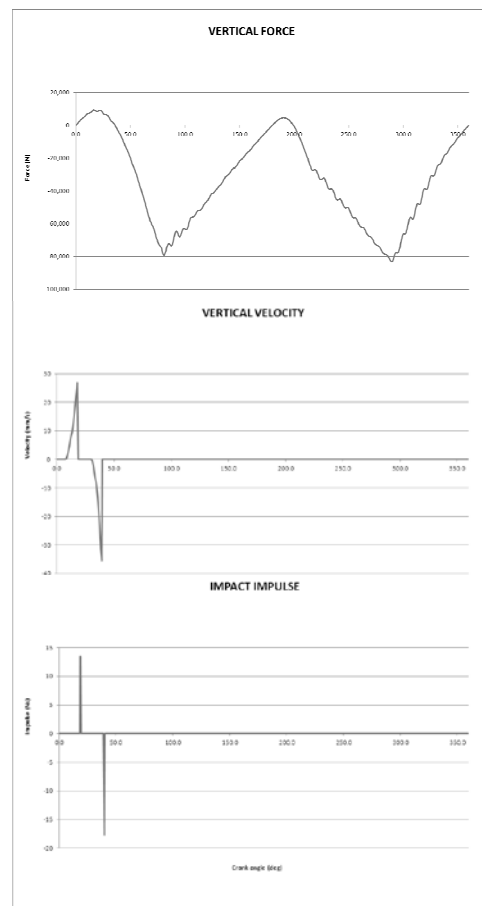
Figure 14: Vertical force at crosshead, crosshead vertical velocity, crosshead position, impact locations at full load

Localization of reciprocating compressor components faults using on-line dynamic correlation of impulsive vibration signatures with calculated forces and displacements at individual running gear components,
Gaia Rossi; GE MEASUREMENT & CONTROL
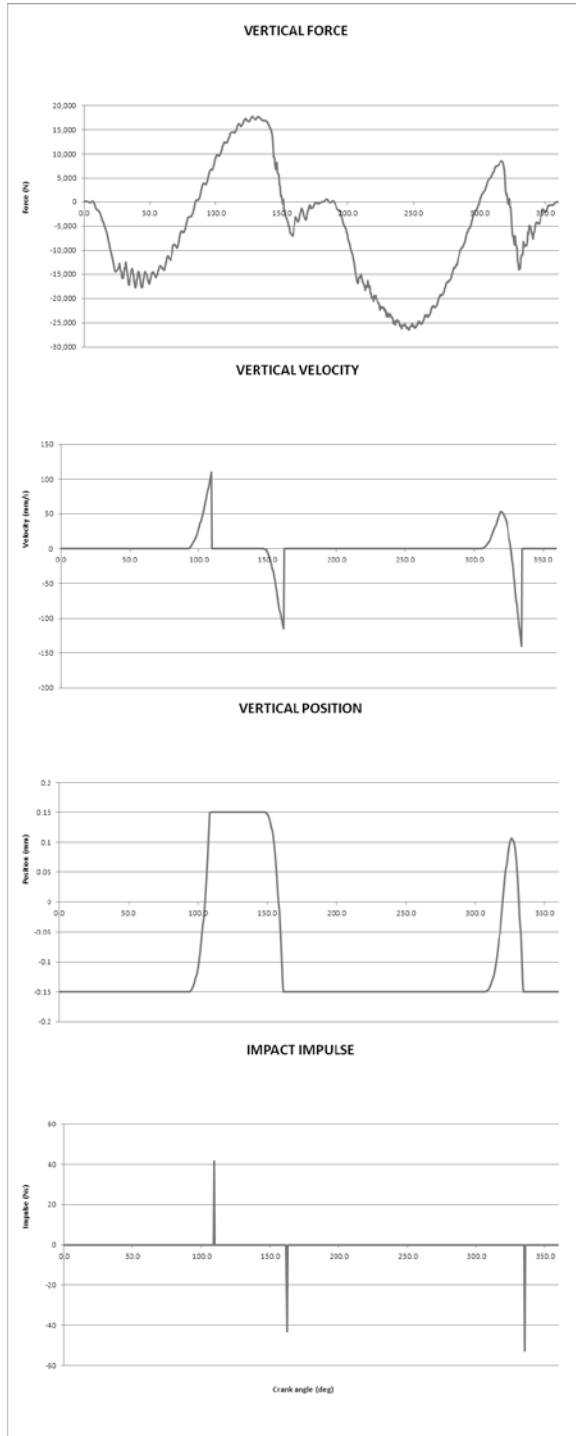
Figure 15: *Vertical force at crosshead, crosshead vertical velocity, crosshead position, impact locations at part load (valve stepless unloader)*
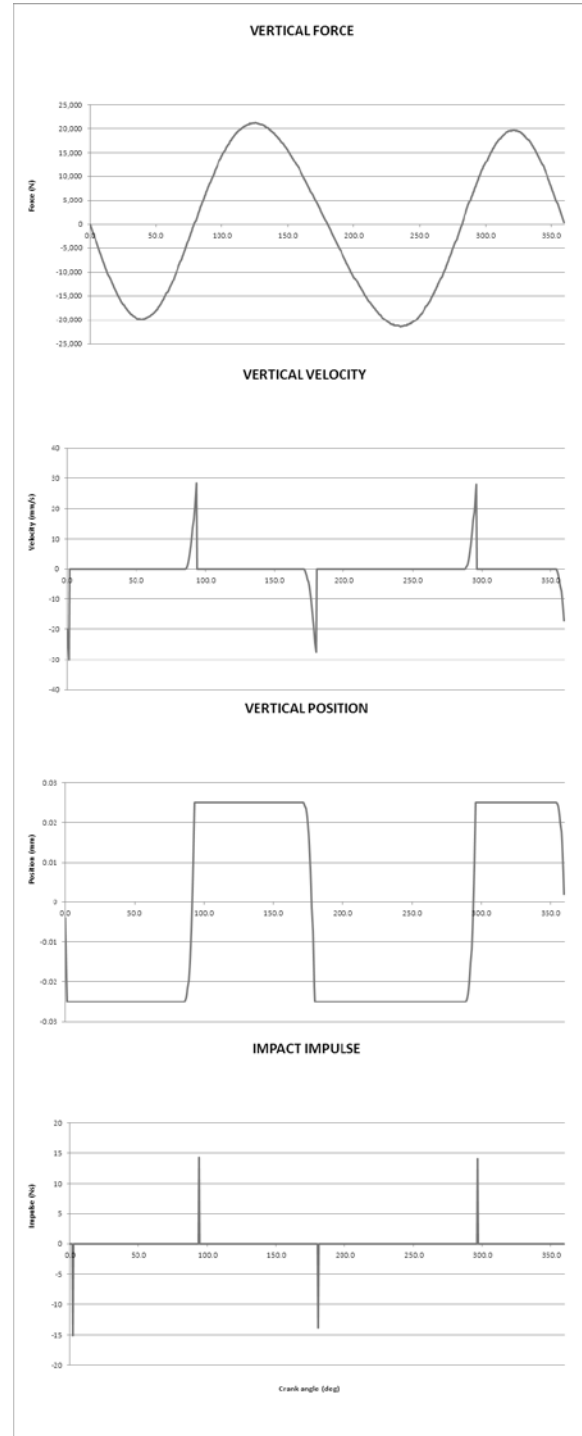
Figure 16: *Vertical force at crosshead, crosshead vertical velocity, crosshead position, impact locations at no load test run*

CONDITION MONITORING

Localization of reciprocating compressor components faults using on-line dynamic correlation of impulsive vibration signatures with calculated forces and displacements at individual running gear components,
Gaia Rossi; GE MEASUREMENT & CONTROL

5   Conclusions

Advances on signal processing and diagnostic software techniques allow on line correlation of multiple synchronized high frequency sampled data providing a powerful tool to pinpoint the malfunction root cause using knowledge based tools and on line information from advanced monitoring systems, which can in turn support diagnostic engineers through automated data correlation and malfunction detection avoiding the need of extensive and time consuming data review.

Online calculation of main forces acting on a reciprocating compressor is a powerful tool not only to monitor load related malfunctions but also to correlate events in vibration signal to a specific component giving the ability to identify the typical malfunctions occurring at these components.

References

[1] Rossi, G., "Vibration Analysis for Reciprocating Compressors (Part 1) ", Orbit Magazine ,Vol. 32, No. 2, Apr 2012
Howard, B.F., "Loose Piston Detection for Reciprocating Compressors", Compressor Tech Two, April 2009.
[2] API Standard 618, Fifth Edition, "Reciprocating Compressors for Petroleum, Chemical, and Gas Industry Services", American Petroleum Institute, 2007.
[3] Howard, B.F., "Loose Piston Detection for Reciprocating Compressors", Compressor Tech Two, April 2009.

8th Conference of the EFRC
September 27th / 28th, 2012, Düsseldorf

BLUEPOCKET®:

Stepless Mass Flow Control Using Fixed Clearance Pockets – a New Solution Using an Old Idea

Dr.-Ing. Klaus Hoff
Dr.-Ing. Georg Flade
Central Division of Technology
NEUMAN & ESSER GmbH & Co KG
Übach-Palenberg, Germany
klaus.hoff@neuman-esser.de
georg.flade@neuman-esser.de

Dr.-Ing. Osman Kurt
EWE Netz GmbH
Oldenburg, Germany
osman.kurt@ewe.de

8th Conference of the EFRC
September 27th / 28th, 2012, Dusseldorf

Abstract:

The idea to implement stepless mass flow control using fixed clearance pockets is very old. To realize it a fast switching valve is necessary controlling the activity of the clearance pocket. In the presented invention, process gas is used to control this valve. The valve has a control chamber, where a process gas pressure between suction pressure and discharge pressure is maintained, controlling the switching times of the valve. The design of the valve follows well known compressor valve designs enabling fast operation, high durability and high efficiency.

BLUEPOCKET: Stepless mass flow control using fixed clearance pockets – a new solution using an old idea,
Klaus Hoff, Georg Flade, Osman Kurt; NEUMAN & ESSER GMBH & CO KG, EWE NETZ GMBH

1   Introduction

The mass flow of reciprocating compressors can be controlled by using different principles. There are different ways to classify these principles, one of them is shown in **Figure 1.**
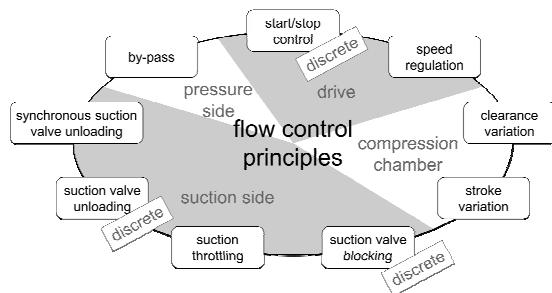
Figure 1:   Feasible flow control principles

All these principles are well known for many decades. But in the last years we saw leaps in technology when combining traditional compressor engineering and state of the art technology derived from other applications. Examples of this general development are electronic frequency converters for compressor drives or electronically controlled suction valve unloading.

The approach described in this paper also follows this scheme, as an old idea was used and modified with the help of up-to-date technology.

2   Mass Flow Control by Using Clearance Pockets - State of the Art

2.1   Standard Solutions

Mass flow control by using clearance pockets is one of the most energy effective principles of adjusting the compressor performance. Fixed clearance pockets are very common. The standard solutions enable a stepwise mass flow control, in which the mass flow reduction depends on the pressure ratio of the compressor stage. **Figure 2** shows a standardized solution using a pneumatically actuated plug valve.
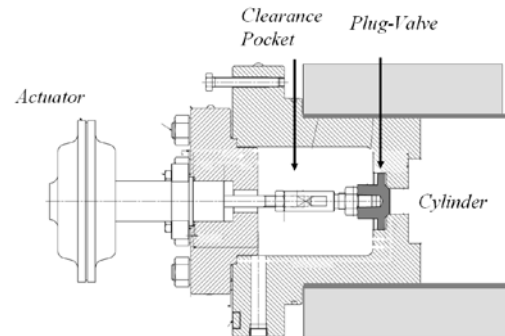
Figure 2:   Fixed clearance pocket with plug valve

To realize stepless mass flow control variable clearance pockets can be used. A manually operated piston adjusting the clearance pocket size is shown in **Figure 3**.
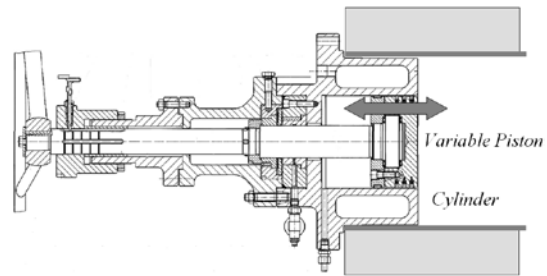
Figure 3:   Variable clearance pocket with manually operated piston

It is possible to add a mechanical drive to the variable pocket solution and to embed this system into the PLC. However, an automatable solution will be of high complexity.

2.2   Former Inventions Enabling Stepless Mass Flow Control with Fixed Clearance Pockets

Solutions for stepless mass flow control using fixed pockets have been known for many years. One of them was patented in Germany (DE 664566) in 1935. A fast operating valve opens and closes the connection from cylinder to the pocket during the compression phase and during the expansion phase. To adjust the compressor mass flow, the switching time of the valve has to be adapted. In the invention mentioned above, this problem is solved by using a variable spring force, which controls the valve operation. The scheme of the invention is shown in **Figure 4**.

BLUEPOCKET: Stepless mass flow control using fixed clearance pockets – a new solution using an old idea, *Klaus Hoff, Georg Flade, Osman Kurt; NEUMAN & ESSER GMBH & CO KG, EWE NETZ GMBH*
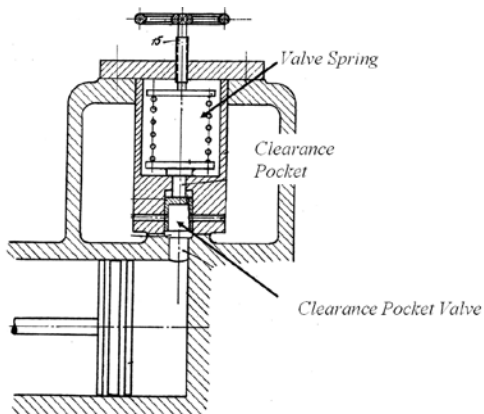
Figure 4:   Solution for stepless mass flow control with fixed pocket clearance (from patent DE664566)

In the solution patented in DE664566 each compression cycle starts with an opened clearance pocket valve. The cylinder side is connected to the clearance pocket. At a certain cylinder pressure, the spring loaded valve closes and the cylinder side operates without the pocket. During the expansion phase the valve opens at almost its closing pressure. The resulting pV-chart is shown in **Figure 5** (upper chart).

To adjust the compressor mass flow, it is also possible to invert the solution. This means to start the compression with a closed pocket valve, opening it during the compression phase and reclosing the valve during the expansion phase. The resulting pV-chart is shown in **Figure 5**. (lower chart)
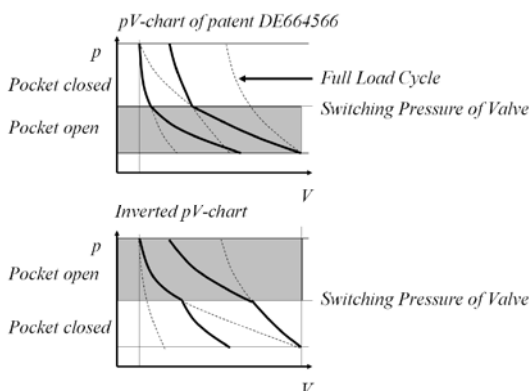
Figure 5: pV-charts for different solutions

3   New Invention – Setting the Switching point by Control Pressure

The former inventions use springs with a variable loader for adjustment. A different method of setting the valve switching point is to use a control

pressure. By means of control pressure it is possible to activate the pocket in the lower pressure range (see **Figure 5** upper chart) or in the higher pressure range (see **Figure 5** lower chart). The schemes of these solutions are illustrated in **Figure 6** and **Figure 7**.
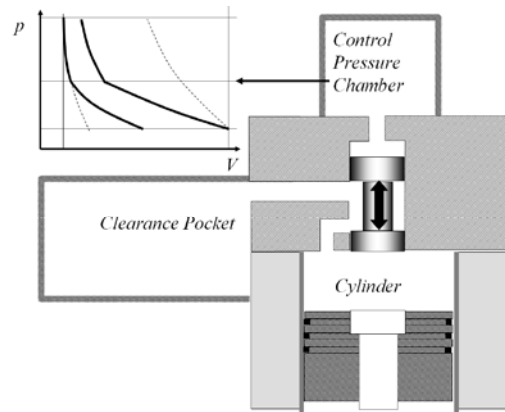
Figure 6:   Solution with activated clearance pocket at lower pressure range. (pV-chart at top left)
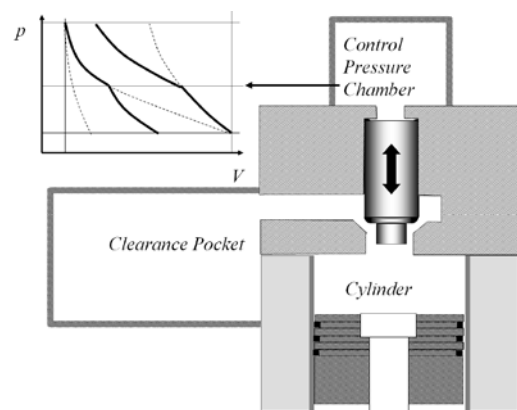
Figure 7:   Solution with activated clearance pocket at upper pressure range. (pV-chart at top left)

In both cases the pressure in the control chamber (control pressure) determines the switching pressure of the clearance pocket valve. In the first case (**Figure 6**): The lower the control pressure, the higher the compressor mass flow. In the second case (**Figure 7**): The higher the control pressure, the higher the mass flow.

Figure 8 shows the correlation between control pressure and mass flow using a solution according to **Figure 7**. In this calculation example the pressure ratio is 3, the normal cylinder clearance is 20% and the isentropic coefficient is 1.4. The mass flow is calculated using

BLUEPOCKET: Stepless mass flow control using fixed clearance pockets – a new solution using an old idea,
Klaus Hoff, Georg Flade, Osman Kurt; NEUMAN & ESSER GMBH & CO KG, EWE NETZ GMBH

$$p \cdot V^{\kappa} = const$$

The size of the clearance pocket is designed such, that the mass flow gets down to zero if the switching pressure equals the suction pressure.

Control Pressure (0 = Suction Pressure, 1 = Discharge Pressure)
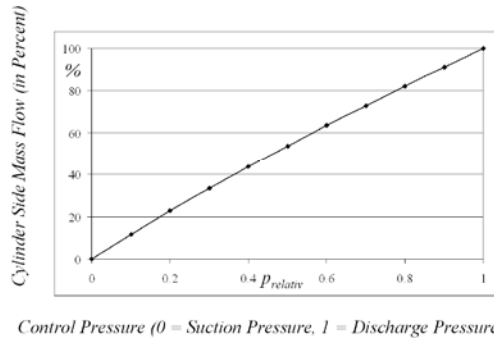
Figure 8: Mass flow as a function of control pressure

The control pressure is the actuating variable to adjust the compressor mass flow. Hence the control pressure has to be adjusted to change the operational point. If the operational point should be kept, the control pressure has to be maintained at a certain level. The adjusting and the keeping of the control pressure level can easily be done using process gas as controlling medium. The control chamber is connected to the suction side or to the discharge side of the cylinder by solenoid or pneumatic valves depending on whether the control pressure has to be lowered or increased. These valves are activated by the pressure monitoring system of the control chamber. The scheme of the pressure monitoring system of the control chamber is shown in **Figure 9**.
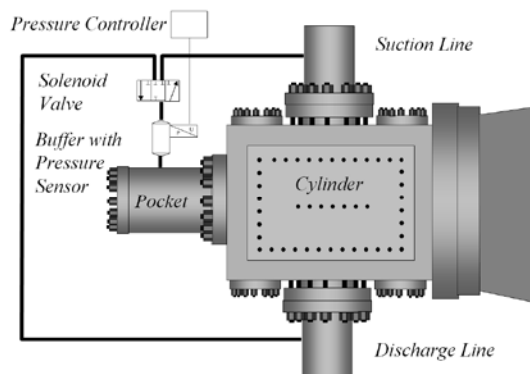
Figure 9: Pressure monitoring system of the control chamber

4   Design of Test Compressor

4.1   Valve Design

Standard solutions are available for the pressure monitoring system including solenoid or pneumatic valves, pressure sensor and control circuits.

The clearance pocket valve itself is a new development. The design requirements of the valve are very similar to those of normal compressor valves:

- Fast operation and short reaction time

- High operating life

- Low pressure loss for high compressor efficiency

- Low additional fixed clearance for high volumetric efficiency at maximum compressor load.

These requirements are conflicting as short reaction time and high durability need low valve lifts and low pressure loss requires a high cross-sectional valve area. The answer to all requirements is a valve design which is very similar to well known Poppet valves. The valve design complies with the scheme shown in **Figure 7.** The additional pocket is active at lower pressures in the cylinder. The design of the valve is shown in **Figure 10**.
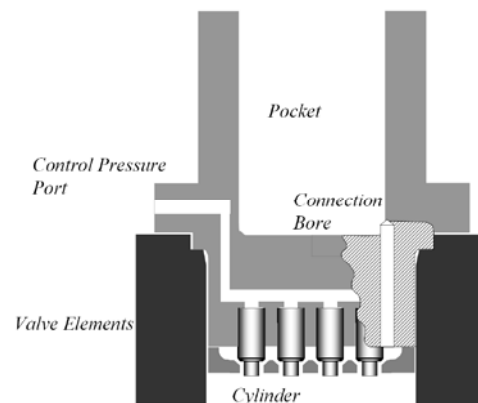
Figure 10: Design of the clearance pocket valve

4.2   Dimensioning and Calculation

Although the design of all compressor parts apart from the cylinder covers complies with NEA standard, the calculation of the compressor has to be adapted. As the pV-charts are changing, rod loads, load reversals for crosshead bearings etc. have to be rechecked. The static and dynamic strength of the clearance pocket unit including the valve have to be simulated with FEM **(Figure 11).**

137

DESIGN & ENGINEERING

BLUEPOCKET: Stepless mass flow control using fixed clearance pockets – a new solution using an old idea,
Klaus Hoff, Georg Flade, Osman Kurt; NEUMAN & ESSER GMBH & CO KG, EWE NETZ GMBH
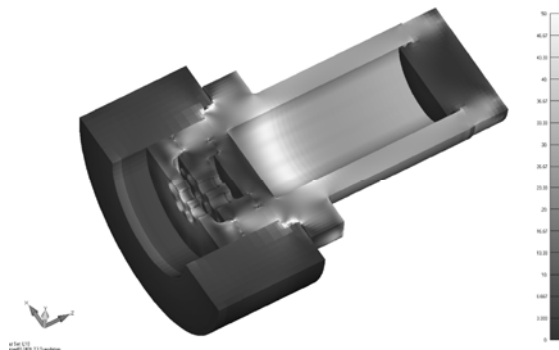
Figure 11: FEM-simulation of the clearance pocket unit

To ensure the durability of the valve elements, the dynamic of these elements has to be checked. Since low impact velocities are essential for a long life time, the allowable valve lift was determined by a simulation of the valve element dynamics.

Since there are different operating points, the simulation of dynamics has to be carried out for several conditions. The simulation shows that, the higher the pressure transient in cylinder, the higher the impact velocity of the valve elements. A sample chart of the cylinder pressure over the crank angle for 100% load including the cylinder pressure transient is shown in **Figure 12**. The switching points of the valve resulting in the highest impacts are marked for opening and for closing.
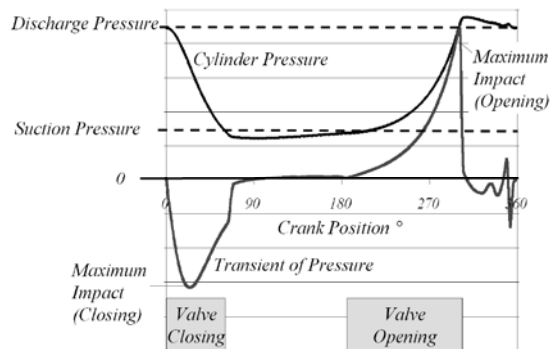
Figure 12: Sample chart of cylinder pressure over crank angle (100% load) including pressure transient; Valve switching points with highest impact velocities marked.

The valve lift was designed such that the impact velocity is in an acceptable range in every operating state.

The valve elements were made of well established materials for compressor valve elements (especially for standard Poppet valves).

5 Conclusion

The presented solution using a fast switching clearance pocket valve controlled by process gas represents a reasonable additional solution for compressor mass flow adjustment.

The new valve can be designed using well known compressor valve principles. Apart from the valve, well known standard technologies like solenoid or pneumatic valves, pressure sensors or control circuits can be used. The system is very simple, and retrofitting of existing compressors is possible.

The new system does not need any auxiliary hydraulic equipment, which is not allowed for some applications. A measurement of crank position is also not necessary.

How the golden age of gas is challenging the reciprocating compressor business

by:

Dr. Gunther Machu, Dr. Tino Lindner-Silwester and Dr. Bernhard Spiegl
HOERBIGER Compression Technology Holding
Donaucity Strasse 1, 1220 Vienna
Austria
Gunther.machu@hoerbiger.com

8th Conference of the EFRC
September 27th / 28th, 2012, Düsseldorf

Abstract:

Natural gas has become the major player in the consideration of current and future demand for energy. Reciprocating compressors play a key role in the exploration, production and distribution of natural gas. The technical challenges to overcome originate mainly from two areas: (1) on the one hand natural gas has a significantly higher global warming potential than CO2 (factor of ~ 21 to 23), therefore any fugitive emissions from compression equipment have to be avoided. (2) On the other hand, the increasing pressure for cost effective, competitive compression equipment led to compressor designs running at significantly higher speeds than ever before, with much increased throughput for a given equipment size hence impacting the reliability and efficiency. In this paper we will show innovative solutions to these challenges on the valves and rings & packing side enabling environmentally friendly and efficient compression of natural gas.

How the golden age of gas is challenging the reciprocating compressor business, *Dr. Gunther Machu,*
Dr. Tino Lindner-Silwester, Dr. Bernhard Spiegl; HOERBIGER COMPRESSION TECHNOLOGY HOLDING

1 Introduction

In recent years, oil has become increasingly difficult to exploit and thus more and more expensive, mainly because countries involved are politically unstable, or deep water drilling is needed to keep up with demand.

Therefore natural gas, in the past more treated as a by-product of oil production and often flared next to the well, has massively covered ground in recent years as the primary substitute to oil, not only for heating and cooking purpose, but also vehicle fueling, in the chemical industry and even as a source to produce liquids again in gas to liquid conversion plants (GTL).

Reasons for this trend are manifold. Natural gas is a very clean fuel, and recently also the cheapest. Compared to other fuels such as furnace oil, petrol, diesel or coal when being burnt it produces the least amount of carbon oxide, nitrogen oxide, sulphur oxide and even particulates.

Therefore, it has been adopted to fuel vehicles (CNG) by many Asian countries in megacities as a very effective solution to drastically improve air quality.

These facts have and will boost the demand for natural gas, considering the fact that transportation is the fastest growing energy consumer in the upcoming years, especially in Asia.

Now the bulk of conventional natural gas production has been historically in the US / Canada as well as Russia (CIS) and Middle East. Many of these gas fields suffer from a decreasing gas pressure, hence the need for efficient gas compression to boost the field pressure to pipeline levels.

Because of high oil prices alternative technologies have been developed to also access unconventional gas resources, the so called shale gas plays. The two key technologies which enable a commercially feasible extraction of shale gas are horizontal drilling and fracturing (please refer to figure 1.).

With this new technology at hand, all of a sudden massive shale gas reserves were discovered all around the world, leading to a massive boom especially in the US.
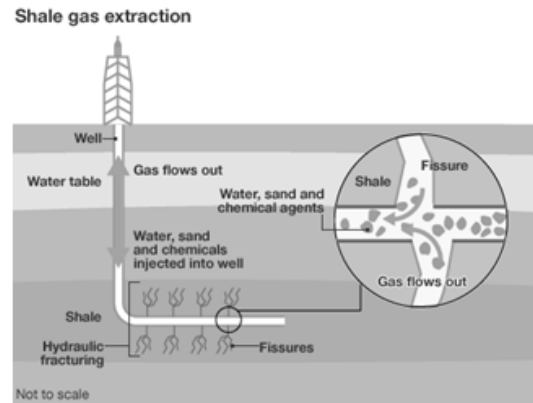
Figure 1: horizontal drilling and fracturing to extract shale gas
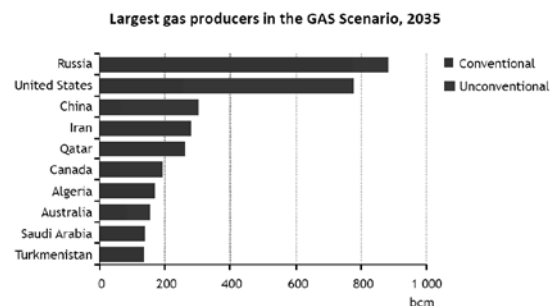
Figure 2: The mix of conventional vs. unconventional natural gas production, 2035

Comparing the future mix of conventional vs. unconventional natural gas production (pls. refer to figure 2), it is easy to see the growing importance of shale gas. Reliable sources state that global resources exceed 250 years of current production!

Hence, the golden age of natural gas has started.

But there is a major environmental impact which is easily overlooked: natural gas is among the few gases which affects global warming and has to be considered in regards of its global warming potential when emitted into the atmosphere.

The equivalent global warming potential (GWP) in relation to CO2 is about 21 ~ 23 times higher. Hence, 1kg fugitive emission of natural gas has an equal GWP as 21 kg CO2.

This megatrend towards natural gas leads to quite challenging reciprocating compressor designs. The two major technical challenges to overcome are

(a) massively increased power density – small compressor footprint but highest speed

(b) prevention of fugitive emission

DESIGN & ENGINEERING

How the golden age of gas is challenging the reciprocating compressor business, *Dr. Gunther Machu,*
Dr. Tino Lindner-Silwester, Dr. Bernhard Spiegl; HOERBIGER COMPRESSION TECHNOLOGY HOLDING

Hence, in this paper we will follow the flow of natural gas from the wellhead via the gas network to the end user and describe in detail solutions to the technical challenges of the reciprocating equipment used in the various stages.

2   The flow of natural gas

2.1   Wellhead

As said previously, there is an increasing trend to shale gas production. These smaller wells impose major challenges:

(a) a lot of liquids, particulates (sand) and H2S is coming along with the gas

(b) the wells deplete much faster than a conventional well, i.e. the wellhead pressure changes quickly

Typically, reciprocating compressors cope very well with varying operating conditions and all sorts of particulates / liquids in the medium. As the wells deplete fast, compressors furthermore need to be easy to move around. This has led to small footprint, trailer mounted compressors running at high speeds (2100rpm and more) for maximum throughput with respect to size.

Furthermore, these compressors are sitting in the middle of nowhere, thus requiring a good level of reliability.

Summing up, small, flexible high speed units capable of reliably dealing with liquids and debris are needed.

For the compressor valves, this translates into the requirement of

1. highest efficiency at a given valve size to minimize power losses at the required speeds

2. reliable operation in the presence of liquid and debris

The first requirement eliminates any kind of poppet valve, as these valves typically only utilize about 12% of the given pocket area as effective flow area. Plate valves are more favorable, reaching already about 16 -17 % effective flow area. A ring valve does reach about 20% efficiency, but is more expensive and difficult to realize for the small valve sizes needed here.

The solution to the problem is a profiled plate valve, using a nonmetallic sealing element with an aerodynamically shaped contour sitting on a profiled seat to reach about 25% effective flow area in relation to the available pocket area.

The beauty of a profiled plate valve is, that it combines the simplicity and cost effectiveness of a plate valve with the efficiency of a high end ring valve.

As the indicated valve power losses of a reciprocating compressor are proportional to the square of the effective flow area, a profiled plate valve is saving about 60% of the valve losses a standard plate valve would produce: $(0.16^2)/(0.25^2) \sim 0.41$. Less power losses mean lower overcompression, less temperature and thus making higher compression speeds possible.

Additionally, the nonmetallic profiled plate can easily absorb liquids and embed particulates without leading to failure, as can be seen in figure 3 below:
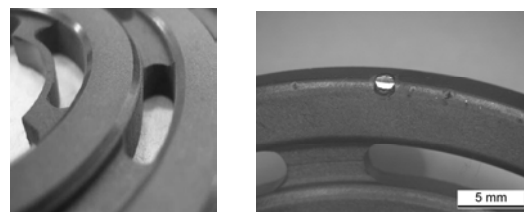
Figure 3: The profiled sealing element (left), and the ability of special designed polymers to absorb any kind of hard particulates, without subsequent damage.

The CP valve design favorably combines all the above required features and was described in more detail at the 2010 EFRC conference in Florence, IT.

On the test bench, runs with a compressor speed of 3100 rpm have been performed, with very satisfying results.

Profiled plate valves will revolutionize the design of wellhead compressors and are the clear path into the future.

2.2   Gas gathering, gas processing

From the various wellheads, gas is collected by gas gathering compressors, which become increasingly bigger, including the gas processing plant recip. In the gas processing plant, natural gas is cleaned and desulphurized and prepared for pipeline transmission.

The trend to increase compressor speeds mainly to reduce initial investment cost is clearly evident here, posing similar challenges to the compressor valves as described in the previous section. Profiled

How the golden age of gas is challenging the reciprocating compressor business, *Dr. Gunther Machu,*
Dr. Tino Lindner-Silwester, Dr. Bernhard Spiegl; HOERBIGER COMPRESSION TECHNOLOGY HOLDING

plate valves are the clear answer here as well, but of course the needed valve sizes are bigger and go up to about 200mm valve diameter. Power consumption of the reciprocating compressors can reach up to 2MW, and these machines are all double acting. Here, power savings due to efficient profiled plate valves like the CP valve can be huge, translating into tens of thousands of Euros saved per year.

With double acting compression, a new problem is on the table – what to do with the (so far) unavoidable packing leakage? Packing leakage means natural gas emitted into the air via the vent line, resulting in an equivalent CO_2 footprint of an average sized compressor equipped with conventional rod seals of easily 1000 tons CO_2 equiv. per year!

Not only the public, but also governments are more and more aware of these facts, resulting in increasing pressure to tighten up emission legislation.

Hence, a solution is needed for the rod seals.

The authors' answer is the BCD (balanced cap design) packing ring. It has been presented in detail at the last EFRC conference 2010 by T. Lindner – Silwester et al (2). The BCD ring is comprised of four segments (figure 4). On the high-pressure-facing side of the ring (left-hand side of figure 4), four radial gaps are formed by these segments that make the ring single-acting. On the low-pressure-facing side of the ring, two wear-compensating gaps are formed between the two main segments 1. These gaps are sealed by the cap segments 2 in axial and radial direction.
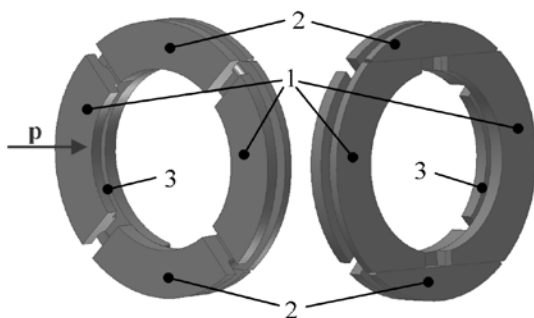
Figure 4: The new low emission BCD packing ring

Thus, the ring is gastight without the necessity of having an additional ring in front to cover any gaps.

Summing up, the BCD is characterized by the following features:

- Maintenance of high sealing efficiency over lifetime.

- High lifetime due to low wear rate and optimum utilization of ring material.

- Low generation of frictional heat due to pressure-balancing and small axial ring width.

- Robust one-ring design that consumes less space and therefore allows for shorter packing cases.

Low generation of frictional heat and a shorter overall packing length are very favourable in terms of lifetime for high speed compression units.

This design has been released 2010 to the market, and so far excellent field evidence of the claimed performance has been reported:

(a) emissions prove to be more than 70% less than with conventional R/T style rings. Many sites even report no detectable leakage at all, including gassed up stand still conditions, which is typical for natural gas compressors.

(b) Lifetime in demanding applications like non lube fuel gas boosters, or non lube CNG compressors is more than threefold as before with conventional ring designs.

2.3 Gas transmission, storage

This area is an interesting one. So far, reciprocating compressors were the obvious machine of choice in the previously described applications.

With gas transmission and also storage, more and more competition from turbo compressors is evident. This has led to a race turbo vs. recip, with the outcome that reciprocating compressors are becoming huge, delivering flow rates previously only known from turbo equipment.

This is achieved by increased sizes of cylinders and increased rotating speed, imposing huge challenges on the efficiency but also reliability of the compressor valves. Especially for gas storage applications, a major benefit of the reciprocating compressor is put into use: the great flexibility to various operating conditions.

DESIGN & ENGINEERING

How the golden age of gas is challenging the reciprocating compressor business, *Dr. Gunther Machu,*
Dr. Tino Lindner-Silwester, Dr. Bernhard Spiegl; HOERBIGER COMPRESSION TECHNOLOGY HOLDING

During summertime, the storage has to be filled, resulting in greatly varying discharge pressure. Also, gas from different pipelines, coming in at various suction pressures is used. By means of a stepless control system like the HydroCOM, exact flow rates can be set and energy is saved.

For these high pressure, high flow compressors which need stepless regulation the CM valve was introduced to the market in 2007, and published in detail at the 5th EFRC conference in 2007 by B. Spiegl et al[3].

Figure 5: The CM valve, featuring a multitude of finely spaced rings for optimum efficiency

Similar to the profiled plate valve, this valve allows to push the envelope of existing compressor designs and helps to defeat the turbo compressor, offering the end user all the benefits of a recip: energy efficiency, reliability, flexibility.

Using this valve type, end users have reported up to 70.000 € energy savings per year compared to plate type valves!

Similar to the previously discussed applications, emissions (packing leakage) is of huge concern. In various gas transmission and storage applications the BCD packing ring has proved to significantly reduce leakage. Customers who had leakage meters installed at the vent line were concerned initially when the new BCD rings were fitted. The meter didn't show any read out – the BCD leakage was found to be below the measuring range of the used device!

Interestingly, in all the previously mentioned applications with the advent of high speed compression a new problem emerged which initially did not receive a lot of attention: the efficiency of the installed oil wiping rings was less than suboptimal. Customers reported oil losses as high as 3 – 4 litres (~ 1 gallon) per day. This is not only an environmental concern, but also a cost factor, especially in the area of field gas compression, where new drums of oil have to be carried to remote locations way too often.

Furthermore, problems have been reported of traditional wiper rings "eating" the piston rods.

These are unfortunately inherent problems of classical oil wiper designs, which rely on a sharp edge to "scrape" the oil off the rod. To retain a sharp edge, metallic ring designs have to be used. These are typically very stiff, hence they

- either do not conform well to the rod in case of slight mismatch leading to massive amounts of oil loss or

- or scrape the oil off the rod too efficiently, thereby leaving no lubrication film and thus ruining the rod
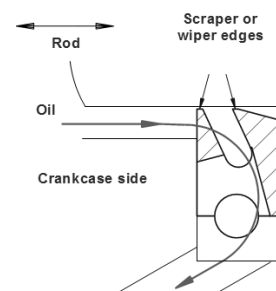
Figure 6: Classical wiper, scraping the oil from the rod

Hence, the authors started a research program to come up with a new oil scraper design. In the course of that research, a paradigm shift was performed, and the new OFD wiper was born (OFD = oil film dynamics). Basically, there are two approaches to achieving zero net leakage of oil: a) aiming at scraping all the oil off the rod during the outstroke or b) letting a controlled amount of oil pass the wiper during the outstroke and ensuring that the same amount of oil gets transferred back again during the instroke.

The working principle of the new OFD wiper is based upon approach b). For a wiper to work in this way, use must be made of so-called elasto-hydrodynamic (EHD) effects. Such effects come into play when the deformations of the seal ring

have a pronounced effect upon the dynamics of the oil film and vice versa. Since the oil pressure levels typically arising when oil gets wiped off a rod are comparatively low, for EHD effects to become effective the material the wiper is made of must not be too stiff. Hence, the OFD wiper is made of filled polymers. With the wiper sealing profile being fully lubricated during operation not only a high sealing efficiency but also a high lifetime can be achieved.

The non-metallic ODF wiper is depicted in Fig. 7. The ring consists of a straight-cut L-shaped cover ring "2" that surrounds a straight-cut insert ring "1" in such a manner that no leakage paths are formed.

How the golden age of gas is challenging the reciprocating compressor business, *Dr. Gunther Machu,*
Dr. Tino Lindner-Silwester, Dr. Bernhard Spiegl; HOERBIGER COMPRESSION TECHNOLOGY HOLDING
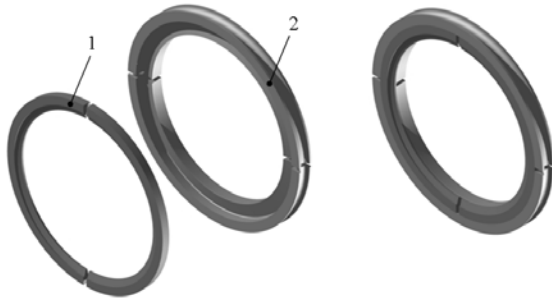
Figure 7: The new non-metallic OFD wiper. The straight-cut insert ring "1" is surrounded by the straight-cut cover ring "2".

In house testing and field experience show that the new OFD wiper offers the following advantages:

- Superior sealing efficiency by making use of EHD effects

- Long lifetime and high reliability

- Optimum rod conformity guaranteed

2.4 CNG

The final stage in the distribution of natural gas to the end user relevant for reciprocating compression equipment is the CNG car fuelling station.

CNG is either distributed via trucks carrying NG bottles at ~250bar pressure which are offloaded at the station (leading to greatly varying suction pressures for the compressor), or favourably via a low pressure gas pipeline network.

Gas is then discharged to the vehicle tank at around 250 bar.

Challenges involving CNG compression equipment are

1) increasing gas demand, but small footprint of the compressor required (space constraints in large cities)

2) frequent start / stop operation, with longer periods of pressurized standstill

3) more and more customers asking for non lube compression, as any lube oil in the vehicle tank will destroy the engine's gas injections.

Ad 1): means bigger power density (and the need for efficient compressor valves such as a profiled plate valve). Furthermore, for delivery rates >

1200sm³/h, double acting compressors are needed. Hence, a rod packing has to be used. (2) Conventional rod seals will leak during pressurized standstill. Where to vent the gas leakage, especially in crowded city centers?

A proper answer already has been mentioned in the previous section: the BCD packing ring has proven its low leakage performance also in pressurized standstill.

Item 3) technically leads to the fact, that all of a sudden a not too difficult commodity application becomes quite challenging, especially in the light of ever increasing rotational speeds. Especially the higher stage piston rings are exerted to very high loads, while at the same time piston ring blow by could affect the delivery performance. Furthermore, the involved rod diameters are small, which leads to the question, which material for the rings should be used? A stiff, tribologically not favourable PK grade which mechanically could cope with the high loads, or a soft, well conforming PTFE material which shows very low wear but could easily extrude?

The following image shows how a standard, gastight piston ring design looks after 200h in the last stage (250bar) at 1800rpm in a small nonlube CNG compressor:

All rings extruded, overstressed, molten.

The right answer to these challenges is provided by the BCR piston / ring combo, which has been specifically developed for this kind of service:
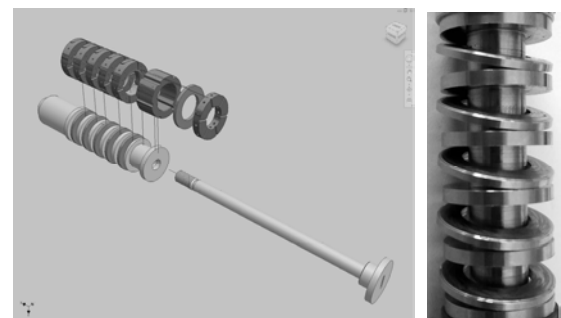
Figure 8: The patented BCR piston / ring combo, featuring floating, solid backup rings machined out of the main piston body

DESIGN & ENGINEERING

How the golden age of gas is challenging the reciprocating compressor business, *Dr. Gunther Machu,*
Dr. Tino Lindner-Silwester, Dr. Bernhard Spiegl; HOERBIGER COMPRESSION TECHNOLOGY HOLDING
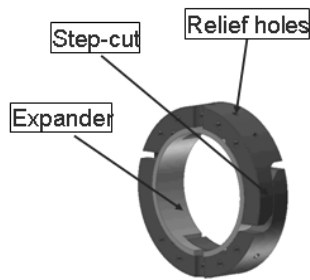
Figure 9: Gastight pressure balanced BCR piston ring

The BCR piston / ring combo features solid, free floating backup rings machined out of the main piston body.

The advantages of this design are

- the solid backup ring allows precise adjustment of the piston clearance independent of the piston diameter and makes the use of PTFE materials possible even at very high pressures.

- Simultaneously the solid backup ring also solves the problem of adjusting the rider ring clearances of step pistons. Typically, the clearance is determined by the bigger rider ring, which results in too much play and the risk of piston - liner contact of the smaller piston.

- The gastight BCR piston ring significantly reduces the piston ring blow by. Measurements in demanding non lube applications showed an increase of 7% of delivery rate.

This design has proven to yield the promised advantages already in several applications.

3   Outlook

As has been shown in the previous sections, that the next generation profiled plate valves provide the path into the future for efficient, reliable compression of natural gas.

Regarding the problem of vented gas emissions, the BCD packing ring provides a first, very important step towards very low emissions by reducing gas leakages in the order of 70 – 90 % as compared to traditional designs.

Well, the next step is clear: zero emission. We will not disclose any more details here, but HOE is already deep into the development of a zero emission packing, and the first customer test is

already running successful since February 2012. The zero emission packing will be the scope of a paper to be presented at the next EFRC conference.

4   Conclusion

Natural gas is the fossil energy carrier of the 21st century, providing a clean, environmentally friendly alternative to oil at a very affordable price level, found almost everywhere around the globe. With regards to reciprocating compressors, it poses some technical challenges which are not easy to overcome. The authors are very confident that with ongoing development and recent technological advances, the path into the future of efficient, reliable compression looks bright and very promising.

References

[1] Next generation valve technology for high speed compressors, B. Spiegl, G. Machu, M. Testori, 7th Conference of the EFRC

[2] The BCD packing ring – a new high performance design, Tino Lindner-Silwester, Christian Hold, 7th Conference of the EFRC

[3] The role of improved valve technology in the utilization of natural gas resources, B. Spiegl, G. Machu, P. Steinrueck, 5th Conference of the EFRC

Analysis of the Movements
of the Valve Sealing Elements

by:

F. Manfrone, A. Raggi
Dott.Ing.Mario COZZANI S.r.l.
Arcola (SP)
Italy
info@cozzani.com

8th Conference of the EFRC
September 27th / 28th, 2012, Düsseldorf

Abstract:

This paper reports the research activity results, both theoretical and experimental, carried out by Dott. Ing. Mario Cozzani s.r.l. on automatic valves.

Usually the mathematical equations used in simulation software to study the valve behavior consider the movements of the sealing elements as unique and perfectly axial. However in the real application, the flow is not evenly distributed, consequently it may cause pitch and roll effects and non-synchronized movements of the sealing elements with negative impact on the valve life time and performance.

The authors explain how this research activity contributed to increase the knowledge of the valve physical phenomena and how the acquired knowledge enabled to improve the internal Company calculation software and valve selection criteria. They showed as well the strict interaction between cylinder design and valve design which requires a strong cooperation between compressor OEM and valve manufacturer.

Analysis of the Movements of the Valve Sealing Elements, *F. Manfrone, A. Raggi;* DOTT.ING MARIO
COZZANI S.R.L.

1 Introduction

The aim of this research activity is to investigate the physical phenomena which influence the reciprocating compressor valve behaviour and thus optimizing the simulation software used during the design phase. This software is usually based on the simultaneous solving of several differential equations describing the valve sealing element motion and the flow through the valve.

The lack of some input data and the need to control the computational time impose some simplifying hypothesis such as to consider uniform pressure distribution inside the cylinder, fully axial valve sealing element movement and just an equivalent single shutter of equal mass/springing instead of more concentric rings.

The paper shows how the presence of heavy section reduction due to the pocket valves, flow deviations in suction/discharge phase and the piston masking effect generate not uniform pressure and velocity distributions. Consequently, this produces force unbalances that modify the theoretical axial motion introducing pitch and roll movements, which can be the cause of stress increase. The activity confirms that a correct valve design cannot be done without considering the cylinder which it is installed to. The computational time increase is compensated by a better power losses evaluation.

Starting from the results presented in Prague at EFRC Conference in 2007. Dott. Ing. Mario Cozzani Srl has carried out a series of research activities in order to go into more detail regarding the mathematical correlations between geometrical parameters (internal and external to the valves) and the pressure losses especially focusing on the pocket valve effects.

This research has been done through both advanced CFD mesh motion analysis and experimental tests on a compressor using instrumented valves for pressures, temperatures and sealing elements movement data acquisition.

The mathematical models used in PROVAL, the dynamic simulation software developed by Cozzani Company for its own valve design, have been implemented by more detailed equations for disk/rings movements and gas flow in order to consider the effects explained before.

The work has confirmed the utility of advanced software in the design of automatic valves and cylinders, and it has shown the need of a closer and closer synergy between valve and compressor designing.

2 Compressor equipment and preliminary experimental results

The experimental activity has been carried out using a two stage reciprocating compressor (*Figure 1*) with inverter.

The compressor has been equipped with pressure and temperature transducers for data acquisition inside the cylinder, suction/discharge chambers, and inlet/outlet piping.
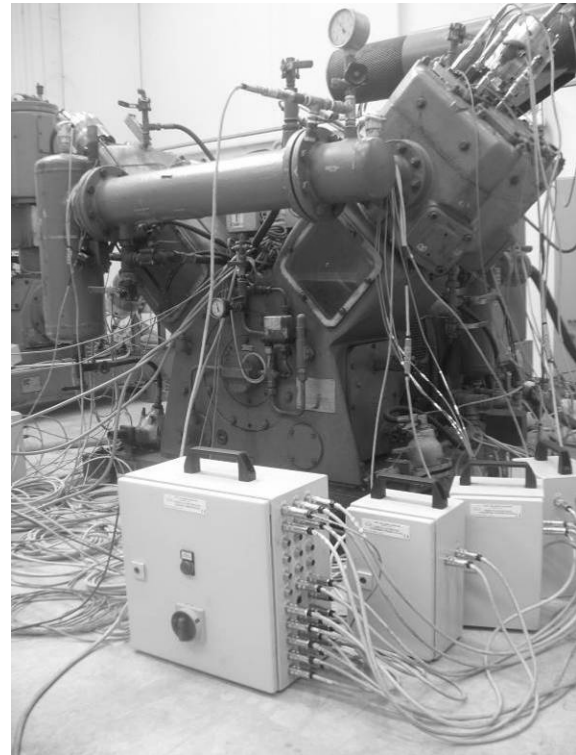
Figure 1: Compressor and Cozzani acquisition System

A position sensor installed on the crankshaft measures the TDC.

As in this case, the two cylinder ends are characterized by different pocket valve geometries as shown in *Figure 2*, both discharge sides have been equipped in order to evaluate the influence of this element on valve behaviour.
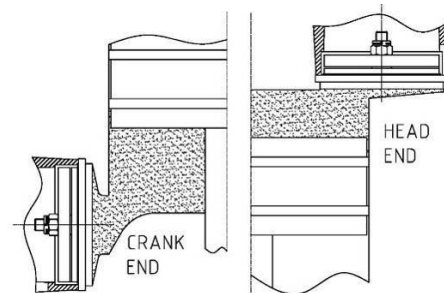
Figure 2: HE and CE cylinder schemes

DESIGN & ENGINEERING

Analysis of the Movements of the Valve Sealing Elements, *F. Manfrone, A. Raggi;* DOTT.ING MARIO COZZANI S.R.L.

Valve disc/rings motion acquisitions have been obtained through special plate type discharge valves in *Figure 3* realized for the installation of 4 inductive proximity sensors.
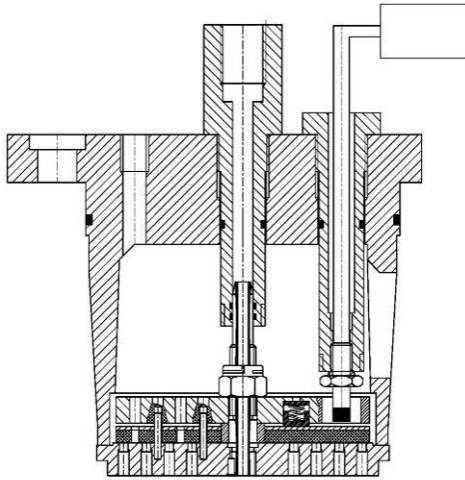
Figure 3: Discharge Valve-Cage scheme for data acquisition

An acquisition sensor board sends the signals to a PC where dedicated software developed by Cozzani Company for the design and the performance of its products (*Figure 4*) is installed.
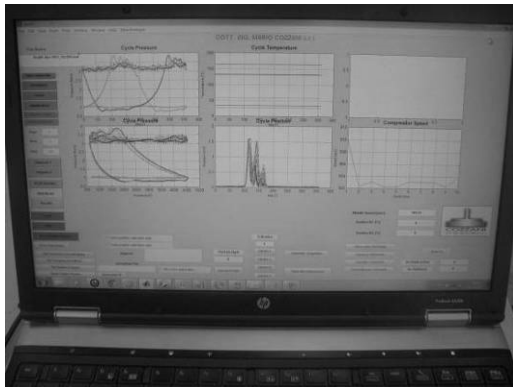
Figure 4: PC with Cozzani acquisition software "ACQVAL"

The software allows a quick data processing and provides several graphs such as PV diagrams, pressure trends and valve sealing elements positions function of crank angle/time. In addition numerical results such as pressure drops and power losses due to the valves, indicated power and valve opening/closure crank angle are available.

Figure 5 and *Figure 6* show the disk movements of the two discharge plate valves installed in the cylinder ends. The proximity sensors of the head end valve located in the cylinder top provide trends which are almost overlapped and this suggests an essentially axial plate motion. On the contrary the acquisition of the crank end valve highlights that a

part of the disk monitored by sensors 3-4 detaches from the guard before the other (sensors 1-2) and this indicates pitching and rolling phenomena during the valve closing phase.
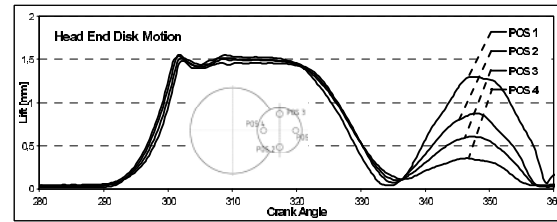
Figure 5: Head end valve plate position
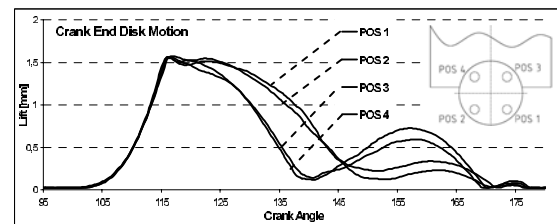
Figure 6: Crank end valve plate position

In order to verify that this phenomenon is really due to the pocket valve geometry, the proximity sensor positions have been changed and several acquisitions have been done.

All the tests have shown that the differences between the two cylinder end valve behaviours are due to the different pressure distributions, results of the pocket valve geometries.

Trends like the one in *Figure 6* point out the presence of localized impact phenomena on the plate edge: these are very interesting because if not considered they can reduce sealing element life.

3   Dynamic CFD Approach

As the high piston velocity generates inertia terms that cannot be estimated through steady state simulations, the phenomena shown in the previous chapter have been investigated by means of CFD approach.

The attention has been focused on the compression phase by doing a 3D model reproducing cylinder bore, valve housings, discharge valve and outlet duct.

In order to obtain pressure, velocity and temperature distributions during every time step, the analysis have been performed in transient conditions by SST turbulent solver and geometry motion.

Analysis of the Movements of the Valve Sealing Elements, *F. Manfrone, A. Raggi;* DOTT.ING MARIO
COZZANI S.R.L.

The piston motion is obtained by deforming
geometry and consequently the mesh of the
cylinder fluid domain in accordance with the piston
motion equation.

The mesh is composed by hexahedral elements
which allow a homogeneous compression without
elements distortion close to the Top Dead Centre.
On the contrary the valve fluid domain has been
meshed by using tetrahedral elements for a better
fitting to its geometry.

Figure 7 and *Figure 8* show the velocity streamline
distribution for two different steps of the
compression.
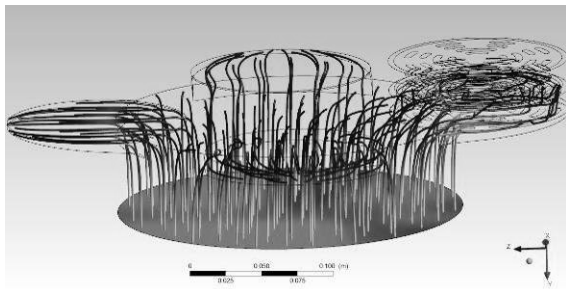
*Figure 7: Velocity streamlines for HE cylinder
close to BDC*
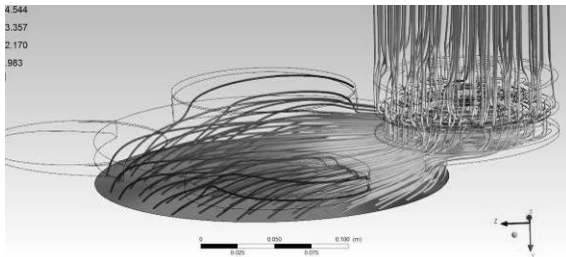
*Figure 8: Velocity streamlines for HE cylinder
close to TDC*

During the compression the discharge valve is kept
closed until the differential pressure between
cylinder and outlet piping exceeds the spring load
acting on the sealing element.

This is possible thanks to last generation solver
integrated with HPC capability.

The results of the dynamic analysis for the head end
and crank end outputs are expressed in terms of
pressure, velocity and temperature fields. That
allows assessing average mass flow at any
transversal surface. *Figure 9* shows the trend of the
average mass flow versus crank angle.
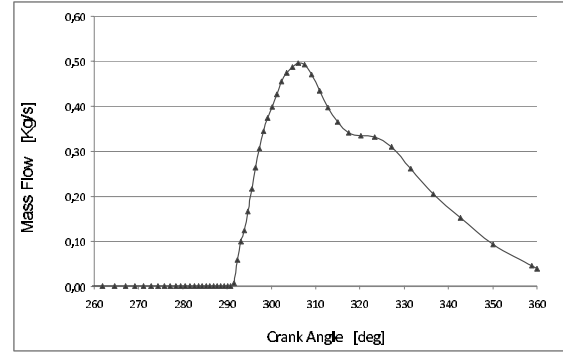
Figure 9: Mass flow vs crank angle

The analysis of the pressures on the valve plate
surface (*Figure 10*) highlighted different
distributions in the two cylinder ends. In the
cylinder head end symmetrical distribution
produces a force resultant centred on the valve axis;
consequently only axial component of plate
movement is present. On the contrary, in the crank
end the force resultant is located in the upper half
of the disk where there is higher pressure
concentration. This generates an imbalance of the
plate that explains the sealing element movement
shown in *Figure 6*.
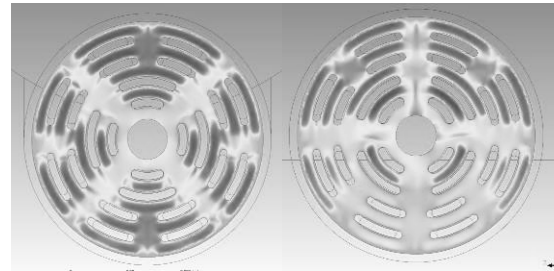
a) Head End plate   b) Crank End plate

Figure 10: Pressure on the disk

4   Fluid dynamics Coefficients

The accuracy of a mathematical model is based on
the precision of the coefficients used to describe the
system.

Two of the most important coefficients are flow K_S
and drag C_d coefficients, which can be calculated
by means of the following formula:

$$K_S = \frac{\dot{m}_{real}}{A_r P_{in} \sqrt{\left[\left(\frac{P_{out}}{P_{in}}\right)^{2/k} - \left(\frac{P_{out}}{P_{in}}\right)^{(k+1)/k}\right] \frac{2k}{R \cdot (k-1) \cdot T_{in}}}}$$

$$C_d = \frac{F}{A_{shutter} \cdot (P_{in} - P_{out})}$$

Analysis of the Movements of the Valve Sealing Elements, *F. Manfrone, A. Raggi;* DOTT.ING MARIO
COZZANI S.R.L.

The first one describes a fluid-dynamic efficiency
of the valve and the second one defines the reaction
of the sealing element to the pressure (the higher
the C_d is and the better the valve opening/closure
with low differential pressure is).

Starting from the results shown at the EFRC
conference in 2007 in Prague, a new series of CFD
analysis has been carried out in order to improve
the knowledge in coefficient calculation function of
valve and cylinder parameters.

At the beginning the attention has been focused on
the valve, coupling it with two straight ducts.
Considering the high number of simulations
necessary for this investigation Cozzani Company
developed an automatic CFD steady state simulator
capable of generating a 3D model starting from
geometry data stored in a database, meshing,
applying the boundary conditions, solving it and
showing the results (*Figure 11*)
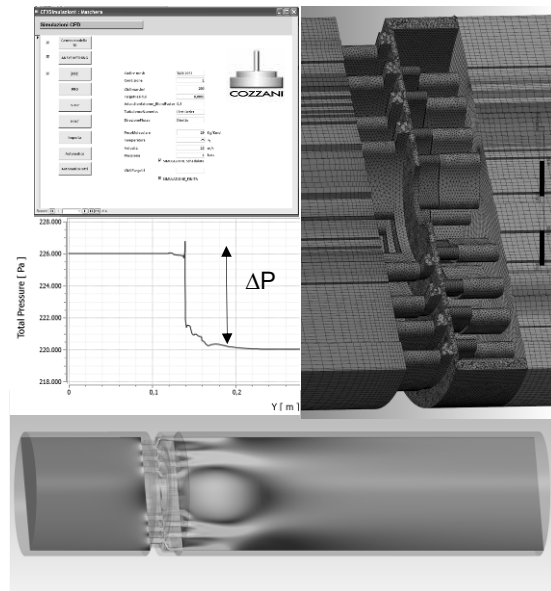
Figure 11: Automatic CFD valve analysis

Analysis results allowed defining a series of
mathematical correlations of the fluid-dynamic
coefficients with the valve parameters (lift, channel
dimensions, sealing element geometry, etc…).
Later, the model has been updated by adding
cylinder chamber and pocket valve (*Figure 12*) in
order to study the coefficients in a configuration
closer to reality.

New geometrical parameters have been introduced
in order to consider the influence of pocket valves
and their positions inside the cylinder, on flow and
drag coefficients. In this way, new mathematical
correlations have been obtained.
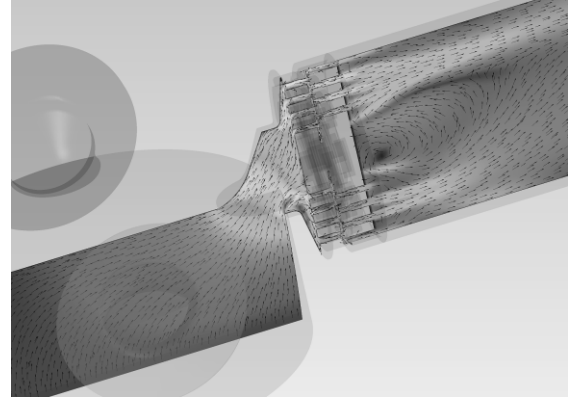
*Figure 12: CFD simulation for Cylinder, valve,
housing*

5   Restitution Coefficient

In order to simulate the valve sealing element
motion it is necessary to introduce in addition to the
fluid dynamic coefficients another one, which
considers their dynamics during the impact with
seat and guard.

In the case of a pure axial movement it is sufficient
to consider the valve sealing element bounce back
with a velocity v_2 opposite in sign to the velocity
before the collision v_1 and modulus decreased by
the coefficient C_R, as defined by:

$$v_2 = -C_R \cdot v_1$$

In case of a non-zero impact angle (*Figure 13*) the
valve sealing element movement after the bouncing
has both axial and rotational velocity components
(v2 and ω2) and their value can be calculated
introducing two restitution coefficients for
translation and rotation (C_{RA} e $C_{R\theta}$) and applying
the conservation of energy.

Two equations can be written:

$$v_2 = C_{RA} \cdot f(M, D, J, \theta, v_1, \omega_1)$$
$$\omega_2 = C_{R\theta} \cdot g(M, D, J, \vartheta, v_1, \omega_1)$$

M, D and J are mass, diameter and moment of
inertia of the sealing element.
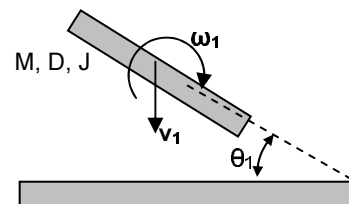
Figure 13: Non-zero impact angle motion

150

DESIGN & ENGINEERING

Analysis of the Movements of the Valve Sealing Elements, *F. Manfrone, A. Raggi;* DOTT.ING MARIO COZZANI S.R.L.

These new coefficients have been calculated through several experimental tests carried out on a special test bench (*Figure 14*) with proximity sensors able to measure the motion before and after the sealing element collision with a surface in free falling conditions and non-zero impact angle.
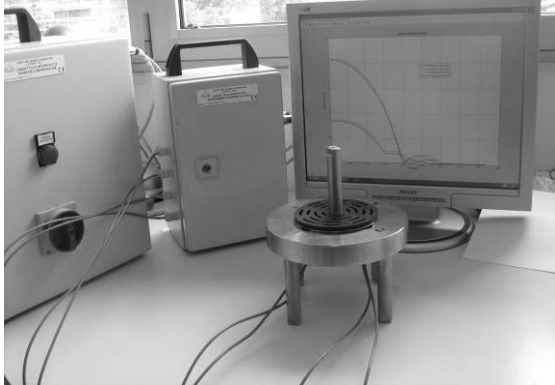
Figure 14: Workbench for free falling impact tests

New correlations for impact have been introduced into the software and the comparison between experimental and simulation results (*Figure 15*) have shown a very good adaptation of the model to reality.
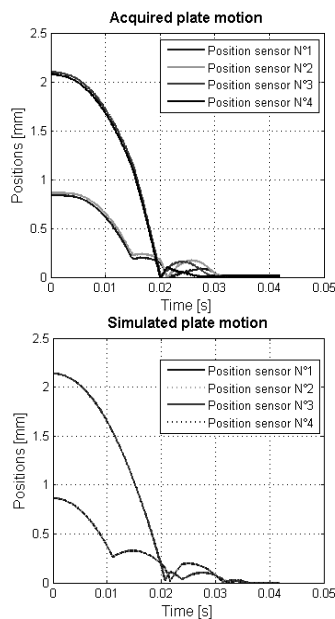
Figure 15: Comparison between impact experimental tests-simulation for a valve plate in free falling conditions.

6 PROVAL software development

The activities described in the previous chapters have allowed a closer examination of the physical phenomena regarding the valves, giving very useful suggestions about how to upgrade the correlations used in the dynamic simulations software.

Figure 16 shows the theoretical disk movement of a discharge valve plate done through the previous simulation software version.
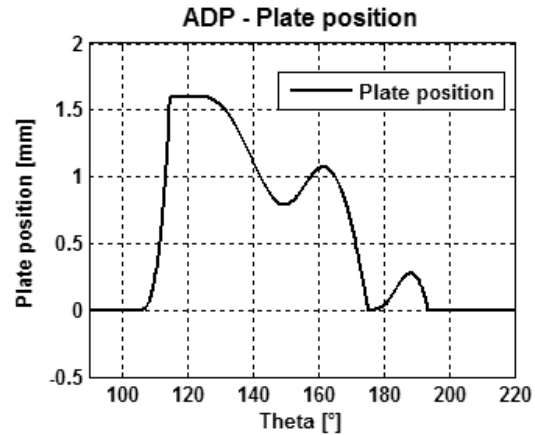
Figure 16: Plate movement (only axial)

In the new software version the hypothesis of fully axial sealing element movement and uniform inlet pressure distribution have been exceeded.

The new matrixes of coefficients, deduced through the CFD analysis of chapter 4, consider the pocket valve geometries and positions and allow writing a series of flow equations and equilibrium equations for force and moment on the sealing element. In addition to that knowing the impact angle it is possible to calculate the restitution coefficients and solve the motion equations.

The software solves the N·i·j differential equations simultaneously where N is the number of system state variables (density, temperature, angular and axial position/velocity, etc…).

In this way the software considers the asymmetries produced by the gas forces and can analyse the motion of each sealing element allowing the evaluation of possible pitch and roll movements like the ones highlighted in *Figure 17*.

DESIGN & ENGINEERING

Analysis of the Movements of the Valve Sealing Elements, *F. Manfrone, A. Raggi;* DOTT.ING MARIO COZZANI S.R.L.
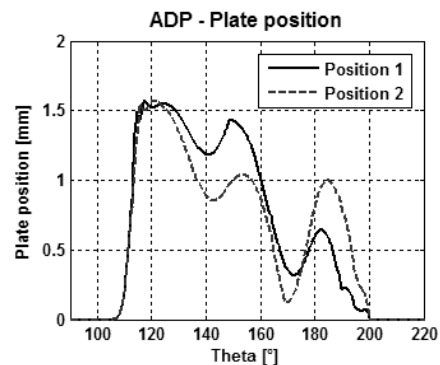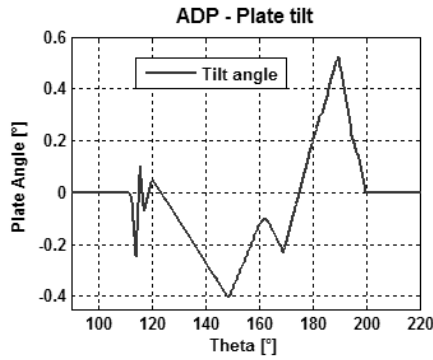
Figure 17: Plate movement and tilt angle

The software upgrade also allows a more accurate evaluation of suction/discharge phase pressure drops and power losses considering the different influences of different pocket valves.

Figure 18 shows the simulated discharge pressure increase due to the pocket valve.
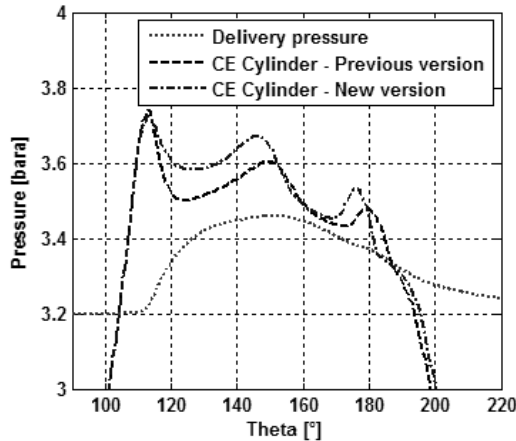
Figure 18: Cylinder Pressure

An additional comparison between new and previous software versions can be done about power losses. In *Figure 19* there is a comparison regarding power consumption for the two cylinder ends described in chapter 2.
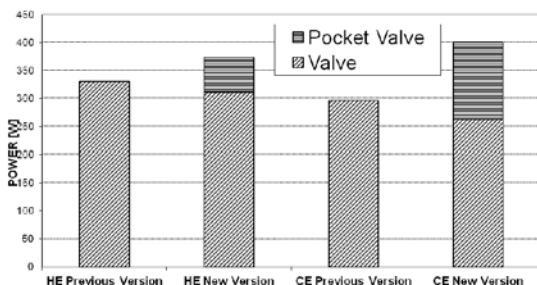
Figure 19: Discharge side power losses

Power losses due to the pocket valve in crank end cylinder are higher than the ones in the head end. This can be explained considering the different geometries of *Figure 2*. On the contrary the power

losses due to the valve itself substantially don't change.

7 Results and analysis of experimental tests

The PROVAL software modifications explained in the previous chapter have been validated through several experimental tests on the compressor shown in chapter 2 and pressure, temperature and sealing element motion data have been acquired.
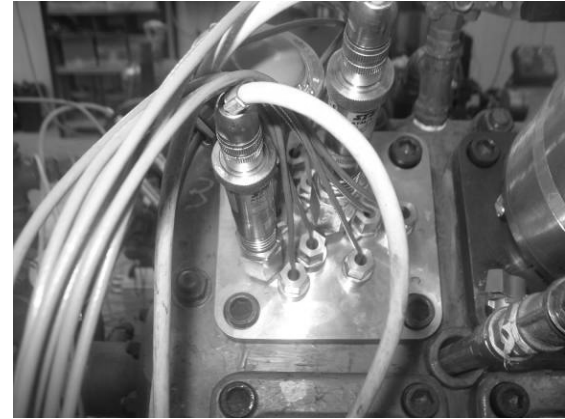
Figure 20: Head end cylinder equipped with ring type valves

The tests have been carried out equipping the two cylinder ends with different valve types with proximity sensors for the sealing element position monitoring and repeating them for different compressor speeds.

Figure 21: Plate type valve for experimental tests

First of all, the attention has been focused on the plate type valves. The disk movements have been shown in *Figure 5* and *Figure 6* of Chapter 2. It has been noticed how the different pocket valve geometries influence the dynamic valve behaviour, generating pitch and roll effects that are more evident in the crank end.

Analysis of the Movements of the Valve Sealing Elements, *F. Manfrone, A. Raggi;* DOTT.ING MARIO COZZANI S.R.L.

In *Figure 22* plate positions and tilt angles trend for the crank end cylinder at two different compressor speeds (600 and 1200 rpm) are shown .The pictures highlight that pitch and roll phenomena are present for all the speed range and their influence doesn't change (the maximum value of the tilt angle is the same at 600 and 900 rpm). In addition to that, it is shown that the number of disk oscillations decreases with increasing compressor speed.
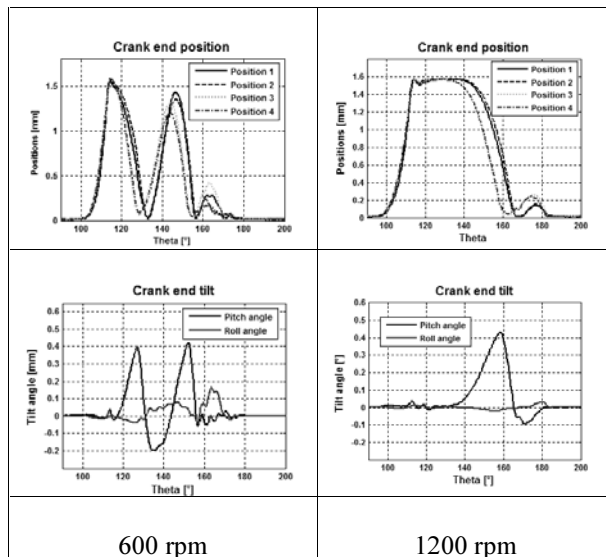
Figure 22: Crank end disk motion at 600 rpm and 1200 rpm

Afterwards, the tests continued installing ring valves equipped with 3 proximity sensors for each ring.
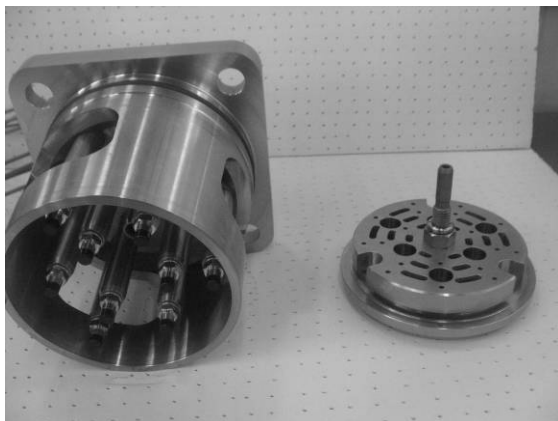
Figure 23: Ring type valve for experimental tests

Figure 24 shows the pressure trends for ring type valves installed in the crank and head ends, whilst *Figure 25* shows the ring motions
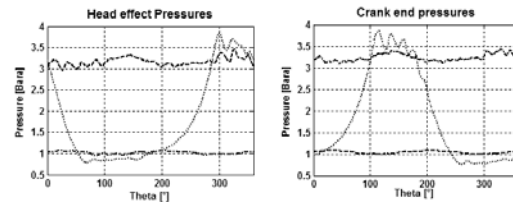
Figure 24: Pressure measures form experimental tests for ring type valves

a) – Head End   b) – Crank End

Figure 25: Position measures from experimental tests for ring type valves

In the graphics of *Figure 25* it is possible to notice that the internal ring motion is almost fully axial and the pitch and roll phenomena that appear at the beginning of the valve closure are more evident on the external rings.

These phenomena can be explained considering that the central part of the valve is affected by a direct and uniform flow, which is minimally influenced by the pocket valve geometry. On the contrary, the external parts of the valve are more influenced by the pocket valve shape. This has been also highlighted by the CFD simulations (*Figure 26).*
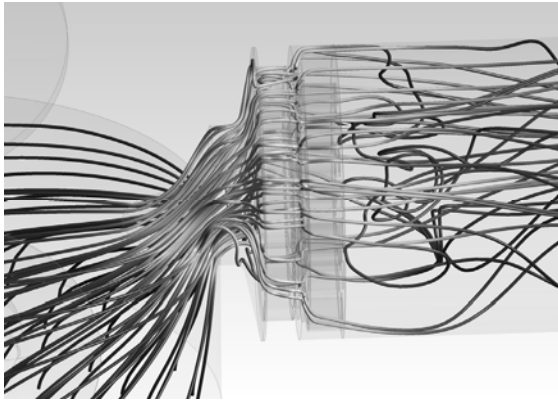
*Figure 26: Velocity stream lines in a ring type
valve*

This produces a non-uniform pressure distribution
on the external rings and consequently angular
moment, which leads to the movements of Figure
25.

8 Comparison between simulation and experimental tests results

The last phase of the research activity has been the
comparison of results from the new version of the
simulator software PROVAL with the data acquired
during the experimental tests. The comparisons of
some features are explained below.

Figure 27 shows the pressure trends inside the
cylinder and in the suction/discharge valve cages.
There are some divergences regarding the discharge
side related to possible resonances that the model
doesn't take in account.
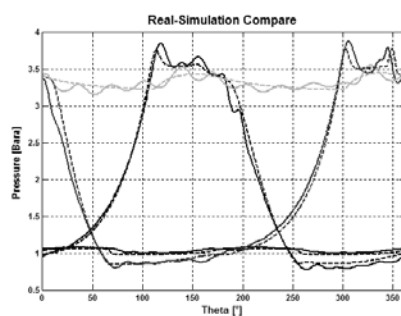
*Figure 27: Comparison between simulated and
measured pressures at 800 rpm*

Figure 28 shows the temperature trends in the
suction/discharge valve cages and in the related
piping. The temperature acquisitions are constant
because the sensors cannot catch the phenomenon
due to its fast variation. However the average
values of the simulated temperatures in a cycle are
very close to the experimental data.
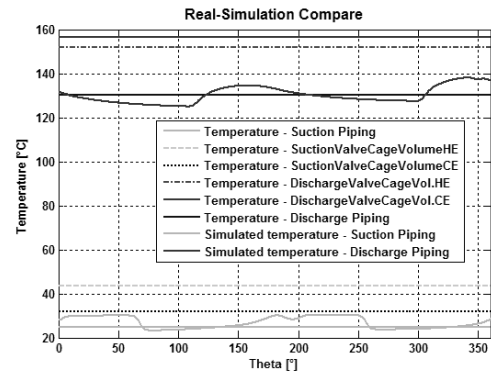
*Figure 28: Comparison between simulated and
measured temperature at 800 rpm*

Figure 29 shows the comparison regarding disk
motion. In order to carry out a comparison with the
outputs of the 4 proximity sensors used to acquire
the plate motion, the simulated position values of
these points have been calculated starting from the
values of centre of mass and angular rotation given
by the software. It is possible to notice good
matching with software response in detecting the
detachment points of the disk from the guard and so
to simulate the pitch and roll effects.
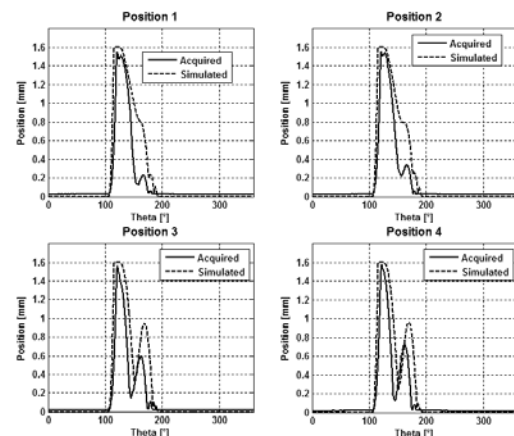
*Figure 29: Comparison between simulated and
acquired positions at 800 rpm*
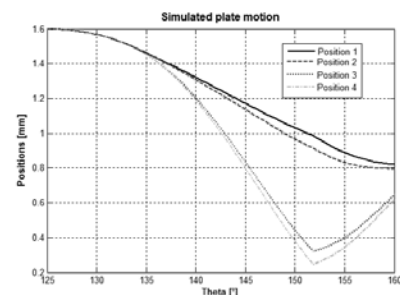
Figure 30: Detail of simulated positions

In Figure 31 there is a comparison regarding the
power losses. The influence of the pocket valve on

DESIGN & ENGINEERING

Analysis of the Movements of the Valve Sealing Elements, *F. Manfrone, A. Raggi;* DOTT.ING MARIO COZZANI S.R.L.

the discharge phase power consumption is 26% for the crank end and 11.5% for the head end.
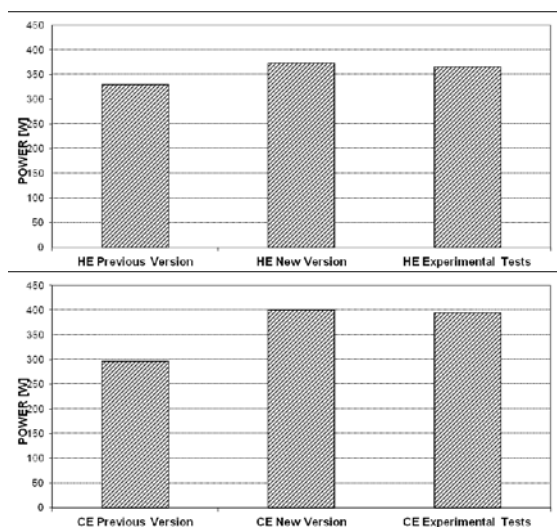
Figure 31: Comparison between simulated and measured power losses in the discharge phase for both the ends

9 Conclusions

This research activity carried out by Dott. Ing. Mario Cozzani s.r.l. has shown the utility of theoretical and experimental approach for the investigation of the physical phenomena related to valves.

Thanks to advanced CFD mesh motion analysis and rig test, it has been possible to understand how the pocket valve influences the flow on the sealing elements.

The activity shows how the asymmetries produced by pocket valves are the cause of disk/ring pitch and roll motions.

The new matrixes of flow and drag coefficients allowed the writing of more precise functions for the upgrading of dynamic valve simulation software "PROVAL".

Through this new software version Cozzani Company can simulate both axial and rotational motion of the single valve sealing elements.

The evaluation of the impact angles/velocities of rings/disks gives very useful information to valve designers in order to choose the right valve set up (springing, lift etc…) according to the materials used.

The new software version can also evaluate the additional power losses due to the valve housings (a combination of geometry of passages between cylinder and housing and interaction with the valve itself).

The activity has confirmed the need of a strict synergy between valve and compressor makers starting from the first phase of the design.

References

1 - Ansys CFX User's Guide
2 - Matlab User's Guide
3 - S.Rosati, "Fisica Generale I"
4 - E.Latrofa, "Fisica tecnica - Termodinamica", 1994
5 - Gas Processors Supplier Association, "Engineering Data Book", 1998
6 - API Standard 618 "Reciprocating Compressors for Petroleum, Chemical and Gas Industry Services", 5th Edition, December 2007
7 - Nafems, Lorenzo Bucchieri, " Fondamenti di fluidodinamica computazionale", 2000
8 - L. Postrioti, "Definizione e rilievo del coefficiente d'efflusso e del numero di Swirl/tumble", 2006
9 - M. Schiavone, F. Manfrone, E. Giacomelli, "Evaluation of the Coefficients used for simulation for Cylinder Valves for Reciprocating Compressors ", EFRC-Conference 2007 Prague.
10 - R. Aigner, H. Steinruck "Internal Flow and Valve Dynamics in a Reciprocating compressor", July 2007
11 - Silcock, Don. "Reciprocating Compressor Instrumented for Machinery Management," Orbit Magazine, June 1996
12 - Smith, Tim. "Quantum Chemical Uses Reciprocating Compressor Monitoring to Improve Reliability," Orbit Magazine, June 1996

8th Conference of the EFRC
September 27th / 28th, 2012, Düsseldorf

EFRC

**EUROPEAN FORUM
for RECIPROCATING
COMPRESSORS**

Increasing the capacity of reciprocating compressors for LDPE plant

by:
Hisung Lee
LDPE section
Samsung Total Petrochemical Ltd.
Daesan
Korea
hisung.lee@samsung.com

and
Dr. Charles D. Beals
Executive Vice President
Engineers and Constructors International, INC.
Baton Rouge
USA
cbeals@eci-la.com

and
Manfred Strässler
Components, Service, Support
Burckhardt Compression AG

Winterthur
Switzerland
manfred.straessler@burckhardt
compression.com

8th Conference of the EFRC
September 27th / 28th, 2012, Düsseldorf

Abstract:

Improved reactor performance for LDPE plants leads to enhanced conversion rates. This potential can only be utilized if equipment such as Booster/Primary, Hyper compressor and extruder is adapted to the new throughput.

The optimal solution is derived in an iterative process involving owner, operators, process licensor and contractors. The compressor manufacturer has to propose different options for increasing the capacity of the compressors make the necessary changes to the auxiliary equipment and piping systems and provide the engineering services and, in many cases, conduct a pulsation and vibration study.

Samsung Total Petrochemicals Co. Ltd., Daesan, Korea, successfully realized a project for a 25% capacity increase which was realized by replacing the electric motors, modifying cylinders and adjusting the auxiliary equipment for the Booster/Primary (B/P) and the Hyper compressor. Since the product from a tubular LDPE reactor is a blend of the polymers that are made as the reaction progresses down the tube, the increased Hyper compressor capacity required significant modification to the reactor to keep the product delivered to the end user the same. Without these modifications, the final product may not have met the end user's requirements, resulting in loss of sales. After the reactor was configured, many other systems required modifications that were necessary to make them compatible with the increased Hyper capacity and reactor configurations.

Increasing the capacity of reciprocating compressors for LDPE plant, *Hisung Lee, Dr. Charles D. Beals, Manfred Strässler;* SAMSUNG TOTAL PETROCHEMICAL LTD, ECI INTERNATIONAL INC, BURCKHARDT COMPRESSION AG

1   Introduction

The LDPE plant operated by Samsung Total Petrochemicals in Daesan, Korea was built in 1989. The rated capacity of the plant is 100 KT/Y. Samsung employed the Mitsubishi Process. The responsible EPC contractor was Hitachi.

The heart of the plant, the tubular reactor, was originally designed for a Hyper compressor throughput of 46 t/hr. Initially the plant used a combination of oxygen and peroxide to initiate polymerization in the reactor. It was designed to produce EVA up to a concentration of 11.3% [wt]

The Hyper compressor was designed for a final discharge pressure of 2750 bar running with a rotating speed of 200 RPM. It was driven by a Jeumont Schneider motor rated with 9500kW. The high pressure piping was delivered by Böhler.

Burckhardt Compression also supplied the Booster/ Primary compressor and its auxiliaries on a turnkey basis. The Booster/Primary unit is a typical API horizontal 6 crank motor driven reciprocating compressor with a shaft speed of 400 RPM. The main driver is a Jeumont Schneider motor rated at 1800 kW.

Market demand and the availability of additional ethylene allowed Samsung Total Petrochemicals Co (STC), located in Daesan, Korea, to consider upgrading the output of the LDPE plant.

Around 2005/2006 STC, anticipating the future possibility of increased feed stock, requested Engineers and Constructors International, Inc. (ECI) located in Baton Rouge, Louisiana, to perform a feasibility study to identify "spare margins on all existing equipment which could be exploited to increase the operating rate of both the homopolymer and EVA Resins." ECI was able to identify and evaluate several incremental steps that would provide increased throughputs. Each of these steps required different degrees of modification and different levels of investment for various plant systems. The elimination of oxygen allowed ECI to suggest a reconfiguration of the Hyper compressor that provided additional feed to the reactor. Once this was confirmed by Burckhardt, the reactor had to be reconfigured to assure the product that was made after the project was completed was identical to the product that was currently being provided to the end users. Since increased gas rate and change in reactor configuration affect many other plant systems, a systematic approach was undertaken to assess these impacts on ALL plant systems. The increased rate and production rate affects systems such as the gas to polymer separation; the booster and primary compressor, the cooling in the HP recycle system and the product extrusion and handling systems. All of these effects required detailed evaluation. When there were questions regarding equipment performance at the higher expected rates, STC ran plant tests to assure the equipment would deliver the required performance. This was particularly important in the product handling systems such as the extruder and downstream equipment. Many different reactor configurations, each resulting in a different level of investment and different capacities, were evaluated and offered to STC.

Almost 3 years after the initial screening studies were completed STC selected the alternate that best fit their corporate needs and forecasts. ECI then completed the final design of the high pressure systems involved in this alternate. At the same time, Daewoo, a highly qualified Korean contractor, was contracted by the STC project management team to provide engineering for all non-high-pressure areas as well as all needed services for the construction work at the plant. Of course critical equipment manufacturers such as Burckhardt also played a key role in the successful implementation of this project. The major modifications to the Hyper compressor allowed STC to benefit from the significant operational and design improvements that have been made by Burckhardt since the original STC project in 1986. These improvements are discussed in detail later in this paper.

Once all engineering was completed, the STC project management team along with ECI, Daewoo, and Burckhardt developed a project execution strategy.

Burckhardt Compression received the first engineering contract to study the debottlenecking potential of compressors in 2006. Samsung wanted to increase the throughput of Hyper compressor from originally 46t/h to 62t/h and with a EVA content of 28% [wt] and the B/P compressor from 5,000/20,000 kg/h to 7,800/30,000 kg/h respectively.

ECI Baton Rouge approached Burckhardt Compression in 2009 requesting an update of the study. A comprehensive RFQ was issued with a clear description of scope.

Several meetings between Samsung, ECI and Burckhardt Compression resulted in a scope of hardware supply. Several components of the LDPE plant had to be upgraded.

Approximately two years after the implementation of the final phase, the critical components such as reactor tubing, compressor parts and motors were delivered to site. The onsite installation was, in a typically efficient Korean way, successfully completed after 1.5 months. The pre-commission was completed in 1 month so STC was able to start production a mere 3 months after the initial shutdown. Plant performance has since met or exceeded all expectations.

Increasing the capacity of reciprocating compressors for LDPE plant, *Hisung Lee, Dr. Charles D. Beals, Manfred Strässler;* SAMSUNG TOTAL PETROCHEMICAL LTD, ECI INTERNATIONAL INC, BURCKHARDT COMPRESSION AG

2 Debottlenecking of Hyper compressors

2.1 Main measures

Hyper compressors typically allow plunger diameter changes and/or stroke adaptations.
However, these modifications are normally limited to the plunger diameter increase and the replacement of the main driver. The versatile cylinder design of the Burckhardt Hyper allows easy diameter changes of plungers without affecting HP pipe connections. The cylinder modifications allowed STC to install a new LP packing design and a new multi-poppet valve with a spherical suction valve seat. The new driver power was increased from 9,500 kW to 12,000 kW. The new rated mass flow of the Hyper compressor is 62t/h (a 35% increase). As discussed later, some of the high pressure piping around the compressor had to be changed in order to keep the pulsations predicted by the pulsation study at an acceptable level.
Specifically, for the STC project, the cylinder sizes were changed as follows.

Plunger diameter	1st stage		2nd stage	
[in mm]	Old	New	Old	new
Stream "A"	103.5	111	88	94.5
Stream "B"	88	106.5	78	94.5

Chart 1: Comparison old/new plunger diameters

2.2 Adaptation of cylinders for Hyper compressors

The design of the compressor cylinder allows the plunger diameter to be changed without affecting the position of the high pressure pipe connections. The modification was therefore limited to the replacement of the high pressure packing, the combined suction discharge valve and the low pressure packing.
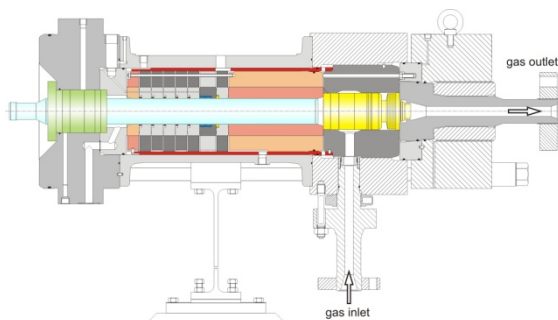
Figure 1: Hyper compressor Cylinder. Highlighted parts have been replaced or machined.

2.2.1 High pressure cartridge

The high pressure packing is configured as a cartridge. The outer diameter remains the same for all admissible plunger diameters. Consequently, the shrink fit between the inner and outer ring has to be calculated for each application. In this case an especially corrosion resistant material has been selected to be suitable for the EVA application.
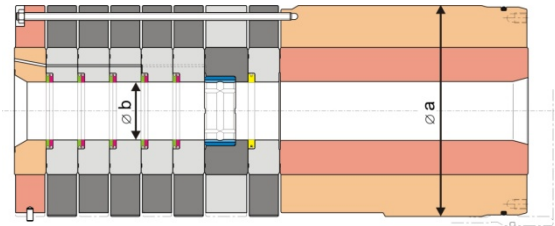
Figure 2: High pressure cartridge. Outer diameter "a" still original. Inner diameter "b" modified to suit new plunger diameters

2.2.2 Multi-poppet valves with spherical valve body

Initially the Hyper was equipped with the "old style" multiple poppet valves. The suction valve body shows a fairly flat shaped cavity towards the compression chamber. Fretting corrosion between the shrunk liner and the valve seat was initiated by relative movement during the compression cycle. Several different geometries were investigated with the FEA (Finite Element Analysis) method. As a result, the valve seat is built with a more spherical shape. A minor increase of death volume due to spherical shaped suction valve body of 2nd stage valve was compensated for by installing longer plungers.
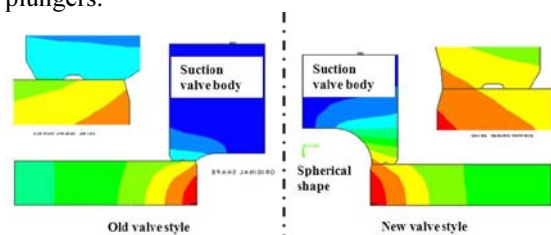
Figure 3: Figure to left showing flat shape of suction valve body. Figure right showing suction valve body with spherical shape

2.2.3 New low pressure packing

The Hyper compressor was equipped with a low pressure packing designed around 1985. In the meantime the low pressure packing design has been further improved by N_2 buffering. The N_2 buffer reduces the ingress of cylinder lubricating oil into the cooling flushing oil.

159

Increasing the capacity of reciprocating compressors for LDPE plant, *Hisung Lee, Dr. Charles D. Beals, Manfred Strässler;* SAMSUNG TOTAL PETROCHEMICAL LTD, ECI INTERNATIONAL INC, BURCKHARDT COMPRESSION AG
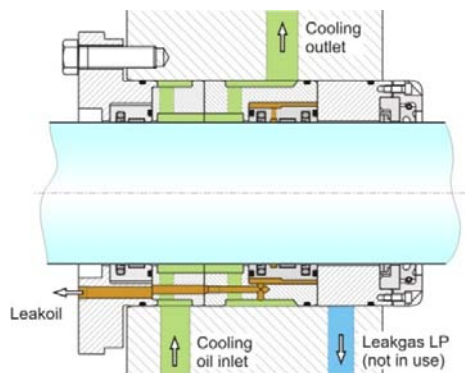
Figure 4: Old low pressure packing without N2 buffering system
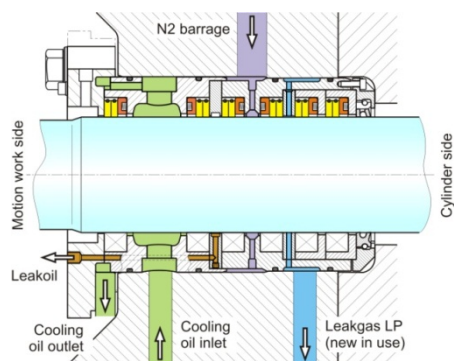
Figure 5: New low pressure packing with N2 buffering system

2.2.4 New galvanic coated connecting rod bearings

Connecting rods were originally fitted with conventional try metal bearings with a 1mm layer of Babbitt metal. Higher load to bearings suggested replacement of conventional bearings with new bearings with only a flash galvanized Babbitt layer, which are far less sensitive against breaking out of Babbitt metal. No machining was required to install the new type of bearings. However, previously installed 25micron oil filters had to be replaced by 10 micron filters.

2.3 Additional engineering services

2.3.1 Compressor performance calculations

Extensive thermodynamic calculations had to be performed with the proprietary sizing program for all operating cases to explore the set points of pressure and temperature switches as well as the correct settings of the bursting disks.

2.3.2 Torsion analysis

Since the main driver had to be replaced, a torsional analysis of the drive system had to be executed. All

information about the motor shaft design was provided by the motor manufacturer.

2.3.3 Pulsation study Hyper compressor

In 1990, the original pulsation study was done on the Analog Simulator.

A second pulsation study was conducted to confirm that the revamped system conformed to the same pulsation limits/pulsation levels despite the increased mass flow.

The re-engineered system was analyzed using the digital simulation program PULSIM developed by the TNO/TPD Institute in Delft (NL).

All operating cases were investigated. Pulsations above the original pulsation level have to be reduced through changes in the piping system or by the installation of orifices.

To reduce the pulsation on the suction side of the 2nd stage we recommended increasing the piping diameter in the common suction line from 55mm to 200mm over a length of about 2.5m.

This modification reduces the pulsation for the whole line but especially for the suction part of the 2nd stage.

For the remaining piping system the installation of orifice plates was sufficient to reduce the pulsations to below the given limits.

The overall pressure drop is still within the same range of the original design.

The comparison between original design and the debottlenecked design is shown on Chart 2.

Homopolymer operation				
Location	Pulsation ptp [%] original design line A	Pulsation ptp [%] after debottlenecking. Line A	Pulsation ptp [%] original design line B	Pulsation ptp [%] after debottlenecking. Line B
Common suction line	9.9	4.5	NA	NA
Compressor 1st stage suction flange	6.3	8.4	5.0	7.2
Compressor 1st stage discharge flange	7.7	11	5.4	10
Intercooler	4.1	7.5	9.7	8.6
Compressor 2nd stage suction flange	10.6	15	9.9	9.0
Compressor 2nd stage discharge flange	8.0	8.3	6.2	6.7
Inlet reactor	2.1	1.8	2.1	1.9
Pressure drop [bar]	48	23.23	37.1	21.58

Chart 2: Comparison Hyper pressure pulsation before/after debottlenecking. Partial increase in HP piping diameter improved situation with regard to pulsation considerably. In fact, the line pressure drop was reduced, saving energy

2.3.4   Vibration study

The purpose of the vibration study is to check the dynamic behavior of the piping system at worst case pulsation loads. Besides vibration amplitude and vibration velocity, stresses and support forces are checked. In general the following limits are to be maintained.

	calculated	Admissible limit
Max. displacement ptp	0.82mm	1mm
Max. velocity [RMS]	23.4mm/s	30.0mm/s
Reaction force	32.2 N/mm^2	45 N/mm^2

Chart 3: Comparison calculated to admissible
values.

The investigation of the piping showed no severe problems with vibrations. One reason for this is the reduced pulsation level that was achieved through the modifications recommended in the pulsation study. The existing support types displayed very rigid properties, no modification of the supports was necessary.

2.4   Replacement of the existing main driver

Hyper compressors are typically installed on a table top foundation. Major modification to the table top foundation is almost impossible since the compressor block and the motor block form one solid piece of concrete, reinforced by iron. The originally delivered main driver was manufactured by Jeumont Schneider, France. This manufacturer has ceased its activities in the meantime, which created a new situation for the project team. ABB was ultimately selected to design a motor to match the existing foundation pit as it fulfilled all requirements.

Figure 6: Lifting out existing main driver

Figure 7: Assembly of new main driver

Figure 8: Lifting of main driver through open roof
into position

2.5   Debottlenecking of auxiliary equipment

As discussed earlier, equipment in a high pressure LDPE plant typically has very long deliveries. For this reason a debottleneck project such as this one must be carried out by engineering companies such as ECI that can identify critical long delivery items so they can be ordered and onsite in time to ensure smooth coordination with all other project work. Once an operating LDPE plant shuts down, it must start up again at the appropriate time in order to keep critical customers supplied. Without this capability, an operator's market position will surely be compromised.

Figure 9: Highlighted area for new intercooler
bundle stream "B"

RETROFIT

Increasing the capacity of reciprocating compressors for LDPE plant, *Hisung Lee, Dr. Charles D. Beals, Manfred Strässler;* SAMSUNG TOTAL PETROCHEMICAL LTD, ECI INTERNATIONAL INC, BURCKHARDT COMPRESSION AG

Figure 10: Installation of additional intercooler bundle for stream "A"

3 Debottlenecking of Booster/Primary Compressor

The B/P compressors used for the LDPE process are standard API 618 reciprocating compressors. The discussed compressor is a six crank compressor with a three stage booster section installed on two cranks with one double acting piston for first and one step piston for second and third stage. The primary part is installed on four cranks with two double acting first stage cylinders and two step pistons for second and third stage. The primary section is split into two streams. (Figure 11 1 top view of B/P compressor) To increase the capacity of an API 618 compressor the manufacturer usually has the option to either increase the speed and/or to install larger cylinders. In most cases the extension of the stroke is the most expensive option.

An increase of the speed of the compressor is only possible as long as the average piston speed stays within acceptable limits.

Besides an increase in speed from 400 RPM to 450 RPM, new cylinders for the 1st and 2nd stage of the booster and two 1st stage cylinders for the primary with increased bore were required. The increased mass flow required the replacement of the intercoolers and of the pulsation bottles. Space constraints made the whole job quite demanding.
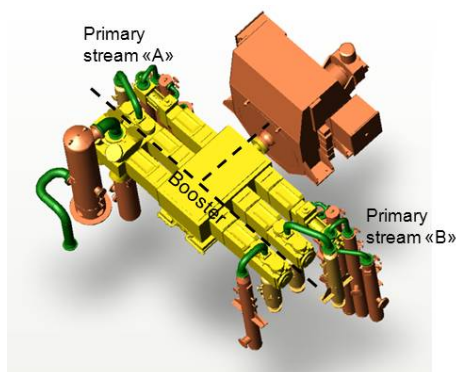
Figure 11: Top view of B/P compressor

3.1 Design of new cylinders for B/P compressor

The narrow crank distance demanded meticulous analysis and planning during the redesign of the 1st stage booster and 1st stage primary cylinder in order to allow side-by-side installation of both cylinders. Existing nozzle inlet and outlet positions had to be maintained since the position of the discharge pulsation dampers could not be adjusted due to space constraints.
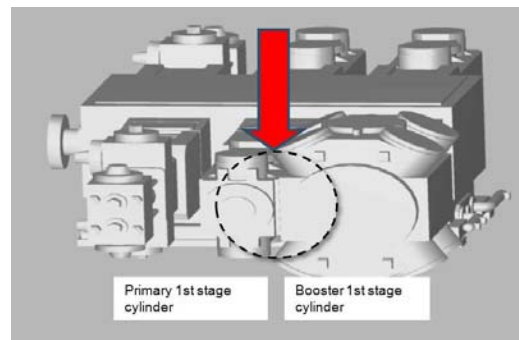
Figure 12: Space constraints between compressor cylinders

3.2 Pulsation and Vibration studies of Booster/Primary compressor

3.2.1 Pulsation study

The B/P compressor underwent partial cylinder replacement, which required modifications to pulsation dampers. Space constraints made the installation of optimized pulsation dampers more challenging.

The original damper volumes were designed for a pressure pulsation level of 4% ptp. To reach this pulsation level after debottlenecking seven out of ten pulsation dampers had to be replaced with higher volume dampers.

The Pulsation study showed that with optimized orifices the pulsation level could be maintained throughout the piping system.

3.2.2 Vibration study

Basis of the vibration study are isometric drawings produced by Daewoo Engineering Co. Ltd. Korea. The investigation of the piping showed no severe problems with vibrations. As for the Hyper compressor, the displacement, velocity and stress forces were checked and found to be below our limits. Therefore no modifications were required. One reason for the low vibration level was the reduced pulsation level, which was achieved by making the modifications recommended in the pulsation study.

RETROFIT

Increasing the capacity of reciprocating compressors for LDPE plant, *Hisung Lee, Dr. Charles D. Beals, Manfred Strässler;* SAMSUNG TOTAL PETROCHEMICAL LTD, ECI INTERNATIONAL INC, BURCKHARDT COMPRESSION AG

3.3   Auxiliary equipment

Auxiliary equipment for the B/P compressor is designed for its original purpose. Components such as intercoolers, dampers and separators can sometimes handle a minor increase in mass flow. All components had to be checked for operational suitability after the increase in mass flow. Burckhardt Compression delivered all required information to perform the heat load calculations of existing heat exchangers. The verification of the capability of a heat exchanger should preferably be performed by the heat exchanger OEM or an experienced engineering company. Pulsation damper volume adjustments must be taken into account to keep the pulsation within acceptable limits. Quite often, compromises are required because space limitations do not allow for the installation of a perfectly sized damper. Our preliminary volume calculations revealed most of the damper volumes were too small to maintain pulsations within acceptable level. New pulsation dampers were designed with untypical dimensions. Optimal configuration of 2/3 to 1/3 could not be maintained because of space restrictions resulting in the accumulation of liquids (oil & condensate) during operation. A separate drain system was introduced to overcome this problem.
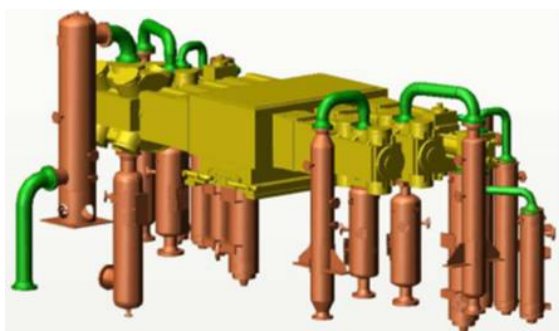
Figure 13: Graphic shows original pulsation dampers
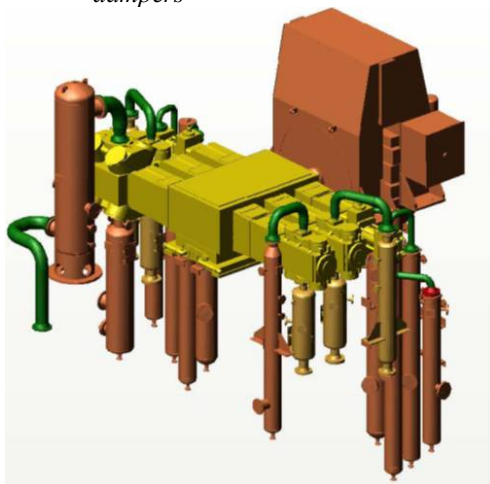
Figure 14: Graphic shows elongated pulsation dampers

Daewoo Engineering was the appointed supplier for the auxiliary equipment. Burckhardt Compression delivered sketches for new pulsation dampers. Coolers as well as dampers were procured in Korea through Daewoo.

Correctly sized separators are essential for B/P compressors running on a high EVA content to ensure safe operation. Fortunately the existing separators were still suitable. Process gas piping had to be rerouted in order to accommodate the new pulsation dampers and to keep mean gas velocities within acceptable limits.

3.4   Replacement of existing main driver

The main driver of the B/P compressor was replaced with a new driver running with a speed of 450 RPM and a power rating of 2500kW compared with 400 RPM /1800kW previously. The new motor was made to fit into the existing foundation pit. Only the motor sole plates had to be changed.

Previously installed coupling bolts had to be replaced by a new coupling system. (Dictated by space constraints due to a wider motor casing)

Burckhardt Compression used two **Superbolt®️ Expansion Bolts** for the transmission of sheering torque and the 8 conventional bolts for the tension. This system reduced the installation time considerably since no new coupling holes had to be reamed.
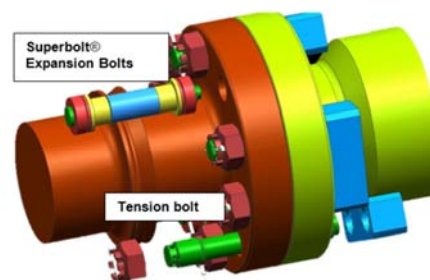
Figure 15: Installation of Superbolts for coupling

4   Site installation and commissioning

Highly professional site organization was the key factor for ensuring smooth execution without accidents.

- To be able to lift heavy equipment such as the main driver of the Hyper compressor, a 600 t crane had to be installed. The weight of the heaviest part was 118t.
- The onsite installation was successfully completed after 1.5 months.
- Pre-commissioning was finished within 1 month.

163

RETROFIT

Increasing the capacity of reciprocating compressors for LDPE plant, *Hisung Lee, Dr. Charles D. Beals, Manfred Strässler;* SAMSUNG TOTAL PETROCHEMICAL LTD, ECI INTERNATIONAL INC, BURCKHARDT COMPRESSION AG

- Samsung started the PE production 3 months after start of construction
- The plant performance is well within expected output.
- Equipment vibration was reduced considerably. No actual measurements were taken for comparison purposes.

5   Conclusion

Debottlenecking of existing LDPE plants requires a huge effort in engineering.

Upgrading a Hyper compressor is easier to accomplish compared to Booster/Primary compressors.

Hyper compressor cylinders can accommodate minor plunger diameter alterations without influencing the main dimensions of a cylinder. Bottlenecks are quite often caused by the HP piping system. Replacing HP piping is a rather expensive task. Accepting higher pulsations within the system has a negative impact on the lifetime of components.

Upgrading Booster/Primary compressors is a more complex process. This type of compressor is typically built for a specific duty. Replacing cylinders with larger-sized cylinders has a detrimental impact on pulsation dampers, intercoolers and other auxiliary equipment. Professional management of such contracts is the key to success. Major surprises leading to higher costs can be avoided by executing thorough engineering right from the start. Utilizing professional services of highly specialized engineering companies is highly recommended. Communication between all players is essential to avoid misunderstandings.

Design and manufacturing of a new large bore compressor cylinder

by:

Lau Koop

Technology Department

Howden Thomassen Compressors BV

Rheden,The Netherlands

lk@thomassen.com

8th Conference of the EFRC

September 27th / 28th, 2012, Düsseldorf

Abstract:

The demand for large bore cylinders on reciprocating compressors has increased recently. Typical applications are: Low pressure Hydrogen, LNG 1st and 2nd stage, CO2 and ammonia for the fertilizer industry. The bore of cylinders for these applications, ranges up to 1200 mm. The large frame ratings now available on reciprocating compressor frames, allow for the application of large bores at a relative high differential pressure per stage. New cylinders have to be designed for this. This paper describes the design and manufacturing of such large bore cylinders.

1   Introduction

Piston compressors can be used, by their large flexibility, in many applications. API 618 compressors are traditionally only applied in oil and gas, refinery and petrochemical industry. The requested capacity and pressures usually fit in the existing cylinder diameters up to approximately 800 mm. Even in some compressor specifications limits on the maximum piston diameter are given.

Especially in the application for Hydrogen compression the last decades larger piston compressors have been developed. In this case, larger means higher admissible gas forces on the piston rod, and high drive power up to 20 Mw. If these large frames can be applied in applications where the initial pressure is very low, such large volumes can be compressed that the piston compressor can take over a part of the operating envelope of a centrifugal compressor. This can be desirable, especially when the process requires a large flexibility and/or energy efficiency is of utmost importance.

Possible applications for these cylinders are:
- Hydrogen for Aromizing and Octanizer Units
- Hydrogen rich gas from CCR.
- 1st and 2nd stage CO2 capture and storage,
- 1st and 2nd stage LNG boil off.

For all these applications cylinder diameters up to 1200 mm can be used. In 2008, Howden Thomassen compressors initiated the development of a range of large bore cylinders suitable for the large compressors. They became available for operation in 2010.
In this paper the different development stages and the most important design criteria are summarised. The development of the Thomassen CH cylinder has been carried out using modern FEM and CFD calculation programmes. Mile stones in the development:
- Size and design
- Determination of casting ranges
- Efficiency; flow path optimization, flow resistance.
- FEM strength calculations
- Piston design.
- Special tools for handling the very heavy covers and valves.
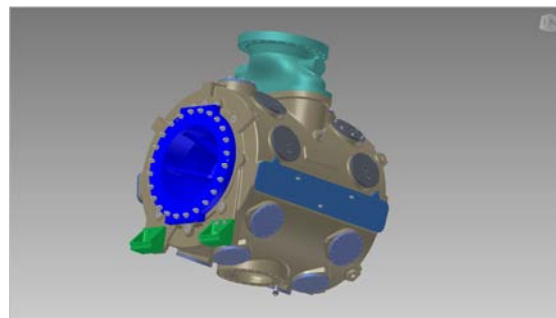
Figure 1

2   Size and design

2.1   General

The cylinders are designed in compliance with the directives according to API 618 5th edition. This means a replaceable lining, liquid cooling, and bottom discharge connection of the process gas. The die cast parts are made of nodular cast iron or cast steel.

The liner material can be adapted to the requirements of the process regarding the temperatures and corrosivity. One of the design requirements was to maintain a short running length of the piston. This was done to keep the piston mass low.

2.2   Cylinder diameters and frame sizes

For each compressor type a selection table is available. In these tables the selection of a particular cylinder type, the design pressure of the required cylinder diameter, and the associated cylinder type is indicated. This selection is automated in the selection program and visualized in Figure 2.
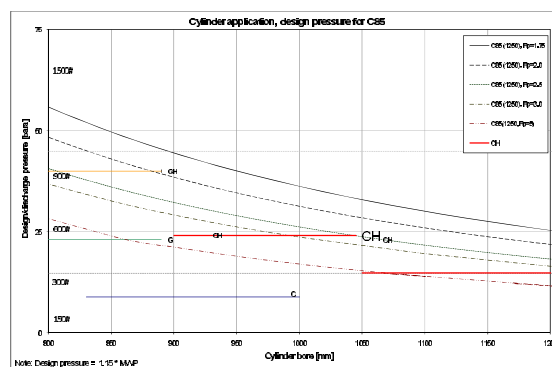
Figure 2: compressor selection diagram

The rating of our largest frame allows for a maximum diameter of 1200 mm at a design pressure of 14.8 bara (150# rating), and a maximum of 1040 mm for a design pressure of 24 bara.

2.3 Cylinder diameter ranges

The exterior dimensions of the cylinder is largely determined by two parameters: the size and number of suction and discharge valves and the size of the pipe connections on the suction and discharge side.

The cylinders are divided into two main dimensions. A diameter range of 900-1040 mm and a range of 1050-1200 mm. the cylinder bore size within a master is adjusted by adjusting the cooling water space.

2.4 Compressor valves

The number of valves and the size are limited by the available circumferential length of the liner. It was specified that the cylinder had to be designed for heavy gases too. This requirement makes it necessary to restrict the flow resistance. The shape of the channels in cylinder around the valves are optimized. A special design of the valve ports was created to minimize the resistance. The flow resistance in the valves itself can be minimized by the choice of the number, the type, and the dimensions of the valves.

The most economic design is to optimize the number of valves. This means that the largest valves available from valve suppliers is applied. In the CH cylinders 4 suction and 4 discharge valves per side can be installed.
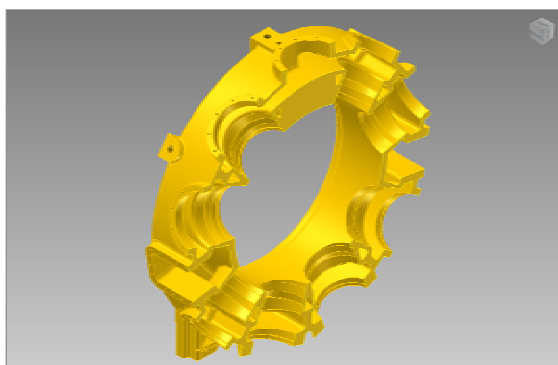
Figure 3: Cylinder valve section

2.5 Cylinder process connections

The size of the cylinder process gas connections are based on the maximum piston speed and the maximum density of the gas. The suction connection of the largest cylinder then comes out at 28 ". The application of a round flange would create long cylinder. Some designs leave a solution with double connection. Others make the connection elliptical. A transitional piece to a round flange is then required. The shape of this transitional piece requires calculations to be carried out to meet the pressure rating. However, the

relatively low pressures make this application possible without using large wall thicknesses.

It was decided to choose a separate transitional piece to the pipe flange.

3 Casting

During the entire design process there has been close contact with the foundry. Together with 3D design we have made use of rapid prototyping models to scale.
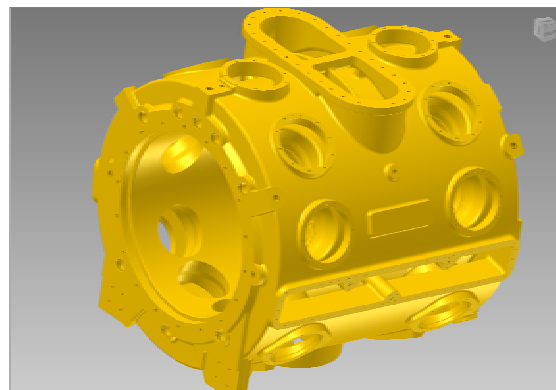
Figure 4: Bare cylinder casting
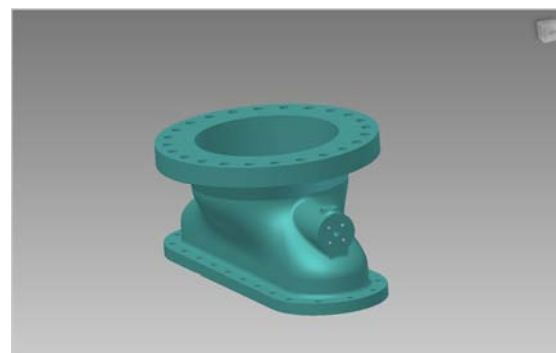
Figure 5: Casting of transition piece

4 Calculations

The dimensions of the cylinder are relatively large. The necessary amount of cast material amounts to about 12 tonnes. Finite Element calculations can therefore give great benefits by reducing the amount of material at locations where this is not necessary.

Computational Flow Dynamic calculations are done to the channels in the cylinder to optimize for the flow resistance and valve behaviour.

4.1   FEM strength calculations

4.1.1   Cylinder

The cylinders must be designed for:

1. The internal pressure
2. The tensile and compressive force caused by the differential pressure in axial sense.
3. The load on all bolt connections
4. The stress as a result of the preload of the valves on the seat and in the glands
5. The design pressure in the cooling water space
6. Hoisting
7. Cylinder supports
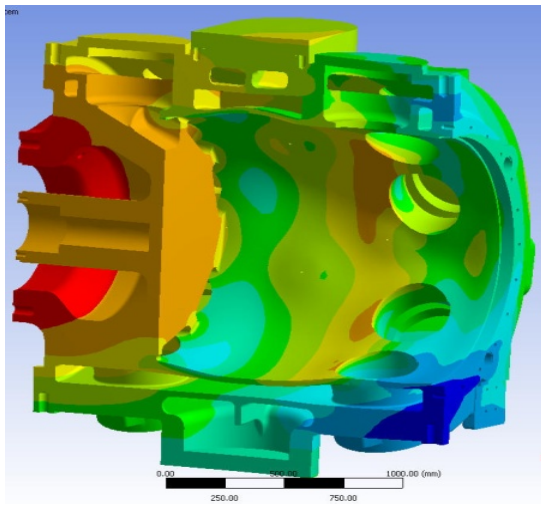
Figure 6: Deformation under Pressure

The cylinder has passed the design process several times loadings. In several locations, especially around the valve ports, adaptions are done to decrease the stress.
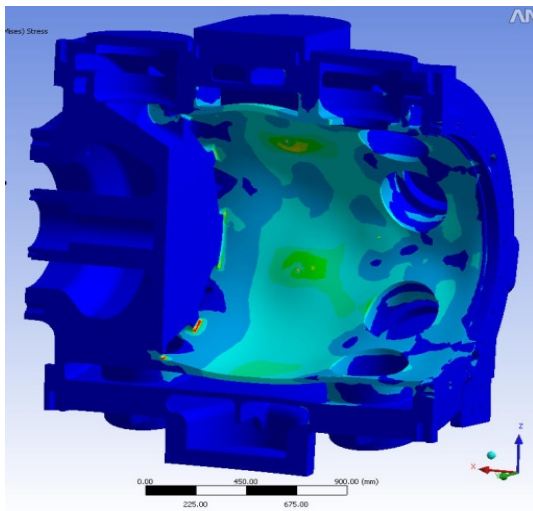
Figure 7: Von Mises Stress under Pressure

For vibrations of the cylinder, it is important that the distortion remains low. It turns out that only the inner wall, under the influence of the varying pressures exhibits some distortion. The rest of the cylinder deforms very little which will influence the vibration behaviour of the cylinder positively.

4.1.2   Piston

The cylinders are designed for the largest frame size compressor, the pistons must be designed for the associated gas forces. The gas forces deform the piston. Long bolts at the perimeter of the piston are required to keep the piston halves together under load.
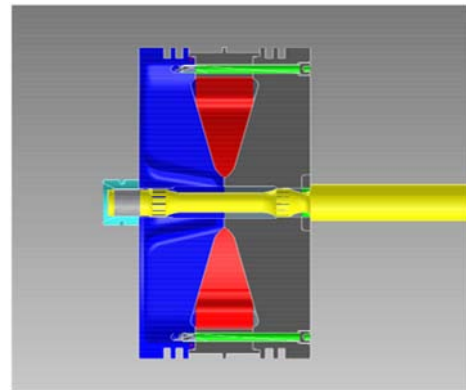
Figure 8

4.2   CFD calculations
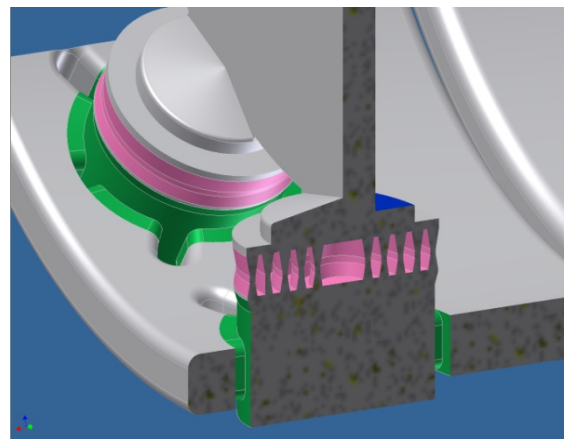
Figure 9: CFD model conventional valve location

4.2.1   Conventional valve locations

Traditionally, the valves are radially positioned in the cylinder, whereby the center of the valve is located under the edge of the cover. When the piston rapportages the end of the stroke, the gas has to flow back partially under the piston. It is known that this configuration causes a relative large pressure drop, and consequently   an increase in

168

pressure in the cylinder. In order to optimize the flow, CFD calculations of the cylinder, channels, and valve spaces have been done. The images show the flow regime. It turns out that in the traditional configuration, the available flow area of the discharge valve is not fully used. The largest velocities occur in the middle, where the available passage is smallest. This means that the flow induced forces on the centre rings is high.
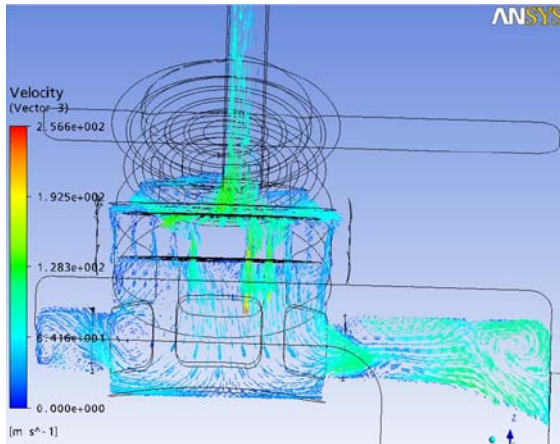
Figure 10: CFD results conventional valve location

4.2.2 Modified valve location
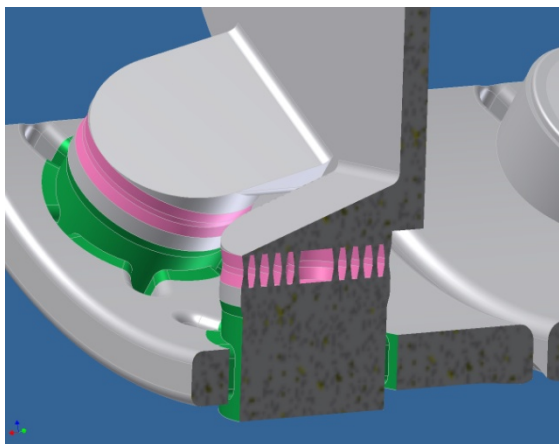
Figure 11: CFD model actual valve location

In this configuration the valve ports have been moved, When the valves have been moved to a location outside the running area of the piston, the flow channel will not be covered by the piston. The flow regime changes completely and the gas flow is well distributed over the surface of the compressor valve (see figure 12). This results in a decreased pressure drop, and stabile operation of the valve rings.
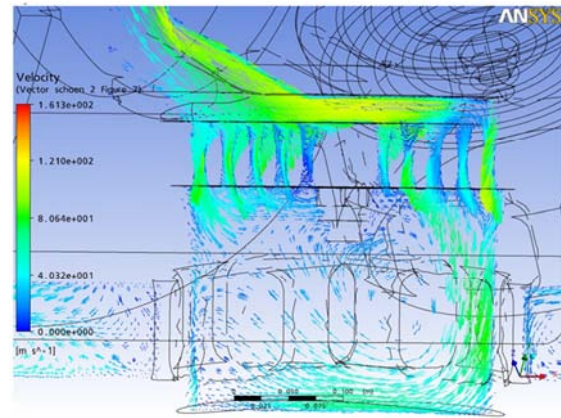
Figure 12

4.2.3 Cylinder channels

The cylinder is fitted with 4 suction and 4 discharge valves at each side. The discharge opening of each valve is released in a common space. It appears that the flow coming from the upper valve, disturbs the proper flow of the adjacent one. (see fig 13). This has been solved by the installation of a baffle, integrated in the casting. This solution leads to a proper inflow (or outflow) to or from the valves, and the valve rings will operate more stable and reliable.

The pressure drop in the valves and cylinder channels affect the pressure gradient inside on the piston front, inside the cylinder. Especially during the discharge stroke the absolute pressure near the suction valves is relatively low, and near the discharge valves the pressure is relatively high. This effect is intensified when the flow resistance in the valves and channels is high.
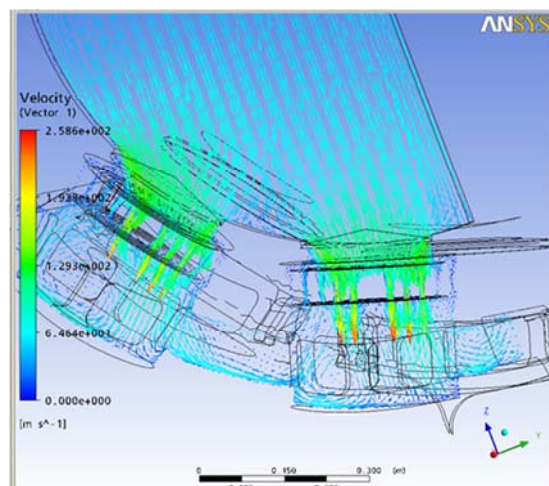
Figure 13

The table below shows the pressure drop (% of
absolute pressure) for the two valve locations.

Location/valve position	Standard	Alternative
Vertical piston gradient	5.8%	5.0%
Valve inlet	5%	2.5%
valve	3.3%	1.7%
Valve outlet/cylinder flange	1.7%	1.7%
Total pressure loss	10.0%	5.9%

5   Modelling and casting

After the design was ready, a model is made by
means of fast prototyping on a reduced scale. This
miniature model is used as a guide for the
discussion on the manufacturing of the real model.

Figure 14

Later on the real model, consisting of 60 pieces,
was composed and shipped to the foundry.

Figure 15

Howden Thomassen Compressors owns the cast
model.

Figure 16

6   Special Tools

Every part of the new cylinders is too heavy to lift
by hand. API 618 states the following in paragraph
7.11.1: When special tools and fixtures are needed
to disassemble, assemble or maintain the unit, they
shall be included in the quotation and furnished as
part of the initial supply of the machine, together
with complete instructions for their use. For
multiple unit installation, the quantities of special
tools and fixtures shall be agreed by the purchaser
and the vendor. These or similar special tools shall
be used during shop assembly and post-test
disassembly of the equipment.

Howden Thomassen has developed special tools
according the above requirement.

6.1   Installation suction valves and covers

Figure 17

Figure 18

6.2   Discharge valve installation

Figure 19

7   Applications

Figure 20 shows a compressor fitted with three large bore cylinders, diameter   1130mm. It is designed for Hydrogen rich gas.
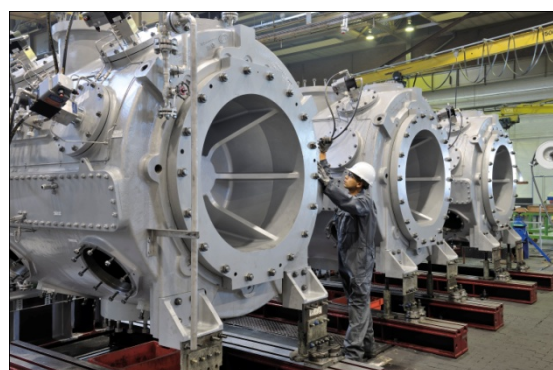
Figure 20

In figure 21 a compressor is a multistage Hydrogen compressor is shown. The 1st   stage cylinder is a large bore cylinder, diameter 990mm.

Figure 21

8   Conclusion

- The development or adaptation of a compressor cylinder takes a considerable investment in product development and technical realization. The right choice has to be made for which power and framesize the cylinders have to be designed for. The investment and development on these large high power cylinders allows Howden Thomassen Compression to quote energy efficient, low pressure cylinders.

- The large frames such as the C-45 and C-85 compressor can now be efficiently used for low pressure applications and high volumes.

- In order to obtain a technically sound, and economic design the application of FEM and CFD is inevitable.

- API 618 requires the design of special tools for the maintenance. These tools must be safe to handle and user friendly.

- The large dimensions and complexity of the cylinder, requires adequate coordination and consultation between designers, the machining group and the foundry.
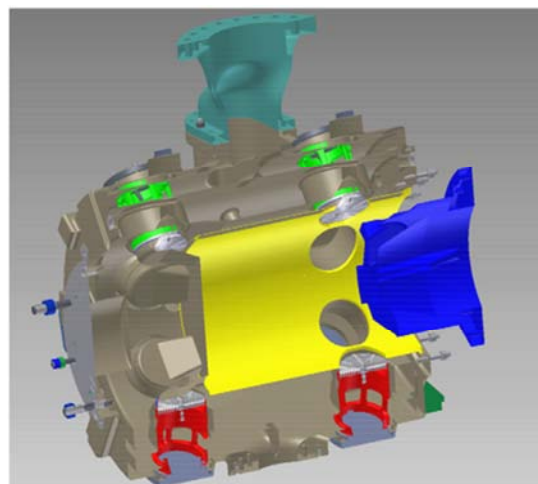
Increasing the reliability and reducing vibration of a 35 year old compressor by replacing the frame housing with an optimised design using the FEA method

by
Mr Ralf Krich,
Manager Engineering Western Europe
HOERBIGER Kompressortechnik Europa Services GmbH
HOERBIGER Service GmbH,
Walsrode
ralf.krich@HOERBIGER.com

8th Conference of the EFRC
September 27th / 28th, 2012, Düsseldorf

Abstract:

During more than 34 years of operation the 3 stage high pressure air compressor produced by the company Halberg was used in a chemical plant in Western Germany.
Installed in 1977 the original compressor had a welded frame housing manufactured without foundation supports for the crosshead guides. Also after modifications 1978 the frame was still not sufficiently rigid in order, to run as smoothly as expected from a four throw boxer design is normally working. During these years several repair sessions and minor modifications were carried out. Several cracks in the housing were repaired by welding. In 2007 a new installation using epoxy grout could not solve the problem in general either. However the cylinders of second and third stage could be to run with lower vibration by the implementation of extreme stiff steel structures for these two cylinders. To overcome the continued problems the authors analysed the installation and the original design. By engineering, manufacturing and installing a complete new welded frame housing employing optimized 3D design and calculation methods including FEA the authors could reduce vibration levels, increased safety margins and thus improve reliability of the compressor. In addition improved cylinder support helped to run the compressor at lower vibration levels, even without the additional steel structure between the two high pressure cylinders.

RETROFIT

Increasing the reliability and reducing vibration of a 35 year old compressor by replacing the frame housing with an optimised design using the FEA method, *Ralf Krich;* HOERBIGER SERVICE GMBH

1   Introduction

The compressor operates in a chemical plant, being part of a chemical group who is a leader in speciality chemicals and operates in all important global markets.

This high pressure Halberg air compressor , which has been modified and upgraded by an international

team from HOERBIGER specialists, is part of a sewage treatment system at the Uerdingen plant. (Picture 1)
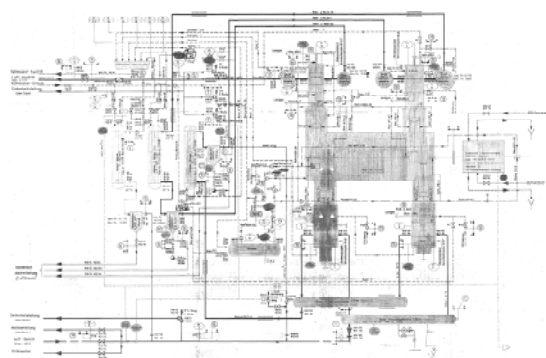
Picture 1: Piping and Instrumentation

The sewage treatment is belonging to an Hexane-oxidation process. Organic compounds from this process are burnt with at 280 to 350°C and at 150 to 200 bar. The combustion air is initially compressed by 2 smaller booster compressors to 10 bar. The high pressure compressor HPC is than subsequently compressing this air to the final pressure in 3 stages.

It is a single unit and thus required to run continuously year after year. Service intervals have been extended as much as possible, but several problems kept the compressor owner and their respective service companies busy, for many years.

2   History

The compressor HPC (Picture 2) was bought, from Halberg in Ludwigshafen in 1976.

At this time Halberg had a lot of experience with single crank compressors and had recently started to build vertical and horizontal machines with multiple cranks. As Halberg had no pattern to produce a casting for this compressor size, the 4-crank boxer design got welded steel frame. The attached list (Table 1) gives a short overview of problems this compressor caused over 25 years.

June 1976	Order to Halberg
July 1977	Compressor Delivery
March 1978	Compressor start-up
April 1978	additional steel structure assembled between cylinder stage 2 and 3
May 1978	First cracks in piping, piping modifications
June 1978	First cracks in frame housing
July 1978	second modifications in piping layout

August 1978	analogue piping study
September 1978	Assembly of Orifices, reduced vibration
December 1978	New cracks at frame housing
March 1980	Cracks at cylinder support stage 3 Discussion about new frame in cast version.
August 1980	Decision to run with reduced pressure (160bar)
February 1981	Crack at pulsation dampener Stage 3
August 1983	Repair of pressure vessel
Till 1986	several problems with valves
July 1987	Bypass piping cracked
September 1988	Major revision
June 1994	Major revision 2nd and 3rd stage re-bored with 0,5 mm bigger diameter to get new running surface
November 1996	
May 2001	Major Revision
June 2001	Crack at crosshead guide cyl.1. welded
July 2005	vibration measurements
June 2006	vibration measurements
July 2007	Major revision of the foundation, several repair work, new grouting
July 2007	E-motor realigned and vibration measurement
July 2008	Crack at cylinder connection stage 2 welded
July 2010	Service and repair welding
September 2010	HOERBIGER Customer Information Day Düsseldorf
December 2010	Pulsation study and measurements
January 2011	HOERBIGER visit customer for Inquiry new frame housing

Table 1: Event list for compressor HPC

Looking for a permanent remedy for the persistent frame problems the customer became aware that the frame of this unit has been unique.

Picture 2: Compressor HPC in January 2011, view to 1st stage cylinders

3   The design process

Thus the customer invited the authors to perform design check of the original design and to come up with a proposal to re-manufacture the compressor frame, fitting the existing foundation, all compressor internals, such as crank, bearings, cylinders, pistons etc. and all connections.

To start this investigation the customer provided sets of the original drawings.

Increasing the reliability and reducing vibration of a 35 year old compressor by replacing the frame housing with an optimised design using the FEA method, *Ralf Krich;* HOERBIGER SERVICE GMBH
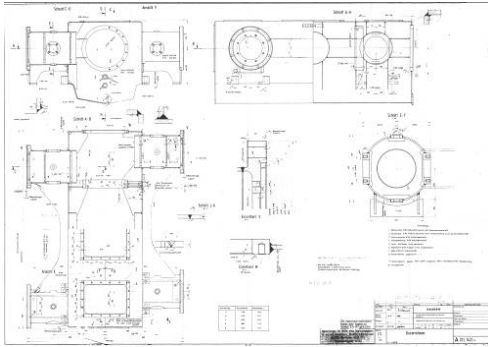
Picture 3: Halberg manufacturing drawing

Part of this documentation was a manufacturing drawing from Halberg (Picture 3) which helped to analyze the design to find the problematic spots and to re-design a new frame with matching dimensions.

With many years of experience in engineering and production of reciprocating compressors components and systems, the authors were able to identify the principle design flaws and to check the feasibility of delivering a solution within a suitable time window and compliant with all other requirements.
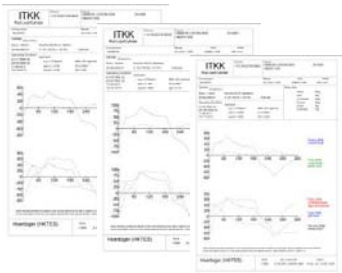
Picture 4: HOERBIGER Rodload calculation

In a primary study the drawings, the history, the process and all other data were analyzed. The authors started to calculate internal and external forces (Picture 4+7) and to re-check the foundation as well. Within this study the principle ideas were streamlined in order to get a clear understanding about how the final design could look like, even though the complete design and stress calculation was not finished in the pre-study.

Picture 5: Details from original frame

The fixation of all 4 crosshead guides, in the main housing, was found to be too weak. (Picture 5) Originally the crosshead guide housings were designed in round shape and these crosshead guides have been mounted using ribs, that were welded at 90° to the main force direction. These guides were welded onto both side walls, just by having additional reinforcements in shaft direction, on both sides of the wall.

In the first drawings these guides were not having any vertical support to the foundation at all, as to be seen in the cross sectional drawing (Picture 6)
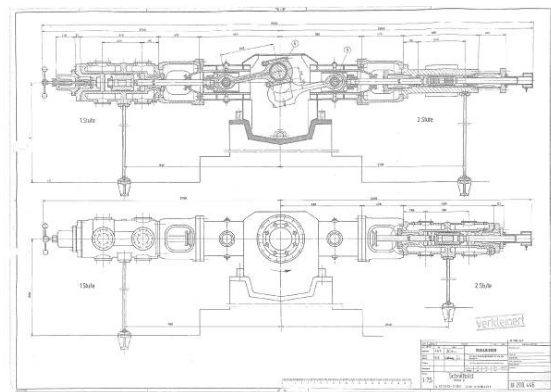
Picture 6: Compressor cross sectional drawing

Picture 7: Data preparation for FEA study

The forces, introduced by the cylinders, had to pass across these housings. Combined with the lever-arms the forces result additional in moments (Picture 7) which were leading to high bending effect within these two side walls.

Increasing the reliability and reducing vibration of a 35 year old compressor by replacing the frame housing with an optimised design using the FEA method, *Ralf Krich;* HOERBIGER SERVICE GMBH

4 The new design modifications

There were no stringers which could lead the forces to the opposite side and therefore they were ending in the weak top area or foundation hold points.
Several cracks in the weld lines as results from these internal forces proof the poor design (Picture 8+9).

Picture 8+9: New welding were indicating former cracks

Removing this design flaw, overcoming some other identified design problems and a list of parts to be replaced at the occasion of this upgrade served as the basis for a technical and commercial feasibility study.

The resulting quote included site supervision as well but not field services which were carried out by the customer's service partners.

The detail engineering and design work started in February 2011.

The authors have been working in an international team sharing the work load, specialists located in Vienna (Austria), Heerlen (the Netherlands) and Walsrode (Germany).

Frame internal forces and foundation forces have been analysed, a new frame has been designed using 3D CAD modelling (Picture 10) and checked to withstand all process conditions using FEA (Ansys).

Already in the first design step, the idea of using a rectangular crosshead guide was realised.
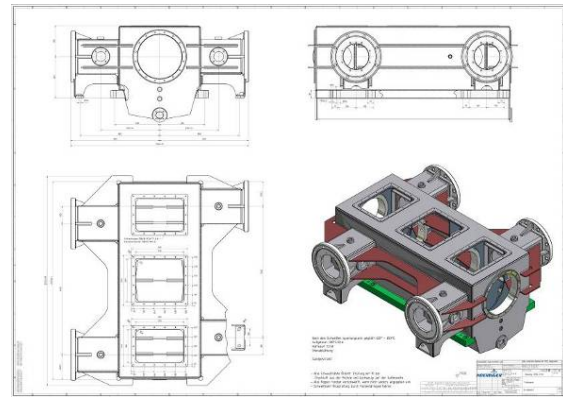
Picture 10: Newly designed frame housing

Using 3 stringers or rips which are connected to the opposite side also including the support for implementation of the main bearing seats, reasonable stress values within the frame have been archived (Picture 11).
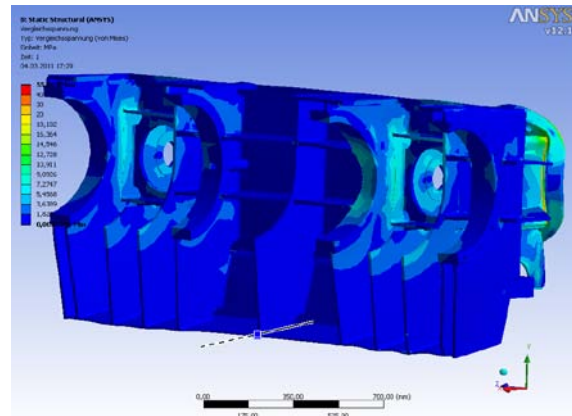
Picture 11: The new designed frame housing-stress plot

Forces supplied by the compressor simulation software were combined with the mechanical design in 3 optimizing steps. The optimization not only reduced stress values on the one hand but minimized production costs on the other hand as well.

The weight of the new frame housing is 2.6 tons instead of 1.8 tons compared the original.
This is less a result just from thicker plates but predominantly from an optimised use of re-enforcements.

To enable a simple welding process, the assembly sequence was checked, welding directions, and number of parts were optimized applying pre-bevelled plates wherever useful (Picture 12). Also collision checks with the con-rods were carried out.
For cutting the steel plates the dxf data files were directly used, avoiding redundant manual work.

RETROFIT

Increasing the reliability and reducing vibration of a 35 year old compressor by replacing the frame housing with an optimised design using the FEA method, *Ralf Krich;* HOERBIGER SERVICE GMBH

Picture 12: Assembly of all parts checked before starting the cutting and welding process

To avoid the risk of any new trouble the customer required an extremely short delivery time, which left no choice for any other production method than welding.

To further shorten delivery time an approach of overlapping design- and purchasing has been carried out. The design and FEA work had to run parallel to the production process. Plate and other bare material could be ordered before the design was completed.

Before starting machining of parts the final FEA study (Picture 13) has been completed considering all findings and design modifications.

Parallelization of design and manufacturing as well employing shift labour the originally quoted delivery time of 17 weeks has been cut to 11 week.

Picture 13: Picture of maximum displacements as a result from FEA study

5   Foundation modification

Alike for the change for the crosshead guide design, our knowledge on the installation of compressors led to the modifications was to be applied to the foundation.

In principle, there were 3 major areas for improvement:

1.) The design of the cylinder support was not rigid enough, to keep the cylinders in place during operation. Quite similar to a few other designs on the market, expecting that thermal expansion is more relevant to proper compressor installation, than reduction cylinder-vibration. (Picture 13+14)

Picture 13+14: Cylinder pendulum support

2.) The foot connection cleats to fix the frame to the foundation bolts were too small and could not provide the optimum force transmission from the crosshead-guide and the bearings into the foundation, at least assuming that this 4-crank boxer is not balanced concerning the opposite weight of piston and rod.

Picture 15: Foot cleats for foundation bolts

3.) During the last major overhaul the re-grouting was made under the foot cleats and also under the oil-sump as to be seen in original cross sectional drawing. (Picture 16) The thermal expansion might have introduced additional stress into the side walls.

176

RETROFIT

Increasing the reliability and reducing vibration of a 35 year old compressor by replacing the frame housing with an optimised design using the FEA method, *Ralf Krich;* HOERBIGER SERVICE GMBH

Picture 16: Epoxy grouting under oil-sump

It is worth mentioning that because of the new design the steel structures applied between cylinders 2 and 3 for the reduction of vibration by Halberg already in 1978 became obsolete.

These stiffening structures (Picture 17+18) definitely have reduced vibrations but may have introduced additional stress into the frame housing.

Picture 17+18: Additional Cylinder supports from 1978 delivered by Halberg

The cylinder supports were replaced by A-type steel supports which are fixed to the same steel beams inside the concrete. These supports are rigid, mainly in shaft direction, but can allow some thermal expansion. (Picture 19, 20 and 31).
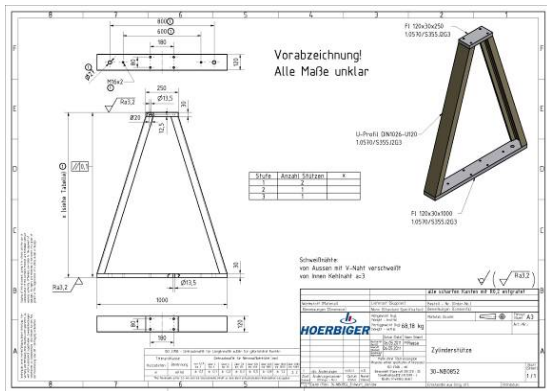
Picture 19: New cylinder support A-shape
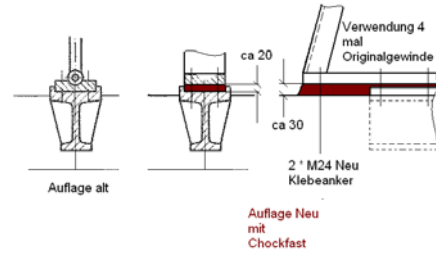
Picture 20: fixation of cylinder supports on foundation

The new frame housing got 2 massive, full length steel bars, welded on the top side to the sidewall and at the bottom to the oil sump bevel plate.
The bars are fully machined and can distribute the loads perfectly into the foundation. (Picture 10,13 and 21)

Picture 21: one of 2 foundation rails after the planing

Concerning the grouting it has been agreed with the customer to eliminate bonding between the oil-sump and the epoxy grout. Fortunately at the last grouting in 2007 it had been decided to use an aluminium foil to separate the epoxy from the steel. Otherwise it would have been extremely difficult to remove the old frame from the foundation. Only for aesthetic reasons the foundation under the oil sump got a new epoxy layer but this time with a 20 mm elastic material under the frame. (Picture 22)
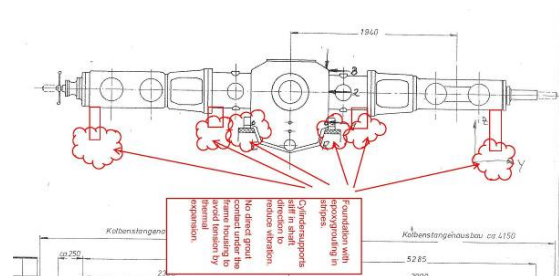
Picture 22: grouting areas agreed

177

RETROFIT

Increasing the reliability and reducing vibration of a 35 year old compressor by replacing the frame housing with an optimised design using the FEA method, *Ralf Krich;* HOERBIGER SERVICE GMBH

6 Scope of work

In addition to the engineering work the delivery scope included

1) The welded, heat treated and machined frame housing out of Carbon Steel S355J2+N

2) cover, studs and gaskets.

3) leakage test

4) paint in – and outside

Picture 23: frame during welding

Picture 24: frame painted at machining

5) Assembly of crankshaft, con-rods, bearing supports, crosshead liner, crossheads at HOERBIGER in Heerlen

6) A-shape cylinder support

Picture 25: crankshaft preassembled

7) 4* Main bearings

8) Machining main bearings assembled at

HOERBIGER in Heerlen

Picture 26: machine bearings in new housing

9) 2* Holding bolts for bearing supports

10) Honing crosshead liner stage 1

11) Dimensional check of distance pieces

12) Magnetic particle test main bearing support

13) Inspection of con-rod bearings

14) 3* re-grinding piston-rods

15) 4* re-machining crosshead pins

16) 2* turning centre main bearing supports

Picture 27: re-machined bearing support

RETROFIT

Increasing the reliability and reducing vibration of a 35 year old compressor by replacing the frame housing with an optimised design using the FEA method, *Ralf Krich;* HOERBIGER SERVICE GMBH

17) Magnetic particle test crankshaft

18) Oil connection oversize

19) crosshead liner machined outside

20) Transportation

21) Re-machining top cover for oil system

22) 4*Oil connection

23) Turning bearing support pump end

24) 8* Anchor bolt-holes re-bored

25) 8* BCD Packings (Picture 28)

Picture 28: HOERBIGER BCD Packing

26) 4* HOERBIGER Oil scraper

27) 1 set of HOERBIGER valves for all stages

28) Clearance pocket modifications

7   Timeframe

Engineering and production of the new frame housing have been realized starting mid of February, 2011 to mid of May, 2011. Parallel to the last production days, the old compressor was taken from the foundation. From beginning May 2011 to mid of June 2011 the compressor frame housing was changed and the reassembled compressor started including all additional work which came up in between and described in chapter 8.

8   Additional Obstacles

During the order-fulfilment some unforeseen items required quick decisions and solutions.

8.1   Mismatching bearing oil connections

Based on the original drawing, the new design had to match with several dimensions. There was no plan for additional measurements as all involved parties were sure that the frame was manufactured by Halberg to this drawing. During disassembly of both centre bearing supports it was found that the oil connection holes were not in line, and the oil connection bolts could not be installed (Picture 29). To get new connections realised, it was necessary

to re-bore the eccentric holes with a bigger diameter and produce special fitting bolts

Picture 29: old frame showing connection bolt hole not in the middle

8.2   Mismatching foundation bolts

Based on the same drawing the foundation holes were drilled, but during production of the original frame someone must have decided to bore 980 mm instead of 960 mm.

However the new frame with its big foundation rails got enough material to allow also the re-boring (picture 30).
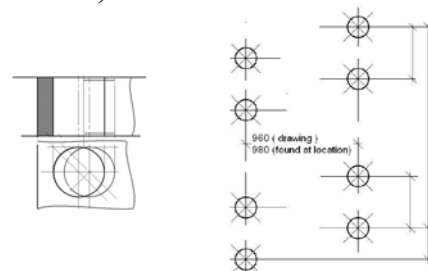
Picture 30: old frame foundation holes not machined to original drawing

8.3   Un-sufficient E-Motor Power for 100% Capacity

Originally the HP compressor was equipped with manual operated clearance pockets. For years these were used always open and the force to close them would have destroyed the spindles. The customer requested a modification, which would allow continuously running at 100%. A system using internal plugs which replaced the spindle has been provided. During 100% operation the electric motor got increasing winding temperature got excessively high, indicating that the motor has been too weak from the very start. For this reason the old clearance pocket system was assembled again and the compressor is running at reduced capacity but at maximum pressure.

RETROFIT

Increasing the reliability and reducing vibration of a 35 year old compressor by replacing the frame housing with an optimised design using the FEA method, *Ralf Krich;* HOERBIGER SERVICE GMBH

8.4   3Not fitting crosshead liner

After disassembly it was found that the crosshead liner stage 2 has a too big outer diameter. It got than clear that during the maintenance work in 2007 the clearance between this liner and the guide was too big and therefore this liner was coated outside. As the 4 new crosshead guides were all designed with the same identical diameter it was logical to re-machine the outer diameter of this liner to match with the original clearance at all 4 guides.

8.5   Pulsation in 3rd stage discharge line at start up

After the upgrade the plant was totally down in all stages.
For this reason the compressor had to build up his own system pressure which should reach 180 to 200 bar.
During this process the compressor is more or less acting like a single stage unit for a while, rather than working in two stages and finally with all 3 stages. The stages which are not involved into the compression are just passed by the through flowing gas. About the period of starting to compress in all 3 stages only the discharge line of stage 3 was shaking and some piping supports got loose. After reaching the maximum pressure, the complete piping got quiet. The reason for this behaviour is not yet totally clear, but due to the fact that the compressor is running very seldom within these conditions, the investigations were not completed yet to this point.

9   Vibration Monitoring

In addition to the engineering and delivery of this major upgrade the authors measured the vibration values (velocity RMS) at several places marked in the attached drawing. (Picture 31)
The measurements were carried out before and after the upgrade of the compressor frame and foundation modifications.
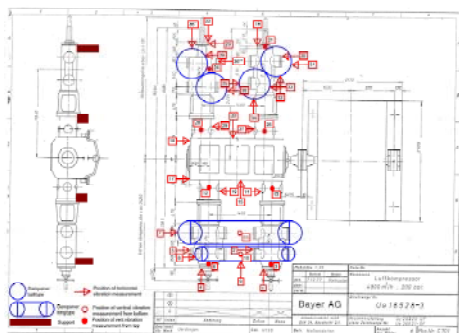
Picture 31: drawing with marked vibration measurement points

The overall values found (Picture 32), were low in comparison with allowable values like the recommended values from the EFRC but also compared with values from other similar sized compressors. For the new design- except for very few values at one dampener and at crosshead guide stage 2 all other values were much lower than before.
The exception at crosshead guide 2 can be explained by the fact that the huge steel stiffening structure between cylinder stage 2 and 3 has been taken away. As an average result, the level was reduced by about 19% for in total 39 values.
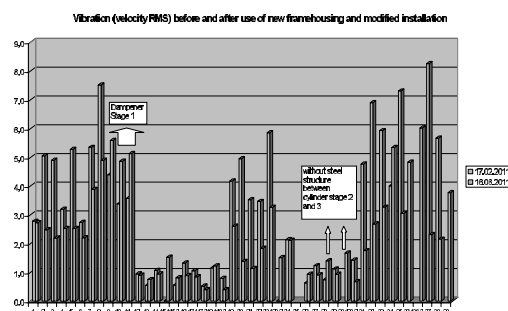
Picture 32: Diagram with RMS values before and after modification

10   Conclusion

The HP compressor is now running for more than one year (Picture 33) without problems. With the supply of , new frame housing, designed with the modern state-of-the-art engineering techniques, the problems that have occurred for many years, have entirely disappeared.
The excellent cooperation between the customer and the authors solved one long lasting problem, which has not been solved in the past
Accumulated experience, systematic engineering, understanding the detail of reciprocating compressor fundamentals, providing key parts and delivering comprehensive services, creates customer value. This project was one of several important initiatives on the path to support the compressor owners and operators in making compressors more reliable and efficient.

Picture 33: with new frame housing and cylinder supports

8th Conference of the EFRC
September 27th / 28th, 2012, Düsseldorf

EFRC

EUROPEAN FORUM
for RECIPROCATING
COMPRESSORS

Experience with Electromagnetic Stepless Flow Control Systems

By

R. Aigner, L. Sasse, E. Glück, A. Allenspach

Burckhardt Compression AG

Winterthur

Switzerland

roland.aigner@burckhardtcompression.com

8th Conference of the EFRC
September 27th / 28th, 2012, Düsseldorf

Abstract:

Experiences with electromagnetic stepless flow control systems are discussed. The mechanical design of the unloading device, electrical equipment, and control strategy aspects are considered and benefits of different approaches are shown. Technical challenges are highlighted and ways to optimize the system are discussed. Experiences with the system in operation on various compressors (in-house and field tests) are shown. Findings from these tests and resulting relevant technical improvements are described. Comprehensive measurement results are shown. The impact of the stepless reverse flow control on the compressor is discussed for the complete control range and all control strategies.

1   Introduction

The operation of large reciprocating compressors often requires energy- and cost-efficient ways to adjust mass flow and/or to ensure certain pressure levels at the intermediate stages or at the outlet of the compressor. In 2010 a new approach for capacity control systems was presented[1]. Especially the development, the basic principles and the main design issues of the new stepless flow control system have been shown. Here, only a small overview is given and that data is updated where necessary.

The further development and improvement of the capacity control system has not come to a halt. Long-term testing showed that the guide bushes used in the magnetic actuator cannot guarantee the specified lifetime. An alternative guidance bearing had to be found. In this paper guide bushes with different contact material pairings, linear rolling bearings and guidance springs will be discussed and advantages and drawbacks highlighted.

Not only the mechanical part but also the electronic part of the flow control system has undergone a complete redesign. It turned out that the commercial products had limited functionality. Most notably the Ethernet data connection between the master controller and slave controllers at each suction valve proved to be the bottleneck of the system. Therefore, proprietary electronics with a new fieldbus have been developed and are presented here.

Finally, the results of measurements and field tests are discussed. On the basis of measurements of a compressor in operation the influence of the flow control system on the compressor is shown. Different control strategies are compared.

2   Existing System

The basic idea of the stepless flow control system is that the already suctioned gas is delivered back to the suction line. Therefore, it is no longer available for the subsequent compression and delivery to the discharge line. The mass flow of the compressor or the interstage pressure decreases depending on the stage controlled. This procedure can be performed either during one or more subsequent full strokes as "intermittent flow control" or only during a certain portion of the compression phase, as so-called "stepless reverse flow control".

Each conventional suction valve is equipped with an unloading device (Figure 2.1). The fingers of the unloader reach the sealing elements of the valve through the valve seat and can push them against the valve guard (open valve). The unloader itself can be pushed down by the plunger of the magnetic actuator. In the initial position, the magnetic actuator is deactivated and the spring holds the unloader and the armature of the magnet in the uppermost position. In this state, the valve works without any influences. The armature is pulled down if an electric current (provided by the power electronics) is running through the coil of the magnet and the plunger pushes the unloader down[3]. The unloader, in turn, pushes against the valve plate, and therefore, the valve can be kept open, even if the pressure force of the gas flow tries to close the valve[5, 6, 7]. The movement of the armature is determined by the amount of current running through the coils of the solenoid. Here a controller electronic calculates the necessary amount of current. Most of all it is important that the impact velocities of the moving parts are kept below a certain level to guarantee high durability and low noise levels [4].
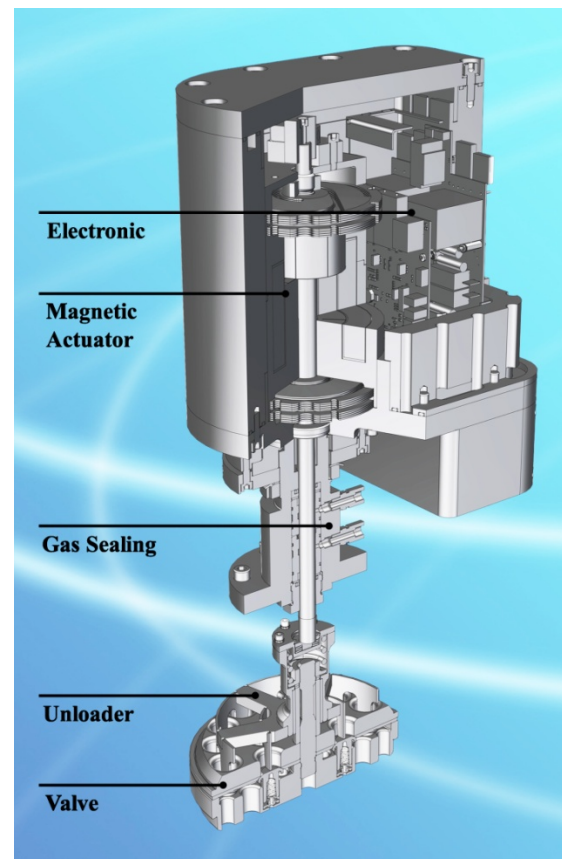
Figure 2.1: Unloading device

FLOW CONTROLS

Experience with Electromagnetic Stepless Flow Control Systems, *R. Aigner, L. Sasse, E. Glück, A. Allenspach;*
BURCKHARDT COMPRESSION AG

3   Optimal Axial Guide

The main part of the stepless flow control system is the magnetic actuator. Its armature provides the necessary axial force to move the rod and further on the unloader to keep the suction valve open. During the lifetime of an unloading device the moving parts reach one billion cycles. With a maximum speed in each cycle of 1m/s and a maximum acceleration of 200m/s² they must cover a distance of 10 000 km. In addition to an axial force the magnet delivers a small radial force due to imperfections in the symmetry and in the magnetic material used.

With these demanding specifications for the linear bearing many different approaches were tested to select the optimal solution.
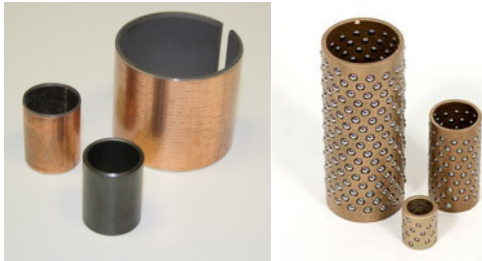
Figure 3.1: Conventional Bush guides and linear ball bearings

3.1   Guide Bush

These conventional bearings have been tested with a wide variety of available contact pair materials and coatings. Steel / Bronze (various), Steel / Graphite, Steel / DLC (Diamond Like Carbon) and Steel / Plastic (various) are possible combinations, to name but a few [8]. In this case the most promising guide bush consisted of Graphite - Bronze (Figure 3.1). Figure 3.2 shows the measured gap width and trend line dependent on the cycles in operation. As the wear increases the radial force increases as well and the wear process speeds up. The prediction shows that at about 300 million oscillation cycles the gap width would exceed tolerable limits. Moreover, the debris can influence the operation of the magnet.

3.2   Linear rolling bearings

Commercially available linear rolling bearings (Figure 3.1) feature very high precision and low wear. However, they cannot fulfill some of the specifications needed in this application. Namely, the limits for the maximum acceleration are below the actual maximum acceleration. Moreover, the space requirements are rather high compared to the guide bush.

3.3   Guidance Spring

The guidance spring is a rolled up leaf spring (Figure 3.3). This alternative bearing allows small axial movements as the outer and inner ring are fixed. The deviations in radial and tangential direction are negligible small. They have been used for years in compressor plate valves, most notably in oxygen applications where this is the only bearing which cannot produce any sparks. The radial stiffness is multiplied by using more guidance springs in one package separated by disc washers (Figure 3.4).

Figure 3.2: Gap width of bronze bush dependent on the oscillation cycles in operation. Thin, black line represents the predicted trend

Figure 3.3: Guidance spring

Figure 3.4: Package of guidance springs mounted on magnet

Experience with Electromagnetic Stepless Flow Control Systems, *R. Aigner, L. Sasse, E. Glück, A. Allenspach;*
BURCKHARDT COMPRESSION AG

3.4 Choosing the right bearing

The comparison of the three different approaches is shown in Table 3.1. Although the guidance spring is by far the most expensive bearing the advantages outweigh the drawbacks. Most notably the theoretically infinite lifetime makes it the perfect bearing for the stepless flow control system.

Category	Guide bush	Rolling Bear.	Guid. spring
Space requirements	👍	👎	👎
Max. Acceleration	👍	👎	👍
Max. Velocity	👍	👍	👍
Wear	👍	👎	👍
Precision	👍	👍	👍
Durability	👎	👎	👍
Cost	👍	👍	👎

Table 3.1: Comparison of different guides

4 New Electronic and Software Architecture

4.1 Hardware Concept

In the new stepless flow control system the commercial electronics were replaced with an in-house development. The advantages are: customized functionality, customized size and placement of connectors and different components can be combined, to name but a few. The higher development costs are outweighed by much lower costs for higher batch numbers.

Figure 4.1 shows the main components of the capacity control system and their connections. Each valve controller is equipped with a hard-real-time control system, consisting of a main control board (digital signal processor) and an optimized power electronic for controlling the unloader device. Here additional monitoring sensors can be connected to the main control board. The master control is provided by an industrial PC with connections to all of the valve controllers and to a data logger. It contains a small real-time operating system that monitors and controls the complete system. The master controller prepares control and sensor data and stores it in the data logger. The junction box contains an additional main control board which processes the crankshaft trigger signal and provides the system with the calculated crank angle. The long term data can be analyzed both on site and remotely. An optional compressor monitoring system (PROGNOST® NT) can be connected to the stepless control system.

4.2 Software Concept

The modular object-oriented software is set up to self-monitor and to perform error checks on-line. The master control can thereby monitor the sub-modules (valve controllers, available connections, etc.) in an effective manner. Furthermore, when an error occurs, the master control can attempt to solve the problem without shutting down the compressor (see Section 5.7).

Figure 4.1: Setup of new electronics for the stepless flow control system

4.3 Fieldbus Evaluation

The fieldbus between the master controller and every valve controller must have fast cycle times and a large bandwidth. With these requirements in mind, several options have been evaluated. From these options, the EtherCAT fieldbus has been chosen for the stepless flow control system.

EtherCAT (Ethernet for Control Automation Technology) is a high performance Ethernet based fieldbus system. It was developed to apply Ethernet to automation applications which require short data update times (cycle times) with low communication jitter for synchronization purposes.

EtherCAT takes an approach to packet handling called "processing on the fly". The Ethernet packet or frame is no longer received, then interpreted and copied as process data at every slave. Instead, the packet data is sent through a telegram travelling in a ring. The slave devices read the data addressed to them while the telegram passes through the device.

FLOW CONTROLS

Experience with Electromagnetic Stepless Flow Control Systems, *R. Aigner, L. Sasse, E. Glück, A. Allenspach;*
BURCKHARDT COMPRESSION AG

Similarly, input data are inserted while the telegram passes through. The frames are only delayed by a fraction of a microsecond in each slave, and many slaves can be addressed with just one frame.

With EtherCAT in the stepless flow control system all necessary data can be transferred in real time (Figure 4.2). For example, the trigger signal of the crankshaft is only processed in the junction box and is transferred via EtherCAT to every valve controller with almost no jitter. Additional sensor signals can be transmitted, such as pressure or temperature signals.
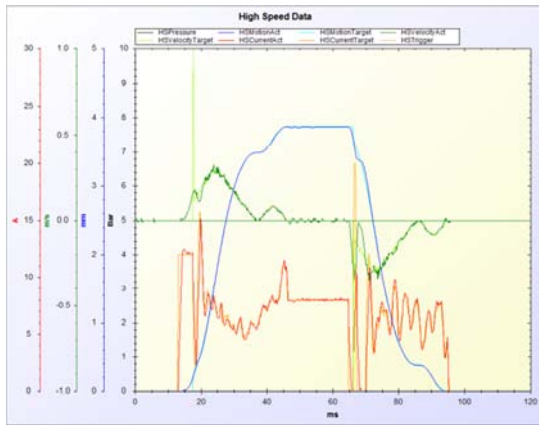
Figure 4.2: On-line high speed data of a valve control

5 Control Strategy

The stepless flow control system has a big impact on the design, operation, and maintenance of a compressor and its components[2]. The chosen control strategy can have the most important influence. This flow control system has the capability of using a wide range of different control philosophies, so the advantages, drawbacks, risks and restrictions of each should be taken into account when choosing one. The control strategy to be used can be chosen on three levels:

For the first level, each suction valve is equipped with an actuator. With this, Intermittent Flow Control (IFC), Reverse Flow Control (RFC) or a combination of both strategies can be used. In the second level, different control approaches within one compressor stage can be used. The third and final level is an overall control strategy that applies to the whole compressor. Here the regulation design of the single stages are synchronized and determine the interstage pressures.

The desired control strategy can also vary with mass flow, operating point of the compressor, or desired benefits.

Some of the possible targets are:

- High energy efficiency

- Low vibrations due to pulsations

- Minimized control offset

- Low gas temperature changes in the lines

- Extended usable mass flow range.

- High durability

Mechanical restrictions must be taken into account when choosing a strategy. Various factors such as rod reversal or resonances in the drive train can limit the feasible control strategies considerably.

The results, diagrams and tables in this chapter are taken from the measurements conducted at the first field compressor. This compressor has two stages and each stage has two compression chambers (for a detailed description see Section 6.1). With this setup, the following control strategies can be used:

Reverse flow control (RFC): The closing time of each suction valve can be individually adjusted. The Closing Crank Angle (CCA) specifies the crank angle after the dead center when the suction valve is completely closed.

Intermittent Flow Control (IFC): In this case three crank shaft revolutions are combined to form a total cycle. From this cycle, six different mass flows can be set (Table 5.1). The more revolutions used for the total cycle, the more flow capacity operating points are available.

Total cycle 1st compress. Chamber			Total cycle 2nd compress. chamber			Mass Flow [%]
1	2	3	1	2	3	
●	○	○	○	○	○	83.3
●	○	●	○	○	○	66.7
●	○	●	●	○	○	50
●	●	●	●	○	○	33.3
●	●	●	●	●	○	16.7
●	●	●	●	●	●	0

Table 5.1: Flow capacity system using intermittent flow control. Here a dot indicates the cycle where the suction valve is kept open

Unloader: In this special case of the intermittent flow control, 50% of the mass flow is delivered by keeping the suction side of half of the compression chambers continuously open. In the case of four compression chambers per stage, 25% and 75% flow rate can be delivered using a similar strategy.

FLOW CONTROLS

Experience with Electromagnetic Stepless Flow Control Systems, *R. Aigner, L. Sasse, E. Glück, A. Allenspach;*
BURCKHARDT COMPRESSION AG

Compressor Stage Strategies: Different regulation designs can be applied to suction valves of the same stage with this stepless flow control system, such as a combination of unloader and reverse flow control.

5.1 Validity of the Measurement Results

The measurement results of the control methods described in this chapter were confirmed by simulations. Although only one field test is presented here, the same results occurred for other field tests conducted. Moreover, it turns out that extension to bigger compressors with more stages or compression chambers do not add any new problems or difficulties. On the contrary, it gives rise to more control scheme possibilities. For compressors with only one compression stage or one compression chamber per stage not all the control strategies mentioned are applicable.

5.2 Efficiency of Capacity Control

The energy efficiency of the different control strategies can be displayed using the power-mass flow diagram (Figure 5.1). The deviation of the actual power consumption from the ideal curve is due to additional losses of the capacity control system. These losses are produced when the already suctioned gas is pushed back through the valves into the suction line. In this case the valve losses are rather high and therefore the deviation from the ideal capacity control is rather high.

The difference between the reverse flow control and the intermittent flow control is low. In terms of efficiency the unloader strategy is the best.
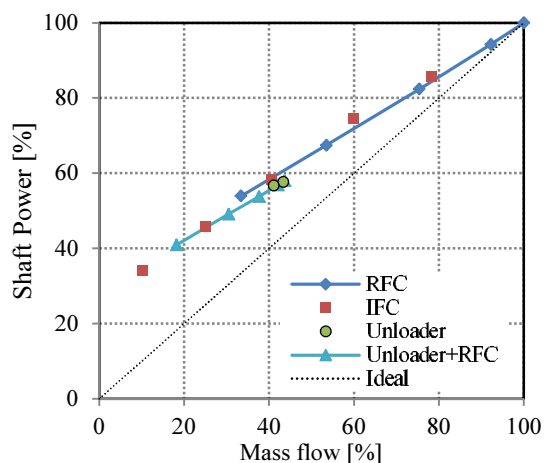
Figure 5.1: Power consumption of the compressor depending on the mass flow and the flow control method used (RFC...Reverse Flow Control, IFC...Intermittent Flow Control, Unloader and Combination of Unloader and RFC)

5.3 Pressure in the Suction and Discharge Lines

To evaluate the influences of the different control strategies on the pressure pulsations, the pressure is measured directly before and after the compressor flanges for discharge and suction. Depending on the regulated mass flow there is an influence on the pressure pulsations for all control strategies. At this compressor plant the peak to peak discharge pressure is increased between 40% and 80% of the maximal mass flow for the intermittent flow control regime and a reduction for the reverse flow control regime (Figure 5.2). The unloader control strategy reduces the peak to peak discharge pressure.

The situation is reversed for the suction side (Figure 5.3). The reverse flow control leads to an increase of the peak to peak suction pressure pulsation and the intermittent flow control leads to a decrease. Deployment of the valve lift unloader results in a very low peak to peak value (two to three times lower compared to 100% mass flow).

Figure 5.2: Pressure in the discharge line. Peak to peak value depending on the mass flow and the flow control method used (RFC...Reverse Flow Control, IFC...Intermittent Flow Control, Unloader)

To get a deeper understanding of the effects from each control strategy on the pressure pulsations, the values must be analyzed in the frequency domain. In fact, even the allowable pressure pulsations depend on frequency, according to API 618[9]. The higher the frequency, the lower the limit.

According to reference [0] the reverse flow control may increase the pressure pulsations at higher frequencies in the domain of around 200 to 600Hz. However, the intermittent flow control changes the pressure pulsation frequency as well. Due to the fact that for this compressor three cycles are one

FLOW CONTROLS

Experience with Electromagnetic Stepless Flow Control Systems, *R. Aigner, L. Sasse, E. Glück, A. Allenspach;*
BURCKHARDT COMPRESSION AG

repeating period, the minimum exciting frequency is divided by 3 compared to the reverse flow control case. Figure 5.4 shows the pressure pulsations in the frequency domain at the discharge side for the 60% mass flow RFC case and the 66.7% mass flow IFC case. At compressor speed (16.5Hz) or multiple thereof both control strategies excite pressure pulsations at a similar level. But for the IFC there are as well pulsations at frequencies at one third of the compressor speed or multiple thereof. At 7/3 of the compressor speed there is the highest amplitude, which leads to the comparably higher peak to peak pressure pulsations for the IFC. The reason for this peak is that a quarter wave length at this frequency is equal to the piping length between discharge valve and discharge damper, and therefore acoustic resonance occurs.

Another acoustic phenomenon arises as the intermittent flow control is deployed. The operator of the compressor is confronted with different and unfamiliar compressor acoustic emissions. Although the compressor is in perfect health the untrained operator may come to a different conclusion.

Figure 5.4: Amplitudes of pressure pulsations for different frequencies for the 60% mass flow reverse flow control case and the 66.7% mass flow intermittent flow control case.

5.4 Cycle Irregularity

The cycle irregularity δ is given by

$$\delta = \frac{\omega_{max} - \omega_{min}}{\omega_m},$$

where ω denotes the angular velocity and the subscripts max, min and m stand for maximum, minimum and mean value, respectively. The measurement results show that reverse flow control has only a small impact on the inverse cycle irregularity (Figure 5.5), whereas the intermittent flow control decreases the inverse cycle irregularity considerably. For small compressors with small flywheels, the IFC causes the inverse cycle irregularity to fall below tolerable values; however, for lower mass flows this cycle irregularity does not cause any problems. The unloader capacity control reduces the cycle irregularity only slightly in this case.

Figure 5.3: Pressure in the suction line. Peak to peak value depending on the mass flow and the flow control method used (RFC…Reverse Flow Control, IFC…Intermittent Flow Control, Unloader)
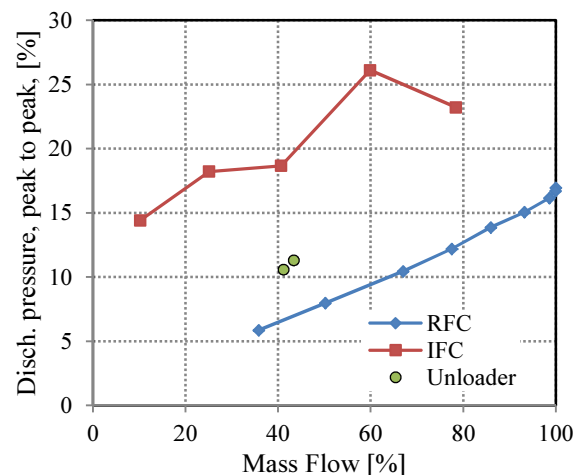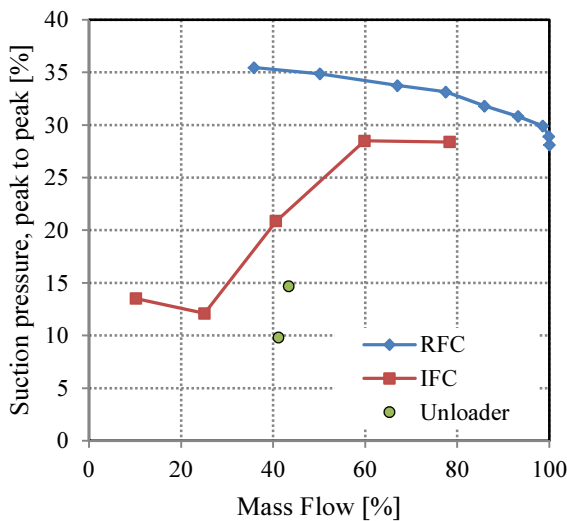

Figure 5.5: Cycle irregularity depending on the mass flow and the flow control method used (RFC…Reverse Flow Control, IFC…Intermittent Flow Control, Unloader)

Experience with Electromagnetic Stepless Flow Control Systems, *R. Aigner, L. Sasse, E. Glück, A. Allenspach;* BURCKHARDT COMPRESSION AG

5.5 Gas Temperature Changes and Compressor Heating

During reverse flow control the suctioned gas gets in contact with the hot wall of the cylinder and heats up during the suction phase. After dead center the compression phase starts and the already suctioned gas is pressed back into the suction line. Additionally, valve losses occur that further heat up the gas. The suction temperature rises with decreasing mass flow as more of the hot gas is pressed back into the suction line (Figure 5.6).

Similar processes take place when using the intermittent flow control or unloader capacity control system, but here the cylinder walls stay cooler as the gas does not reach the high discharge temperature in every cycle. In the cycles where the suction valve is kept open, the gas has approximately the suction temperature. For high and moderate mass flows the suction temperature stays unaffected. At very low capacities (high reverse mass flows) increasing temperatures due to valve losses are not negligible and therefore the suction temperature rises considerably. In case of 0% mass flow, where all suction valves are kept open all the time, the suction temperature rises very quickly (Figure 5.7). In most compressors the suction temperature would exceed safety limits within a few minutes.
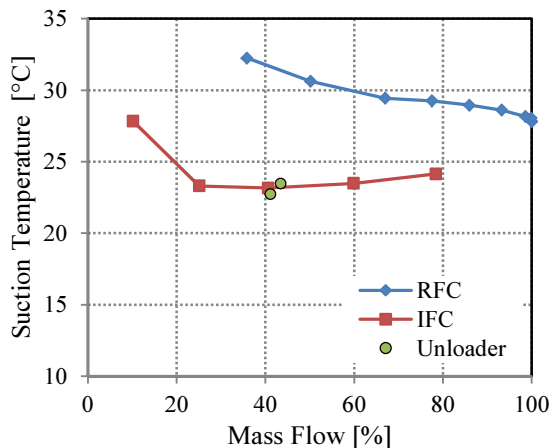
Figure 5.6: Suction Temperature depending on the mass flow and the flow control method used (RFC...Reverse Flow Control, IFC...Intermittent Flow Control, Unloader)

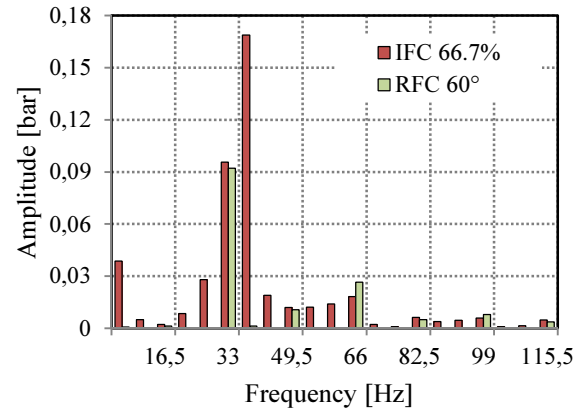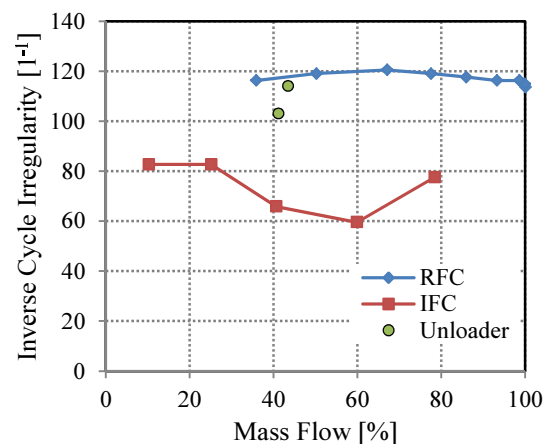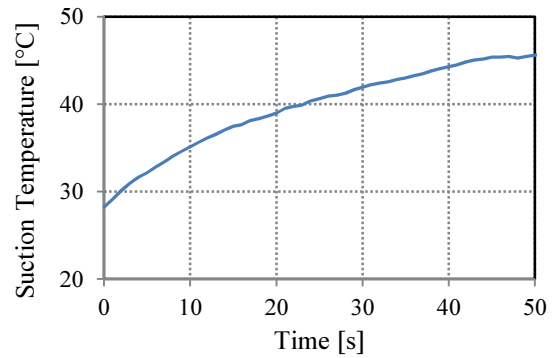*Figure 5.7: Suction Temperature. At t=0 s the mass flow rate was reduced to 0% by keeping all suction valves fully open*

5.6 Influence on the Interstage Pressure

Intermittent flow control and unloader capacity control have no or very little influence on the interstage pressure when the same setup is deployed in each stage. Using reverse flow control, however, can have a huge impact on the interstage pressure. When setting the Closing Crank Angle (CCA) to the same value in both stages the interstage pressure will rise with decreasing mass flows (increasing CCA). The reason for that can be found in the increasing relative cylinder clearance for the higher stages. In most cases increased interstage pressure leads to a decreasing energy efficiency (Figure 5.8). Moreover, changed interstage pressures shift the rod loads and could lead to compressor damage in the worst case.

With the stepless flow control system any interstage pressure can be achieved by applying different settings for each stage (e.g. different CCAs). The suction valves of the first stage determine the mass flow, whereas the interstage pressures are determined by the settings of the consecutive suction valves. In order to avoid any difficulties the interstage pressure could be kept constant at the design point. In our case the interstage pressure is 2.3 bar at the design point (100% mass flow), and when the interstage pressure is kept at that point, the energy efficiency increases considerably (Figure 5.8). Reducing the interstage pressure even further than the design point leads to lower power consumption. The lower limits of the pressure are defined by mechanical and safety restrictions. In this case the lowest pressure achievable was 2.1 bar.

Experience with Electromagnetic Stepless Flow Control Systems, *R. Aigner, L. Sasse, E. Glück, A. Allenspach;*
BURCKHARDT COMPRESSION AG

*Figure 5.8: Shaft power depending on mass flow
for different interstage pressures*

5.7   Emergency Control Strategy

In the event of a total system failure of the capacity control, the unloaders of the suction valves return to an initial position so that the suction valves operate normally and the compressor delivers 100% mass flow. Usually a backup bypass valve ensures that the capacity still can be controlled.

If not all unloaders encounter problems and shut down, the master control decides whether changing the overall control strategy can yield a limited but functional capacity control system. Table 5.2 lists possible emergency control strategies with various uncontrolled stages for this field test compressor.

1st Stage		2nd Stage		Control
Ch.1	Ch.2	Ch.1	Ch.2	Range
○	○	○	○	100%..0%
●	○	○	○	100%..50%
●	○	●	○	100%..50%
●	●	○	○	None (100%)

*Table 5.2: Available control range for different
errors. Here a dot indicates a
compression chamber (Ch.) with faulty
flow controller that has been stopped*

6   Field Tests

6.1   University of Applied Science and Arts, Northwestern Switzerland
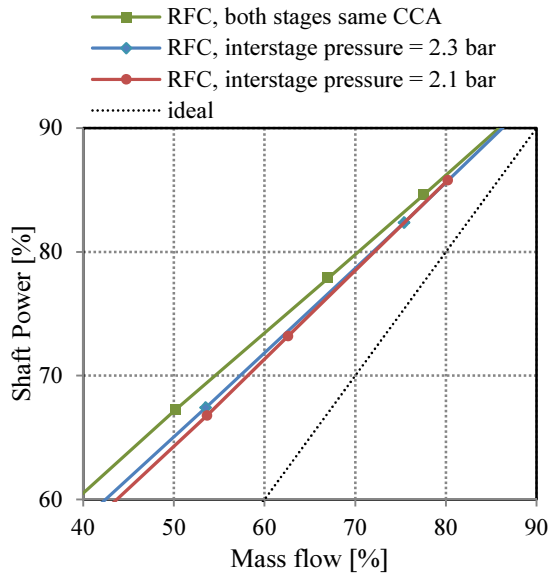
This small two-stage compressor runs at about 1000 rpm and compresses air from 1 to 7 bar. The two double acting cylinders are equipped with one suction valve for each compression chamber. At full load this compressor uses 76kW to deliver about 750 kg/h of compressed air. It is well equipped with the latest sensor technology[11,12]. The aim of this field test was to get independent and very accurate measurement data.

6.2   Refrigeration Application, Switzerland

In this refrigeration application the two-stage compressor runs at about 1000 rpm and compresses ammonia from 1 to 10 bar. The compressor operates 8 to 16 hours a day, at which the mass-flow demand fluctuates significantly between 100% and 50%.

In the past speed control was used to control the capacity. A frequency converter regulated the frequency of the asynchronous motor. However, it turned out that at certain frequencies the vibrations of the compressor and the pulsations were above specified limits. The operator shut down the frequency converter.

In October 2011 a prototype of the stepless flow control system was installed. The capacity control has operated without any problems since then.

7   Summary and outlook

Further development, optimizations and improvements of the stepless flow control system were presented in detail. In addition measurement results and experiences with compressors in operation were shown.

An alternative axial guide bearing was introduced. It turned out that for this application the guidance spring is the best choice. Above all the unlimited lifetime (and therefore no maintenance cost) is the biggest advantage.

Not only the mechanical part but also the electronic part has been redesigned. Here the data connection between each unloading device and the master controller was changed from Ethernet to EtherCAT. Furthermore the commercial electronics were replaced with a proprietary solution. Now hard-real-time control is possible.

The field tests on two different compressors unveiled some interesting influences of the stepless flow control system on the compressor operation. In particular, the influence of the different control strategies was shown. The efficiency of the reverse flow control and the intermittent flow control were shown to be very similar. The unloader control strategy proved to be the most energy efficient. However, at low mass flows a combination of different flow control strategies is best. The stepless

flow control can increase the pulsation in the suction and discharge lines. This leads to higher peak to peak pressures at certain mass flows. As this occurs, the suction temperature increases. For very low mass flows this temperature rise limits the application of flow controls where suctioned gas is pressed back to the suction line.

In the near future, field tests will be conducted on bigger compressors and in explosive areas.

8 Acknowledgements

References

[1] Aigner, R., Voser, A., Allenspach, A. (2010): Development of a Stepless Flow Control System, 169-178.

[2] Workshop documentation of the 5th EFRC-Conference (2007): Capacity Control.

[3] Kallenbach, E., Eick, R., Quendt P., Ströhla, T., Feindt, K., Kallenbach, M. (2008): Elektromagnete. Vieweg Teubner.

[4] Hoffmann W., Peterson, K., Stefanopoulou, A. G. (2003): Iterative learning control for soft landing of electromechanical valve actuator in camless engines. IEEE trans on control system technology, 11(2), 174–184.

[5] Costagliola, M. (1950): The Theory for Spring Loaded Valves for Reciprocating Compressors. J. Appl. Mech, 415-420.

[6] Aigner, R. Meyer, G., Steinrück H. (2005): Valve Dynamics and Internal Waves in a Reciprocating Compressor. 4th EFRC-Conference, 169-178.

[7] Aigner, R. (2007): Internal Flow and Valve Dynamics in a Reciprocating Compressor. Dissertation TU Vienna.

[8] Czichos, H.,Habig, K. (2010): Tribologie-Handbuch. Vieweg Teubner.

[9] API Standard 618 (2007) Fifth edition, p58.

[10] Korst, H., Bocatus, W. (2005): Noise Reduction at a NAM-compressor Station. 4th EFRC Conference Antwerp.

[11] Egli, Ph. (2011): Experimentelle Untersuchung des Kolbenkompressors Burckhardt Laby 2K105. Bachelor Thesis, University of Applied Science and Arts, Northwestern Switzerland.

[12] Scheibling, T. (2011): Experimentelle Untersuchung und Bilanzierung des Kolbenkompressors Burckhardt Laby 2K105. Bachelor Thesis, University of Applied Science and Arts, Northwestern Switzerland.

New concept for electrical stepless compressor capacity-control system

by:

Bernhard Spiegl, Peter Dolovai, Tino Lindner-Silwester
Research & Development
HOERBIGER Ventilwerke GmbH & Co KG
Vienna
Austria
bernhard.spiegl@hoerbiger.com

8th Conference of the EFRC
September 27th / 28th, 2012, Düsseldorf

Abstract:

Stepless capacity-control has almost become standard for newly built and existing compressors in demanding applications. For reasons of energy saving and process control the concept of reverse-flow regulation with HydroCOM has by far the highest market share of all applied technologies. Nevertheless, in spite of the broad success of this electro-hydraulic system, there is a demand in the market for a system requiring less installation and maintenance efforts. In accordance with the industry trend of replacing hydraulic systems with electrically actuated systems, different attempts to come up with an oil-free electrical capacity-control system have been made recently. In this paper the challenges to be met by an electrical system are outlined and a specification for such a system is derived on the basis of long-term application experience with stepless capacity-control systems. A fundamental research project was initiated to screen all possible types of electrical actuation principles. Within this project, the evaluation of several different working principles has led to the identification of two systems considered to be worth the efforts of further developing them up to prototype stage. Final prototype testing revealed one of these two systems to be overall superior. This completely oil-free, ATEX-certified electrical system, being capable of covering the whole application range of the existing HydroCOM system, has been installed in a challenging application. The performance of the system has met the high expectations.

New concept for electrical stepless compressor capacity-control system, *Bernhard Spiegl, Peter Dolovai, Tino Lindner-Silwester;* HOERBIGER VENTILWERKE GMBH & CO KG

1   Introduction

The wish for a stepless capacity-control dates back to the beginning of modern compressor technology. Nowadays several different options are available for controlling the capacity of a reciprocating compressor. The most commonly used are:

- Bypass regulation
- Suction valve On / Off unloaders
- Variable volume clearance pockets
- Variable speed control
- Reverse-flow regulation (RFR) with pneumatical or electrical preloading
- Stepless capacity regulation with reverse-flow regulation and timed electro – hydraulic valve unloading
- Variable stroke compressor

This paper is devoted to purely electrically-actuated systems that make use of the reverse-flow principle for capacity control. First concepts of electrically-actuated valve unloaders date back to the late 1930's.
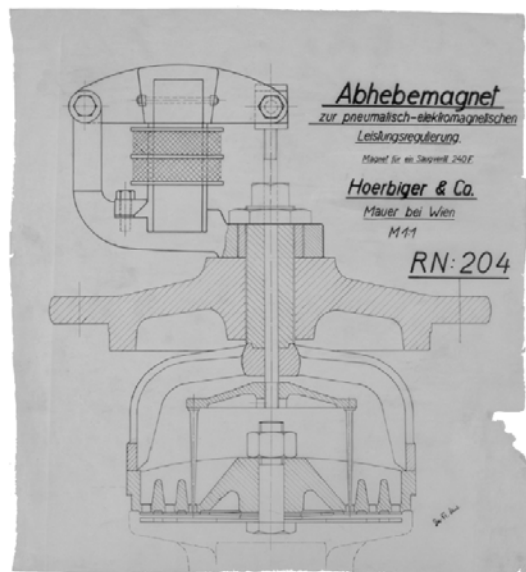

Fig. 1: First electromagnetic unloading system for compressor valves (HOERBIGER Museum, patented 1930)

Later on, the functionality of the system was enhanced so that it could be used as a stepless capacity RFR system with magnetic preloading. This allowed for a variance in capacity of 60% to 100%. The system can be seen in detail in the HOERBIGER Museum in Vienna. In the 1940´s several compressors were equipped with that system.

However, this early concept was stopped and the force-generation switched to pneumatic actuation for RFR systems until the late 1990's when the HydroCOM system, being capable of controlling the capacity over the entire range, replaced the RFR systems almost completely.

HydroCOM is an electrohydraulic system where the required high actuation force is generated hydraulically. The hydraulic actuation principle has lots of advantages so that it was chosen for the HydroCOM system:

- One central oil-supply unit feeds decentralized actuators
- Proven and cost-attractive technology
- New high-speed valve and solenoid technology available
- Full control over impact speeds
- Unloader actuator is cooled by hydraulic oil

In some applications the efforts for installing the hydraulic piping and the required maintenance for the hydraulic pump are seen as critical and cost driving. Thus, in accordance with the industry trend of replacing hydraulic systems with electrically actuated systems, different attempts to come up with an oil-free electrical capacity-control system have recently been made [1], [2], [3] and are still ongoing [2], [3].

Electrical actuators are considered as more cost efficient and easier to handle than hydraulic actuators. With the decrease in cost of power electronics and the availability of powerful processor technology the attractiveness of electrically actuated systems has been increasing significantly over the last years.

In what follows, a specification for a new electrical stepless capacity-control system is derived. Different electrical actuation principles are then compared to each other and evaluated on the basis of this specification. Prior to this, the challenges to be met when applying the reverse-flow principle are briefly discussed.

2   The reverse-flow principle

As outlined, utilizing the reverse-flow principle for controlling the capacity of reciprocating compressors has proven to be both efficient and reliable. However, long-term experience has shown that special care has to be taken in the design of such a capacity-control system in order to meet the high demands being placed on compressor reliability. In order to elucidate the challenges to be faced when applying the stepless reverse-flow control approach, a closer look shall be taken into the reverse-flow phase.

New concept for electrical stepless compressor capacity-control system, *Bernhard Spiegl, Peter Dolovai, Tino Lindner-Silwester;* HOERBIGER VENTILWERKE GMBH & CO KG

A typical pressure-volume diagram is shown in Fig. 2 where the suction valve is kept open by an unloader, actuated by a suited actuator, for a well-defined period of time during the reverse-flow phase. Hence, only the required amount of gas is compressed with the remainder being pushed back into the suction plenum.
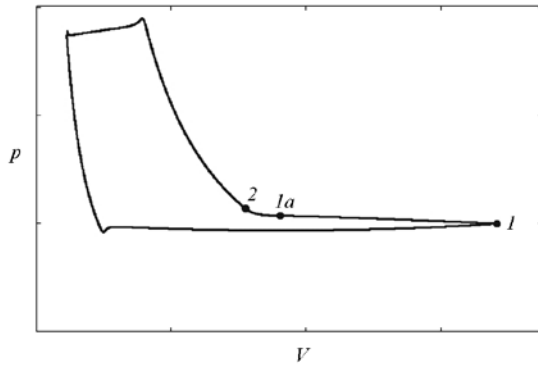

Fig. 2: Pressure-volume diagram at part-load operation of compressor. Reverse flow phase starting at 1 and ending at 2, closing event of suction valve initiated at 1a and ending at 2

The same scenario is shown in Fig. 3 where the evolution of the pressure differential Δp_V across the valve with crank angle is depicted.
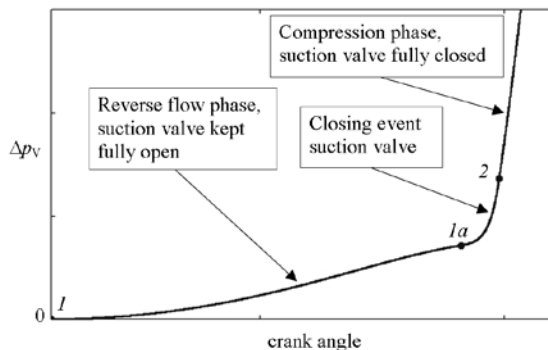

Fig. 3: Rise of differential pressure Δp_V across suction valve with crank angle during reverse-flow phase (1→2) and subsequent compression phase starting at 2 from where on the suction valve is fully closed

Herein, $\Delta p_V = p_{cyl} - p_s$ is the difference between cylinder pressure p_{cyl} and the pressure level in the suction plenum p_s. This pressure difference is required for pushing gas back into the suction plenum through the suction valve. As can be seen in Fig. 3, this differential pressure (typically) vanishes at bottom dead centre 1 and rises in accordance with the increasing mass flow rate through the suction valve brought about by the increase in piston speed.

At a certain crank angle (point 1a), determined by the required amount of compressed gas, the closing event of the suction valve is initiated by releasing the actuation force upon the unloader. Owing to the inertia of the unloader the closing event takes a finite time Δt_c during which there is a steep rise in the pressure differential. This steep rise arises from the decrease in the suction valve´s effective flow area during the closing event.

Since the reverse-flow force F_{flow} acting on the valve sealing element is proportional to the differential pressure across the valve, there is also a steep increase in the reverse-flow force during the closing event of the suction valve. With the inertia of the valve sealing element being negligible compared to the inertia of the unloader, the inertial forces of the sealing element do not have a noticeable impact on the closing event dynamics so that the force $F_{unloader}$ exerted by the unloader onto the sealing element balances F_{flow} (plus the valve spring forces) during the (first instances of the) closing event to an excellent approximation. As a consequence, the valve sealing element gets deflected and bending stresses arise during the reverse-flow phase.

As can be seen in Fig. 4, these sealing element deflections lower the effective flow area of the suction valve which in turn increases the reverse-flow force. Hence, deflections of the sealing element may have a significant impact on the reverse-flow force F_{flow} and thus on the stress level the sealing element is exposed to. The relative importance of these deflections on F_{flow} depends on the stiffness of the sealing element and on the lift of the valve.
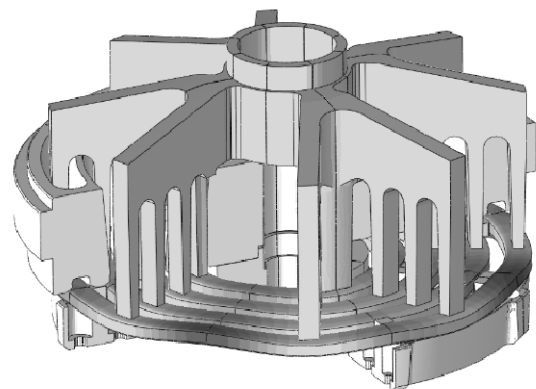

Fig. 4: Deflection of sealing elements (here: ring valve) arising from reverse-flow force (exaggerated view)

During the valve closing event 1a→2, the first contact between the valve seat and the sealing element occurs at the location of maximum deflection at a particular instant 1b (cf. Fig. 5).

New concept for electrical stepless compressor capacity-control system, *Bernhard Spiegl, Peter Dolovai,
Tino Lindner-Silwester;* HOERBIGER VENTILWERKE GMBH & CO KG

From this time on 1b→2, a certain part of the reverse-flow force is balanced via contact of the sealing element with the valve seat with the remainder part $F_{unloader}$ being balanced by the unloader fingers (cf. lower part of Fig. 5). Even though the differential pressure continues to rise in the interval 1b→2, the load support of the seat typically lowers both the stress level in the sealing element and $F_{unloader}$.
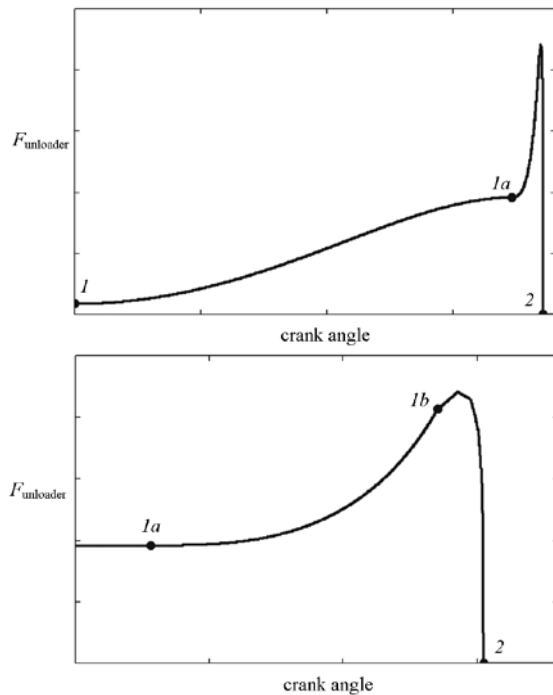

*Fig. 5: Typical behaviour of contact force $F_{unloader}$
between sealing element and unloader
fingers during reverse-flow phase. Upper
part: gradual rise from bottom dead centre
1 to start of closing event 1a followed by
steep rise during closing event with
subsequent steep drop down to zero when
suction valve is fully closed at 2. Lower
part: Detailed view of closing event
showing instant 1b of first contact between
sealing element and valve seat*

Apart from preventing the sealing-element bending-stress level from exceeding allowable limits it is also crucial to keep the closing impact speeds sufficiently low. Whereas the maximum sealing-element bending-stress level tends to get reduced by lowering the closing event time duration Δt_c, decreasing the impact speeds tends to increase this time duration.

Reconciling these opposing requirements thus requires a careful control of the motion of the unloader during the closing event. Within the interval 1→1a the actuation force F_{act} exerted on the unloader must always exceed $F_{unloader}$ while at 1a the unloader has to be de-activated sufficiently quickly

in order not to cause any detrimental delays in the closing event. Since the unloading force rises rapidly during the closing event as shown in Fig. 5, it is crucial for ensuring a soft valve impact that the actuator is capable of providing very high breaking forces in a very dynamic manner.

Note that these breaking forces have to be considerably higher than the force required to keep the suction valve open (=value of $F_{unloader}$ at 1a, Fig. 5).

3 Comparison of different electric actuation principles, derivation of specification for new system

There is a broad variety of different electric actuation principles. However, not all of these meet the basic requirements for this application. Potential candidates are:

- Piezo electric actuators
- Simple solenoid with or without springs
- Modified solenoid designs with or without springs
- Double-acting magnets with springs
- Lorentz force actuators
- Linear motor actuators
- Highly dynamic torque motor with ball screw spindle actuator
- Hybrid actuators – an intelligent combination of different principles

In order to evaluate the different principles a specification to be met by the preferred system has to be derived. This is done on the basis of field experience with more than 800 electro-hydraulic systems and by extrapolating the future needs of the industry which leads to the following basic specification:

- Handling of compressor speeds up to 1500 rpm
- Maximum unloader forces during valve unloading of 7000 N and load spikes up to 14000 N.
- Valve closing time duration < 4 ms
- Full control of unloader motion to keep unloader speed within defined limits independent of compressor speed and load
- Actuator temperature < 100°C, no external cooling allowed
- Withstanding the vibration levels
- Actuator capable of handling sealing element wear and thermal expansions up to ±5 mm in total
- 48000 hours of service-free operation
- No mechanical adjustments on actuator

FLOW CONTROLS

New concept for electrical stepless compressor capacity-control system, *Bernhard Spiegl, Peter Dolovai,*
Tino Lindner-Silwester; HOERBIGER VENTILWERKE GMBH & CO KG

- Completely oil-free design
- One actuator fits all applications
- Easy installation and service in remote locations
- EX certification for H_2 applications
- Diagnostic functions preferred
- "Plug and Play" design preferred

3.1 Piezo electric actuators

Over the last 10 years Piezo actuators have found their way into the high-volume market for high-speed diesel injectors. Their inherently high actuation speed, accuracy, and energy efficiency would basically make them very attractive for use as an actuator for suction valve unloading. Unfortunately the size of the actuator stack cannot be produced on high-volume production equipment which requires handmade actuators that are no longer cost-efficient.

Apart from high costs there is another severe disadvantage, namely the thermal expansion of the Piezo stack itself and its short stroke. In diesel injectors the diesel oil is used as stroke amplifier compensating thermal expansion. In an oil-free actuator this is no longer an option which makes this actuator principle not the preferred one for the considered application.

3.2 Simple solenoid with or without springs

Simple solenoids (see Fig. 6, concept a) as used by Kopecek [1] have different pros and cons. Even though the achievable peak force level is high, the highly nonlinear relation between force and stroke makes controlling the motion of the unloader very challenging. In order to handle installation tolerances and wear (between unloader and valve plate or valve plate and seat), the solenoid needs to be large in size in order to provide sufficient safety margin for a reliable operation. However, increasing the size makes the solenoid slow so that a full control of the closing motion is no longer possible.

3.3 Modified solenoids

An easy way to achieve a more favourable relation between force and stroke of a solenoid is to change the form of the air gap (see Fig. 6, concepts b and c) as also mentioned by Aigner in [2]. This gives a significant improvement in controllability of the actuator especially when combined with a spring. In a certain limited application window, active control of the unloader motion becomes then possible by means of a fast-response position sensor and state-

of-the-art power electronics in conjunction with advanced control strategies.
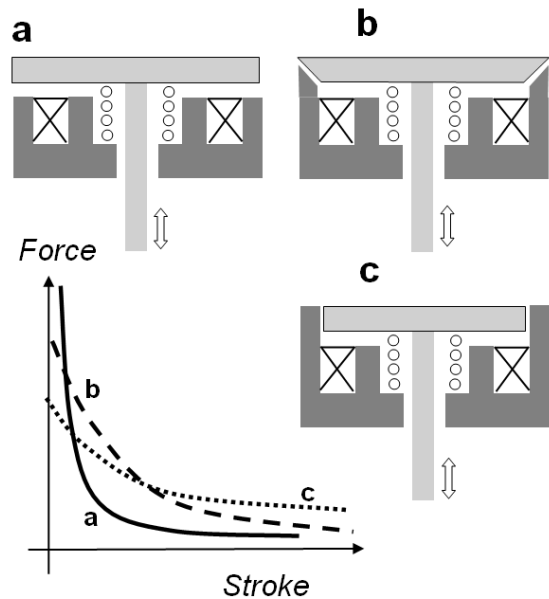
Fig. 6: Different types of solenoids and their basic relations between force and stroke

The limitation arises from the change in the magnetic circuit. The more favourable force - stroke relation goes hand in hand with reduced peak forces. In order to provide high peak forces while retaining high dynamics the actuator needs to be limited in size while operated with higher currents. However, the ohmic losses and eddy current losses heat up the actuator in high force applications, thus necessitating external cooling.

Additionally the changes in the air gap give rise to an instable middle position as well as to considerable lateral forces. The latter have to be handled without causing wear and friction. Achieving 48000 hours of service-free operation with this design constitutes a great challenge.

3.4 Double-acting magnets with springs

An attractive approach [3] for the considered application is to use two solenoids acting against each other with one anchor plate in combination with stop springs (Fig. 7). Such a concept is used in fully electric valve trains in the automotive industry. Using two solenoids allows for a better control of the closing and opening motion of the unloader. The end-stop springs store large portions of the kinetic energy in an efficient manner and help accelerate the actuator from its end positions. A highly dynamic actuator with good energy efficiency is achievable.

Fig. 7: Double-acting solenoid with springs,
Lorentz-force actuator

In order to utilize the system in a best possible manner the springs need to be selected to fit to the occurring reverse-flow forces. Since these forces vary strongly from application to application, the spring selection becomes very challenging – as soon as the system operates outside its design point, the performance is noticeably reduced. In general it is difficult to meet the "one fits all" requirement which is often of essential importance in remote locations.

In addition, the spring reduces the maximum achievable unloading force. In combination with tolerance and wear effects the effective maximum level of unloading force for continuous unloading is either severely limited or calls for large actuator sizes which in turn degrades controllability.
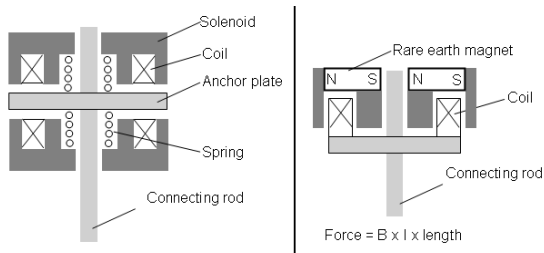
3.5 Lorentz-force actuators

This type of actuator is often referred to as "Voice Coil" or "Loudspeaker" actuator (see Fig. 7). The working principle is simply a coil moving in a magnetic circuit. There is a linear relation between force and current. The actuator´s response is very fast (up to 200 Hz) since no magnetic field needs to be built up. With the cost-attractive availability of powerful rare-earth magnets this old technology has come again into focus for industrial applications.

Even though, for a given size, the achievable peak forces are very high, there is a severe limitation in the achievable unloading forces during continuous operation due to thermal overheating. In order to achieve high forces the air gaps need to be small – this always leads to tradeoffs with respect to the maximum coil cross-section and ohmic losses.

However, not only the thermal management, but also the fact that the moving coil is exposed to strong vibrations and impacts is critical.

3.6 Linear motor actuators

Usually linear motors are flattened brushless direct current motors (BLDC) with rare-earth magnets. Even state-of-the-art linear motors would become unacceptably large in size. Besides, continuously

handling high reverse-flow forces leads to significant ohmic losses, thus necessitating external cooling devices.

3.7 Highly dynamic torque motor driving ball-screw spindle

An attractive concept as far as handling tolerances, wear, and providing easy installation procedures are concerned is a highly-dynamic torque motor with ball-screw spindle. A powerful torque motor with optimised inertia was designed. Due to the system´s inherent linearity, a good controllability during valve unloading and closing is achievable. The high efficiency of the actuator permits the generation of energy during the valve closing event when the unloader gets pushed back.
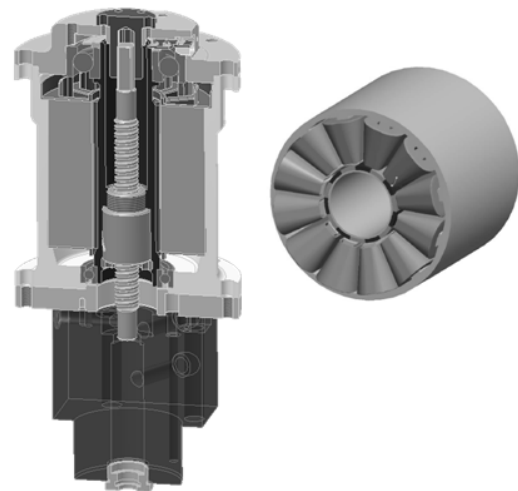
Fig. 8: Highly dynamic torque actuator with ball
screw

The main disadvantages of this concept are related to wear and the reliability of the ball screw. Even if, based on data sheets figures, the ball screw is capable of handling the occurring static and dynamic loads, the strong acceleration at the beginning of the valve closing event will give rise to sliding motions of the roller balls so that wear inevitably sets in. The reverse-flow force spikes cause accelerated wear as well that can hardly be predicted.

Even though the system showed good performance while not exhibiting significant wear in most of the tests, further development of the concept was stopped since an estimation of the failure probability revealed 48000 hours of service-free operation not to be achievable in a reliable manner. An increased size of the ball screw would have led to higher inertia and thereby to slower valve closing speed – thus causing higher force spikes that again reduce lifetime.

FLOW CONTROLS

New concept for electrical stepless compressor capacity-control system, *Bernhard Spiegl, Peter Dolovai,
Tino Lindner-Silwester;* HOERBIGER VENTILWERKE GMBH & CO KG

3.8   Hybrid actuator

A hybrid actuator incorporates different design elements of the above-mentioned principles in an intelligent manner, thereby combining advantages and overcoming limitations.

	Piezo Actuator	Simple Solenoid	Modified Solenoid	Double Magnets	Lorentz Force Act.	Linear Motor	Spindle Actuator	Hybrid Actuator
Dynamic potential	+++	+	+	+ +	+++	+	~	+ +
Min. closing time (*)	< 1ms	< 2 ms	< 3 ms	< 2ms	< 2 ms	< 4 ms	< 5 ms	< 3 ms
Force Potential(*)	+++	+	~/+	~/+	~	~	+	+ +
Max. Force (*)	>8 kN	~ 5 kN	~ 4 kN	~ 3 kN	~ 2 kN	~ 2 kN	< 4 kN	~ 8 kN
Controllability of motion	+++	-/~	~/+	~/+	++	+	+/~	+ +
Thermal Management	+++	+	~	+	~	~	+	+ +
Install. & wear sensitivity	~	~	~/+	~/+	+	++	++	+++
Wear & Reliability	~	+ +	~	~	~	+	-	+ +
Oil freeness	no	yes	yes	yes	yes	yes	no	yes

(*) at given size, continuous operation at 20 Hz, not external cooling, surface temperature < 100°C, including 1 mm wear tolerance

Fig. 9: Comparison of applicable actuation principles and benchmarking with respect to specification

Since the hybrid actuator approach performed best not only in simulations but also in real-world testing, this concept was chosen as the proper fully electrical alternative to HydroCOM. The following sections exclusively refer to this hybrid actuator concept.

4   Control concept

As outlined in section 2, the concept of reverse-flow capacity-control poses some challenges on the motion of the unloader.

- Small impact speed when the unloader gets in contact with the open suction valve sealing element.
- Sufficiently fast suction-valve closing event while keeping impact speeds low.

Without loss of generality a set trajectory can be defined which maps all above-mentioned requirements. Hence, a controller providing proper performance in terms of tracking a reference trajectory perfectly suits this need.
Due to the system layout and working principle of the new hybrid actuator there are several static system properties and dynamic system informations which can be used for the design of a position control loop.
The actuator force is, to a good approximation, quasi-statically related to the air gap height and the magnetomotive force, the magnetomotive force itself being a function of air gap height and linked magnetic flux. These two relationships, derived within an initial optimization process of the

magnetic circuit, are available in (invertible) lookup tables, see Fig. 10 and 11.
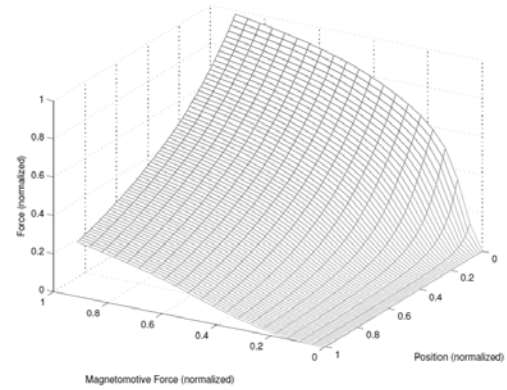
Fig. 10: Actuator force map
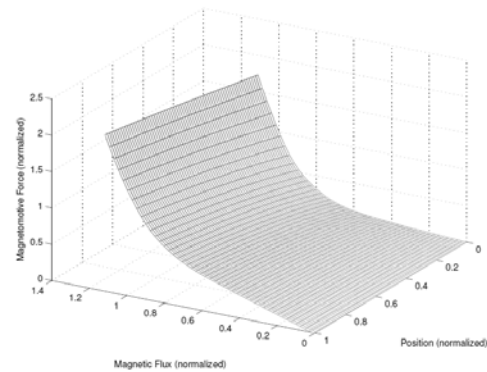
Fig. 11: Magnetomotive force map

The controller output serves as reference value for the voltage applied to the magnetic circuit. The differential equation describing the dynamics of the magnetic circuit is also available. Thereby the input – output behaviour of the actuator, namely applied voltage to actuator force, is known. The controller structure is designed with the purpose of utilizing any available system information for improving the overall controller performance and stability. The block diagram of the controller is depicted in Fig. 12.
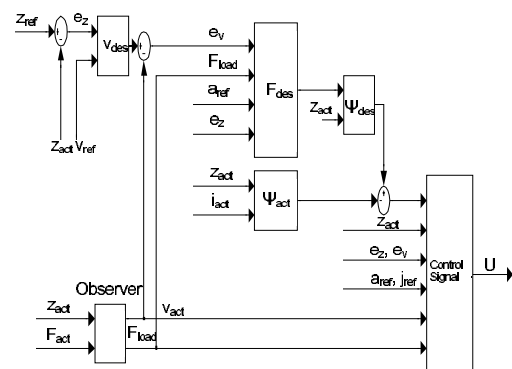
Fig. 12: Position control loop block diagram

As can be seen all relevant system information is collected to derive the control law.

The control error e_z based on position deviation and reference speed v_{ref} is used to calculate a desired speed v_{des}. Comparison of the desired speed with the actuator speed v_{act} gives a control error e_v based on speed deviation.

In a second step, a desired actuator force is calculated based on the position control error e_z, on speed control error e_v, on the reference acceleration a_{ref}, and on the reverse-flow force F_{load}. Making use of the inverse magnetomotive and actuator force maps a desired value of the magnetic flux Ψ_{des} can be determined. The desired magnetic flux is compared to the map-based actual value of the magnetic flux.

Finally, the controller output is calculated using a) the deviation of the desired from the actual flux, b) the actuator position z_{act}, c) the position control error e_z, d) speed control error e_v, e) the reference acceleration a_{ref}, f) the reference jerk j_{ref}, g) the actuator speed v_{act} and h) the reverse-flow force F_{load}.

This specific choice of signals and arrangement enables the utilization of backstepping methods which allows to form a Control Lyapunov Function for the system and to derive a control law. As a consequence, the closed loop is unconditionally stable in the sense of Lyapunov.

Since not all signals and system information utilized in the controller are directly available in terms of measurements, a respective observer is required. This observer needs to estimate the instantaneous values of those properties not accessible to direct measurements such as the reverse-flow force F_{load} and the actuator speed v_{act} (the latter quantity would require differentiation of the position signal which involves unacceptably high numerical errors). Therefore, a high-gain disturbance observer is implemented for the reverse-flow estimation and an ordinary Kalman filter is used for the estimation of the actuator speed, both using the measurable quantities actuator position z_{act} and the (map-based) actuator force F_{act} as input.

In Fig. 13 a simulation result is depicted, showing tracking performance, impact speeds, and controller output for a compressor at 50% capacity, 720rpm, and a reverse flow peak of 3400N.
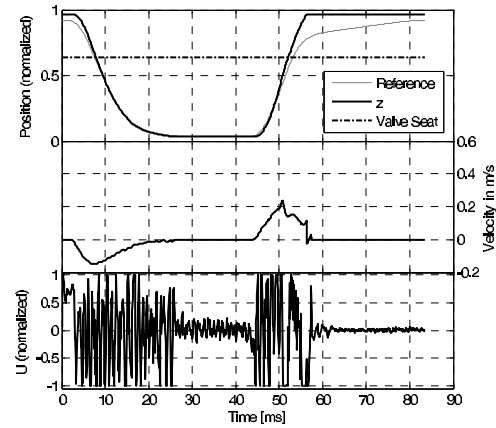
Fig. 13: Simulation of motion and speed of unloader and of controller output

5   Thermal Management

It is crucial to keep the temperature levels of the actuator and the power electronics below certain limits (system performance, reliability, ATEX conformity). Several measures have been taken to minimize the heat generation of the system:

- Optimization of the magnetic circuit with respect to minimal copper losses.
- Automatic clearance compensation that allows actuator to work permanently in its optimum operating range.
- Adaptive control concept. The copper losses of the actuator can be estimated online and hence passed to a cost function, which, considering the performance boundary conditions, can be minimized by adjustment of the reference trajectory.
- Power electronics designed such that switching losses of the driver components are minimized.

As a result of all these measures, no external cooling device is required any more. The heat generated within the actuator gets transferred away solely via conduction to the suction-valve cover, while all heat losses generated within the electronics compartment are transferred away via convective heat transfer to the ambient atmosphere. Fig. 14 shows a thermal FE simulation of the actuator.

New concept for electrical stepless compressor capacity-control system, *Bernhard Spiegl, Peter Dolovai,*
Tino Lindner-Silwester; HOERBIGER VENTILWERKE GMBH & CO KG

Fig. 14: Thermal simulation of new actuator

6   Test bench system

The capacity-control system does not only consist of the actuator, but also of the power electronics. Testing of these components can of course be done on a real-world compressor. However, the characteristics of the reverse-flow force (magnitude, rise rate) can barely be varied on a compressor. Therefore a test bench system capable of emulating different compressor loads was developed.

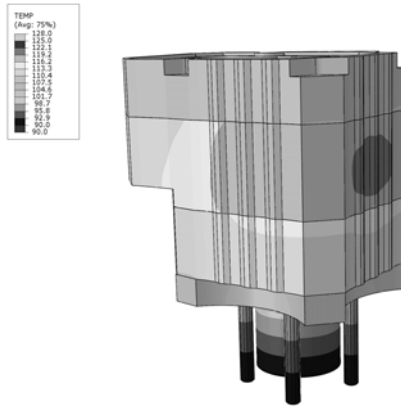The challenge in designing a proper test system is to find a working principle which provides loads in close resemblance to those occurring on a compressor during the reverse-flow phase. A mirrored system with an electromagnetic actuator of more or less the same design was found to be the perfect load emulator, see Fig. 15.
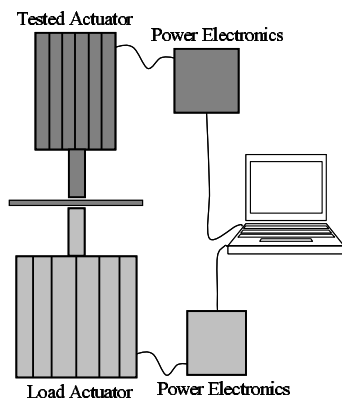

Fig. 15: Principle test system layout

A huge variety of operating conditions (reverse-flow force, compressor speed, valve lift,…) covering the system´s whole application range can be emulated with this test bench. The test bench has proven to be a very valuable tool in the pre-development phase allowing for first functional tests of the actuator and power electronics, model validation, optimization of the position control loop, and for long-time endurance tests of the overall system. Fig. 16 depicts an unloader-motion

trace measured on the test bench emulating a compressor at 50% capacity, 720rpm, with a reverse flow peak of 4000N.
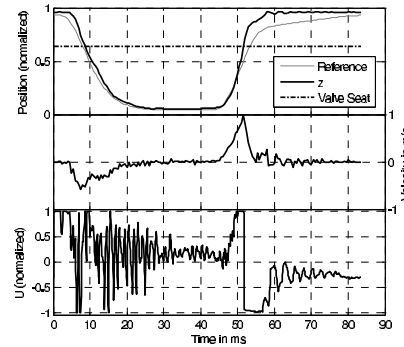
Fig. 16: Motion and speed of unloader and
controller output during one cycle at test
bench operation

7   Customer test installations

Whereas valuable insight has been gained on this test bench, running the system on a real-word compressor is still crucial, especially when it comes to embedding the actuator and its power electronics into the overall capacity-control system architecture. The very first compressor installation was done on an ARIEL compressor. The new capacity-control system was additionally installed on a gas storage plant, replacing two hydraulic actuators. The ATEX requirements for Zone 1 are met by the actuator. An LMF compressor was equipped with the new system. On one cylinder side, two new electrical actuators were installed, whereas the opposing cylinder is still equipped with hydraulic actuators. This shows that the new capacity-control system fits into already available system architecture, making use of the same BUS communication and the same load signals coming from the PLC. An additional monitoring system was also installed. Fig. 17 shows the actuator of the new capacity-control system attached to the compressor on the gas storage site.
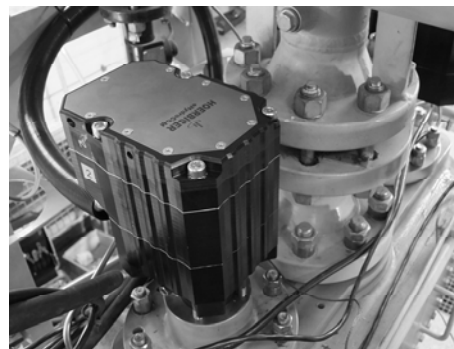
Fig. 17: New actuator installed on gas storage plant

So far the new system has been running flawlessly.

New concept for electrical stepless compressor capacity-control system, *Bernhard Spiegl, Peter Dolovai, Tino Lindner-Silwester;* HOERBIGER VENTILWERKE GMBH & CO KG

8   Summary and outlook

Reverse-flow regulation is still a very attractive option for stepless capacity control. Based on comprehensive field experience, a specification for a fully electrical capacity-control system was derived. Different applicable actuation principles were screened and simulated. The two most promising concepts were developed up to prototype stage. Final prototype testing revealed one of these two systems to be overall superior.

This completely oil-free, ATEX-certified electrical system, being capable of covering the whole application range of the existing HydroCOM system, was presented with laying emphasis on the crucial areas of control concept and thermal management. The system has been running successfully on test rigs and compressors.

The new concept will go into global field-testing phase covering the whole application envelope within the next two years with special focus on oilfree and critical units. The new system will help bring down the costs of installation, maintenance, and operation for the OEM and the enduser.

References:

[1] Kopecek, H., Klockow, H., Schmitz M. (2008): Development and Test of an Electrical Valve Actuator for Reverse Flow Capacity Control of Reciprocating Compressors. 6th EFRC-Conference, 98-104

[2] Aigner, R., Voser, A., Allenspach, A. (2010): Development of a Stepless Flow Control System 7th EFRC-Conference, 120-129

[3] Schiavone, M., Raggi, A. (2008): Electromechanical Actuator for Reciprocating Compressor Stepless Control. 6th EFRC-Conference, 180-187

BLUESTROKE
A Variable Stroke Flow Control for Reciprocating Compressors

by:

Dr. Mike Hüllenkremer
Central Division of Technology
Neuman & Esser GmbH & Co KG
Übach-Palenberg
Germany
Mike.Huellenkremer@Neuman-Esser.de

Dr. Osman Kurt
EWE Netz GmbH

8th Conference of the EFRC
September 27th / 28th, 2012, Düsseldorf

Abstract:

For reciprocating compressors many options of controlling the flow exist. Among these options, there are some which have a good performance in terms of efficiency at full load conditions. Nevertheless, efficiency drops down at part load condition for most control mechanisms.

This paper will explain the most known control options for reciprocating compressors and will classify them in terms of efficiency. It will be demonstrated that a control mechanism which could reduce the stroke of the compressor should be a very effective and efficient way of adjusting the flow.

The paper will also show the technical design of such a control principle.

BLUESTROKE. A Variable Stroke Flow Control for Reciprocating Compressors, *Mike Hüllenkremer;*
NEUMAN & ESSER GMBH & CO KG

1 Introduction

One of the advantages of reciprocating compressors is the perfect ability to adjust their performance to varying flow and pressure conditions. Varying suction and/or discharge pressure conditions are automatically adjusted by this type of compressors. Since reciprocating compressors are generally equipped with plate or ring valves which are actuated just by the differential pressure, varying pressure conditions are automatically adjusted in the compression cycle. Of course, varying pressure conditions have an influence on the flow, but almost no influence on the efficiency. This statement is even valid for multiple stage compressors. The compressor just reacts by interstage pressure adjustment.

Another advantage is that many options of controlling the flow exist. Among these options, there are some which have a good performance in terms of efficiency at full load condition. Nevertheless, the efficiency drops down at part load condition for most control mechanisms. This paper follows the aim to point out an efficient control mechanism that is able to reduce flow Q to at least 50 % of the nominal flow Q_0.

2 Example Compressor

The conclusions drawn in this paper based on calculations done for an exemplary compressor of the Neumann & Esser type 1 SVL 320. This describes a reciprocating compressor that

- is used for a single process,
- has lubricated cylinders,
- is a horizontal machine and
- has 4 cranks.

Its main technical data are:

- Power P 2300   kW
- Rod Force F 388   kN
- Stroke $s_{100\%}$ 300   mm
- Relative Cylinder Clearance ε_0 0.28   —

Originally it has been dedicated to natural gas storage operation with an isentropic exponent κ of natural gas of 1.31 and an intermediate pressure ratio ψ of 4.2

3 Flow Control Principles

A huge variety of flow controls for reciprocating compressors exist. **Figure 1** gives an overview. As to see they are already classified by their underlying working principle.
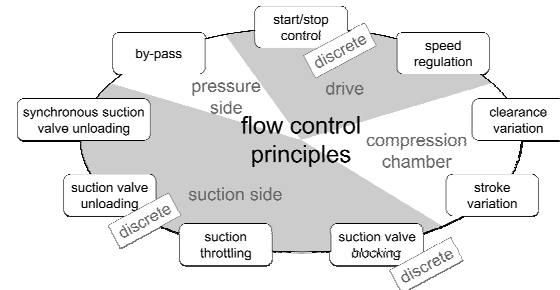
Figure 1:   Feasible flow control principles

Mainly 4 working principles exist:

1. Acting on the drive. It allows to reduce speed or turn the drive temporarily off.

2. Changing compressor cycle parameters like clearance or stroke.

3. Manipulations on the suction side by unloading or blocking the suctions valves or by a throttle in the suction line.

4. Acting on the pressure side by by-passing the gas back to the suction line.

Controls like start/stop control, suction valve blocking or suction valve unloading do not allow a continuous flow control. Therefore they will be excluded from further considerations.

4 Benchmarking

Figure 2 gives a first qualitative efficiency ranking of the introduced flow controls.

Figure 2:   Energetic benchmark of continuous variable flow controls

BLUESTROKE. A Variable Stroke Flow Control for Reciprocating Compressors, *Mike Hüllenkremer;*
NEUMAN & ESSER GMBH & CO KG

Without any doubt by-passing is energetically worse as it consumes 100 % power independent of the flow delivered. On the contrary, best results are gained by speed regulation. As the compressors power consumption *P* is calculated by

$$P = w \cdot \omega \cdot \prod_i \eta_i$$

where *w* is the thermodynamics process work, ω the drives angular velocity and η_i are efficiency factors, it becomes obvious that reducing the drives velocity has a strong impact. In contrast to all other controls there is almost no saving gained in the thermodynamics process work. This is stated by a look at the *pV*-chart (**Figure 3**), wherein the thermodynamics process work is proportional to the enclosed chart area. Only the valve losses, which result from gas friction and are proportional to the squared piston velocity, are slightly reduced.

Figure 3: p*V-chart comparison between full and half load using speed regulation*
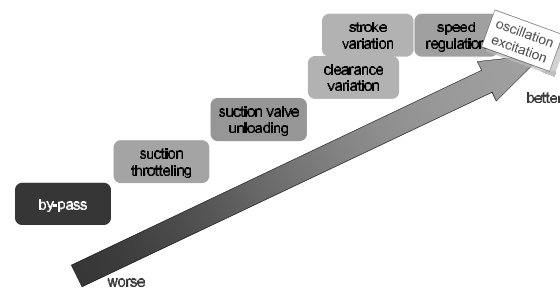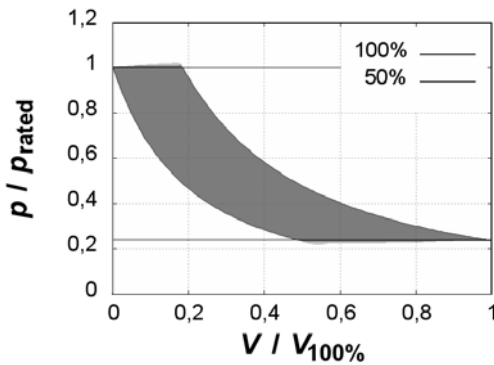
Disadvantageous is the effect of the increased leakage between the pressure chambers due to the longer lasting compression cycles. Also converters show increased losses in part load operations. But the main problem applying a speed regulation is that the drive represents a major source of vibrations. Therefore it is very common to forbid one or more speed ranges in order to prevent a catastrophic resonance. Altering the cylinder clearance is another very energy efficient control measure. It can be achieved by additional pocket clearances or a continuously adaptable volume, imaginable as movable cylinder ends, e. g. a piston instead of a fixed cap. The additional clearance extends the gas' compression and expansion and by this reduces the suction and discharge time. Its impact on the volume flow depends on gas composition and pressure ratio ψ. The bigger the pressure ratio ψ and the smaller the isentropic exponent κ the stronger the effect becomes. The comparison between the highlighted areas in the *pV*-chart (**Figure 4**) states almost half the energy is saved.
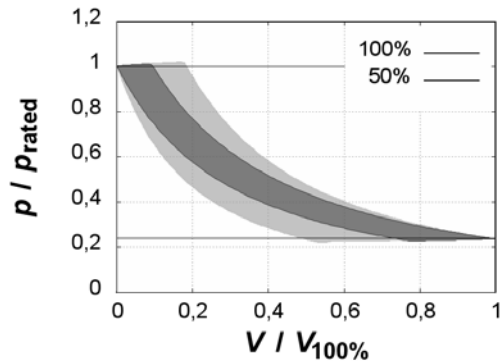
Figure 4: p*V-chart comparison between full and half load with altered cylinder clearance*

A suction throttle reduces the suction pressure and by this increases the pressure ratio. This again leads to longer lasting compression and expansion phases and therefore less discharge.

The energy dissipated by the throttle has to be fed back to the gas by the compressor. In the *pV*-chart (**Figure 5**) this extra work is identifiable as the additional enclosed area below the suction line pressure level. It is obvious that the efficiency of the suction throttle control is not as optimal as it is for the cylinder clearance variation.
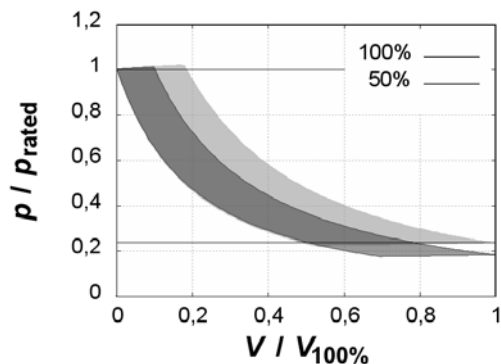
Figure 5: p*V-chart comparison between full and half load utilizing a suction throttle*

A synchronized suction valve unloader acts directly on the rings or the plate of the suction valve. It is designed to extend the valves opening period beyond the suction phase. Consequently the gas cannot be compressed and the piston starts to push it back into suction line instead. The unloader will allow the valve to close once the gas is reduced to the required volume. By this, only the work needed to compress the required gas is carried out. The only losses result from gas friction while passing the valves. In the *pV*-chart (**Figure 6**) they are visible as hysteresis around the suction pressure level. The smaller the molar mass of the gas composition is, the bigger the losses become. They are independent of the pressure ratio. Therefore the relative losses increase for small pressure ratios and

FLOW CONTROLS

BLUESTROKE. A Variable Stroke Flow Control for Reciprocating Compressors, *Mike Hüllenkremer;*
NEUMAN & ESSER GMBH & CO KG

vice versa. Still the synchronized suction valve unloader is a relative energy efficient flow control system.

Figure 6: pV-*chart comparison between full and half load using synchronous suction valve unloader*

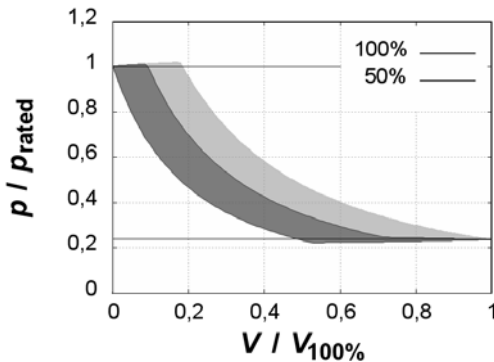The principle of the variable stroke flow control is easy: smaller stroke leads to less output. Its impact is amplified because the reduced stroke also leads to an increase in cylinder clearance. Compared to the preceding controls it shows several advantages:

1. Only the gas required is sucked into the cylinder. No gas transfer back to the suction line is needed, no extra valve losses occur. Valve losses are even decreased because the reduced stroke leads to slower piston movement!

2. It is effective without additional cylinder volume.

3. No energy is dissipated to decrease pressure.

4. No additional oscillating excitation occurs due to this control mechanism.

These advantages can be verified by a look at the *pV*-chart (**Figure 7**), which also already promises good energy efficiency.
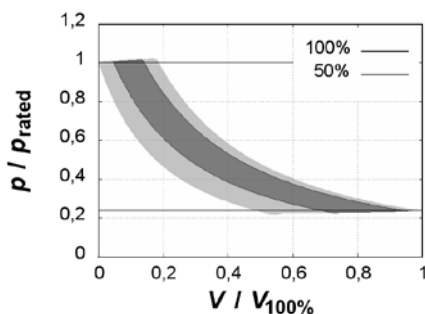
Figure 7: pV-*chart comparison between full and half load varying the stroke*

The efficiency of the stroke variation becomes even more obvious when compared to the other flow controls, s. **Figure 8**. The variable stroke flow control comes off even better than the controls by cylinder clearance and synchronized suction valve unloading. Only the speed regulation control is more efficient, but as mentioned before, often has to spare out one or more speed ranges.
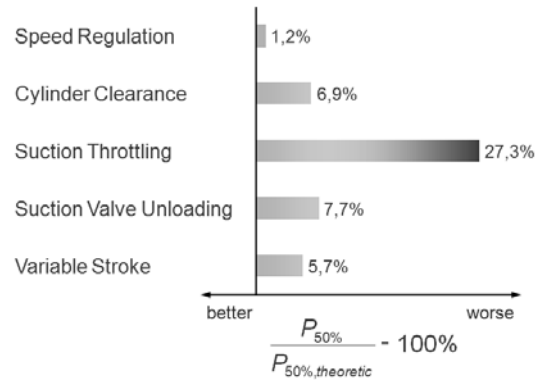
Figure 8: *Comparison of power consumption relative to half power of full load operation*

5 Variable Stroke Control Design

Before a compressors stroke altering mechanism can be designed, the required stroke difference that matches the targeted volume flow has to be determined. In the example demonstrated here we were aiming at 50 % of the nominal volume flow. Following the stroke-flow-characteristics in **Figure 9**, a reduction to 89 % of the nominal stroke is sufficient. Referring to the example compressor with a nominal stroke s_0 of 300 mm this corresponds to a stroke difference of 33 mm.
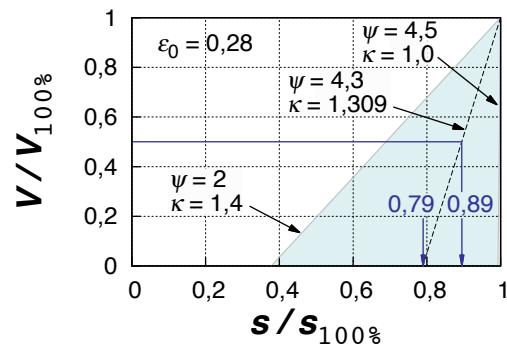
Figure 9: *Stroke-flow-characteristics for variable stroke*

Our literature research for appropriate mechanisms led to several hits, most of them belonging to the field of combustion engines. Some examples are depicted in **Figure 10**. It emerged that an extended crank drive is the most promising solution as it

FLOW CONTROLS

BLUESTROKE. A Variable Stroke Flow Control for Reciprocating Compressors, *Mike Hüllenkremer;* NEUMAN & ESSER GMBH & CO KG

allows sufficient stroke differences and stepless adjustability, without frequent actuator intervention.
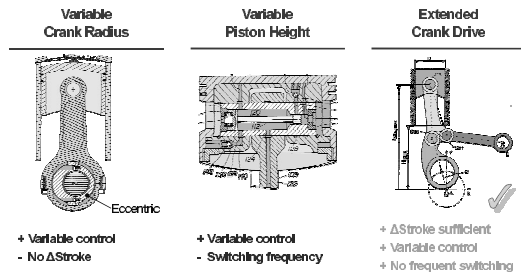
Figure 10: Examples of mechanisms altering the compression behavior

From an academical point of view, the final solution basically is a planar six-bar linkage with the crankcase as its first ternary link (link with 3 joints). Its second ternary link is not clearly identifiable because 2 of its joints are coaxial. Therefore it is impossible to categorize whether it has a Stephenson or a Watt topology.

Described in simple words the solution is a crank-rocker mechanism, being built up of the crankcase, the fully rotating crank, the lower con-rod and the back and forth moving rocker (s. **Figure 11**), with an attached two-bar link with sliding joint made up of the upper con-rod and the crosshead.
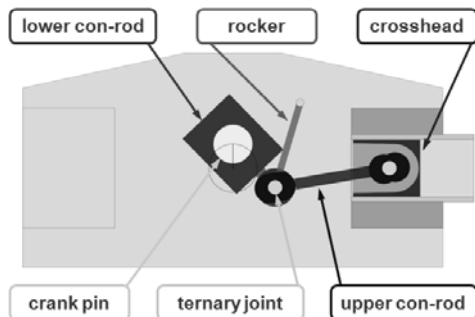
Figure 11: Variable stroke control: main parts and design principle

In this linkage the position of the joint between rocker and crankcase decides about the stroke and the mean position around which the crosshead oscillates. These kinematic properties are easily calculated from geometry.

Searching a suitable solution is an iterative process in which several steps have to be taken:

1. Define rod lengths. As a consequence the possible whereabouts of the rockers joint are bounded because of the linkage functionality.

2. Rasterize search domain and calculate crossheads movement mean position and stroke.

3. Identify isolines (curve of a constant value) of crossheads movement mean position and stroke.

4. Apply boundary conditions like
   a. design space
   b. allowed forces
   c. …

5. Identify optimal solution. For double acting reciprocating compressors this should be a curve of (almost) constant crosshead mean position. This ensures both pressure chambers are served equally. The curve should cross as many stroke isolines as possible to realize the maximal stroke difference. In the end, a linear curve would allow the use of a linear guide to bear the rocker joint.

The described work is best done by a computer. An exemplary solution is shown in **Figure 12**.
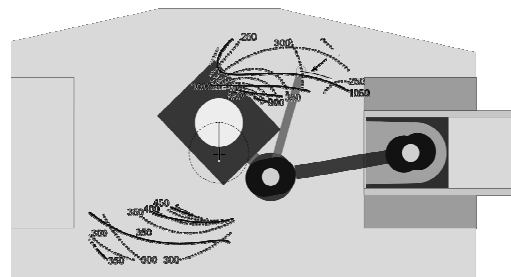
Figure 12: Variable stroke flow control linkage with information on stroke (dotted red isolines) and mean piston position (continuous blue isolines)

Following, an impression of the real design of our patented principle is given. **Figure 13** shows the bare linkage, **Figure 14** when built into the crankcase. The rocker joint is mounted on the slide of a linear bearing which is actuated by a hydraulic cylinder. The cylinder is able to move and hold the rocker joint in any position along the linear bearing axis, thereby utilizing the new drive-trains continuous flow control capability, s. **Figure 15** to **Figure 17**.

Figure 13: Linkage design of variable stroke flow control

BLUESTROKE. A Variable Stroke Flow Control for Reciprocating Compressors, *Mike Hüllenkremer;*
NEUMAN & ESSER GMBH & CO KG
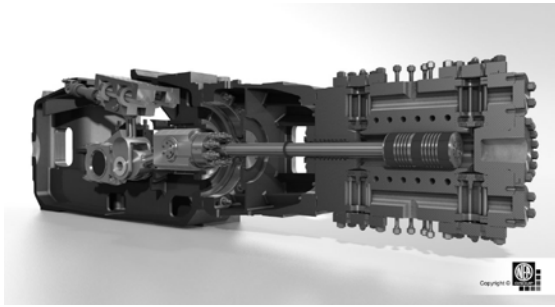
Figure 14: Built-in variable stroke flow control
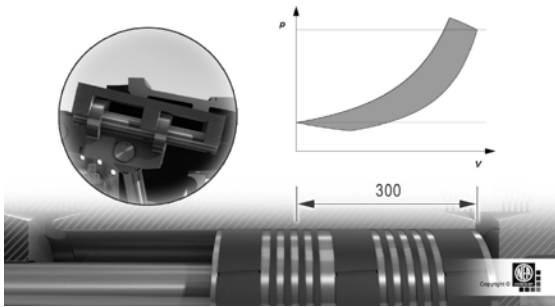
Figure 15: Variable stroke flow control in full load operation
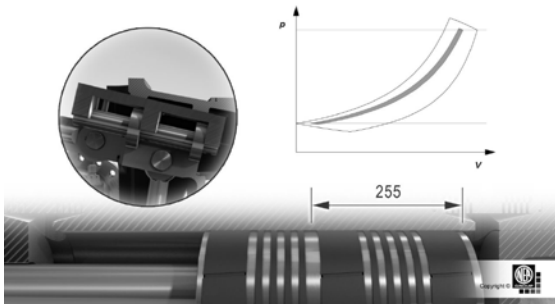
Figure 16: Variable stroke flow control in minimum load operation
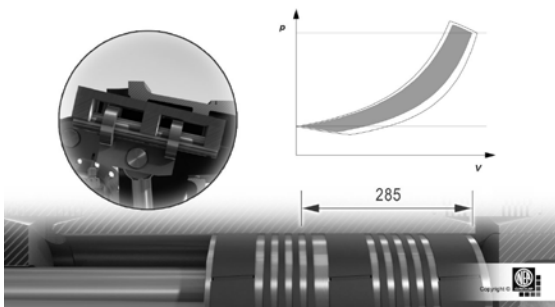
Figure 17: Variable stroke flow control between full and minimum load operation

As a matter of course the crankcase has to undergo some modifications with respect to mounting surfaces. Cylinder and valves are available in ex-proof design.

The lubricating system is illustrated in **Figure 18**. It is fed through the main crankshaft bearing and the crosshead liner. The oil is passed on to the following part via the bearings as it is widely established.
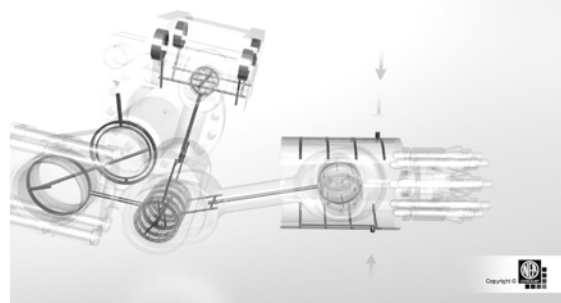
Figure 18: Lubricating system of the variable stroke flow control

6   Conclusion

The aim was to develop a continuous flow control for reciprocating compressors with excellent energetic efficiency in full load as well as in part load operation. In the analysis of known control principles a variable piston stroke emerged as promising solution. It works by altering the stroke, amplifying its effect through the inherent simultaneous increase of the cylinder clearance. Thus it only sucks in the gas required without the disadvantages known from other controls, like additional valve losses, an increasing mechanical oscillation excitation or intentional energy dissipation. With these characteristics its good performance in the direct energetic efficiency comparison was no surprise.

The research on how to implement a variable stroke resulted in 6-bar linkage with 1 sliding joint as a replacement for the common known slider-crank mechanism. The linkages kinematic characteristics are adjusted by the position of the rocker joint. A layout procedure to find a suitable adjusting curve has been presented. One of its main constraints was to keep the mean piston position constant in order to ensure an equally impact on both working compartments of the double acting cylinder.

Finally the implemented design of our BlueStroke control has been presented. A linear guide operated by a hydraulic cylinder is used to position the rocker bearing. They are already available in ex-proof design. Thus the variable stroke flow control is an interesting alternative to already established continuous flow controls for reciprocating compressors.

8th Conference of the EFRC
September 27th / 28th, 2012, Düsseldorf

EFRC

EUROPEAN FORUM
for RECIPROCATING
COMPRESSORS

High-frequency radiated noise in a reciprocating compressor installation: analysis and mitigation

by:

Joachim Golliard and Leonard van Lier
TNO - Department of Fluid Dynamics
Delft, The Netherlands
joachim.golliard@tno.nl

Vasillaq Kacani
Leobersdorfer Maschinenfabrik GmbH
Leobersdorf, Austria
Vasillaq.Kacani@lmf.at

8th Conference of the EFRC
September 27th / 28th, 2012, Düsseldorf

Abstract:

This paper will present an installation problem observed at commissioning of two identical reciprocating compressors. During operation at 100% and 75% load, a high frequency whistling was observed around the machines, posing a serious issue with noise exposure to personnel. The noise was also radiated efficiently to the environment via the coolers installed outside of the building. The noise sources were identified after a field survey including measurement of high-frequency pulsations and vibrations at different loads. The restriction orifices located at the inlet of the line chokes of the discharge dampers were confirmed as sources. This was based on the fact that the frequency of the tone would depend linearly on the gas velocity at the discharge side, without any dependence on the flow velocity, pressure and temperature at the suction side. The interaction between flow instability in the orifice and higher-order acoustic modes in the discharge damper proved to be very important for finding the root cause of the noise. The dampers were modified to change the location of the restriction orifices towards a different location in the discharge piping, while keeping a similar low-frequency pulsation damping effect. This solved the high-frequency noise problem.

High-frequency radiated noise in a reciprocating compressor installation: analysis and mitigation,
Joachim Golliard, Leonard van Lier, Vasillaq Kacani; TNO - DEPARTMENT OF FLUID DYNAMICS,
LEOBERSDORFER MASCHINENFABRIK GMBH

1   Introduction

For new reciprocating compressor installations, pulsation and mechanical analysis according to the API 618 standard are common engineering practice. The scope of the analysis is explicitly limited to identification and mitigation of pulsation and vibration issues, caused by the intrinsic pulsations of the compressors. The overall focus is at structural integrity at lower frequencies. Normally the dominant frequencies occurring in these systems are typically low (<50 Hz). For special systems, such as high-speed reciprocating compressors and/or systems with reverse flow capacity control, the frequency range of interest may reach up to a few hundred Hz. In the majority of cases, a robust pulsation and mechanical analysis ensures a trouble-free system, with respect to low-frequency pulsations and vibrations. The API 618 standard does not address pulsation issues that are caused by other sources than the reciprocating compressor itself. The most common type of pulsation source (apart from the reciprocating compressor) are flow-induced pulsations. In the majority of cases, these flow-induced pulsations are caused by T-joints connecting the main piping to closed side branches. At these closed side branches, flow instability (periodic vortex shedding at the inlet) can couple with acoustic resonances (typically ¼λ standing waves) in the closed side branch, leading to a strong source of pulsations [2, 3]. The frequency of this source depends on the flow speed and the diameter of the side branch. Most known cases concern system with large flows and large side branch diameters. As a consequence, these flow-induced pulsation problems mainly occur in turbo-compressors (which have in general larger flows and larger pipe dimensions). If such a flow-induced pulsation problem at closed side branches occurs, the dominant frequencies are typically low (~20 Hz and lower). In any case, API 618 (nor any other industrial standard) explicitly stipulates a design evaluation strategy, leaving it to the operator and engineer contractor to decide on the required level of analysis. A less common type of flow-induced pulsation sources concerns whistling of orifice plates [4]. Also in this case, flow instability (vortex shedding at the orifice) and coupling with acoustic resonances (such as small-bore side branches or higher-order acoustic modes in the piping) leads to strong pressure pulsations. However, given the more confined dimensions of the piping and orifice configuration, this phenomenon occurs at much higher frequencies, typically at a few hundred Hz up to a few kHz. This higher frequency make the identification and mitigation of these problems more problematic than low-frequency problems.

First, for a design evaluation, more sophisticated simulation tools are required, being able to predict acoustic sources and propagation in the 3D regime. Second, the level of details required to do simulations is of another order than the amount of detail required for "normal" pulsation analysis. When 3D acoustic simulation tools are required, also computational effort will be excessively large, making it virtually impossible to evaluate a large envelope of possible process conditions. High-frequency in-line pulsations are transferred to radiated noise via the pipe wall efficiently: the pipe wall is relatively transparent to high-frequency noise. Also, the human ear is very sensitive at frequencies around 1 kHz, and noise levels at this frequency are severely penalized in noise legislation. In short, a full-proof identification in the design stage of potential whistling orifice is very problematic, while the consequences may be very serious. Finally, a complicating factor is that this phenomenon occurs relatively rarely, with only a handful of cases reported over the past decade. This paper describes such a case. For the pulsation and mechanical analysis, it started as 'business as usual'. However, upon commissioning a very persistent noise issue occurred, that required an elaborate additional analysis to identify the root cause and find a robust mitigation strategy. This process was painstaking, but eventually successful.

2   Compressor configuration and operational aspects

Two one-stage LMF Compressors Model B252 with two axis horizontal type are installed in Schönkirchen, Austria. The installation compresses sour natural gas from the reservoir and the gas is transported to a treatment facility further downstream. The compressor installation is operated by ÖMV. The compressors are designed for sour gas service. The partial pressure of H_2S varied from 42kPa at suction side to 162kPa at discharge side of the compressor. Therefore the gas service falls within region 3 in NACE MR0175 [5] and the materials are according to this code and user specifications.

The compressors and the separator vessel are mounted indoors, in a compressor building, see figure 1. The compressor building has no acoustic treatment of the walls and is therefore highly reverberating.

High-frequency radiated noise in a reciprocating compressor installation: analysis and mitigation,
Joachim Golliard, Leonard van Lier, Vasillaq Kacani; TNO - DEPARTMENT OF FLUID DYNAMICS,
LEOBERSDORFER MASCHINENFABRIK GMBH

Figure 1: Compressor installation inside the building

Further, the operating conditions of the compressors are highly variable:

- Variable gas composition
- Suction pressure varied from 21 bar abs to 61 bar abs.
- Compressor speed range 300 to 600rpm (VSD)
- Bypass operation
- Suction valve unloaded 25%, 50% and 75% load
- Single operation 25%, 50%, 75% 100% load
- Parallel operation of two compressors 25%, 50%, 75% 100% load

The compressors are designed for all specified load steps and fully unloaded condition.

Due to the wide range of operating parameters the compressor design is checked specially regarding the required capacity, power consumption, piston rod load, gas rod load, inertia load, torsional critical speed etc.

Figure 2 shows the flow capacity for one compressor and a typical power curve for one stage compressor versus the suction pressure for different compressor speeds at a constant discharge pressure of 81 bar abs. The circle in the diagram specifies the design point of the compressor at 595rpm and suction pressure 40bar abs.

Figure 3 and 4 show the maximum, respectively minimum, forces (plus compression and minus tension) during a complete crank shaft revolution - as a function of the suction pressure at different compressor speeds for a constant discharge pressure. The gas force is calculated from the actual internal cylinder pressure using the valve and passage losses and real gas data. The horizontal lines represent the 100% respectively 80% of

maximum allowable rod load. Figure 5 shows the maximum discharge temperature.
These are the main data to determine the allowable parameter ranges of compressor units.

To avoid any overload of the compressor – such as: maximum allowable rod load, rated power of electric motor, maximum allowable discharge temperature, minimum required rod reversal angle/magnitude etc. - certain parameters are disabled for continuous service.

Based on the calculated data the so-called panhandle diagrams are prepared for an automatic control of both compressors during the start-up, shut down as well as continuous operation.
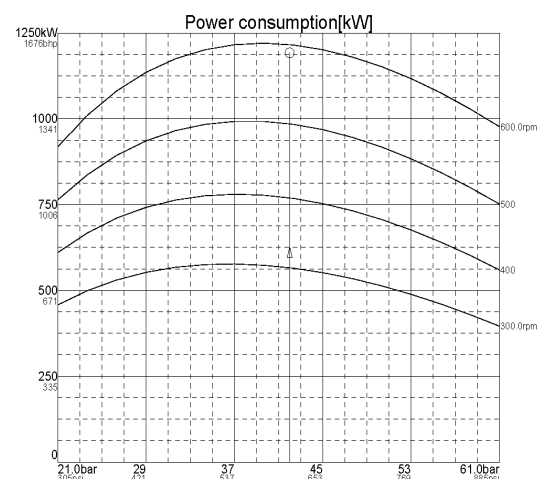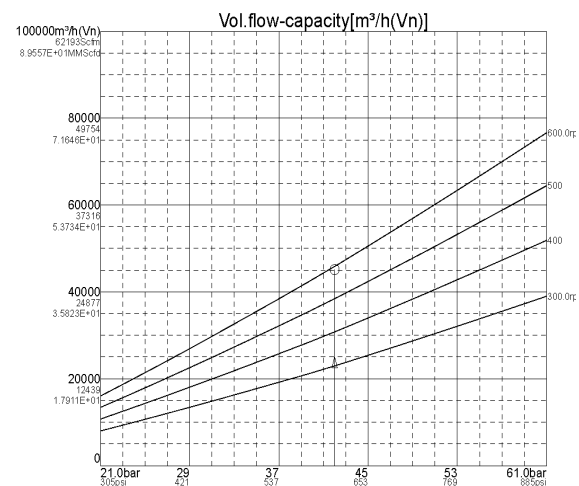

Figure 2: Flow capacity, m³/h(Vn) and power consumption

High-frequency radiated noise in a reciprocating compressor installation: analysis and mitigation,
Joachim Golliard, Leonard van Lier, Vasillaq Kacani; TNO - DEPARTMENT OF FLUID DYNAMICS,
LEOBERSDORFER MASCHINENFABRIK GMBH

Figure 3: Combined rod load

Figure 4: Gas forces

Figure 5: Maximum discharge temperature

3 Initial pulsation analysis and damper design

The operating range of the compressor system is large: variable suction pressure, various load steps, variable speed, variable gas composition and both single/parallel operation of the compressors. It was decided to adopt a API 618, design approach 3 pulsation analysis. This is the most elaborate design approach, including pulsation and analysis and mechanical analysis, paying special attention to cover the complete operating envelope. The scope also included a dynamic compressor valve analysis, in which the impact of pulsations on the compressor valve behavior is analyzed (avoiding excessive valve impact velocities and valve fluttering). In addition to the optimization of the pulsation dampers, the pulsation analysis of the piping and the mechanical response analysis, TNO's scope of work also included the piping flexibility (static stress) analysis. This is convenient, since this facilitates the iteration loops that typically occur between the piping flexibility analysis (minimize static stress, aiming at maximum flexibility) and the mechanical response analysis (minimize dynamic vibrations, aiming at minimum flexibility).

As usual, the pulsation analysis embarked with an evaluation of the pulsation dampers (damper check). At this stage in the project, the field piping is not yet known, and a simplified boundary condition is applied to represent the field piping. During the damper check, API 618 stipulates a safety margin of 30% on the allowable pulsation levels, to allow for the effect of acoustic resonances that may occur in the field piping. This safety margin is a reasonable estimate, but may not always be sufficient to fully mitigate the resonances occurring in the field piping. In that case, additional measures may be required, such as restriction orifices at the line connection of the dampers or orifices in the field piping. Of course, modifications to the pulsation damper design in a late stage of the project should be avoided as much as possible.

During the damper check in this project, various modifications were evaluated and proposed. These included increasing the volume of the damper, and by adding orifice plates at the cylinder connections. More important, a 8" line choke was added at the outlet of the discharge dampers (extended outlet), to minimize the transfer of high-frequent pulsations to the pipe system. After various iteration steps, a satisfactory performance for all process conditions was computed.
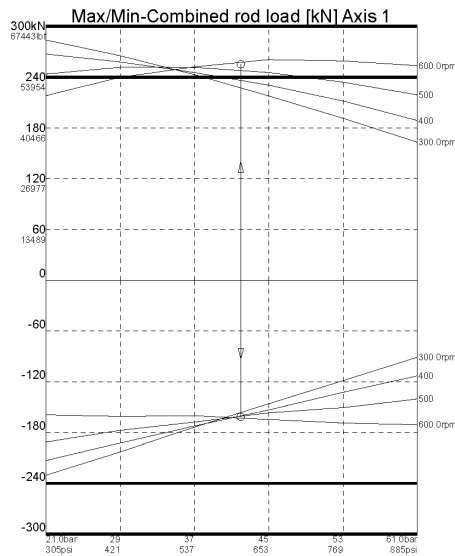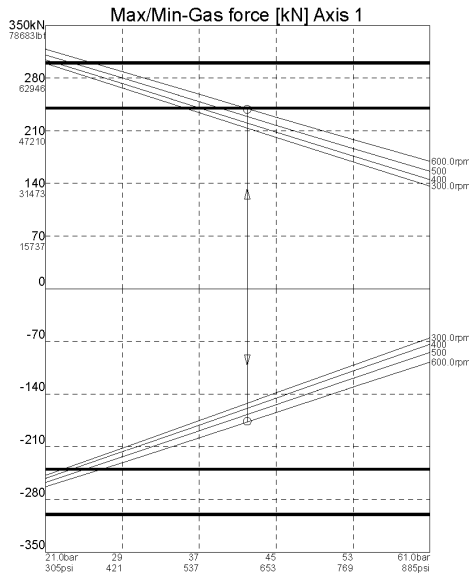
High-frequency radiated noise in a reciprocating compressor installation: analysis and mitigation,
Joachim Golliard, Leonard van Lier, Vasillaq Kacani; TNO - DEPARTMENT OF FLUID DYNAMICS,
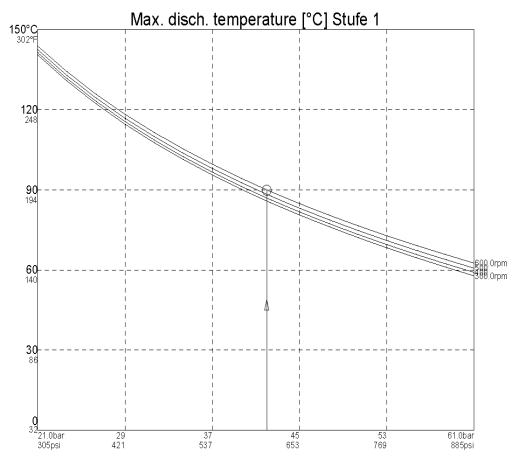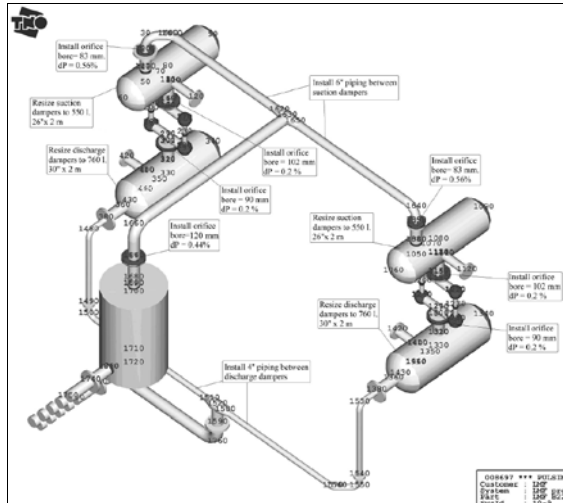LEOBERSDORFER MASCHINENFABRIK GMBH

Figure 6: Simulation model of dampers and skid piping

Because also the skid piping was already known at an early stage of the project, this piping was included in the evaluation of the dampers (figure 6). It appeared that due to acoustic resonances in the skid piping, a significant exceeding at the discharge side occurs. This exceeding can be mitigated most efficiently by adding orifice plates near the pulsation dampers. Due to the relatively high compressor speed, the frequency of the exceeding pulsations is relatively large (~100 Hz), and acoustic wavelengths are subsequently small. In this case, the placement of a restriction orifice at the damper flange may not be effective. Note that an orifice is most effective when placed close to a large volume, such as a pulsation damper. If the orifice is placed at $1/4\lambda$ from the volume, it will not be effective. Since the exceeding in the field piping occurred near the 10th harmonic of the compressor speed, the restriction orifices need to be placed very close to the damper volume. Due to the additional length of the line choke, the outlet flange of the damper was not suited for placing the orifice, being too far from the damper volume to obtain efficient suppression of these high-frequency pulsations. After discussion with LMF it was decided to install the restriction orifice at the inlet of the line choke. With a bore of 85 mm, the flow velocities in the orifice contraction are large, but not excessively high.

As a next step, the field piping was included in the simulation model (see figure 7). Meanwhile, the design of the pulsation dampers had been modified, using a smaller size for the line-choke at the discharge dampers (from 8" to 4"). The orifice bores were updated accordingly to 56 mm, see figure 8. This modification leads to high local flow velocities in the orifice contraction, making it more liable to strong noise production.
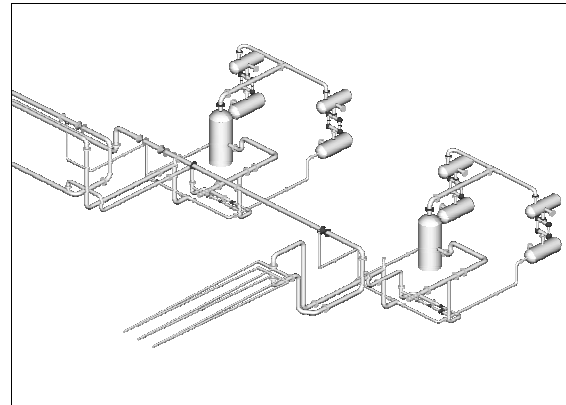
Figure 7: Simulation model field piping
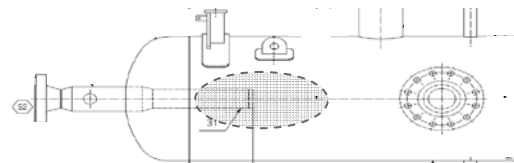
Figure 8: Detail of discharge pulsation damper with orifice plate at the inlet of line choke

In the field piping exceeding of the allowable pulsation levels was observed in the relief lines. This exceeding could be mitigated by placing restriction orifices at the inlet of the relief lines

After the pulsation analysis, the supporting layout was evaluated in the mechanical response analysis. Several additional supports were recommended. At some locations in the pipe system a conflict between the static stress analysis (aiming at maximum piping flexibility) and the mechanical response analysis (aiming at minimum piping flexibility) occurred. To resolve this conflict, spring hold-down supports were recommended. A spring hold-down support provides sufficient dynamic fixation (by means of increased friction at the support-structure interface) while still allowing for thermal expansion by means of adequate clearances in the bolt holes. Figure 9 shows a typical arrangement.

The analysis was finalized in 2009 and the design of the piping was issued "for construction".

Within TNO's scope of work, also a commissioning field survey was included, containing pulsation and vibration measurements. This field survey is meant to confirm that the actual pulsation and vibration levels in the installation are consistent with the simulations and compliant with the allowable levels.

High-frequency radiated noise in a reciprocating compressor installation: analysis and mitigation,
Joachim Golliard, Leonard van Lier, Vasillaq Kacani; TNO - DEPARTMENT OF FLUID DYNAMICS,
LEOBERSDORFER MASCHINENFABRIK GMBH

Figure 9: Typical spring hold-down support

4   High frequency noise issue

Upon commissioning of the compressor station, excessive noise radiation was reported by the operator. Preliminary observations by plant personnel suggested that the noise was originating from the cylinder connection of the discharge dampers. A field survey of the noise and pulsations in the piping was organized at short notice, in September 2010. In-line pressure pulsations were measured at 6 positions in the suction piping, the bypass section and the discharge piping. During this first survey, only one of the two compressor was running, and the pulsations were measured for three different conditions, chosen as being characteristic of the operational range of the compressor. The three conditions corresponded to different suction pressures (23 bar, 43 and 60 bar), while the discharge pressure was constant to 73 bar. The load of the compressor was 75% for the suction pressures 23 bar and 60 bar, and 100% for the suction pressure of 43 bar. Due to operational limitations, most of the gas was recycled and the bypass valve was mostly in open position during this survey.

The low-frequency pulsations measured during this survey were within acceptable levels for all the conditions at all positions in the suction, discharge and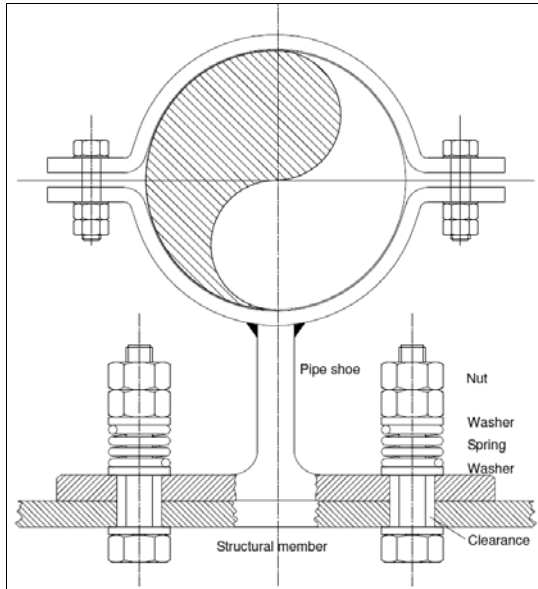 bypass piping. However, due to the large recycling, the loads were not completely characteristic of actual operational conditions. As a consequence only a limited part of the operating envelope could be investigated.

During the field survey, high-amplitude noise levels were recorded at 4.3 kHz (figure 10).
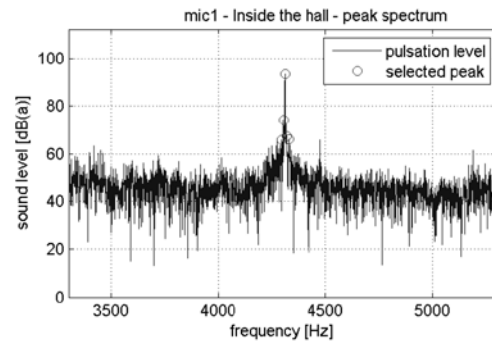
Figure 10: Noise spectrum, dominated by strong tonal noise at 4310 Hz

This high-frequency whistling tone was confirmed to be originating from the recycle line. When gradually closing and re-opening the recycle valve, a spectrogram was recorded. See figure 11, where the frequency is plotted versus time. Red color means a large noise, blue color a low noise. The amplitude of the noise is modulated (source strength scales with flow) and a lock-in is clearly observed (the dominant frequency remains constant, as a consequence of the constant resonance frequency).
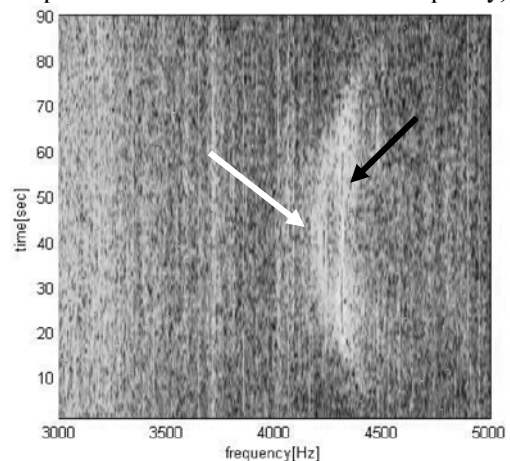
*Figure 11: Spectrogram while closing and re-opening the recycle valve.
White arrow: source frequency modulating with flow.
Black arrow: flow-independent resonance frequency*

The flow-induced noise issue in the recycle line can be controlled by reducing the flow speed (avoiding excessive bypassing).

Still, the operators reported large amplitude noise in the building where the compressors are installed, and close to the cooling exchangers outside. This remaining noise was also at a high frequency (800-1500 Hz), and occurred also with closed recycle valve. This noise posed an urgent environmental issue, to both personnel and surroundings neighbors.

5   Troubleshooting analysis of the noise problem

To investigate further the high-frequency noise issue, a second field survey took place in April 2011. The goal of this survey was to identify and characterize the root cause of noise to eventually eliminate it. The starting hypotheses for the source of the noise were the following:

- Higher harmonics of the compressor pulsations;
- The valves of the compressor;
- Flow-induced pulsations in the suction piping, the discharge piping or in the bypass piping.

The objectives of the survey were:

- Reproduce the problem
- Precise its nature (frequency)
- Precise at what operating conditions it happens
- Determine origin of problem: locate source and determine source mechanism.

Since flow-induced pulsations were one of the suspected possible sources, the measurement program was for a large part related to modifications of the flow velocities in the different parts of the piping. The mass flows in each part of the system were monitored in parallel to the noise around the compressors, the pulsations in the piping, and the vibrations of the piping at selected locations. Combined with the pipe cross sections and the density variations due to operational condition, the actual gas velocities could thus be computed in each part of the system. Actual gas velocity is the key parameter for flow-induced pulsations.

The first observation was that a tonal noise was measured in the compressor building at 75% load (one cylinder double acting and the other cylinder single acting) and 100% load (both cylinders double acting), while no whistling noise was measured at 50% load. When observed, the tonal noise was characterized by a frequency between 765 Hz and 785 Hz, depending on the cases, and a second tone at double the frequency. The noise measured with two microphones close to the two cylinders of the compressor is reported for 50% load in figure 12 and for 75% in figure 13. In figure 13, it also apparent that the microphone located close to the double-acting cylinder measures higher amplitude noise than the other one. It was also measured that the total noise level around 785 Hz was the largest at 100% load. This was a first indication that the noise source was probably associated with cylinders working in double action. However, this could still be true for any of the identified possible noise-source mechanisms.
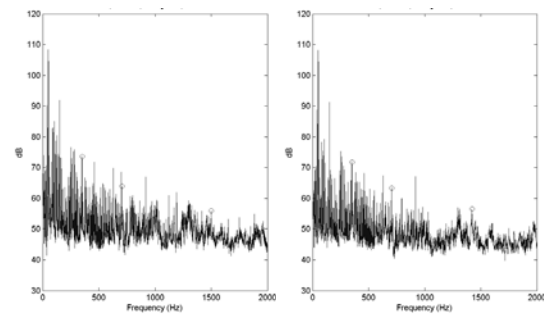
Figure 12: Noise measured by microphones close to each cylinder of the compressor in service at 50% load. Left plot: Microphone close to single-acting (SA) cylinder 1; Right plot: Microphone close to single-acting (SA) cylinder 2
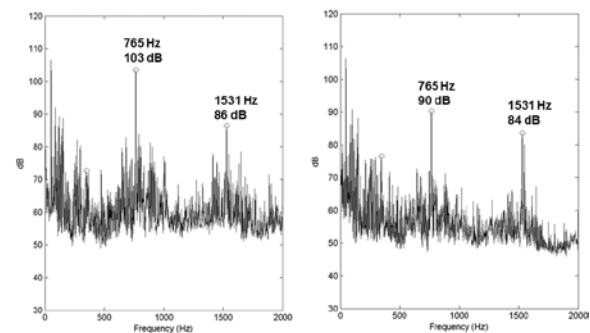
Figure 13: Noise measured by microphones close to each cylinder of the compressor in service at 75% load. Left plot: Microphone close to double-acting (DA) cylinder 1; Right plot: Microphone close to single-acting (SA) cylinder 2

Furthermore, as long as the load was 75% or 100%, variations of the suction pressure (between 50 bar and 59 bar) would not have any effect on the occurrence of the whistling. The only effect of the suction pressure was that, al lower pressures, the frequency of the tone would switch to larger frequencies.

In figure 14, the pulsations measured in the suction piping are reported for the same measurement as reported in figure 13. The spectra reported in this figure don't show large pulsations, and definitely not any peak at 765 Hz.

High-frequency radiated noise in a reciprocating compressor installation: analysis and mitigation,
Joachim Golliard, Leonard van Lier, Vasillaq Kacani; TNO - DEPARTMENT OF FLUID DYNAMICS,
LEOBERSDORFER MASCHINENFABRIK GMBH

Figure 14: In-line pulsations measured close to the inlets of suction damper during operation at 75% load. Right plot: Pulsations measured close to inlet of damper of cylinder 1 (DA); Pulsations measured close to inlet of damper of cylinder 2 (SA)

The pulsations measured close to the outlets of the discharge dampers are presented in figure 15 (50% load) and figure 16 (75% load). In both figures, large peaks are observed. At 50% load, the peak is observed at 460 Hz, while at 75% load, peaks are observed at 358 Hz and 765 Hz (and at the double frequency of 765 Hz: 1631 Hz). The 765 Hz peak at 75% load corresponds to the high-frequency noise measured around the compressors (figure 13). However, no peak is measured in the noise at 460 Hz for the 50% load (figure 12) and no peak is observed at 358 Hz in the noise measured at 75% load (figure 13). This is summarized in table 1.
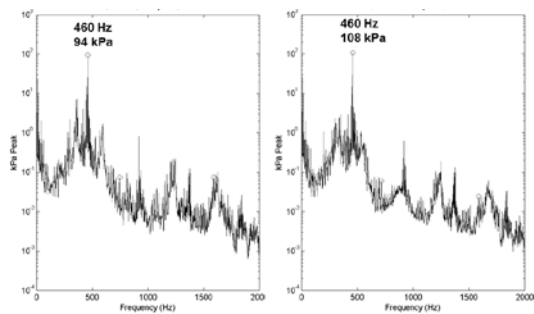
Figure 15: Pulsations measured at outlet of discharge damper at 50% load. Left plot: pressure measured at outlet of discharge damper of cylinder 1; Right plot: pressure measured at outlet of discharge damper of cylinder 2
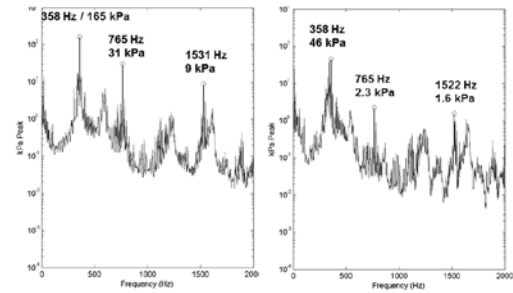
Figure 16: Pulsations measured at outlet of discharge damper at 75% load. Left plot: pressure measured at outlet of discharge damper of double-acting (DA) cylinder 1; Right plot: pressure measured at outlet of discharge damper of single-acting (SA) cylinder 2

Load	Tone frequencies	Actual velocity in discharge piping of		frequency / actual flow velocity
		cylinder 1	cylinder 2	
50%	460 Hz	19 m/s	19 m/s	24 m^{-1}
75% (high suction pressure)	358 Hz and 765 Hz	34 m/s	16 m/s	22 m^{-1} 22 m^{-1}
75% (low suction pressure)	365 Hz and 781 Hz	32 m/s	17 m/s	21 m^{-1} 24 m^{-1}
100%	785 Hz	30 m/s	29 m/s	26 m^{-1}

Table 1: Summary of the frequency of the observed tones in the spectra of pulsations measured close to the outlet of the discharge dampers
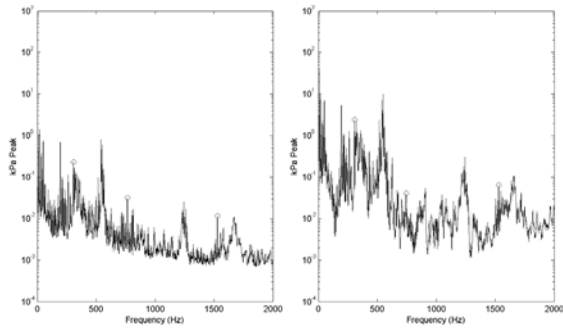
In this table, the actual flow velocity in the outlet of the discharge damper is also presented. If one considers that, for 75% load, the lower (resp. higher) frequency tone is associated with the lower-frequency (resp. higher-frequency) tone, it appears that the ratio between the tone frequency and the actual flow velocity is almost constant. This type of feature is characteristic of flow-induced whistling. The root cause was thus identified as a flow instability located in the discharge piping of each cylinder of the compressor.

However, two questions remained:
- Where were the sources exactly ?
- Why are the pulsations tones at lower frequencies (around 360 Hz and 460 Hz) not audible as noise around the compressor?

To search for the location of the sources, a Strouhal-number analysis was done. This consists in considering all the "obstacles" in the pipe (restrictions, T-joints, diffusers, …) and determine, on basis of their dimensions and of the gas velocity

High-frequency radiated noise in a reciprocating compressor installation: analysis and mitigation,
Joachim Golliard, Leonard van Lier, Vasillaq Kacani; TNO - DEPARTMENT OF FLUID DYNAMICS,
LEOBERSDORFER MASCHINENFABRIK GMBH

at that location, if a flow instability can be present there which would whistle at the same frequency as the measured tones. This requires to compute the actual flow velocity at all these points, and to know accurately the internal dimensions of the piping, restriction orifices, vessels, side branches, etc. Each of these obstacle have a different typical Strouhal number as a potential source of flow-induced pulsations. These typical Strouhal numbers are summarized in Table 2 for restriction orifices and Tee-joints.

Elements	Sr definition	Characteristic length	Characteristic flow speed	Sr value
Tee-joint	$f D_{sb} / U_{pipe}$	Diameter of side branch D_{sb}	Velocity in main pipe U_{pipe}	~ 0.5
Restriction orifice	$f t / U_{jet}$	Plate thickness t	Velocity in orifice U_{jet}	~ 0.2

Table 2: Strouhal number definition and values for sources of flow-induced pulsations at Tee-joints with grazing flow [2,3] and restriction orifices[4]

This analysis enabled to identify the restriction orifices located at the inlet of the line chokes of the discharge dampers (see Figure 8) as the source of whistling, and to eliminate all the other obstacles and restriction orifices in the discharge piping as potential sources. It appeared that the restriction orifice had been produced out of a thicker plate than normal (20 mm), which increased its whistling potentiality. The downstream edge of the orifice was not bevelled as is common practice for thicker orifice plates. This source would then couple efficiently with circumferential acoustical modes in the damper on the one side, and with acoustic modes in the downstream piping on the other side. The fact that the tones observed around 360 Hz and 460 Hz in the discharge piping was not measured as noise radiated around the compressor was attributed to the fact that the piping acts as a high pass filter, as described in VDI 3733 [1]

6 Modifications to eliminate the root cause source

Based on the analysis presented in the preceding section, it was decided to cut the line chokes close to the restriction orifices (effectively removing these). Some other pulsation reduction devices then had to be used to achieve sufficient damping of the pulsations. The two options considered for that purpose were the following:
- Reduction of the internal diameter of the line chokes, to introduce a pressure drop equivalent to the original restriction orifice, while avoiding any whistling potentiality;
- Installation of a restriction orifice at the outlet flange of the discharge damper.

The second option was chosen for ease of installation and for durability reasons. Due to the less efficient position in the piping, this restriction orifice had to have a larger pressure drop than the restriction orifice originally installed. However, since the measurements made at commissioning had provided the relation between the pulsation levels and the vibration levels, a less conservative approach could be taken for the allowable pulsation levels, and thus for the dimensioning of these orifices.

After removal of the orifices and installation of the new orifices at the outlet flanges, it was confirmed that the high-frequency noise had disappeared. Furthermore, a final field survey in November 2011 confirmed that the pulsation and vibration levels were all within allowable limits.
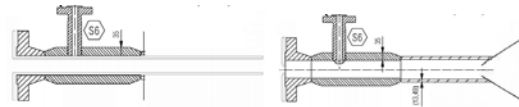
Figure 17: Modifications considered to remove orifice responsible for noise generation and to replace it by another pulsation-reduction device (below left: line choke with reduced internal diameter; below right: orifice plate at outlet flange)

7 Conclusions

- Issues with whistling orifices occur seldom, but the consequences (radiated noise) can pose a serious issue with respect to noise emission to personnel and environment.
- Reproducing the noise issue and finding the exact location of the source is not easy: this requires detailed measurement techniques, a well-controlled setting of operational parameters and numerical analysis.
- Correlating the measured in-line pulsations with noise levels and with controlled variation in the operational parameters, enabled a robust root cause analysis.
- The noise originated from flow instability in the orifice at the inlet of the line choke in the discharge dampers.
- At the orifice, a sharp contraction in flow occurs. Furthermore, the local flow velocities in the orifice are high. In addition, the applied orifice design has a very large thickness of 20mm.
- Coupling between the flow instability in the orifice with higher-order acoustic resonances (circumferential modes in the damper) result in strong tonal noise generation.

High-frequency radiated noise in a reciprocating compressor installation: analysis and mitigation,
Joachim Golliard, Leonard van Lier, Vasillaq Kacani; TNO - DEPARTMENT OF FLUID DYNAMICS,
LEOBERSDORFER MASCHINENFABRIK GMBH

- Based on the root-cause analysis, efficient options for mitigation measures have been proposed.
- The chosen approach was to remove the orifice from the line choke and to add an orifice at the damper flange instead. This location is less effective to suppress compressor pulsations, and subsequently, a high pressure loss is required.
- The pulsation analysis was updated with the final proposed layout and acceptable pulsation levels were found.
- A final field survey confirmed that the noise issue had disappeared, while pulsation and vibrations were within allowable levels.

8   Acknowledgement

9   References

[1] VDI 3733, Noise at pipes, 1996

[2] Tonon, D., Hirschberg, A., Golliard, J. and Ziada, S., Aeroacoustics of pipe systems with closed side branches, International Journal of Aeroacoustics, volume 10, number 2&3, 2011.

[3] Belfroid, S.P.C., Peters, M.C.A.M., Schiferli, W., Flow-induced pulsations caused by split flow in T-branch connections. 6th FSI, AE and FIV Symposium, Vancouver, Canada, 2006.

[4] P. Testud, Y. Aurégan, P. Moussou, and A. Hirschberg. The whistling potentiality of an orifice in a confined flow using an energetic criterion. Journal of Sound and Vibration, 325, 2009.

[5] NACE, Petroleum and natural gas industries – Materials for use in H_2S-containing environments in oil and gas production, 2010.

Vibrations at natural gas storage facilities during combined operation of reciprocating and turbo compressors

by

Dr.-Ing. Jan Steinhausen

KÖTTER Consulting Engineers GmbH & Co. KG

Bonifatiusstraße 400, 48432 Rheine, Germany

jan.steinhausen@koetter-consulting.com

8th Conference of the EFRC
September 27th / 28th, 2012, Düsseldorf

Abstract:

The current trend for constructing new and revamping existing underground natural gas storage facilities shows that the combined operation of reciprocating and turbo compressors is occurring more frequently. As a part of engineering during the planning phase, exceeding gas pulsations and resulting mechanical piping vibrations should be avoided by theoretical computations. This paper will give an overview of an approach for a procedure when both compressor types are combined. Usually, the theoretical approach has to meet different requirements for each compressor type. It is a well known fact that reciprocating compressors can sometimes cause significant gas pulsations in the connected piping. But what are the possible consequences of these for a turbo compressor that is operated at the same time? The specific aspects due to the combined operation of reciprocating and turbo compressors are discussed.

Vibrations at natural gas storage facilities during combined operation of reciprocating and turbo compressors,
Dr.-Ing. Jan Steinhausen; KÖTTER CONSULTING ENGINEERS GMBH & CO. KG

Due to the situation on the gas market, the technical demands on the equipment for the operation of natural gas storage facilities have increased in the last years. High flexibility is required, especially regarding the amount of natural gas to be stored and withdrawn (thus volume flow) at different pressure ratios. In the recent years, it can be observed that the concept of reciprocating and turbo compressors operating in parallel is being pursued more often, when new storage facilities are constructed (see figure 1) or existing ones are extended and/or revamped. It is a well known fact that reciprocating compressors can sometimes cause significant gas pulsations in the connected piping. But what are the possible consequences of these for a turbo compressor that is operated at the same time?

Figure 1: Construction of a new natural gas storage facility

A so-called "pulsation study" is often performed for new facilities with reciprocating compressors. Using theoretical models, the expected pulsation level due to the oscillating compressor is predicted. Being performed during the planning phase, the aim of the pulsation study is to avoid high gas pulsations and accordingly mechanical vibrations of the piping caused by pulsations. At the heart of the study is the acoustic modelling of the pulsation source itself, i.e. the cylinders of the compressor. Based on technical drawings of the reciprocating compressor, acoustic models are built for the piston, the cylinder, the valves and the gas passages. Subsequently, models are made for the piping, the dampers, the coolers, the gate valves etc. The API standard 618 (Reciprocating Compressors for Petroleum, Chemical and Gas Industry Services, API standard 618, 5th edition, 2007) describes the way and the extents of pulsation studies and gives guidelines for allowable pressure pulsations. Typically, the gas pulsations occur at the rotational frequency of the compressor (typically 200 rpm up to 1,000 rpm) and multiples of this (the higher harmonics).

The situation is different for studies for turbo compressors. The compressor's rotational frequency and blade passage frequency (rotational frequency x number of blades) does not play an important role

in the occurrence of piping vibrations. Firstly, the excitation frequency range lies distinctly higher, with rotational speeds between 6,000 rpm and 15,000 rpm. Secondly, because of the different mode of operation of the turbo compressor, the pulsation amplitudes are small compared to those caused by a reciprocating compressor. During normal operation of turbo compressor facilities, undesired pressure pulsations in the piping are primarily caused by flow induced excitation. They are mainly caused by vortex shedding at T-joints, where a non-flown through side branch is "whistled". The vortex shedding frequency depends on the geometry and - among others - on the flow velocity. When the frequency of the vortex shedding is the same as the acoustic natural frequency of the side branch (coincidence), high gas pulsations can occur (acoustic resonances). Especial critical are those acoustic resonances that occur close to structural natural frequencies of the piping system.

Summing up, the pulsation studies for both different types of machines reciprocating and centrifugal compressors follow a different approach. But when in a new or in an extended facility both compressor types are implemented, it is obvious to connect both approaches. Initially, both types of pulsation study are performed more or less separately. That means: 1. Investigating the gas pulsations caused by the operation of the reciprocating compressor and 2. Investigating the flow induced excitation that occurs during operation of the turbo compressor.

For this, the complete piping system on the suction and discharge side of the compressor is considered. Thus, also the pressure pulsations caused by the reciprocating compressors at the connecting flanges of the turbo compressors are calculated. For the parallel operation with a turbo compressor, whose steady operating point lies close to the surge line, these pressure pulsations should not exceed this limit. As a conservative approach for an allowable pulsation level at such an operating point, the margin can be used that exists between operating point and surge line for steady operation of the turbo compressor, see figure 2.

Vibrations at natural gas storage facilities during combined operation of reciprocating and turbo compressors,
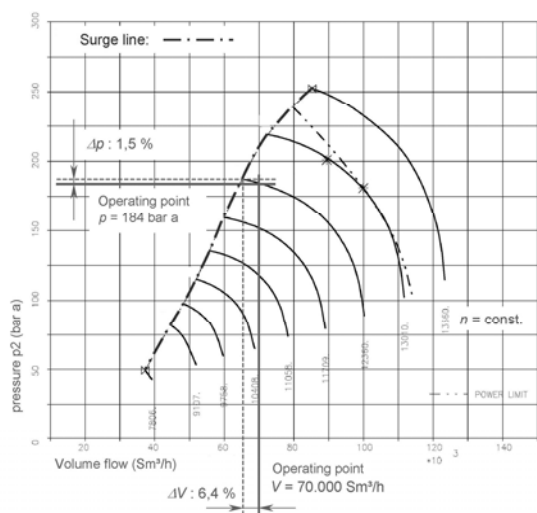*Dr.-Ing. Jan Steinhausen;* KÖTTER CONSULTING ENGINEERS GMBH & CO. KG

Figure 2: Performance map of a turbo compressor with an operating point close to the surge line – Example of assigning allowable pressure and volume flow pulsations

Figure 3: Structural-mechanical model (FEM) of a piping system near a turbo compressor – the arrows indicate the exciting gas pulsation forces

For natural gas storage facilities, which shall be extended, it is a fundamental advantage to investigate the pulsation and vibration levels of the status quo by measurements in the non extended plant before performing the calculations. Independent if the extension involves a reciprocating or centrifugal compressor. Because firstly, measurements can reveal sections with critical vibration levels. The second reason is that measurements can validate and tune the acoustic modelling for the existing facility. With this, reliable statements can be made for the extended facility. In the past, the combination of measurements and modelling has shown to be beneficial especially for older facilities. Uncertainties in the modelling due to lacking information of the older facility could thus be compensated.

The structural piping layout close to a turbo compressor is often relatively flexible, e.g. when the connecting pipeline "descends from above" towards the compressor. Such a pipeline section is relatively susceptible for excitation by pressure pulsations from a parallel operating reciprocating compressor. Therefore, these sections are generally examined more closely in the structural-mechanical calculations of a pulsation study. For the assessment of vibrations due to gas pulsations, the acoustic forces at e.g. bends and T-joints, which are calculated in the acoustic study, are used as excitation (input) for the structural mechanical model, see figure 3.

In case the structural mechanical calculations show that the allowable guidelines (for vibration velocity, vibration displacement or the dynamic part of the stresses in the material) are exceeded, the guidance of the piping can be modified, e.g. by adding a support or by increasing the stiffness of an already existing support etc.

The experience with pressure pulsation and piping vibration measurements after start-up of natural gas storage facilities shows that the parallel operation of reciprocating and turbo compressors can be in principle trouble-free (from the vibration-technical point of view). However, it remains recommendable to carry out a pulsation study during the planning phase, which is adapted to the requirements for both machine types and if necessary to carry out measurements upfront.

Impact of pulsations on flow metering accuracy: identification and remedies

Leonard van Lier

TNO, Department of Fluid Dynamics

Delft, The Netherlands

leonard.vanlier@tno.nl

Rob Crena de Iongh

Nederlandse Aardolie Maatschappij B.V.

Assen, The Netherlands

Rob.crenadeiongh@shell.com

8th Conference of the EFRC
September 27th / 28th, 2012, Düsseldorf

Abstract:

In the compressor installation of the NAM (Nederlandse Aardolie Maatschappij BV, a 50/50 Shell/ExxonMobil joint venture) at Kootstertille, natural gas is produced from a depleting field. Two 2-stage reciprocating compressors are used to compress the gas to grid pressure. Due to the depletion of the field, the actual flow has collapsed to approximately 10% of the initial capacity. The initial design of the restriction orifice plates in the system is not adequate anymore for the strongly declined flow. As a consequence, pulsation issues could be expected. Indeed, at specific compressor speeds, vibrations of the discharge piping, near the turbine flow meter are observed during annual (visual) inspection. Concern is raised by the end user, if the flow meter accuracy may suffer from pulsation and vibrations.

To investigate the impact of compressor pulsations on the flow meter accuracy, a field survey was undertaken, measuring pulsations and vibrations over the full speed range of the compressors. The pressure pulsation levels were compared with a PULSIM simulation model and a good correspondence was found. Next, the simulation model was used to predict the flow pulsations near the flow meter. Information from the manufacturer and the ISO/TR 3313 standard was applied to quantify the additional measurement error due to the pulsating flow. Even though the pressure pulsation levels near the flow meter were negligibly low, the flow pulsations lead to a significant error (up to 4%) for specific compressor speeds.

To avoid issues with the accuracy of the flow meter, a new design of the restriction orifices was recommended, using the simulation model. With the new restriction orifices, the flow metering error is reduced to acceptable levels. In addition, the pulsation and vibration levels near the compressors (that were significant) are also reduced with the new orifice design.

Impact of pulsations on flow metering accuracy: identification and remedies, *Leonard van Lier, Rob Crena de Iongh;* TNO - DEPARTMENT OF FLUID DYNAMICS, NEDERLANDSE AARDOLIEMAATSCHAPPIJ BV

1   Introduction

Reciprocating compressors are reliable and robust compressors, that can be operated over a very wide range of applications. However, a reciprocating compressor is an intrinsic source of pulsations. These pulsations are periodic fluctuations in pressure and flow. Due to acoustic resonances in the piping, these pulsations can be amplified. Strong pulsations can cause many issues in process installations. For example, pressure pulsations cause dynamic shaking forces on the piping. When in-line pulsation frequencies coincide with mechanical resonance frequencies in the piping structure, strong vibrations may occur. High cyclic stresses and even fatigue failure may be the ultimate consequence. Furthermore, strong pressure pulsations can have a negative impact on the compressor's performance and may lead to issues with compressor valves. In case of low flows (for example in depleting gas fields), the dynamic fluctuation of the flow can lead to flow reversal. When flow reversal occurs near a non-return valve, 'hammering' of the valve may lead to reduced lifetime.

The API 618 standard addresses these issues and stipulates a strategy to mitigate any adverse effects due to pulsations in the design phase of a project [1]. For critical systems (high power, high pressure) the most robust design approach shall be applied, including:

- A pulsation analysis, ensuring an optimal design of pulsation dampers, piping and orifice plates.

- A mechanical response analysis, ensuring an optimal design of the supporting.

- A dynamic compressor valve analysis, ensuring an optimal design of the compressor valves.

- A compressor manifold analysis, ensuring an optimal mechanical design of the compressor, for example the crank shaft balancing, frame construction, damper- and cylinder supports.

In the latest revision of the API 618 standard, special attention is paid also to the impact of pulsations on the accuracy of flow meters. The impact of pulsations on flow meters may be very significant, but often remains unnoticed in the field.

This paper addresses the impact of pulsations on flow metering equipment. First a short introduction is given on the generation and propagation of pulsations. Also the relation between pressure pulsations and flow pulsations is discussed. Next, the impact of flow pulsations on various types of flow meters is discussed. Finally, we present an example case, in which flow pulsations caused a significant degradation of the flow meter accuracy. A combined approach of measurements and simulations was applied, in order to quantify the error in the flow meter due to pulsation, and to evaluate recommendations to improve the flow meter's accuracy.

2   Generation and propagation of pulsations

In reciprocating compressors, the process gas is pressurized by periodic piston movement. The piston is driven by for example an electric driver or a gas engine. Due to the reciprocating action of the piston and the compressor valves, a 'discontinuous' or pulsating flow is obtained.
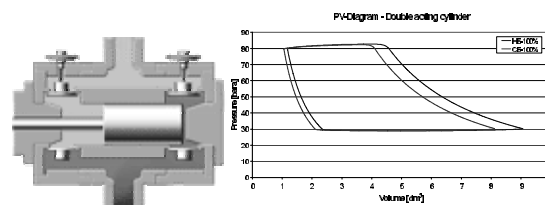
Figure 1: Compressor cylinder (left) and PV-diagram (right)

Figure 1 shows a typical compressor cylinder. Due to the periodic piston movement, the gas in the cylinder is compressed. Due to the compressor valves' action, the inflow from the suction side and the exhaust into the discharge piping is effectuated. The thermodynamic effects during intake, compression and exhaust are typically represented in a P-V-diagram. In case of a single-acting cylinder, 1 compression stroke occurs per revolution. In case of a double-acting cylinder, 2 compression strokes occur during one crank revolution. The head-end stroke and crank-end stroke are generally (slightly) different, due to the presence of the piston rod on the crank-end side and the different clearances.

Figure 2 illustrates the typical flow pulses on the suction side and discharge side, for a double-acting cylinder.

Impact of pulsations on flow metering accuracy: identification and remedies, *Leonard van Lier, Rob Crena de Iongh;* TNO - DEPARTMENT OF FLUID DYNAMICS, NEDERLANDSE AARDOLIEMAATSCHAPPIJ BV

Figure 2: Flow pulses of a double-acting cylinder

The pulse at the suction side are out-of-phase with the pulses at the discharge side. The suction pulses are broader and of lower amplitude, while the discharge pulses are smaller and of higher amplitude. The area below the curves is the same, due to mass conservation. The frequency spectrum of the pulses in figure 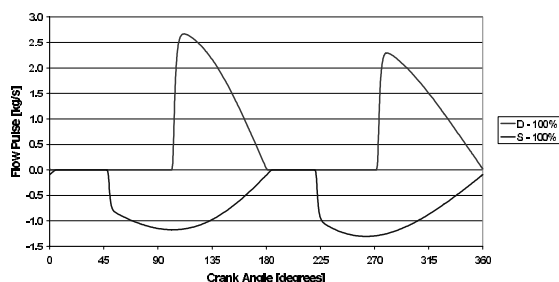2 are dominated by the second harmonic of the compressor speed. Also the higher, even harmonics (4th, 6th, 8th …) will be identified in the spectrum. Note that the head-end and crank-end pulses are not identical, due to differences in clearance and the piston rod. Therefore, also the odd harmonics (1st, 3rd, 5th, …) will be noticeable in the frequency spectrum.

Note that pulsations occur at both discharge side and suction side. It is often wrongly concluded that pulsations are generated at the discharge side only.

The pulsations propagate through the piping as pressure waves, at the speed of sound. The speed of sound depends primarily on the composition and temperature of the process gas.

To reduce the transfer of pulsations from the compressor to the process piping, a careful design of the pulsation dampers is mandatory. An analysis of the performance of the pulsation dampers ("damper check") is the first step in a pulsation analysis, according to the API 618 standard. An ideal pulsation damper has and optimal balance between reduced transfer of pulsations, low shaking forces on the damper and minimal pressure loss. Based on the specific project requirements, the damper design may range from an empty volume bottle to a complex manifold damper, including baffle plates, chokes, intruded pipes and perforated plates.

Damping mechanisms reduce the amplitude of the pressure waves, while traveling in the piping. The damping of pressure pulsations in the piping is generally low. Thus, pulsation issues may arise at remote distances from the pulsation source (compressor). Therefore, a careful analysis of the whole piping system is required.

Pressure waves will reflect on discontinuities in the piping, for example at a change in cross section of a pipe (pulsation damper) or at a change in temperature (cooler). Due to the reflections, a superposition of upstream and downstream travelling pressure waves will occur. Due to this superposition, a strong amplification of the pulsations will occur, under specific conditions: a phenomenon known as *acoustic resonance*. Upon acoustic resonance a so-called standing wave will develop, where the maxima and minima in pulsation amplitude depend on the position in the piping. Depending on the damping, the amplification upon resonance can be factor 10-20 in the main piping, carrying flow. In closed side branches, without mean flow, the amplification due to acoustic resonance can be even more spectacular (factor 100). Obviously, upon acoustic resonance, high shaking forces may act on the piping. To reduce the amplitude of the standing wave in resonance conditions, frequently orifice plates are applied. Orifice plates suppress the resonant amplification of the pulsations with a mild pressure loss. Goal of an API 618 pulsation analysis is to find the optimal location for orifice plates and the best balance between reduction of pulsations and pressure loss.

3 Pressure pulsations and flow pulsations

A pulsating flow induces also a pulsation pressure, which is generally a small disturbance on the mean pressure. The relation between the flow and pressure pulsations is governed by the conservation laws for mass, momentum and energy and the boundary conditions of the system. In resonance conditions, the locations of maximum pressure pulsations coincide with the locations of minimum flow pulsations. This alternating effect is illustrated in figure 3: the nodes in the pressure coincide with the anti-nodes in the flow and vice versa.
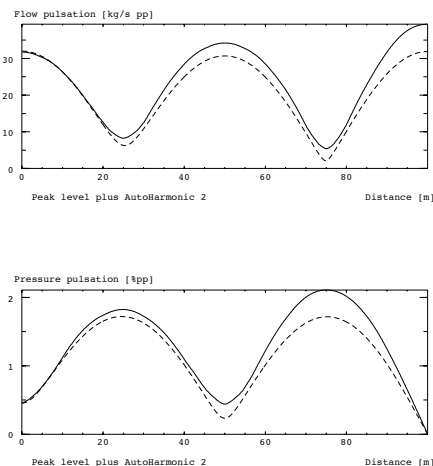

Figure 3: Standing wave patterns for flow pulsations (top) and pressure pulsations (bottom)

Impact of pulsations on flow metering accuracy: identification and remedies, *Leonard van Lier, Rob Crena de Iongh;* TNO - DEPARTMENT OF FLUID DYNAMICS, NEDERLANDSE AARDOLIEMAATSCHAPPIJ BV

Another striking difference between pressure and flow pulsations is the ratio of the fluctuation with respect to the mean quantity. In general, pressure pulsations are a relatively small disturbance on the mean pressure: typically a few percent. However, flow pulsations may be substantial in comparison with the mean flow. Especially in systems with a small mean flow, such as depleting gas fields, the fluctuation may be in the order of the mean flow, or even larger. As a consequence, a periodic backflow may occur, occurring at a typical frequency of a few Hz. Issues caused by pressure pulsations, such as pulsation-induced vibrations, are typically judged by the pressure pulsation *amplitude*. However, issues caused by flow pulsations, such as check valve hammering and flow meter errors, are judged by the ratio of the flow pulsation and the mean flow.

4   Impact of flow pulsations

The 5th edition of the API 618 standard addresses the allowable flow metering error due to pulsations in the following generic way:

- Maximum 1.00% error, for non-custody transfer meters;
- Maximum 0.125% error for custody transfer meters.

Depending on the type of flow meter, this criterion is easily violated in low-flow systems. Thus, the target of API 618 may be very ambitious, in some cases. In any case, a quantitative prediction of the measurement error due to pulsations is very important input information for system designers and operators.

Note that the error caused by pulsating flow is an *additional* metering error, to be added to other errors, that can be quantified in standard calibration procedures.

In case of the most conventional types of flow meters (differential pressure and turbine flow meters), a pulsating flow leads to a positive offset in the flow reading. That means that the flowmeter systematically indicates a flow that is higher than the actual flow. This effect can be best understood by considering a Δp flow meter. The static pressure drop over an orifice plate or venturi is measured, and from a calibration curve the static flow is determined. The relation between pressure and flow is a quadratic formula:

$$p = K \cdot \frac{1}{2} \rho U^2 ,$$

with K a constant, depending on the orifice bore.

Figure 4 illustrates the quadratic relation between pressure drop and flow. Assuming a perfectly

smooth mean flow, the relation between the observed pressure drop and the actual flow is unambiguously defined: a pressure drop of 1.2 mbar corresponds to 10 m/s, in this example.
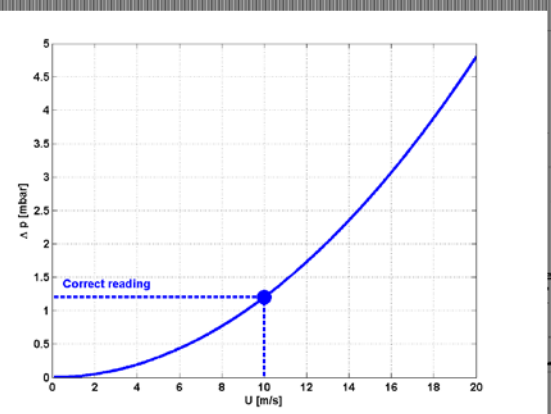
Figure 4: Pressure drop as a function of flow

Now, the flow is disturbed by a periodic fluctuation with an amplitude of 10 m/s peak-to-peak. The corresponding fluctuating in pressure drop is described by the quadratic curve and is *not symmetric* with respect to the actual pressure drop. A 'slow' differential pressure sensor yields the time-average value of the maximum and the minimum of the fluctuating pressure drop, which is *higher* than the pressure drop of the undisturbed flow. This effect is illustrated in figure 5. Now the reading of the flow is also too high, in this case by more than 10%.

Figure 5: Error due to fluctuating flow

This systematic error in differential pressure flow meters is commonly referred to as square-root-error E_T, and is described in the ISO/TR 3313 standard [2]:

$$E_T = \sqrt{1 + \left(\frac{U_{RMS}}{U_{mean}} \right)^2} - 1$$

Impact of pulsations on flow metering accuracy: identification and remedies, *Leonard van Lier, Rob Crena de Iongh;* TNO - DEPARTMENT OF FLUID DYNAMICS, NEDERLANDSE AARDOLIEMAATSCHAPPIJ BV
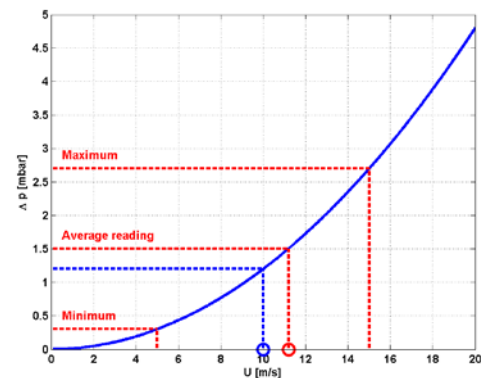
Note that, in general, a differential pressure sensor responds to the RMS values of the fluctuating pressure signal, instead of to the peak value.

Note that this simple relation for the square-root error is only valid for purely harmonic fluctuations. In case the pulsations are not exactly sinusoidal, no simple analytical relations are available to quantify the effect of pulsations on the measurement error.

Also other types of flow metering devices may suffer from unsteady flow conditions. For example, turbine flow meters have different response (due to rotor inertia) to accelerating and decelerating flow. Similar formulas (but more complex) can be derived for the measurement error of turbine flow meters. The following table summarizes the main effects, for various types of flow meters. It also includes some references to applicable international standards:

Type	Error	Standard	Standard Error	Criterion
Differential pressure: orifice, nozzle, venture	Square-root, gauge line	ISO 5167 (API 2530)	ISO/TR 3313	U'<5% RMS
Turbine	Inertia of rotor and fluid	ISO 9951	ISO/TR 3313	U'<3.5% RMS
Ultrasonic	Aliasing	ISO/TR 12765	-	-
Vortex	Lock-in	ISO/TR 12764	ISO/TR 3313	U'<3% RMS
Coriolis	Lock-in	ISO 10790	-	-

Besides the direct influence of the pulsating flow, also pulsation-induced pipe vibrations may disturb the flow meter. Vortex flow meters are the most notorious, because the vortex shedding frequency (which is a direct measure for the flow speed) is greatly influenced by vibrations. For other flow meters, the effect of vibrations is presumably less relevant.

Reciprocating compressors are not the only source of pulsations. Other types of pulsation sources can disturb the operation of flow metering equipment as well. Reference [3] gives various examples of flow metering disturbance by turbo-compressors (pulsations at the blade-passing frequency of the impellers) and flow-induced pulsations at closed T-branches. Finally, broadband ultrasonic noise due to highly turbulent flow through a control valve can disturb ultrasonic flow meters.

5 Identification of high flow pulsations

One of the major obstacles to resolve potential issues due to flow pulsations is the difficulty to identify excessive flow pulsations in the field.

Flow pulsations can be significant, even if the pressure pulsations are low. As a consequence, issues with flow pulsations are not easily identified in the field, because piping vibrations (caused by pressure pulsations) may be very low.

Simple sensors to directly measure the flow pulsations only exist in laboratory environment. In principle, flow pulsations could be measured by applying the so-called "2-microphone method" [4]. However, in industrial applications, this measurement technique is highly impractical, because a large number of sensors at prescribed locations is required, to be able to resolve the flow pulsations over given frequency range.

When the amplitude of the flow pulsations is such, that flow reversal occurs, it may be noticed by the operator that non-return valves start hammering. Thus, also concern may be raised on the impact of flow pulsations on the flow meter's accuracy. Unfortunately, the flow meter's accuracy starts to degrade at relatively low flow pulsation levels, well before flow reversal and non-return valve hammering occurs.

Furthermore, in gradually depleting conditions, the slowly growing error in the reading of the measurement devices remains generally unnoticed by the operator.

Finally, the periodic calibration procedures of the flow meters do not highlight potential issues either. In the laboratory, during 'standard' calibration procedures, the flow meter is not evaluated under pulsating conditions. Furthermore, it is very difficult to reproduce with an individual calibration test in a laboratory, the real system's pulsations as observed in the field.

To enhance the awareness and allow for early identification, we propose that the potential impact of pulsations shall be an explicit point of attention in any pulsation analysis of gas systems that may decline over time, including the near-future and far-future operating conditions.

If problems are suspected in the field, we recommend to verify with measurements the root cause of the pulsations. In some cases this may be a reciprocating compressor or a plunger pump. In other cases, in metering streets the piping layout

Impact of pulsations on flow metering accuracy: identification and remedies, *Leonard van Lier, Rob Crena de Iongh;* TNO - DEPARTMENT OF FLUID DYNAMICS, NEDERLANDSE AARDOLIEMAATSCHAPPIJ BV

contains typically many closed side branches (valve manifold). Such a valve manifold is liable to Flow-Induced Pulsations, due to vortex shedding at the inlet of the side branch in combination with acoustic resonances in the side branch. Also the most notorious configuration of a double side branch, separated by 2 times the side branch length can exist. This tandem side-branch configuration may cause excessive Flow-Induced Pulsations, see figure 6 [5]. Of course, identification of the Root Cause (reciprocating compressor, turbo compressor, flow-induced pulsations, valve noise etcetera) is of utmost importance for the design of effective solutions.
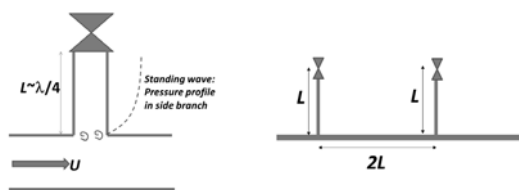

Figure 6: Flow-induced pulsations due to vortex shedding at T-joint (left) and tandem configuration of side branches (right)

6   Strategies to reduce flow pulsations

A trivial recommendation is to avoid depleting conditions. Increasing the flow will limit the negative effects for two reasons: (1) the mean flow increases so the ratio of pulsating flow to mean flow decreases, (2) the efficiency of orifice plates, pipe wall friction and other damping effects will increase with increasing flow.

Relocation of the flow meter to a location in the pipe system with minimal flow pulsations is in theory a valid approach. However, in reality, one has only very limited flexibility to relocate flow meters. Furthermore, the location of the minima in the flow pulsation amplitude is generally ill-defined. For different frequencies, the minima occur at different locations. Therefore, especially in systems with a Variable Speed Drive System (VSDS) and/or variable process conditions, the overall effect of relocation will be disappointing.

An effective way to reduce flow pulsations is by introducing secondary volume bottles, in addition to the existing pulsation dampers. The additional volume has a buffering effect on the pulsations from the compressor and reduces the transfer to the piping and the flow meter. In addition, if the system between the primary and secondary bottles is well designed, a Helmholtz resonator with a sufficiently low cut-off frequency can be realized. Such a system will provide effective damping of pulsations with frequencies above the cut-off frequency.

Unfortunately, the implementation of secondary bottles is a large expenditure, that is commercially not always viable in a highly depleted gas field. Of course, it shall be robustly confirmed that indeed the pulsations from the compressor are the culprit for the flow meter disturbance. Otherwise, secondary pulsation bottles may not be effective at all.

In depleting gas installation, the original orifice plates may not be effective, due to the declined flow and the subsequently lower pressure drop. Refitting of the orifice plates is then an effective approach to reduce pulsations. The orifices are refitted with smaller bores, to obtain again an appreciable pressure drop. The refitting of the orifice plates may have a limiting effect on the system's operation flexibility. For example, when a new gas well is tied in into the installation, the pressure drop over the refitted orifices may become excessive. Special care should be taken to consider future operating scenarios and evaluate the impact on pressure loss in the system.

Modifications to the flow meter, to correct for the fluctuating conditions are not straightforward. This is only easily done, if a purely sinusoidal fluctuation is observed (which is not generally true) and when the sensor is sufficiently fast to track the fluctuating signal. Based on the maximum amplitude and the frequency of the fluctuating reading, a first-order correction could be applied. Diagnostic tools, to be operated by experienced personnel are available for field inspection. However, in industrial flow meters, the technology is not common practice yet and a robust implementation requires additional research and development.

7   Field case

In the northern part of The Netherlands a depleting gas field is operated by NAM. With declining suction pressure, additional compression is required. Two parallel 4-cylinder reciprocating compressors are installed. The compressors are identical and are operated in a 2-stage configuration (2 cylinders for each stage). The compressors have a variable compressor speed, driven by a E-motor with VSDS. With the initial flow capacity, the 2 compressors were operated in parallel (A+B). In recent years, the compressors are operated in single operation (A or B). The flow has dropped to about 10% of the initial capacity, while the design of pulsation dampers and orifice plates has remained unchanged since the initial installation.

The gas is compressed from 5 bar to approximately 63 bar discharge pressure. At the discharge side, the

Impact of pulsations on flow metering accuracy: identification and remedies, *Leonard van Lier, Rob Crena de Iongh;* TNO - DEPARTMENT OF FLUID DYNAMICS, NEDERLANDSE AARDOLIEMAATSCHAPPIJ BV

flow is passed through a turbine flow metering street.

During a visual site inspection, vibrations were observed in the pipe leading upstream of the flow metering street, presumably caused by pulsations by the reciprocating compressors. Concern was then raised about the impact of these pulsations on the accuracy of the turbine flow meter.

TNO was asked to investigate this potential issue and supply recommendations to improve, if required. The following project proposal was agreed upon:

- Field survey, measurement of pulsations and vibrations over the full speed range of the compressors.
- Pulsation analysis, using TNO's PULSIM software.

The field survey shall confirm that the pulsations are caused by the reciprocating compressors and not by another source. The measured pressure pulsation level will be compared to the allowable levels according to the API 618 standard. The measured vibrations will be compared to the EFRC guideline for allowable vibrations, and with allowable vibration levels according to the flow meter's manufacturer.

Since only pressure pulsations can be determined directly by measurements, a numerical model is needed to predict the flow pulsation levels. This is the purpose of the second step (pulsation analysis). For the numerical simulation, TNO's software tool PULSIM is used. The predicted pressure pulsation levels are compared with the measured results from the field survey. In case a satisfactory match is observed, the numerical model can be used (a) to predict the flow pulsations near the flow meter and quantify the subsequent measurement error and (b) to formulate and evaluate recommendations to reduce the flow pulsations and enhance the flow meter's accuracy.
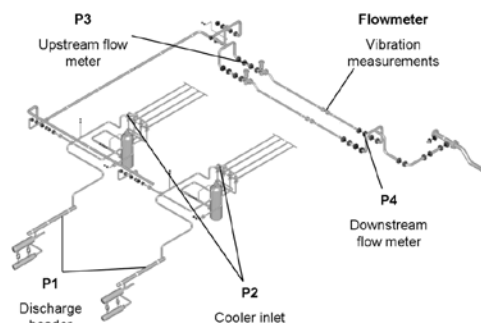

Figure 7: Simulation model with indication of field survey measurement locations

Figure 7 illustrates the simulation model. Only the discharge part of the 2nd stage, containing the flow meter, is included in the model. The compressors, the coolers and the KO drums are easily identified. Further downstream, two parallel metering streets are observed. Only one metering street is operated, the other being blocked-in. Upstream of the flow meter, a filter is present. Figure 7 contains also the locations for pressure pulsation measurements, applied during the field survey. Pulsations are measured near the compressors, near the KO drums and upstream/downstream of the flow meter.

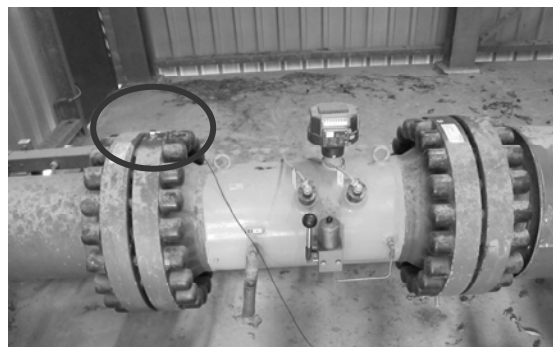*Figure 8: Parallel flow metering streets with filters and flow meter enclosure*

Figure 9: Turbine flow meter with accelerometer

The compressors and the flow meter are separated by a pulsation damper, a discharge header and a large KO drum. Normally, no strong pulsations are expected close to the flow meters. This is confirmed by measurement of the pressure pulsations: near the flow meter the pressure pulsations are less than 10% of the allowable level according to API 618. Also the vibrations on the flow meter are low (< 1mm/s RMS).

Spectral analysis of the pulsations confirmed that the pulsations are indeed originating from the reciprocating compressors. Furthermore, the dominant harmonic component in the spectrum (1st harmonic) suggested that the system is running at part load: 50% load by unloading of suction valves at the cylinder head ends. However, the DCS suggested that the compressors are running at full load. More detailed inspection confirmed that the

Impact of pulsations on flow metering accuracy: identification and remedies, *Leonard van Lier, Rob Crena de Iongh;* TNO - DEPARTMENT OF FLUID DYNAMICS, NEDERLANDSE AARDOLIEMAATSCHAPPIJ BV

solenoids on the actuators are not connected and that the valves are disabled.

The pulsation levels in the system depend strongly on the compressor speed. The full speed range allowed by the VSDS was investigated: 181-357 rpm (during normal operation, the system is operated at a narrower speed range), see figure 10.
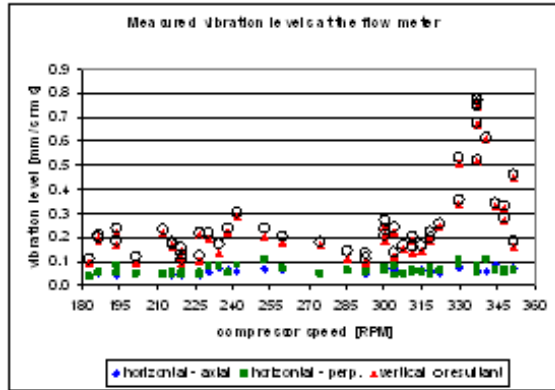

Figure 10: Vibration levels on flow meter as a function of compressor speed

The conditions investigated during the field survey were also studied with the simulation model. The results for the pressure pulsations show a satisfactory correspondence, both in terms of amplitude and dependence on the compressor speed. No 'adjustment' or calibration of input parameters was needed in the simulations to obtain a good match. Typical results are illustrated in figure 11 and 12.

With this satisfactory correspondence between measurements and simulations, the numerical model can be used to predict the flow pulsations near the flow meter.
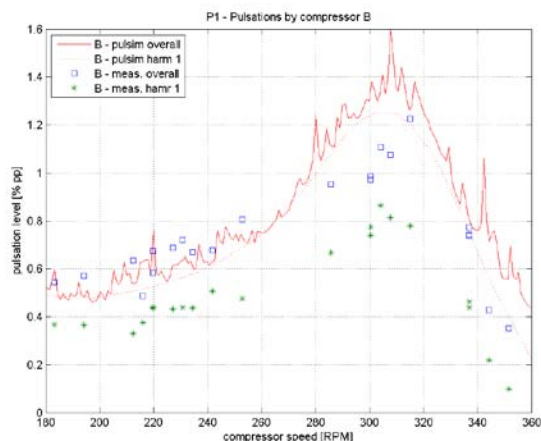

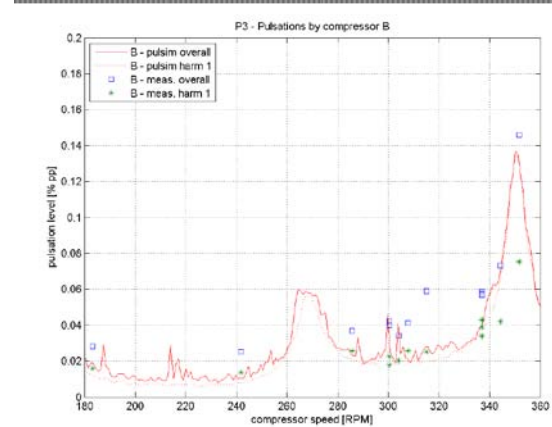*Figure 11: Measured and simulated pressure pulsation levels near the compressors*

Figure 12: Measured and simulated pressure pulsation levels near the flow meter

The predicted flow pulsations near the flow meter are shown in figure 13.
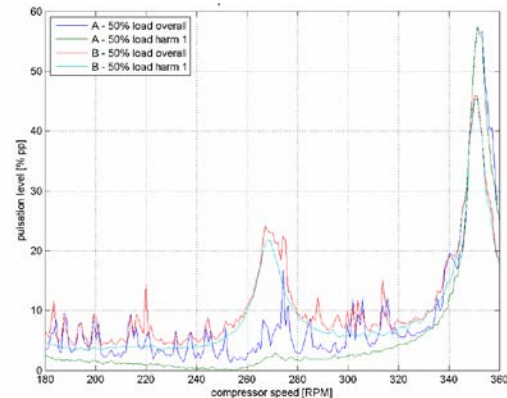

Figure 13: Simulated flow pulsation levels near the flow meter: contribution for compressors A and B

The flow pulsation levels are significant: more than 50% peak-to-peak, of the mean flow. Furthermore, the amplitude again strongly depends on the compressor speed. Finally, the flow pulsation spectrum is fully dominated by the first harmonic of the compressor speed (~5 Hz at the maximum amplitude). This observation enables the usage of simple formula's to quantify the impact of the flow pulsations on the metering accuracy. According to the manufacturer's specification, the following relation is applicable for the error due to flow pulsations E_Q. This relation is consistent with the more complex relation, according to ISO/TR 3313:

$$E_Q = \frac{1}{2} I^2,$$

with $I = \dfrac{\Delta Q}{Q_0}$ the ratio of (mass) flow pulsation

amplitude ΔQ to mean mass flow Q_0.

Impact of pulsations on flow metering accuracy: identification and remedies, *Leonard van Lier, Rob Crena de Iongh;* TNO - DEPARTMENT OF FLUID DYNAMICS, NEDERLANDSE AARDOLIEMAATSCHAPPIJ BV

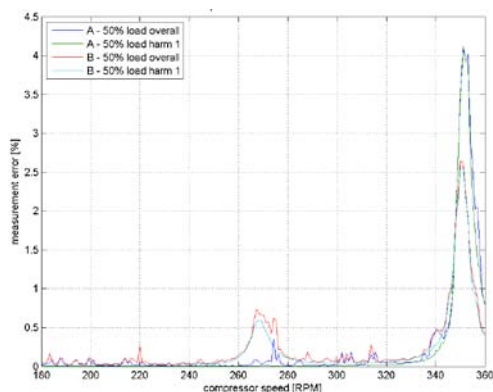The calculated flow metering error is shown in figure 14.

Figure 14: Calculated flow meter error E_Q due to pulsations from compressors A and B

The maximum calculated error is 4%, occurring at 350 rpm. This speed is not within the normal operation range of the system. However, also at lower speeds, an error of 0.5% is calculated. Therefore, recommendations to reduce the measurement error have been evaluated, using the simulation model.

In the existing system, restriction orifice plates are installed at the line connection of the 2nd stage discharge pulsation dampers.
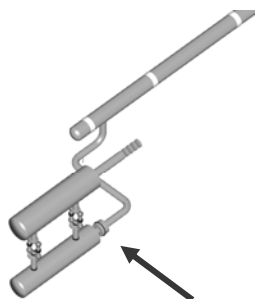

Figure 15: Restriction orifice plate at the line connection of 2nd stage discharge damper

However, due to the depleted conditions, the pressure loss over the orifices, at 50% load conditions, has dropped to 0.03%. To increase the performance of the orifices, a new design with a reduced bore was suggested. The bore was optimized, yielding a pressure drop of approximately 1%. These modified orifices bores were evaluated with the PULSIM simulation model, and proved to be very effective. The metering error in the modified layout is well below 0.1% over the full range of compressor speeds.

8   Conclusions

- Pulsating flow may result in a systematic error in the reading of flow meters.
- The occurrence of pulsating flow is easily overlooked in practical systems: even when pressure pulsations are low, flow pulsations may still be considerable. This is especially critical in low-flow conditions, such as depleting gas fields.
- Reliable simulation tools exist to identify issues with degraded metering accuracy due to pulsating flow, in an early stage of the design.
- These simulation tools shall be applied during the design stage to identify and mitigate pulsation issues with flow meters, for near-future and far-future operating conditions of the system.
- For operational systems, a combination of measurements and simulations proves to be a reliable approach to identify flow pulsations.
- Based on information from the manufacturer or from industrial standards, the metering error can be quantified for many types of flow meters.
- The simulation models can also be fruitfully used to evaluate modifications to improve the flow meter's accuracy.

9   References

[1] API 618 5th edition, "Reciprocating Compressors for Petroleum, Chemical, and Gas Industry Services", December 2007.

[2] ISO/TR 3313 Measurement of fluid flow in closed conduits – Guidelines of the effects of flow pulsations on flow-measurement instruments, ISO Technical Report, Third edition, 1998.

[3] E. van Bokhorst and M.C.A.M. Peters, "Optimization of flow measurements in a pulsating flow – experience from field measurements", 19th International North Sea Flow Measurement Workshop, 22-25 October 2001, Kristiansund, Norway. [3] E. van Bokhorst and M.C.A.M. Peters, "Optimization of flow measurements in a pulsating flow – experience from field measurements", 19th International North Sea Flow Measurement Workshop, 22-25 October 2001, Kristiansund, Norway.

Impact of pulsations on flow metering accuracy: identification and remedies, *Leonard van Lier, Rob Crena de Iongh;* TNO - DEPARTMENT OF FLUID DYNAMICS, NEDERLANDSE AARDOLIEMAATSCHAPPIJ BV

[4] M. Åbom & H. Bodén: "Error Analysis of two-microphone measurements in ducts with flow", Journal of the Acoustical Society of America (83), p. 2429-2438, 1988.

[5] M.C.A.M. Peters, A. Hirschberg, J. Bruggeman, *et al*: "High amplitude vortex-induced pulsations in a gas transport system", Journal of Sound and Vibration 184(2), p. 343-368, 1995.

8th Conference of the EFRC
September 27th / 28th, 2012, Düsseldorf

EFRC

EUROPEAN FORUM
for RECIPROCATING
COMPRESSORS

Uncut Ring Technology
for Compressor Packing

by:

Martin, Craig

Applications Engineering Supervisor

Cook Compression

Jeffersonville, Indiana

USA

cmartin@cookcompression.com

8th Conference of the EFRC
September 27th / 28th, 2012, Düsseldorf

Abstract:

Traditional compressor rod packing utilizes segmented rod rings held together with a garter spring. Most packing arrangements are based on the "BT" pair of a radial-cut ring pinned to a step-tangent-cut ring. Segmental packing has gaps that allow the rings to float and to self-adjust. This allows them to seal well even as they wear, and has worked well in most applications for many years. However, there are disadvantages inherent in their fundamental design.

The "BT" ring is always in contact with the rod and is pressure-loaded against the rod, such that significant frictional heat is generated within the packing. This frictional heat raises the temperature of the rod and of the packing rings. Because PTFE and PEEK materials exhibit wear rates that increase as a function of temperature, this frictional heat causes accelerated packing ring wear. As the elements that contribute to this friction become more severe, the wear rate of the packing increases. These elements include gas temperature, pressure, speed and lubrication. With the increasing demand for non-lubricated packing, this is becoming a more critical issue.

Uncut Ring Technology offers a solution to the problem of rapid packing wear. This solution adds two rings to the "BT" pair that seal in a different manner. These added backup rings have clearance over the rod until increasing gas pressure causes the rings to sequentially close down on the rod. This results in a sharing of the pressure load between the rings in the groove, with an overall reduction in the frictional load.

The paper will show that laboratory trials and extensive field testing have exhibited marked decreases in piston rod temperatures with this packing ring style. This in turn results in longer service times and improved reliability. Furthermore, gas leakage is reduced significantly. These advantages will be demonstrated with supporting experimental data and case studies. The potential benefits are significant, especially considering trends toward higher pressures and faster speeds, particularly in non-lube operation.

1   Introduction

As customers seek to do more with their equipment, operating conditions of reciprocating compressor packing are becoming more aggressive. Piston speeds are increased in order to improve capacity; pressures are escalated due to process demands, and more and more users are choosing to run with no packing or cylinder lubrication. These trends make it more and more difficult to achieve good packing reliability.

Increased pressures and speeds tend to impact the packing by increasing frictional heat generation from the rod rings. Unless this additional heat is removed by water cooling or other means, the end result is that packing runs hotter. Unfortunately, wear rates of plastics are proportional to a power of the operating temperature, meaning that higher packing temperatures mean shorter packing life.

Much research has been dedicated to packing materials, with the goal of improving the frictional properties of rod rings. While this work is critical and has done much to improve packing reliabilities, it is also prudent to address the mechanical design of the rod rings. For over 100 years, most packing designs have utilized tangent-cut rings or radial-cut/butt-tangent-cut pairs as the primary sealing device. There are, however, opportunities to utilize new sealing technologies to improve packing performance and reliability.

Uncut Ring Technology provides a different sealing methodology that helps to achieve those improvements. This technology has been successfully applied both to primary seal rings and to pressure breakers to reduce packing leakage and to improve packing service life.

2   Function of Traditional Packing Rings

Traditional packing, for many years, has been based on tangent-cut rings or radial-cut/butt-tangent-cut pairs.

Tangent-cut rings are susceptible to leakage with temperature variations due to the potential for thermal growth of the tangent segments, which can lift the adjacent segment off the rod. Radial-cut/butt-tangent-cut pairs are oriented and pinned such that the end gaps are offset. The butt-tangent ring, because of its offset tangent cut, can tolerate a wide range of temperatures without leaking excessively. However, the frictional heat generated,

and thus the wear experienced, is proportional to the pressure differential across the ring.

Rigid backup rings are often employed with these ring styles. These backup rings have butted ends and have sufficient clearance over the rod such that they have only incidental contact with the rod and do not participate in sealing. The primary reason to use a backup ring is to prevent extrusion of the primary seal ring material, which is usually PTFE or PEEK. Typically at pressures above about 48 bar lubricated or 34 bar non-lubricated, backup rings are required to prevent extrusion and premature failure of rod rings.

A secondary function of the backup ring, particularly in the case of metallic backup rings, is to assist in temperature management by conducting some heat away from the rod into the packing cups.
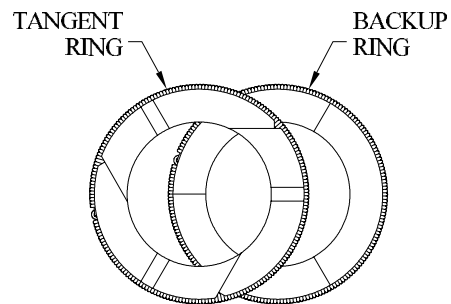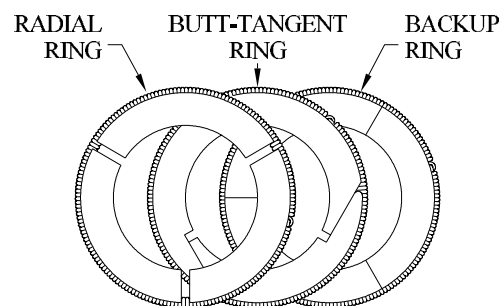

Figure 1: Tangent-Cut Rod Ring

Figure 2: Radial-Cut/Butt-Tangent-Cut Pair

3   Function of Uncut Packing Rings

3.1   Close Down of Uncut Rings Under Pressure

Central to Uncut Ring Technology is that an uncut ring can actually close down under pressure to effect a seal. When correctly designed, an uncut ring will close and approach or contact the rod for a portion of the piston stroke. Several variables are critical to this operation, however.

First, the ring must be dimensioned properly relative to the piston rod diameter such that the correct change in ID of the ring is achieved. Second, the material must be carefully chosen on the basis of the compressive modulus. This ensures that the ring can close under the correct pressure range. It also determines the resulting load against the rod once the ring has closed. This load should be sufficient to seal but should not be excessive. An excessive load could lead to increased friction and rapid wear.

For example, consider a ring being designed for a 2.000" rod at 35 bar pressure. A basic carbon-filled PTFE may have a theoretical close-down of 0.010" with a resulting 35.1 bar load against the rod. A stiffer PEEK blend may have only a 0.004" theoretical close-down, resulting in a 29.1 bar load against the rod.

The desired load against the rod will depend on the wear resistance of the ring material being used, as well as the variables that impact the frictional properties of the situation, including lubrication (or lack thereof), temperatures and pressures.

Figure 3 below demonstrates the ability of a ring to close down and seal. An uncut pressure breaker is compared to a traditional radial-cut pressure breaker. The X-axis shows maximum cylinder pressure, while the Y-axis represents the pressure drop across the ring.
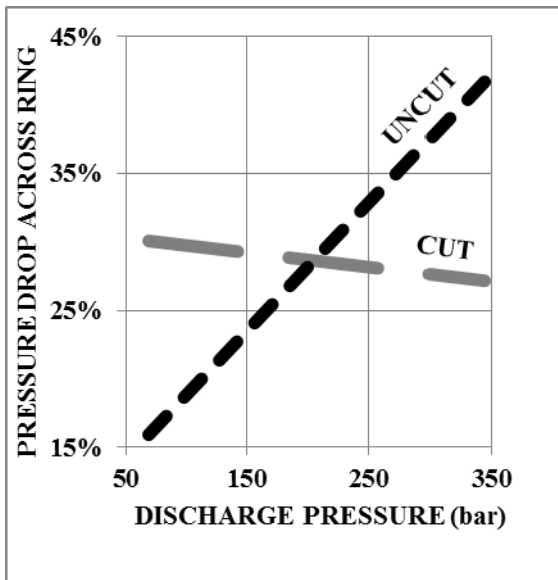

Figure 3: Sealing Effect of Collapsed Ring

Note that as the pressure increases, the pressure drop across the uncut ring increases, while the pressure drop across the cut ring does not. This represents the fact that the uncut ring closes and is loading more heavily against the rod with increasing pressure, restricting gas leakage.

3.2 Sequential Close Down in Ring Assemblies

Rod rings, either pressure breakers or primary seal rings, can use this ability to close down to improve the overall performance of a groove of packing. Because the cylinder pressure is constantly changing during one piston stroke, a rod ring assembly can be tailored to maximize the benefits of Uncut Ring Technology.
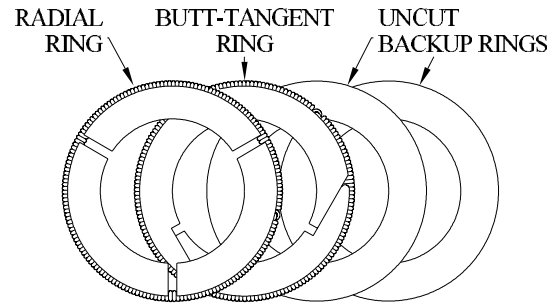

Figure 4: Seal Ring Assembly Using Uncut Rings

A typical seal ring assembly will utilize a radial/butt-tangent pair along with two uncut backup rings. In this case, the radial/butt-tangent ring pair provides effective sealing at lower pressures, while the uncut rings take the load at higher pressures.

At the beginning of the stroke, the pressure drop exists across the radial/butt-tangent pair. This pair seals against the rod under gas load and the garter spring load.
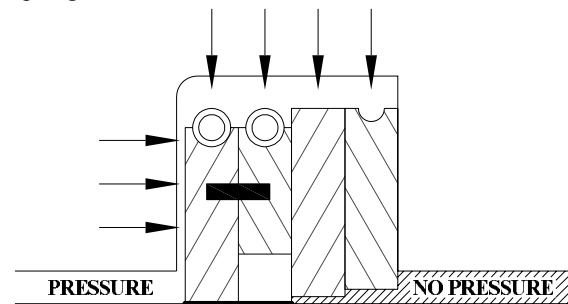

Figure 5: Radial/Butt-Tangent Pair Seals at Low Pressure

As the pressure increases during the stroke, the first uncut ring begins to close down until it eventually seals. At this point there is no longer a pressure drop across the radial/butt-tangent pair, and these rings are no longer pressure loaded. The pressure drop now exists only across the first uncut ring.
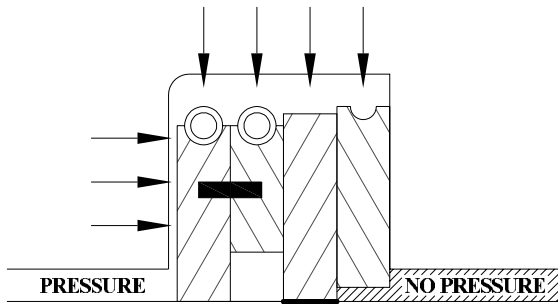
Figure 6: First Uncut Ring Seals at Moderate Pressure

As the pressure finally reaches a maximum in the cylinder, the second uncut ring closes down. As before, the pressure drop moves to this last ring, relaxing the other rings in the groove.
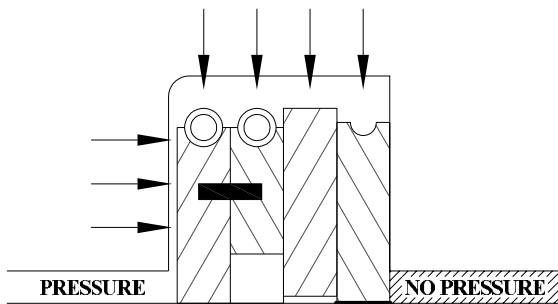

Figure 7: Second Uncut Ring Seals at High Pressure

This sequential sealing is accomplished by designing each uncut ring to close down at the proper point within the stroke. The end result is that the pressure load is transferred from one ring to the next during the stroke, such that the amount of time that any single ring is loaded against the rod is significantly reduced.

4 Benefits of Uncut Ring Technology

4.1 Reduction in Frictional Load

The sequential loading that occurs within the ring groove results in several benefits for packing performance and life. Firstly, each ring spends less time loaded against the piston rod. Whereas a traditional packing ring spends the entire stroke pressure-loaded, in this arrangement, each ring is loaded only for a portion of the stroke. This in turn reduces the overall frictional load of the ring assembly.
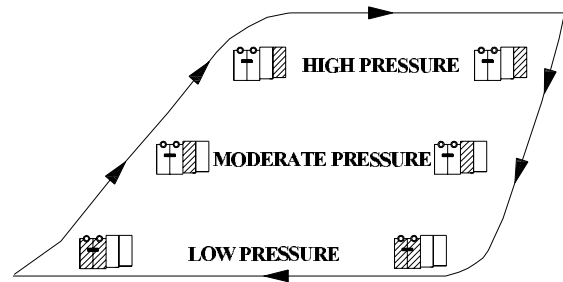

Figure 8: Sequential Loading of Rings During Stroke

In addition, as noted above in Chapter 3.1, because the gas pressure load is acting against the compressive strength of the uncut ring material, some of the pressure is expended in closing the ring. This reduces the resulting load against the rod. This is advantageous because the radial/butt-tangent pair is sealing only at low pressures, and as pressures increase, the uncut rings seal, but at a reduced load. This again reduces the overall frictional impact of the ring assembly.

Finally, because the uncut rings seal tightly against the rod, the uncut ring assembly seals more effectively than a traditional packing ring assembly. When installed in a packing case, this results in a highly effective seal at the first packing groove. The other packing grooves, as a result, are thus unloaded and generate very little frictional heat.

See Figures 9 and 10 below. Figure 9 shows that in a case packed with traditional rod ring assemblies, each groove of packing takes a portion of the total pressure load as pressure is gradually reduced. Figure 10 shows that in a case packed with uncut ring assemblies, the first groove of packing takes almost the full pressure load. This, once again, reduces the overall frictional load of the packing when using uncut ring assemblies.
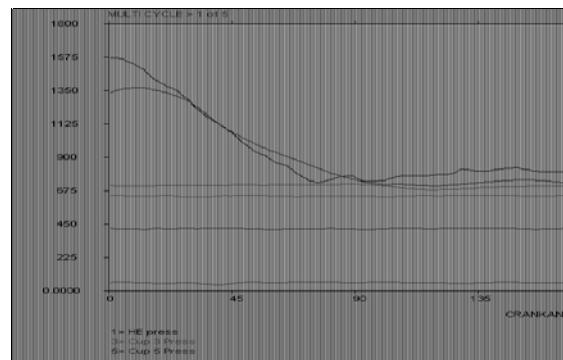

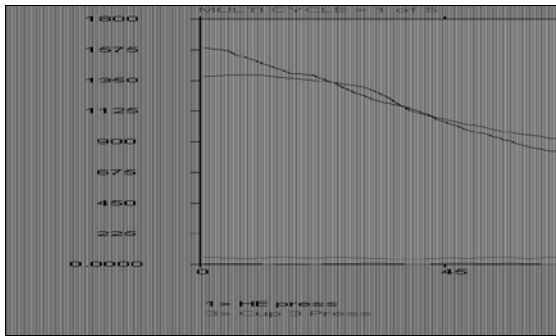*Figure 9: Pressure Distribution in Traditional Packing*

Figure 10: Pressure Distribution with Uncut Packing Technology

The net result of these reductions in frictional heat is a decrease in heat generated and thus in rod temperature. Note below that not only does the uncut packing run significantly cooler, but it increases less with pressure.
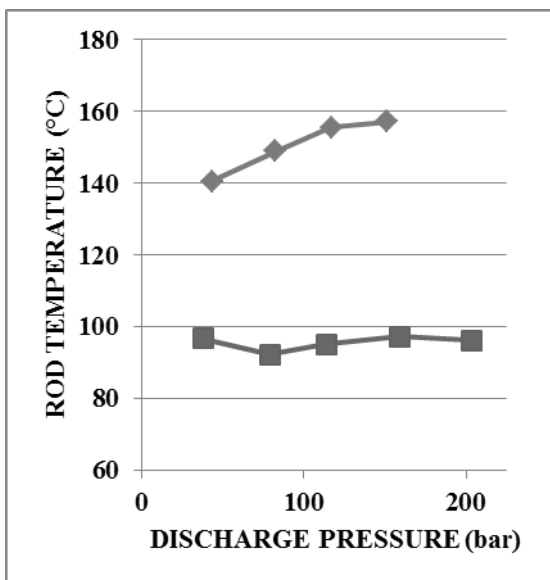

Figure 11: Rod Temperature Reduction with Uncut Ring Technology

Because packing wear rates are directly impacted by rod temperature, these reductions in frictional loading result in an overall improvement in packing life.

4.2   Reduced Leakage

As was mentioned above, this method of sealing is much more effective than traditional packing. This allows significant reductions in packing leakage and is beneficial wherever leakage has been a problem or where emissions are closely monitored.

4.3   More Efficient Packing

Because uncut ring assemblies seal more effectively and run longer than conventional designs, fewer grooves of packing are required. Whereas in the past a packing case needed several grooves to effectively contain pressure for the required amount of time, only a few grooves are now needed.

Pressure	Traditional Packing	Uncut Ring Technology
> 140 bar	5 – 7 Rings	4 – 5 Rings
55 – 140 bar	4 – 6 Rings	3 – 4 Rings
20 – 55 bar	3 – 5 Rings	3 – 4 Rings
< 20 bar	2 – 4 Rings	2 – 3 Rings

5   Case Studies

Although the laboratory results shown above illustrate the benefits of Uncut Ring Technology, field data exists to demonstrate its effectiveness in real applications.

5.1   Case Study 1 – Leakage and Temperature Reductions

A gas-transmission customer had multiple 4-throw compressors running on a single site, all of which were experiencing packing leakage on most throws. The packing was using typical radial/butt-tangent pairs with backup rings. Packing was not worn, but was still leaking. Attempts to troubleshoot the problem were unsuccessful.

Packing on nearly all throws was replaced with Uncut Ring Technology. The same packing materials were used, and leakage on all throws went to zero (below measurement threshold). Data is shown in the table below. Leakage is reported in SCFM (standard cubic feet per minute).

	Traditional Packing	Uncut Ring Technology
Unit 1		
Throw 1	0.0	0.0
Throw 2	0.8	0.0
Throw 3	1.5	0.0
Throw 4	0.3	0.0
Unit 3		
Throw 1	1.6	0.0
Throw 2	0.0	0.0
Throw 3	1.9	0.0
Throw 4	0.6	0.0
Unit 5		
Throw 1	2.1	0.0
Throw 2	1.9	0.0
Throw 3	0.0	0.0
Throw 4	0.8	0.0
Unit 6		
Throw 1	0.0	0.0
Throw 2	0.8	0.0
Throw 3	0.5	0.0
Throw 4	0.0	0.0
Unit 7		
Throw 1	0.7	0.0
Throw 2	0.4	0.0
Throw 3	0.5	0.0
Throw 4	2.7	0.0
Unit 2		
Throw 1	2.5	0.0
Throw 3	1.3	0.0
Unit 15		
Throw 1	1.6	0.0
Throw 3	0.8	0.1

In addition, rod temperatures were measured on several throws, both before and after this conversion. Significant reductions were reported.

	Traditional Packing	Uncut Ring Technology
Unit 2		
Throw 1	107°C	67°C
Throw 3	107°C	71°C
Unit 15		
Throw 1	84°C	71°C
Throw 3	85°C	63°C

5.2   Reliability Improvement

A high-speed, non-lube fuel gas booster was experiencing short packing life.   Packing was literally lasting only days. Packing was running at 46 bar, 3.6 m/s. Radial/butt-tangent pairs made up the packing set. Several fixes were attempted, none were successful. Premium non-lube materials from multiple vendors were tried, all unsuccessful.

Finally, the case was re-fitted with Uncut Ring Technology. Premium materials were also used, but these were the same materials that had previously failed with standard ring types.

After installing the upgraded packing, life was extended and now has better than 10000 hours.

6   Conclusion

Uncut Ring Technology gives us new tools to improve packing performance and life.   A completely different method of sealing results in more effective leakage control and significantly reduced frictional heat.

These improvements allow a level of reliability previously unavailable to us, particularly in difficult non-lube applications.

7   Acknowledgements

Friction-surface coatings in dry-running piston compressors - benefits and risks

by:

Dr. Norbert Feistel
Research and Development
Burckhardt Compression AG
CH-8404 Winterthur
Switzerland
norbert.feistel@burckhardtcompression.com

8th Conference of the EFRC
September 27th / 28th, 2012, Düsseldorf

Abstract:

Due to increasing demands on the reliability of process-gas compressors, measures to protect the counter-body surfaces of the sealing and rider rings are becoming increasingly important. In this regard, the influences of different coatings on the processes involving dry-running friction contact are not clear. Bench tests with dry-running sealing systems have revealed notable changes in surface texture, typically accompanied by severe wear of the sealing elements after just 500 hours of testing in the case of some coatings, despite high hardness values significantly in excess of 1000 HV. In addition to surface topography, the chemical resistances of the various coatings appear to be an important factor influencing the formation of transfer film. Especially with high pressure loads, all coatings recommended for use in corrosive media achieved poorer wear rates compared to nitrided-steel piston rods.

Friction-surface coatings in dry-running piston compressors - benefits and risks, *Dr. Norbert Feistel;*
BURCKHARDT COMPRESSION AG

1   Introduction

The application of coatings to prevent damage during compression of corrosive gases has proven successful over many years. Due to ever-increasing demands on the reliability of process-gas compressors, coatings are now also being used increasingly in the absence of corrosive media to protect surfaces subjected to tribological loads. API 618[1] recommends wear-reducing coatings for piston rods, regardless of the base material. A wear-resistant coating inside the cylinder might also become necessary in case of a high load exerted on the sealing system, a use of piston and rider rings with abrasive fillers, or a presence of abrasive contaminations in the gas.

Today's complex set of requirements concerning the use of coatings in process-gas compressors and involving, in particular, a diversity of gases, gas mixtures and impurities, are met through numerous combinations of coating materials and processes. Especially in the case of dry-running piston compressors, the interactions taking place between the friction pair and ambient medium must be considered too. The coating's surface texture, of importance to stable dry-running conditions, also raises questions about optimal parameters and feasibility. To be taken into account furthermore is the large bandwidth of parameters influencing production of the desired coating quality.

2   Requirements for friction-surface coatings in dry-running piston compressors

A sound knowledge of materials as well as detailed information regarding the load parameters involved are needed to determine the most appropriate combination of coating material and procedure for a given application. High corrosion resistance and/or high wear resistance are required depending on the specific application. The maximum permissible layer thickness which already precludes individual coating processes or at least necessitates use of a special intermediate layer is of importance depending on whether a new coating or repair of a worn component is involved. In addition to the piston rod's outer coating, the diameter of the cylinder to be coated on the inside can range from less than 50 mm to more than one meter. Finally, also to be considered in the case of oil-free compression is the suitability of the friction surface's coating for dry-running operation with a broad spectrum of filled plastic materials.

2.1   Corrosion resistance

Coatings of the highest possible chemical resistance are used to avoid damage to the metallic friction surfaces inside the cylinder and the piston rod during compression of corrosive gases such as chlorine, hydrogen chloride, hydrogen sulphide etc. Especially ceramic coatings such as chromium (III) oxide (Cr_2O_3) have proven suitable for such applications for many years.

In addition to ceramics, hard-metal coatings are being used increasingly for compression of corrosive media. In the most common variant of friction-surface coating comprising tungsten carbide in a cobalt matrix, however, the base cobalt constitutes a weakness in terms of corrosion resistance. To mitigate this drawback, about one-third of the metallic cobalt matrix is replaced with chromium. In reciprocating compressors, these WC/CoCr coatings quickly proved successful in many applications involving corrosive media. Another very corrosion-resistant variant of a hard-metal coating is chromium carbide in a matrix of nickel and chromium. Suitable especially for high-temperature applications, this wear-resistant layer has performed well in the chemical and aerospace industries, and is also used now as a friction-surface coating in compressors.

Ceramics and hard metals suitable for corrosion protection are usually applied through thermal coating. Due to the nature of this process, however, thermal spray coatings always exhibit a porosity whose degree is influenced, in particular, by the type of process employed. The porosity ranges from 0.5 % in the case of very dense layers to more than 2 %. Through these pores and microcracks in the spray coating, corrosive media can penetrate as far as the substrate. To prevent this kind of underlying corrosion, it is necessary to implement additional measures such as surface sealing, thermal after-treatment by means of self-fluxing alloy powders, or use of a dense, corrosion-resistant intermediate layer between the base material and coating. Intermediate layers comprising, for example, nickel-chromium-molybdenum alloys or chemically deposited nickel are employed as diffusion barriers. Available finally as an alternative coating process is high-temperature CVD, in which repeated spraying and annealing of a ceramic suspension followed by sealing also makes it possible to create a layer almost free of pores.

Friction-surface coatings in dry-running piston compressors - benefits and risks, *Dr. Norbert Feistel;*
BURCKHARDT COMPRESSION AG

2.2 Wear resistance

Dry-running materials with abrasive fillers such as ceramics, glass or carbon fibre can already cause severe wear-related damage on counter-body surfaces made of cast iron. If abrasive gas contaminations such as aluminium oxide are involved additionally, the wear resistance limits of even high quality nitrided steel are rapidly exceeded[7]. Even hard chrome coatings offer no protection here. The only remedy in this case is to use a coating with a significantly higher wear resistance. The highest possible degree of hardness, in particular, is usually favoured during selection of this kind of wear-protection coating. Thin layers deposited using the PVD or CVD process, and possessing a maximum thickness of only a few micrometers, theoretically offer a very good perfor-mance. The well-known titanium nitride layers are specified to have micro-hardness values of over 2000 HV. The extremely hard diamond-like carbon (DLC) coatings have significantly higher micro-hardness values of 4000 - 6000 HV. However, high hardness values alone are no guarantee of adequate protection for the base material, for example, if requirements for bonding strength are not met so that the layer fails by flaking during operation.

In addition to ceramic coatings with a high hardness of about 2000 HV, some hard-metal coatings have proven themselves superbly during operation with the afore-mentioned alumina particles present in the gas flow. Though a hard metal comprising 88 % WC and 12 % Co has a hardness of just 1300 to 1400 HV, the heterogeneous structure of this sintered composite of hard carbides in a soft metal matrix has proven to be wear-resistant even in the presence of very hard gas impurities.

2.3 Coating quality

Requirements for the quality of a friction-surface coating are described by coating specifications, which stipulate agreed limiting values for the layer's composition, thickness, hardness, porosity, tensile adhesive strength etc. In actual fact, however, a coating's properties depend on a variety of further parameters. In the case of thermal spraying, for example, the coating's quality is also influenced to a large extent by the process, spray gun, fuel, application rate, etc. In dependence on these boundary conditions, the coater selects a powder of the most appropriate particle size. Despite a constant powder composition, any change to these parameters can significantly affect coating quality, as Figure 1 already shows in terms of the differences between the structures of two WC/Co coatings applied using different processes. The coating applied using a detonation process has a

much coarser structure, with carbide sizes ranging from 10 to 25 µm (bottom), whereas a WC/Co coating of a nearly identical composition applied by high velocity oxygen fuel spraying (HVOF), exhibits a very fine structure with carbide sizes ranging from just 4 to 5 µm[9].
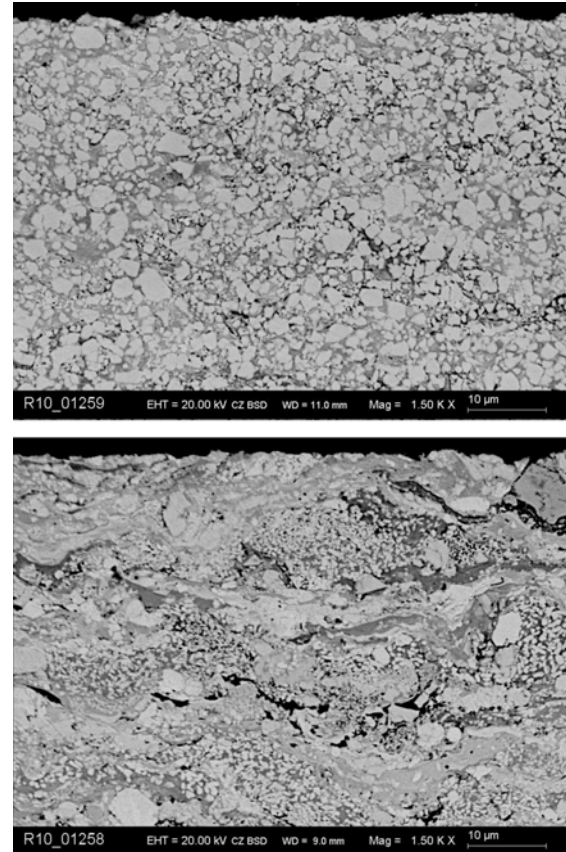

Figure 1: WC/Co coatings applied using a detonation process (bottom), and using high velocity oxygen fuel spraying (HVOF) [9]

Process-specific variations in the coating quality are not always avoidable in practice. From a critical value onward, the internal coating of a cylinder of a small diameter can no longer be applied using the process, spray gun or powder particle size optimal for a piston rod's outer coating, for example. To achieve reproducible coating qualities, it is therefore essential that all process parameters, the preparation of the substrate surface and the after-treatment of the coating are defined by means of a spraying instruction, in addition to defining a coating specification[2, 3].

2.4 Suitability for dry-running operation

Practice has shown that cast iron or nitrided steel as the counter-body material in dry-running applications achieves a very good service life for the sealing and rider rings. At least the same expectations are placed on friction-surface coatings.

RINGS & PACKINGS

Friction-surface coatings in dry-running piston compressors - benefits and risks, *Dr. Norbert Feistel;*
BURCKHARDT COMPRESSION AG

The requirement to produce a functional friction pair from various available dry-running materials is therefore a key criterion which significantly restricts the choice of available coatings.

Key requirements for friction-surface coatings intended for dry-running can generally be described as follows:

- Resistance to local, high temperatures above 300 °C
- Highest possible thermal conductivity
- Favourable properties for formation of a stable transfer film
- Favourable influence on tribochemical processes

The thermal conductivity values of eligible friction-surface coatings might differ notably from those of conventional metallic counter-body materials. For instance, carbon-based coatings exhibit significantly better values. WC/Co coatings also have a very good thermal conductivity. Ceramics range from materials with excellent thermal conductivity, such as silicon carbide, to insulators (e.g. zirconia).

An optimal roughness range instead of an extremely smooth surface has proven successful during dry-running[7]. Appropriate precise surface finishing by means of grinding, lapping, honing etc. is required after the application of the coating. At present, it is unclear whether proven roughness values for metallic counter-body materials can be implemented for specific coatings, and whether the resultant combinations have optimal effects.

Attention must also be drawn to the fact that tribochemical processes take place during dry frictional contact, significantly influencing friction and wear, and can thus have a positive effect, for example, through formation of a protective layer on the sealing elements' running surface[6]. However, adequate empirical data regarding tribochemical interaction with a variety of combinations of filled plastic materials and gases are not available for all coatings. Especially in the case of ceramics with a low chemical activity, as well as coatings with pronounced anti-adhesive properties, such as hard chrome and composite materials made of nickel-phosphorus with embedded PTFE particles, significant differences to conventional metallic counter-body materials can be expected. Particularly with regard to coatings containing PTFE, it is necessary to note that they are not identical to the tribochemically modified transfer film formed during operation, and therefore do not advance the process of transfer film formation, but instead can affect it negatively.

3   Friction-surface coatings in practice

The afore-mentioned requirements for friction-surface coatings in dry-running piston compressors are now met mainly by hard-metal and ceramic layers applied by a thermal spray process. This method offers the greatest variation in terms of coating materials as well as layer properties and thicknesses, thereby holding a lot of potential especially for the repair of worn friction surfaces.

Hard-metals are handled differently than ceramics, however. Thus, hard-metals are now favoured increasingly as piston-rod coatings. For instance, their lower impact sensitivity compared to ceramics has a positive effect highly valued during everyday handling. In addition, hard-metal powders applied using the HVOF technique can be used to produce very dense, low-porosity layers. Spraying of ceramic layers requires higher temperatures, achievable by plasma processes. However, smaller spray-gun dimensions here also make it possible to realize internal coatings of cylinders with a diameter of slightly less than 50 mm. Optimized multi-component systems are also continually broadening the scope of applications for ceramic coatings. An alternative process to thermal coating of cylinders with small diameters is the high temperature CVD method.

Despite the additional costs, the application of friction-surface coatings in reciprocating compressors has increased significantly. For example, coated piston rods are increasingly replacing nitrided piston rods, which were still widespread until a few years ago, especially in dry-running applications involving low loads. When investing in such surface finishing, however, customers expect added value in the form of notably longer lifespans of the coated components.

Operational experience with coatings has shown that demands placed on them, especially in terms of increased wear protection compared to uncoated friction surfaces, are usually fulfilled in a most excellent manner. However, practical experiences with the performance of dry-running packings in practice have been mixed. In applications involving pressure differences in excess of about 20 bar, packings occasionally had a very short service life, the piston rod exhibiting conspicuous, very smooth surface areas. Figure 2 shows the average wear rate of all sealing elements forming part of dry-running packings of a hydrogen compressor with a pressure difference of 54 bar. Evidently, the wear rate deteriorates continuously despite constant conditions for assembly and operation of the packings, until premature failure of the fourth sealing system. Each packing was operated on the

RINGS & PACKINGS

Friction-surface coatings in dry-running piston compressors - benefits and risks, *Dr. Norbert Feistel;*
BURCKHARDT COMPRESSION AG

same rod with a hard metal coating, which was in excellent condition except for a low roughness along the packing rings' friction path.
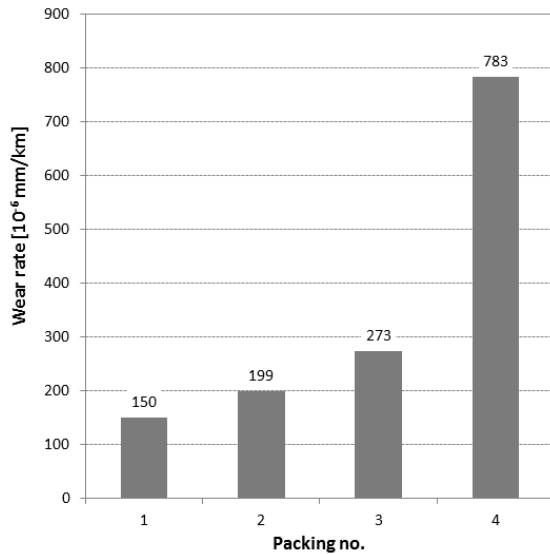

Figure 2: Average wear rates of four packings for sealing a piston rod coated with hard metal

4 Interactions between dry-running material and counter-body surface

Insights into the phenomena observed on coated piston rods in practice were to be provided by bench tests on a dry-running compressor. For this purpose, the compressor's 550-mm long tail rod with a diameter of 50 mm was coated with the hard metal WC/Co using both the detonation as well as the HVOF process. For comparison with the two chromium-free coatings, the hard metal WC/CoCr containing chromium was applied to another piston rod, also using the HVOF process. Finally, a quaternary ceramic consisting of aluminium oxide, chromium oxide, zirconium oxide and titanium oxide was included in the test series. A piston rod made of nitrided steel served as a reference for a metallic counter-body surface. An arithmetical mean deviation Ra in the range from 0.20 to 0.30 μm was specified for all surfaces (Table 1).

A suction pressure of 16 barg, final pressure of 40 barg and average piston velocity of 3.18 m/s were specified as the load parameters for the tests conducted with dry nitrogen. Used in each case was only one sealing element comprising PTFE/PPS polymer blend in a cooled packing, to ensure clearly defined conditions during subjection of the piston rod to friction power. The PTFE/PPS polymer blend selected for the packing rings and filled with graphite and carbon fibre[7] has proven to be non-abrasive in many applications, even in combination with cast iron of a low hardness. Each

test was to have a duration of 500 hours, though this was not possible with the WC/CoCr-coated piston rod. In this case, test had to be interrupted due to a sudden rise in the temperature of the sealing element's chamber (Figure 3).
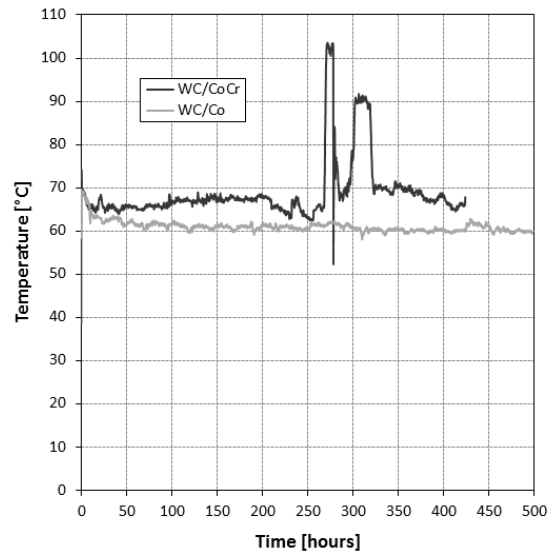

Figure 3: Temperatures measured in the sealing element's chamber, for piston rods coated with WC/CoCr and WC/Co using the HVOF process

The removed sealing element had been thermally damaged by the excess temperature, and therefore had to be replaced with a new one. On the piston rod, the roughness in the region of the sealing element's friction surface had declined significantly; this is clearly visible in comparison with the surface in its new state (Figure 4). There was another temperature rise later on, and the test eventually had to be cancelled after 424 hours due to high leakage. The piston rod's friction surface was polished smooth and glossy (Figure 4, bottom).

Such steep rises in temperature to values above 100°C were not observed in the other tests. Here, the chamber temperatures remained stable in the range between 60 to 70 °C after running in. Figure 3 therefore only shows the temperature profile of the piston rod coated with WC/Co (HVOF process) for the purpose of comparison.

Especially during the running-in period of a dry-running friction pair, surface topography is altered through breakage of roughness peaks, deposition of wear particles and reorganization of surfaces, even on extremely hard counter-body materials. Because these effects can vary highly along the friction surface, roughness measurements in this region usually provide results which fluctuate greatly. Consequently, zones exhibiting minimal roughness were sought and evaluated on the surfaces of all piston rods.

RINGS & PACKINGS

Friction-surface coatings in dry-running piston compressors - benefits and risks, *Dr. Norbert Feistel;*
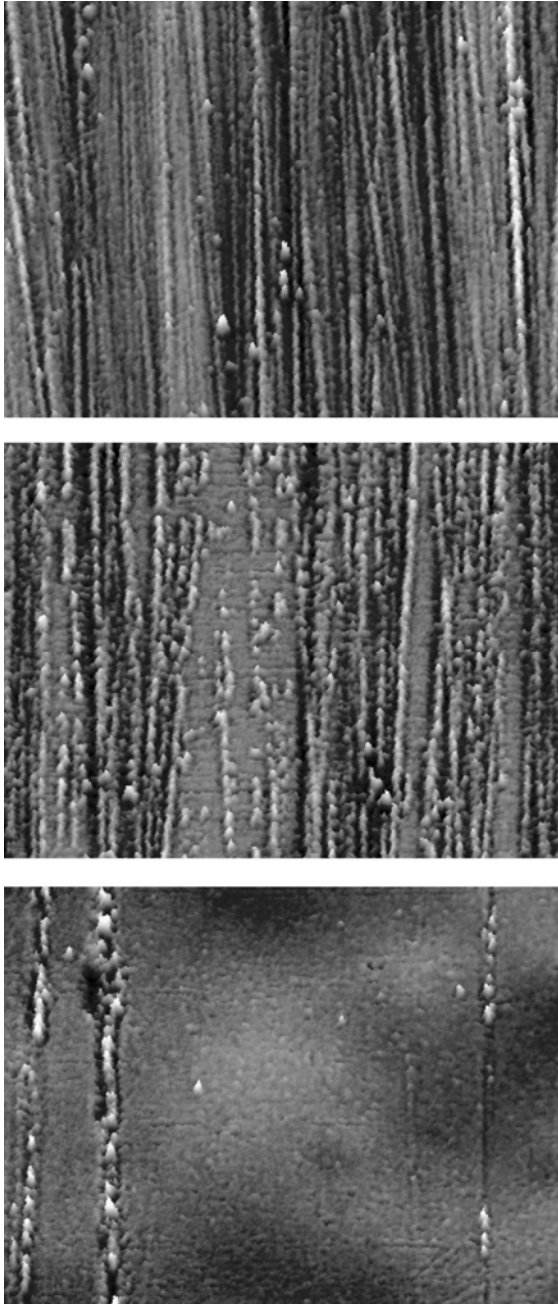BURCKHARDT COMPRESSION AG

Figure 4: Friction surface of a piston rod coated with WC/CoCr in the new condition (top), after an operating period of 270 hours (centre) and after 424 hours (edge length 300 * 225 µm)

Comparing the thus obtained arithmetical mean deviation of the profile Ra to the values in the original state reveals a reduction in the case of all surfaces, except the ceramic coating (Figure 5). On this coating, formation of the transfer film even led to a slight increase in the Ra value. Especially evident is the reduction in roughness on the WC/CoCr-coated piston rod, although it turned out to have the highest hardness values (Table 1). The two chromium-free hard-metal coatings and even the nitrided steel exhibit a much smaller drop in Ra values.

A further result shown in Figure 6 comprises the wear rates of the sealing elements operated on the various surfaces under otherwise identical conditions. The lowest value was obtained in the test of the ceramic-coated piston rod. Very good results were also obtained with the two chromium-free hard-metal variants. The wear rates of the sealing elements are also significantly lower than that of the nitrided steel surface. The highest wear rate was established in the test of the WC/CoCr-coated piston rod involving high chamber temperatures at times, and revealing the greatest drop in the Ra value.
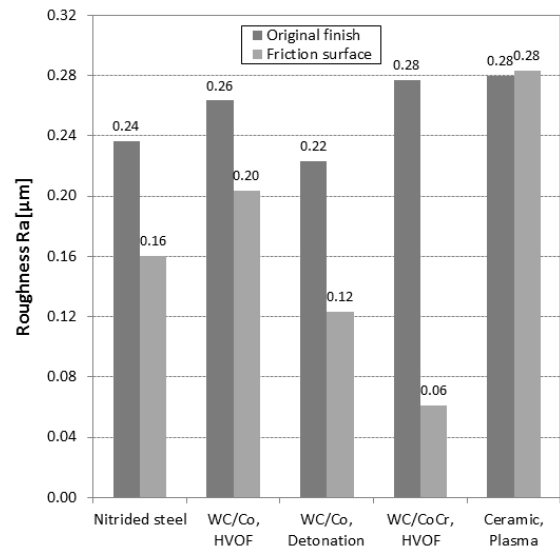

Figure 5: Ra values measured on the friction surfaces of different counter-body materials, compared with the original finish in each case
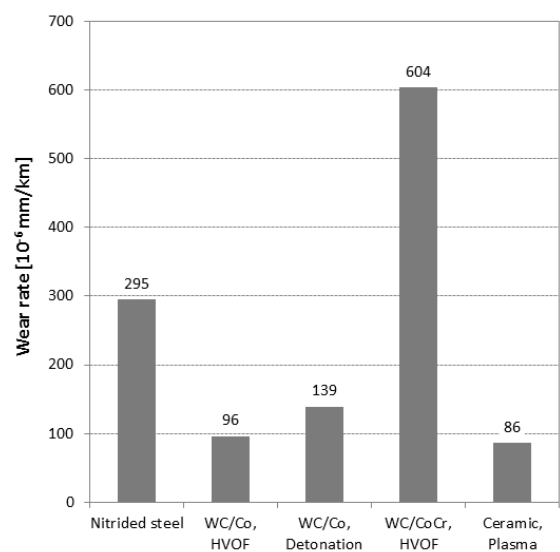

Figure 6: Wear rates of a single packing ring in dry nitrogen on various counter-body materials

Friction-surface coatings in dry-running piston compressors - benefits and risks, *Dr. Norbert Feistel;*
BURCKHARDT COMPRESSION AG

5   Analysis of influencing parameters

Although a functional design of counter-body surfaces is of particular importance for the dry-running friction pair comprising soft and hard, the surface of the hard counter-body material is usually described only by specifying a permissible range for the Ra value. Ignored in this case is the known fact that the arithmetical mean deviation of the profile Ra is totally unsuitable for characterizing surfaces, as it does not permit any distinction between different profiles. Peaks and valleys are treated equally during determination of the Ra value. The arithmetical mean deviation of the profile is therefore only suitable as a quality control para-meter if the character of the roughness is known[8].

Several surface texture parameters permit a characterization of surfaces and therefore serve to supplement the results of an Ra measurement. This is achievable, for example, by means of the following parameters:

- Ratio of core roughness depth Rk to average roughness depth Rz (DIN)
- Ratio of average peak-to-valley height Rp to average roughness depth Rz (DIN)
- Relative material ratio of the profile Rmr

Especially in the case of the porous ceramic coatings applied using the plasma process, the surface after completion of processing might be characterized by a plateau-like roughness profile comprising a high proportion of valleys attributable to the pores (Figure 7). However, the upper limit of the permissible Ra value is often exceeded by this kind of surface. While an inadmissibly large Ra value of a profile with a pronounced proportion of peaks leads to high abrasive wear on the soft dry-running sealing element, it is not necessarily a drawback in the case of a plateau-like roughness profile. A quick initial conclusion about the nature of the roughness profile can be drawn from the ratio between the core roughness depth Rk and the average roughness depth Rz (DIN)[8]. In practice, surfaces achieving a value of less than or equal to 0.25 in terms of this ratio have also proven successful in dry-running if their Ra value exceeds the permissible upper limit (Table 1).

Conclusions about the characteristics of the various piston rod surfaces can also be drawn from the material ratio of the profile Rmr indicated in Table 1. In each case, the material ratio was determined with a reference line c0 shifted by about 2 % with respect to the highest peak at an profile section level of c1 = Rz/4. A comparison between the Rmr values of the three hard-metal layers reveals that the material ratio of the WC/CoCr-coated piston rod is significantly lower than that of the two chromium-free variants, and only slightly higher than the minimum value of 31.3 % ascertained for the nitrided-steel piston rod. The highest value of 82.1 % was obtained with the ceramic coating.
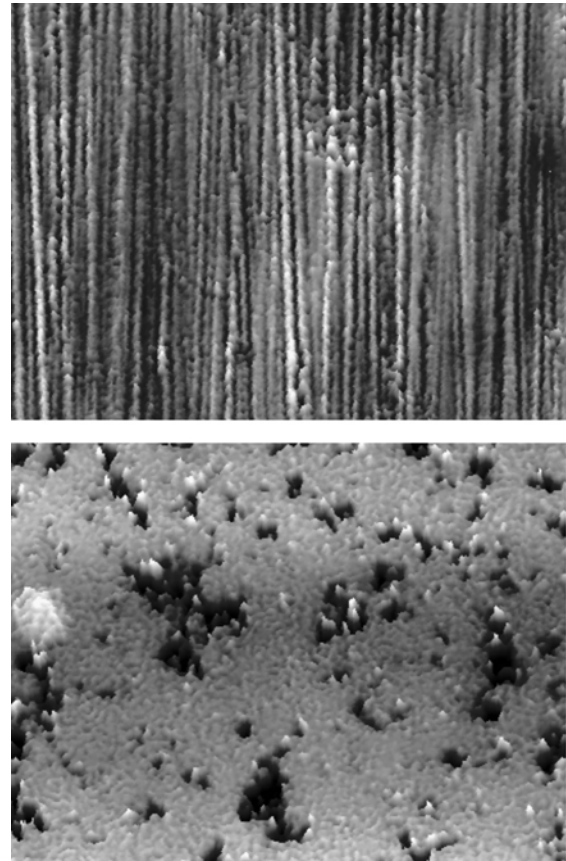

*Figure 7: Porous surface of a ceramic applied using a plasma process (bottom) compared to a nitrided steel surface (edge length 300 * 225 μm)*

Counter-body material	Nitrided steel	WC/Co	WC/Co	WC/CoCr	Ceramic
Coating process	-	HVOF	Detonation	HVOF	Plasma
Hardness HV0.3	731	1128	1156	1279	926
Ra [μm]	0.237	0.263	0.223	0.277	0.280
Rz (DIN) [μm]	1.797	2.093	1.793	1.957	2.487
Rk [μm]	0.773	0.840	0.667	0.933	0.303
Ratio Rk / Rz	0.430	0.401	0.372	0.477	0.122
Rmr [%]	31.29	46.86	53.47	32.15	82.12

Hardness as average from 10 measurements, roughness parameters as average from 6 measurements by profile method [4, 5]

Table 1: Hardness and roughness values of the tested counter-body materials

A comparison of the surface topographies of both layers applied by means of the HVOF process reveals that the piston rod coated with WC/CoCr has a coarser structure (Figure 8, bottom). Powder with a particle size of -45 +15 μm was employed for both hard-metal variants; as a result, the carbides present in the WC/CoCr coating and sized about 3 μm were slightly smaller compared to the sizes of 4 to 5 μm in the chromium-free coating.
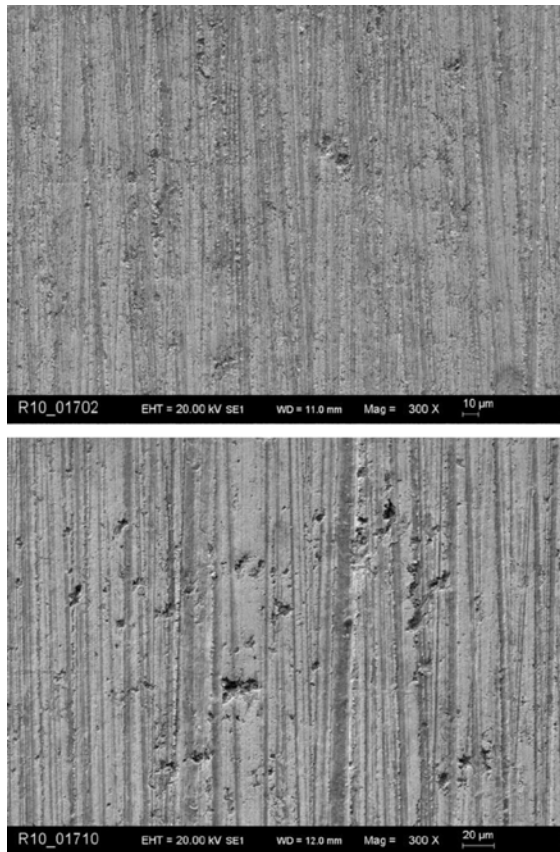
RINGS & PACKINGS

Friction-surface coatings in dry-running piston compressors - benefits and risks, *Dr. Norbert Feistel;* BURCKHARDT COMPRESSION AG

Figure 8: Different surfaces after processing of a WC/Co coating and a WC/CoCr coating (bottom) [9]

The differences in surface topographies observed after processing can therefore hardly be explained by their structure, but rather by the different composition of the matrix material and the resultant material properties. Whereas the cobalt content of the chromium-free variant is 12 % by weight, it drops to 8 % by weight in the WC/CoCr-powder, and is supplemented there by a chromium content of 4 % by weight. The chromium content has a negative effect on the composite's toughness, apparently making it difficult to produce a surface profile with a high material ratio, and resulting in the observed coarse surface topography[9].

An analysis of the test results obtained with the ceramic coating and the two chromium-free WC/Co coatings shows that plateau-like surfaces with the greatest possible material ratio offer favourable conditions for dry-running. Plateau-like structures can be realized, for example, by levelling the roughened profile's peaks using a suitable superfinishing process, thereby creating a surface with a dominant proportion of valleys.

6 Influence of coatings on the performance of dry-running sealing systems

The single-ring test results concerning the influence of various coatings' surface texture on the performance of dry-running sealing systems were studied in more detail in a hydrogen compressor. For this, the piston rods possessing a diameter of 50 mm were coated with both hard-metal variants with and without a chromium content using the HVOF process, and their surfaces furnished with highest possible material ratio Rmr in an additional superfinishing process. Table 2 shows that this was achieved more successfully with the chromium-free coating. To counter the conspicuously high roughness loss on the WC/CoCr-coated piston rod, slightly lower Ra values in the range from 0.15 to 0.25 µm were selected for all surfaces. A conventionally finished piston rod made of nitrided steel again served as a reference for a metallic surface.

A suction pressure of 14 barg, final pressure of 40 barg and average piston speed of 3.41 m/s were specified for the tests, conducted in the first stage of a horizontal compressor which was operated with dry hydrogen (dew point of about -65 °C). The piston rod sealing system in each case comprised a cooled packing of six packing rings made of a PTFE/PPS polymer blend. An operating period of 500 hours was planned for each test.

Counter-body material	Nitrided steel	WC/Co	WC/CoCr	CrC/NiCr
Coating process	-	HVOF	HVOF	HVOF
Rmr, original finish [%]	33.89	64.36	40.60	43.58
Ra, original finish [µm]	0.220	0.227	0.170	0.237
Ra, friction surface [µm]	0.157	0.140	0.102	0.077

Table 2: Roughness values of the counter-body materials tested in dry hydrogen

In this series of tests, too, the WC/CoCr-coated piston rod's behaviour was conspicuous. Though the test in this case did not pose any problems, the average wear rate of the six packing rings was more than twice that of the chromium-free variant, and higher by about one third even compared to the result obtained for the nitrided-steel piston rod (Figure 9), despite the higher material ratio Rmr.

Accordingly, laboratory analyses were conducted to reveal whether friction and wear are influenced not only by different surface topographies, but also the different compositions of the two hard-metal variants via tribochemical interactions between the friction pair and the ambient medium[9]. However, investigations carried out using energy dispersive X-ray analysis (EDX) and micro-probe analysis

Friction-surface coatings in dry-running piston compressors - benefits and risks, *Dr. Norbert Feistel;*
BURCKHARDT COMPRESSION AG

(WDX) revealed no differences, such as a depletion of oxygen or chromium, between the coatings' used and original areas. Nor was there any change in the layer structure near the surface. The test series was nonetheless supplemented by a further hard-metal coating which, like WC/CoCr, is highly resistant to corrosion. Though the average wear rate of the sealing elements operated on this CrC/NiCr-coated piston rod is somewhat lower than the result obtained for the WC/CoCr coating, it is still significantly higher compared with the values obtained for the chromium-free hard-metal variant and the nitrided-steel piston rod. In addition, the friction surface of the CrC/NiCr-coated piston rod exhibited a significant decrease in Ra value from 0.237 to just 0.077 μm (Table 2). This loss of surface roughness was accompanied by formation of a striking, silver-coloured layer on the sealing elements' friction surfaces (Figure 10).
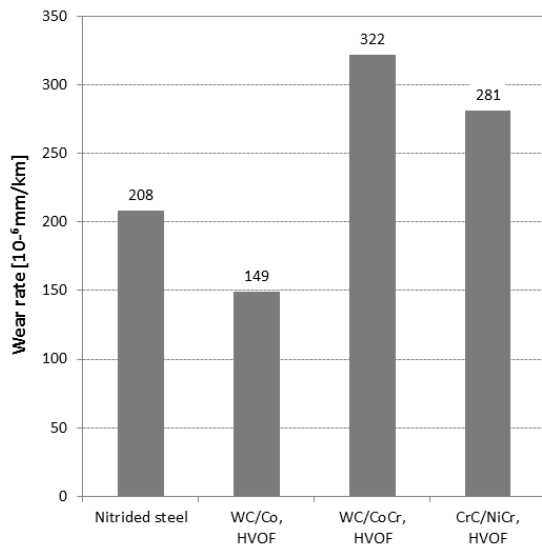

Figure 9: Average wear rates of packings in dry hydrogen on various counter-body materials

Figure 10: Silver-coloured layer on the friction surface of a dry-running packing ring after operation on a CrC/NiCr-coated piston rod

The quaternary ceramic which successfully passed the single-ring tests also has an excellent corrosion resistance. Due to the very good results obtained at a final pressure of 40 barg, this coating was to subsequently prove its dry-running suitability under a significantly higher load comprising a suction pressure of 40 barg and a final pressure of 100 barg in the hydrogen compressor's second stage. The sealing system employed here comprised a cooled packing with a total of ten packing rings made of a PTFE/PPS polymer blend and optimized for this application.

Already during the test, unfavourable operating characteristics were indicated by conspicuously high temperatures on the piston rod's surface and at the outlet for leakage gas and cooling water. The average wear rate of the sealing elements operated on the ceramic coating is more than twice the value obtained for a conventional piston rod made of nitrided steel (Figure 11). This poor result was confirmed in a repeated test. At variance to the compact structure of the transfer film observed in all other tests, both tests here revealed a large amount of loose, powdery particles on the ceramic coating's surface.
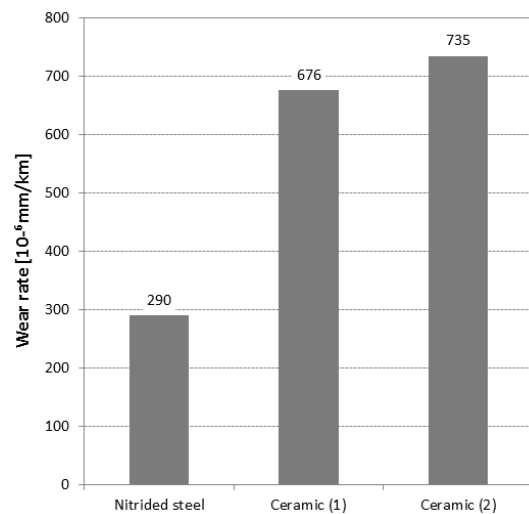

Figure 11: Average wear rates of two packings operated on a ceramic coating in comparison to a nitrided-steel piston rod

7   Summary and conclusions

Despite high hardness values significantly in excess of 1000 HV, the arithmetical mean deviation of the profile Ra of some hard-metal coatings dropped by more than 0.1 μm in the region of the sealing element's friction surface after only 500 hours. This change in surface texture was typically accompanied by high wear rates on the packing rings, thereby confirming the observations made in practice.

Friction-surface coatings in dry-running piston compressors - benefits and risks, *Dr. Norbert Feistel;*
BURCKHARDT COMPRESSION AG

structure of the hard-metal composite. For example, hard-metal coatings with a pure cobalt matrix exhibited a considerably smaller decline in roughness than those with a matrix material containing chromium.

Another important factor influencing roughness loss is the counter-body surface's topography. The tests showed that plateau-like surfaces with the highest possible material ratio Rmr offer favourable conditions for dry-running, besides reducing roughness losses. Coating composition turns out to play an influential role here too, a generation of such surfaces with the highest possible material ratio Rmr being more successful in the case of WC/Co coatings than in the case of the two hard-metal variants WC/CoCr and CrC/NiCr.

These WC/Co coatings possessing a high material ratio Rmr also exhibited lower wear rates compared with the tests of a conventional piston rod made of nitrided steel. A quaternary ceramic tested as an alternative to hard-metal coatings, and possessing a significantly higher material ratio Rmr yet due to its porous surface topography, achieved the best test results with a final pressure of 40 barg. After the load pressure was increased to 100 barg, however, the ascertained wear rates were reproducibly worse compared to the result obtained for the nitrided-steel piston rod.

Large amounts of loose particles on the counter-body surface suggest that the corrosion-resistant ceramic coating adversely affects a formation of transfer film. In addition to surface topography, variations in chemical resistance among the coatings therefore also appear to be an important factor influencing wear characteristics. Especially with high pressure loads, all coatings recommended for use in corrosive media achieved poorer wear rates than a nitrided-steel piston rod, despite higher values for the material ratio Rmr.

Notation

PTFE	Polytetrafluorethylene
PPS	Polyphenylensulfide
CVD	Chemical vapour deposition
PVD	Physical vapour deposition
HVOF	High velocity oxygen fuel
DLC	Diamond-like carbon
Ra	Arithmetical mean deviation of the profile (AA, CLA)
Rz (DIN)	Average roughness depth
Rk	Core roughness depth
Rp	Average peak-to-valley height (Rpm)
Rmr	Relative material ratio of the profile
c0	Reference level
c1	Profile section level

References

[1] American Petroleum Institute
Reciprocating Compressors for Petroleum, Chemical, and Gas Industry Services
API Standard 618, Fifth Edition
Washington, D.C. 20 005, December 2007

[2] DIN EN 15311
Thermisches Spritzen – Bauteile mit thermisch gespritzten Schichten –
Technische Lieferbedingungen
Beuth-Verlag GmbH, Berlin, Juni 2007

[3] DIN EN 15648
Thermisches Spritzen – Bauteilbezogene Verfahrensprüfung
Beuth-Verlag GmbH, Berlin, April 2009

[4] DIN EN ISO 3274
Geometrische Produktspezifikation – Oberflächenbeschaffenheit: Tastschnittverfahren
Nenneigenschaften von Tastschnittgeräten
Beuth-Verlag GmbH, Berlin, April 1998

[5] DIN EN ISO 4287
Geometrische Produktspezifikation – Oberflächenbeschaffenheit: Tastschnitt-verfahren – Benennungen, Definitionen und Kenngrößen der Oberflächenbeschaffenheit
Beuth-Verlag GmbH, Berlin, Juli 2010

[6] Tomschi, U.:
Verschleißverhalten von Trockenlaufwerkstoffen für Abdichtelemente in Kolbenkompressoren
Dissertation Universität Erlangen-Nürnberg, 1995

[7] Feistel, N.:
Dry-running sealing systems in practice – new challenges by new materials
5th EFRC-Conference, Prague, Czech Republic 2007, 51 – 62

[8] Volk, R.:
Rauheitsmessung
Beuth Verlag GmbH, Berlin Wien Zürich, 2005

[9] Kühnert, B.:
Schichtbeurteilung von Kolbenstangen
Unveröffentlichter Bericht von Sulzer Innotec, Winterthur, 2010

Reciprocating Sealing Elements – Importance of Material and Layout

Dr. Marc Langela
STASSKOL GmbH
39418 Staßfurt,
Germany
marc.langela@stasskol.de

8th Conference of the EFRC
September 27th / 28th, 2012, Düsseldorf

Abstract:

In compressor applications sealing elements manufactured from Polytetrafluorethylene (PTFE) and Polyetheretherketone (PEEK) compounds with additives for reinforcement and self-lubrication are frequently used. The life-time of the sealing elements is sometimes the bottleneck towards a sufficient service time between two routine maintenances. In industrial process applications the wear behavior of sealing materials can be strongly influenced by the characteristics of the application. In consequence, choosing the right material is a crucial task for the reliability of compressor systems. In order to do so, parameters like gas composition, dew point and many more have to be considered carefully.

The layout of the sealing elements is the second important parameter in order to maximize the service-time of the compressor operation as well as the reliability of the process. The right choice has to be made out of a broad variety of sealing ring designs in order to maximize the life-time of the spare parts and in order to keep leakage rates down to a minimum value. This also adds to the compressor reliability, especially when dealing with reactive gases.

In order to improve the performances of materials and sealing ring designs, several tribological investigations as well as compressor tests were conducted on compounds with different filler and solid lubricant concentrations. Choosing the right additives is important for optimizing sealing materials and the right concentrations of the additives have to be found. The development of new materials and new layouts and their testing at real-life conditions enables an important process for improving the performance of reciprocating sealing elements and to increase the reliability of reciprocating compressor systems.

1   Introduction

Reciprocating compressors are widely used to compress gaseous media for industrial applications, for example at chemical plants for hydrogenation reactions, polymerizations or Polysilicon productions. These are fully-integrated and automated industrial processes, which are running continuously and therefore a failure in compressor operation can cause unexpected and expensive down-time.

In consequence, the reliability is one of the most important properties of reciprocating compressor systems. The crucial items in respect to reliability are often the spare parts of the bare compressor such as piston rings, guide rings, piston rod packings, intermediate packings and oil wiper packings (see Figure 1 a to d).
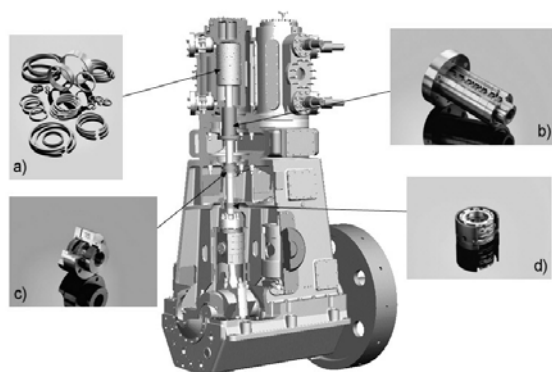
Figure 1: Spare parts of reciprocating compressors

The spare parts especially the sealing elements have to be optimized in respect to sealing efficiency and life-time in order to achieve maximum reliability. This optimization strongly depends on the customer's application as both, the layout of the sealing element and the material of the sealing element has to be tailored to the process parameters of the compressor system. In this paper we will explain the crucial aspects to make the right choice of material and layout.

2   Sealing element layout

At reciprocating compressors sealing elements are used to seal different compression chambers and different gas areas against each other. Thereby the working principle of piston rings as well as of piston rod sealing elements is correlated to the pressure difference between the "high pressure side" and the "low pressure side". The pressure difference is responsible for pushing the sealing element against the wall of the chamber or groove and for sealing against the cylinder wall or piston rod.

The leakage rate can be influenced by the design of the radial cuts as shown for piston rings in Figure 2 and for piston rod sealing rings in Figure 3. At both Figures the gas tightness of the ring design increases from the left side to the right.
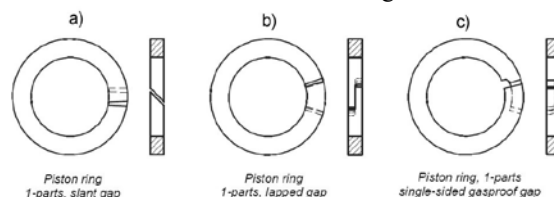

Figure 2: 3 different layouts of piston rings: slant gap (a), overlapped gap (b) and gas-tight (c)
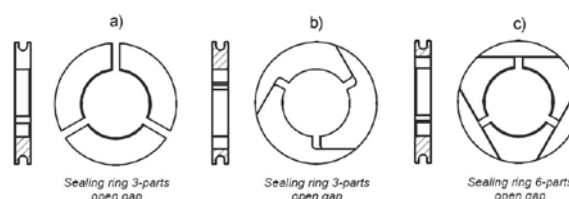

Figure 3: 3 different piston rod sealing rings: 3-piece with radial cut (a), 3 piece with tang. cut (b) and a 6 piece ring design

The choice of the sealing ring layout depends on several operational parameters like the molecular weight of the gas, possible impurities within the gas, suction and discharge pressure, suction and discharge temperature, etc. For example at high pressure applications a gas tight piston ring might not always be the best choice because it will result in a high pressure difference at the first sealing element. High pressure differences will cause high forces of the sealing surface against the cylinder wall as explained above. This high mechanical load together with high frictional energies can cause excessive wear of the sealing material in use. Therefore, it might be better to use a ring design with a certain leakage or a combination of gas tight and non-gas tight piston rings. The same is true for piston rod packings, were a combination of different sealing ring layouts might be the optimum solution.

Another example is a reactive gas like a monomer gas. At these applications a sealing ring layout with an open gap can cause reduced life-time of the sealing elements as the gaps can be filled up by polymer precipitate. The sealing element can no longer adjust to the piston rod and the sealing efficiency decreases.

3 Sealing element material

In most of the applications Polytetrafluorethylene (PTFE) is used as matrix material for the sealing elements. There are several grades available with different fillers and lubricants such as glass fibres, carbon fibres, carbon black, graphite, molybdenum disulfide, etc. Especially at dry-running applications the material composition in dependence of the parameters of the operation is crucial for wear resistance of the material and thus for the life-time of the sealing elements. Wear resistance is never a material property; it's always a property within a tribological system.

The tribological system consists of the sealing material itself, the counter surface material (piston rod or cylinder wall), the process gas and the lubricant (if lubrication is applied). The system is influenced by its operational conditions like temperature, average velocity, pressures, etc. A sealing material can be very good within one tribological system for one application but it might fail in another application where one or more properties or parameters of the tribological system are different. Thus, sealing materials always have to be chosen by taking all aspects of the target application into account in order to maximize life-time and reliability.

As an example, two of the most important parameters are the composition of the gas and its moisture content (dew point). The gas system can be described by a splitting it into oxidizing gases, inert gases and reducing gases which can be wet, dry or bone-dry in respect to their moisture content. The tribological behaviour is influenced by a tribological film that is formed on the counter surface during the operation and this film formation and stability depends on the gas system.

As a result, a broad variety of sealing materials is available at most of the suppliers of sealing elements for reciprocating compressors which are optimized for specific gas systems and it's very important to do the right choice depending on the operating conditions of the compressor.

4 Material development

The development of materials with increased wear resistances is the key for further maximization of the reliability of compressor applications. Sealing materials like Polytetrafluorethylene (PTFE) and Polyetheretherketone (PEEK) can be optimized by tribological characterization of material compositions with different concentrations of fillers and/or lubricants.

For effective material development, it is highly important that the results from tribological testing can be compared to the material performance at the real compressor applications. In general, the transferability of polymer testing into the target application is the pre-dominant factor for optimizing material compositions.

At tribological characterizations, three main factors (*Test Rig Design, Materials* and *Test Conditions*) of the so-called "tribological system" have to be reproduced and designed according to the target application. Therefore, a test rig was developed (see Figure 4) that enables the determination of the wear resistances under reciprocating sliding conditions with parameters that are as close as possible to compressor applications.

Figure 4: Reciprocating tribometer

However, even the most sophisticated experimental setup can never provide 100 % comparability to the "reality of the field". In order to overcome this weakness we also have also to concentrate on other material properties than only on pure wear rates and we have to determine how these properties are interconnected to result in the observed material performances at the compressor applications.

5 Summary

We emphasized the importance of choosing reciprocating sealing elements with the right layout and the right material in order to maximize the performance and the reliability of a reciprocating compressor system. Especially the wear resistance of sealing materials depends on the properties and parameters of the tribological system.

In consequence, layout <u>and</u> materials have to be chosen carefully by taking all aspects of the application into account.

8th Conference of the EFRC
September 27th / 28th, 2012, Düsseldorf

EFRC

EUROPEAN FORUM
for RECIPROCATING
COMPRESSORS

Educating reciprocating compressor engineers at the EFRC

by:

Dr.-Ing. Siegmund V. Cierniak
RWE Deutschland AG
Essen
Germany
Siegmund.Cierniak@RWE.com

Chairman of the EFRC Educating Committee

8th Conference of the EFRC
September 27th / 28th, 2012, Düsseldorf

1 Why do we educate reciprocating compressor engineers?

The design, selection, operation and maintenance of reciprocating compressors makes the education and training of different types of engineers a must. Due to these facts all compressor manufacturers, packagers and end users have a need for highly qualified, educated and skilled engineers. Our branch need now and in the future, well educated and highly motivated graduates from the best universities and colleges.

The EUROPEAN FORUM for RECIPROCATING COMPRESSORS - EFRC is creating co-operation between the members of EFRC, other compressor makers, packagers, subsuppliers users and the well known universities, colleges, institutes and their students.

2 Some examples of these co-operative efforts:

- common supported thesises
- presentations – made by people from companies at the universities
- excursions to workshops and facilities in our branch
- practical work of students in firms
- information about jobs for graduates
- sponsoring of first class results of student's (thesis', etc.)
- realisation of workshops as platform for recent students and graduates
- publication of studies, theses, research work

3 What EFRC members are already doing:

- participating in EFRC promotion committee
- hosting of excursions
- organizing of internships
- sponsoring of events
- subsidizing highly qualified students and graduates

4 Advantages for EFRC members:

- access to qualified engineers
- influence on the education of students
- part time jobs of students

5 Important results of the EFRC activity „Educating reciprocating compressor engineers"

5.1 Autumn 2000: EFRC Workshop "The Netherlands and Belgium"

Picture 1: Professor Will's speech at the Students excursion 2000

Tour on the facilities of

- NEUMAN & ESSER GmbH,
  Übach-Palenberg / Germany

- WÄRTSILÄ Nederland BV,
  Zwolle / The Netherlands

- THOMASSEN Intern. BV,
  Rheden / The Netherlands

- BASF AG,
  Antwerp / Belgium

- TNO Inst. of Applied Physics,
  Delft / The Netherlands

Picture 2: BASF AG, Antwerp / Belgium

5.2 Spring 2002: EFRC Workshop "Northern Germany"

- Natural Gas Underground Storage Kraak (near Schwerin / Germany)
 "HEINGAS Hamburger Gaswerke GmbH" / compressors "ARIEL / HGC"

- Natural Gas Underground Storage Hamburg-Reitbrook
 "HEINGAS Hamburger Gaswerke GmbH" / compressors "ARIEL / HGC"

Picture 3: Workshop participants at the Natural Gas Underground Storage Kraak Germany

Workshop's tasks

A computerized simulation program „Reciprocating Compressors in Natural Gas Underground Storages" > "Selection and sizing"

Picture 4: Tour on the facilities of the Tarnow site Poland

5.3 Spring 2004: EFRC Workshop "Poland"

Beginning of June 2004 the EFRC organized an event which was once again very successful.

Picture 5: Students in front of the lab of the Wroclaw University / Poland

App. 30 students from Austria, Czechia, Germany, Poland and the Netherlands travelled to Poland and visited the universities of Wroclaw and Krakow and its laboratories and also the compressor plants at the natural gas pipeline station of Tarnow and at the natural gas gathering station of Zanok. The participants had a very interesting training course reg. reciprocating compressor technology.

Picture 6: The group of students in front of the Krakow University / Poland

Workshop's tasks

Diagnostics of leaking valves in reciprocating compressors.

5.4 Spring 2006: EFRC Workshop "Switzerland and Italy"

One of the statutory tasks of EFRC is to educate young people to the design operation and management of reciprocating compressors.

In June 2006 EFRC the 4th workshop for students in reciprocating compressors sciences happened. We had a trip to some famous plants.

- Burckhardt Compression AG, Winterthur / Switzerland

- Polymeri Europa S.p.A., Ferrara / Italy

- General Electrics Oil and Gas Nuovo Pignone S.p.A., Firenze / Italy

Picture 7: Tour on the facilities of Burckhardt Compression AG Winterthur / Switzerland

Picture 8: Training of the students in the premises of General Electrics Oil and Gas Nuovo Pignone S.p.A., Florence / Italy

Picture 9: The group of students in the premises of General Electrics Oil and Gas Nuovo Pignone S.p.A. in Florence / Italy

5.5 Spring 2008: EFRC Workshop "Vienna / Austria"

In May 2008 EFRC arranged the 5th Students' workshop, this time in Vienna / Austria.

Picture 10: The group of students in the premises of Leobersdorfer Maschinenfabrik AG Leobersdorf / Austria

The group of students guided by Dr. Siegmund Cierniak / RWE and Andre Eijk / TNO visited the following companies:

- LMF Leobersdorfer Maschinenfabrik AG Leobersdorf / Austria

- Hoerbiger Ventilwerke GmbH & Co KG Vienna / Austria

- BOREALIS Polyolefine GmbH Schwechat / Austria

- OMV Raffinerie AG Schwechat / Austria

Picture 11: The OMV-refinery in Schwechat/
Austria

At the end of the workshop the 25 students from seven different nations (Germany, Switzerland, India, Austria, Poland, England, The Netherlands) were assigned with a theoretical task to develop in the following 4 weeks with the understanding that the three best homeworks would be compensated with a prize.

Picture 12: The group of students, listening to a
presentation in the premises of
HOERBIGE Ventilwerke , Vienna /
Austria

5.6 Spring 2010: EFRC Workshop "United Kingdom"

During the time between May 25 and May 28, 2010 a group of approximately 25 students came over to England and participated in the 6th EFRC Students' workshop.
Due to the fact that all former workshops had been so successful everything went according the well experienced procedures:

- Tour of facilities
- Presentations
- Tasks (home work)

Picture 13: The route of EFRC's Students
Workshop 2010 in the United Kingdom

Picture 14: Down-town Chester the home of
COOK-Compression

Picture 15: Students at LNG-facilities in Isle of
Grain

Picture 16: Isle of Grain (LNG – Terminal)

Students from Poland, Turkey, Austria, Germany, Greece, Holland and England participated in the workshop and visited the LNG-plant Isle of Grain (Burckhardt-compressors), Dresser-Rand, COOK Compression and the Shell-refinery in Stanlow.

257

5. 7   Spring 2012: EFRC Workshop "France"

EFRC created a workshop in France, organized by an EFRC-internal task force.

Picture 17: EFRC task force: Siegmund Cierniak, Christiane Hammer, Ullrich Hesse, André Eijk, Edmond Marchand

May 29, 2012
Charles-de Gaulle-Airport Paris
>meet of all participants (11:00 h)

C-P-I
Bavay

May 30, 2012

HOWDEN
Nogent-sur-Oise

ATLAS CREPELLE
Lille

May 31, 2012
TOTAL Refinery
Le Havre

June 1, 2012
École Nationale Superiéure
Paris
> End of workshop (15:00 h)

A very exiting tour was created with many interesting presentations and as a result we do have to state clearly: all participants were very much satisfied and learnt a lot about the technology of reciprocating compressors.

Picture 18: Students, being happy in Paris

The goal for the attending students was – as all the times - to present a report (home work) to a committee of EFRC members and getting an award and once again very attractive prizes for the 3 best students.

1st prize	A free of charge compressor training course at Ariel's in Mount Vernon /Ohio/USA + a free of charge participating at 2012's EFRC conference in Dusseldorf / Germany
2nd prize	500,00 € cash + a free of charge participating at 2010's EFRC conference in Dusseldorf / Germany
3rd prize	a free of charge participating at 2010's EFRC conference in Dusseldorf / Germany

Evaluations of the individual works were made by EFRC members from Technische Universität Dresden / Germany and RWTH Rheinisch Westfälische Technische Hochschule, Aachen / Germany.

6   Next EFRC Workshop 2012

- Spring 2014 in Ukraine (Україна)

- Details will be published in Fall 2013

7 Prize winners 2012

1st prize

Martin Krieck

e-mail:
martin.krieck@rwth-aachen.de

RWTH Aachen University

Aachen
GERMANY

2nd prize

Martin Sinkwitz

e-mail:
martin.sinkwitz@web.de

RWTH Aachen University

Aachen
GERMANY

3rd prize

Johannes Strecha

e-mail:
johannes.strecha@tuwien.ac.at

Vienna University of Technology

Vienna
AUSTRIA

Temperature Reduction of the Piston Rod
in non-lubricated Piston Compressors by
Internal Cooling

by:

Christiane Hammer, Gotthard Will, Ullrich Hesse

Bitzer-Stiftungsprofessur für Kälte-, Kryo- und Kompressorentechnik

Institut für Energietechnik

Technische Universität Dresden

Dresden

Germany

christiane.hammer@tu-dresden.de

8th Conference of the EFRC
September 27th / 28th, 2012, Düsseldorf

Abstract:

Especially in non-lubricated piston compressors the wear of the piston rod packing rings is a problem that needs to be considered when it comes to the schedule of maintenance and also to the calculation of costs. Due to the demands of high gas pressure and leak-tight sealing the frictional heat of the rings are causing high temperatures in the area of the piston rod packing. High temperatures are – among other factors – one reason for an increase of wear and thus for a lifetime reduction of the packing. To increase this lifetime – and so to increase the time between two technical services – the idea of an internal cooling of the piston rod with a phase changing medium was created at the Technische Universität Dresden (TU Dresden). As a project between the EFRC R&D Working Group and TU Dresden this subject is investigated. Therefor a test bench with a balanced opposed compressor by Leobersdorfer Maschinenfabrik (LMF) was set up and measurements shall be taken. Also with the help of a model test rig fundamental research on heat transfer of a fluid inside a filled oscillating cavity are made and are validated with a thermal ANSYS simulation.

EFRC

Temperature Reduction of the Piston Rod in non-lubricated Piston Compressors by Internal Cooling,
Christiane Hammer, Gotthard Will, Ullrich Hesse; TECHNISCHE UNIVERSITÄT DRESDEN

1   Introduction

Nowadays the demand of non-lubricated piston compressors is bigger than ever before. It is not possible to imagine the pharmaceutical, chemical and food industry without these types of compressors. The delivery of gas with high purity at high pressures is only possible with non-lubricated pistons and packings. So several components have much higher temperatures compared to the ones in lubricated compressors due to higher friction and the omission of the cooling effect of the lubricant.

Especially the piston rod packing heats up enormously because of the friction with the piston rod. These high temperatures lead to a reduction of the lifetime of the packing elements. So the task for every manufacturer and scientist that works on the subject of non-lubricated piston compressors is to reduce influences on the packing, rider rings the piston rings that enlarge the possibility of an early wear and failure of the sealing components. To define this radial wear Δr the approach of Kriegel[3] is used according to equation (1) and (2):

$$\Delta r = L \cdot \overline{p_r} \cdot K \qquad (1)$$

$$K = K_0 \cdot K_T \cdot K_C \cdot K_R \cdot K_\varphi \qquad (2)$$

Here factor K_0 is a characteristic value for the material at reference conditions. The other factors depend on the reference conditions itself: temperature of the sliding path T, average piston speed c_m, roughness of the sliding path R and dew point of the working medium φ. So the goal of research must be to reduce every factor to its minimum. In fact, we cannot change the type of gas. Also, the speed is given in most cases because of the drive. During the last decades there was a lot of optimization about the roughness of the sliding path. The result was, that too rough is negative and also to smooth is negative, so here an optimum range was found. So that last factor is the temperature.

A lot of research was made within the last years to develop cooling concepts for the piston rings and packing. These arrangements include mainly cooling channels inside the housing of the packing or cylinder that lead to a better heat transfer from the sealing elements to the surrounding. Also other ideas came up from several manufacturers. They all have the same problem: a separate cooling cycle is necessary for the compressor. This means: more costs, more parts, problems of leakage of the cooling medium, problems with plugging of the pipes and so on. All of these issues led to the development of a new patent for the reductions of the piston rod temperature.

2   Principle of Internal Cooling

2.1   Basic Idea

At the Technische Universität Dresden a concept was created with the focus on piston and piston rod cooling of reciprocating compressors oscillating and translational movement of the piston and the piston rod[5].   Figure 1 shows the basic setup of the idea of the cooling system:
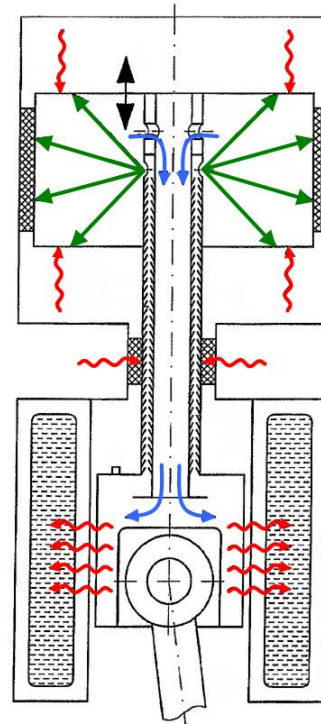

Figure 1: Patent idea: Cooling Device for Piston compressors[5]

Piston, piston rod and cross head are designed with internal cavities, which are connected to each other. Enclosed inside this cavity is a working fluid for the transport of heat. This leads to an efficient heat transport between the hot parts (piston and upper part of the piston rod) and the colder crosshead.

In the figure above the rod is divided into two parts: one channel for the liquid and one channel for the vapour. This shows only one possibility of the internal setup (here with internal structures). Other options are: just one channel (basic and most simple construction) and also constructions with check valves that should support the direction of the fluid flow. For the transport of the liquid a new heat pipe type is employed which will be explained in chapter 2.2.

Temperature Reduction of the Piston Rod in non-lubricated Piston Compressors by Internal Cooling,
Christiane Hammer, Gotthard Will, Ullrich Hesse; TECHNISCHE UNIVERSITÄT DRESDEN

2.2 Principle of Operation

For this new principle for a temperature reduction of the piston rod and the piston an old knowledge is used. The function of a heat pipe should be explained with the help of figure 2:
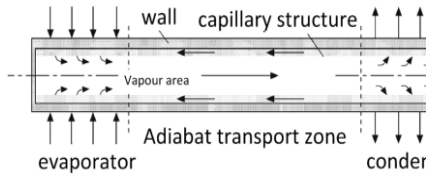

Figure 2: Setup of a heat pipe [6]

A heat pipe is a heat exchanger with high effect. A liquid medium is transported to an area of high temperatures and evaporates. The resulting vapour flows back to the "cold end" of the heat pipe and condenses. So the cycle is closed and can start anew. Due to the fact that vapours always flow to a colder area because of its physics, the only "critical" factor is the transport of the liquid to the "hot end". In most heat pipes this is done by capillary structures (see figure 2). The liquid is transported by the capillary forces in most cases at the internal wall of the heat pipe. Between the evaporator and condenser is – in most cases – the adiabatic transport zone. Heat pipes have the advantages of a huge heat transport capability (also at small temperature differences), short reaction time and a compact and simple construction. The array of application is from temperatures of 5 K to 2200 K.

2.3 Construction for non-lubricated compressors

So the heat pipe effect is an efficient method for the application in the non-lubricated compressor industry. The difference between the described "basic" heat pipe and the principle that is used in the patent is that there are no capillary structures. In reciprocating piston compressors there is no need for capillary forces due to the fact that the movement of the piston and the acceleration itself transports the liquid working medium to the hot areas. [5]

The focus of the patent is the piston and piston rod cooling. But to keep the challenge in a frame that is feasible it was decides to concentrate the investigation to the Temperature Reduction of the Piston Rod. The on-going project is financed by the EFRC R&D Working Group. The investigation includes an examination of a real compressor system designed by LMF, which is a balanced opposed compressor. As an additional idea of the TU Dresden a model test rig was set up where basic investigations of the internal heat transport

coefficient are made. The evaluation of the measurements will be supported by the simulation tool ANSYS.

3 Model Test Rig "Alpha"

3.1 Motivation and Construction

A real compressor system including the piston, piston rod, sealing elements and cross head is only hardly accessible for measurements. Due to the fact that the piston rod moves back and forth and rubs against the sealing elements a direct temperature measurement is rather difficult. There are several ways of measuring the piston rod temperature indirectly, but the accuracy of these results is controversial[1]. Also a definition of the frictional heat input of every sealing element and the amount of heat that flows into the sealing element or the opposite metal is hard to find.

That is the reason why pre-investigations are made with the help of a model test rig "Alpha". These experiments deal with the thermal impact of a piston rod that is designed as a heat pipe with an accurate measurement of the temperatures.

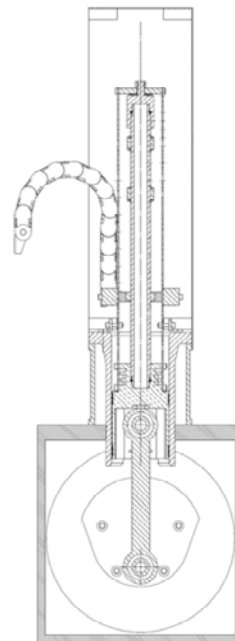A crankshaft driving mechanism was used for the construction of test rig "Alpha":

Figure 3: Section View of Test Rig "Alpha"

The pipe is driven by an engine with a variable speed up to 600 min^{-1}. The stroke of the driving mechanism is 100 mm. Because of the weight the pipe is made of titanium with an external diameter of 35 mm and an internal diameter of about 24 mm. At an interval of 30 mm thermocouples measure the temperature of the pipe in a depth of 2 mm. Also two mantled thermocouples are placed inside the

EFRC

Temperature Reduction of the Piston Rod in non-lubricated Piston Compressors by Internal Cooling,
Christiane Hammer, Gotthard Will, Ullrich Hesse; TECHNISCHE UNIVERSITÄT DRESDEN

cavity for the detection of the internal temperatures of the working fluid. Due to the fact that a measurement with sealing elements leads to the problems that were already mentioned, the heat input of the packing and the working chamber are simulated by two heating devices in the upper third of the titanium pipe.

The heating devices are mounted to the pipe and create the typical heat input of the packing and piston rings. The challenge of a direct measurement in a moving system could be solved with the help of a so called energy chain by igus® that is mounted on a guidance of the pipe. Here the cables of the heating devices and the thermocouples are guided in defined chambers inside this energy chain. So the mechanical stress produced by the movement of the pipe is no longer a problem for the cables. The final set up of test rig "Alpha" is shown in figure 4.
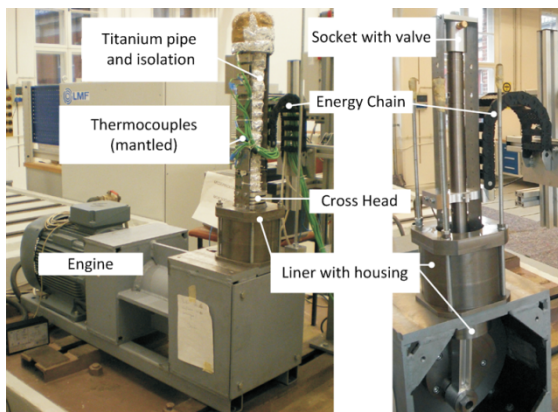
Figure 4: Set up Model Test Rig "Alpha"

The pipe itself is mounted at the bottom to the crosshead that was designed especially for this test rig. A socket with a valve for evacuation and filling of the pipe is mounted to the upper end.

To adjust the heat input of the heating devices an adjustable transformer is used. The pipe is completely isolated so that the heat loss can be minimized. This is really important for the evaluation of the measurements. As described the heat input is defined, furthermore there is a heat flow to the upper and the lower part of the pipe and also inside the cavity. These temperatures are measurable and so the heat flow can be defined. A difficulty is the heat loss to the surrounding. To make this as low as possible an effective isolation was installed and the temperatures on the outside surface are measured directly after stopping of the machine.

3.2 Results and Perception

The first stage of the experiments with test rig "Alpha" was the determination of the heat transfer coefficient at the outside of the isolated pipe. During these tests there was only air inside the pipe. Air is one of the worst heat conductors so the influence of the heat transfer inside the pipe is neglected. The measurements of the temperatures of the pipe, inside the pipe and on the outside of the isolation were taken at different speeds and different heat input. The results were evaluated with the help of a steady state thermal ANSYS simulation that will be explained in chapter 4.2. The next step was the use of a medium that has a better heat transport efficiency. The concept should be realized in all different types of reciprocating compressors, so – in best case – the use of a non-dangerous working fluid is desired. The first guess was a water-air mixture. A certain amount of water was filled into the titanium pipe and the measurements started once again with different speeds and different heat inputs. The result of such a measurement is shown in figure 5.
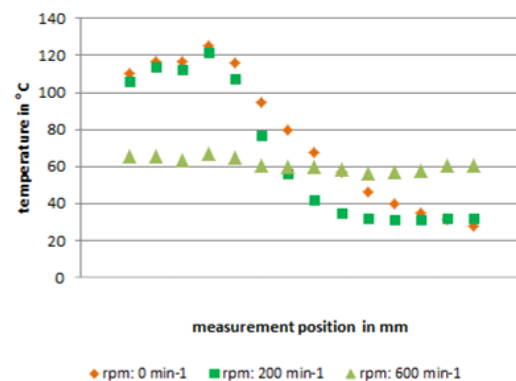

Figure 5: Measurement Test Rig "Alpha", internal cooling with water-air-mixture[3]

The two locations of heat input can easily be seen. At downtime the highest temperatures were recorded. The effect of the cooling is only small at a small speed of 200 min^{-1}. This leads to the assumption, that there is a certain range of speed of compressors where the cooling effect doesn't work in an efficient way and that the cooling is dependant from the acceleration of the piston rod. At 600 min^{-1} the internal cooling works perfectly. The high temperature levels do not exist anymore but there is almost a constant temperature along the pipe.

EFRC

Temperature Reduction of the Piston Rod in non-lubricated Piston Compressors by Internal Cooling,
Christiane Hammer, Gotthard Will, Ullrich Hesse; TECHNISCHE UNIVERSITÄT DRESDEN

4   Calculation of the temperature distribution

4.1   Model test Rig "Alpha"

For a detailed description of the temperature conditions inside the pipe and on the surface of the pipe a coupling of measured values and calculation is necessary. The analysis was made with a steady state thermal ANSYS simulation.

This analysis was made step by step – once with the user interface ANSYS Workbench, which is a graphical interface and with ANSYS APDL[2], a computer language based ANSYS version. Working with ANSYS APDL allows a much easier definition of suitable parameters. Although the handling seems – at a first glance – more complicated than with ANSYS Workbench, it was recommended to use this way for solving the calculation because the interaction with the ANSYS program via "batch files" is possible.

Due to the fact that almost every component of test rig "Alpha" is rotationally symmetric, a 2D-calculation is possible. This leads to much smaller calculation time and thus it is possible to set a finer grid for the calculation. So the first step was to transfer the 3D-construction into a 2D-model for the calculation (see figure 6).
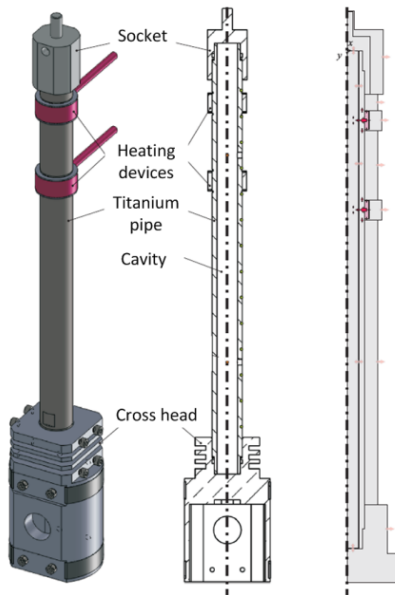
Figure 6: Transfer 3D-model to 2D-model[2]

With the originated 2D-model, a steady state calculation was possible to simulate the thermal conditions of the model test rig and to define the heat transfer coefficients inside and outside the titanium pipe.

The first step for the simulation was the examination of the heat transfer coefficient on the outside of the isolation of the pipe at different speeds and heat inputs. The assumption was made that – at similar temperatures on the surface – the heat transfer coefficient on the outside is independent from the temperature difference between the surface and the surrounding (see [4]). So if the heat transfer coefficient on the outside of the pipe is known, future changes of the temperature of the pipe surface can be affiliated to the effect of the heat pipe – which means the internal heat transfer coefficient.
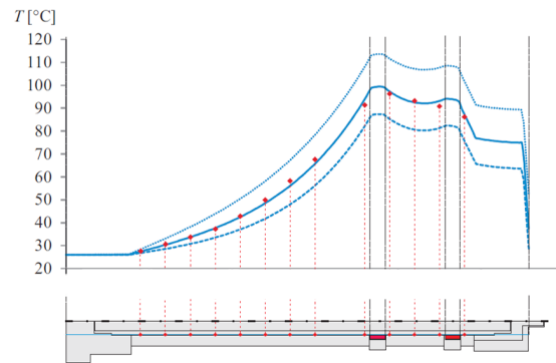

Figure 7: Evaluation of external heat transfer Coefficient by parameter study[2]

With the help of the measured values and a parameter study it was possible to detect the correct heat transfer coefficients on the outside of the pipe (see figure 7).

With this knowledge it is now possible to evaluate the processes inside the pipe.

4.2   Process Gas Compressor

A balanced opposed compressor by Leobersdorfer Maschinenfabrik (LMF) was set up at the TU Dresden to evaluate the cooling method at a real system (see figure 8 and 9).
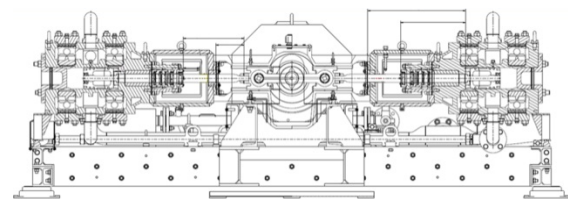

Figure 8: Section View: Balanced opposed compressor (LMF)

The compressor is a 1-stage, double acting machine with two cylinders.

It is set up with temperature and pressure sensors in the suction, discharge and working chambers.

EFRC

Temperature Reduction of the Piston Rod in non-lubricated Piston Compressors by Internal Cooling,
Christiane Hammer, Gotthard Will, Ullrich Hesse; TECHNISCHE UNIVERSITÄT DRESDEN

Figure 9: Balanced opposed compressor

The packing is constructed and provided by Stasskol. Here the temperatures and pressures after each sealing ring and the temperature measurement of the piston rod with a method developed by STASSKOL are detectable. Also the temperature of the oil surrounding the crosshead and the leakage and discharge gas can be measured.

At the time of the submission of this paper no measured data were available. So only the theoretical part of the simulation will be described in the next passage.

Also for the simulation of the thermal behaviour of the balanced opposed compressor ANSYS APDL was used. In this case a transient thermal simulation was set up. A transient calculation was chosen because of the assumption that the fast periodic changes of frictional heat – owed to the changing pressure inside the sealing chambers – would lead to a transient behaviour of the surface temperature of the piston rod.

Once again the 3D-model was transferred into a 2D-model with a rotationally symmetric calculation. With the help of a calculation of the conditions inside the working chamber and first assumptions about the impact of the sealing elements and their frictional heat an excel-sheet was prepared as an input list for the transient boundary conditions of the piston rod.
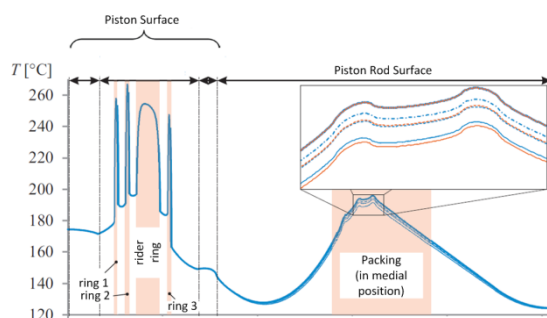
Figure 10: Transient Thermal Simulation balanced opposed compressor[2]

In this case no frictional heat was calculated in ANSYS but the assumed amount of heat that is produced by the friction is an input value (area related heat q) for the transient simulation. Within the scope of a student work also the influence of the grid structure was considered which has large impact on the accuracy of the calculated values and the calculation time.

The programmed batch file makes it possible to define a value for the distance between the calculated crankshaft angle and the number of periods that should be calculated. In figure 10 the results of a transient simulation of the surface temperature of the piston and the piston rod at 1450 min^{-1} and a discharge pressure of 3 bar is shown (with different grid sizes).

To reduce the calculation time it is necessary to define the starting values of each node as close as possible to the stationary end condition. After several simulations with an optimized net it was found out that the transient calculation is not necessary if the starting conditions and the averaged boundary conditions are as close as possible to reality. The effect of the transient boundary conditions on the temperature gradient in radial direction within the first millimetres is smaller than ever imagined because of the heat conduction and inertia of the piston rod material.

5   Conclusion

The method of an internal cooling constitutes an efficient and simple constructible way of a temperature reduction of the piston rod. Because of the lower slipway temperature an increase of the lifetime of the sealing elements inside the packing is not far to seek. Within a research project several investigations are taken. Two test rigs were set up for measurements and the results are evaluated by the FEM software ANSYS. So the influence of several parameters can be evaluated and so an outlook for other machine types or boundary conditions can be made in the future.

6   Acknowledgements

_____

EFRC

Temperature Reduction of the Piston Rod in non-lubricated Piston Compressors by Internal Cooling,
Christiane Hammer, Gotthard Will, Ullrich Hesse; TECHNISCHE UNIVERSITÄT DRESDEN

[1]Feistel, N.: Comparative measurements of the
piston rod surface temperature during operation;
2nd symposium EFRC; 2001

[2]Klotsche, K.: Simulation stationärer und
instationärer Wärmeleitung und Wärmeübergang
in der Kolbenstange zur Bestimmung der
Kolbenstangentemperatur mit ANSYS; Großer
Beleg; TU Dresden; 2012

[3]Kriegel, G.: Beitrag zur Berechnung des
Radialverschleißes von Trockenlaufkolbenringen.
Dissertation Technische Universität Dresden,
1977

[4]Lindner-Silvester,T.: Advances in fundamental
understanding of the dynamic sealing action in
packing systems; 5th EFRC Conference; 2007

[5]Patent DE 10 2007 00 652 A1

[6]VDI Wärmeatlas, 10. Auflage; 2006

Compressor Foundation Analysis Tool (COFANTO)

by:

André Eijk, TNO Fluid Dynamics
Sven Lentzen, Flavio Galanti, Bruno Coelho, TNO Structural Dynamics
Delft, The Netherlands
(andre.eijk@tno.nl)
(sven.lentzen@tno.nl)
(bruno.zuadacoelho@tno.nl)

8th Conference of the EFRC
September 27th / 28th, 2012, Düsseldorf

Abstract:

Reciprocating compressors are generally supported on a heavy concrete foundation. In spite of the large inertia and stiffness of the foundation, problems can occur due to interaction between the mechanical installation and the foundation. Two types of problems may occur. In the first type, the interaction is such that excessive vibration levels occur in the entire concrete structure including compressor frame, cylinders, dampers and piping that can lead to alignment problems and unallowable crankcase deformations.

In the second type, failure of the connections between compressor and foundation may occur due to poor design. These problems have often been identified after construction of the plant.

Foundations for reciprocating compressors are different than for rotating compressors (high speed, small rotating unbalance) and it appeared that the design of foundations for reciprocating compressors was at a poor level the last 20 years. The new generation of designers exhibits limited experience in the dynamic design of foundations, especially for reciprocating compressors. In most of the designs the soil-structure interaction is not included, even though it can have a large effect on the dynamic design. It is also known that existing foundations are used for new larger compressors without adjusting the foundation and has often led to vibration problems and failures of foundation and compressor system components.

Within the R&D group of the EFRC a simple tool has been developed to check the preliminary or existing design of a reciprocating compressor foundation with respect to dynamic loads in an early stage of the project. This tool enables the plant commissioner to perform a check without repeating the detailed analyses already carried out by the design engineers.

The paper focuses on the theoretical background of the program, especially the soil foundation interaction and comparison with field measurements is presented.

Compressor Foundation Analysis Tool (COFANTO), *André Eijk, Sven Lentzen, Flavio Galanti, Bruno Coelho;*
TNO – FLUID DYNAMICS, TNO - STRUCTURAL DYNAMICS

1   Introduction

Reciprocating compressors are generally supported on a heavy concrete foundation. The design of such a foundation is carried out by a civil engineer, following the calculations of the dynamic loads generated by the compressor and driver.
In spite of the large inertia and stiffness of the foundation, problems can occur due to interaction between the mechanical installation and the foundation. Two types of problems may occur. In the first type, the interaction is such that excessive vibration levels occur in the entire concrete structure including frame, cylinders, dampers and piping which can lead to alignment problems and unallowable crankcase deformations. In the second type, failure of the connections between compressor and foundation may occur due to poor design. These problems have often been identified after the construction of the plant.

Foundations for reciprocating compressors are different than for rotating compressors (high speed, small rotating unbalance) and it appears that the design of foundations for reciprocating compressors has been performed at a poor level the last 20 years.

The new generation of designers exhibits limited experience in the dynamic design of foundations, especially for reciprocating compressors. In most of the designs the soil-structure interaction is not included, even though it can have a large effect on the dynamic design. It is also known that existing foundations are used for new larger compressors without adjusting the foundation that has regularly led to vibration problems.

In a paper published during the EFRC conference in Antwerp[1], it was shown that placing a new compressor on an existing foundation has led to an overloading of the foundation. This was caused by the fact that not all relevant dynamic parameters were included in the calculations of the existing foundation for the new compressor.

To solve this problem a rigorous, expensive and time consuming modification of the concrete foundation was necessary to decrease the dynamic loads on the system, see also photo in figure 1. These kind of problems should be avoided in a very early stage of the project.

The design of foundations of reciprocating compressors becomes more and more important due to:
- operation at higher speeds leading to higher unbalanced loads,

- more compressors operating at larger speed ranges; higher change on excitation of natural frequencies,
- more compressors operating at variable process conditions; e.g. compressors used for underground gas storage systems have more fluctuating dynamic loads,
- more compressors running at higher power leading to higher unbalanced loads, and
- hyper compressor installations which require special attention due to the rather high unbalanced loads.

For that reason the research group of the EFRC has initiated a project to develop a compressor foundation analysis tool program, named COFANTO to provide the plant commissioner and the OEM of reciprocating compressors a simple and easy to use tool to check the preliminary or existing design of a reciprocating compressor foundation with respect to dynamic loads in an early stage of the project. This tool should enable the plant commissioner to perform a check without repeating the detailed analyses carried out already by the design engineers.

Figure 1: Modification of foundation

2   Calculation tool COFANTO

2.1   Introduction

COFANTO is a program for carrying out a simplified dynamic response analysis of a compressor and its foundation. The program serves as a tool to check whether the design of a compressor foundation is susceptible to excessive vibrations during operation of the compressor. The tool is recommended to be used by those who intend to install a compressor and who want to verify whether the combination of selected compressor and foundation is feasible. It is used to predict the vibration levels indicatively and by no means it is intended for the actual design of foundations nor as a substitute for the required engineering calculations.
Basic machine configurations can be selected in combination with either a mat foundation or pile

EFRC

Compressor Foundation Analysis Tool (COFANTO), *André Eijk, Sven Lentzen, Flavio Galanti, Bruno Coelho;*
TNO – FLUID DYNAMICS, TNO - STRUCTURAL DYNAMICS

foundation. The machine can consist of a separate driver and compressor, both of which are connected to the same foundation block. Loads are specified for each operating speed either in terms of a time history over a single cycle or as amplitudes for each harmonic of the operating speed. The program calculates the vibration response of the compressor, driver and foundation in terms of displacement, velocity and accelerations for each specified load case. The program generates graphs of the time history of the response as well as a summary containing the maximum, minimum, peak-peak, mean and r.m.s. values. These values can be compared with recommended threshold values, e.g. EFRC Guidelines for vibrations in reciprocating compressor systems[2].

The tool is assembled from existing soil/ground interaction software and models that have been developed by TNO in earlier projects on the dynamics of soil. In these projects the dynamics of soil has been based on Wolf's[3] theory and has been proved to be a good approach. The tool has been developed for slab type foundations and for foundation mounted on piles, including soil structure interaction effects and dynamic impedance functions describing a frequency dependent soil/foundation response. Simple mass-damper-spring-dashpot systems can be included to describe various parts or modes of vibration of the foundation/compressor system.

The final result of the check is that one of the following flags is assigned to the foundation: correct, marginal or wrong. If the design is marginal or wrong, it is advised to carry out detailed calculations to check the design into more detail.

2.2   Theory of underlying model

2.2.1   Spring-mass-damper model

The underlying model is based on multiple spring-mass-damper systems, see Figure 2.
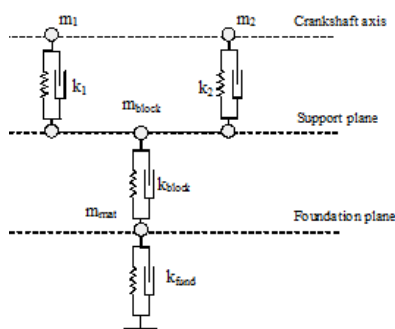
Figure 2: Basic model of machine and foundation

Each node in the model exhibits six degrees of freedom, namely three translations and three rotations. Therefore, for the machine and the driver a mass matrix is assumed containing the mass in the three translational directions and the moment of inertia computed for each rotational direction.

As the machine and the driver are not necessarily positioned at the Centre Of Mass (COM) of the block or the mat (depending on whether a block is present), a rigid link between the contact point and the COM of the block or the mat is introduced. Therefore an additional node is introduced at the contact point. The rigid links translates the translation and rotation of the COM of the block or mat into a motion of the contact point.

It is further possible to model anti-vibration mounts (AVM's) between the machine and block or mat and between the driver and block or mat. The anti-vibration mounts can be modelled as translational and rotational springs and viscous dampers. The viscous dampers are assumed to be hysteretic, which makes it possible to model a constant damping factor in the whole frequency domain of interest.

The block can be isolated from the mat by springs and dampers as well. It is also possible to replace the block (and possibly the isolation) by a table top. The table top consist of a rigid mass including moments of inertia. The legs of the table top are summarised into one spring stiffness and damping ratio for the translations and rotations of all three directions.

Finally, the machine and the driver (and possibly including block or table top) are supported by the mat. The mat is modelled as a rigid mass with the appropriate moments of inertia.

2.2.2   The foundation

The mat serves as a foundation for the machine and it is supported by the soil and in certain cases also by piles. The system soil/piles can be replaced by a single spring-damper system for the translation and rotation in all three directions. Alternatively the point compliance transfer function (for all translations and rotations) of the soil with piles can be determined according to the models described by Wolf[3]. Since the Wolf-model delivers the dynamic behaviour in the frequency domain, the total simulation is performed in the frequency domain, where the spring-mass-damper system of paragraph 2.2.1 is connected to the Wolf-model in series. In the following the principle of the Wolf-model is explained. For further detailed information on the model the reader is referred to[3].

The Wolf-model is based on the assumption that the mechanical behaviour of a disk, of any shape, on a half-space, see figure 3, can be modelled by a circular disk on an infinite cone as shown in

EFRC

Compressor Foundation Analysis Tool (COFANTO), *André Eijk, Sven Lentzen, Flavio Galanti, Bruno Coelho;*
TNO – FLUID DYNAMICS, TNO - STRUCTURAL DYNAMICS

figure 4. An elaborate discussion on the foundations of this assumption can be found in[5] and[6].

The opening angle and the cut of the cone can be determined depending on the disk geometry and the soil characteristics. The determination is performed such that the wave behaviour in the cone-model represents the wave behaviour in the half-space, taking into consideration for instance the reflections on the boundaries of the layers.
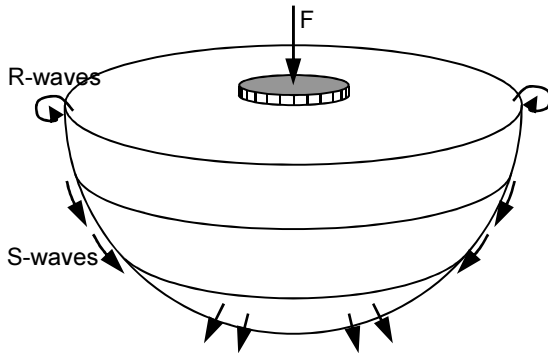
Figure 3: Excited disk on a half-space generating compressive (P), shear (S) and Rayleigh (R) waves
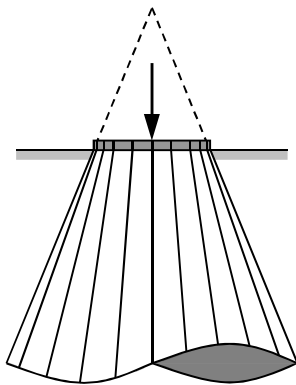
Figure 4: Infinite cone model describing the mechanical behaviour of a half-space

It is therefore also possible to replace a layered half-space with a cone-model. The advantage of using a cone-model can be found in the simplified analytical solution based on a one-dimensional rod theory.

In order to model piles in a half-space it is important to initially consider a disk enclosed in the half-space, see figure 5.
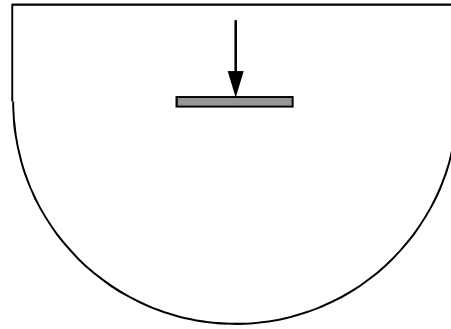
Figure 5: Excited disk enclosed by a half-space

The excited disk generates waves that are reflected from the free surface. It is therefore important to replace the half-space with a double cone-model to incorporate the reflections as shown in figure 6.
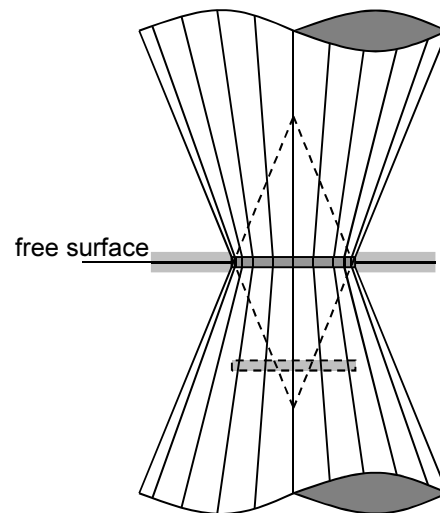
Figure 6: Infinite double cone model describing the mechanical behaviour of an excited disk embedded in a half-space

As the embedded disk is assumed to be infinitesimally thin, an embedded pile or rod can be modelled by connecting a series of embedded disks.

To analyse the dynamic behaviour of a group of piles with their heads connected by a rigid cap (the mat) and with vertical axes, the interaction of the individual piles via the soil has to be taken into consideration. It is for instance incorrect to add the dynamic stiffnesses of the individual piles in order to obtain the dynamic stiffness of the pile group. While forcing one pile down, other piles will follow. Therefore while forcing all piles simultaneously, the pile displacement is larger than predicted with simply adding the stiffnesses.

In [7] and [8] it has been discussed that the pile-soil-pile interaction, which is strongly frequency dependent, can be accurately incorporated into the cone-model concept by incorporating so-called dynamic-interaction factors. These interaction factors are always determined between two piles.

While the source-pile (s) is dynamically excited, the response of both piles is determined using wave analysis, and the ratio between the response of the receiver-pile (r) and the source-pile describes the interaction factors.
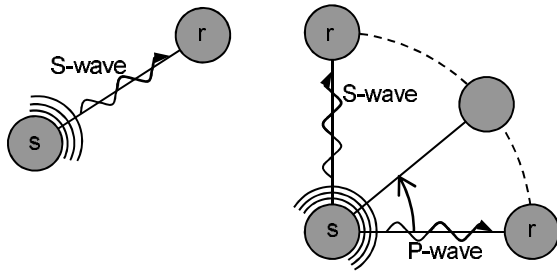

Figure 7: Cylindrical waves emitted from the source pile and propagating towards the receiver (left: vertical waves, right: horizontal waves)

In figure 7, the source- and the receiver-pile are shown from above. It can be seen that the source-pile emits shear and compressive waves which interact with the receiver-pile. For the vertical movements only shear waves are responsible for the pile-interaction. The interaction factor does not depend on the relative angle between the piles, but rather on the distance between them.

On the right side of figure 7, the waves responsible for the horizontal interaction are shown. Considering the motion left-right motion (relative to the illustration) it can be seen that the compressive waves are responsible for the interaction when the relative location of the receiver-pile is in the direction of the motion. When the relative position of the receiver-pile is perpendicular to the motion, then the shear waves are responsible for the interaction. For the horizontal coupling, thus, the relative angle between the receiver- and the source-pile is an influencing factor.

When all interaction factors between all the possible combinations of pile-pairs are computed, and when the dynamic-stiffness coefficients of the single piles are known, the dynamic-stiffness matrix for harmonic loading of the pile group can be determined using the standard matrix formulation of structural analysis.

2.2.3   Check of the Wolfs model

The Wolf model was validated by means of comparison with a Finite Element Model (FEM) calculation. The Finite Element Model is built with 20 node brick elements, whereas infinite elements are used for the boundaries, in order to minimize wave reflection. A linear elastic formulation is adopted for the material behaviour, and the damping is assumed to be hysteretic. The system of equations is solved in the frequency domain.

The test case consists of 4 different layers of soil combined with a compressor mounted on a concrete slab with pile foundation. The finite element model is shown in figure 8.
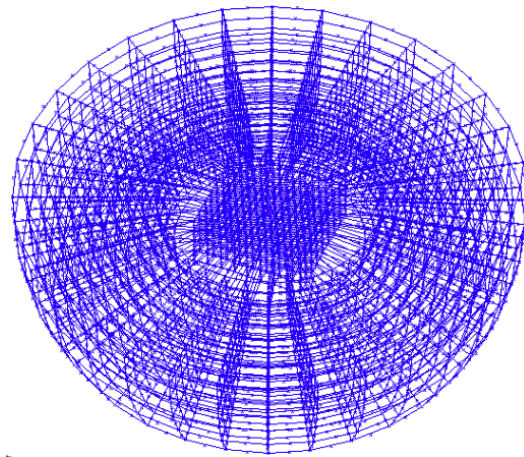

Figure 8: Finite element model

Figure 9 presents the comparison between the results of the horizontal compliance for the two models. It can be concluded that a good agreement is found for both models in all directions. The peak occurs at a similar frequency with a similar response. The static response (as the frequency tends towards zero) is also in agreement.
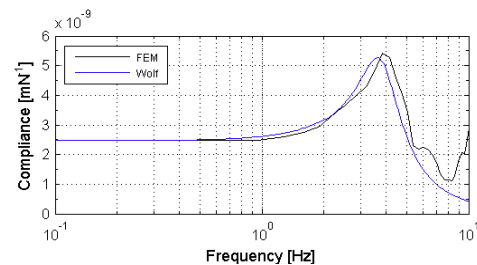

Figure 9: Comparison of horizontal compliance between Wolf and FEM model

2.3   Program structure

The core of the program is developed in MATLAB and a GUI (Graphical User Interface) is developed specially to control the core. The GUI has the following main functions: geometry input, loads definition, calculation control and output. In the following subchapters each of the main functions is described in detail.

2.3.1   Model input

The available components to build the model have are grouped as follows, see also figure 10:
1. Machine: compressor and driver
2. Interface: rigid or flexible
3. Support: none, block, block on flexible elements and table top
4. Foundation: pile or mat

EFRC

Compressor Foundation Analysis Tool (COFANTO), *André Eijk, Sven Lentzen, Flavio Galanti, Bruno Coelho;*
TNO – FLUID DYNAMICS, TNO - STRUCTURAL DYNAMICS

The input parameters for each of the different components are:

Machine:
- Total mass
- Mass moments of inertia in 3 directions
- Position in the X, Y and Z direction

Interface
- Translation and rotation spring stiffness in 3 directions
- Damping ratio

Block support
- Position in the X, Y and Z direction
- Density
- Mass moments of inertia in 3 directions

Table top support
- Young's modulus
- Width of columns
- Cross section area
- Number of columns
- Column length
- Damping ratio

Mat
- Dimensions
- Density

Springs
- Translation and rotation spring stiffness in 3 directions
- Damping ratio

Piles
- Young's modulus
- Cross section diameter
- Length
- Density
- Number of piles
- Position 3 directions

Soil
- Number of layers
- Shear modulus
- Density
- Poisson's ratio
- Damping ratio
- Thickness
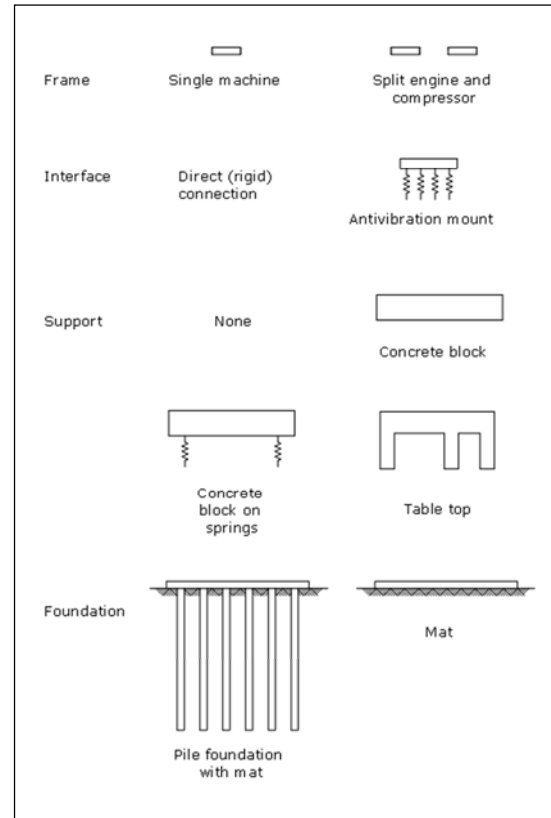
Figure 10: Available components
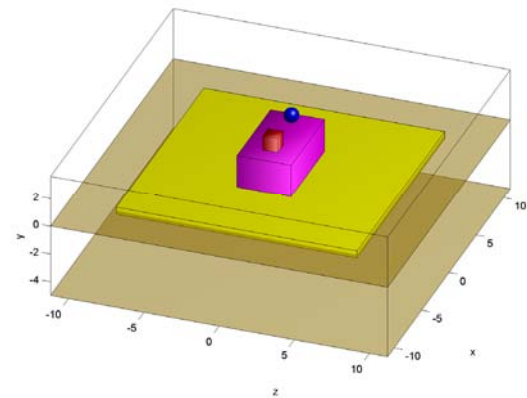
Figure 11: Example of a COFANTO model

2.3.2 Load input

A number of load cases can be considered which can be specified either in the frequency or in the time domain. Loads can be specified acting from the compressor as well as from the driver. In both cases the loads are assumed to act in the centre of mass (COM) of the respected component. Other loads, e.g. pulsation-induced forces, can also be considered but in that case these loads should be "converted" to act in the COM of the compressor or driver.

Compressor Foundation Analysis Tool (COFANTO), *André Eijk, Sven Lentzen, Flavio Galanti, Bruno Coelho;*
TNO – FLUID DYNAMICS, TNO - STRUCTURAL DYNAMICS

2.3.3   Results Output

The results will be presented both in tabular and graphical form. The generated text file will contain the results of the vibration displacement, vibration velocity and vibration acceleration levels in maximum, minimum, mean, peak-to-peak and r.m.s. (root means square) values. The r.m.s. values will be compared with a specified criterion, e.g. "EFRC Guidelines for Vibrations in Reciprocating Compressor Systems"[2]

Further on the results file will contain the reaction loads on the support block if present. Otherwise these are the loads applied on the mat.

In the final part of the analysis, the user has the opportunity to inspect the response in a graphical way. Graphs are available with mechanical natural frequencies, time wave form of the input loads, reaction loads, vibration displacement, vibration velocity and vibration acceleration levels of which an example is shown in figure 12.
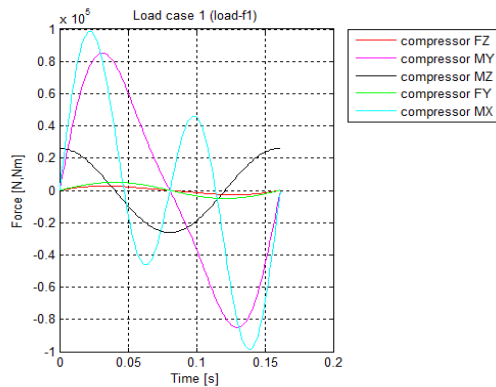
Figure 12: Example of a loads time waveform

3   Validation models

3.1   Introduction

To check the results of the program, two test cases has been carried out. For both test cases, vibration measurements have been carried out in the field for both test cases on a reciprocating compressor system.

3.1.1   Test case 1

System description:
- 3-stage compressor with 3 cylinders and one dummy
- E-motor drive: 2759 Kw
- Fixed speed of 495 rpm (8.25 Hz)
- Compressor and driver mounted on a block
- Block mounted on mat
- Mat mounted on concrete piles
- Input forces: compressor unbalanced forces of 1 and 2 times compressor speed

The COFANTO model is shown in figure 13.
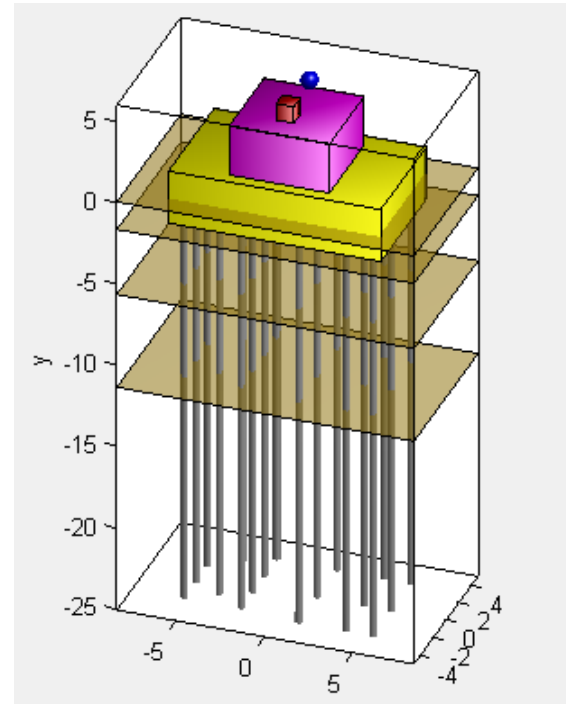
Figure 13: COFANTO Model (Red: machine, blue: driver, magenta: block, yellow: mat, grey: piles, brown: soil layer surfaces)

Discussion of results

The compliance transfer function on the block in the rod direction is shown in figure 14. From this figure it can be concluded that a mechanical natural frequency does not coincide with the frequency of the excitation loads of one (8.25 Hz) and two (16.5 Hz) times the compressor speed.

A picture with the maximum calculated peak-to-peak vibration displacement of the block is shown in figure 15. The maximum calculated vibration displacement of 0.035 mm peak-to-peak is in the rod direction and is caused by the unbalanced moment in the horizontal plane (moment around the vertical axis) of one time the compressor speed. This value is within the A/B evaluation zone of the EFRC Guidelines. This means that as a result of the COFANTO calculations the foundation should be flagged "correct" which is also according to the field experience because no problems have been encountered.

Compressor Foundation Analysis Tool (COFANTO), *André Eijk, Sven Lentzen, Flavio Galanti, Bruno Coelho;*
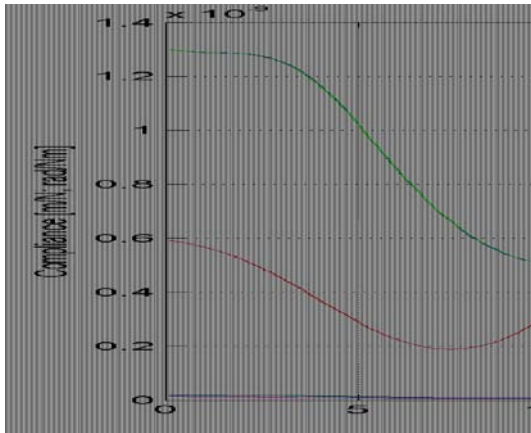TNO – FLUID DYNAMICS, TNO - STRUCTURAL DYNAMICS

Figure 14: Compliance transfer function of the foundation block in Z direction (4-TZ)
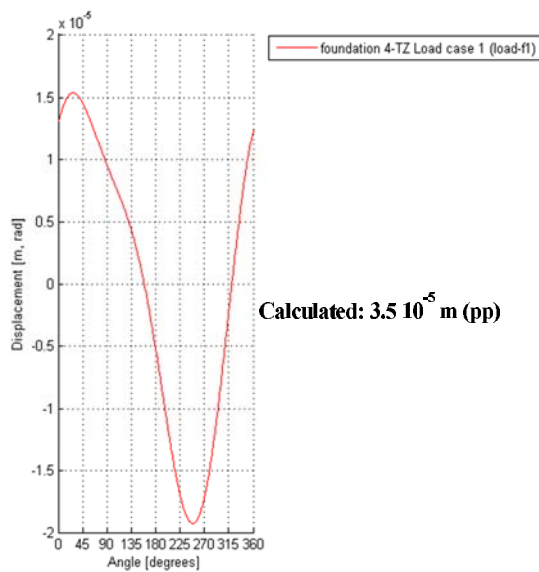

Figure 15: Calculated vibration displacement on the foundation block

The results of the measurements for this location are shown in figure 16. The measured vibration displacement is 0.05 mm peak-to-peak (pp). This pictures shows also higher frequency components that are probably caused by the pulsation-induced pulsation forces acting on the pulsation dampers and on the cylinder passage volumes. This means that the vibration displacement caused by only the unbalanced mechanical loads will be lower as measured.

The ratio of the measured and calculated value at this location is 1.43 and will even be lower when the effect of the pulsation-induced forces will be taken into account. For dynamic calculation of foundations where the soil/foundation interaction can have an important effect, the results between measurements and calculations show a good agreement with this check tool.

General conclusions are:
- Results of calculations and measurements are in good agreement.
- Pulsation-induced forces can have an important effect on the vibrations of the foundation and should be included.
- Another test case has shown similar results
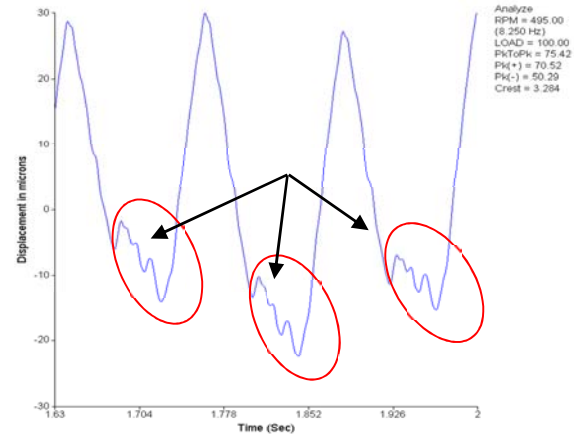
Figure 16: Measured vibration displacement on the foundation block

4   Summary and conclusions

Due to higher excitation loads, more variable process conditions, large range in variable speeds, the dynamics loads on the reciprocating compressor foundations become more challenging.

Together with the fact that field experiences have shown that there is a lack of knowledge in the dynamic design of foundations this has led to more failures of foundations and compressor components. All dynamic loads must be considered in the dynamic design of a compressor system. Modification of an incorrect designed foundation is not so easy and can be very expensive and time consuming.

For that reason the research group of the EFRC had decided to develop an easy to use tool which can be used to check the preliminary dynamic design of a foundation in a very early stage of the project.

This check tool, named COFANTO, enables the plant commissioner to perform a check without repeating the detailed analyses carried out already by the design engineers. The soil/foundation interaction has an important effect on the dynamic properties of the system and this special feature has been included in the program.

Field measurements have shown that the results of COFANTO are in good agreement.

Pulsation-induced forces can have an important effect on the vibrations of the foundation and test results have shown that these forces should also be included in the dynamic design of foundations of reciprocation compressors.

EFRC

Compressor Foundation Analysis Tool (COFANTO), *André Eijk, Sven Lentzen, Flavio Galanti, Bruno Coelho;* TNO – FLUID DYNAMICS, TNO - STRUCTURAL DYNAMICS

5   Acknowledgements

References

[1] Gast, S, Borsig ZM, Rainer, P.M. TOTAL Refinery Germany, "Modification of a reciprocating compressor due to process changes in the TOTAL refinery in Spergau/ Germany", 4th EFRC Conference, June 2005 Antwerp.

[2] Eijk, A, "EFRC Guidelines for vibrations EFRC Guidelines for Vibrations in Reciprocating Compressor Systems", 6th Conference of the EFRC (www.recip.org)

[3] Wolf, J.P. "Foundation vibration analysis using simple physical models", Prentice Hall, Englewood Cliffs, 1994.

[4] API RP 686 Recommended Practices for Machinery Installation and Installation Design, 1st edition April 1996.

[5] Weck, J.W. and Wold, J.P., "Cone models for nearly incompressible soil", Earthquake Engineering and Structural Dynamics, 22 (1993): 649-663.

[6] Weck, J.W. and Wold, J.P., "Why cone models can represent the elastic half-space", Earthquake Engineering and Structural Dynamics, 22 (1993): 759-771.

[7] Dobry, R. and Gazetas G., "Simple method for dynamic stiffness and damping of floating pile groups", Géotechnique, 38 (1988): 557-574.

[8] Makris, N. and Gazetas, G., "Dynamic pile-soil-pile interaction, part II: lateral and seismic response", Earthquake Engineering and Structural Dynamics, 21 (1992): 145-162.

8th Conference of the EFRC
September 27th / 28th, 2012, Düsseldorf

The Importance of Motor Dynamics in Reciprocating Compressor Drives

by:

Gerhard Knop
Central Division of Technology
NEUMAN & ESSER GmbH & Co. KG
Übach-Palenberg
Germany
gerhard.knop@neuman-esser.de

8th Conference of the EFRC
September 27th / 28th, 2012, Düsseldorf

Abstract:

In drive train technology the exceptional torque dynamics of reciprocating compressors are well known. There are not many other driven machines which show the same height of torque fluctuations. Most often, reciprocating compressors are driven by induction and synchronous motors. They react on these compressor torque dynamics with their own air gap torque variations and that way return a significant effect on the torsional vibration behavior of the shafting system and coupling. Usually the influence of the motor can be considered to be more important than the influence of the compressor. Still, even today one encounters torsional vibration simulations which ignore the motor influence completely.

This paper gives an overview on the motor dynamic performance and the different ways, on how they can be included in the torsional vibration simulation. It compares simulation results with and without motor dynamics showing their enormous differences.

Contents:

1   Introduction

Because of their enormous torque variations, reciprocating compressors introduce torsional vibrations into the drive train which must be thoroughly investigate by simulation before the machines are put into operation. In the early past, but interestingly sometimes even today, the reacting torque of the driving induction or synchronous motor was considered to be constant at steady state operation (meaning without motor dynamics).

This assumption most often leads to completely incorrect shafting torque dynamics and gives no information on electric current fluctuations. Both quantities however, are the key design features of a drive train (API 618, paragraphs 7.1.1.7+7.1.2.6[13]).

Torque dynamics must be limited in order to
• avoid coupling overloading or early rubber wear
• avoid shaft fractures
• avoid rotor and stator mechanical overloading

Electric current fluctuations must be limited to
• avoid excessive mains loading and flicker
• avoid frequency converter thermal overloading
• or semiconductor malfunction

The motor reactions on torsional vibrations can be in a way that shaft torque variations are much amplified or attenuated. This divers behavior is investigated in this report.

Focus is on induction motors which are much more frequently used than synchronous motors. However, some general findings apply for synchronous motors in a similar way.

Motor dynamics were introduced into the drive train simulation many years ago[10]. Today they are becoming more and more important because of the following reasons which require more calculation correctness with more sophisticated simulation models.

a) Higher compressor rotational speeds are more often selected than years ago. This increases the probability of torsional resonances.

b) The use of speed control is more often considered which always results in resonant conditions that need to be properly investigated.

c) Due to much more accurate strength evaluation of the compressor axes parts on the basis of Finite Element Analyses (FEA), the rod loads went up a lot without loss of operational reliability. As the rod load acts on the crankshaft adding bending stress to the torsional loading, the accuracy of the drive train simulation must follow that of the compressor axes in order to get equivalent strength evaluation safety.

d) Better drive train simulations allow reduction of flywheel size and weight which means reduced compressor main bearing load, reduced crankshaft bending load and reduced lateral vibration tendency.

e) More complete and sophisticated drive train simulation means increase of reliability. It can be recognized that the number of coupling or shafting failures due to incomplete simulation models (no motor dynamics) has gone down to practically zero.

2   Visualization of Motor Behavior

Motors react on torsional vibrations. If the torque of the compressor were constant, the motor air gap torque would be constant as well. The fluctuating compressor torque however produces angular deflections of the rotor within its magnetic field which causes the motor air gap torque to change its height accordingly.

Although physically not correct, one can illustrate this context by the motor and compressor torque vs. speed diagrams as given in Fig. 1.
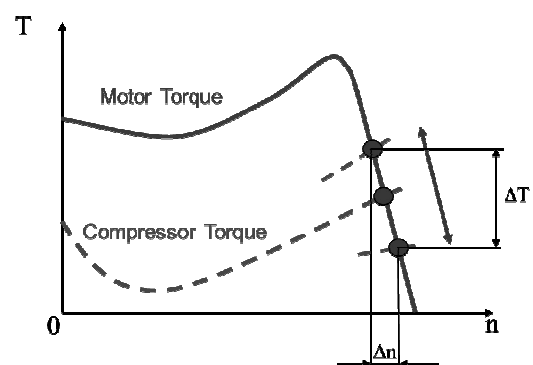

Fig. 1: Illustration of motor torque reaction on compressor torque variations (n = speed)

The correctness lacks in the fact that the motor curve is no static entity but changes its shape permanently depending on the dynamics. Furthermore, the motor reacts not directly on the compressor torque, but on the motor shaft oscillations which are again depending on the mass-

elastic characteristics of the coupling and shafting system between compressor and motor.

The resulting motor air gap torque variations represent an external excitation, same as the compressor torque, influencing the torsional vibrations of the drive train. This feedback can be visualized by replacing the motor air gap magnetic field in a simulation model by a mechanical spring and damper as shown in Fig. 2. If the motor really followed the static curve as given in Fig. 1, there would be only dampening and no spring characteristic because of the pure speed dependence. However in reality, as shown further below in this report, there is also considerable spring behavior.
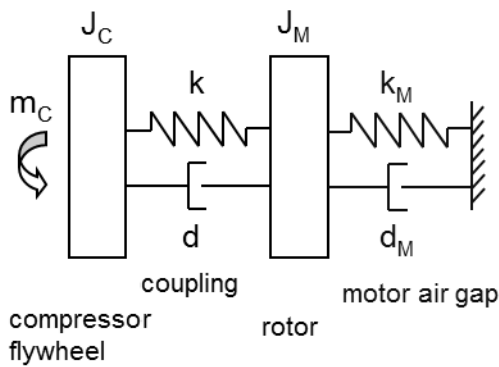
Fig. 2: Representation of the motor air gap torque by mechanical spring and viscous damper

J_C = compressor inertia (flywheel)
J_M = motor inertia (rotor)
k = coupling stiffness
d = coupling viscous damping
k_M = motor magnetic field stiffness
d_M = motor magnetic field viscous damping
m_C = compressor torque

Although this illustration may be somehow typical for *mechanical* engineers to explain electro-magnetic issues, it is physically not far away from reality.

The following thoughts show why the motor air gap torque is so important for the torsional performance.

Fig. 3 gives the typical mode shape of the lowest torsional natural frequency of flexibly coupled machinery.

The highest torsional deflection (φ_4) occurs at the rotor whereas it is very low at the compressor crank (φ_1). Therefore the highest excitability is given at the rotor which is represented by the high kinetic vibration energy (E_{KIN4}) that follows

$$E_{KINi} = \frac{1}{2} J_i \cdot \dot{\varphi}_i^2 . \qquad\qquad J = \text{inertia}$$
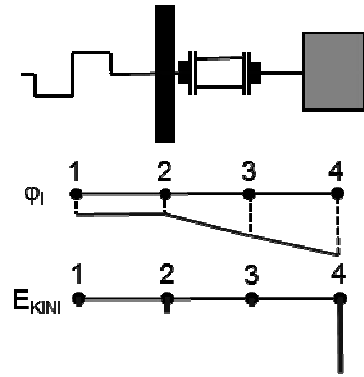

Fig. 3: Mode shape and kinetic vibration energy
  φ_i = *angular deflection of inertia #i*
  E_{KINi} = *kinetic vibration energy of inertia #i*

This means that the returning excitation of the motor must be considered to be more important than that of the compressor even though it is normally much smaller in amplitude.

3   Calculation Methods [1 to 12]

Today it is common practice to solve the given differential equations by numerical integration. This allows simple inclusion into software and fast calculation of results. When motor dynamics are considered, the mechanical set of equations of the drive train is completed by the following electro-magnetic part of the motor.

Voltage and magnetic flux equations: (Eq. 1)

$$u_1 = i_1 \cdot R_1 + \frac{d\Psi_1}{dt}$$

$$0 = i_2 \cdot R_2 + \frac{d\Psi_2}{dt}$$

$$\Psi_1 = i_1 \cdot L_1 + i_2 \cdot L_h e^{jp\beta}$$

$$\Psi_2 = i_2 \cdot L_2 + i_1 \cdot L_h e^{-jp\beta}$$

The motor air gap torque results from:

$$m_M = \frac{3}{2} p \cdot \text{Im}\left\{\Psi_2 \cdot i_2^*\right\} \qquad\qquad \text{(Eq. 2)}$$

R = Ohm's resistance, L = inductivity
Ψ = magnetic flux
u = voltage, i = current
β = angle between rotor and stator coil
p = number of pole pairs
Index 1 = stator, Index 2 = rotor
m_M = motor air gap torque
j = imaginary number, Im = imaginary part
* = conjugated complex

As convenient the numerical integration may be, it lacks in one important quality: The results are little descriptive! Often the results have to be accepted as they are without being able to explain special phenomena which have been observed.

What is missing is the insight on the dynamic behavior of the drive train: *Why* is it performing like that?

This insight can be much better gained by applying *analytical* solutions. These require simplification and linearization of the system (Eq. 1+2) which can often be done without too much loss of accuracy.

Doing so, one can get the following simple equation for an induction motor (from now on, all variables are considered to be phasors used in a frequency domain calculation):

$$m_M = \frac{M_{St}}{1 + j\omega T_L} \cdot s \qquad \text{(Eq. 3)}$$

m_M motor torque (air gap torque)
M_{St} constant with torque dimension
s motor slip
j imaginary number
ω angular frequency of the given harmonic
T_L electrical time constant

This equation represents the relation between motor torque m_M and motor slip s, with a phase shift according to the denominator including the imaginary number j.

The slip phasors can be expressed by the angular velocity phasor $\dot{\varphi}_M$ acc. to

$$\dot{\varphi}_M = \Omega_s s$$

(Ω_S = angular frequency of magnetic field)

This relates to the angular deflection φ_M acc. to

$$\dot{\varphi}_M = j\omega\varphi_M .$$

The equations above show that the motor torque can be also considered as a parallel connection of mechanical spring k_M and a viscous damper d_M as displayed in Fig. 2. It shows that, other than the static motor curve of Fig. 1 may imply, there is not only dampening d_M but also spring behavior k_M.

$$m_M = k_M \cdot \varphi_M + d_M \cdot \dot{\varphi}_M \qquad \text{(Eq. 4)}$$

$$k_M = \frac{\dfrac{M_{St}}{\Omega_s} \cdot \omega^2 T_L}{1 + \left(\omega T_L\right)^2} \qquad \text{(Eq. 5)}$$

$$d_M = \frac{\dfrac{M_{St}}{\Omega_s}}{1 + \left(\omega T_L\right)^2} \qquad \text{(Eq. 6)}$$

Nomenclature is acc. to Fig. 2 and (Eq. 3.)
M_{St} and T_L can be derived from the equivalent circuit components.
The factors k_M and d_M are frequency (ω) dependent.

4   Soft Coupling and Motor - Two friends

The most amazing influence on the torsional vibration behavior of the motor dynamics can be observed at drive trains being equipped with high flexible (rubber in shear type) couplings.
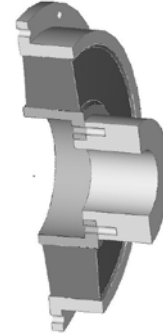

Fig. 4: High flexible (rubber in shear) coupling

It can be noted that the lowest natural frequency is enormously increased and the coupling torque dramatically reduced, even if in resonance!

Applying the analytical derivations of the previous chapter, the following 2 differential equations can be written down:

$$J_C \cdot \ddot{\varphi}_C + d\left(\dot{\varphi}_C - \dot{\varphi}_M\right) + k\left(\varphi_C - \varphi_M\right) = m_C$$

$$J_M \cdot \ddot{\varphi}_M - d\left(\dot{\varphi}_C - \dot{\varphi}_M\right) + d_M\dot{\varphi}_M - \\ - k\left(\varphi_C - \varphi_M\right) + k_M\varphi_M = 0 \qquad \text{(Eq. 7,8)}$$

Nomenclature is acc. to Fig. 2.

Without motor influence k_M and d_M, they produce the well know un-damped natural frequency of a 2-mass oscillator:

$$\omega_0 = \sqrt{k \cdot \left(\frac{1}{J_C} + \frac{1}{J_M}\right)} \qquad \text{(Eq. 9)}$$

However, when including the "air gap stiffness" k_M, this frequency goes up and a second one appears.

$$\omega_{0_{12}} = \sqrt{-\frac{p}{2} \pm \sqrt{\left(\frac{p}{2}\right)^2 - q}} \qquad \text{(Eq. 10)}$$

$$p = -\left(\omega_{0CM}^2 + \omega_{0C}^2 + \omega_{0M}^2\right), \quad q = \omega_{0M}^2 \cdot \omega_{0C}^2$$

$$\omega_{0M}^2 = \frac{k_M}{J_M}, \quad \omega_{0C}^2 = \frac{k}{J_C}, \quad \omega_{0CM}^2 = \frac{k}{J_M}$$

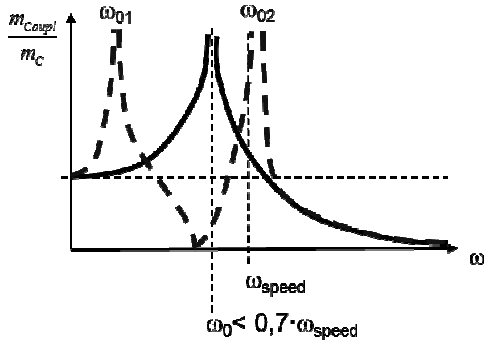Fig. 5 compares both transfer functions of the (firstly) un-damped system.

Fig. 5: Effect of motor dynamics on natural frequency (un-damped system); blue and dashed includes motor influence, solid and black is without. m_{Coupl}/m_C is coupling torque related to compressor excitation torque.

It is still widespread practice when selecting a coupling to evaluate the natural frequency without motor influence ω_0 and place it below the speed angular frequency ω_{speed} (typically $\omega_0 < 0.7 \cdot \omega_{speed}$).

Fig. 5 however shows that the real natural frequency may be then in the range of the speed frequency, meaning near resonance!

The amount of difference between both (with and without motor influence) depends on the inertia ratio J_M/J_C (motor/compressor) and torsional spring ratio k_M/k (air gap magnetic field/coupling).

Fig. 6 quantifies this relation where the abscissa gives typical stiffness relations of high flexible couplings (their stiffness k is much below the magnetic field stiffness k_M!).
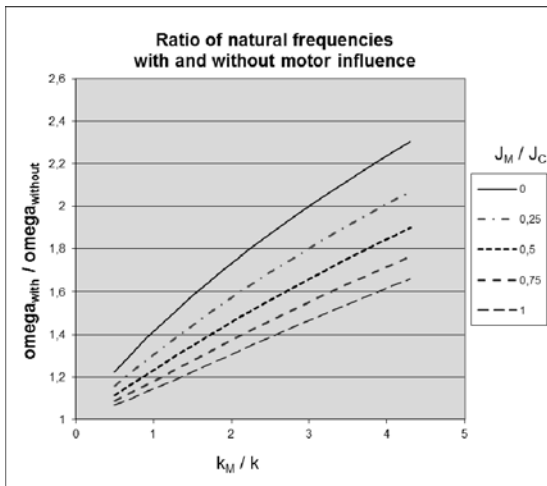
Fig. 6: Ratio of natural frequencies with and without motor influence
J_M/J_C = inertia ratio motor / compressor
k_M/k = torsional stiffness ratio mag. field / coupling

It can be noted that the real natural frequency can be easily higher by a factors of 1.5 or more than the value calculated by the "classical" approach without motor influence!

This circumstance may cause some worries, but when performing the quantification of the dynamic coupling torque loading, it turns out that these can be reduced to very low values by selecting a suitable coupling-flywheel combination for the given motor characteristics. This applies also for resonance conditions as shown in the example of Fig. 8.

Note that the 1st angular natural frequency at ≈ 15 s^{-1} cannot be met as it is too low.
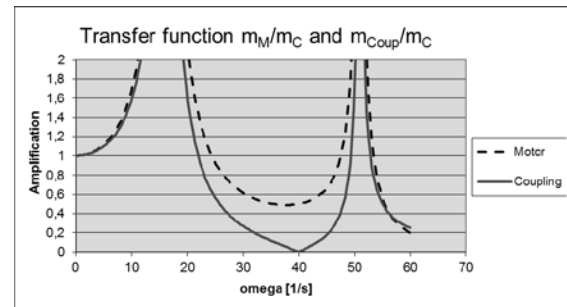

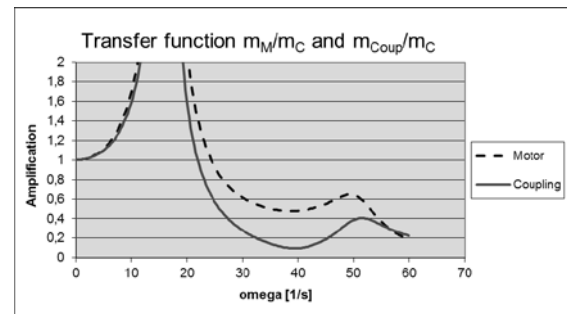*Fig. 7: Transfer function without damping*

Fig. 8: Transfer function including damping
m_M/m_C = motor air gap torque / compressor excitation torque (Note: m_M is also a measure of electric current fluctuations)
m_{Coupl}/m_C = coupling torque / compressor excitation torque

These transfer functions reflect some very interesting findings:

- There is an angular frequency at which the dynamic coupling load is almost zero. At Fig. 7, this is at 40 s^{-1}. It can be shown that

this frequency results from $\omega = \sqrt{\dfrac{k_M}{J_M}}$ and

is therefore only dependent on motor characteristics! This means that if by chance the speed angular frequency matches this point, the coupling load will always be low and this independent of the selected coupling stiffness!

- The resonance at around 52 s^{-1} is extremely attenuated (Fig. 8).

- This attenuation is bought by rather high motor air gap torque variations which correspond to electric current fluctuations.

The amount of minimum current fluctuations depends again on the inertia ratio J_M/J_C and torsional spring ratio k_M/k. Fig. 9 shows that for that respect, the rotor inertia should be as low as possible.
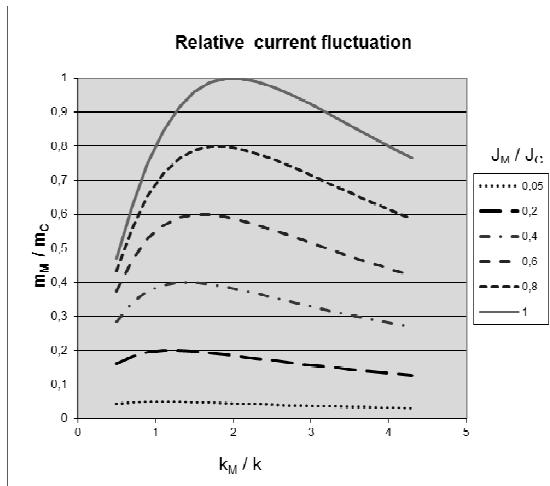

Fig. 9: Minimum relative motor air gap torque variations, corresponding to minimum motor current fluctuations

Note: The term "minimum" refers to the frequency of the minimum motor torque. In the example motor of Fig. 8, this is at around 38s^{-1}. The current fluctuations cannot be lower than that.

All these findings can only be gained by applying analytical calculation approaches. Numerical simulation would give equal or probably more accurate results for the individual configuration, but would produce little insight and understanding of what is actually happening.

5 Negative Damping

There is another interesting effect that can only be understood by using analytical approaches. Especially if all-steel disc type couplings are installed (which are always torsionally pretty rigid) it can be sometimes observed, that coupling and motor shaft torque variations go significantly up without much external excitation.
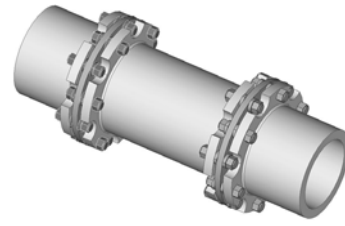

Fig. 10: All-steel disc type coupling

This may happen during startup as shown in Fig. 11 (at 3.5 sec.) or during steady state operation as shown further below. These are self-induced vibrations which are driven by the feedback of the motor.
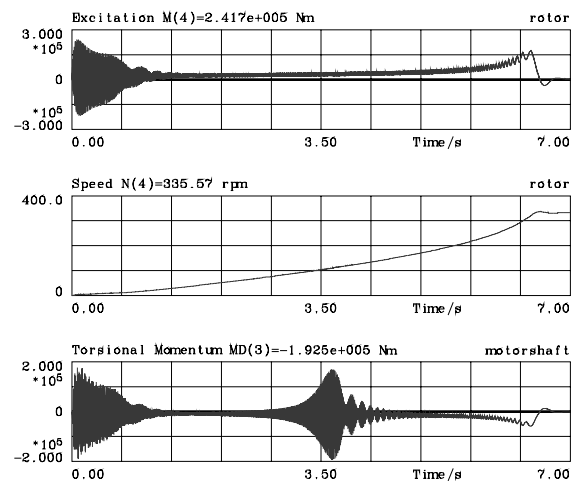

Fig. 11: Self-induced vibrations during startup

If the motor magnetic field is replaced by spring and damper, the self-induced vibrations can be illustrated as *negative damping*[8,9]. The term damping in this context must not be considered in its physical meaning of energy dissipation but just in the phase shift between excitation and vibration. Where positive damping results in attenuation of vibrations in resonance near condition, negative damping would amply the vibrations due to unfortunate phase shift.

The simple analytical approach of the motor torque given in (Eq. 3) cannot produce negative damping as can be easily recognized by the equation of d_M (Eq. 6). In order to include these negative damping effects, less simplifications need to be applied when deriving analytical approaches from the original set of differential equations (Eq. 1+2) as had been done by Jordan, Müller and Seinsch already back in 1979 and 1980[8,9]. Especially the Ohm's resistance of the rotor coil R_1 can no longer be neglected.

Fig. 12 and 13 show the R_1 dependence on spring stiffness and viscous damping for an example motor. R_1 is given here as the dimensionless variable α ($\alpha = 0.01$ for this motor). Different curves relate to different vibration frequencies. The lowest frequency f = 16.2 Hz is the motor speed.

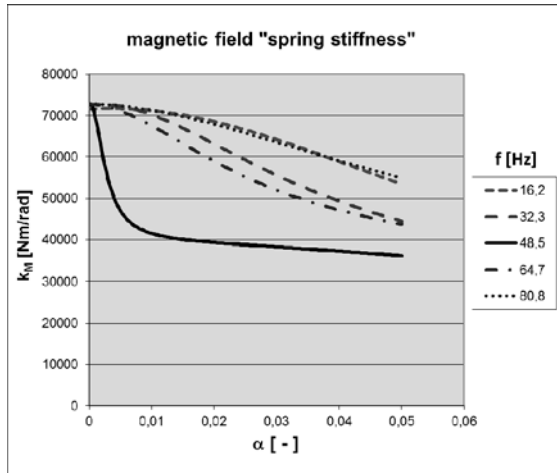The Importance of Motor Dynamics in Reciprocating Compressor Drives, *Gerhard Knop;* NEUMAN & ESSER GMBH & CO. KG

Fig. 12: Magnetic field "spring stiffness" as a function of the dimensionless stator Ohm's resistance α and vibration frequency f. (example motor of the drive train addressed to below)
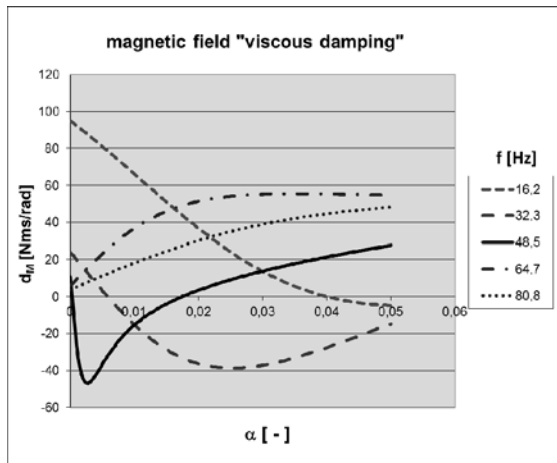

Fig. 13: Magnetic field "viscous damping" as a function of the dimensionless stator Ohm's resistance α and vibration frequency f. (example motor of the drive train addressed to below)

It can be recognized that the spring stiffness in the range of the given dimensionless Ohm's resistance $\alpha = 0.01$ is only little influenced by α and f except for the frequency f = 48.5 Hz which is close to the mains frequency 50 Hz.

Note: Having f approach 50 Hz, k_M would be around 40000 Nm/rad at $\alpha = 0$, so approximately only 50% compared to other frequencies.

Damping is very much influenced by α, especially at high frequencies. There are even areas with negative damping values!

The damping curves of Fig. 13 appear somewhat chaotic at first glance, but after a closer look they obey the following behavior.

Low frequency curves like 16.2 Hz of Fig. 13 start at very high and positive damping values, go down with increasing α and have their minimum in the negative area but in an α range that is far beyond typical motor values.

With increasing frequency, the minimum moves further to the left, meaning to lower and more realistic α values.

At a frequency right below the mains frequency, the minimum is at $\alpha = 0$. Above mains frequency, there is no longer negative damping and the curves go up with increasing α.

For the given example motor $\alpha = 0.01$ both frequencies 32.3 Hz and 48.5 Hz (2nd and 3rd harmonic) show negative damping.

The possible consequences of negative damping are demonstrated in the following figures that show an actual drive train equipped with an all-steel disc type coupling that produced a natural frequency of around 42 Hz. It is placed right between the 2nd and 3rd harmonic of the speed frequency[10].

Fig. 12 and 13 also belong to this motor.

Data of this example drive are:
U_N = 6000 V star (voltage supply)
P_N = 515 kW (motor rated power)
s_N = 0.9% (nominal slip)
2p = 6 (number of poles)
f_N = 50 Hz (mains frequency)
I_N = 61 A (rated amps)
R_1 = 1.28 Ω (Ohm's resistance of stator coil)
R_2 = 0.54 Ω (Ohm's resistance of rotor coil)
$X_{1\sigma}$ = 5.2 Ω (stray reactance of stator coil)
$X_{2\sigma}$ = 7.4 Ω (stray reactance of rotor coil)
X_m = 134.6 Ω (main reactance)
J_M/ J_C = 0.136 (ratio rotor / compressor inertia)
k = 2.53 MNm/rad (coupling stiffness)

Note: The coupling stiffness is in the same range as the crankshaft and motor shaft stiffness (meaning very rigid).

This drive train was engineered in year 1998 and put into operation shortly after. The all-steel disc type coupling failed after few running hours and was then replaced by an elastomeric coupling.

When incorrectly assuming the motor air gap torque to be constant like shown in Fig. 14, the coupling and motor shaft dynamic torque loading is rather low.

In reality (Fig. 15) however, the torque variations are much amplified by the unfortunate feedback of the motor ("negative damping"). The torque amplitudes in coupling and motor shaft are 5-times higher compared to Fig. 14!

The Importance of Motor Dynamics in Reciprocating Compressor Drives, *Gerhard Knop;* NEUMAN & ESSER GMBH & CO. KG

This example shows how important the inclusion of the motor electro-magnetic differential equations is. They should never be neglected!
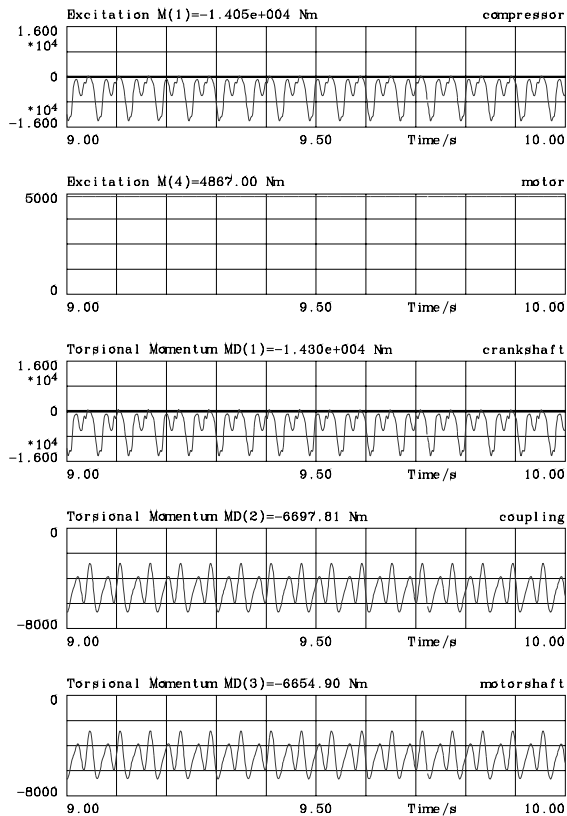

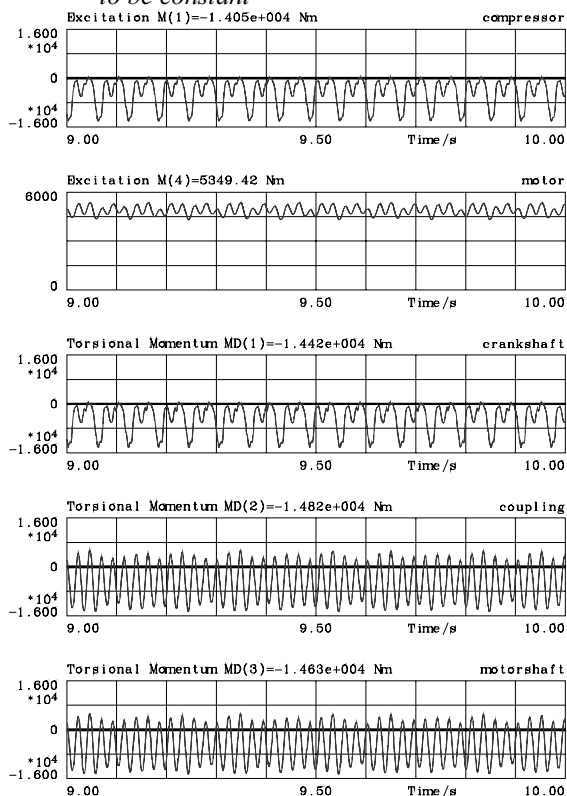Fig. 14: Motor air gap torque incorrectly assumed to be constant

Fig. 15: Motor air gap torque considered by its electro-magnetic characteristics

Note:

When using high-flexible rubber-in-shear couplings, the resulting natural frequencies are typically in a range that cannot provide negative damping. When properly chosen, they would even attenuate the shaft torque loading to an almost constant value due to the effects described in the previous chapter.

Fig. 16 shows the results for the same drive train as for Fig. 15, only equipped with high flexible coupling.
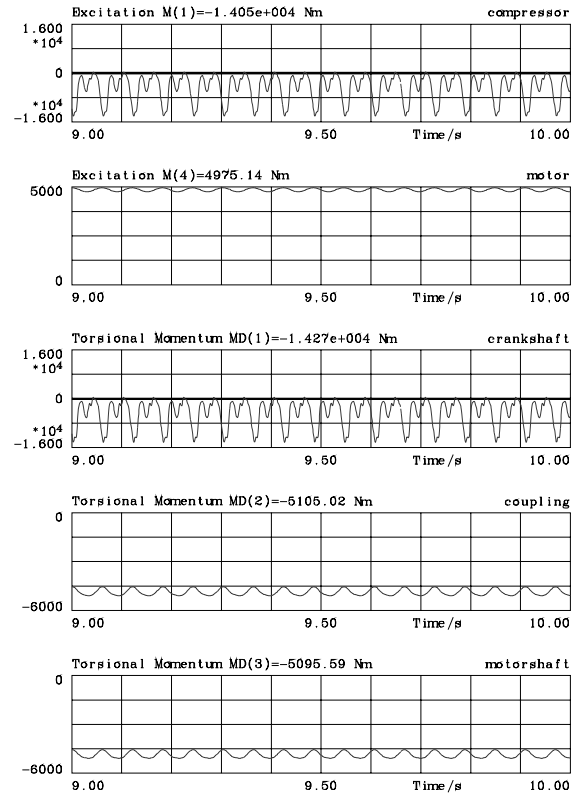

Fig. 16: Drive train equipped with high flexible coupling

Comparing the previous results yields:

Fig. 14	All-steel disc coupling, Motor torque incorrectly assumed constant	3800 Nm
Fig. 15	All-steel disc coupling, Real motor torque	19000 Nm
Fig. 16	High flexible coupling, Real motor torque	540 Nm

Tab. 1: Peak-to-Peak coupling and motor shaft torque

6   Variable Frequency Drives

Chapters 4 and 5 showed two examples of the immense effect of the motor air gap torque which reduces or increases torsional vibrations and shafting torque load depending on the given drive train configuration.

If a frequency converter is used to feed the motor, this motor air gap torque is much affected by the respective frequency converter control method and therefore may improve or worsen the situation significantly. The established control principle is called vector control or field oriented control. There are the following options:

a) Control of motor current fluctuations. In this case the motor air gap torque is smoothened in the same way as the motor current. If the control is fast enough, the behavior approaches that of a constant motor air gap torque.

b) Control of the rotational speed fluctuations. In order to reduce speed variations, the motor air gap torque must vary accordingly. Therefore, smooth speed is bought by varying current and shaft torque.

c) Setting the control very slow so that no fluctuations are controlled down. In this case the motor behaves in the same way as if connected directly to the mains, only with different frequency and voltage supply.

It must be noted that, same as with direct mains supply, for VFD drives it is not only the dynamic shafting torque but also the motor electric current fluctuations that have to be considered during the drive train design. The frequency converter allows only limited peak current values in order to avoid thermal overloading or malfunction of the semiconductor elements[5].

Reflecting all the matters said before, it comes clear that the control aim of the frequency converter must be properly chosen and communicated between all parties involved.

7   Conclusions

It could be demonstrated that the motor dynamics represent the major influence on the torsional vibrations of drive trains, especially on the shaft torque loading and on electric current pulsations.

As it was not common practice to consider motor dynamics for the drive train simulations in the early past, its inclusion has resulted into increased equipment reliability. This has become even more important today, as modern compressor installations provide a stronger demand on calculation accuracy then they used to do, due to better strength utilization.

Therefore, the motor electro-magnetics should always be included into the calculations.

When using torsionally soft couplings, the torque loading can be brought down to very low values due to the motor reaction. Motor and soft coupling represent a very good team, producing very robust systems that show only small torque pulsations at coupling and shafting.

When torsionally rigid couplings like all-steel disc type couplings are used, self-induced vibrations may occur with sometimes harmful height. When applying a spring-dampener model for the motor magnetic field, these self-induced vibrations can be considered as negative damping. The resulting shaft and coupling torque variations can be multiples of the values calculated with the false assumption of constant motor torque!

At Variable Frequency Drive (VFD) the frequency converter control method must be thoroughly chosen in order to promote or reduce the motor magnetic field influence, depending on the individual requirements.

It is usually the compressor manufacturer who is in charge of the drive train design (API 618 6.7.1[13]). As compressor and motor can only be simulated in a single combined simulation model, it helps a lot if the dynamic motor behavior is well understood by the compressor manufacturers, allowing them to optimize the drive train on every relevant aspect.

As a summary, it can be stated that in every compressor train which is driven by an electric motor, the electro-magnetic motor characteristics represent the most important parameters in terms of torsional vibrations, torque dynamics and mains electrical loading.

8   References and Literature

[1] Bühler, Einführung in die Theorie geregelter Drehstromantriebe, Band 1, Birkhäuser Verlag 1977

[2] Schröder, Elektrische Antriebe 1, Springer 1994

[3] Steinhart, Dynamik elektrischer Antriebe, Hochschule Aalen WS 08/09

[4] Vogel, Elektrische Antriebstechnik, 6. Auflage, Hüthig 1998

[5] Cierniak, Funke, Wendt, Optimizing the drive system for variable speed electric motor driven reciprocating compressors; EFRC 2003 Wien

[6] Seinsch, Über die Bestimmung der Drehzahl- und Leistungsschwankungen bei Drehstromantrieben für Kolbenverdichter , Conti-Elektro Berichte Jan./Jun.1967

[7] Seinsch, Ausgleichsvorgänge bei elektrischen Antrieben, Teubner 1991

[8] Heinz Jordan, Jörg Müller, Hans Otto Seinsch; Über elektromagnetische und mechanische Ausgleichsvorgänge bei Drehstromantrieben; Wiss. Ber. AEG-TELEFUNKEN 52 (1979) 5

[9] Heinz Jordan, Jörg Müller, Hans Otto Seinsch; Über das Verhalten von Drehstromasynchronmotoren in drehelastischen Antrieben; Wiss. Ber. AEG-TELEFUNKEN 53 (1980) 3

[10] Knop, Entwicklungsschritte bei der drehschwingungsgerechten Auslegung von Antriebssträngen mit Kolbenverdichtern, 5. Kötter Workshop Kolbenverdichter, 2001

[11] Jordan, Lorenzen, Taegen, Erzwungene Pendelungen von Asynchronmaschinen, ETZ Heft 20, S. 645-648, 1963

[12] Wenzke, Zur Ableitung der dynamischen Kennlinie des Asynchronmotors im Hinblick auf die Berechnung von Schwingungserscheinungen in Antriebsanlagen, Wiss. Zeitung TH Magdeburg 14 Heft 5/6 Seite 517-523, 1970

[13] API 618 5th edition, Reciprocating Compressors for Petroleum, Chemical, and Gas Industry Services, December 2007

Practical experience from torsional vibration measurements and analysis of reciprocating compressors - Case studies

by

Dr.-Ing. Johann Lenz and Dr.-Ing. Fikre Boru

KÖTTER Consulting Engineers GmbH & Co. KG

Bonifatiusstraße 400, 48432 Rheine, Germany

lenz@koetter-consulting.com, boru@koetter-consulting.com

8th Conference of the EFRC
September 27th / 28th, 2012, Düsseldorf

Abstract:

Reciprocating compressors are unavoidable classical solutions in the field of natural and process gas compression with the ability to function over a wide range of operating conditions. The dynamic design of the reciprocating compressor is complicated due to the large number of conditions that have to be satisfied. Since, high torsional dynamic stress is often not recognised until damages appear, it is advisable to conduct a detailed torsional vibration analysis when planning a new drive train or modifying an existing one. In this paper, the different measures to influence the torsional behaviour of reciprocating compressors is presented with the help of four case studies.

TORSIONAL VIBRATIONS

Practical experience from torsional vibration measurements and analysis of reciprocating compressors -
Case studies, *Dr.-Ing. Johann Lenz, Dr.-Ing. Fikre Boru;* KÖTTER CONSULTING ENGINEERS
GMBH & CO. KG

1 Theoretical background

The working principle of the reciprocating
compressor leads to torsional loading in the
crankshaft. This torsional loading is then
transmitted to the optional flywheel, the coupling
and the driving motor. Besides the working
principle of the compressor, a lot of factors
influence the torsional loading of the drive train.
The excitation loads responsible for the torsional
fatigue loading are explained below.

The piston rod force F_P can be calculated from the
cylinder gas forces and the simplified dynamic
forces of the piston and piston rod masses as
follows:
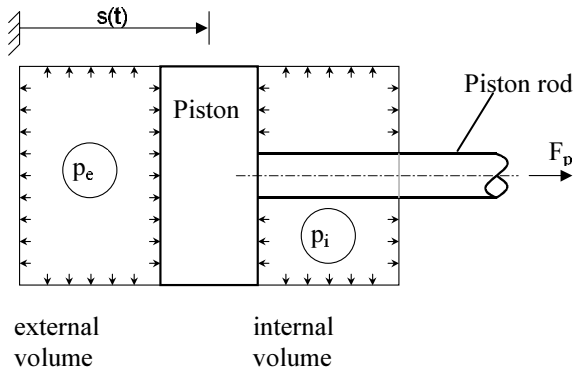
Figure 1: Simplified cylinder

Piston rod force $F_P(t)$:

$$F_p(t) = m_p \cdot a_p(t) + p_i(t) \cdot A_i - p_e(t) \cdot A_e$$

where

m_p = piston and piston rod mass

a_p = piston acceleration

p_{ie} = internal, external cylinder pressure

A_{ie} = internal, external piston area

From the piston rod force and the dynamic force of
the crosshead and the reciprocating mass of the
connecting rod, one can calculate the radial (F_r) and
tangential (F_t) forces (as a function of the crankshaft
angle) acting on the crosshead pin. The tangential
force component is responsible for the torque
loading of the crankshaft.

Figure 2 depicts the piston rod force and the
resultant moment load of a single crankshaft of a
typical slowly rotating natural gas reciprocating
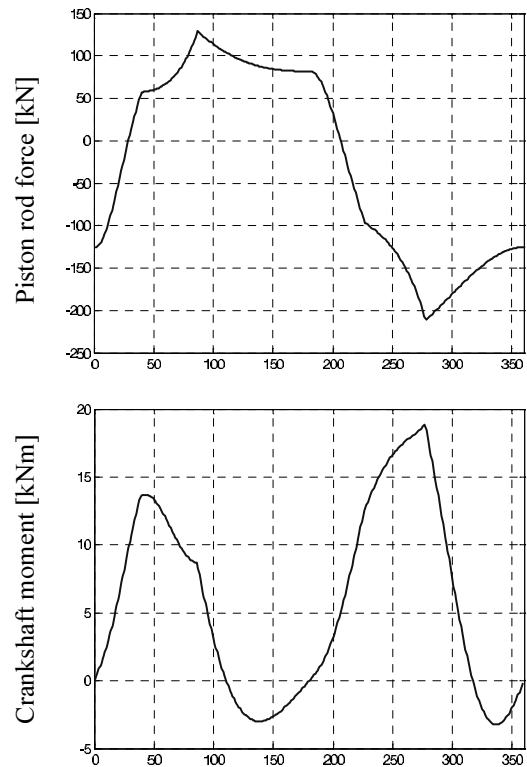compressor for one complete crankshaft revolution.

*Figure 2: Piston rod force and crankshaft moment,
variation of a typical natural gas piston
compressor as a function of crank angle*

In order to analyse the resulting torsional vibration,
the spectrum of the dynamic components of the
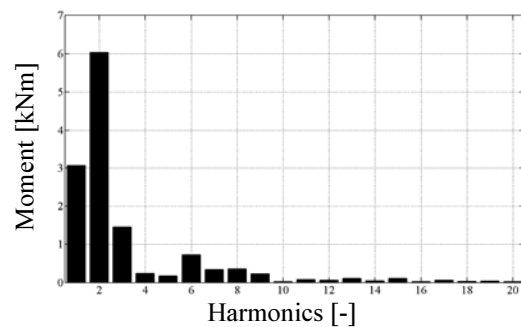torque is generated as shown in figure 3.

Figure 3: Spectrum of excitation torque

The torque spectrum is composed of a number of
harmonic components which are multiples of the
compressor rotational speed. The value of these
harmonic components depends on the operating
condition of the compressor.

The torque spectrum presented above acts on the
"torsionally flexible" drive train. The drive train is
composed of a number of elements having moment
of inertia, torsional damping and torsional stiffness
properties.

Before installation of reciprocating compressors, a torsional vibration study should be conducted in order to check if the allowable loadings are not violated by the planned operation of the compressor. Besides the allowable load levels of the drive train components, the allowable maximum vibration amplitude and the allowable safety margin between resonance and excitation frequency have to be checked.

The results of the torsional vibration analysis depend on the quality of the equivalent physical model and the consideration of the different conditions, which may arise during operation of the compressor. The model should be accurate enough so that it is sensitive to the smallest changes, for example a different coupling manufacturer. In practice, it is advisable to check the torsional vibration level by measurements during commissioning of the drive train.

2 Case studies

2.1 Problems after retrofit with an active suction valve unloader

Since the retrofit of an active suction valve unloader to a reciprocating compressor led repeatedly to failures of its coupling, a basic investigation of the torsional vibration was conducted on an equivalent drive train to determine the influence of the unloader. The analysed reciprocating compressor is a 2-stage, boxer-type compressor with 2,100 kW coupling power having a loaded operating speed range from 600 rpm to 1,000 rpm. In order to broaden the range of the volume flow, an active unloader was retrofitted on both stages of the drive train. An equivalent torsional physical (figure 4) and mathematical model was generated. The first two eigenvalues and their corresponding eigenforms are shown in the Campbell diagram (figure 5).
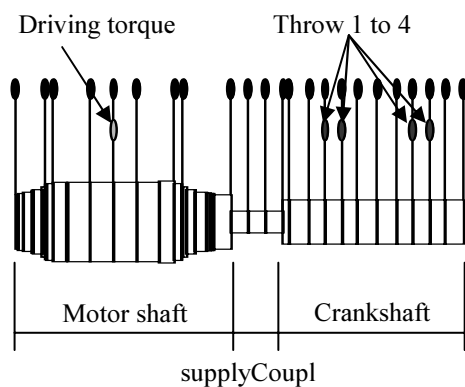

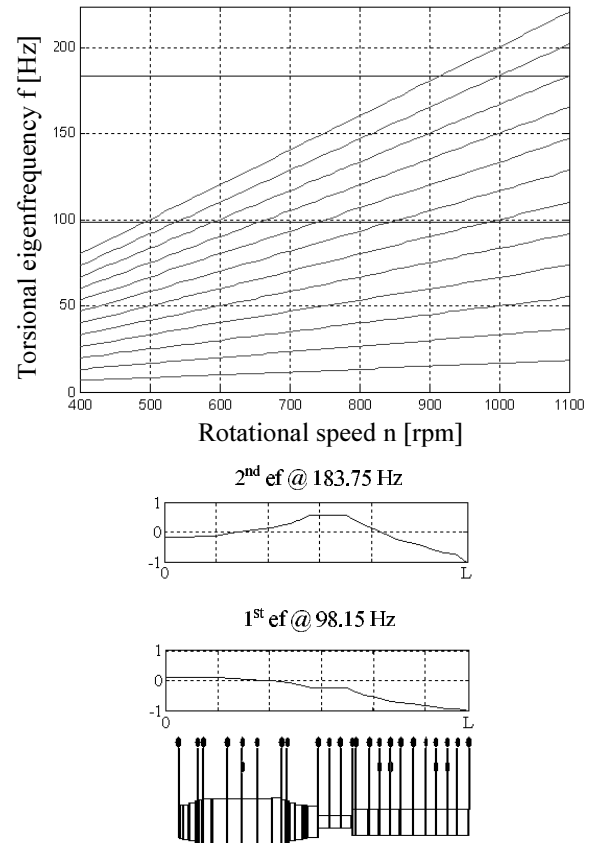*Figure 4: Torsional physical model of the investigated drive train*

Figure 5: Campbell diagram as well as 1st and 2nd torsional eigenform at the drive train

The suction valve unloaders influence the excitation torque spectrum of the drive train. Figure 6 shows the torque spectra for different settings of the unloaders. The dynamic response of the drive train was analysed for the unloader settings. In figure 7, the torque amplitude in the coupling element is given for an operation between 400 rpm and 1,100 rpm.
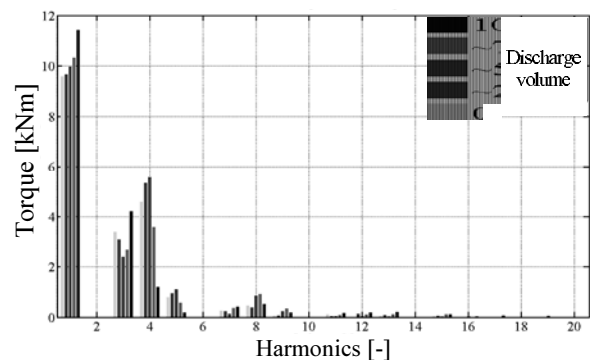

Figure 6: Torque spectra of the 2nd throw (2nd stage) of the 4-cylinder reciprocating compressor operating at 750 rpm
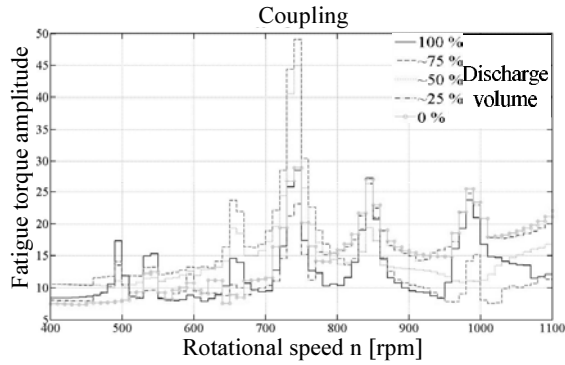
289

Practical experience from torsional vibration measurements and analysis of reciprocating compressors - Case studies, *Dr.-Ing. Johann Lenz, Dr.-Ing. Fikre Boru;* KÖTTER CONSULTING ENGINEERS GMBH & CO. KG

Figure 7: Torque amplitude of the coupling for different settings of the suction valve unloader, operation speed between 400 rpm and 1,100 rpm

Figure 7 shows that the dynamic torque of the coupling was considerably higher for the 75 % setting than for 100 % (i. e. deactivated unloader). This was due to the change in the 8th harmonic of the excitation, which interfered with the 1st torsional eigenfrequency.

This example shows that - depending on the system damping and the selected rotational speed - large dynamic torque may result from the activation of the unloaders. Hence, it is always advisable to conduct a torsional vibration analysis before retrofitting an existing reciprocating compressor with an active suction valve unloader.

2.2 Resonance of the connecting shaft

Reciprocating compressors are often applied for liquefaction of natural gas. Damage at the metal disc coupling of ten similar 2-stage reciprocating compressors was registered after different operation life time. The compressors with a coupling power of 350 kW were operated at a constant rotational speed of 600 rpm. The drive train consists of an electric motor connected to the compressor (with two double acting cylinders) by two metal disc couplings, an interconnecting shaft and a flywheel (figure 8).
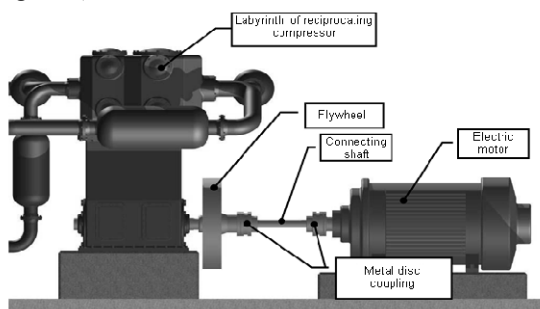

Figure 8: Two-stage reciprocating compressor with metal disc coupling and connecting shaft

For the preliminary investigation of the possible source of the problem, the calculated torsional eigenfrequencies of the drive train were presented in the Campbell diagram in figure 9.
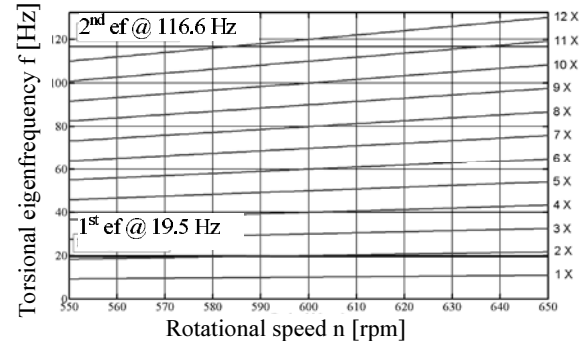

Figure 9: Campbell diagram with calculated eigenfrequencies (ef.) to determine the possible resonance speed

It can be seen that in the neighbourhood of the operation speed of 600 rpm there is an interference between the 1st torsional eigenfrequency (19.5 Hz) and the 2nd excitation harmonic. The torsional vibration at the connecting shaft was measured as shown in figure 10. Figure 11 shows the amplitude spectrum of the measured torque.
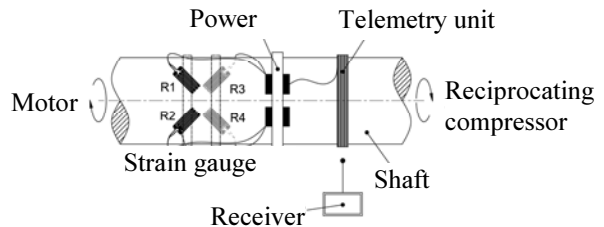

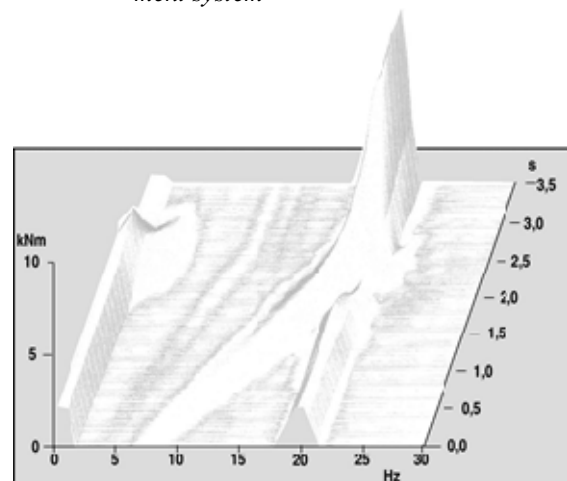*Figure 10: Principle layout of a torque measurement system*

Figure 11: Amplitude spectrum of the torque for start-up of the compressor

Practical experience from torsional vibration measurements and analysis of reciprocating compressors - Case studies, *Dr.-Ing. Johann Lenz, Dr.-Ing. Fikre Boru;* KÖTTER CONSULTING ENGINEERS GMBH & CO. KG

During running up of the compressor, a large torsional resonance at about 20 Hz was recorded. To describe the torsional mode, a vector diagram of the measured torque was used as shown in figure 12.
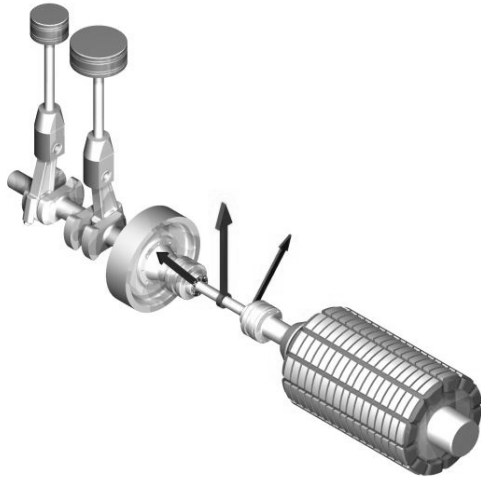

Figure 12: Vector diagram of the measured torque of the drive train

From the vector presentation it can be seen that the main torsional deformation occurs in the connecting shaft. As an easy corrective measure the diameter of the connecting shaft was increased. This moved the calculated 1st torsional eigenfrequency up to 26 Hz. Since this corrective measure was implemented at all compressors, there have not been coupling failures due to torsional vibration anymore.

2.3 Influence of damping

Expanding the operation speed range of two reciprocating compressors for a natural gas storage resulted in a failure of the lubrication system (driven by the crankshaft) of both drive trains after a short operation life time. A measurement showed that torsional resonance vibration was the cause for this failure. For this drive train, the customer decided to run the drive train at constant speeds of 750 rpm, 850 rpm and 1,000 rpm. Such decisions limit the flexibility of the plant, hence other possible solutions are discussed below.

An alternative is to replace the metal disc coupling which is almost rigid and has a very low damping, with an elastic coupling in order to torsionally decouple the motor shaft from the crankshaft. Additionally, the elastic coupling brings damping into the drive train. However, the application of elastic coupling results in changing the dynamic property. Hence, a careful torsional analysis is required before such an implementation.

Below, a principle investigation of the coupling effect is presented for a six-cylinder natural gas (reciprocating) compressor with an elastic coupling and flywheel. A torsional finite element model is developed for the drive train. Then, an appropriate metal disc coupling is selected. Figures 13 and 14 show calculated eigenfrequencies and eigenforms of the drive train with the elastic (figure 13) and the metal disc (figure 14) coupling.
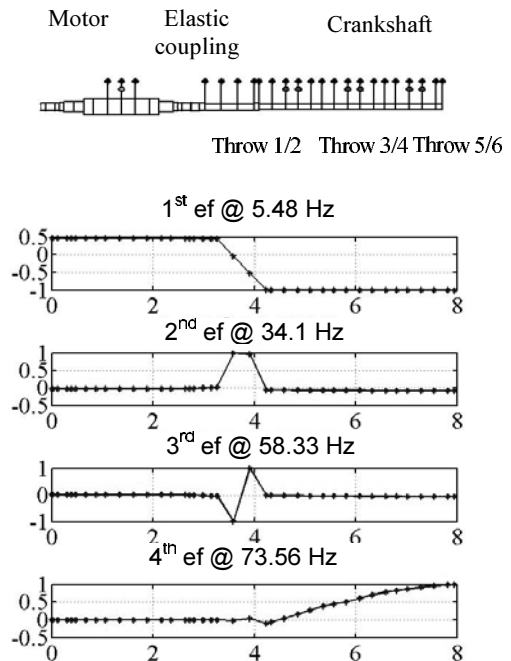

Figure 13: Calculated eigenvalues of a six-cylinder reciprocating compressor with elastic coupling
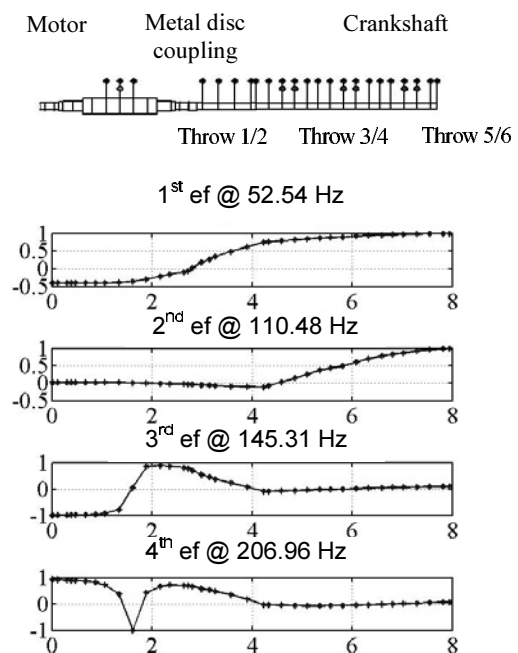

Figure 14: Calculated eigenvalues of a six-cylinder reciprocating compressor with metal disc coupling

Practical experience from torsional vibration measurements and analysis of reciprocating compressors -
Case studies, *Dr.-Ing. Johann Lenz, Dr.-Ing. Fikre Boru;* KÖTTER CONSULTING ENGINEERS
GMBH & CO. KG

One can see that the elastic coupling gives three natural frequencies below the 1st crankshaft natural frequency. These natural frequencies are torsional vibrations within the coupling and hence do not exist in the system with metal disc coupling. Using an elastic coupling the excitation of the eigenmodes with large twisting within the coupling leads to a large power dissipation which may lead to an overheating of the coupling elements resulting in coupling failure. Hence, an additional control of the power dissipation is unavoidable for systems with elastic coupling. The 1st crankshaft eigenfrequency of the drive train with metal disc coupling is 52.5 Hz, whereas that of the drive train with elastic coupling is 73.6 Hz. Figure 15 shows the Campbell diagram of both assemblies to determine the possible resonance operation speeds between 450 rpm and 1,150 rpm.
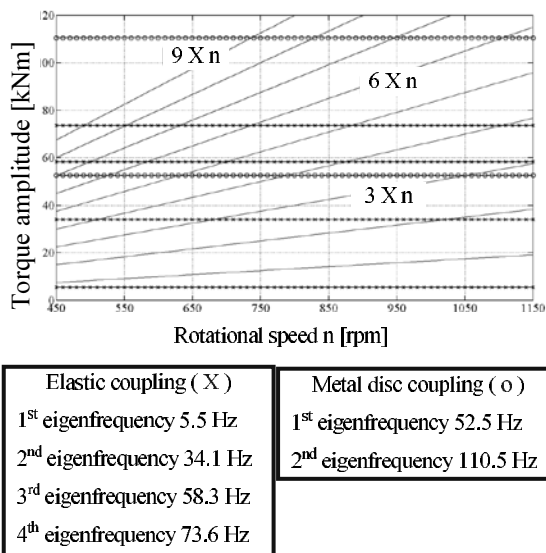

Elastic coupling (X)	Metal disc coupling (o)
1st eigenfrequency 5.5 Hz	1st eigenfrequency 52.5 Hz
2nd eigenfrequency 34.1 Hz	2nd eigenfrequency 110.5 Hz
3rd eigenfrequency 58.3 Hz	
4th eigenfrequency 73.6 Hz	

Figure 15: Campbell diagram of the drive train with elastic and metal disc coupling

In reciprocating compressors with variable operation speed, it is not possible to completely avoid the excitation of all eigenfrequencies due to higher harmonics of the rotation frequency. One way to maintain the torsional amplitude within an acceptable limit is to use a coupling with damping properties. The effect of different coupling damping on the dynamic torsional response of the drive train (discussed above) is shown in figure 16.
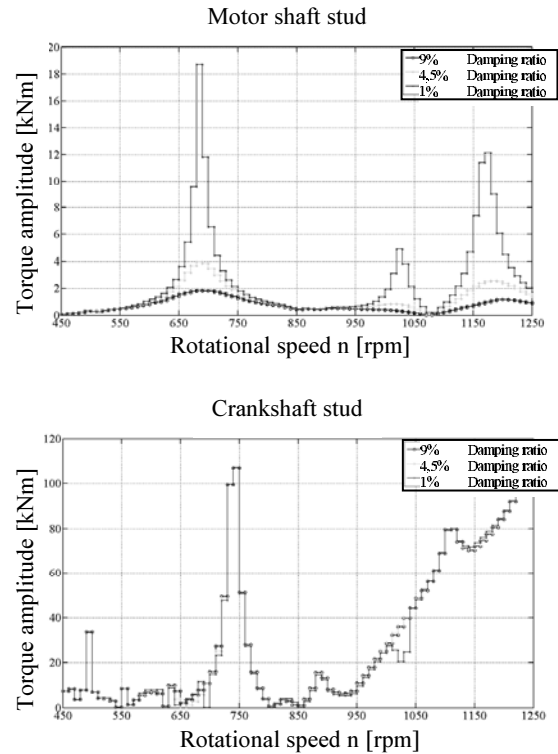

Figure 16: Comparison of the torsional loading of the motor shaft stud (top) and crankshaft stud (bottom) for different damping ratio

The calculation results show that damping ratio has a crucial influence in attenuating the torque amplitude level in the motor shaft stud. Unlike the motor shaft stud, the torque level in the crankshaft stud is irresponsive to variation of the coupling damping ratio. At the resonance speed of around 750 rpm in the crankshaft stud the 4th eigenfrequency is excited by the 6th harmonics. Since the coupling elements are almost static (nodes) for the 4th eigenform, the variation of coupling damping ratio plays an insignificant role for this resonance.

2.4 Influence of dynamic absorber

There are different ways to reduce the dynamic torque at the resonance speed of 750 rpm. One possible method is the installation of either an undamped or damped torsional dynamic absorber directly on the crankshaft. An undamped torsional dynamic absorber removes the 4th eigenfrequency but results in two new eigenfrequencies, one above and one below the previous value. As shown in figure 17, the dynamic torque level at the two new resonance speeds (resulting from the new eigenvalues) is significantly lower than the previous level. Including damping to the absorbers will further reduce the torque level as illustrated in figure 18.
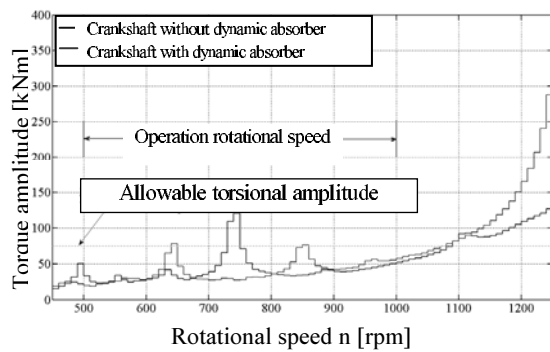
Practical experience from torsional vibration measurements and analysis of reciprocating compressors - Case studies, *Dr.-Ing. Johann Lenz, Dr.-Ing. Fikre Boru;* KÖTTER CONSULTING ENGINEERS GMBH & CO. KG

Figure 17: Torque level at the crankshaft stud with and without torsional dynamic absorber
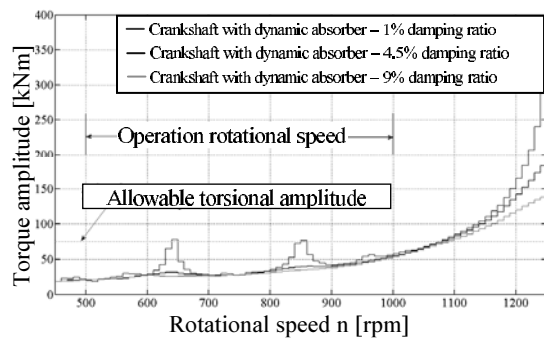

Figure 18: Influence of damping on the torsional dynamic absorber on the torque level

3   Conclusion

Torsional vibration at reciprocating compressors cannot be identified on site with simple measuring methods like e. g. measurement of the casing vibration. Often high torsional dynamic stress is not recognised until damages appear. Hence, it is advisable to conduct a detailed torsional vibration analysis when planning a new drive train or modifying an existing one. Different tools to influence the torsional vibration behaviour of a reciprocating compressor are possible. We recommend to check the results of the analysis by a strain gauge measurement to ensure the safety of the plant.

Flywheel and induction motor sizing for reciprocating compressors

by:

Pedreira Javã
Downstream
Petrobras
Rio de Janeiro
Brazil
javap@petrobras.com.br

8th Conference of the EFRC
September 27th / 28th, 2012, Düsseldorf

Abstract:

Reciprocating compressors are prone to high cyclic loads. The high required performance rely on a good design focusing a torque oscillation applied by the driver. In the first part of this this job, dynamic model of reciprocating is presented. Newton-Euler method[1][2][3] is used to get motion equations. In the second part, numerical results are presented. Simulations are used for calculate the driving moment as function of crankshaft motion. These results illustrate the effect of the flywheel and motor on its dynamics and is used for induction motor selection and flywheel sizing for optimizing crankshaft torque fluctuation and power consumption reduction.

1   Introduction

The most common cause of crankshaft failure is fatigue. In order for fatigue to occur, a cyclic tensile stress is necessary.

Two types of force act within the reciprocating compressor, namely: gas and inertia forces. Piston motion generates crankshaft angular position-varying pressures that act on the head and crank end sides. Inertia force has an alternate nature as well, resulting from time-varying acceleration of reciprocating masses. Each crank throw represents a rotating unbalance as rotation produces varying vertical and horizontal forces as a sinusoidal function. Such forces will be transmitted to crankshaft as strong time-varying torque provided by the driver. So, reciprocating machines produce significantly more torsional excitation than rotating machine such as pumps and centrifugal compressors.

Many combinations of drivers, piston sizes, load conditions, flywheel, couplings can affect the torsional characteristics of the entire system.

This work will focus in the magnitude of torque fluctuation and in the role of flywheel and motor sizing for minimizing that. Newtonian-Eulerian mechanics is used to get motion equations of compressor parts and, numerical methods are used to solve a second order non-linear differential equation.

2   Kynematics Analysis

It will be specified three referential coordinate systems *RS*, depicted at figure 1, and their respective rotation matrices.

- Inertial system *RS I* with axis *X, Y, Z* with origin at *O*;

- Moving system *RS F* with origin at *O* and axis X_1, Y_1, Z_1 rotating with the crankshaft *OA*

$$
{}^{I}T^{F} = \begin{bmatrix} \cos\theta & -\sin\theta & 0 \\ \sin\theta & \cos\theta & 0 \\ 0 & 0 & 1 \end{bmatrix}
$$

$$
{}^{I}\vec{\omega}_{F} = {}^{F}\vec{\omega}_{F} = \begin{Bmatrix} 0 \\ 0 \\ \dot{\theta} \end{Bmatrix} \tag{1}
$$

where superscripts at left and right of rotation matrix *T* refer to *RS* of origin and destiny, respectively, and $\vec{\omega}$ is *RS* angular speed with left superscript referring to where the vector is written.

- Moving system *RS Q* with origin at *B* and axis X_2, Y_2, Z_2 rotating with connecting rod *AB*

$$
{}^{I}T^{Q} = \begin{bmatrix} \cos(-\beta) & -\sin(-\beta) & 0 \\ \sin(-\beta) & \cos(-\beta) & 0 \\ 0 & 0 & 1 \end{bmatrix} =
$$

$$
= \begin{bmatrix} \cos\beta & \sin\beta & 0 \\ -\sin\beta & \cos\beta & 0 \\ 0 & 0 & 1 \end{bmatrix}
$$

$$
{}^{I}\vec{\omega}_{Q} = {}^{Q}\vec{\omega}_{Q} = \begin{Bmatrix} 0 \\ 0 \\ -\dot{\beta} \end{Bmatrix} \tag{2}
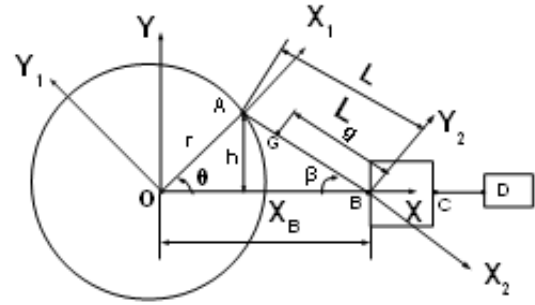$$

Figure 1: Reciprocating compressor and referential coordinate systems

Applying trigonometric relations at *OAB* triangle, one obtains

$$
h = r\sin\theta; \qquad x_B = r\cos\theta + \sqrt{l^2 - h^2} \text{ thus}
$$

$$
x_B = r\cos\theta + \sqrt{l^2 - r^2\sin^2\theta} \tag{3}
$$

Differentiating (3) twice, one obtains acceleration of points *B, C* and *D* in (4) .

$$
\ddot{x}_B = -r\sin\theta(1 + a\cos\theta)\ddot{\theta} - r(\cos\theta + a\cos(2\theta))\dot{\theta}^2 \tag{4}
$$

where $a = r/l$.

Usually the ratio a is about 0.2. So, $a^2 \sin^2 \theta \cong 0$, what simplifies a lot the algebra involved.

We also have that $\sin \beta = h / l$. Thus

$$\beta = \arcsin(a \sin \theta) \qquad (5)$$

Differentiating (5) leads to connecting rod angular speed

$$\dot{\beta} = a\cos\theta\dot{\theta} \qquad (6)$$

Differentiating (6) leads to connecting rod angular acceleration as following

$$\ddot{\beta} = a\cos\theta\ddot{\theta} - a(a^2 - 1)\sin\theta\dot{\theta}^2 \qquad (7)$$

Connecting rod gravity center acceleration $^I\vec{a}_G$ is given by (8) by using $RS\,Q$.

$$^I\vec{a}_G = {}^I\vec{a}_B + {}^I\vec{\omega}_Q \times {}^I\vec{\omega}_Q \times {}^I\vec{l}_G + {}^I\dot{\vec{\omega}}_Q \times {}^I\vec{l}_G \qquad (8)$$

where,

$^I\vec{\omega}_Q$ and $^I\dot{\vec{\omega}}_Q$ - angular velocity and acceleration of $RS\,Q$

$^I\vec{l}_G$ - vector position of gravity center of connecting rod, written in $RS\,I$

thus

$$^I\vec{a}_B = \begin{Bmatrix} \ddot{x}_B \\ 0 \\ 0 \end{Bmatrix} ; \qquad ^Q\vec{l}_G = \begin{Bmatrix} -l_G \\ 0 \\ 0 \end{Bmatrix} \qquad (9)$$

$$^I\vec{\omega}_B = \begin{Bmatrix} 0 \\ 0 \\ -\dot{\beta} \end{Bmatrix} ; \qquad ^I\dot{\vec{\omega}}_B = \begin{Bmatrix} 0 \\ 0 \\ -\ddot{\beta} \end{Bmatrix} \qquad (10)$$

$$^I\vec{l}_G = {}^IT^Q \, {}^Q\vec{l}_G = \begin{Bmatrix} -l_G \cos \beta \\ l_G \sin \beta \\ 0 \end{Bmatrix} \qquad (11)$$

Performing the vector cross products in (8) yields

$$^I\vec{\omega}_Q \times {}^I\vec{\omega}_Q \times {}^I\vec{l}_G = \begin{Bmatrix} l_G \dot{\beta}^2 \cos \beta \\ -l_G \dot{\beta}^2 \sin \beta \\ 0 \end{Bmatrix} \qquad (12)$$

$$^I\dot{\vec{\omega}}_Q \times {}^I\vec{l}_G = \begin{Bmatrix} l_G \ddot{\beta} \sin \beta \\ l_G \ddot{\beta} \cos \beta \\ 0 \end{Bmatrix} \qquad (13)$$

Adding the three parcels yields

$$^I\vec{a}_G = \begin{Bmatrix} \ddot{x}_B + l_G\left(\ddot{\beta} \sin \beta + \dot{\beta}^2 \cos \beta\right) \\ l_G\left(\ddot{\beta} \cos \beta - \dot{\beta}^2 \sin \beta\right) \\ 0 \end{Bmatrix} \qquad (14)$$

Thus, the horizontal component a_{Gx} of acceleration connecting rod gravity center is

$$a_{Gx} = \ddot{x}_B + l_G\left(\ddot{\beta} \sin \beta + \dot{\beta}^2 \cos \beta\right) \qquad (15)$$

3   Dynamic analysis

In order to perform reciprocating compressor dynamic analysis is necessary to construct a free-body diagram of each component, namely: piston, rod, crosshead, connecting rod and crankshaft. Such diagram is shown at figure 2.
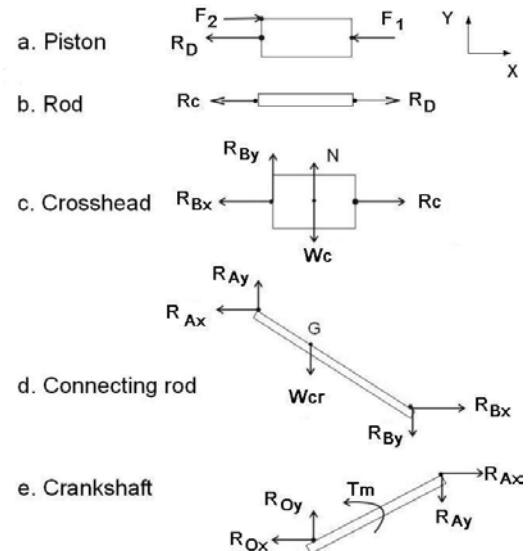

Figure 2: Free-body diagram

3.1   Piston

Observing figure *2a* and applying Newton's Second Law, one obtains

$$\sum F_x = F_2 - F_1 - R_D = m_p a_D \qquad (16)$$

$$R_D = F_g - m_p a_D \qquad (17)$$

where $\sum F_x$ - sum of forces at X direction

F_1 and F_2 – gas forces at head and crankshaft sides, respectively

$F_g = F_2 - F_1$ - resultant gas force as crankshaft angular position function $F_g = f(\theta)$

m_p – piston mass

$$a_p = \ddot{x}_B \quad \text{– piston acceleration} \qquad (18)$$

3.2   Rod

Observing figure *2b* and applying Newton's Law, one obtains

$$\sum F_x = R_D - R_C = m_{cr} a_D \qquad (19)$$

where m_{cr} - connecting rod mass

$$a_D = \ddot{x}_B \quad \text{- rod acceleration.}$$

Substituing *(17)* in *(19)* yields

$$R_C = F_g - (m_p + m_{cr})a_D \qquad (20)$$

3.3   Crosshead

Observing Figure *2c* and applying Newton's Law yields

$$\sum F_x = R_C - R_{Bx} = m_c \ddot{x}_B \qquad (21)$$

where m_c is crosshead mass

Substituing *(20)* in *(21)* yields

$$R_{Bx} = F_g - m\ddot{x}_B \qquad (22)$$

where $m = m_p + m_r + m_c$

3.4   Connecting rod

Observing figure 2d and applying Newton's Law leads to

$$\sum F_x = R_{Bx} - R_{Ax} = m_{cr} a_{Gx} \qquad (23)$$

where m_{cr} is connecting rod mass.

Substituting *(15)* and *(22)* in *(23)* yields:

$$R_{Ax} = F_g - m_t \ddot{x}_B - m_{cr} l_G \left(\dot{\beta}^2 \cos\beta + \ddot{\beta} \sin\beta\right) \qquad (24)$$

where $m_t = m + m_{cr}$

The reaction force R_{Ay} will be found by applying Euler Equation and thus

$$\sum \vec{M}_B = {}^Q\dot{\vec{H}}_B + {}^Q\vec{l}_G \times (m_{cr}\,{}^Q\vec{a}_B) \qquad (25)$$

where

J_{cr} - connecting rod mass moment of inertia with respect to axis Z_1 and

$$\sum M_B = {}^Q\vec{l} \times {}^Q\vec{R}_A + {}^Q\vec{l}_G \times {}^Q\vec{w}_{cr} \text{ - sum of moments}$$
about point B

$$\vec{H}_B = J_{cr}\omega \text{ - connecting rod angular momentum}$$

${}^Q\vec{l}$ - vector position of point A

${}^Q\vec{w}_{cr}$ - connecting rod weight.

thus

$${}^Q\vec{l} \times {}^Q\vec{R}_A + {}^Q\vec{l}_G \times {}^Q\vec{w}_{cr} = J_{cr}\,{}^Q\dot{\vec{\omega}}_Q + {}^Q\vec{l}_G \times m_{cr}\,{}^Q\vec{a}_B \qquad (26)$$

One has that

$$\bullet \;\; {}^Q\vec{R}_A = {}^QT^{11}\vec{R}_A = \begin{Bmatrix} -(R_{Ax}\cos\beta + R_{Ay}\sin\beta) \\ R_{Ay}\cos\beta - R_{Ax}\sin\beta \\ 0 \end{Bmatrix} \qquad (27)$$

where $\quad {}^{I}\vec{R}_A = \begin{Bmatrix} -R_{Ax} \\ R_{Ay} \\ 0 \end{Bmatrix}$

$$\bullet \quad {}^{Q}\vec{l}_G = \begin{Bmatrix} -l_G \\ 0 \\ 0 \end{Bmatrix} \quad ; \qquad {}^{Q}\vec{l} = \begin{Bmatrix} -l \\ 0 \\ 0 \end{Bmatrix}$$

(28)

$$\bullet \quad {}^{Q}\vec{w}_{cr} = {}^{Q}T^{II}\vec{w}_{cr} = \begin{Bmatrix} w_{cr}\sin\beta \\ -w_{cr}\cos\beta \\ 0 \end{Bmatrix} \qquad (29)$$

where $\quad {}^{I}\vec{w}_{cr} = \begin{Bmatrix} 0 \\ -w_{cr} \\ 0 \end{Bmatrix}$

$$\bullet \quad {}^{Q}\vec{a}_B = {}^{Q}T^{II}\vec{a}_B = \begin{Bmatrix} \ddot{x}_B\cos\beta \\ \ddot{x}_B\sin\beta \\ 0 \end{Bmatrix} \qquad (30)$$

$$\bullet \quad {}^{Q}\dot{\vec{\omega}}_G = \begin{Bmatrix} 0 \\ 0 \\ -\ddot{\beta} \end{Bmatrix} \qquad (31)$$

Performing the vector cross products indicated in *(26)* yields

$$J_{cr}\begin{Bmatrix} 0 \\ 0 \\ -\ddot{\beta} \end{Bmatrix} + \begin{Bmatrix} 0 \\ 0 \\ -l_G m_{cr}\ddot{x}_B\sin\beta \end{Bmatrix} =$$

$$= \begin{Bmatrix} 0 \\ 0 \\ l(R_{Ax}\sin\beta - R_{Ay}\cos\beta) \end{Bmatrix} + \begin{Bmatrix} 0 \\ 0 \\ l_G w_{cr}\cos\beta \end{Bmatrix}$$

(32)

thus from *(32)* one obtains

$$R_{Ay} = \sin\beta(F_g - bm_{cr}\ddot{x}_B) +$$

$$+ (\frac{J_{cr}}{l} - m_{cr}l_g\sin^2\beta)\ddot{\beta} - m_{cr}l_g\sin\beta\dot{\beta}^2 + bw_{cr}$$

(33)

3.5 Crankshaft

Observing figure 2e and applying Euler Equation leads to

$$\sum {}^{I}M_o = {}^{I}\vec{r} \times {}^{I}\vec{R}_A + {}^{I}\vec{T}_m = J{}^{I}\dot{\vec{\omega}}_c \qquad (34)$$

where

$\sum M_O$ - sum of moments about point *O*

J - sum of mass moment of inertia of flywheel, driver rotor, crankshaft and coupling with respect to axis Z_I

$\vec{T}_m$ - torque applied by the driver and

$${}^{I}\vec{r} = \begin{Bmatrix} r\cos\theta \\ r\sin\theta \\ 0 \end{Bmatrix} ; \quad {}^{I}\vec{R}_A = \begin{Bmatrix} R_{Ax} \\ -R_{Ay} \\ 0 \end{Bmatrix} ; \quad {}^{I}\vec{\omega} = \begin{Bmatrix} 0 \\ 0 \\ \ddot{\theta} \end{Bmatrix}$$

(35)

Substituting *(35)* in *(34)* and performing the vector cross products leads to

$$J\begin{Bmatrix} 0 \\ 0 \\ \ddot{\theta} \end{Bmatrix} = \begin{Bmatrix} 0 \\ 0 \\ -r(R_{Ax}\sin\theta + R_{Ay}\cos\theta) \end{Bmatrix} + \begin{Bmatrix} 0 \\ 0 \\ T_m \end{Bmatrix}$$

(36)

thus

$$J\ddot{\theta} + r(R_{Ax}\sin\theta + R_{Ay}\cos\theta) = T_m \qquad (37)$$

Substituting *(24)* and *(33)* in *(37)* yields

$$\frac{J}{r}\ddot{\theta} + A_1\ddot{x}_B + A_2\ddot{\beta} + A_3\dot{\beta}^2 + A_4 = T_m/r \quad (38)$$

where T_m is the torque applied by the driver and

$$A_1 = \sin\theta[a(bm_{cr} - m_t)\cos\theta - m_t]$$

$$A_2 = \cos\theta(\frac{J_{cr}}{l} - abm_{cr}r\ \sin^2\theta) - am_{cr}l_g \sin^2\theta$$

$$A_3 = m_{cr}l_g \sin\theta(a\cos\theta + 1)$$

$$A_4 = F_g \sin\theta(a\cos\theta + 1) + bw_{cr}\cos\theta$$

Substituting *(4)*, *(6)* and *(7)* in *(38)* yields

$$(f_1(\theta) + J/r)\ddot{\theta} + f_2(\theta)\dot{\theta}^2 + f_3(\theta) = T_m/r$$

(39)

where

$$f_1(\theta) = -a\sin^2\theta(c_1\cos^2\theta + c_2\cos\theta - c_3) + c_4$$

$$f_2(\theta) = \sin\theta[c_5\cos\theta - c_6\sin^2\theta(a\cos\theta + 1) +$$
$$+ r(m_t - c_7\cos\theta)(\cos\theta + a\cos(2\theta)) - c_8]$$

$$f_3(\theta) = F_g\sin\theta(a\cos\theta + 1) + bw_{cr}\cos\theta$$

and,

$$c_1 = ar(2bm_{cr} - m_t)\ ;\quad c_2 = 2a(m_{cr}l_g - m_t l)$$

$$c_3 = m_t l\ ;\qquad c_4 = aJ_b/l$$

$$c_5 = a^2[J_{cr}(a^2 - 1)/l - a^2m_{cr}l_g]$$

$$c_6 = a^2 m_{cr}l_g(a^2 - 2)\ ;\quad c_7 = a(bm_{cr} - m_t)$$

$$c_8 = a^2 m_{cr}l_g$$

For an induction motor, one has the torque curve versus angular speed, so $T_m = f(\dot{\theta})$. Equation *(39)* is a non-linear second order differential equation. It is solved numerically and consists in finding crankshaft angular position and speed as function of time. The angular speed variation is controlled by the flywheel inertia and shall be sized to optimize crankshaft torque fluctuation. Once angular speed as function of time is found, one has the torque motor T_m as function of time. Thus, we have crankshaft torque, used to perform torsional and stress analysis.

4   Numerical simulation

It will be presented two numerical simulations of a hydrogen compressor from a hydro treating unit. It's a horizontal in line compressor with two opposing cylinders. Compressor data is summarized in Table 1.

Numerical simulation will be performed to analyze a hydrogen compressor design. This compressor had the coupling failure some hours after start-up as shown in Figure 3.

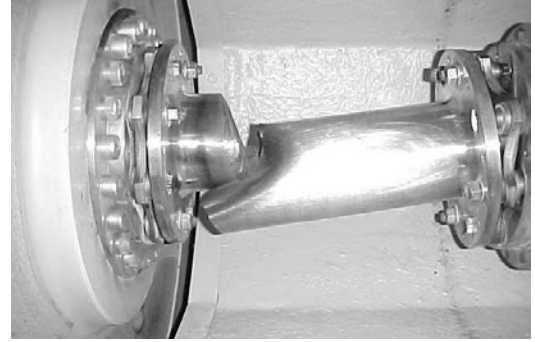Gas forces will be calculated by using ideal gas state equation. Total gas force is shown in Figure 4.

Figure 3: Coupling failure

	1 stg	**2 stg**
Piston diam. (mm)	305.0	220.0
Rod diam. (mm)	70.0	70.0
m_t (kg)	303.0	268.0
m_{cr} (kg)	68.0	68.0
Throw (mm)	180.0	180.0
Ratio a	0.16	0.16
Clearance (%)	11.0	15.0
Suc. pressure (bar g)	20.5	39.4
Disc. pressure	39.5	70.1

Table 1: Compressor data

Figure 4: Total gas force

299